DOKUZ EYLÜL UNIVERSITY

GRADUATE SCHOOL OF NATURAL AND APPLIED SCIENCES

TREATABILITY OF ANTIBIOTICS IN SEQUENTIAL BUOYANT FILTER/AEROBIC AND MULTICHAMBER/AEROBIC SYSTEMS

by

Hakan ÇELEBİ

October, 2012

İZMİR

TREATABILITY OF ANTIBIOTICS IN SEQUENTIAL BUOYANT FILTER/AEROBIC AND MULTICHAMBER/AEROBIC SYSTEMS

A Thesis Submitted to the
Graduate School of Natural and Applied Sciences of Dokuz Eylül University
In Partial Fulfillment of the Requirements for the Degree of Doctor of Philosophy in Environmental Engineering, Environmental Science Program

by
Hakan ÇELEBİ

October, 2012
İZMİR

Ph.D. THESIS EXAMINATION RESULT FORM

We have read the thesis entitled **"TREATABILITY OF ANTIBIOTICS IN SEQUENTIAL BUOYANT FILTER/AEROBIC AND MUTLICHAMBER /AEROBIC SYSTEMS"** completed by **HAKAN ÇELEBİ** under supervision of **PROF. DR. DELIA TERESA SPONZA** and we certify that in our opinion it is fully adequate, in scope and in quality, as a thesis for the degree of Doctor of Philosophy.

Prof. Dr. Delia Teresa SPONZA

Supervisor

Prof. Dr. Ayşegül PALA

Thesis Committee Member

Prof. Dr. Nur OKUR

Thesis Committee Member

Assoc. Prof. Dr. Celalettin ÖZDEMİR

Examining Committee Member

Assoc. Prof. Dr. Görkem AKINCI

Examining Committee Member

Prof.Dr. Mustafa SABUNCU
Director
Graduate School of Natural and Applied Sciences

ACKNOWLEDGMENTS

I am grateful to my supervisor, Prof. Dr. Delia Teresa SPONZA, for her advices to be subject, for all her suggestions and support in every step of my study.

I would like to sincerely thank Prof. Dr. Ayşegül PALA and Prof. Dr. Nur OKUR the committee members of my thesis study, for their strong support, valuable suggestions on my research, and their helps in many aspects of this project.

Moreover, I would like to thank. M.Sc.Env. Eng. Oğuzhan GÖK, Ph.D. Gülden GÖK, M.Sc.Env. Eng Mesut AK and M.Sc.Env. Eng Melik KARA for their valuable helps during my laboratory studies.

I am thankful to Assoc. Prof. Dr. Görkem AKINCI and M.Sc. Adem TÜZEMEN for their help, assistance and moral support during my study.

I am grateful to my family for their support. Their sacrifices are immeasurable and will never be forgotten.

Finally, I specially would like to thank my wife Yudum ÇELEBİ, my daughter Melek Naz ÇELEBİ for his endless support, patience, and love.

Hakan ÇELEBİ

TREATABILITY OF ANTIBIOTICS IN SEQUENTIAL BUOYANT FILTER/AEROBIC AND MULTICHAMBER/AEROBIC SYSTEMS

ABSTRACT

In the context of this thesis, the treatability of oxytetracycline (OTC), amoxicillin (AMX), tylosin (TYL) and erythromycin (ERY), which are toxic and non-degradable antibiotic compounds were investigated in an sequential Anaerobic Multichamber Bed Reactor (AMCBR)/aerobic Continuously Stirred Tank Reactor (CSTR) and sequential Anaerobic Buoyant Filter Reactor (ABFR)/aerobic Continuously Stirred Tank Reactor (CSTR) reactor systems at increasing OTC, AMX, TYL and ERY loading rates and decreasing HRTs. COD, OTC, AMX, TYL and ERY removal efficiencies, total and methane gas productions, methane contents, TVFA, Bic.Alk., TVFA/Bic.Alk. ratios were investigated separately in AMCBR and ABFR at increasing OTC, AMX, TYL and ERY loading rates and decreasing HRTs. High COD, OTC, AMX, TYL and ERY removals were obtained in the AMCBR reactor compared to the ABFR reactor. High methane productions and methane yields were obtained in the AMCBR versus ABFR reactor.

High COD, OTC, AMX, TYL, ERY removal efficiencies and methane gas contents were obtained at high HRTs in the AMCBR and ABFR reactors. TVFA, Bic.Alk., TVFA/Bic.Alk. ratios were found between optimum values in the AMCBR and ABFR reactors through continuous operation. The toxic OTC and AMX were transformed to less toxic intermediate products namely alfa-Apo, beta-Apo OTC and to diketopiperazine, respectively in the AMCBR and ABFR reactors. High acute toxicity yields were obtained with the bioassays performed by *Vibrio fischeri* and *Daphnia magna* in the sequential AMCBR/CSTR reactor systems. The substrate removal in the AMCBR was performed according to Grau-second order, Stover-Kincannon kinetic model. At high OTC concentration the inhibition was explained with Haldane kinetic model. The methane obtained from the AMCBR reactor can be used to recovery a partial part of the expenses utilized in the sequential anaerobic/aerobic reactor with simultaneous OTC, AMX; TYL and ERY removals.

Keywords: anaerobic multichamber bed reactor (AMCBR), anaerobic buoyant filter reactor (ABFR), oxytetracycline (OTC), amoxicillin (AMX), tylosin (TYL), erythromycin (ERY), anaerobic treatment, anaerobic/aerobic treatment, toxicity, kinetic, inhibition, *Daphnia magna*, *Vibrio fischeri*

ANTİBİYOTİKLERİN ARDIŞIK YÜZEN ANAEROBİK FİLTRE/SÜREKLİ TAM KARIŞTIRMALI REAKTÖR VE ÇOK KADEMELİ ANAEROBİK REAKTÖR/ SÜREKLİ TAM KARIŞTIRMALI REAKTÖRLERDE ARITILABİLİRLİKLERİ

ÖZ

Bu tez kapsamında toksik ve zor ayrışabilen antibiyotik bileşiklerden olan oksitetrasiklin (OTS), amoksisilin (AMS), tilosin (TLS) ve eritromisinin (ERT) arıtılabilirliği, ardışık Anaerobik Çok Kademeli Yatak Reaktör (AÇKYR)/Aerobik Sürekli Karıştırmalı Tank Reaktör (SKTR) ve ardışık Anaerobik Yüzen Filtre Reaktör (AYFR)/ Aerobik Sürekli Karıştırmalı Tank Reaktör (SKTR) sistemlerinde, artan OTS, AMS, TLS ve ERT yükleme hızlarında ve altı farklı hidrolik bekleme sürelerinde (HBS) karşılaştırılmıştır. KOİ, OTS, AMS, TLS ve ERT giderme verimleri, toplam ve metan gaz üretimleri, metan içeriği, TUYA, Bik.Alk. ve TUYA/Bik.Alk. oranları değişimleri artan OTS, AMS, TLS ve ERT yükleme hızlarında ve azalan HBS'lerde AÇKYR ve AYFR'de ayrı ayrı incelenmiştir. Yüksek COD, OTS, AMS, TLS ve ERT verimleri AYFR reaktörle karşılaştırıldığında AMCBR reaktör için elde edilmiştir. Yüksek metan üretimi ve metan verimi ABFR reaktöre karşı AÇKYR'de elde edilmiştir.

AÇKYR ve AYFR reaktörlerde yüksek KOİ, OTS, AMS, TLS ve ERT giderme verimleri ve metan gaz içerikleri yüksek HBS'lerde elde edilmiştir. AÇKYR ve AYFR reaktörlerinde, TUYA, Bik.Alk. ve TUYA/Bik.Alk. oranları sürekli işletim süresince optimum değerler arasında kalmıştır. Toksik OTC ve AMX, AMCBR ve ABFR'de sırasıyla, daha az toksik alfa-Apo, beta-Apo OTS diketopiperasin'e ara ürünlerine dönüştürülmüştür. Yüksek akut toksisite verimleri sıralı AMCBR/CSTR reaktör sistemlerinde *Vibrio fischeri* ve *Daphnia magna* tarafından gerçekleştirilen biyoanalizlerle elde edilmiştir. AÇKYR reaktörde substrat giderimi Grau-ikinci dereceden, Stover-Kincannon kinetik modeline göre yapıldı. Yüksek OTC konsantrasyonunda inhibisyon Haldane kinetik model ile açıklanmıştır. AMCBR reaktörden elde edilen metanın bir kısmı eşzamanlı OTS, AMS, TLS ve ERT

giderimleri ile ardışık anaerobik/aerobik reaktörde kullanılan giderlerin bir bölümünde kullanılabilir.

Anahtar Kelimeler: anaerobik çok kademeli yatak reaktör (AÇKYR), anaerobik yüzen filtre reaktör (AYFR), oksitetrasiklin (OTS), amoksisilin (AMS), tilosin (TLS), eritromisin (ERT), anaerobik arıtım, anaerobik/aerobik arıtım, toksisite, kinetik, inhibisyon, *Daphnia magna*, *Vibrio fischeri*

CONTENTS

Page

CHAPTER ONE
INTRODUCTION

1.1 Introduction

Emerging contaminants (ECs) are defined as newly identified or previously unrecognized pollutants, and this group mainly comprises products used in large quantities in everyday life, such as pharmaceuticals and personal care products (PPCPs), endocrine-disrupting compounds (EDCs) and various industrial additives (Chen and Ding, 2008). Pharmaceutical compounds, their byproducts and metabolites can be toxic, mutagenic and carcinogenic for the environment and human health (Chen and Ding, 2008). These compounds are generally recalcitrant to biological treatment and remain in the environment. Oxytetracycline (OTC), tylosin (TYL), erythromycin (ERY) and amoxicillin (AMX) were listed by the Environmental Protection Agency (EPA)'s as "Emerging Contaminants" (EPA, 2010).

Antibiotics are an important group of pharmaceuticals in today's medicine. They are used for the treatment of human and animal diseases and they are used as growth promoter in animal feeding operations. Human and veterinary antibiotics are continually being released into the environment mainly as a result of manufacturing processes, disposal of unused or expired products, and excreta. Veterinary antibiotics may enter into the environment more immediately than does human antibiotics (Sarmah et al., 2006). The existence of antibiotics in the environment and their possible effects on living organisms are giving rise to growing concern. Depending upon their physical and chemical properties, many of antibiotics or their bioactive metabolites end up in soils and sediments (Teixeira et al., 2008). In addition, effluent of sewage treatment plant can constitute a source for antibiotic pollution in the surface and ground water. Bacterial resistance is a significant problem related with the presence of antibiotics in the environment. These compounds have also an important exerting toxic effect to aquatic organisms even in the μg/L and mg/L concentration range that change the ecological balance negatively (Teixeira et al.,

2008). Currently, legal limits for antibiotics in surface water, groundwater, and wastewater have not been established (Sarmah et al., 2006). To assess the environmental risk, extensive data documenting the contamination of the aquatic environment by these pollutants is needed.

Conventional treatment processes are unable to eliminate antibiotics in water and wastewater, thus it is necessary to investigate different treatment technologies for antibiotic pollution control. Different treatment technologies have been recently evaluated for this purpose, including biological treatment (anaerobic: Wu et al. (2011), Chelliapan et al., (2011); aerobic: Lapara et al., (2001), Chang et al., (2008), Chen et al., (2008); sequential anaerobic/aerobic: Buitron et al., (2003)), adsorption (advanced oxidation using ozone and ozone/hydrogen peroxide, hydrogen peroxide/UV, titanium dioksit and Fe^{+3}) (Trovo et al., 2011, Elmolla et al., 2011, Elmolla et al., 2010), membrane filtration such as nano-filtration, reverse osmosis, photo-fenton (Snyder et al., 2007; Watkinson et al., 2007), chemical treatment (coagulation/flocculation) (Suarez et al. 2009, Deegan et al., 2011). The biological treatment processes mentionated above exhibited low antibiotic yields while the advanced treatment processes are costly.

The anaerobic buoyant filter (ABFR) and anaerobic multi chamber bed reactors (AMCBR) are high rate anaerobic reactors. The advantages of anaerobic AMCBR and anaerobic ABFR reactor systems are: better resilience to hydraulic and organic shock loadings, longer biomass retention times, lower sludge yields, and the ability to partially separate between the various phases of anaerobic catabolism (Ghaniyari-Benis et al., 2009).

The literature survey shows that there is a lack on the anaerobic treatment of OTC, TYL, ERY AMX by ABFR and AMCBR reactors. In other words, no study was found in the literature for the AMCBR and ABFR reactor treating the pharmaceutical wastewaters containing OTC, TYL, ERY and AMX.

1.2 The Purpose and Scope of the Study

The general purpose of this Ph.D thesis was to evaluate the performance of the anaerobic multi chamber bed (AMCBR) and anaerobic buoyant filter reactors (ABFR) on the treatment efficiencies of a synthetic pharmaceutical wastewaters and real pharmaceutical wastewaters containing the antibiotics namely OTC, TYL, ERY and AMX. There is not enough knowledge about the treatability of pharmaceutical wastewater under anaerobic conditions for AMCBR and ABFR reactor systems. In other words, no study about the anaerobic treatability of real raw pharmaceutical wastewaters containing antibiotic, no study about the antibiotic removal and inhibition kinetics was encountered using both AMCBR and ABFR reactors. Therefore this thesis was designed to investigate these lacks in the literature. The specific objectives of this study are as follows:

1. To determine the inhibition concentration of OTC, TYL, ERY and AMX which caused 50% decrease in the methanogenic activity (IC_{50}) in batch reactors (the batch studies gives information about the OTC, TYL, ERY and AMX doses will be used in the AMCBR and ABFR reactor through continuous operation. In the first step of this study, the toxic effect of OTC, TYL, ERY and AMX on methane *Archaea* was investigated using anaerobic toxicity (ATA) test,

2. To evaluate short- and long-term effects of low and high OTC, TYL, ERY and AMX concentrations on COD removals and biogas productions in steady-state anaerobic treatment for both reactors in synthetic pharmaceutical wastewaters,

3. To determine the COD subcategories in the anaerobic AMCBR reactor at increasing OTC and AMX concentrations under constant hydraulic retention times (HRT),

4. To determine the effect of compartments located in both reactors, on the total reactor performances based on OTC, TYL, ERY and AMX, COD yields, pH, total volatile fatty acid (TVFA) accumulation, bicarbonate alkalinity (HCO_3) and TVFA/HCO_3 ratios at increasing OTC, TYL, ERY and AMX loading rates under constant HRTs,

5. To determine the total removal efficiencies in sequential anaerobic AMCBR/aerobic completely stirred tank reactor (CSTR) and sequential anaerobic ABFR/aerobic completely stirred tank reactor (CSTR) systems at increasing OTC, TYL, ERY and AMX loading rates under constant HRTs and flow rates,

6. To determine OTC, TYL, ERY and AMX, COD removal efficiencies, total gas, methane gas productions, methane contents in AMCBR and ABFR reactors at decreasing HRTs under constant OTC, TYL, ERY and AMX concentrations,

7. To determine the effect of compartments, located in the reactors, on the total reactor performances based on OTC, TYL, ERY and AMX, COD, pH, TVFA, HCO_3 alkalinity and TVFA/HCO_3 ratios at decreasing HRTs under constant OTC, TYL, ERY and AMX concentrations,

8. To determine the total removal efficiency in sequential AMCBR/CSTR and ABFR/CSTR reactor systems at decreasing HRTs under constant OTC, TYL, ERY and AMX concentration,

9. To determine the acute toxicity effect of OTC, TYL, ERY and AMX on *Daphnia magna* and *Vibrio fischeri* in the sequential AMCBR/CSTR reactor system at increasing OTC, TYL, ERY and AMX loading rates,

10. To determine the metabolites of OTC and AMX through continuous operation of AMCBR and ABFR reactor systems, respectively,

11. To determine the substrate (COD) and antibiotics (OTC, TYL, ERY and AMX) removal kinetics in the AMCBR reactor using Monod, Contois and Stover-Kincannon kinetic models at decreasing HRTs,

12. To determine the inhibition kinetic of OTC in AMCBR reactor using Competitive, Noncompetitive, Uncompetitive and Haldane inhibition kinetic models, at decreasing HRTs,

13. To determine the kinetic model for gas productions and methane gas quality at decreasing HRTs,

This Ph.D. thesis is presented in five chapters: The purposes and scopes of this Ph.D. study were presented in Chapter 1. In the Chapter 2 antibiotics, their sources and properties were summarized. In Chapters 3 and 4 the literature review about antibiotics and treatability studies of OTC, AMX, TYL and ERY antibiotics under anaerobic, aerobic and sequential conditions were mentioned. The section “materials and methods” were explained in Chapter 5. Results and discussions were presented in Chapter 6. The general conclusions and recommendations were presented in Chapter 7.

CHAPTER TWO
ANTIBIOTICS, THEIR SOURCES AND PROPERTIES

2.1 Sources of Emerging Contaminants (ECs)

Emerging contaminants, including a wide range of compounds, are an important issue of study due to the current lack of information about the potential impact associated with their occurrence, fate, and eco-toxicological effects (Suarez et al., 2008; Myers, 2009). ECs are generally classified as pharmaceuticals, personal care products (PPCPs), endocrine disrupting compounds (EDCs) and pesticides and range from a variety of both natural and synthetic organic compounds and also some heavy metals. The main sources of ECs include industrial discharges, wastewater treatment facilities, storm water and agricultural runoffs in addition to leakages by sewer systems/industrial systems and illicit discharges (Figure 2.1).

2.1.1 Antibiotics in the Environment

Antibiotics are substances produced by microorganisms that can destroy or inhibit the growth of other microorganisms. The presence of antibiotics in a natural environment can disturb the ecological balance (Lansky and Halling-Sorensen, 1997) and lead to the development of multiresistant strains of bacteria (Balcioglu and Otker, 2003), making treatment of some diseases difficult. More important, the detection of antibiotics in the environment has raised concern about potential human health effects. The discharge of pharmaceutical wastewater from the process of antibiotic production is one of the most important sources of antibiotics in surface and groundwater. More than 50 million pounds of antibiotics are produced in the United States each year, with about 60% used in human medicine, and the remaining 40% used for veterinary purposes, including growth promotion (32%) and therapeutic use (8%) (Sarmah et al., 2006), as shown in Figure 2.2.

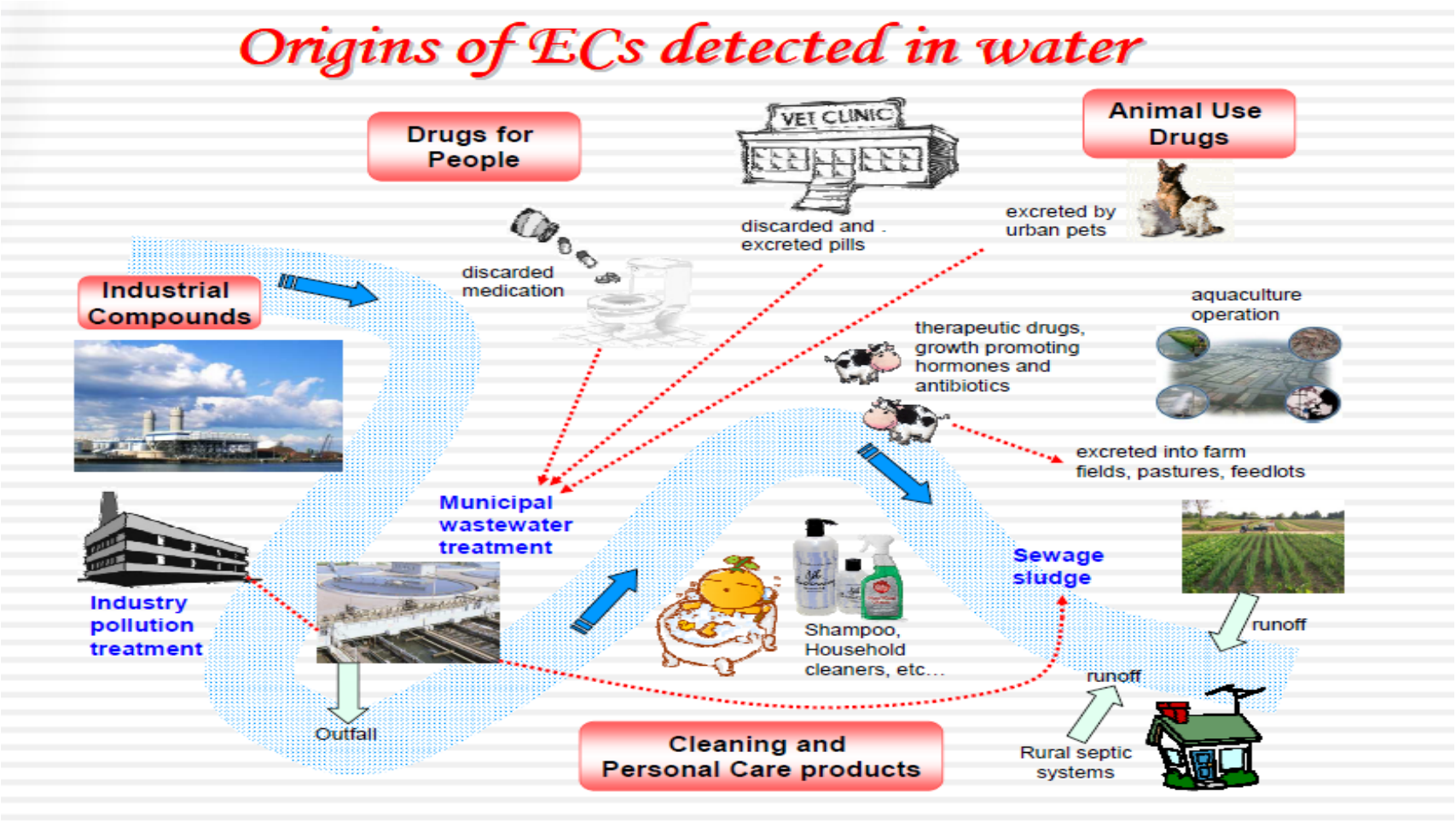

Figure 2.1 Origins of Emerging Contaminants Detected in Water (Chen and Ding, 2008)

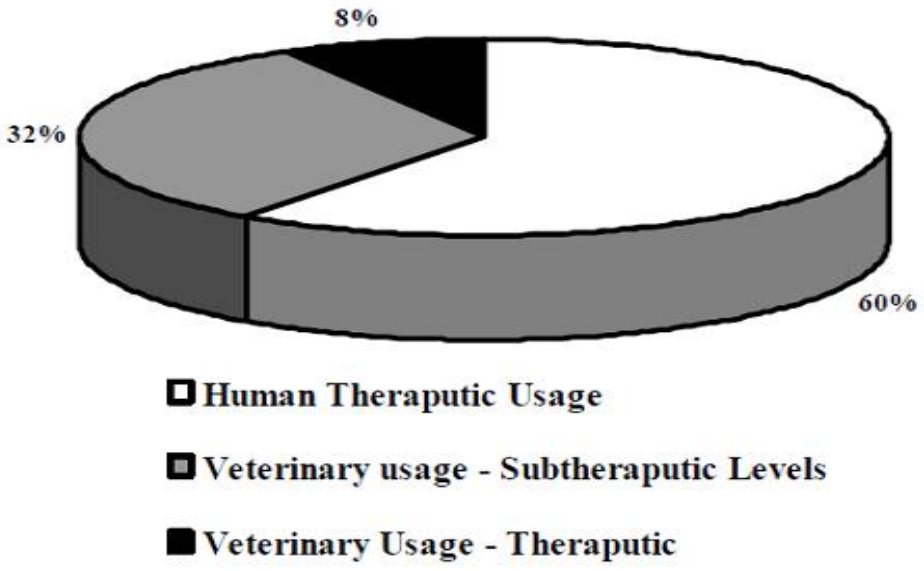

Figure 2.2 Distribution of antibiotics usage in the world-wide (Sarmah et al., 2006)

2.1.1.1 Sources of Environmental Antibiotic Contamination

Antibiotics used in Human Medicine: Antibiotics used in human treatment can enter the environment either by excretion or disposal of surplus drugs into sewage systems. Effluent from wastewater treatment plants (WWTPs) is released into the local aquatic surroundings (Jorgensen and Halling-Sorensen, 2000) as shown in Figure 2.3. Antibiotic residues have been detected in the final effluents of WWTPs in world-wide. Currently, many conventional WWTPs are not designed and operated to remove very low concentrations of contaminants, such as pharmaceuticals, consequently releasing these compounds into surface waters (Kolpin et al., 2002; Daughton and Ternes, 1999; Ternes et al., 2004; Batt, 2006). Recent investigations have identified WWTPs as important point sources for antibiotic contamination of surface waters (Petrovic et al., 2003; Glassmeyer et al., 2005).

Drugs Used in Veterinary Medicine: In the livestock industry, the use of antibiotics as growth promoters as well as therapeutic agents is very common. In a recent survey conducted by the US National Animal Health Monitoring System, approximately 25% of small feedlot cattle operations and 70% of large feedlot

operations used antibiotics in the feed (Golet et al., 2002). A significant portion of the administered antibiotics in animals is excreted in an un-metabolized form. Animal manure containing excreted antibiotics is frequently applied to agricultural fields, where antibiotics may potentially contaminate ground water and eventually enter surface water, as shown in Figure 2.3.

The use of antibiotics both by humans and in the veterinarian field can lead to exposure of the environment by a number of routes (Figure 2.3): The sources of antibiotics can be divided into 11 categories.

1 Water Source (surface)
2 Municipal water treatment facilities-treatment a barrier to some pharmaceuticals
3 Municipal water distribution systems
4 Domestic wastes - pharmaceutical metabolites enter wastewater system.
5 Hospital waste from patients, hospital labs, and pharmacies-both metabolites and pharmaceuticals enter waste water system.
6 Pets treated with medication produce waste-metabolites runoff to storm sewers.
7 Vet clinics, hospitals, pharmacies, labs produce waste-metabolites and discarded pharmaceuticals enter sewers.
8 Farms discard drugs into wastewater and metabolites from treated animals go into runoff
9 Sewage treatment plant destroys some, but not all, pharmaceuticals and metabolites-some discharged into source water; sludge often spread on fields, ultimately resulting in runoff to source water.
10 Municipal compost often spread on fields; metabolites from animal waste, and also from diapers, may be present.
11 Municipal-town groundwater sources and rural wells receive runoff with metabolites from farm animals.

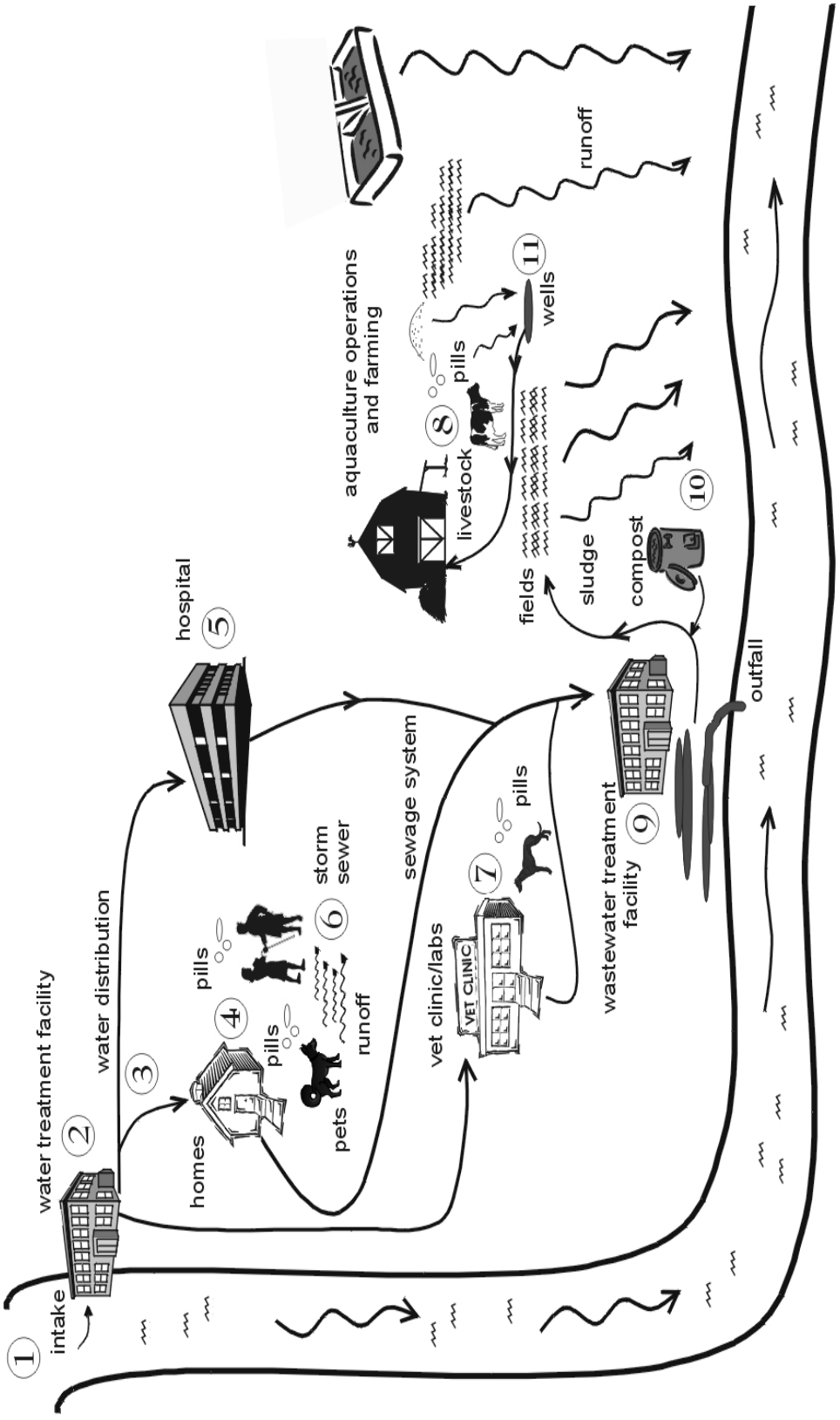

Figure 2.3 Potential exposure routes of antibiotics used in human and veterinary medicine into the aquatic environment (Holtz, 2006)

2.2 Characteristics of the selected antibiotics

For this Ph. D. thesis four antibiotics were selected (OTC, AMX, TYL and ERY). The selection criteria have been as following:

1. High consumption rates in the world-wide;
2. Representation of a variety of therapeutic classes;
3. Reported occurrence in the environment;
4. Reported acute and chronic toxicity;
5. Physical and chemical properties (hydrophobic/hydrophilic);
6. Susceptibility to biodegradation;
7. Availability of validated analytical methods

2.2.1 Structures, Properties, and Behavior of Studied Antibiotics

Among all the emerging contaminants, pharmaceuticals are of the greatest and increasing concern (see Table 2.1). The modes of action, mechanism of resistance, approved in the world-wide of selected antibiotics included in this research are presented in Table 2.1. Furthermore, chemical structures and selected physical properties of the target antibiotics are listed in Table 2.2.

Table 2.1 Classes of pharmaceuticals (Kolpin, 2002; Holtz, 2006)

Therapeutic Class	**Antibiotics and Drugs**
Veterinary and human antibiotics	
*β-lactams	Amoxicillin, Ampicillin, Benzylpenicillin
*Macrolides	Erythromycin, Azithromycin, Tylosin
*Sulfonamides	Sulfamethazine, Sulfadiazine, Sulfaguanidine
*Tetracyclines	Oxytetracycline, Tetracycline
Analgesics, anti-inflammatory drugs	Codeine, Ibuprofen, Acetoaminofen, Diclofenac
Lipid regulators	Bezafibrate, Clofibric acid, Fenofibric acid
Psychiatric drugs	Diazepam
β -blockers	Metoprolol, Propranolol, Timolol, Solatol
Anti-depressants	Fluoxetine
Hormones	Estradiol, Estrone, Estriol, Diethylstilbestrol

Table 2.2 A summary of the chemical structures and selected physical properties of the studied antibiotics.

Tetracycline	**Molecular Weight**	**CAS Number**	**Log K_{OW}**	**Log K_d**	**pKa**	**Structure**
Oxytetracycline (OTC)	460.5 g/mol	79-57-2	0.08	2.5-3.0 in different soils	3.22 7.46 8.94	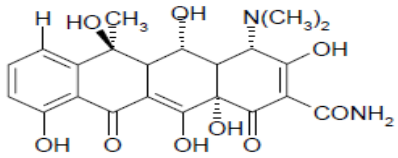
Macrolide	**Molecular Weight**	**CAS Number**	**Log K_{OW}**	**Log K_d**	**pKa**	**Structure**
Tylosin (TYL)	916.1 g/mol	1401-69-0	3.5	2.7-3.9 in soils	7.5	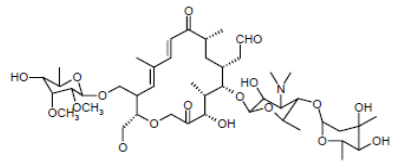
Erythromycin (ERY)	733.9 g/mol	114-07-8	3.06	1.65 at pH 7	8.90	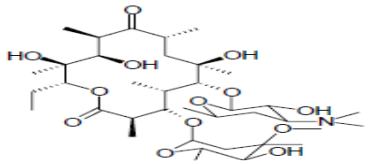
β-Lactams	**Molecular Weight**	**CAS Number**	**Log K_{OW}**	**Log K_d**	**pKa**	**Structure**
Amoxicillin (AMX)	365.4 g/mol	26787-78-0	0.87	2.4-2.8, at pH 7.2	1.06	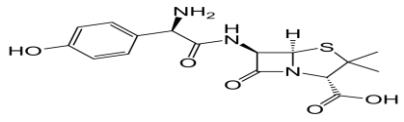

2.2.1.1 Macrolide Antibiotics

Mode of action and resistance mechanism: The macrolide ERY is a naturally occurring antibiotic, with other semi-synthetic derivatives of this compound in use (roxithromycin). Macrolides also exert a bacteriostatic effect, and like the lincosamides, their mode of action is to prevent protein synthesis by binding to ribosomal RNA, and resistance also develops as the result of an alteration to the drug target site. ERY and clindamycin have actually been shown to bind to the same site in bacterial ribosomal DNA, so cross resistance between these two antibiotic classes can also be developed (Walsh, 2003).

Macrolide resistance is also accomplished by the development of efflux pumps, although this mechanism does not affect the lincosomides (DiPersio and DiPersio, 2006).

Approved Uses in the world-wide: ERY is used in human medicine to treat respiratory infections (Walsh, 2003). ERY and TYL are used extensively in veterinary medicine, and are approved for both therapeutic and growth promotion use in cattle, sheep (ERY only), swine, and poultry (USDA/APHIS/Veterinary Services, 1999; FDA, 2006).

Behavior in the Environment: The log K_{OW} values for ERY and TYL indicate that these compounds are slightly hydrophobic (Table 2.2). Log K_d values measured for TYL in different types of soil ranged from 2.7-3.9, which suggests that it will be slightly mobile to immobile in soil systems (Kay et al., 2005). The sorption behavior of other macrolides has been investigated in sewage sludge, however, ERY could not be detected in sludge in comparison to high dissolved concentrations in effluent, therefore it was concluded that sorption of ERY to sewage sludge is negligible (Gobel et al., 2005).

2.2.1.2 Tetracyclines

Mode of action and resistance mechanism: TCs are a naturally occurring class of bacteriostatic compounds their mode of action, like the macrolides and lincosomides, is to prevent protein synthesis by binding to ribosomal RNA, although the TCs have a different target site in the ribosome. The main reported mechanism of resistance against the TCs is the development of efflux pumps (Walsh, 2003).

Approved Uses in the world-wide: Tetracycline (TC) is widely used in human medicine to treat a variety of bacterial infections (USFDA, 2004). TC, OTC, and chlortetracycline (CTC) are approved for use as feed additives and therapeutic agents in dairy and beef cattle, swine, chickens, and turkeys, while OTC and CTC are approved for the same uses in sheep. The tetracyclines (TCs) are the most frequently used feed additives in commercial feedlots (USDA/APHIS/Veterinary Services, 1999).

TCs are a group of broad spectrum antibiotics, commonly used in preventative treatments, and to increase growth efficiency of cattle in many countries by being added to animal feeds (cattle, pig and poultry), fish stocks in aquacultures, and fruit trees. Moreover, the use of TCs is legal and has economical advantages (Jin et al., 2010).

Behavior in the Environment: Based on the calculated log K_{OW} values reported for OTCs, they are not hydrophobic (Table 2.2). However, OTC has been found to sorb strongly to soils (Kay et al., 2005; Kulshrestha et al., 2004) and TC has been found to sorb strongly to sewage sludge (Kim et al., 2005), as indicated by the high log K_d values.

2.3. Environmental Concentrations of Antibiotics in Water

2.3.1 Surface Water

A nation wide survey conducted by the United States Geological Survey (USGS) Toxic Substances Hydrology Program reported the presence of human and veterinary drugs in 80% of 139 streams sampled (Kolpin et al., 2002). These streams consisted of areas susceptible to contamination from various suspected sources, such as downstream from intense urbanization or livestock production. Ciprofloxacin was detected in 2.6% of 115 samples, while enrofloxacin was not detected. At pH below 7.0, ERY is immediately converted into its main degradate, ERY (Yang and Carlson, 2004), and thus is typically quantified as such in environmental samples.

ERY was one of the most frequently detected antibiotics, while tylosin is also one of the most frequently detected veterinary antibiotics in surface water. Trimethoprim was the most commonly detected of all antibiotics tested (27.4%), with concentrations as high as 0.71 μg/L. The sulfonamide used in human medicine, sulfamethoxazole, was detected more often and at higher concentrations than the tested veterinary sulfonamides. TC, OTC and CTC were all detected in surface waters, with concentrations as high as 0.69 μg/L (Kolpin et al., 2002).

2.3.2 Wastewater

Several classes of antibiotics have been detected in different environmental waters at concentrations ranging from ng/L to μg/L. Municipal and hospital wastewaters are the most important sources of human pharmaceutical compounds. Antibiotics concentrations as high as 100 μg/L were found in a hospital sewage water (Lindberg et al., 2004). AMX concentrations between 28 and 82.7 μg/L were measured in a hospital wastewater sample (Benito-Pena et al., 2006).

Concentrations of antibiotics have also been determined in wastewater influent and effluent by the USGS from several wastewater treatment plants (WWTPs) in

Wisconsin, USA, where several tested antibiotics were repeatedly detected (Karthikeyan, and Meyer, 2006). Ciprofloxacin was detected in influent and effluent at concentrations ranging from 0.05 to 0.21 μg/L while erythromycin was also detected at concentrations ranging from 0.07 to 1.2 μg/L. Sulfamethazine was also frequently detected in influent and effluent at concentrations ranging from 0.05 to 1.25 μg/L, while sulfamethazine was detected twice in wastewater influent (out of 25 influent and effluent samples) at concentrations of 0.11 and 0.21 μg/L. Trimethoprim was detected in 16 wastewater samples, with concentrations as high as 1.3 μg/L (Karthikeyan, and Meyer, 2006). Bacteria resistant to ciprofloxacin, ERY, and the ERY-TYL combination have also been detected in WWTPs (Costanzo et al., 2005). TC was detected in wastewater influent, effluent, and one groundwater monitoring well in Wisconsin at concentrations ranging from 0.05 to 1.2 μg/L (Karthikeyan, and Meyer, 2006). Not only have TC resistant bacteria been detected in WWTPs (Costanzo et al., 2005), but resistant genes have been detected in animal wastewater as well. A recent study identified tetracycline antibiotic resistant genes from eight different classes of genes in wastewater lagoons from a swine production facility (Chee-Sanford et al., 2001). Another survey conducted in Germany by Hirsch et al., (1999) analyzed effluents from several WWTPs, in which five antibiotics were repeatedly detected, with concentrations ranging from 0.32 to 6.0 μg/L and frequency of detection as high as 100%. Several of the same antibiotics were also detected in surface waters, with concentrations ranging from 0.03 to 1.7 μg/L and a detection frequency as high as 60%.

2.3.3 Ground Water

Although antibiotics have been widely detected in wastewater and surface water, their findings in ground water has been limited. The same study by Hirsch et al. (1999) also investigated ground water samples, and out of 59 samples analyzed, only sulfamethazine (up to 0.16 μg/L) and sulfamethoxazole (up to 0.47 μg/L) were detected in two samples. Lindsey et al., (2001) also examined surface and ground water samples for the presence of TC and sulfonamide antibiotics, and of the six groundwater samples tested, only one revealed sulfamethoxazole (0.22 μg/L). The

most prevalent detection of antibiotics in groundwater was found surrounding a landfill used as a disposal for waste from the pharmaceutical industry, with concentrations of sulfonamides as high as 10440 μg/L close to the landfill (Holm et al., 1995). With the exception of one groundwater monitoring well revealing a detection of TC on one sampling date (Karthikeyan, and Meyer, 2006), sulfonamides have been so far the only antibiotic reported in groundwater.

CHAPTER THREE
LITERATURE REVIEW

Biological treatment methods have traditionally been used for the treatment of pharmaceutical wastewater (Samuel Suman Raj and Anjaneyulu, 2005; Deegan et al., 2011). They may be subdivided into aerobic and anaerobic processes. Aerobic applications include activated sludge, membrane batch reactors and sequence batch reactors (LaPara et al., 2001; Samuel Suman Raj and Anjaneyulu, 2005; Noble, 2006; Chang et al., 2008 and Chen et al., 2008). Anaerobic methods include anaerobic sludge reactors, anaerobic film reactors and anaerobic filters (Gangagni et al., 2005; Enright et al., 2005; Chelliapan et al., 2011; Oktem et al., 2007; Sreekanth et al., 2009). The wastewater characteristics play a key role in the selection of biological treatments (Deegan et al., 2011).

The advantages of anaerobic treatment over aerobic and advanced processes is its ability to deal with high strength wastewater, with lower energy inputs, sludge yield, nutrient requirements, operating cost, space requirement and improved biogas recovery. However, because a wide range of natural and xenobiotic organic chemicals in pharmaceutical wastewaters are recalcitrant and non-biodegradable to the microbial mass within the conventional treatment system are removed with low yields (Deegan et al., 2011).

3.1 Literature Review for the Treatment of OTC

The treatment performance of wastewater containing OTC was investigated in an up-flow anaerobic sludge blanket (UASB) reactor (Mohan et al., 2001). The study of UASB reactor's performance was obtained at a HRT of 1 day. A removal of 90% COD and 80% OTC was observed during the acclimation period. Maximum COD and OTC removal efficiencies were 95% and 89%, respectively at a HRT of 1 day.

Nandy et al., (1998) investigated the treatability of herbal pharmaceutical wastewater containing mixed antibiotics in an up flow fixed bed reactor (UFFBR) when molasses was used as carbon source. The organic loading rate was 1.0 kgCOD/m^3d by the influent COD concentration from 5000 mg/L, resulting in a 96% COD removal efficiency in an UFFBR reactor during the operation time (86 days).

Wu et al., (2011) investigated the treatability of OTC in an anaerobic compost system. OTC removal efficiency decreased from 70% to 62% when the initial OTC concentrations were increased from 0 to 85 mg/L at C:N ratio of 9.01. The maximum COD removal efficiency was achieved as 87% at an OTC concentration of 85 mg/L.

Treatment of OTC was carried out using an anaerobic degradation system by Kim et al., (2005). The system was operated at various HRTs (7.4-24 h), SRTs (3-10 days) and at an influent OTC concentration of 200 mg/L. The removal efficiency of OTC was varied between 75% and 85%.

Heidari et al., (2011) investigated the treatment of OTC under anaerobic conditions. 105 mg OTC/L was completely degraded at a HRT of 1 day in the anaerobic sequencing batch reactor (SBR). The maximum COD removal efficiency was achieved as 90% at an OTC concentration of 105 mg/L.

3.2 Literature Review for the Treatment of AMX

An up-flow anaerobic sludge blanket (UASB) reactor was used for the pre-treatment of pharmaceutical wastewater containing 6-aminopenicillanic acid (6-APA) and amoxicillin (AMX) at COD loading rates varying between 12.57 and 21.02 kg/m^3d. The COD, 6-APA and AMX yields were 52.2%, 26.3% and 21.6%, respectively (Chen et al., 2011).

Zhou et al., (2006), 67% total COD yield was obtained in a high-strength pharmaceutical wastewater containing 3.2 mg/L AMX in an anaerobic contact reactor (ACR), after 120 days operation time, at HRTs varying between 1.25 and 2.5 days.

The treatment performance of a wastewater containing AMX was investigated in a hybrid up flow anaerobic sludge blanket (HUASB) reactor at a HRT of 2 days and at an influent COD concentration of 13000-15000 mg/L (Sreekanth et al., 2009). Maximum COD removal efficiencies varied between 65% and 75%, respectively at a HRT of 1 day.

In this study, the anaerobic treatability of AMX was investigated in an anaerobic biological contact reactor (BFR) at an AMX concentration of 78 mg/L by Deng et al., (2012). The AMX removal efficiency was 82% at a HRT of 1.56 days.

Pallavi et al., (2009) investigated the treatability of AMX under anaerobic conditions. AMX removal efficiency was found as 65% when the initial AMX concentration were increased from 0 to 89 mg/L, at a HRT of 1.95 days while the maximum COD removal efficiency was 90%.

3.3 Literature Review for the Treatment of TYL

The performance of an up-flow anaerobic stage reactor (UASR) treating pharmaceutical wastewater containing tylosin (TYL) and avilamycin (AVL) was investigated at a HRT of 4 days and at an OLR of 1.86 kg COD/m^3d by Chelliapan et al. (2006). Maximum COD, TYL and AVL removal efficiencies were 70%, 85% and 75%, respectively.

An up-flow anaerobic stage reactor (UASR) was used to treat a macrolide antibiotic of TYL (200 mg/L) at a HRT and OLR of 4 days and 1.88 kg COD/m^3.d by Chelliapan et al., (2011). The maximum COD removal efficiency was 92%.

A laboratory-scale anaerobic sequencing batch reactor (ASBR) was operated using a glucose-based synthetic wastewater to study the effects of TYL (0, 1.67, 167 mg/L) from swine wastewater (Shimada et al., 2008). The maximum COD removal efficiency was observed as 96% at a HRT of 1.67 days at an influent TYL concentration of 1.67 mg/L.

Chelliapan et al., (2011) investigated the treatability of TYL in an up-flow anaerobic stage reactor (UASR). TYL removal efficiency was found as 85% when the initial AMX concentration were increased from 100 to 800 mg/L, at a HRT of 4 days. The maximum COD removal efficiency was achieved as 93% at a TYL concentration of 600 mg/L.

3.4 Literature Review for the Treatment of ERY

The treatment performance of wastewater containing ERY was investigated in an anaerobic hybrid reactor (AHR) (Nandy and Kaul, 2001). The hybrid reactor was consisted of a trickling filter (TF) and an aeration tank (AT) giving a combination of attached growth and suspended growth systems. The maximum COD and ERY removal efficiencies were found as 95% and 79%, respectively at a HRT of 1.5 days.

In this study, the anaerobic treatability of 200 mg/L ERY was investigated in an anaerobic sequence batch reactor (ASBR) by Amin et al., (2006). The COD removal was 99% at an OLR of 2.9 kgCOD/m^3d.

In a study performed by Kim et al., (2008) 85% azithromycin removal efficiency was observed for the anaerobic degradation of 100 mg/L azithromycin concentration in pharmaceutical wastewater after 2.4 days HRT at SRTs varying between 10 and 20 days, at a pH of 7.46.

Busetti and Heitz, (2011) investigated the treatability of ERY under anaerobic conditions. ERY removal efficiency was 90% at an initial ERY concentration of 100 mg/L, at a HRT of 2 days.

CHAPTER FOUR
AEROBIC, ANEROBIC AND SEQUENTIAL SYSTEMS FOR THE TREATMENT OF ANTIBIOTC WASTEWATERS

Conventional aerobic technologies based on activated sludge processes are dominantly applied for the treatment of industrial wastewater due to the high efficiency achieved, the possibility for organic matter removal and the high operational flexibility. In the past, aerobic processes were very popular for biological treatment of wastewater in the 1960s. However, the energy predicament in the early 1970s brought about a significant change in the methodology of wastewater treatment. Energy preservation in industrial processes became a major concern and anaerobic processes rapidly emerged as an acceptable alternative (Chelliapan et al., 2011). One of the important advantages of anaerobic degradation is the energy production during the reactor in the form of methane. Moreover, when high organic loading rates are accommodated and the area needed for the reactor is small. The sludge production is low, when compared to aerobic methods, due to the slow growth rates of anaerobic bacteria (Seghezzo et al., 1998). Anaerobic wastewater treatment is considered as the most cost-effective solution for organically polluted industrial waste streams (Van Lier et al., 2001). Toxic and recalcitrant industrial wastewaters (pharmaceutical, petrochemical etc.), that were previously believed not to be suitable for anaerobic reactors, are now effectively treated.

At high toxic pollutant concentration such as pharmaceuticals, antibiotics, drugs and polyaromatic organics the aerobic technologies can not be effective. Although aerobic microorganisms under aerobic conditions can easily transform such organic intermetabolites even to CO_2 and H_2O it is difficult to achieve complete antibiotic degradation using only aerobic biological processes (Chen et al., 2008). Furthermore, the conventional aerobic technologies have some disadvantages including high capital and operational costs. Therefore, to antibiotic treatment, reliable and cost-effective treatment technologies should be adopted.

Various physico-chemical and biological techniques may be used for the treatment of pharmaceutical wastewaters, but each method has technical and economic limitations (Elmolla et al., 2011). Many physico-chemical methods, such as adsorption, coagulation and advanced oxidation, have been used to treat the pharmaceutical wastewaters containing antibiotics (Elmolla et al., 2011; Suarez et al. 2009; Deegan et al., 2011). Although high antibiotic removal can be achieved, physico-chemical methods have some disadvantages including high cost. The relatively inexpensive anaerobic biologic treatment methods may be preferred for antibiotic treatment as an alternative to the physico-chemical and advanced oxidation methods, with low land requirement and methane production.

In comparison with conventional aerobic technologies, the sequential anaerobic/aerobic reactor system consumes distinctly less energy, produces less excess sludge and is less complex in operation (Kassab et al., 2010). Sequential anaerobic/aerobic processes are a viable alternative for the treatment of xenobiotic compounds (antibiotics, drugs et.) which are difficult to treat by traditional processes (Speece, 1996). The mineralization of some recalcitrant pollutants (antibiotics, drugs etc.) has been possible by using the sequential anaerobic/aerobic reactor system. Therefore, a sequential anaerobic/aerobic reactor system is required to complete the mineralization of antibiotics (Arıkan et al., 2006). Thus, many researchers have adopted sequential anaerobic/aerobic reactor systems for complete biodegradation of antibiotics (Buitron et al., 2003).

4.1 Properties of the Anaerobic Reactors Used in This Study

In recent years, at increasing attention was given to the anaerobic process for the treatment of industrial wastewaters. This process has advantages such as design simplicity, use of non-sophisticated equipment, high treatment efficiency, high methane production, low excess sludge production and low operating and capital cost (Sato et al., 2006). The successful application of anaerobic technology for the treatment of industrial wastewaters depends on the development of high rate bioreactors (Liu et al., 2010; Wu et al., 2011).

4.1.1 Anaerobic Multichamber Bed Reactor (AMCBR)

Nowadays, many researches have focused on anaerobic reactors for the treatment of wastewater. As one of the high-rate anaerobic reactors, the AMCBR reactor was extensively used in treating industrial wastewaters (Liu et al., 2010). The AMCBR reactor was initially developed at "Sardar Patel University" and it can be described as a series of anaerobic fixed-bed reactors (AFBRs) (Patel and Madamwar, 2001). As the name suggests, it consists of a series of vertical baffles to force the wastewater to flow under and over them as it passes from the inlet to the outlet. AMCBR reactor has been developed using different combination of bedding materials in different chambers (Patel and Madamwar, 2001). Best performance has been obtained at 37 ^{0}C under the combination of pumice stone and bone chair as supporting materials (Patel and Madamwar, 1998). The performance of the AMCBR reactor while treating a variety of wastewaters has been well reviewed in the literature (Patel and Madamwar, 1998; Patel and Madamwar, 2001). The AMCBR reactor can be used to treat various wastewaters, in particular, low and high strength wastewater and other refractory wastewaters (petrochemical, salty cheese whey wastewater) (Patel and Madamwar, 1998; Patel and Madamwar, 2001).

The AMCBR reactor which is a high rate bioreactor has many advantages compared to the other anaerobic reactors such as simple design due to no special gas or sludge separation, lower sludge generation, longer biomass retention times, lower hydraulic retention time and higher stability to organic and hydraulic shock loads (Patel and Madamwar, 2001). The most significant advantage of the AMCBR is its ability to separate acidogenesis and methanogenesis longitudinally down the reactor. This can permit different bacterial population to dominate each compartment, acidification predominating in the first compartment section and methanogenesis dominant in the third compartment. The separation of acetogenic and methanogenic phases causes an increase in protection against toxic materials and higher resistance to changes in environmental parameters such as pH, temperature, organic loading (Patel and Madamwar, 1998).

4.1.1.1 Applications of the AMCBR Reactor for the Treatment of Industrial Wastewaters

Very limited studies were determined in literature concerning the treatment of industrial wastewater with AMCBR reactor. AMCBR reactor systems were studied by Patel and Madamvar, (2001) to treat the petrochemical industrial wastewater. The effect of operational parameters such as hydraulic retention time (HRT), organic loading rate (OLR) and pH was investigated on single and multichamber in the AMCBR reactor. The maximum COD removal efficiency was measured as 95% while the methane yield was 0.37 m^3/m^3 d at an OLR of 20.4 kg COD/m^3 d. Patel and Madamvar, (1998) investigated the treatability of salty cheese whey wastewater in the AMCBR reactor system at a HRT of 2 days. The maximum COD removal efficiency and methane content were achieved as 83% and 68%, respectively at a HRT of 2 days.

The literature survey shows that there is a lack on the anaerobic treatment of the antibiotics by AMCBR reactor.

4.1.2 Anaerobic Buoyant Filter Bed Reactor (ABFR)

The development of modern high-rate anaerobic industrial wastewater treatment reactors, like the up-flow anaerobic sludge bed, fixed film and fluidized bed reactors has made anaerobic degradation with most competitive treatment technology for high and medium strength biodegradable industrial wastewaters. However, all modern high-rate anaerobic reactor systems have severely reduced capacity for the treatment of wastewater with insoluble and complex organic substrates, usually termed as ‘‘complex wastewater’’. Therefore, the efficient treatment of industrial wastewaters depends on the development of new high rate bioreactors.

The ‘‘Anaerobic Buoyant Filter Bioreactor’’ (ABFR) being developed by the Environmental Technology Programme at Regional Research Laboratory (Thiruvananthapuram, India). This is an attempt to enhance the loading rate and

treatment efficiency of complex wastewater in anaerobic reactors. The ABFR reactor has an upper chamber and a lower chamber. Between the two chambers there is a buoyant filter bed in the mixed liquor of the ABFR. The filter media is made from expanded polystyrene balls. Best performance has been obtained at 37 ^{0}C when the polystyrene balls were used as supporting material. The performance of the ABFR reactor has been well reviewed in the literature for the treatment of a variety of wastewaters (Haridas et al., 2005). The ABFR reactor can be used to treat complex wastewaters (dairy industry and lipid-rich wastewater etc.) (Haridas et al., 2005; Panicker et al., 2008).

The ABFR reactor has been compared with traditional anaerobic reactors include higher resilience to hydraulic and organic shock loads, longer biomass retention times and lower sludge yields (Haridas et al., 2005). There are no requirement special settling properties for the biomass. The most significant advantage of ABFR is its ability to separate acidogenesis and methanogenesis. The reactor behaves as a two-phase system (upper and lower chamber). This design characteristic permits separation of more sensitive anaerobic population (methanogens).

4.1.2.1 Applications of the ABFR Reactor for the Treatment of Industrial Wastewaters

Very limited studies were determined in literature concerning the treatment of industrial wastewater with ABFR reactor. Haridas et al., (2005) investigated the treatability of lipid-rich complex wastewaters in the ABFR reactor system at an OLR of 10 kg COD/m^{3}d. The maximum COD removal efficiency was 85% at an OLR of 10 kg COD/m^{3}d. Anaerobic treatment of complex wastewater was investigated by Panicker et al., (2008) in an ABFR reactor. 90% COD removal efficiency was obtained at a HRT of 3.25 hours and at an OLR of 4.5 kg/m^{3}d.

No study was found in the literature for the ABFR reactor treating the pharmaceutical wastewaters containing antibiotics.

4.2 Sequential System for the Treatment of Wastewaters

Sequential anaerobic/aerobic biological treatment using mixed bacterial populations is a promising technology for the treatment of antibiotic containing pharmaceutical wastewaters in recent years (Bonakdarpour et al., 2011; Buitron et al., 2003). In this system, the pharmaceutical wastewater containing antibiotic is first subjected to an anaerobic biological treatment which results in the reduction, and the consequent degradation of the antibiotic ending with an aerobic step. This second step provides ultimate biodegradation of both COD and antibiotic. Some reduction in the antibiotic load also occurs under anaerobic conditions (Zhou et al., 2009). At high organic and antibiotic loadings the antibiotic could not be effectively removed under anaerobic conditions due to their recalcitrant nature of the antibiotics and some intermetabolite products. The antibiotics and their metabolites remaining from the anaerobic reactor can be potentially biodegraded under aerobic conditions. Therefore, the major role of the aerobic reactor is the reduction of antibiotic concentrations to the environmental standards for their discharge (Bonakdarpour et al., 2011).

4.2.1 Applications of Sequential Anaerobic/Aerobic Reactor System for the Treatment of Industrial Wastewaters

There are limited numbers of reports available on the treatment of pharmaceutical wastewater using sequential anaerobic/aerobic reactor systems. The treatment performance of pharmaceutical wastewater was investigated in sequential anaerobic/aerobic reactor systems at a HRT of 3.25 hours, at influent COD concentrations varying between 28400 and 72000 mg/L and at OLR varying between 4.6 and 5.7 kg/m^3d (Buitron et al., 2003). A maximum COD removal efficiency of 97% was observed.

CHAPTER FIVE
MATERIALS AND METHODS

5.1 Experimental Set-up for Batch Reactors

5.1.1 Lab-scale Anaerobic Batch Reactor for Anaerobic Toxicity Assay (ATA)

The anaerobic batch experiments were performed in a 150 ml capacity round bottom dark glass serum bottles consisting of narrow mouth and suitable inlet arrangement. The configuration of the anaerobic batch reactor is represented in Fig. 5.1. The gas outlet is connected through rubber tubing to the liquid displacement system to measure the gas production. The entire test was conducted at 37±1°C in a temperature controlled incubator. The entire system is checked thoroughly for gas leakages.

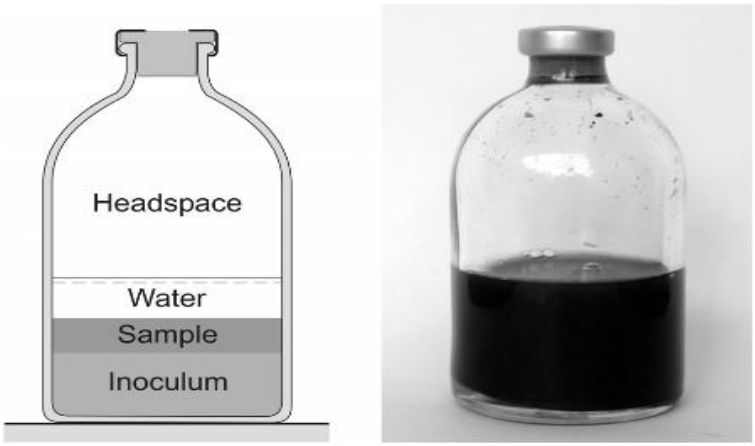

Figure 5.1 Anaerobic batch reactors for anaerobic toxicity assay (ATA)

5.1.2 Lab-scale Anaerobic Batch Reactor for Specific Methanogenic Activity Measurement (SMA)

The studies were performed in dark glass serum bottles sealed with 5 mm butyl rubber septum, kept in place, by a screw cap. Each reactor has 150 ml of total volume with an effective volume of 75 ml. The entire test was conducted at 37±1°C in a temperature controlled incubator. The gas outlet is connected through rubber tubing to the liquid displacement system to measure the gas production. Contents of the serum bottles were mixed by swirling manually after every gas measurement.

5.1.3 Batch Reactors for Abiotic Tests

5.1.3.1 Adsorption Test

The studies were performed in 250 ml glass serum bottles sealed with 5 mm butyl rubber septum, kept in place, by a screw cap. The configuration of the batch reactor used in the adsorption test was presented in Figure 5.2. All batch experiments were conducted at 37±1°C in a temperature controlled incubator.

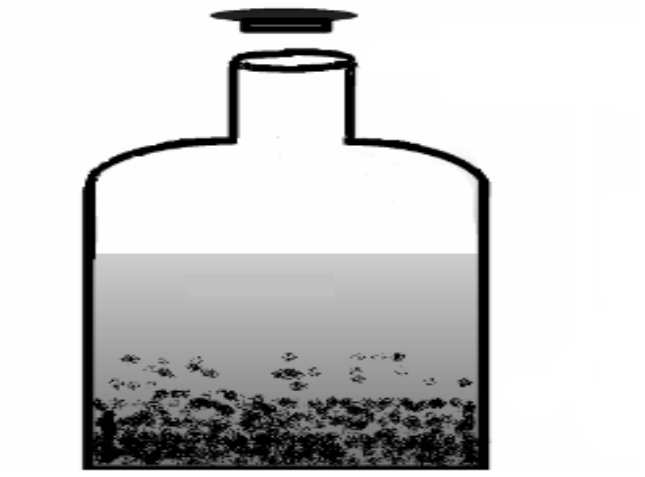

Figure 5.2 Configuration of anaerobic batch reactors for adsorption test

5.1.3.2 Volatilization Test

The anaerobic closed-batch reactors were used in the study. The experiments were conducted at 37±1°C temperature in a controlled incubator. The closed-system batch reactors have a volume of 250 ml and made in from glass with teflon-faced septa at the center of the sealing caps.

5.1.3.3 Antibiotic Accumulation Inside Granular Sludge

The anaerobic batch experiments were performed in 250 ml capacity amber glass vials with septa screw caps. The entire test was conducted at 37±1°C in a temperature controlled incubator.

5.1.4 Batch Reactors for Biotic Tests

5.1.4.1 Biodegradation Experiments

The anaerobic batch reactors were used in the study. The batch biodegradation experiments were conducted at 37±1°C in a temperature controlled incubator. The anaerobic batch reactors have a volume of 250 ml and made in from glass with 5 mm butyl rubber septum, kept in place, by a screw cap.

5.2 Experimental Set-up for Continuous Operation Processes

In this study, continuously fed anaerobic multichamber bed reactors (AMCBR) and anaerobic buoyant filter reactors (ABFR) connected with aerobic completely stirred tank reactor (CSTR) systems were used. The schematic diagram of the reactor systems are shown in Figure 5.3 and 5.4. The effluent of the ABFR and AMCBR reactors were used as the influent of the aerobic CSTR reactors.

5.2.1 Sequential Anaerobic Multichamber Bed Reactor (AMCBR)/Completely Stirred Tank Reactor (CSTR) System

A continuously fed stainless steel anaerobic AMCBR and an aerobic CSTR reactor were used in sequence for the experimentation (Figure 5.3). The effluent of the anaerobic AMCBR reactor was used as the influent of aerobic CSTR reactor. The AMCBR reactor were constructed with the following specifications: reactor inside dimensions; reactor length 40 cm, reactor height 25 cm, reactor width 20 cm and the total volume of the AMCBR (without support material) was 4.5 L. Round openings with a diameter of 2.5 cm from the backside of the stainless steel sheets separated the compartments. These openings were placed at the bottom to create sufficient contact between biomass and substrate. The influent feed was pumped using peristaltic pump. The outlet of AMCBR was connected to a glass U-tube for controlling the level of wastewater. The produced gas was collected via porthole in the top of reactor. The operating temperature of the reactor was maintained constant at 37±1 ^{o}C by placing the AMCBR reactor on a heater. A digital temperature probe located in the middle part of the second compartment showed the constant operation temperature.

Two different types of support materials were used in different chambers so as to support the growth of both acidogenic and methanogenic organisms for separation of the two phases namely acidogenesis and methanogenesis. Chamber 1 was bedded with 300 g pumice stone (extremely porous, glassy, extrusive igneous rock) of size 5x5x5 mm for fast growing of acidogens, where chamber 2 contained total 315 g mixed pumice stone and animal bone with equal size of approximately 125 mm^3. Chamber 3 was exclusively bedded with 330 g animal bone (crushed bone burned at an Owen at 400 ^{o}C) of size approximately 125 mm^3 with a specific surface area of 53.35 m^2/g and a specific volume of 0.244 cm^3/g of support material for fast growing of methanogens (Figure 5.3(a)). The AMCBR reactor was operated in such a way that the feed was pumped continuously in an upward direction in the first chamber. The effluent from the first chamber was allowed to flow down into the second chamber, which further moved upward in to the third chamber as shown in Figure 5.3 and Figure 5.3(b) in the AMCBR reactor.

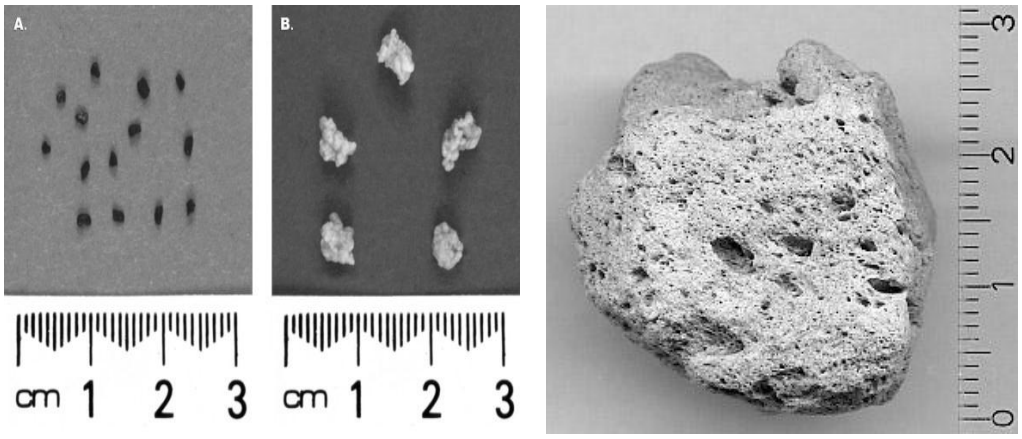

Bone chair Pumice stone

Figure 5.3(a) Two different type of support materials used in AMCBR reactor

Figure 5.3(b) AMCBR reactor internal appearance

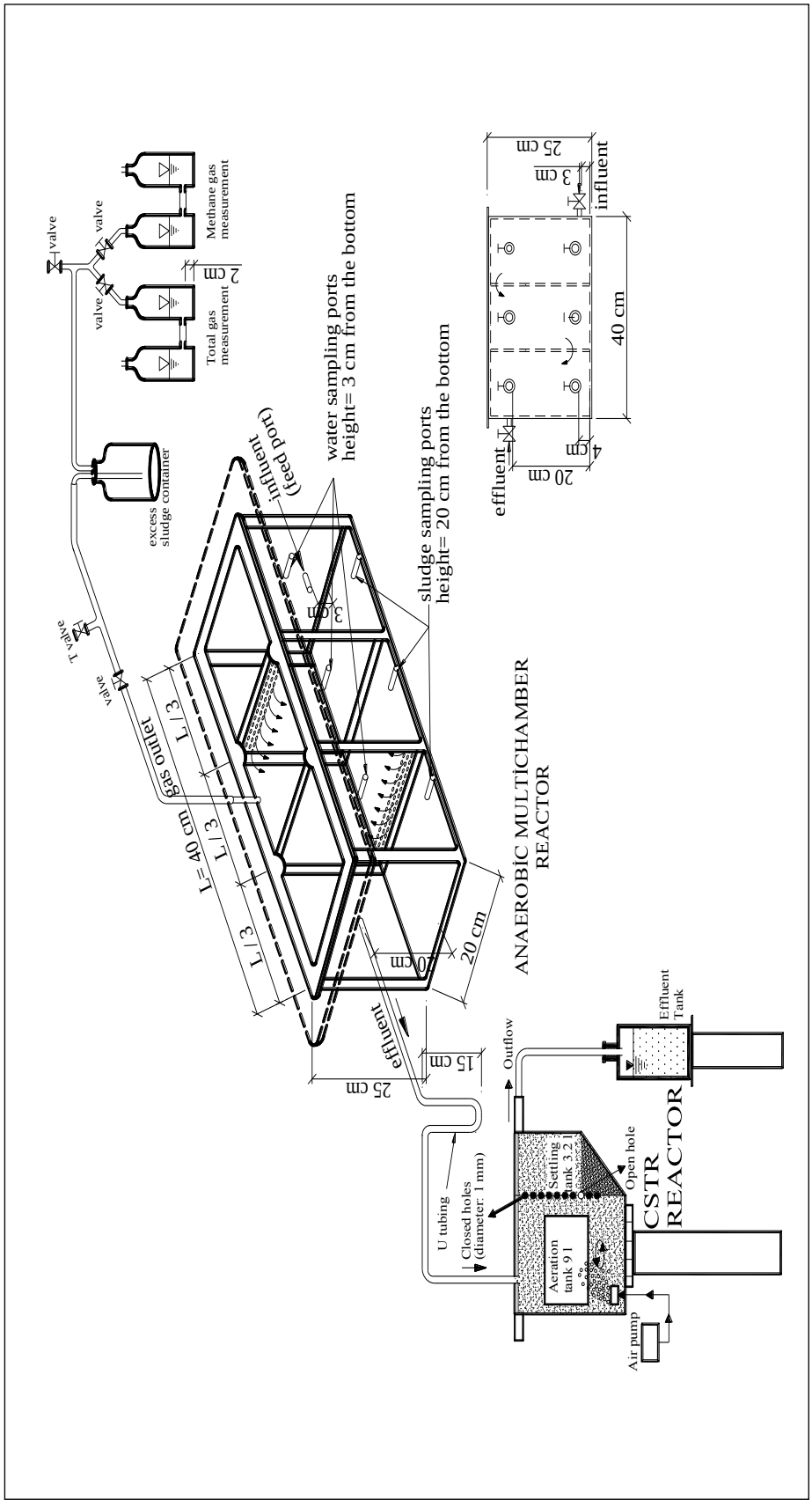

Figure 5.3 Schematic diagram of lab-scale AMCBR/CSTR sequential reactor system

The CSTR reactor consisted of an aerobic tank (effective volume = 9 L) and a settler with a volume of 1.2 L. The effluent wastewater from the aeration tank to the sedimentation tank passed through holes in a plate inclined at 45o to the horizontal axis. Effluent leaving the sedimentation tank was collected in an effluent tank. The effluent of the AMCBR reactor was used as the influent of the CSTR reactor (Figure 5.3).

5.2.2 Sequential Anaerobic Buoyant Filter Reactor (ABFR)/Completely Stirred Tank Reactor (CSTR) System

A continuously fed anaerobic ABFR reactor having 14 cm diameter and 1.48 m height was employed made in of stainless steel. The total effective reactor volume of the ABFR was 12 liter. The schematic configuration of the reactor system is shown in Figure 5.4. The operating temperature of the reactor was maintained constantly at $37 \pm 1\ ^{0}C$ by placing the ABFR reactor on a heater. All analysis was performed in the samples taken from the sampling ports. The effluent of the ABFR was collected in a container. The feeding medium was kept in a refrigerator and it was pumped from the bottom of the reactor. A gas–liquid separator, with a peripheral effluent launder was provided at the top of the upper chamber. The filter bed in the ABFR reactor made in by polystyrene balls with an internal diameter of 2.6 cm and a length of 43 cm move through wastewater and flow between the upper and lower chambers (is expanded and floated) of the ABFR. The polystyrene balls with a porosity of 42.2% and a void ratio of 0.73 are illustrated in Figure 5.4(a).

Figure 5.4(a) Properties of the support material used in the ABFR reactor

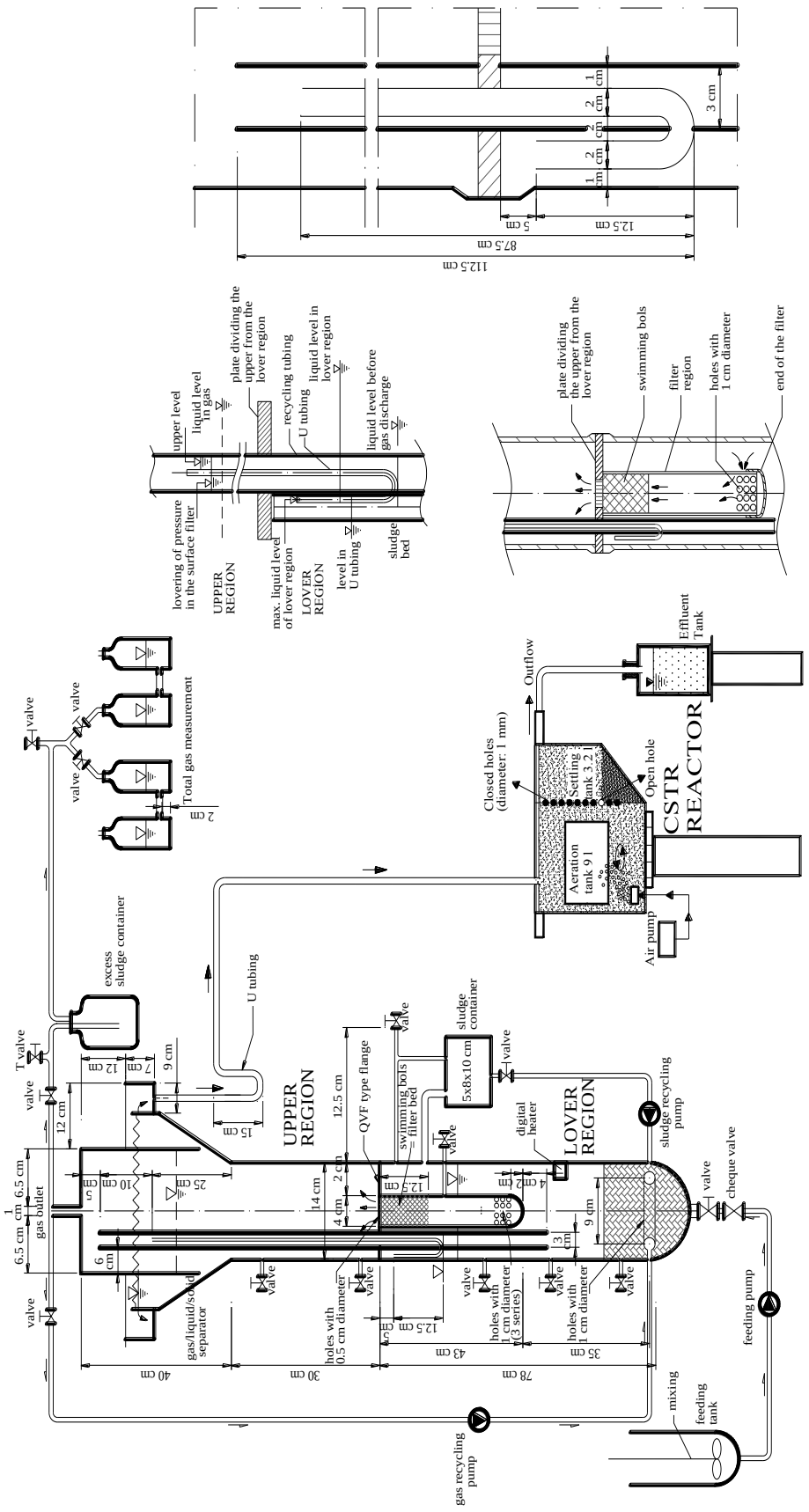

Figure 5.4 Schematic configuration of lab-scale ABFR/CSTR sequential reactor system

During the operation of the ABFR, the gas formed due to bioconversion and the gas recirculated by a pump collected in the lower chamber forcing liquor into the upper chamber through the filter chamber. As a result of filtration action biosolids and sludge are captured in the buoyant filter. Gas release causes a rapid backflow of filtered liquor from the upper chamber to the lower chamber causing the buoyant filter bed to fluidize and expand downward. The solids captured in the buoyant filter are washed out “back flushed”, into the lower chamber. The interval between successive back flushing is adjusted so as to prevent excessive build-up of the filter pressure drop.

During the course of the reactor operation, the ABFR was modified with an excess sludge recirculation facility for the lower chamber in order to improve mixing. An excess sludge collection vessel is connected to the lower chamber through a large nozzle. Excess sludge along with mixed liquor overflows into the vessel during back flushing. The gas vent facility ensures quick filling of the scum collection vessel. It is pumped back into the reactor through nozzle feed using pump. The pumping rate is adjusted so that vessel is emptied before the next filling during back flushing when empty pump merely function to circulate gas in the lower chamber providing additional agitation. The liquor in the lower chamber is mixed by the gas recirculation pump. The pumping rate of gas can be adjusted to change the interval between back flushing so as to provide the longest possible filter run before back flushing (Figure 5.4(b)).

a) external b) internal

Figure 5.4(b) Buoyant Filter Reactor internal and external appearances

The CSTR reactor consisted of an aerobic tank (effective volume = 9 L) and a settler with a volume of 1.2 L made in stainless steel. The effluent wastewater from the aeration tank to the sedimentation tank passed through holes in a plate inclined at 45o to the horizontal axis. Effluent leaving the sedimentation tank was collected in an effluent tank. The effluent of the ABFR reactor was used as the influent of the CSTR reactor (Figure 5.4).

5.3 Operational Conditions

5.3.1 Operational Conditions in Batch Reactor for ATA and SMA Tests

Study 1: In the first step of this study, the toxic effects of OTC, AMX, TYL and ERY antibiotics on methane *Archaea* was investigated using ATA test under batch conditions in the beginning of the study in order to determine the IC_{50} (The OTC, AMX, TYL and ERY concentrations which caused 50% decrease in the methanogenic activity) values of the OTC, AMX, TYL and ERY antibiotics. The batch studies gives information about the OTC, AMX, TYL and ERY doses will be used in the AMCBR and ABFR reactor through continuous operation.

Four different antibiotics of batch reactor experiments were performed in anaerobic conditions for daily methane gas productions with anaerobic biodegradation. The daily methane gas productions in the solution were measured throughout 2 days. The anaerobic batch experiments were done in triplicate samples. All of the experiments were performed in 150 ml serum bottles. The anaerobic sludge, Vanderbilt mineral medium, molasses ($C_6H_{12}NNaO_3S$), $NaHCO_3$, antibiotics (OTC, AMX, TYL and ERY) was inoculated into each bottle. Table 5.1 shows the feeding protocol for anaerobic batch reactors. The operational conditions of this batch study were given in Table 5.2.

Table 5.1 The feeding protocol in anaerobic batch reactors for ATA and SMA tests

Parameters	Control in reactor		Value of parameters in reactor		concentrations in the reactor	
	Value	Unit	Value	Unit	Value	Unit
Anaerobic granulated sludge MLVSS	4	ml/150 ml	4	ml/150 ml	3000	mg/L
Molasses	7.5	ml/150 ml	7.5	ml/150 ml	4000	mg/L
Vanderbilt mineral medium	0.25	ml/150 ml	0.25	ml/150 ml	0.25	ml
$NaHCO_3$	7.5	ml/150 ml	7.5	ml/150 ml	5000	mg/L
$C_2H_3NaO_2S$	1.0	ml/150 ml	1.0	ml/150 ml	667	mg/L
Antibiotics (OTC, AMX, TYL, ERY)	-[a]	ml/150 ml	0.8- 1.7- 2.5- 3.3 4.2 5.0- 5.8- 6.7	ml/150 ml	50-100-150-200-250 300-350-400	mg/L
Total volume	75	ml/150 ml	75	ml/150 ml	-	-

[a]: (-) without antibiotics, control

Table 5.2 The operational conditions for batch ATA test

parameters	**Unit**	**Values**		
		Minimum	Mean	Maximum
Flow rate	ml/day	75	75	75
reactor volume	ml	150	150	150
COD	mg/L	3000	3500	4000
HRT	days	2	2	2
Organic loading rate	gCOD/L.d	1.5	1.75	2.00
F/M ratio	gCOD/gMLVSS. d	0.50	0.60	0.65
MLVSS	mg/L	2800	3000	3100
Operational days (OTC, AMX, TYL, ERY)	days	2	2	2
Concentration of antibiotics (OTC, AMX, TYL, ERY)	mg/L	50; 100; 150; 200; 250; 300; 350; 400		

Study 2: The SMA is an indicator of methanogenic activity of the biomass forming granules. The SMA points out the gas productions, based on COD, per each gram of anaerobic biomass through anaerobic operation. The SMA test was used to determine the potential methane production rates of the anaerobic sludges. The SMA test was conducted in 150 ml serum bottles at 35 ^{0}C under anaerobic conditions. The microorganisms, molasses ($C_6H_{12}NNaO_3S$), Vanderbilt mineral medium, antibiotics (OTC, AMX, TYL and ERY) doses were added to the serum bottles in the same manner as those used in the ATA test. The operating parameters for the batch reactor were summarized in Table 5.3.

Table 5.3 The operational conditions for batch SMA test

parameters	**Unit**	**Values**		
		Minimum	Mean	Maximum
Flow rate	ml/d	4.05	4.05	4.05
reactor volume	ml	150	150	150
COD	mg/L	3000	3500	4000
HRT	days	37	37	37
Organic loading rate	gCOD/L.d	0.08	0.09	0.11
F/M	g COD/g MLVSS d	0.03	0.03	0.04
MLVSS	mg/l	2800	3000	3100
Operational days (OTC, AMX, TYL, ERY)	days	37	37	37
Concentration of antibiotics (OTC, AMX, TYL, ERY)	mg/L	50; 100; 150; 200; 250; 300; 350; 400		

[a]: Minimum; [b]: Mean; [c]: Maximum; [d]: Flow-rate (l/d); [e]: Organic loading rate (gCOD/L.d)

5.3.2 Operational Conditions in Batch Reactor for Biotic and Abiotic Tests

Study 3: These sets of batch studies were performed in order to determine the main degradation mechanisms (biotic and abiotic) of antibiotics (OTC, AMX, TYL, and ERY) under anaerobic conditions in lab-scale anaerobic batch reactors. The operational conditions of this anaerobic batch study were given in Table 5.4.

Table 5.4 Operational conditions for Biotic and Abiotic Studies in batch reactors

PARAMETERS	UNIT	VALUES								
		Biodegradation test			Volatilization test			Adsorption test		
		Min[a]	Mean[b]	Max[c]	Min[a]	Mean[b]	Max[c]	Min[a]	Mean[b]	Max[c]
Q[d]	ml/day	10.00	10.00	10.00	10.00	10.00	10.00	10.00	10.00	10.00
reactor volume	ml	250	250	250	250	250	250	250	250	250
HRT	days	27	27	27	18	18	18	25	25	25
COD	mg/L	3000	3500	4000	3100	3400	3950	3000	3500	4000
OLR[e]	gCOD/L.d	0.11	0.13	0.15	0.17	0.19	0.22	0.12	0.14	0.16
F/M	(gCOD/g MLVSS.d)	0,04	0.05	0.06	-	-	-	0.07	0.08	0.09
MLVSS	mg/L	2500	2750	3000	-	-	-	1700	1850	2000
Operational days for OTC	days	28	28	28	15	15	15	22	22	22
Operational times for AMX	days	27	27	27	18	18	18	24	24	24
Operational times for TYL	days	27	27	27	18	18	18	24	24	24
Operational times for ERY	days	27	27	27	18	18	18	24	24	24
Antibiotic Concentration (OTC, AMX, TYL, ERY)	mg/L	100	100	100	100	100	100	100	100	100
ALR[f] (OTC, AMX, TYL, ERY)	g/L.d	0.04	0.04	0.04	0.04	0.04	0.04	0.04	0.04	0.04

[a]: Minimum; [b]: Mean; [c]: Maximum; [d]: Flow-rate (l/d); [e]: Organic loading rate (gCOD/l.d); [f]: Antibiotic loading rate (g/l.d)

5.3.3 Operational Conditions in Continuous Reactors

5.3.3.1 Operational Conditions for Sequential AMCBR/CSTR System

Study 4: Start-up is important in anaerobic treatment. A successful start-up allows the acclimation and phase separation of bacteria in the anaerobic reactor. Once the biomass has been established, either as a granular particle, while the reactor operation is quite stable (Speece, 1996). A start-up period led to a more complete biological degradation of the toxic substances such as antibiotics and a better adaptation of the biomass for the degradation of the antibiotic. The AMCBR was operated through 45 days without OTC to acclimate the granular sludge to the AMCBR. The operational conditions for this study were given in Table 5.5.

Table 5.5 Operational conditions of the AMCBR reactor at start-up period (without OTC)

Parameters	**Units**	**Values**		
		Minimum	**Mean**	**Maximum**
Flow rate	L/d	2		
Volume	L	4.5		
COD concentration of molasses-COD	mg/L	3950	3990	4010
HRT	d	2.25		
Organic loading rate of molasses-COD	g.COD/L.d	1.76	1.77	1.78
F/M ratio	g.COD/g.VSS. d	0.02	0.03	0.04
VSS	g/L	56	60	63
SRT	d	30	32	34
Operational days	d	45		
ORP	mV	-350	-360	-370
Temperature	^{0}C	36	37	38

Study 5: The adaptation period is very important since the bacterial population used as seed is going to be exposed to the AMX in an anaerobic environment of the AMCBR reactor. In order to acclimation the partially granulated biomass in the AMCBR reactor, the anaerobic reactor was operated with synthetic wastewater through 45 days without AMX for reach to steady state conditions. The operational conditions of continuously study were given in Table 5.6.

Table 5.6 Operational conditions of the AMCBR reactor at start-up period (without AMX)

Parameters	**Units**	**Values**		
		Minimum	**Mean**	**Maximum**
Flow rate	L/d	2		
Volume	L	4.5		
COD concentration of molasses-COD	mg/L	3965	3983	4000
HRT	d	2.25		
Organic loading rate of molasses-COD	g.COD/L.d	1.76	1.77	1.78
F/M ratio	g.COD/g.VSS. d	0.02	0.03	0.04
VSS	g/L	49	52	54
SRT	d	38	40	42
Operational days	d	45		
ORP	mV	-350	-360	-370
Temperature	^{0}C	36	37	38

Study 6: This step contains the start-up period of the anaerobic AMCBR reactor in the without of TYL. The value of the operational conditions for AMCBR reactor was summarized in Table 5.7.

Table 5.7 Operational conditions of the AMCBR reactor at start-up period (without TYL)

Parameters	**Units**	**Values**		
		Minimum	**Mean**	**Maximum**
Flow rate	L/d	2		
Volume	L	4.5		
COD conc. of molasses-COD	mg/L	3984	3996	4008
HRT	d	2.25		
Organic loading rate of molasses-COD	g.COD/L.d	1.77	1.78	1.79
F/M ratio	g.COD/g.VSS. d	0.03	0.04	0.05
VSS	g/L	55	57.5	60
SRT	d	41	43	45
Operational days	d	60		
ORP	mV	-350	-360	-370
Temperature	^{0}C	36	37	38

Study 7: The AMCBR was operated through 90 days without ERY to acclimate the granular sludge. The operational conditions were given in Table 5.8.

Table 5.8 Operational conditions of the AMCBR reactor at start-up period (without ERY)

Parameters	**Units**	**Values**		
		Minimum	**Mean**	**Maximum**
Flow rate	L/d	2		
Volume	L	4.5		
COD conc. of molasses-COD	mg/L	3975	3990	4005
HRT	d	2.25		
Organic loading rate of molasses-COD	g.COD/L.d	1.77	1.78	1.78
F/M ratio	g.COD/g.VSS. d	0.03	0.04	0.04
VSS	g/L	50	55	60
SRT	d	43	47	51
Operational days	d	90		
ORP	mV	-350	-360	-370
Temperature	^{0}C	36	37	38

Study 8: The AMCBR reactor was continuously operated with OTC concentrations. A CSTR reactor followed the AMCBR reactor was used for sequential operation of AMCBR and CSTR reactors. In this study, effects of increasing OTC concentrations on the removal efficiencies of the OTC, COD and gas productions, TVFA were investigated in a sequential system. The effluent of the AMCBR was used as feed in the CSTR reactor. The operational conditions for this run were given in Tables 5.9 and 5.10 for AMCBR and CSTR reactor.

Table 5.9 Operational conditions of the AMCBR reactor at increasing OTC concentrations

Parameters	**Units**	**Values**
Flow rate	L/d	2
Volume	L	4.5
COD concentration of molasses-COD	mg/L	3900; 3917;3925;3950;3960; 3978; 3990; 4000
OTC concentration	mg/L	50; 100; 150; 200; 250; 300; 350; 400
COD originating from the OTC-COD	mg/L	40; 60; 80; 90; 100; 110; 120; 140
Total COD concentration	mg/L	3940; 3977; 4005; 4040; 4060; 4088; 4110; 4140
HRT	d	2.25
Organic loading rate of molasses-COD	g.COD/L.d	1.73; 1.74; 1.74; 1.75; 1.76; 1.77; 1.77; 1.78
Organic loading rate of OTC-COD	g.COD/L.d	0.02; 0.03; 0.04; 0.04; 0.04; 0.05; 0.05; 0.06
Total organic loading rate	g.COD/L.d	1.75; 1.77; 1.78; 1.79; 1.80; 1.82; 1.82; 1.84
F/M ratio	g.COD/g.VSS. d	0.030; 0.030; 0.029; 0.031; 0.031; 0.032; 0.032; 0.033
VSS	g/L	58.33; 58.89; 60.00; 58.49; 58.14; 57.07; 56.25; 56.00
SRT	d	98; 99; 101; 98; 97; 96; 95; 94
Operational days	d	263
ORP	mV	-370
Temperature	^{0}C	37

Table 5.10 Operational conditions of the CSTR reactor at increasing OTC concentrations

Parameters	**Units**	**Values**
Flow rate	L/d	2
Volume	L	9
COD concentration of molasses-COD	mg/L	280; 296; 305; 456; 502; 578; 640; 900
OTC concentration	mg/L	2.5-3-3-6-3-3-70-85
COD originating from the OTC-COD	mg/L	4.00; 5.60; 6.00; 6.40; 6.80; 8.00; 8.80; 9.60
Total COD concentration	mg/L	300; 350; 354; 500; 365; 205; 485; 800
HRT	d	4.5
Organic loading rate of molasses-COD	g.COD/L.d	0.06; 0.07; 0.07; 0.10; 0.11; 0.13; 0.14; 0.20
Organic loading rate of OTC-COD	g.COD/L.d	$0.88x10^{-3}$; $1.24x10^{-3}$; $1.33x10^{-3}$; $1.42x10^{-3}$; $1.51x10^{-3}$; $1.78x10^{-3}$; $1.96x10^{-3}$; $2.13x10^{-3}$
Total organic loading rate	g.COD/L.d	0.06; 0.07; 0.07; 0.10; 0.12; 0.13; 0.15; 0.21
F/M ratio	g.COD/g.MLVSS.d	0.02; 0.02; 0.02; 0.03; 0.04; 0.04; 0.05; 0.08
MLVSS	g/L	3; 3.5; 4; 3.6; 3.2; 3.0; 2.8; 2.6
SRT	d	20
Operational times	d	106
ORP	mV	+90
Temperature	^{0}C	20

Study 9: The AMCBR reactor was continuously operated with 50-100-150-200-250-300 mg/L AMX concentrations. In this run the effects of increasing AMX concentrations on the performance of the AMCBR reactor (COD, AMX, TVFA, HCO_3 alkalinity and gas productions) was investigated. The operational condition for the AMCBR reactor was summarized in Table 5.11.

Table 5.11 Operational conditions of the AMCBR reactor at increasing AMX concentrations

Parameters	**Units**	**Values**
Flow rate	L/d	1
Volume	L	4.5
COD concentration of molasses-COD	mg/L	4000; 4005; 4010; 3990; 4000; 4025
AMX concentration	mg/L	50; 100; 150; 200; 250; 300
COD originating from the AMX-COD	mg/L	25; 35; 40; 45; 55; 65
Total COD concentration	mg/L	4025; 4040; 4050; 4035; 4055; 4090
HRT	d	4.5
Organic loading rate of molasses-COD	g.COD/L.d	0.88; 0.89; 0.89; 0.88; 0.88; 0.89
Organic loading rate of AMX-COD	g.COD/L.d	$5.5x10^{-3}$; $7.78x10^{-3}$; $8.88x10^{-3}$; $1x10^{-2}$; $1x10^{-2}$; $2x10^{-2}$
Total organic loading rate	g.COD/L.d	0.88; 0.89; 0.89; 0.89; 0.89; 0.90
F/M ratio	g.COD/g.VSS. d	0.02; 0.02; 0.02; 0.03; 0.03; 0.03
VSS	g/L	55; 58; 45; 40; 35; 30
SRT	d	90; 95; 74; 66; 57; 49
Operational days	d	186
ORP	mV	-370
Temperature	^0C	37

The effluent of the AMCBR was used as feed in the CSTR reactor. In this step of the study the effects of increasing AMX concentration (50-100-150-200-250-300 mg/L) were investigated on the performance of the aerobic CSTR reactor with continuous operation. The operational conditions for this study were given in Table 5.12.

Table 5.12 Operational conditions of the CSTR reactor at increasing AMX concentrations

Parameters	Units	Values
Flow rate	L/d	1
Volume	L	9
COD concentration of molasses-COD	mg/L	338; 345; 302; 562; 600; 786
AMX concentration	mg/L	7; 7.4; 8; 8.7; 9.2; 11
COD originating from the AMX-COD	mg/L	3.5; 3.7; 4; 4.35; 4.6; 5.5
Total COD concentration	mg/L	342; 349; 306; 566; 605; 792
HRT	d	9
Organic loading rate of molasses-COD	g.COD/L.d	0.03; 0.03; 0.04; 0.06; 0.07; 0.09
Organic loading rate of AMX-COD	g.COD/L.d	$0.38x10^{-3}$; $0.41x10^{-3}$; $0.44x10^{-3}$; $0.48x10^{-3}$; $0.51x10^{-3}$; $0.61x10^{-3}$
Total organic loading rate	g.COD/L.d	0.03; 0.03; 0.04; 0.06; 0.07; 0.09
F/M ratio	g.COD/g.MLVSS. d	0.01; 0.01 ; 0.01; 0.02; 0.03; 0.04
MLVSS	g/L	2.7; 3.0; 3.5; 3.0; 2.8; 2.5
SRT	d	20
Operational days	d	73
ORP	mV	+86
Temperature	^{0}C	22

Study 10: Table 5.13 and 5.14 showed the operational conditions for AMCBR and CSTR reactor system treating TYL. In this step, sequential AMCBR and CSTR system were operated through 285 days in order to investigate the effect of increasing TYL concentrations on TYL and COD removals, gas production, TVFA and Bicarbonate Alkalinity variations. The effluent of the AMCBR reactor was used as feed in the influent of CSTR reactor. The SRT in the CSTR reactor was adjusted to 20 days.

Table 5.13 Operational conditions of the AMCBR reactor at increasing TYL concentrations

Parameters	**Units**	**Values**
Flow rate	L/d	2
Volume	L	4.5
COD concentration of molasses-COD	mg/L	3900; 3905; 3917; 3986; 4000; 4100
TYL concentration	mg/L	50; 100; 150; 200; 250; 300
COD originating from the TYL-COD	mg/L	25; 35; 40; 65; 75; 100
Total COD concentration	mg/L	3925; 4005; 3957; 4051; 4075; 4200
HRT	d	2.25
Organic loading rate of molasses-COD	g.COD/L.d	1.73; 1.74; 1.74; 1.77; 1.78; 1.82
Organic loading rate of TYL-COD	g.TYL/L.d	0.01; 0.02; 0.02; 0.03; 0.03; 0.04
Total organic loading rate	g.COD/L.d	1.74; 1.76; 1.76; 1.80; 1.81; 1.86
F/M ratio	g.COD/g.VSS. d	0.03; 0.03; 0.04; 0.04; 0.05; 0.05
VSS	g/L	50; 58; 48; 45; 40; 35
SRT	d	101; 117; 97; 91; 81; 71
Operational days	d	189
ORP	mV	-360
Temperature	^{0}C	37

Table 5.14 Operational conditions of the CSTR reactor at increasing TYL concentrations

Parameters	**Units**	**Values**
Flow rate	L/d	2
Volume	L	9
COD concentration of molasses-COD	mg/L	11.90; 96.45; 96.45; 146.25; 296; 450.20
TYL concentration	mg/L	3; 15; 22; 30; 35; 50
COD originating from the TYL-COD	mg/L	3.10; 3.25; 3.55; 3.75; 4.10; 4.80
Total COD concentration	mg/L	15; 100; 100; 150; 300; 455
HRT	d	4.5
Organic loading rate of molasses-COD	g.COD/L.d	0.10; 0.10; 0.11; 0.15; 0.16; 0.20
Organic loading rate of TYL-COD	g.TYL/L.d	$0.68x10^{-3}$; $0.72x10^{-3}$; $0.78x10^{-3}$; $0.83x10^{-3}$; $0.91x10^{-3}$; $1.07x10^{-3}$
Total organic loading rate	g.COD/L.d	0.10; 0.10; 0.11; 0.15; 0.16; 0.20
F/M ratio	g.COD/g.MLVSS. d	0.03; 0.03; 0.03; 0.04; 0.05; 0.08
MLVSS	g/L	3; 3.5; 4; 3.2; 3; 2.47
SRT	d	20
Operational days	d	96
ORP	mV	+90
Temperature	^{0}C	22

Study 11: In this step of the study the effects of increasing ERY concentrations on the performance of the continuous anaerobic AMCBR were investigated. The operational conditions for this step were given in Table 5.15. The effluent of the AMCBR reactor was used as the influent of the aerobic CSTR reactor. The ERY concentrations were increased steply from 50, 100, 150, 200, 250 to 300 mg/l through continuous operation of 98 days. The operational conditions for the aerobic CSTR reactor were summarized in Table 5.16.

Table 5.15 Operational conditions of the AMCBR reactor at increasing ERY concentrations

Parameters	**Units**	**Values**
Flow rate	L/d	3
Volume	L	4.5
COD concentration of molasses-COD	mg/L	4000
ERY concentration	mg/L	50; 100; 150; 200; 250; 300
COD originating from the ERY-COD	mg/L	20; 40; 60; 80; 100; 120
Total COD concentration	mg/L	4020; 4040; 4060; 4080; 4100; 4120
HRT	d	1.5
Organic loading rate of molasses-COD	g.COD/L.d	2.67
Organic loading rate of ERY-COD	g.ERY /L.d	0.01; 0.03; 0.04; 0.05; 0.07; 0.08
Total organic loading rate	g.COD/L.d	2.68; 2.70; 2.71; 2.72; 2.74; 2.75
F/M ratio	g.COD/g.VSS. d	0.04; 0.04; 0.04; 0.05; 0.05; 0.05
VSS	g/L	60; 62; 65; 60; 56; 52
SRT	d	98; 101; 106; 98; 92; 85
Operational days	d	192
ORP	mV	-360
Temperature	^{0}C	37

Table 5.16 Operational conditions of the CSTR reactor at increasing ERY concentrations

Parameters	Units	Values
Flow rate	L/d	3
Volume	L	9
COD concentration of molasses-COD	mg/L	393; 400; 425; 468; 635; 876
ERY concentration	mg/L	5.30-5.52-6.00-6.50-7.05-9.12
COD originating from the ERY-COD	mg/L	2.12; 2.21; 2.4; 2.6; 2.82; 3.65
Total COD concentration	mg/L	395; 402; 427; 471; 638; 880
HRT	d	3
Organic loading rate of molasses-COD	g.COD/L.d	0.13; 0.13; 0.14; 0.16; 0.21; 0.29
Organic loading rate of ERY-COD	g.ERY/L.d	$0.71x10^{-3}$; $0.74x10^{-3}$; $0.80x10^{-3}$; $0.86x10^{-3}$; $0.94x10^{-3}$; $3.04x10^{-3}$
Total organic loading rate	g.COD/L.d	0.13; 0.13; 0.14; 0.16; 0.21; 0.29
F/M ratio	g.COD/g.MLVSS.d	0.03; 0.03; 0.03; 0.04; 0.06; 0.10
MLVSS	g/L	4; 4.5; 5; 4; 3.5; 3
SRT	d	20
Operational times	d	98
ORP	mV	+90
Temperature	^{0}C	22

Study 12: In this run antibiotic treatabilities were studied in a sequential system at different HRTs. In this study, the COD, antibiotic removal, gas productions were investigated at increasing flow rates. Furthermore the effects of compartments on the reactor performances was determined by measuring COD yields, TVFA, HCO_3 variations at decreasing HRTs. In this study, the effect of HRT on the OTC, COD yield, TVFA, HCO_3 variations was investigated in sequential system. The effluent of the AMCBR was used as feed in the CSTR. The operational conditions for this run were given in Tables 5.17 and 5.18 for AMCBR and CSTR reactors, respectively.

Table 5.17 Operational conditions of the AMCBR reactor at different HRTs

Parameters	**Units**	**Values**
Flow rate	L/d	0.82; 1.00; 2.00; 3.00; 4.00; 5.00
Volume	L	4.50
COD concentration of molasses-COD	mg/L	3980
OTC concentration	mg/L	100
COD originating from the OTC-COD	mg/L	60
Total COD concentration	mg/L	4040
HRT	d	5.50; 4.50; 2.25; 1.50; 1.13; 0.90
Organic loading rate of molasses-COD	g.COD/L.d	0.73
Organic loading rate of OTC-COD	g.OTC/L.d	0.01
Total organic loading rate	g.COD/L.d	0.74
F/M ratio	g.COD/g.VSS.d	0.01
VSS	g/L	50
SRT	d	158
Operational days	d	208
ORP	mV	-360
Temperature	^{0}C	37

Table 5.18 Operational conditions of the CSTR reactor at different HRTs

Parameters	**Units**	**Values**
Flow rate	L/d	0.82; 1.00; 2.00; 3.00; 4.00;5.00
Volume	L	9.00
COD concentration of molasses-COD	mg/L	300
OTC concentration	mg/L	2.5
COD originating from the OTC-COD	mg/L	0.60
Total COD concentration	mg/L	300
HRT	d	10.97; 9; 4.5; 3; 2.25; 1.8
Organic loading rate of molasses-COD	g.COD/L.d	0.03
Organic loading rate of OTC-COD	g.COD/L.d	$0.55x10^{-4}$
Total organic loading rate	g.COD/L.d	0.03
F/M ratio	g.COD/g.MLVSS.d	0.01
MLVSS	g/L	3.0
SRT	d	20
Operational days	d	208
ORP	mV	+90
Temperature	^{0}C	20

Study 13: The effect of HRT on the performance of AMCBR/CSTR reactor system was investigated in a synthetic wastewater containing 150 mg/L of AMX. The influent COD, AMX concentrations were kept constant at 4000 mg/L and 150 mg/L, respectively, during continuous operation of 189 days. The HRT was decreased from 5.5 to 4.5, 2.25, 1.5, 1.13 to 0.9 d in the AMCBR reactor while the HRTs decreased from 9 to 1.8 days in the aerobic CSTR reactor depending to flow rate entering to the CSTR reactor from AMCBR. The operational conditions for the AMCBR and aerobic CSTR reactor were summarized in Tables 5.19 and 5.20.

Table 5.19 Operational conditions of the AMCBR reactor at different HRTs

Parameters	**Units**	**Values**
Flow rate	L/d	0.82; 1.00; 2.00; 3.00; 4; 5
Volume	L	4.5
COD concentration of molasses-COD	mg/L	4000
AMX concentration	mg/L	150
COD originating from the AMX-COD	mg/L	40
Total COD concentration	mg/L	4040
HRT	d	5.5; 4.5; 2.25; 1.5; 1.13; 0.9
Organic loading rate of molasses-COD	g.COD/L.d	0.73;
Organic loading rate of AMX-COD	g.COD/L.d	$7.3x10^{-3}$
Total organic loading rate	g.COD/L.d	0.73
F/M ratio	g.COD/g.VSS.d	0.01
VSS	g/L	55
SRT	d	197
Operational days	d	189
ORP	mV	-370
Temperature	^0C	37

Table 5.20 Operational conditions of the CSTR reactor at different HRTs

Parameters	**Units**	**Values**
Flow rate	L/d	0.82; 1.00; 2.00; 3.00; 4; 5
Volume	L	9
COD concentration of molasses-COD	mg/L	316
AMX concentration	mg/L	9
COD originating from the AMX-COD	mg/L	4
Total COD concentration	mg/L	325
HRT	d	11; 9; 4.5; 3; 2.25; 1.8
Organic loading rate of molasses-COD	g.COD/L.d	0.03
Organic loading rate of AMX-COD	g.COD/L.d	$0.82x10^{-3}$
Total organic loading rate	g.COD/L.d	0.03
F/M ratio	g.COD/g.MLVSS.d	$8.11x10^{-3}$
MLVSS	g/L	3.7
SRT	d	20
Operational days	d	189
ORP	mV	+90
Temperature	^{0}C	20

Study 14: Tables 5.21 and 5.22 showed the operational conditions for sequential anaerobic AMCBR and aerobic CSTR reactor system treating TYL. In this step, sequential reactor system were operated through 205 days in order to investigate the effect of decreasing HRTs on TYL and COD removal performances, on gas production, TVFA, HCO_3 variations of sequential AMCBR/CSTR system. The effluent of the AMCBR reactor was used as feed in the influent of CSTR reactor. Solid retention time (SRT) in the CSTR reactor was adjusted to 20 days.

Table 5.21 Operational conditions of the AMCBR reactor at different HRTs

Parameters	**Units**	**Values**
Flow rate	L/d	0.82; 1.00; 2.00; 3.00; 4; 5
Volume	L	4.5
COD concentration of molasses-COD	mg/L	3905
TYL concentration	mg/L	100
COD originating from the TYL-COD	mg/L	35
Total COD concentration	mg/L	4005
HRT	d	5.5; 4.5; 2.25; 1.5; 1.13; 0.9
Organic loading rate of molasses-COD	g.COD/L.d	0.71
Organic loading rate of TYL-COD	g.TYL/L.d	$6.37x10^{-3}$
Total organic loading rate	g.COD/L.d	0.71
F/M ratio	g.COD/g.VSS.d	0.01
VSS	g/L	50
SRT	d	217
Operational days	d	205
ORP	mV	-360
Temperature	^{0}C	37

Table 5.22 Operational conditions of the CSTR reactor at different HRTs

Parameters	Units	Values
Flow rate	L/d	0.82; 1.00; 2.00; 3.00; 4; 5
Volume	L	9
COD concentration of molasses-COD	mg/L	217
TYL concentration	mg/L	8
COD originating from the TYL-COD	mg/L	3
Total COD concentration	mg/L	225
HRT	d	10.97; 9; 4.5; 3; 2.25; 1.8
Organic loading rate of molasses-COD	g.COD/L.d	0.02
Organic loading rate of TYL-COD	g.TYL/L.d	$0.73x10^{-3}$
Total organic loading rate	g.COD/L.d	0.02
F/M ratio	gCOD/gMLVSSd	0.01
MLVSS	g/L	3
SRT	d	20
Operational days	d	205
ORP	mV	+90
Temperature	^{0}C	20

Study 15: A CSTR reactor following the AMCBR reactor was used to investigate the effects of decreasing HRTs on the removal efficiencies of the OTC, COD and gas productions (total, methane) in a continuous mode sequential AMCBR/CSTR system. The effluent of the AMCBR was used as the feed in the CSTR reactor. The operational conditions for this run were given in Tables 5.23 and 5.24 for AMCBR and CSTR reactors, respectively for ERY antibiotic.

Table 5.23 Operational conditions of the AMCBR reactor at different HRTs

Parameters	**Units**	**Values**
Flow rate	L/d	0.82; 1.00; 2.00; 3.00; 4; 5
Volume	L	4.5
COD concentration of molasses-COD	mg/L	3500
ERY concentration	mg/L	100
COD originating from the ERY-COD	mg/L	40
Total COD concentration	mg/L	3540
HRT	d	5.5; 4.5; 2.25; 1.5; 1.13; 0.9
Organic loading rate of molasses-COD	g.COD/L.d	0.64
Organic loading rate of ERY-COD	g.ERY/L.d	$7.3x10^{-3}$
Total organic loading rate	g.COD/L.d	0.65
F/M ratio	g.COD/g.VSS.d	0.01
VSS	g/L	40
SRT	d	198
Operational days	d	292
ORP	mV	-360
Temperature	^{0}C	37

Table 5.24 Operational conditions of the CSTR reactor at different HRTs

Parameters	Units	Values
Flow rate	L/d	0.82; 1.00; 2.00; 3.00; 4; 5
Volume	L	9
COD concentration of molasses-COD	mg/L	375
ERY concentration	mg/L	5.00
COD originating from the ERY-COD	mg/L	2.00
Total COD concentration	mg/L	377
HRT	d	10.97; 9; 4.5; 3; 2.25; 1.8
Organic loading rate of molasses-COD	g.COD/L.d	0.03
Organic loading rate of ERY-COD	g.ERY/L.d	$0.45x10^{-3}$
Total organic loading rate	g.COD/L.d	0.03
F/M ratio	gCOD/gMLVSS d	$7.5\ x10^{-3}$
MLVSS	g/L	4
SRT	d	20
Operational times	d	292
ORP	mV	+90
Temperature	^{0}C	20

Study 16: In this study the anaerobic treatability of a real raw pharmaceutical wastewater was investigated in an AMCBR and ABFR reactor during 73 and 68 days of operation periods, respectively. Table 5.25 (a) and 5.25 (b) show the operational conditions of AMCBR reactor treating real raw pharmaceutical wastewater. The performance of AMCBR reactor system was monitored at a HRT of 2.25 days.

Table 5.25 (a) Operational conditions of the AMCBR reactor at real raw pharmaceutical wastewater

Parameters	**Units**	**Values**
Flow rate	L/d	1, 2, 3
Volume	L	4.5
COD concentration of molasses-COD	mg/L	15102± 750
OTC and AMX concentration	mg/L	65±3; 65±3
COD originating from the OTC and AMX-COD	mg/L	33
BOD_5 concentration	mg/L	3620±130
BOD_5/COD ratio	unitless	0.24±0.01
Total Nitrogen concentration	mg/L	6.50±0.3
Total Phosphate concentration	mg/L	5.00±0.1
HRT	d	4.5, 2.25, 1.5
Organic loading rate of molasses-COD	g.COD/L.d	3.40
Organic loading rate of OTC and AMX-COD	g.COD/L.d	0.01
Total organic loading rate	g.COD/L.d	3.37
F/M ratio	g.COD/g.VSS. d	14.10
VSS	mg/L	237
SRT	d	30
Operational days	d	73
ORP	mV	-360
Temperature	^{0}C	37

Table 5.25 (b) Operational conditions of the ABFR reactor for real raw pharmaceutical wastewater

Parameters	**Units**	**Values**
Flow rate	L/d	1, 2, 3
Volume	L	12
COD concentration of molasses-COD	mg/L	15102±750
OTC and AMX concentration	mg/L	65±3
COD originating from the OTC and AMX-COD	mg/L	33
BOD_5 concentration	mg/L	3620±130
BOD_5/COD ratio	unitless	0.24±0.01
Total Nitrogen concentration	mg/L	6.50±0.3
Total Phosphate concentration	mg/L	5.00±0.1
HRT	d	12, 6, 4
Organic loading rate of molasses-COD	g.COD/L.d	1.26
Organic loading rate of OTC and AMX-COD	g.COD/L.d	$2.75x10^{-3}$
Total organic loading rate	g.COD/L.d	1.26
F/M ratio	g.COD/g.VSS. d	9.10
VSS	mg/L	237
SRT	d	33
Operational days	d	68
ORP	mV	-360
Temperature	^0C	37

5.3.3.2 Operational Conditions for Sequential ABFR/CSTR System with Synthetic Wastewater

Study 17: Start-up is often considered to be the most unstable and difficult phase in anaerobic degradation. Therefore, the main objective of this study is to observe and evaluate start-up performance of ABFR using synthetic wastewater at various organic loading rates. The performance of ABFR was evaluated based on the COD yields and methane production. The ABFR was operated through 63 days without

OTC to acclimate the granular sludge to the ABFR. The operational conditions for this study were given in Table 5.26.

Table 5.26 Operational conditions of the ABFR reactor at start-up period (without OTC)

Parameters	**Units**	**Values**		
		Minimum	**Mean**	**Maximum**
Flow rate	L/d	2		
Volume	L	12		
COD concentration of molasses-COD	mg/L	3990	4045	4100
HRT	d	6		
Organic loading rate of molasses-COD	g.COD/L.d	0.66	0.67	0.68
F/M ratio	g.COD/g.VSS.d	0.01	0.02	0.03
VSS	g/L	36	38	39
SRT	d	22	25	27
Operational days	d	63		
ORP	mV	-350	-360	-370
Temperature	^{0}C	36	37	38

Study 18: Start-up period in anaerobic process is considered to be very critical for anaerobic reactor. This study is focused on the start-up period of anaerobic degradation. In order to acclimation the partially granulated biomass in the ABFR, the anaerobic reactor was operated with synthetic wastewater through 55 days without AMX for reach to steady state conditions. The operational conditions of continuously study were given in Table 5.27.

Table 5.27 Operational conditions of the ABFR reactor at start-up period (without AMX)

Parameters	Units	Values		
		Minimum	Mean	Maximum
Flow rate	L/d	2		
Volume	L	12		
COD concentration of molasses-COD	mg/L	4000	4100	4200
HRT	d	6		
Organic loading rate of molasses-COD	g.COD/L.d	0.66	0.68	0.70
F/M ratio	g.COD/g.VSS.d	0.01	0.01	0.02
VSS	g/L	39	40	41
SRT	d	30	31	33
Operational days	d	55		
ORP	mV	-350	-360	-370
Temperature	^{0}C	36	37	38

Study 19: This step contains the start-up of the ABFR in the without of TYL. The value of the operational conditions for ABFR reactor was summarized in Table 5.28.

Table 5.28 Operational conditions of the ABFR reactor at start-up period (without TYL)

Parameters	Units	Values		
		Minimum	Mean	Maximum
Flow rate	L/d	2		
Volume	L	12		
COD conc. of molasses-COD	mg/L	3800	3900	4000
HRT	d	6		
Organic loading rate of molasses-COD	g.COD/L.d	0.63	0.65	0.66
F/M ratio	g.COD/g.VSS.d	0.01	0.02	0.03
VSS	g/L	28	29	30
SRT	d	21	25	30
Operational days	d	60		
ORP	mV	-350	-360	-370
Temperature	^{0}C	36	37	38

Study 20: The anaerobic ABFR reactor was operated through 60 days without ERY to acclimate the anaerobic granular sludge to the anaerobic ABFR reactor. The operational conditions for this study were given in Table 5.29.

Table 5.29 Operational conditions of the AMCBR reactor at start-up period

Parameters	**Units**	**Values**		
		Minimum	**Mean**	**Maximum**
Flow rate	L/d	2		
Volume	L	12		
COD concentration of molasses-COD	mg/L	4100	4200	4300
HRT	d	6		
Organic loading rate of molasses-COD	g.COD/L.d	0.68	0.70	0.72
F/M ratio	g.COD/g.VSS.d	0.01	0.02	0.02
VSS	g/L	40	41	42
SRT	d	43	46	47
Operational days	d	60		
ORP	mV	-350	-360	-370
Temperature	^{0}C	36	37	38

Study 21: The ABFR reactor was continuously operated with 50-100-150-200-250 mg/L OTC concentrations. In this study, effect of increasing OTC concentrations on the removal efficiencies of the OTC, COD and gas productions were investigated in a sequential ABFR/CSTR system. The effluent of the ABFR was used as feed in the CSTR reactor. The operational conditions for this run were given in Tables 5.30 and 5.31 for ABFR and CSTR reactors, respectively. The SRT in the CSTR reactor was adjusted as 20 days by discarding a certain amount of sludge volume from the aeration stage of the aerobic CSTR reactor.

Table 5.30 Operational conditions of the ABFR reactor at increasing OTC concentrations

Parameters	**Units**	**Values**
Flow rate	L/d	2
Volume	L	12
COD concentration of molasses-COD	mg/L	3900; 3950;3975;3990;4060
OTC concentration	mg/L	50; 100; 150; 200; 250
COD originating from the OTC-COD	mg/L	25; 50; 75; 100; 125
Total COD concentration	mg/L	3925; 4000; 4050; 4090; 4185
HRT	d	6
Organic loading rate of molasses-COD	g.COD/L.d	0.65; 0.66; 0.67; 0.68; 0.69
Organic loading rate of OTC-COD	g.COD/L.d	$4.17x10^{-3}$; $8.33\ x10^{-3}$; $1x10^{-2}$; $2x10^{-2}$; $3x10^{-2}$
Total organic loading rate	g.COD/L.d	0.65; 0.66; 0.68; 0.70; 0.72
F/M ratio	g.COD/g.VSS.d	0.02; 0.02; 0.01; 0.02; 0.02
VSS	g/L	38; 40; 42; 36; 37
SRT	d	64; 68; 71; 61; 63
Operational days	d	183
ORP	mV	-370
Temperature	^0C	37

Table 5.31 Operational conditions of the CSTR reactor at increasing OTC concentrations

Parameters	**Units**	**Values**
Flow rate	L/d	2
Volume	L	9
COD concentration of molasses-COD	mg/L	380; 396; 405; 566; 612
OTC concentration	mg/L	9; 11; 12; 13; 15
COD originating from the OTC-COD	mg/L	7.2; 8.8; 9.6; 10.4; 12
Total COD concentration	mg/L	387; 405; 415; 576; 624
HRT	d	4.5
Organic loading rate of molasses-COD	g.COD/L.d	0.08; 0.09; 0.10; 0.13; 0.14
Organic loading rate of OTC-COD	g.COD/L.d	$1.6x10^{-3}$; $1.95x10^{-3}$; $2.13x10^{-3}$; $2.31x10^{-3}$; $2.67x10^{-3}$
Total organic loading rate	g.COD/L.d	0.08; 0.09; 0.10; 0.13; 0.14
F/M ratio	g.COD/g.MLVSS.d	0.03; 0.03; 0.02; 0.05; 0.07
MLVSS	g/L	2.5; 3.1; 3.8; 2.6; 1.96
SRT	d	20
Operational times	d	183
ORP	mV	+90
Temperature	^{0}C	20

Study 22: The ABFR reactor used in this experimental study was operated continuously throughout 156 days. In this study the study of the effects of increasing AMX concentrations (50-100-150-200 mg/L) on the performance of the anaerobic ABFR reactor was investigated. The operational conditions for the ABFR reactor were summarized in Table 5.32. In this step of the study the effects of increasing AMX concentration were investigated on the performance of the aerobic CSTR reactor. The operational conditions for this study were given in Table 5.33**.**

Table 5.32 Operational conditions of the AMCBR reactor at increasing AMX concentrations

Parameters	**Units**	**Values**
Flow rate	L/d	2
Volume	L	12
COD concentration of molasses-COD	mg/L	4000; 4100; 4010; 4200
AMX concentration	mg/L	50; 100; 150; 200
COD originating from the AMX-COD	mg/L	25; 35; 40; 45
Total COD concentration	mg/L	4025; 4135; 4050; 4245
HRT	d	6
Organic loading rate of molasses-COD	g.COD/L.d	0.66; 0.68; 0.67; 0.70
Organic loading rate of AMX-COD	g.COD/L.d	$4.2x10^{-3}$; $5.83x10^{-3}$; $6.67x10^{-3}$;$1\ x10^{-2}$
Total organic loading rate	g.COD/L.d	0.66; 0.68; 0.67; 0.71
F/M ratio	g.COD/g.VSS.d	0.01; 0.01; 0.02; 0.03
VSS	g/L	45; 50; 41; 37
SRT	d	74; 82; 67; 61
Operational days	d	156
ORP	mV	-370
Temperature	^{0}C	37

Table 5.33 Operational conditions of the CSTR reactor at increasing AMX concentrations

Parameters	**Units**	**Values**
Flow rate	L/d	2
Volume	L	9
COD concentration of molasses-COD	mg/L	438; 545; 602; 700
AMX concentration	mg/L	7.00; 7.40; 8.00; 8.70
COD originating from the AMX-COD	mg/L	3.50; 3.70; 4.00; 4.35
Total COD concentration	mg/L	442; 549; 606; 704
HRT	d	4.5
Organic loading rate of molasses-COD	g.COD/L.d	0.01; 0.12; 0.14; 0.16
Organic loading rate of AMX-COD	g.COD/L.d	$0.77x10^{-3}$; $0.82x10^{-3}$; $0.88x10^{-3}$; $0.96x10^{-3}$
Total organic loading rate	g.COD/L.d	0.01; 0.12; 0.14; 0.16
F/M ratio	g.COD/g.MLVSS.d	0.01; 0.03; 0.05; 0.06
MLVSS	g/L	2.0; 3.5; 3.0; 2.5
SRT	d	20
Operational days	d	156
ORP	mV	+90
Temperature	^{0}C	20

Study 23: Tables 5.34 and 5.35 showed the operational conditions for sequential reactor system at increasing TYL concentrations. During the operation period, pH and gas production were measured daily, COD, TYL, TVFA and Bicarbonate Alkalinity concentrations in effluents were monitored weekly. The effluent of the ABFR reactor was used as feed in the influent of aerobic CSTR reactor. The SRT in the aerobic CSTR reactor was adjusted to 20 days.

Table 5.34 Operational conditions of the ABFR reactor at increasing TYL concentrations

Parameters	**Units**	**Values**
Flow rate	L/d	2
Volume	L	12
COD concentration of molasses-COD	mg/L	3900; 4105; 3948; 4326
TYL concentration	mg/L	50; 100; 150; 200
COD originating from the TYL-COD	mg/L	25; 35; 40; 65
Total COD concentration	mg/L	3925; 4140; 3988; 4391
HRT	d	6
Organic loading rate of molasses-COD	g.COD/L.d	0.65; 0.68; 0.66; 0.72
Organic loading rate of TYL-COD	g.TYL/L.d	$4.17x10^{-3}$; $5.83x10^{-3}$; $6.67\ x10^{-3}$; $1x10^{-2}$
Total organic loading rate	g.COD/L.d	0.65; 0.68; 0.66; 0.73
F/M ratio	g.COD/g.VSS.d	0.02; 0.01; 0.02; 0.03
VSS	g/L	40; 48; 40; 35
SRT	d	98; 110; 98; 86
Operational days	d	176
ORP	mV	-360
Temperature	^{0}C	37

Table 5.35 Operational conditions of the CSTR reactor at increasing TYL concentrations

Parameters	**Units**	**Values**
Flow rate	L/d	2
Volume	L	9
COD concentration of molasses-COD	mg/L	573; 675; 712; 787
TYL concentration	mg/L	9.3; 10.5; 11; 9.5
COD originating from the TYL-COD	mg/L	3.10; 4.25; 5.55; 3.10
Total COD concentration	mg/L	576; 679; 718; 790
HRT	d	4.5
Organic loading rate of molasses-COD	g.COD/L.d	0.13; 0.15; 0.16; 0.18
Organic loading rate of TYL-COD	g.TYL/L.d	$0.68x10^{-3}$; $0.94x10^{-3}$; $1.23x10^{-3}$; $0.68x10^{-3}$
Total organic loading rate	g.COD/L.d	0.13; 0.15; 0.16; 0.18
F/M ratio	g.COD/g.MLVSS. d	0.04; 0.04; 0.08; 0.11
MLVSS	g/L	3; 3.5; 2.0; 1.65
SRT	d	20
Operational days	d	176
ORP	mV	+90
Temperature	^{0}C	20

Study 24: The operational conditions for this step including influent concentrations of ERY, COD concentrations were measured in the reactor throughout 184 days of operation are depicted in Table 5.36. During the operation period, pH and gas productions were measured daily while the COD, TYL and TVFA concentrations in the effluent samples were monitored weekly. In this step performed with CSTR reactor the effect of increasing ERY concentrations on treatment efficiencies of the aerobic CSTR reactor was investigated. The operational conditions for the aerobic CSTR reactor were summarized in Table 5.37.

Table 5.36 Operational conditions of the AMCBR reactor at increasing ERY concentrations

Parameters	**Units**	**Values**
Flow rate	L/d	2
Volume	L	12
COD concentration of molasses-COD	mg/L	4100
ERY concentration	mg/L	50; 100; 150; 200
COD originating from the ERY-COD	mg/L	20; 40; 60; 80
Total COD concentration	mg/L	4120; 4140; 4160; 4180
HRT	d	6
Organic loading rate of molasses-COD	g.COD/L.d	0.68
Organic loading rate of ERY-COD	g.ERY /L.d	$3.33x10^{-3}$; $6.67\ x10^{-3}$; $1x10^{-2}$; $1\ x10^{-2}$
Total organic loading rate	g.COD/L.d	0.68; 0.69; 0.69; 0.70
F/M ratio	g.COD/g.VSS.d	0.02; 0.01; 0.02; 0.03
VSS	g/L	40; 42; 35; 30
SRT	d	88; 92; 77; 66
Operational days	d	184
ORP	mV	-360
Temperature	^{0}C	37

Table 5.37 Operational conditions of the CSTR reactor at increasing ERY concentrations

Parameters	Units	Values
Flow rate	L/d	2
Volume	L	9
COD concentration of molasses-COD	mg/L	493; 500; 625; 668
ERY concentration	mg/L	6.00; 6.50; 7.05; 9.12
COD originating from the ERY-COD	mg/L	2.5; 2.8; 3.12; 3.89
Total COD concentration	mg/L	496; 503; 628; 670
HRT	d	4.5
Organic loading rate of molasses-COD	g.COD/L.d	0.10; 0.11; 0.14; 0.15
Organic loading rate of ERY-COD	g.ERY/L.d	$0.55x10^{-3}$; $0.62x10^{-3}$; $0.69x10^{-3}$; $0.86x10^{-3}$
Total organic loading rate	g.COD/L.d	0.13; 0.13; 0.14; 0.16; 0.21; 0.29
F/M ratio	g.COD/g.MLVSS.d	0.03; 0.03; 0.03; 0.04; 0.06; 0.10
MLVSS	g/L	4; 4.5; 5; 4
SRT	d	20
Operational days	d	184
ORP	mV	+90
Temperature	^{0}C	20

5.3.3.3 Operational Conditions for Substrate Removal and Inhibition Kinetic Models

Study 25: In this step, different kinetic models such as Monod, Contois, Stover-Kincannon, Grau-second order, Zero order, First order and Second order to the experimental date obtained from the continuous operation of anaerobic reactors were applied to determine the suitable substrate removal kinetic and relevant kinetic constants under different HRTs. Furthermore different gas production models such as Modified Stover-Kincannon; kinetic was used in order to obtain the total and methane gas productions and relevant kinetic constants. This study was designed to

investigate the type of inhibition (Competitive, Noncompetitive and Uncompetitive, Haldane), the effect of increasing antibiotics concentrations on kinetic coefficients, maximum substrate removal rate (R_{max}), half saturation constant (K_S), and antibiotic (OTC, AMX, TYL and ERY) inhibition constants (K_I) during the substrate (molasses) removal.

In this run, the effect of increasing antibiotic (Study 8, Study 9, Study 10, Study 11 for AMCBR and Study 21, Study 22, Study 23, Study 24 for ABFR) and different HRTs (Study 12, Study 13, Study 14, Study 15 for AMCBR) on the OTC, AMX, TYL and ERY and COD removal performances, gas productions, pH, TVFA, HCO_3 alkalinity variations was investigated in sequential AMCBR/CSTR and ABFR/CSTR system containing OTC, AMX, TYL and ERY. The effluent of the AMCBR and ABFR was used as feed in the CSTR reactor.

5.4 Wastewater Characterization

5.4.1 Composition of the Synthetic Wastewater Used in the Batch Reactors

4 ml of anaerobic granulated sludge containing a MLVSS concentration of 3000 mg/L was added separately into the serum bottles. Then 7.5 ml molasses ($C_6H_{12}NNaO_3S$; produced by boiling sugar cane waste) with a COD concentration of 4000 mg/L, 1 ml sodium thioglycollate ($C_2H_3NaO_2S$) (0.07%), 7.5 ml $NaHCO_3$ (5000 mg/L) 0.25 ml Vanderbilt mineral medium and 0.8, 1.7, 2.5, 3.3, 4.2, 5.0, 5.8, 6.7 ml synthetic wastewater containing increasing concentration of OTC, AMX, TYL and ERY were added to the serum bottles. The composition of Vanderbilt mineral is given in Table 5.38.

Table 5.38 Composition of Vanderbilt mineral medium (Speece, 1996)

Compounds	**Concentrations (mg/L)**
NH_4CI	400
$MgSO_4$	400
KCI	400
$Na_2S.9H_2O$	300
$(NH_4)_2HPO_4$	80
$CaCI_2.2H_2O$	50
$FeCI_2.4H_2O$	40
$CoCI_2.6H_2O$	10
KI	10
$(NaPO_3)_6$	10
Sistein	10
$AlCI_3.6H_2O$	0.5
$MnCI_2.4H_2O$	0.5
$CuCI_2$	0.5
$ZnCI_2$	0.5
NH_4VO_3	0.5
$NaMoO_4.2H_2O$	0.5
H_3BO_3	0.5
$NiCI_2.6H_2O$	0.5
$NaWO_4.2H_2O$	0.5
Na_2SeO_3	0.5

5.4.2 Composition of the Synthetic Wastewater Used in the Continuous Reactors

OTC concentration varying between 50, 100, 150, 200, 250, 300, 400 mg/L and AMX, TYL and ERY concentration varying between 50, 100, 150, 200, 250, 300 mg/l were used throughout continuous operation of the AMCBR and ABFR reactors (Table 5.39). Molasses was used as the primary substrate giving a COD concentration of 4000 mg/L. The molasses was obtained from the Pakmaya Yeast Beaker Factory in İzmit, Turkey. The COD equivalence of the increasing of OTC (50, 100, 150, 200, 250 300, 350, 400 mg/L), AMX (50, 100, 150, 200, 250, 300 mg/L), TYL and ERY (50, 100, 150, 200, 250, 300 mg/L) concentrations were 20,

40, 60, 80, 100, 120, 140, 160 mg/L; 5, 10, 12, 25, 45, 65 mg/L; 10, 20, 30, 40, 50, 60 mg/L, respectively. The composition of the Vanderbilt mineral medium was given in Table 5.39. The anaerobic conditions were maintained by adding 667 mg/L of Sodium Thioglycollate (0.067%) which is proposed between 0.01-0.2% (w/w) for maintaining the strick anaerobic conditions (Speece, 1996). The alkalinity and neutral pH were adjusted by addition of 5000 mg/L $NaHCO_3$.

Table 5.39 Composition of the synthetic wastewater

Parameters	**Units**	**Concentrations of Synthetic Wastewater**		
		Min[a]	Mean[b]	Max[c]
COD_m[d]	mg/L	3000-3100	3400-3500	3950-4000
BOD_5	mg/L	660-713	885-910	1110-1160
BOD_5/COD	unitless	0.22-0.23	0.25-0.26	0.28-0.29
$NaHCO_3$	mg/L	-	5000	-
$C_2H_3NaO_2S$	mg/L	-	667	-
Total Nitrogen	mg/L	5.00-5.12	6.33-6.68	7.65-8.24
Total Phosphorus	mg/L	4.86-5.00	5.24-5.52	5.62-6.03
OTC	mg/L	50-100	150-250	300-400
AMX	mg/L	50-100	150-200	250-300
TYL	mg/L	50-100	150-200	250-300
ERY	mg/L	50-100	150-200	250-300
VM[e]	65 ml/150 ml			
pH	unitless	6.3-6.5	6.9-7.0	7.2-7.4

[a]: Minimum; [b]: Mean; [c]: Maximum; [d]: Molasses COD concentration; [e]: Vanderbilt medium solution

5.4.3 Composition of the Raw Pharmaceutical Wastewater Used in the Continuous Reactors

The pharmaceutical wastewater was supplied by Mustafa Nevzat Pharmaceutical Industry Inc, Istanbul, Turkey. The characteristics of the raw pharmaceutical wastewater containing the antibiotics are given in Table 5.40. The inorganic content of the pharmaceutical wastewater is mainly composed of metals and elements. The metal and element content of the pharmaceutical wastewater is shown in Table 5.41.

Table 5.40 The characteristics of the real raw pharmaceutical wastewater

Parameters	**Units**	**Concentrations of raw pharmaceutical wastewater**		
		Min[a]	Mean[b]	Max[c]
pH	Unitless	5.00-5.20	5.80-6.00	6.40-6.60
TSS	mg/L	338.17-340.27	341.02-342.30	345.66-347.00
VSS	mg/L	235.12-236.87	237.24-239.00	241.12-243.02
COD	mg/L	13710-14200	14876-15102	15800-16000
BOD	mg/L	3148-3161	3457-3620	4028-4110
BOD/COD	Unitless	0.22-0.23	0.23-0.24	0.24-0.25
Phenol	mg/L	1.92-2.08	3.02-3.14	4.12-4.24
Total Nitrogen	mg/L	4.80-5.00	6.20-6.50	8.30-8.50
Nitrate	mg/L	9.48-9.86	12.26-12.53	15.00-15.21
Nitrite	mg/L	0.10-0.12	0.15-0.17	0.20-0.22
Ammonia	mg/L	3.00-3.12	3.50-3.61	4.00-4.14
Total Phosphate	mg/L	4.20-4.35	4.80-5.00	5.20-5.50
OTC	mg/L	65	65	65
AMX	mg/L	65	65	65
TYL[d]	mg/L	-	-	-
ERY[e]	mg/L	-	-	-

[a]: Minimum; [b]: Mean; [c]: Maximum; [d,e]: Not available

Table 5.41 Metal and Element composition of raw pharmaceutical wastewater

Parameters	**Units**	**Concentrations of raw pharmaceutical wastewater**		
		Minimum	**Mean**	**Maximum**
Al	mg/L	0.27-0.28	0.29-0.30	0.31-0.32
Ba	mg/L	0.01-.0.02	0.02-0.03	0.03-0.04
Ca	mg/L	36.05-36.48	38.00-38.11	39.56-39.75
Cd	mg/L	0.03-0.04	0.04-0.05	0.05-0.06
Co	mg/L	0.06-0.07	0.07-0.08	0.08-0.09
Cr	mg/L	0.01-0.02	0.02-0.03	0.03-0.04
Cu	mg/L	0.05-0.06	0.06-0.07	0.07-0.08
Fe	mg/L	3.00-3.02	3.12-3.26	3.50-3.54
Li	mg/L	0.01-0.02	0.01-0.02	0.02-0.03
Mg	mg/L	90.00-90.12	91.47-92.24	94.35-95.00
Mn	mg/L	21.42-21.65	22.00-23.5	24.68-25.02
Mo	mg/L	0.01-0.02	0.02-0.03	0.03-0.04
Na	mg/L	198-200	208-210	220-222
Ni	mg/L	0.04-0.05	0.05-0.06	0.06-0.07
Pb	mg/L	0.03-0.04	0.04-0.05	0.06-0.07
Sn	mg/L	0.17-0.19	0.19-0.20	0.21-0.23
Zn	mg/L	0.24-0.25	0.26-0.28	0.29-0.30

5.5 Sources of the Seed Sludge

5.5.1 Batch Reactors

Partially granulated anaerobic sludge was used as seed in anaerobic batch reactors. The seed anaerobic sludge was obtained from an anaerobic up flow anaerobic sludge blanket reactor (UASB) containing acidogenic and methanogenic partially granulated biomass taken from the Pakmaya Yeast Beaker Factory in Izmit,

Turkey. The mixed liquor volatile suspended solid (MLVSS) concentration of seed sludge in the anaerobic reactor was measured between 2800 and 3000 mg/L by adding 4 ml of granulated sludge having a MLVSS concentration 12 mg/L

5.5.2 Seed Properties Used in the AMCBR, ABFR and CSTR throughout Continuous Studies

Partially granulated anaerobic sludge was used as seed in the AMCBR and ABFR reactors. 20% of the reactor volumes were filled with partially granulated anaerobic sludge. The seed sludge was obtained from an anaerobic up flow anaerobic sludge blanket reactor (UASB) containing acidogenic and methanogenic partially granulated biomass taken from the Pakmaya Yeast Beaker Factory in Izmit, Turkey. The Activated sludge culture was used as seed for the aerobic CSTR reactor and it was taken from the activated sludge reactor of Pakmaya Yeast Beaker Factory in Izmit. The MLVSS concentration of the seed sludge in AMCBR and ABFR reactor were adjusted as 50 g/L and 60 g/L, respectively. The MLSS and MLVSS in the aerobic CSTR reactor were adjusted between 4-4.5 g/L and 3-4 g/L, respectively.

5.6 Analytical Methods

5.6.1 Chemical Oxygen Demand (COD) Measurements

COD was determined with Close Reflux Method following the Standard Methods 5220-D (APHA-AWWA-WEF, 2005) using an Aqua mate thermo electron corporation UV visible spectrophotometer. First the samples were centrifuged for 10 min at 9000 rpm. Secondly, 2.50 ml volume wastewater samples were treated with 1.50 ml 10216 mg/L $K_2Cr_2O_7$ with 33.30 g/L $HgSO_4$ and 3.50 ml H_2SO_4 which contains 0.55% (w/w) Ag_2SO_4. Thirdly the closed sample tubes were stored in a 148°C heater (thermo reactor, CR 4200 WTW, 2008) for 2 h. Finally, after cooling, the samples were measured at 610 nm with an Aqua mate thermo electron corporation UV visible spectrophotometer. The Closed Reflux Method COD was

used to measure the COD in synthetic wastewater before and after anaerobic/aerobic sequential treatments.

5.6.1.1 COD Calibration Curves

KPH was used to prepare the standard solutions 17 gKPH/L which is equivalent to 20 gCOD/L (see Table 5.42, 5.43 and 5.44; Figure 5.5).

Table 5.42 Absorbance data for COD calibration 1

Concentration of COD (mg/L)	**Wavelength**			
	Absorbance values measured at a wavelength of 610 nm)			
	Analysis 1	Analysis 2	Analysis 3	Average
0	0.000	0.000	0.000	0.000
200	0.054	0.042	0.042	0.046
500	0.093	0.091	0.096	0.093
1000	0.170	0.179	0.172	0.174
2000	0.318	0.336	0.338	0.331
3000	0.502	0.481	0.498	0.494

Table 5.43 Absorbance data for COD calibration 2.

Concentration of COD (mg/L)	**Wavelength**			
	Absorbance values measured at a wavelength of 610 nm)			
	Analysis 1	Analysis 2	Analysis 3	Average
0	0.000	0.000	0.000	0.000
100	0.048	0.049	0.057	0.051
200	0.063	0.069	0.068	0.067
500	0.114	0.117	0.114	0.115
1000	0.202	0.189	0.216	0.202
2000	0.338	0.367	0.335	0.347
3000	0.488	0.511	0.499	0.499

Table 5.44 Absorbance data for COD calibration 3.

Concentration of COD (mg/l)	**Wavelength (A610nm[a])**			
	Absorbance values measured at a wavelength of 610 nm)			
	Analysis 1	Analysis 2	Analysis 3	Average
0	0.000	0.000	0.000	0.000
100	0.013	0.014	0.022	0.016
200	0.028	0.034	0.033	0.032
500	0.079	0.082	0.079	0.080
1000	0.167	0.154	0.181	0.167
2000	0.303	0.332	0.300	0.312
3000	0.453	0.476	0.464	0.464

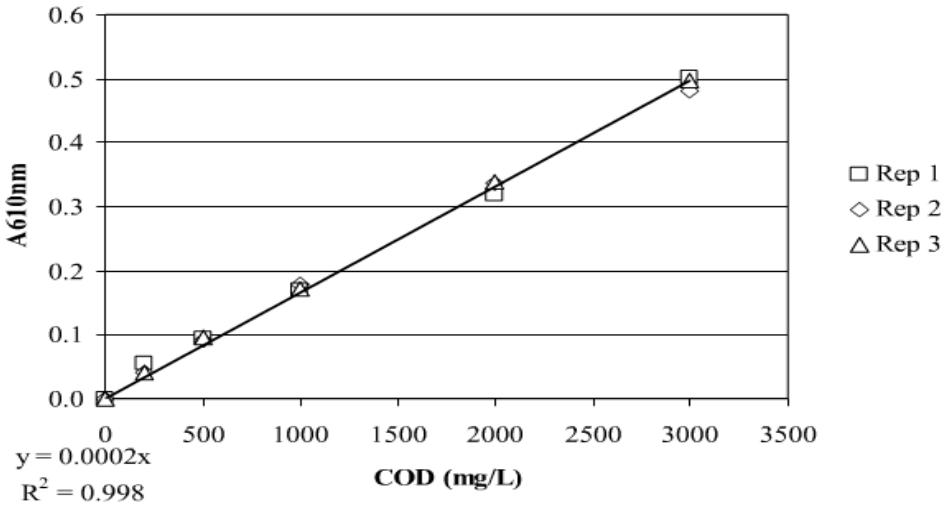

(a)

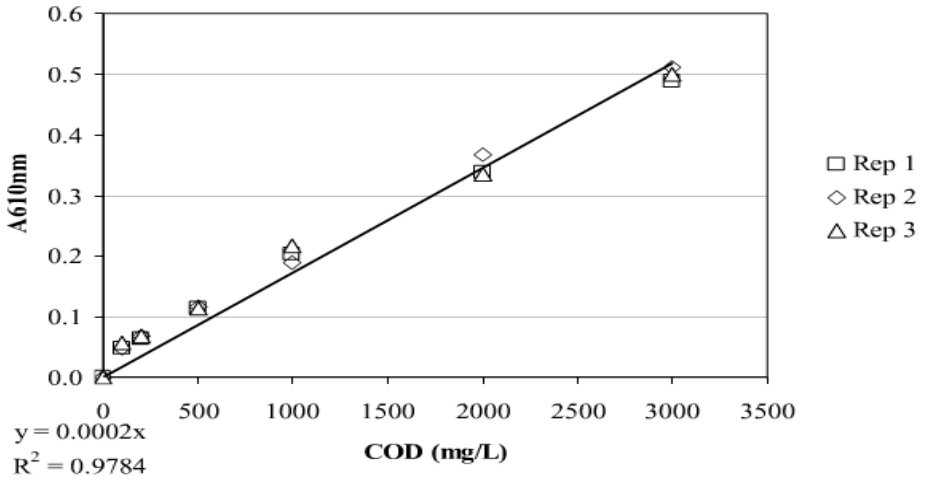

(b)

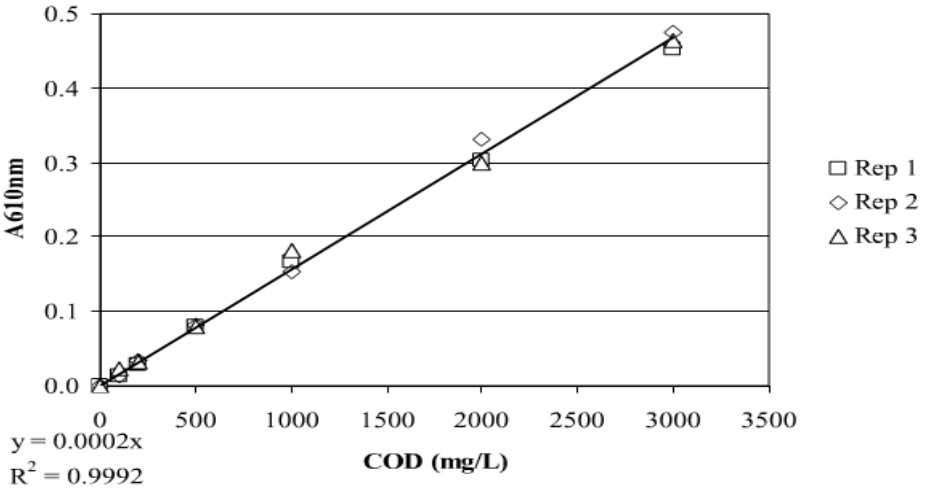

(c)

Figure 5.5 COD calibration plots.

5.6.1.2 COD Subcategories

The inert COD, slowly degradable COD and readily degradable COD were measured following the methods proposed by Ekama et al., (1986). The soluble inert COD was measured using the glucose comparison method. This method involves running three batch reactors, two with the wastewater to be studied and the third with glucose. One of the wastewater reactors has the total COD, and the second has the

total soluble COD, whereas the initial COD in the glucose reactor is adjusted to equal COD value. The experimental studies are performed until all the biodegradable COD is depleted, where the COD profiles reach a plateau and stay unchanged. The difference between glucose COD and wastewater COD gives the inert COD. The readily biodegradable COD is measured with Eq. 5.1:

$$\frac{Dissolved\ O_2\ Change}{(1-Y)} \qquad \text{Eq. (5.1)}$$

Y is the yield and it is equal to the ratio [produced biomass (VSS)/removed soluble COD] which was obtained from the experimental data. Slowly biodegradable COD is measured with Eq. 5.2:

$$Soluble\ COD - (Readily\ Biodegradable\ COD + Inert\ Soluble\ COD) \qquad \text{Eq. (5.2)}$$

5.6.2 Gas Measurements

The amount of total gas was determined by liquid displacement method everyday using H_2SO_4 (v/v, 2%) and NaCl (w/v, 10%) containing solution (Beydilli, et al., 1998). Methane gas was detected by using a liquid containing 3% NaOH to scrub out the carbon dioxide from the biogas (Razo-Flores et al., 1997). The methane gas percentage in biogas was also determined by Dräger Pac®Ex methane gas analyzer. The H_2S gas was measured using Dräger (Stuttgart, Germany) kits in a Dräger H_2S meter. CO_2 and H_2 gas was measured using (Dräger Pac®Ex) CO_2 and H_2 meter.

5.6.3 Mixed Liquor Suspended Solids (MLSS), Mixed Liquor Volatile Suspended Solids (MLVSS), Suspended Solids (SS) and Volatile Suspended Solids (VSS) in the Anaerobic, Aerobic Reactors and Biofilm Carrier Measurements

Biomass was measured as suspended solid (SS) and volatile suspended solid (VSS) in the anaerobic system and raw pharmaceutical wastewater composition. Biomass in aerobic and anaerobic system was measured as mixed liquor suspended

solids (MLSS) and mixed liquor volatile suspended solids (MLVSS). Assays were performed according to Standard Methods for Examination of Water and Wastewater (APHA-AWWA-WEF 2005) (SM-2540-A-G). Estimate of the VSS on the biofilm carrier (polystyrene balls) were according to Bertino, (2010).

5.6.4 Anaerobic Toxicity Assay (ATA) and Determination of Inhibition Concentration (IC_{50})

ATA test was performed at 35±1°C using serum bottles with a capacity of 150 ml as described by Owen et al., (1979) and Donlon et al., (1995). Serum bottles were filled with 3000 mgVSS/L of biomass, 4000 mg/l of molasses-COD, suitable volume from the Vanderbilt mineral medium, 667 mg/L of sodium thioglycollate providing the reductive conditions and 5000 mg/L of $NaHCO_3$ for maintaining the neutral pH. Before ATA test, the serum bottles were batch operated until the variation in daily gas production was less than 15% at least for 7 consecutive days. After observing the steady-state conditions, increasing concentration of OTC, AMX, TYL and ERY antibiotics were administered to serum bottles as slug-doses from concentrated stock solutions of these chemicals. The effects of OTC, AMX, TYL and ERY antibiotics on methane gas production were compared with the control samples. Inhibition was defined as a decrease in cumulative methane compared to the control sample. IC_{50} value indicates the 50% inhibition of methane gas production in serum bottles containing toxicant. This value shows that the toxicant concentration caused 50% inhibition in the methane gas production.

5.6.5 Specific Methanogenic Activity (SMA) Test

The anaerobic sludge samples were taken from PAKMAYA Yeast Industry. The SMA test was realized in 150 ml serum vials and incubated at 35 °C under anaerobic conditions. Each vial was filled with 15 ml of the partially anaerobic sludge and 35 ml of synthetic wastewater, which contained 4000 mg/L carbon source, 0.5 ml Vanderbilt mineral medium, and 5000 mg/L of $NaHCO_3$ and 20 ml sodium thioglycollate as aforementioned in the ATA test. The total volume was completed to

75 ml by adding distilled water. OTC, AMX, TYL and ERY were not added to control bottles. Serum vials were incubated at 35±1 °C and methane production was recorded for 2 days. At the end of each test, the VSS was measured to detect the biomass concentration. The gas production was determined by inserting a hypodermic needle connected to a calibrated fluid reservoir, through the serum bottle. At 35 °C, 395 ml of methane production is equivalent to 1 g of COD reduction. Maximum specific methanogenic activity was calculated from the total methane production through 2 days with the method proposed by Owen et al., (1979) as follows:

$$SMA\left(gCH_4/gVSS.d\right)=\frac{produce\ \ CH_4\ volume\ \ (ml)\times 395\ ml/LgCOD}{sample\,(ml)\times incubation\ \ (d)\times biomass\ \ conc.\,(g/L)} \quad \text{Eq. (5.3)}$$

5.6.6 pH, Temperature, Dissolved Oxygen (DO) and Oxidation Reduction Potential (ORP) Measurements

The pH, temperature, and dissolved oxygen were measured using pH meter (WWT pH 330), an electronic digital heater and an oxygen meter (WWT Oxi330/SET), respectively. The oxidation reduction potential was measured using Sen Tix ORP digital electrode (WWT pH 330) with an $Ag/AgCl_2$ reference electrode which is saturated with KCl solution and Pt electrode.

5.6.7 BOD_5 Measurement

BOD_5 measurements were carried out in Oxi Top IS 12 system manufactured by the WTW Merck Company. The BOD_5 value was initially estimated based on the COD value experimentally measured or calculated: BOD_5=COD/1.46. The range of expected BOD_5 values was then deduced and hence led to the volumes of sample and nitrification inhibitor (10 mg/L solution of N-allylthiourea) which have to be added to the shake flask of the Oxitop apparatus (APHA-AWWA-WEF, 2005) (SM-5210-A-C).

5.6.8 Bicarbonate Alkalinity and Total Volatile Fatty Acid (TVFA) Measurements

A simple, alkali metric method is described that can be used to determine bicarbonate and TVFA concentrations in anaerobic digesters by a two-stage sequential titration. The TVFA concentrations were measured by using Anderson and Yang, (1992). Samples were titrated by 0.1 N H_2SO_4 then the bicarbonate (HCO_3) and TVFA concentration were determined with a computer program. The measurement steps are given below:

- The pH of the sample was measured with pH probe.
- The sample was titrated with standard H_2SO_4 through two stages (first to pH of 5.1). Titration was continued until the pH of the sample decreased to 3.5 (second stage).
- The bicarbonate and TVFA concentration were calculated using a computer program.

Finally the TVFA and Bicarbonate Alkalinity concentrations were calculated with a computer program by solved the Eq. (5.4) and Eq. (5.5).

$$A_1 = \frac{[HCO_3^-]*([H]_2 - [H]_1)}{[H]_1 + K_C} + \frac{[VA]*([H]_2 - [H]_1)}{[H]_2 + K_{VA}} \qquad \text{Eq. (5.4)}$$

$$A_2 = \frac{[HCO_3^-]*([H]_3 - [H]_1)}{[H]_3 + K_C} + \frac{[VA]*([H]_3 - [H]_1)}{[H]_3 + K_{VA}} \qquad \text{Eq. (5.5)}$$

where A_1 and A_2 are the molar equivalent of the standard acid consumed to the first and second end points; $[HCO_3^-]$ the bicarbonate concentration; [VA] the volatile fatty acid ion concentration; $[H]_{1,2,3}$ the hydrogen ion concentrations of the original sample and at the first and the second end points; K_C is the conditional dissociation constant of carbonic acid; K_{VA} is the combined dissociation constant of the volatile fatty acids (C_2–C_6), this pair of constants was assumed, being 6.6×10^{-7} for bicarbonate and 2.4×10^{-5} for volatile acids (Kuşçu, 2007).

5.6.8.1 $TVFA_s$ Composition Measurements

Individual $TVFA_s$ (acetic, butyric, propionic, lactic acid) in the anaerobic effluent were determined by using a high performance liquid chromatograph (HPLC, Agilent 1100 model) with a prevail organic acid column of 5 μm x 150 mm x 4.6 mm and a UV detector of 220 nm. The carrying medium was 25 mM KH_2PO_4 at pH 2.5 with a flow rate of 1 ml/min (www.alltechWEB.com). The data reported in tables are the means of triplicate tests while the data reported in tables are the means of triplicate samplings and their standard deviations.

5.6.9 Antibiotics Measurements

5.6.9.1 OTC Measurement

For preparation of 1000 mg/L of OTC stock standard; 0.5 g OTC is weighted in a beaker, it was put into a 500 ml of volumetric flask and it was filled with HPLC grade deionized water. 5, 50, 100, 150, 300 mg/L standard OTC solutions were prepared from the 1000 mg/L of OTC Stock Standard (Senyuva et al., 2000).

HPLC Equipment Specifications: A HPLC Degasser (Agilent 1100), a HPLC Pump (Agilent 1100), a HPLC Auto-sampler (Agilent 1100), a HPLC Column Oven (Agilent 1100) and a HPLC Diode-Array-Detector (DAD) (Agilent 1100) were used.

HPLC Conditions for OTC Analysis: A C-18 250 mm x4.6 mm x 5 μm (id), column was used. The mobile phase consisted of the HPLC grade formic acid and the methanol to deionized water ratio was 95:5. The flow rate was 2.5 ml/min, the column temperature was 20 ^oC, the wave length was 287 nm (UV) and the injection volume was 10 μl (Senyuva et al., 2000).

Extraction Procedure: 1 L sample was centrifuged using a filter with a pore size of 0.20 μ. The vial was filled with 2 ml of centrifuged sample and it was injected into sampling ports of the HPLC (Kurosawa et al., 1985).

5.6.9.2 AMX Measurement

For preparation of 1000 mg/L AMX stock standard; 0.5 g AMX is weighted in a beaker, it was put into a 500 ml of volumetric flask and it was filled with HPLC grade deionized water. 5, 50, 100, 150, 300 mg/L standard AMX solutions were prepared from the 1000 mg/L of AMX Stock Standard (Hsu et al., 1992).

HPLC Equipment Specifications: A HPLC Degasser (Agilent 1100), a HPLC Pump (Agilent 1100), a HPLC Auto-sampler (Agilent 1100), a HPLC Column Oven (Agilent 1100) and a HPLC Diode-Array-Detector (DAD) (Agilent 1100) were used.

HPLC Conditions for AMX Analysis: A C-18 150 mm x4.5 mm x 5 µm (id), column was used. The mobile phase consisted of the HPLC grade methanol + phosphate ratio was (75:25). The flow rate was 1 ml/min, the column temperature was 22 ^{o}C, the wave length was 210 nm (UV) and the injection volume was 12 µl (Hsu et al., 1992).

Extraction Procedure: 1 L sample was centrifuged using a filter with a pore size of 0.20 µ. The vial was filled with 2 ml of centrifuged sample and it was injected into sampling ports of the HPLC (Kurosawa et al., 1985).

5.6.9.3 TYL Measurement

For preparation of 1000 mg/L TYL stock standard; 0.5 g TYL is weighted in a beaker, it was put into a 500 ml of volumetric flask and it was filled with HPLC grade deionized water. 5, 50, 100, 150, 300 mg/L standard TYL solutions were prepared from the 1000 mg/L of TYL Stock Standard (Hu et al., 2008).

HPLC Equipment Specifications: A HPLC Degasser (Agilent 1100), a HPLC Pump (Agilent 1100), a HPLC Auto-sampler (Agilent 1100), a HPLC Column Oven (Agilent 1100) and a HPLC Diode-Array-Detector (DAD) (Agilent 1100) were used.

HPLC Conditions for TYL Analysis: A C-18 250 mm x 4.6 mm x 5 µm (id), column was used. The mobile phase consisted of the HPLC grade deionize water + acetonitrile ratio was (85:15). The flow rate was 1.25 ml/min, the column temperature was 25 ^{o}C, the wave length was 254 nm (UV) and the injection volume was 20 µl (Hu et al., 2008).

Extraction Procedure: 1 L sample was centrifuged using a filter with a pore size of 0.20 µ. The vial was filled with 2 ml of centrifuged sample and it was injected into sampling ports of the HPLC (Kurosawa et al., 1985).

5.6.9.4 ERY Measurement

For preparation of 1000 mg/L ERY stock standard; 0.5 g ERY is weighted in a beaker, it was put into a 500 ml of volumetric flask and it was filled with HPLC grade deionized water. 5, 50, 100, 150, 300 mg/L standard ERY solutions were prepared from the 1000 mg/L of ERY Stock Standard (EPA, 1998) (EPA 56371B).

HPLC Equipment Specifications: A HPLC Degasser (Agilent 1100), a HPLC Pump (Agilent 1100), a HPLC Auto-sampler (Agilent 1100), a HPLC Column Oven (Agilent 1100) and a HPLC Diode-Array-Detector (DAD) (Agilent 1100) were used.

HPLC Conditions for ERY Analysis: A C-18 125 mm x 3 mm x 5 µm (id), column was used. The mobile phase consisted of the HPLC grade acetonitrile at pH=3, ammonium acetate+deionize water ratio was (95:5). The flow rate was 0.7 ml/min, the column temperature was 20 ^{o}C, the wave length was 287 nm (UV) and the injection volume was 10 µl (EPA 1998) (EPA 56371B).

Extraction Procedure: 1 L sample was centrifuged using a filter with a pore size of 0.20 µ. The vial was filled with 2 ml of centrifuged sample and it was injected into sampling ports of the HPLC (Kurosawa et al., 1985).

5.6.10 Measurement of Intermediate Products for Antibiotics

α-Apo-OTC and β-Apo-OTC measurements were carried out using a HPLC (Agilent-1100) with a method developed by EPA, 1998 (EPA 1694-1698 Methods). After all samples were centrifuged in centrifuge (SED 5X model) and filtered through a 0.45 μm pore sized teflon filter using disposable syringe (Agilent 5185-5835) all samples were given to the HPLC. Elution consisted of 95% formic acid and 5% methanol. The flow-rate of solvent was adjusted as 1 ml/min. The autosampler was set for an injection volume of 12μl. The chromatographic separation of the sample was performed at 27 °C. Detection was performed at 280 nm wave-length for α-Apo-OTC and β-Apo-OTC.

2-4 diketopiperazine AMX measurement was carried out using a HPLC (Agilent-1100) with a method developed by EPA, (1998) (EPA 1694). After all samples were centrifuged in centrifuge (SED 5X model) and filtered through a 0.45 μm pore sized teflon filter using disposable syringe (Agilent 5185-5835) all samples were given to the HPLC. Elution consisted of 75% methanol and 25% deionize water. The flow-rate of solvent was adjusted as 1 ml/min. The autosampler was set for an injection volume of 12μl. The chromatographic separation of the sample was performed at 22°C. Detection was performed at 212 nm wave-length for 2-4 diketopiperazine AMX.

5.6.11 Total Nitrogen, Total Phosphorus, Ammonium, Nitrite and Nitrate Measurements

The total nitrogen and total phosphorus were determined by using analytical kits (Spectroquant N 1.14537.0001 and Spectroquant PO4-P 1.14729.0001, Merck Chemical Company, Germany) and a NOVA-60 spectrophotometer (Merck). The ammonium, nitrite and nitrate were determined by using analytical kits (Spectroquant 1.14752.0001 NH_4-N, Spectroquant 1.14547.0001 NO_2-N and Spectroquant 1.14773.0001 NO_3-N, Merck Chemical Company, Germany) and a NOVA-60 spectrophotometer (Merck).

5.6.12 Heavy metal and Element Measurements

Heavy metal (Ba, Cu, Cd, Co, Cr, Pb, Sn, Zn, Ni, Al, Mn, Mo) and element (Ca, Fe, Li, Mg, Na) measurements were performed following SM-3120-B using an inductively coupled plasma-optical emission spectrometry (ICP-OES) (Perkin Elmer 2100dv model) (APHA-AWWA-WEF, 2005).

5.6.13 Determination of Acute Toxicity

The aim of the toxicity tests is the determination of effective concentration (EC) to assess the effect of chemical compound, wastewaters on aquatic and terrestrial organisms (Photo 5.5). These concentrations of tested compounds cause the mortality of 50 % testing organisms or 50% inhibition growth rate in relation to control tests. From obtained experimental acute toxicity endpoints (EC_{50}, IC_{50}, and LC_{50}) of acute toxicity tests the quantification of acute toxicity values is calculated.

5.6.13.1 Microtox Acute Toxicity Assay

Toxicity to the bioluminescent organism *Vibrio fischeri* was assayed using the microtox measuring system according to DIN 38412 L34, L341, (Lange, 1994). Microtox testing was performed according to the standard procedure recommended by the manufacturer (Lange, 1994). Specific strains of the *Vibrio fischeri* microtox LCK 491 Kit (Dr. LANGE industrial measurement technique in Germany, 1996) were used for Microtox acute toxicity assay.

DRLANGE LUMIXmini type luminometer (Dr. LANGE Company, 1996) was used for the microtox toxicity assay. Reductions in light intensity at 0^{th}, 5^{th}, 15^{th} and 30^{th} min are chosen to measure the toxicity (Lange, 1994). All samples were serially diluted in 2.00% NaCI (w/v) and each assay was performed at pH=7.00 and a temperature of 15 °C. NaCl (2.00%) was used as the control. Samples containing bacterial luminescence were measured for 0 min, 5 min, 15 and 30 min incubation times in a luminometer, respectively. Inhibition percentage (I %) values refer to

decreasing activity in samples causing inhibitory effect of a test substances and/or a toxic wastewater during the light emission. Color correction was performed according to the DIN 38412 Instructions. The decrease in bioluminescence was indicated the toxic effect of the samples. Toxicity evaluation criteria for luminescent bacteria explained with the percent inhibition effect (H %). The decrease of bacterial luminescence due to the addition of toxic substances was calculated as follows in Eqs. (5.6), (5.7) and (5.8):

$$f_k = \frac{I_t}{I_0} \qquad \text{Eq. (5.6)}$$

Where;

f_k: Temporary correction factor determined from the control measurements.

I_0: Initial values of luminescence of control and test sample (0.50 ml bacterial suspension), I_t: Values measured 0. 5th, 15th and 30th min after 0.5 ml of control or test sample was added to 0.50 ml of bacterial suspension.

$$I_{CI} = \frac{avg\ f_K}{I_0} \qquad \text{Eq. (5.7)}$$

Where;

I_{ct}: I0 value adjusted by the correction factor, Average f_k: The average values of f_k

$$\%\ Inhibition = \left[\frac{\left(I_{CI} - I_t\right)}{I_{CI}}\right] \times 100 \qquad \text{Eq. (5.8)}$$

Toxicity evaluation criteria for luminescent bacteria are presented in Table 5.45. If the percent inhibitory effect (H %) change between 0.00% and 5.00%, the effect is non-toxic. When H % is between 5.00% and 20.00%, the effect is possibly toxic, and when H % is between 20.00% and 90.00 the effect is toxic (Lange, 1994).

Table 5.45 Effect of the samples on the inhibition of luminescent bacteria (Lange, 1994)

Percent Inhibitory Effect (H, %)	**Effect**
0% < H < 5.00%	Non toxic
5.00% < H < 20.00%	Moderate toxic
20.00% < H < 90.00%	Toxic

5.6.13.2 Daphnia magna Acute Toxicity Test

Toxicity was tested using 24 h born *Daphnia magna* as described in APHA-AWWA-WEF, (2005). After preparing the test solution, experiments were carried out using 5 or 10 *Daphnids* introduced into test vessel. These vessels were controlled with 100 ml of effective volume at 7-8 pH, providing minimum dissolved oxygen concentration of 6 mg/L at an ambient temperature of 20-25°C.

Daphnia magna are used in the test (in first start ≤24 h old). A 24 h exposure is generally accepted for a *Daphnia magna.* acute toxicity test. Results were expressed as mortality percentage of the *Daphnids* the immobile animals which were not able to move was determined as the death of *Daphnids* (SM-8711).

5.6.14 Statistical Analysis

ANOVA analysis of variance between experimental data's was performed to detect F and p values. In other words ANOVA test is used to test for differences amount dependent and independent groups. The comparison between the actual variation of the experimental date averages and standard deviation is expressed in terms of F ratio. F is equal (found variation of the date averages/ expected variation of the date averages). p reports the significance level. Regression analysis was applied to the experimental date in order to determine the regression coefficient R^2. The aforementioned test was performed using Microsoft Excel program.

5.7 Properties of Chemicals used in the Study

Oxytetracycline (OTC) $C_{22}H_{24}N_2O_9$

OTC, which is a synthetic wastewater biodegradation, with a purity of ≥ 97.00%, [CAS number: 79-57-2, EC number: 201-212-8, MA: 460.44 g/mol, d: 1.63 g/cm^3], (25 gr plastic bottle, HPLC grade, Product number: 51239, Sigma-Aldrich Company, St. Louis, USA) was applied as a chemical in synthetic wastewater.

Amoxicillin (AMX) $C_{16}H_{19}N_3O_5S$

AMX, which is a synthetic wastewater biodegradation, with a purity of ≥ 97.00%, [CAS number: 26787-78-0, EC number: 248-003-8, MA: 365.41 g/mol, d: 1.63 g/cm^3], (5 gr glass bottle, HPLC grade, Product number: A8523, Sigma-Aldrich Company, St. Louis, USA) was applied as a chemical in synthetic wastewater.

Sodium Hydroxide (NaOH)

Sodium hydroxide (NaOH), which is a synthetic wastewater biodegradation, with a purity of ≥ 99.00%, [CAS number: 1310-73-2, HS code: 2815 11 00, EC number: 215-185-5, EC index number: 011-002-00-6, MA: 40.00 g/mol, d: 2.13 g/cm^3 (at 20°C)], (5.00 kg plastic bottle, pellets for analysis EMSURE® ISO grade, Product number: 1.06498.5000, Merck) was applied as a chemical in synthetic wastewater.

Sodium Chloride (NaCl)

Sodium chloride (NaCl), which is a chemical of synthetic wastewater biodegradation, with a purity of 99.50–100.50%, [CAS number: 7647-14-5, HS code: 2501 00 99, EC number: 231-598-3, MA: 58.44 g/mol, d: 2.17 g/cm3 (at 20°C)], (5000 g, suitable for use as excipient EMPROVE® exp Ph Eur, BP, USP, Product number: 1.06400.5000, Merck) was used as a chemical in synthetic wastewater

Sodium Bicarbonate ($NaHCO_3$)

Sodium bicarbonate ($NaHCO_3$), which is a chemical of synthetic wastewater biodegradation, with a purity of > 99.90%, [CAS number: 144-55-8, HS code: 2836 30 00, EC number: 205-633-8, MA: 84.01 g/mol, d: 2.22 g/cm^3 (at 20°C)], (ACS, Reag, Ph Eur grade, Product number: 1.06329.1000, Merck) was used as a chemical in synthetic wastewater.

Sulfuric Acid (H_2SO_4)

Sulfuric acid (H_2SO_4), which is a chemical of synthetic wastewater biodegradation, with a purity of 95.00-98.00%, [CAS number: 7664-93-9, HS code: 2807 00 10, EC number: 231-639-5, MA: 98.08 g/mol, d: 1.84 g/cm^3 (at 20°C)], (suitable for use as excipient EMPROVE® exp Ph Eur, BP, NF, Ph Franc grade, Product number: 1.00713.2500, Merck) was used as a chemical in synthetic wastewater.

Sodium thioglycollate ($C_2H_3O_2SNa$)

Sodium thioglycollate ($C_2H_3O_2SNa$), which is a chemical of synthetic wastewater biodegradation, with a purity of ≥96.5% (iodometric), [CAS number: 367-51-1, MDL number: MFCD00043386, EC number: 206-696-4, MA: 114.10 g/mol], (Sigma-Aldrich Chemie GmbH) was used as a chemical in synthetic wastewater.

Potassium dichromate ($K_2Cr_2O_7$)

Potassium dichromate ($K_2Cr_2O_7$), which is a chemical of synthetic wastewater biodegradation, with a purity of 99.7%, [CAS number: 7778-50-9, HS code: 2841 50 00, EC number: 231-906-6, MA: 294.19 g/mol, d: 2.69 g/cm^3 (at 20°C)], (suitable for use as excipient EMSURE® ACS, ISO, Reag. Ph Eur, Product number: 1048640500, Merck) was used as a chemical in synthetic wastewater.

Mercury (II) sulfate ($HgSO_4$)

Mercury (II) sulfate ($HgSO_4$), which is a synthetic wastewater biodegradation, with a purity of 99.00%, [CAS number: 7783-35-9, HS code: 2852 10 00, EC number: 231-992-5, EC index number: 080-002-00-6, MA: 296.65 g/mol, d: 6.47 g/cm^3 (at 20°C)], (250 g plastic bottle, for analysis EMSURE® ACS, Product number: 1044800250, Merck) was used as a chemical in synthetic wastewater.

Silver sulfate (Ag_2SO_4)

Silver sulfate (Ag_2SO_4), which is a synthetic wastewater biodegradation, with a purity of 99%, [CAS number: 10294-26-5, HS code: 2843 29 00, EC number: 233-653-7, MA: 311.8 g/mol, d: 5. 45 g/cm^3 (at 20°C)], (250 g plastic bottle, for analysis extra pure, Product number: 1015340250, Merck) was used as a chemical in synthetic wastewater.

Potassium dihydrogen phosphate (KH_2PO_4)

Potassium dihydrogen phosphate (KH_2PO_4), which is a synthetic wastewater biodegradation, with a purity of 99.55%, [CAS number: 7778-77-0, HS code: 2835 24 00, EC number: 231-913-4, MA: 136.08 g/mol, d: 2.34 g/cm^3 (at 20°C)], (500 g plastic bottle, anhydrous 99.995 Suprapur®, Product number: 1051080500, Merck) was used as a chemical in synthetic wastewater.

Potassium hydrogen phthalate ($C_8H_5KO_4$)

Potassium hydrogen phthalate ($C_8H_5KO_4$), which is a synthetic wastewater biodegradation, with a purity of ≥ 99.95%, [CAS number: 877-24-7, HS code: 2917 39 95, EC number: 212-889-4, MA: 204.22 g/mol, d: 1.636 g/cm^3 (at 20°C)], (1 kg plastic bottle, for analysis EMSURE® Reag. Ph Eur, Product number: 1048741000, Merck) was used as a chemical in synthetic wastewater.

Ammonium acetate (CH_3COONH_4)

Ammonium acetate (CH_3COONH_4), which is a synthetic wastewater biodegradation, with a purity of ≥ 98%, [CAS number: 631-61-8, HS code: 2915 29 00, EC number211-162-9, MA: 77.08 g/mol, d: 1.17 g/cm^3 (at 20°C)], (1 kg plastic bottle, for analysis EMSURE® ACS, Reag. Ph Eur, Product number: 1011161000, Merck) was used as a chemical in synthetic wastewater.

Formic acid (CH_2O_2)

Formic acid (CH_2O_2), which is a synthetic wastewater biodegradation, with a purity of 98-100%, [CAS number: 64-18-6, HS code: 2915 11 00, EC number: 200-579-1, EC index number: 607-001-00-0, MA: 46.03 g/mol, d: 1.22 g/cm^3 (at 20°C)], (2.5 l glass bottle, for analysis EMSURE® ACS, Reag. Ph Eur, Product number: 1002642500, Merck) was used as a chemical in synthetic wastewater.

Acetic acid (glacial) ($C_2H_4O_2$)

Acetic acid (glacial) ($C_2H_4O_2$), which is a synthetic wastewater biodegradation, with a purity of 99.9%, [CAS number: 64-19-7, HS code: 2915 21 00, EC number: 200-580-7, EC index number: 607-002-00-6, MA: 60.05 g/mol, d: 1.05 g/cm^3 (at 20°C)], (2.5 l glass bottle, suitable for use as excipient EMPROVE® exp Ph Eur,BP,JP,USP,E 260, Product number: 1000562500, Merck) was used as a chemical in synthetic wastewater.

Lactic acid ($C_3H_6O_3$)

Lactic acid ($C_3H_6O_3$), which is a synthetic wastewater biodegradation, with a purity of ≥ 95%, [CAS number: 79-33-4, EC number: 201-196-2, MA: 90,08 g/mol, d: 1.2 g/cm^3 (at 20°C)], (2.5 l glass bottle, suitable for use as excipient EMPROVE® exp Ph Eur,BP,E 270, Product number: L1750, Sigma-Aldrich Chemie GmbH) was used as a chemical in synthetic wastewater.

Propionic acid ($C_3H_6O_2$)

Propionic acid ($C_3H_6O_2$), which is a synthetic wastewater biodegradation, with a purity of ≥ 99.5%, [CAS number: 79-09-4, EC number: 201-176-3, EC index number: 607-089-00-0, MA: 74,08 g/mol, d: 0.993 g/cm^3 (at 25°C)], (500 ml glass bottle, gradient grade ACS reagent, Product number: 402907, Sigma-Aldrich Chemie GmbH) was used as a chemical in synthetic wastewater.

Butyric acid ($CH_3CH_2CH_2COOH$)

Butyric acid ($CH_3CH_2CH_2COOH$), which is a synthetic wastewater biodegradation, with a purity of 98%, [CAS number: 107-92-6, HS code: 2915 60 19, EC number: 203-532-3, EC index number: 607-135-00-X, MA: 88.1 g/mol, d: 0.96 g/cm^3 (at 20°C)], (2.5 l glass bottle, suitable for use as excipient EMPROVE® exp Ph Eur,BP,JP,USP,E 260, Product number: 8004572500, Merck) was used as a chemical in synthetic wastewater.

Methanol (CH_3OH)

Methanol (CH_3OH), which is a synthetic wastewater biodegradation, with a purity of ≥ 99.9%, [CAS number: 67-56-1, HS code: 2905 11 00, EC number: 200-659-6, EC index number: 603-001-00-X, MA: 32.04 g/mol, d: 0.792 g/cm^3 (at 20°C)], (2.5 l glass bottle, gradient grade for high pressure liquid chromatography LiChrosolv® Reag. Ph Eur, Product number: 1060072500, Merck) was used as a chemical in synthetic wastewater.

Acetonitrile (CH_3CN)

Acetonitrile (CH_3CN), which is a synthetic wastewater biodegradation, with a purity of ≥ 98%, [CAS number: 75-05-8, HS code: 2926 90 95, EC number: 200-835-2, EC index number: 608-001-00-3, MA: 41.05 g/mol, d: 0.786 g/cm^3 (at 20°C)], (2.5 l glass bottle, gradient grade for hyper grade for LC-MS LiChrosolv®,

Product number: 1000292500, Merck) was used as a chemical in synthetic wastewater.

5.8 Kinetic Studies

Kinetic studies using lab scale reactors are essential and also provide useful insight and improved understanding for process control and design of full scale reactors. In this regard, different kinetic models have been proposed and most of them have been successfully tested for determine the kinetic constants relevant to COD and antibiotics in the AMCBR and ABFR reactor systems.

5.8.1 Kinetic Approaches in Anaerobic Continuous Studies

In the present work, the kinetic analysis of treatment of synthetic pharmaceutical wastewater using an AMCBR and ABFR reactors were investigated using models for biodegradation (substrate, biomass), gas and inhibition kinetics as described in the literature (Sponza and Işık, 2004; Liu et al., 2008; Deshpande et al., 2012).

5.8.1.1 Biodegradation Kinetics for Substrate Removals

One of the main aims of this study was to estimate the kinetic parameters of antibiotic and COD removal. Due to this reason the AMCBR and ABFR reactor were operated at six different HRTs to determine the kinetic constants of antibiotic and COD removal through anaerobic treatment.

5.8.1.1.1 Zero Order Reaction Kinetic. A zero-order reaction has a rate which is independent of the concentration of the OTC, AMX, TYL and ERY antibiotics (Capellos and Bielski, 1972). Increasing the concentration of the reacting species will not speed up the rate of the reaction. Zero-order reactions are typically found when a material that is required for the reaction to proceed, such as a catalyst, is saturated by the antibiotics (Capellos and Bielski, 1972). The rate of change in substrate

concentration in the system with assuming zero order models for substrate removal could be expressed in Eq. (5.9) (Benefield, 1980):

$$-\frac{dS}{dt} = \frac{Q}{V} \times S_i - \frac{Q}{V} \times S_e - k_0 \qquad \text{Eq. (5.9)}$$

Under steady-state conditions the rate of change in the substrate (COD) concentration (-dS/dt) is negligible and the Eq. (5.9) can be reduced to Eq. (5.10) as follows**:** S_i and S_e are the substrate concentrations in the influent and effluent samples, respectively.

$$S_i = S_e - k_0 \times HRT \qquad \text{Eq. (5.10)}$$

Where; k_0 is zero order kinetic constant (mg/L.d) and it can be obtained from the slope of the line by plotting Eq. (3.10). S_i and S_e are influent and effluent COD and antibiotic concentrations (mg/L), HRT: hydraulic retention time (d).

5.8.1.1.2 First Order Reaction Kinetic. A first-order reaction depends on the concentration of only one substrate (COD, OTC, AMX, TYL and ERY). The rate of change in substrate concentration in the system with assuming the first order model for substrate removal could be expressed as follows (Jin and Zheng, 2009):

$$-\frac{dS}{dt} = \frac{Q}{V} \times S_i - \frac{Q}{V} \times S_e - k_1 \times S_e \qquad \text{Eq. (5.11)}$$

Under steady-state conditions, the rate of change in the substrate (COD) concentration (-dS/dt) is negligible and the equation given above can be modified as:

$$\frac{S_i - S_e}{HRT} = k_1 \times S_e \qquad \text{Eq. (5.12)}$$

Where; S_i and S_e are the influent and effluent substrate concentration (mg/L); k_1 the first order rate constant, which has a unit of (1/d) and HRT is the hydraulic retention time (d).

The value of k_1 can be obtained by plotting ((Si-Se)/HRT) versus S_e in Eq. (5.12), which is obtained by rearranging Eq. (5.11). k_1 can be obtained by plotting the ((Si-Se)/HRT) versus S_e in Eq.(5.12) (Işık and Sponza, 2005). The slope of the line gives the k_1.

5.8.1.1.3 Second Order Reaction Kinetic. The rate of change in substrate concentration in the system with assuming the second order model for substrate (COD, OTC, AMX, TYL and ERY) removal could be expressed as follows (Benefield, 1980).

$$-\frac{dS}{dt} = \frac{Q}{V} \times S_i - \frac{Q}{V} \times S_e - k_1 \times S_e^{\,2} \qquad \text{Eq. (5.13)}$$

Where; k_2 is the second order kinetic constant (L/mg.d). If Eq. (5.13) is integrated and then linearilized to get the Eq. (5.14):

$$\frac{S_i - S_e}{HRT} = k_2 \times S_e^{\,2} \qquad \text{Eq. (5.14)}$$

The value of k_2 can be obtained by plotting ((Si-Se)/HRT) versus S_e^2 in Eq. (5.14). The slope of the line gives the k_2 value (Kuşçu, 2007).

5.8.1.1.4 Application of Monod Kinetic Model. Originally, exponential growth of bacteria was considered to be possible only when all nutrients, including the substrate, were present in high concentrations. However, it was found later that microorganism grow exponentially even when one nutrient is present only in limited amount (Monod, 1949). Furthermore, the value of the specific growth rate coefficient, μ, was found to depend on the concentration of that limiting nutrient,

which can be the carbon source (substrate), the dissolved oxygen, nitrogen, or any other factor needed by the organisms for growth (Wu, 1985).

The Monod model was used to describe the biodegradation of COD, OTC, AMX, TYL and ERY antibiotics. Eqs. (5.15) to (5.16) represent growth and substrate removals. For AMCBR, ABFR and CSTR reactors with no biomass recycle, microbial and substrate mass balance can be expressed using Eq. (5.15) and Eq. (5.16).

Microbial Mass Balance. A microbial mass balance for the reactor can be described as follows:

$$MCR = MIR + MGR - MDR - MOR \qquad \text{Eq. (5.15)}$$

Where, MCR: Microbial Change Rate; MIR: Microbial Input Rate; MGR: Microbial Growth Rate, MDR: Microbial Death Rate; MOR: Microbial Output Rate

Mathematically, Eq. (5.15) can be written as Eq. (5.16).

$$\frac{dX}{dt} = \frac{Q}{V} \times X_i - \frac{Q}{V} X_e + \mu \times X - k_d \times X \qquad \text{Eq. (5.16)}$$

Where; V is reactor volume (L); Q the flow rate (L/d); X_i and X_e are the influent and effluent biomass concentration (g/L); X is concentration of biomass in the reactor (g/L); μ is specific growth rate (d^{-1}) and k_d is endogenous decay coefficient (d^{-1}).

If it is assumed that the concentration of biomass in the influent can be neglected, at steady-state (dX/dt) = 0, and the HRT (d) is defined as the volume of the reactor divided by the flow rate of the influent, since the relationship between the specific growth rate and the rate limiting substrate concentration can be expressed by the Monod equation (5.17) (Monod, 1949);

$$\mu = \frac{\mu_{max} \times S}{K_s + S} \qquad \text{Eq. (5.17)}$$

Where; K_S is the half-saturation concentration (mg/L). It determines how rapidly μ approaches μ_{max} and is defined as the substrate concentration at which μ is equal to half of μ_{max}. The smaller K_S is the lower the substrate concentration at which μ approaches μ_m. S is substrate concentration, mg/L.

Mathematically, Eq. (5.16) can be written as Eq. (5.18).

$$\frac{Q}{V} \times X_e = X \times (\mu - k_d) \qquad \text{Eq. (5.18)}$$

Both sides of the Eq. 5.18 are divided by the value of X and the other side of the equation is constant with a term of k_d. This mathematical change gives the Eq. 5.19 or Eq. 5.20.

$$\frac{Q \times X_e}{V \times X} + k_d = \mu \qquad \text{Eq. 5.19}$$

or

$$\mu = \frac{1}{SRT} + k_d \qquad \text{Eq. 5.20}$$

Mathematically, Eq. (5.16) and Eq. (5.20) can be written as Eq. (5.21):

$$\frac{\mu_{max} \times S}{K_s + S} = \frac{1}{SRT} + k_d \qquad \text{Eq. 5.21}$$

The value of maximum specific growth rate (μ_{max}) (d^{-1}) and half saturation concentration (K_S) (mg/L) can be obtained by plotting (SRT/1 + (SRT x k_d) versus

1/S in Eq. (5.21) (Kuşçu, 2007). The slope of the line gives the K_S. The intercept point of the line gives the μ_{max}.

Substrate Mass Balance: A substrate mass balance for the reactor can be described as Eq. (5.22):

$$SCR = SIR - SUR - SOR \qquad \text{Eq. (5.22)}$$

Where; SCR: Substrate Change Rate; SIR: Substrate Input Rate; SUR: Substrate Utilization Rate; SOR: Substrate Output Rate

This equation can be rearranged to estimate the effluent substrate concentration at the steady state condition as follows:

$$S = \frac{K_S \times \left(k_d + \frac{1}{SRT} \right)}{\mu_{max} - k_d - \frac{1}{SRT}} \qquad \text{Eq. (5.23)}$$

Where; S is substrate concentration (mg/L). The rate of change in substrate concentration in the system could be expressed with Eq. (5.24):

$$-\frac{dS}{dt} = \frac{Q}{V} \times S_i - \frac{Q}{V} \times S_e - \frac{\mu \times X}{Y} \qquad \text{Eq. (5.24)}$$

Where; (-dS/dt) is defined as the rate of substrate removal (g/L.d). S_i and S_e are influent and effluent substrate concentration (g/L). Y is defined the growth yield coefficient (gVSS/g COD). k_d is the endogenous decay coefficient (d^{-1}).

Under steady-state conditions, the rate of change in the substrate (COD) concentration (-dS/dt) is negligible and by a similar technique to that used for the substrate concentration, the above equation with substituting Eq. (5.24) can be reduced to Eq. (5.25);

$$\frac{(S_i - S_e)}{HRT} = \frac{X}{Y} \times \left(\frac{1}{SRT} + k_d \right) \quad \text{Eq. (5.25)}$$

The above equation can then be rearranged to estimate the effluent biomass concentration under steady-state condition as follows:

$$X = \frac{SRT \times Y \times (S_i - S_e)}{HRT \times (1 + k_d \times SRT)} \quad \text{Eq. (5.26)}$$

The kinetic parameters Y, k_d can be obtained by rearranging Eq. (5.25):

$$\frac{(S_i - S_e)}{HRT \times X} = \frac{1}{Y} \times \frac{1}{SRT} + \frac{1}{Y} \times k_d \quad \text{Eq. (5.27)}$$

The values of Y and k_d can be obtained by plotting ((S_i-S_e)/HRTxX) versus 1/SRT in Eq. (5.25), which is obtained by rearranging Eq. (5.27). k_d can be obtained by plotting the SRT/1+(SRTxk_d) versus 1/S in Eq.(5.27) (Kuşçu, 2007). The value of Y can then be calculated from intercept of the straight line while k_d can be obtained from the slope of the line.

5.8.1.1.5 Anaerobic Degradation of Molasses-COD ($S_{m\text{-}COD}$*) in AMCBR Reactor.* In this study, the anaerobic degradation of molasses-COD ($S_{m–COD}$) and OTC were investigated in an AMCBR and the TVFA productions were monitored. The anaerobic treatment was related to hydrolysis of $S_{m–COD}$ to the soluble molasses-COD ($S_{sm–COD}$), to total volatile fatty acid (S_{TVFA}) by hydrolytic and acidogenic bacteria (X_{acid}), respectively, and transformation of S_{TVFA} into methane (S_{CH4}) by methanogens (X_{meth}) (Eqs. (5.28)-(5.32)) (Zhang et al., 2010). Since the production of hydrogen gas was measured as low as 0.31 mg/L it was not considered in this study. The hydrolysis of molasses-COD can be described by the first-order reaction kinetic (Eq. (5.28)) (Zhang et al., 2010). The description of Eq. (5.28) in the presence of biomass is Eq. (5.29). Both the conversion of $S_{m–COD}$ to S_{TVFA} and the transformation of S_{TVFA} to methane and growth of biomass (μ) follow the Monod

type kinetic model, which has been widely used to describe the process kinetics of anaerobic biodegradation (Siegrist et al., 2002) (Eqs. (5.30)-(5.33)).

Hydrolytic rate constant of molasses-COD (*k*) could be calculated by Eq. (5.28):

$$\frac{dS_{m-COD}}{dt} = -k \times S_{sm-COD} \qquad \text{Eq. (5.28)}$$

Where; S_{m-COD} is molasses-COD concentration (mg/L). k is hydrolytic rate constant of molasses-COD (d^{-1}). S_{sm-COD} is soluble molasses-COD concentration (mg/L).

Hydrolysis of $S_{sm\text{-}COD}$ depending to biomass (X) and specific growth rate (μ) could be given by Eq. (5.29):

$$\frac{dS_{m-COD}}{dt} = \left[\frac{\mu_{hyd} \times S_{sm-COD}}{K_{s-sm-COD} + S_{sm-COD}} \right] \times X_{hyd} \qquad \text{Eq. (5.29)}$$

Where; μ_{hyd} is spesific growth rate of hydrolytic bacteria (d^{-1}). $K_{s-sm-COD}$ is half-saturation constant for soluble molasses COD concentration (mg/L) and X_{hyd} is concentration of hydrolytic bacteria (d^{-1}).

Production of TVFA from $S_{sm\text{-}COD}$ by acidogens could be shown by Eq. (5.30):

$$\frac{dS_{sm-COD}}{dt} = \left[\frac{\mu_{TVFA} \times S_{TVFA}}{K_{s-TVFA} + S_{TVFA}} \right] \times X_{acid} \qquad \text{Eq. (5.30)}$$

Where; μ_{TVFA} is specific growth rate of TVFA producing bacteria (d^{-1}). S_{TVFA} is total volatile fatty acid concentration (mg/L). K_{s-TVFA} is half-saturation constant for TVFA concentration (mg/L). X_{acid} is concentration of acidogens (mg/L).

Growth of acidogenic bacteria depending on substrate ($S_{m\text{-}COD}$) and specific growth rate could be shown by Eq. (5.31):

$$\frac{dX_{acid}}{dt} = \left[\frac{\mu_{acid} \times S_{m-COD} \times X_{acid}}{K_{s-acid} + S_{m-COD}} \right] \quad \text{Eq. (5.31)}$$

Where; μ_{acid} is specific growth rate of acidogens (d^{-1}). K_{s-acid} is half-saturation constant of acidogenic bacteria (mg/L).

Methane gas production from TVFA by methanogens could be given by Eq. (5.32):

$$\frac{dS_{TVFA}}{dt} = \left[\frac{\mu_{meth} \times S_{CH_4}}{K_{s-CH_4} + S_{CH_4}} \right] \times X_{meth} \quad \text{Eq. (5.32)}$$

Where; μ_{meth} is specific growth of methanogens (d^{-1}). K_{s-CH4} is half-saturation constant for CH_4 gas concentration (mg/L). S_{CH4} is methane concentration (mg/L) and X_{meth} is concentration of methane bacteria (mg/L).

Growth of methanogenic bacteria depending on substrate (TVFA) and specific growth rate could be shown by Eq. (5.33). Where; K_{s-meth} is half-saturation constant of methanogenic bacteria (mg/L).

$$\frac{dX_{meth}}{dt} = \left[\frac{\mu_{meth} \times S_{TVFA} \times X_{meth}}{K_{s-meth} + S_{TVFA}} \right] \quad \text{Eq. (5.33)}$$

5.8.1.1.6 Contois Kinetic Model. A similar technique was used to develop a kinetic model based on the Contois equation. The relationship between the specific growth rate and the rate limiting substrate concentration can be expressed by the Contois equation as follows (Contois, 1959):

$$\mu = \frac{\mu_{max} \times S}{\beta \times X + S} \quad \text{Eq. (5.34)}$$

Where; β is the Contois kinetic parameter (g COD/g biomass). μ_{max} is the value of maximum specific growth rate (d^{-1}). By substituting Eq. (5.34) instead of the Monod equation into Eq. (5.16) can be obtained Eq. (5.35):

$$\frac{\mu_{max} \times S_e}{\beta \times X + S_i} = \frac{1}{SRT} + k_d \quad \text{Eq. (5.35)}$$

Substituting Eq. (5.26) into Eq. (5.35) and then rearranging it, the effluent substrate concentration at steady state condition can be expressed using Eq. (5.36):

$$S_e = \left(\frac{\beta \times Y}{(\mu_{max} - k_d) \times SRT + \beta \times Y - 1} \right) \times S_i \quad \text{Eq. (5.36)}$$

In this model, the equation for the effluent biomass concentration has the same expression as Eq. (5.26) due to a similar technique being used. Eq. (5.23) and Eq. (5.26) form the basis of the Monod type model while Eq. (5.36) and Eq. (5.26) form the basis of the Contois type model. If the kinetic parameters are known Eq. (5.17), Eq. (5.26) and Eq. (5.23) can be used to predict the effluent substrate concentration and the microbial biomass concentration under steady state. Similarly, the values of μ_{max}, and β can be obtained by plotting Eq. (5.37), which is obtained by rearranging Eq. (5.35). The value of μ_{max} can be calculated from the intercept of the straight line and finally, β could be obtained from the slope of the line.

$$\frac{SRT}{1 + SRT \times k_d} = \frac{\beta}{\mu_{max}} \times \frac{X}{S_i} + \frac{1}{\mu_{max}} \quad \text{Eq. (5.37)}$$

5.8.1.1.7 Grau Second- Order kinetic Model. The general equation of a Grau second-order kinetic model is illustrated in Eq. (3.38) (Grau et al. 1975; Öztürk et al. 1998).

$$-\frac{dS}{dt} = k_s \times X \times \left(\frac{S_e}{S_i}\right)^2 \quad \text{Eq. (5.38)}$$

If Eq. (5.32) is integrated and then linearilized, Eq. (5.39) will be obtained:

$$\frac{S_t \times HRT}{S_i - S_e} = HRT + \frac{S_i}{k_s \times X} \quad \text{Eq. (5.39)}$$

If the second term of the right part of Eq. (5.39) is accepted as a constant, the Eq. (5.40) will be obtained:

$$\frac{S_t \times HRT}{S_t - S_e} = b \times HRT + a \quad \text{Eq. (5.40)}$$

k_S is second order substrate removal rate constant (L/d) (Eq. 5.39). If Eq. (5.40) rearranged, Eq. (5.41) and Eq. (5.42) will be obtained. This equation could be used to predict the effluent COD and antibiotic (OTC, AMX, TYL and ERY) concentrations.

$$S_e = S_t \times \left(1 - \frac{1}{\left(b + \frac{a}{HRT}\right)}\right) \quad \text{Eq. (5.41)}$$

and

$$A_e = A_i \times \left(1 - \frac{1}{\left(b + \frac{a}{HRT}\right)}\right) \quad \text{Eq. (5.42)}$$

Where; a is equal $S_i/(k_s x X)$ (d) and b are constant (dimensionless). $(S_i-S_e)/S_e$ expresses the substrate removal efficiency and is symbolized as E (efficiency). S_e and S_i are effluent and influent COD concentrations (mg /L). A_e and A_i are effluent

and influent antibiotic concentrations (mg/L). X is the average biomass concentration in the reactor (mg VSS/L). HRT is hydraulic retention time (d).

5.8.1.1.8 Stover-Kincannon Model. In this model, the substrate utilization rate is expressed as a function of the organic loading rate by monomolecular kinetic. A special feature of Stover-Kincannon model is the utilization of the concept of total organic loading rate as the major parameter to describe the kinetics of an anaerobic reactor in terms of organic matter removal and methane production. A Stover-Kincannon model could be used for AMCBR and ABFR reactors as follows (Yu et al., 1998): The substrate utilization versus time can be described with Eq. (5.43);

$$\frac{ds}{dt} = \frac{R_{\max} \times \left(\frac{Q \times S_\iota}{V} \right)}{K_B + \left(\frac{Q \times S_\iota}{V} \right)} \qquad \text{Eq. (5.43)}$$

Where; dS/dt is defined in Eq. (5.44):

$$\frac{ds}{dt} = \frac{Q}{V} \times \left(S_\iota - S_e \right) \qquad \text{Eq. (5.44)}$$

Eq. (5.45) obtained from the linearization of Eq. (5.44) as follows:

$$\frac{V}{Q \times \left(S_\iota - S_e \right)} = \frac{K_B \times V}{R_{\max} \times Q \times S_\iota} + \frac{1}{R_{\max}} \qquad \text{Eq. (5.45)}$$

If the maximum utilization rate (R_{max}) (g/Ld) and the saturation value constant (K_B) (g/L.d) values obtained for COD and antibiotics and were substituted in Eqs. (5.45), (5.46) and (5.47) these equations could be used to predict the effluent COD and antibiotic concentrations, respectively. (QxS_i/V) explain the organic loading rate (OLR) applied to the reactor. Q and V are the flow rate (L/d) and the volume of the anaerobic reactor (L), respectively.

$$\frac{Q \times (S_\iota - S_e)}{V} = \frac{R_{\max} \times \left(\frac{Q \times S_\iota}{V}\right)}{K_B + \left(\frac{Q \times S_\iota}{V}\right)} \quad \text{Eq. (5.46)}$$

$$S_e = S_\iota - \frac{R_{\max} \times S_\iota}{K_B + \left(\frac{Q \times S_\iota}{V}\right)} \quad \text{Eq. (5.47)}$$

5.8.1.2 Biogas Production Kinetics in Anaerobic AMCBR and ABFR Reactors

Methane production is an important parameter for anaerobic treatment systems; therefore, the methane production kinetics should also be determined. Methane production kinetic models were applied to overall of the model reactor. The biogas and methane gas production rates can also be mathematically modeled in terms of substrate removal. The biogas and methane gas productions and quality are dependent on the substrate removal and substrate loading rate. The total gas production rate and methane quality can be mathematically explained in terms of substrate removal. The gas production and quality are dependent on the substrate removal and substrate loading rate.

5.8.1.2.1 Stover-Kincannon Kinetic Model for Biogas in the AMCBR. The model developed by Stover. Eq. (5.43) was arranged and has been applied to determine the total and methane gas productions (Satyanarayan & Kaul, 2002). The total gas production rate could also be explained with Eq. (5.48):

$$G = \frac{G_{\max} \times \left(\frac{Q \times S_i}{A}\right)}{G_B + \left(\frac{Q \times S_i}{S}\right)} \quad \text{Eq. (5.48)}$$

Where, A represents the total disc surface area whereby total biomass concentration immobilized on discs. The simple modification of the original Stover–Kincannon model is the introduction of total organic loading rate, (QxS_i/V) into the Eq. (5.41) instead of (QxS_i/A), resulting in Eq. (5.49).

$$G = \frac{G_{\max} \times \left(\frac{Q \times S_\iota}{V} \right)}{G_B + \left(\frac{Q \times S_\iota}{V} \right)} \qquad \text{Eq. (5.49)}$$

Where, (QxS_i/V) can be expressed as organic loading rate (OLR). This equation could be showed as follows for the total specific gas production rate: G is the specific gas production rate (ml/L.d) and G_{max} is defined as the maximum specific gas production rate (ml/L.d). G_B is the proportionality constant (mg/L.d).

$$G = \frac{G_{\max} \times OLR}{G_B + OLR} \qquad \text{Eq. (5.50)}$$

Eq. (5.50) gives the total specific gas production rate. Where, G, G_{max} and G_B can be explained as biogas production rate (mL/L.d), maximum biogas production rate (ml/L.d) and proportionality constant (mg/L.d), respectively.

The methane production rate can be expressed as follows:

$$M = \frac{M_{\max} \times \left(\frac{Q \times S_i}{V} \right)}{M_B + \left(\frac{Q \times S_i}{V} \right)} \qquad \text{Eq. (5.51)}$$

Where, Q, V, M, M_{max}, M_B and , (QxS_i/V) are defined as the flow rate (L/d) and reactor volume (L), specific methane production rate (mL/L.d), maximum specific methane production rate (mL/L.d), proportionality constant and organic loading rate

(g/L d), respectively. Eq. (5.51) gives the specific methane gas production rate. The specific methane gas production rate could also be explained with Eq. (5.52).

$$M = \frac{M_{\max} \times OLR}{M_B + OLR} \quad \text{Eq. (5.52)}$$

The inverse of the methane production rate is plotted against the inverse of the OLR, a straight line portion of intercept and slope of line gives $1/M_{max}$ and M_B/M_{max}, respectively (Eq. 5.53). Linearization of Eqs (5.49) and (5.51) gives Eqs (5.53) and (5.54) which these equations could be used to determine the kinetic constants for specific total and methane gas productions:

$$\frac{1}{G} = \frac{G_B}{G_{\max}} \times \frac{1}{OLR} + \frac{1}{G_{\max}} \quad \text{Eq. (5.53)}$$

$$\frac{1}{M} = \frac{M_B}{M_{\max}} \times \frac{1}{OLR} + \frac{1}{M_{\max}} \quad \text{Eq. (5.54)}$$

5.8.1.2.2 Van der Meer and Heertjes Model. In this study, Van der Meer and Heertjes kinetic model was applied to evaluate the methane gas production of the anaerobic AMCBR reactor. The following emprical Eq. (5.55) was used (Van der Meer and Heertjes, 1983):

$$G_{CH_4} = k_{sg} \times Q\,(S_0 - S) \quad \text{Eq. (5.55)}$$

Where, k_{sg} is the Van der Meer and Heertjes kinetic constant (mL/mg), and G_{CH4} is the methane gas production (L/d). S_0 and S are explained as the influent substrate concentration (mg/L) and the effluent substrate concentration (mg/L), respectively.

5.8.1.2.3 Michaelis-Menten Model for Methane Gas. The volumetric methane production rates (R_{CH4}) can be obtained through the expression (Wang et al. 2009):

$$R_{CH_4} = \frac{q_{CH_4}}{V} \qquad \text{Eq. (5.56)}$$

Where, R_{CH4} is methane production rates (mL CH_4/d.L), q_{CH4} is the daily methane production (mL CH_4/d) and V is the reactor volume (L).

The experimental method used to determine the substrate concentration (COD_{total} and COD_{dis} analysis) does not distinguish between biodegradable substrate (Wang et al. 2009; Senturk et al., 2010). According to the method used in Martin et al. (1993), the amount of biodegradable substrate could be estimated by plotting $LnCOD_{dis}$ as a function of 1/HRT.

5.8.1.3 Inhibition Kinetic Models for OTC, AMX, TYL and ERY

The main types of inhibition kinetics proposed to describe the effect of a toxicant in anaerobic systems using adjustable biokinetic constants on the Monod equation are competitive, uncompetitive, non-competitive (Pavlostathis and Giraldo-Gomez, 1991) (see Figure 5.6) and Haldane (Andrews, 1968; Haldane, 1965).

Figure 5.6 describes the Competitive, Noncompetitive, and Uncompetitive inhibition. Where; S=substrate and I=inhibitor (OTC, AMX, TYL and ERY) concentrations. The equation is linearized, in other words when 1/V=1/R is plotted against 1/S, a straight line is obtained (Lineweaver-Burk plot). In typical enzyme kinetics reaction enzymes bind substrates and turn them into products. The binding step is reversible while the catalytic step irreversible, which can be written as the following chemical model:

$$S + E \Leftrightarrow ES \rightarrow E + P \qquad \text{Eq. (5.57)}$$

Where: S = substrate; E = enzyme; ES = enzyme-substrate complex; P = product

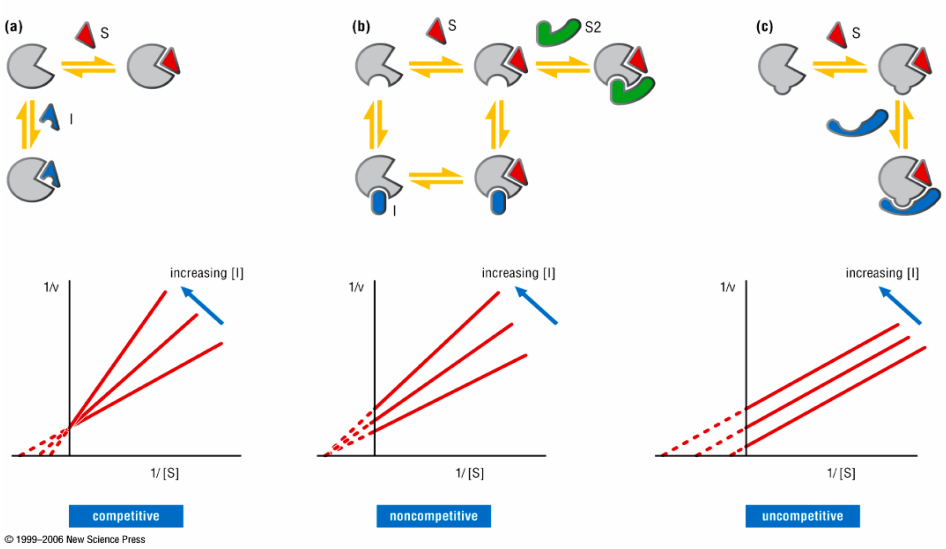

Figure 5.6 Competitive, noncompetitive and uncompetitive inhibitions (Lecture 16, 2012)

Figure 5.6 (a); A competitive inhibitor (I) binds to the same site as does the substrate (S). The inhibitor changes the apparent K_S for the reaction, but not the R_{max} because enough substrate can keep any inhibitor from binding. A Lineweaver-Burk plot for the reaction at various concentrations of the inhibitor reflects this behavior. Figure 5.6 (b); A noncompetitive inhibitor (I) (green) does not bind to the substrate binding site and can bind to both the free enzyme or the ES complex. Usually a noncompetitive inhibitor resembles one substrate (S2) in a two-substrate reaction, as shown here, where both substrates are present on the enzyme at the same time. In the simplest cases, noncompetitive inhibitors don't change the K_S for the first substrate (S), because they don't affect its binding. But providing the concentration of S2 is not high enough to out-compete all the inhibitor, the inhibitor does reduce the R_{max} for the reaction. Figure 5.6 (c); uncompetitive inhibitor (blue) binds only to the ES complex and slows down the reaction probably by inducing a conformational change in the enzyme. Both the apparent K_S and R_{max} are affected proportionally by such an inhibitor, leading to parallel Lineweaver-Burk plots for different inhibitor concentrations (*Lecture 16*, 2012; Lineweaver and Burk, 1934).

5.8.1.3.1 Kinetic Analysis for Competitive, Noncompetitive and Uncompetitive Inhibition. Inhibition models are classified according to the effect of toxic compounds on the maximum reaction rate (R_{max}) and half saturation constant (K_S).

That approach is used for adaptation of substrate removal rate to Monod kinetics. In the presence of increasing concentrations of antibiotic (OTC, AMX, TYL and ERY) the impact of antibiotic is explained by the modified Monod equations. Generally, the effect of antibiotic is related to R_{max} and K_S values. Depending on the type of antibiotic and its concentration the variations in R_{max}, K_S values and the inhibitions were expressed by the following equations (Lehninger, 1977):

Competitive inhibition: A competitive inhibitor is a substance that combines with an enzyme such that it prevents the substrate binding. This could be because enzyme and inhibitor bind to exactly the same site, or partly share a site; the inhibitor could mask or distort the substrate binding site. In any case, inhibitor and substrate binding are mutually exclusive. The inhibition equation is:

$$-\frac{dS}{dt} = -R = -\frac{R_{\max} \times S}{K_S \times \left(1 + \left(\frac{I_A}{K_{IA}}\right)\right) + S} \qquad \text{Eq. (5.58)}$$

Where, R=Substrate utilization rate, (mg/L.d), R_{max}= Maximum substrate utilization rate (mg/L.d); S= Antibiotic concentrations (mg/L); Ks: Half saturation constant for antibiotic (mg/L); I_A= Inhibitor (antibiotic) concentration (mg/L); K_{IA}: Inhibition constant (mg/L)

Noncompetitive inhibition: A simple noncompetitive inhibitor has no effect on substrate binding and vice versa. S and I bind reversibly and independently, but bound inhibitor inactivates the enzyme. The net result is to make it appear as if fewer enzymes are present. The inhibition equation is:

$$-\frac{dS}{dt} = -R = -\frac{R_{\max}}{\left(1 + \left(\frac{K_S}{S}\right)\right) \times \left(1 + \left(\frac{I_A}{K_{IA}}\right)\right)} \qquad \text{Eq. (5.59)}$$

Uncompetitive inhibition: In uncompetitive inhibition, the inhibitor only binds to enzyme that has substrate bound. As with noncompetitive inhibition, there is no substrate concentration that can drive all the inhibitor away (since it binds to the ES complex). Therefore, R is lowered. However, since the inhibitor binds to the ES (ES= Enzim+Susbtrate) complex it favors the equilibrium to this substrate-bound state, and therefore the K_S is decreased.

$$-\frac{dS}{dt} = -R = -\frac{\dfrac{R_{\max} \times S}{\left(1+\left(\dfrac{I_A}{K_{IA}}\right)\right)}}{\left(\dfrac{K_S}{\left(1+\left(\dfrac{I_A}{K_{IA}}\right)\right)}\right)+S} \qquad \text{Eq. (5.60)}$$

If the Eq. (5.58) is linearized, in other words when 1/R is plotted against 1/S, a straight line is obtained. This line will have a slope of K_S/R_{max}, an intercept of $1/R_{max}$ on the 1/R axis, and an intercept of $-1/K_S$ on the 1/S axis. Such a double reciprocal plot has the advantage of allowing much more accurate determination of R_{max} and K_S. The double reciprocal plot can also give valuable information on inhibition. The possible inhibitions of increasing antibiotic concentrations to the slope and to the intercepts and the type of inhibitions are given in Eqs. (5.61) and (5.64) (Table 5.46).

Table 5.46 The slope and to the intercepts and the type of inhibitions

Inhibition model	Slope	Intercept on ordinate	Equation
No antibiotics	$\frac{K_S}{R_{\max}}$	$\frac{1}{R_{\max}}$	5.61
Competitive	$\frac{K_S}{R_{\max}} \times \left(1+\frac{I_A}{K_{IA}}\right)$	$\frac{1}{R_{\max}}$	5.62
Noncompetitive	$\frac{K_S}{R_{\max}} \times \left(1+\frac{I_A}{K_{IA}}\right)$	$\frac{1}{R_{\max}} \times \left(1+\frac{I_A}{K_{IA}}\right)$	5.63
Uncompetitive	$\frac{K_S}{R_{\max}}$	$\frac{1}{R_{\max}} \times \left(1+\frac{I_A}{K_{IA}}\right)$	5.64

5.8.1.3.2 Haldane Inhibition Kinetic Model. High concentrations of substrate can inhibit cell growth, and therefore, estimation of substrate inhibition is an important aspect for biodegradation of toxic compounds. There are several models of cell growth kinetics that have been developed to predict the inhibitory effects of toxic substrates, most of which have been derived from enzymatic reaction kinetics. The Haldane equation (Haldane, 1965), shown below, is a model of substrate inhibition of cell growth kinetics that is in common use. In AMCBR and ABFR reactors containing an inhibitory substrate subjected to degradation by microorganisms, if the bacterial decay is neglected, the changes of substrate concentration (S) and biomass concentration (X) with respect to time (t) can be described, respectively, with Eqs (5.65) and (5.66) (Robinson and Tiedje, 1983):

$$\frac{dS}{dt} = -\frac{\mu \times X}{Y\,obs} \qquad \text{Eq. (5.65)}$$

$$\frac{dX}{dt} = \mu \times X \qquad \text{Eq. (5.66)}$$

Where; Y_{obs}: observed bacterial yield (mg-biomass/mg-substrate). For an inhibitive substrate, μ is usually described by the Haldane or Andrews's model equation as follows (Andrews, 1968):

$$\mu = \frac{\mu_{max} \times S}{K_S + S + \frac{S^2}{K_i}} \qquad \text{Eq. (5.67)}$$

Where μ_{max}=maximum specific growth rate (d^{-1}); Ks=half-velocity concentration (mg/L), and K_i=inhibition constant (mg/L). The higher value of K_i means a less inhibitive substrate. As the value of K_i approaches infinity, Eq. 5.21 reduces to the Monod equation.

5.8.1.3.3 Haldane Inhibition Kinetic for Anaerobic Degradation of Molasses-COD ($S_{m\text{-}COD}$) in the AMCBR Reactor. Inhibition of $S_{sm\text{-}COD}$ degradation by acidogens due to TVFA accumulation could be shown by Eq. (5.68):

$$dS_{sm-COD} = k \times S_{m-COD} - \left[\frac{k_{mh}}{1 + \frac{K_{s-acid}}{S_{sm-COD}} + \frac{S_{TVFA}}{K_{I-TVFA-acid}}} \right] \times I_{pH-acid} \times X_{acid} \qquad \text{Eq. (5.68)}$$

Where; S_{m-COD} is molasses-COD concentration (mg/L). S_{sm-COD} is soluble molasses-COD concentration (mg/L). $K_{s\text{-}acid}$ is half-saturation constant of acidogenic bacteria (mg/L). X_{acid} is concentration of acidogens (mg/L). $I_{pH\text{-}acid}$ is pH inhibition function of acidogens. $K_{I\text{-}TVFA\text{-}acid}$ is inhibition constant of TVFA for acidogens (mg/L).

Inhibition of $S_{sm\text{-}COD}$ degradation and methane bacteria due to TVFA accumulation could be given by Eq. (5.69):

$$\frac{dS_{TVFA}}{dt} = \left[\frac{k_{mh}}{1 + \frac{K_{s-acid}}{S_{sm-COD}} + \frac{S_{TVFA}}{K_{I-TVFA-acid}}} \right] - \left[\frac{k_{TVFA}}{1 + \frac{K_{s-meth}}{S_{TVFA}} + \frac{S_{TVFA}}{K_{I-TVFA-meth}}} \right] \times I_{pH-meth} \times X_{meth} \qquad \text{Eq.(5.69)}$$

Inhibition of methane bacteria due to TVFA accumulation is given by Eq. (5.70). Where; $K_{s\text{-}meth}$ is half-saturation constant of methanogenic bacteria (mg/L). k_{TVFA} is maximum specific utilization rate of TVFA (d^{-1}). $K_{I\text{-}TVFA\text{-}meth}$ is inhibition constant of TVFA for methanogens (mg/L).

$$\frac{dS_{CH4}}{dt} = \left[\frac{k_{TVFA}}{1 + \frac{K_{s-meth}}{S_{TVFA}} + \frac{S_{TVFA}}{K_{I-TVFA-meth}}} \right] \times I_{pH-meth} \times X_{meth} \qquad \text{Eq. (5.70)}$$

Inhibition of OTC biodegradation depending to methane bacteria is given by Eq. (5.71).

$$\frac{dS_{OTC}}{dt} = \left[\frac{k_{OTC}}{1+\frac{K_{s-acid}}{S_{OTC}}+\frac{S_{OTC}}{K_{I-OTC}}}\right] \times I_{pH-acid} \times X_{acid} - \left[\frac{k_{OTC}}{1+\frac{K_{s-meth}}{S_{OTC}}+\frac{S_{OTC}}{K_{I-pH-meth}}}\right] \times I_{pH-meth} \times X_{meth} \quad \text{Eq. (5.71)}$$

Growth of acidogenic bacteria depending on $S_{m\text{-}COD}$ and TVFA inhibition and bacterial death is given by Eq. (5.72)

$$\frac{dX_{acid}}{dt} = Y_{acid} \times \left[\frac{k_{mh}}{1+\frac{K_{s-acid}}{S_{m-COD}}+\frac{S_{TVFA}}{K_{I-TVFA-acid}}}\right] \times I_{pH-acid} \times X_{acid} - k_{d-acid} \times X_{acid} \quad \text{Eq. (5.72)}$$

Growth of methane bacteria depending on TVFA inhibition and bacterial death is given by Eq. (5.73)

$$\frac{dX_{meth}}{dt} = Y_{meth} \times \left[\frac{k_{TVFA}}{1+\frac{K_{s-meth}}{S_{TVFA}}+\frac{S_{TVFA}}{K_{I-TVFA-meth}}}\right] \times I_{pH-meth} \times X_{meth} - k_{d-meth} \times X_{meth} \quad \text{Eq. (5.73)}$$

Haldane inhibition kinetic for substrate could be given by Eq. (5.74)

$$-\frac{dS}{dt} = -R \times \frac{\mu_{\max} \times S \times X}{K_s + S + \left(\frac{S^2}{K_{ID}}\right) \times Y} \quad \text{Eq. (5.74)}$$

Inhibition of acidogenesis by pH is given by Eq. (5.75)

$$I_{pH-acid} = \frac{K_{I-pH-acid}^{2}}{K_{I-pH-acid}^{2} + S_H}$$ Eq. (5.75)

Inhibition of methanogenesis by pH is given by Eq. (5.76)

$$I_{pH-meth} = \frac{K_{I-pH-meth}^{2}}{K_{I-pH-meth}^{2} + S_H}$$ Eq. (5.76)

CHAPTER SIX
RESULTS AND DISCUSSIONS

6.1 Batch Studies

6.1.1 Anaerobic Toxicity Assay Results for OTC, AMX, TYL, ERY

In the first step of this study, the toxic effect of OTC, AMX, TYL and ERY on methane *Archaea* was investigated using ATA test under batch conditions in the beginning of the study in order to determine the IC_{50} (The OTC, AMX, TYL and ERY concentrations which caused 50% decrease in the methanogenic activity) values of the OTC, AMX, TYL and ERY (see Table 5.2, Study 1).

ATAs were performed using serum bottles based on methane gas productions. For each experiment control and test bottles were maintained. All experiments were performed at an incubation temperature of 35 ^{0}C. The serum bottles were incubated 48 h at increasing OTC, AMX, TYL and ERY concentrations (0, 10, 20, 50, 80, 100, 150, 200, 250, 300, 350 and 400 mg/L). These experiments were performed to obtain information on the toxicity of OTC, AMX, TYL and ERY in order to obtain a feed strategy of this compound in the continuous operation of AMCBR and ABFR reactors. ATA were performed to evaluate the toxicity of various concentrations of OTC, AMX, TYL and ERY. The concentrations of OTC, AMX, TYL and ERY were 10, 20, 50, 80, 100, 150, 200, 250, 300, 350 and 400 mg/L. The OTC, AMX, TYL and ERY concentrations caused 50% decreases in the methanogenic activity (decrease of methane gas production) were calculated as IC_{50} values. The IC_{50} values for OTC, AMX, TYL and ERY were found to be 224.18 mg/L, 216.78 mg/L, 192 mg/L and 152 mg/L, respectively as shown in Figures 6.1, 6.2, 6.3 and 6.4. This indicated that the ERY is higher toxic to the OTC, AMX and TYL used in this study.

Ferreira et al., (2007) reported that IC_{50} value of OTC was 11.18 mg/L. In another study, the IC_{50} value for TYL was found as 0.3 mg/L (Blackwell et al., 2007). Gartiser et al., (2007), Lindberg et al., (2007) and Kim et al., (2007) reported that

IC_{50} values of ERY were 67 mg/L, 10.3 mg/L and 30.1 mg/L, respectively. In our study, the IC_{50} values of OTC, AMX, TYL and ERY were higher than IC_{50} values reported by Ferreira et al., (2007), Blackwell et al., (2007), Gartiser et al., (2007), Lindberg et al., (2007), and Kim et al., (2007). This could be attributed to the resistance of partially granulated sludge to OTC, AMX, TYL and ERY. According to IC_{50} values it can be concluded that TYL and ERY exhibited higher toxicity to the granulated anaerobic sludge compared to OTC and AMX. These results showed that the anaerobic partially granulated culture used in our study is more resistant than that used in the aforementioned studies since their IC_{50} values are lower. The anaerobic partially granulated sludge used as seed in this study was not affected significantly by the increasing OTC, AMX, TYL and ERY concentrations, compared to the literature data given above.

The fractal dimension of the granular sludge, 2.79±0.03 mm, was larger than that of some other settling bacteria suggesting that the anaerobic granular sludge (acidogenic and methanogenic bacteria) was more compact and denser (Kuşçu and Sponza, 2009). Anaerobic granules grown on molasses as carbon source for the degradation of OTC, AMX, TYL and ERY showed good resistance to high OTC, AMX, TYL and ERY concentrations in the influent even if unacclimated. The granules exhibited no layered microbial distribution and were packed with different morph type cells intertwined randomly throughout the cross-section (Maszenan et al., 2011). The compact structure of the anaerobic granule protects the microbes residing inside from the inhibitory effects of the OTC, AMX, TYL and ERY. The use of anaerobic granular sludge as seed proved advantageous over the use of suspended growth anaerobic sludge in terms of resistance to toxicity and rapid acclimation as reported by Del Nery et al., (2008).

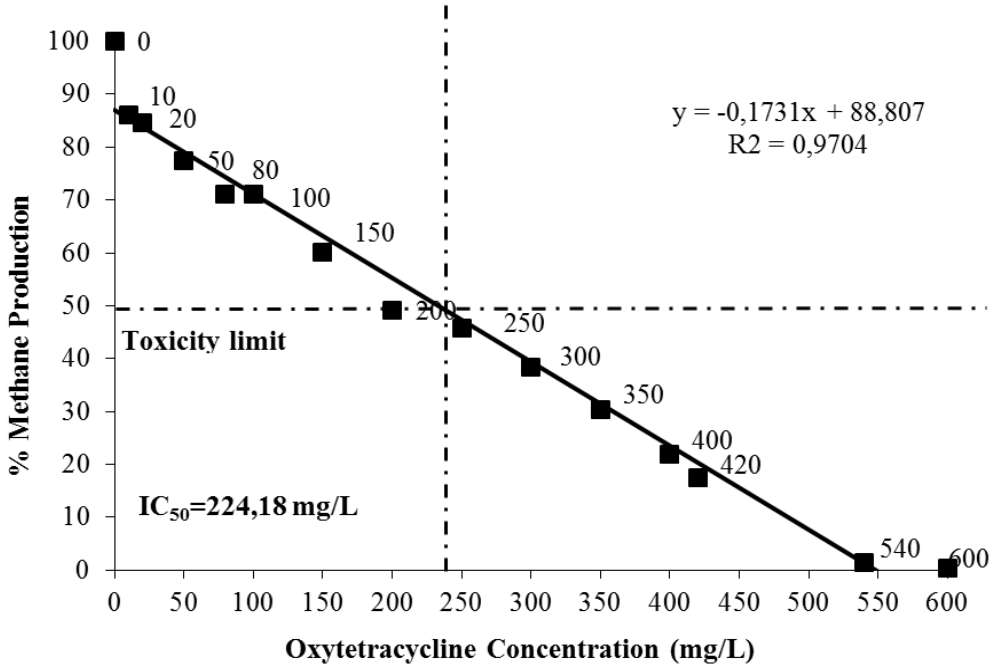

Figure 6.1 IC_{50} value for OTC (IC_{50} = 224.18 mg/L)

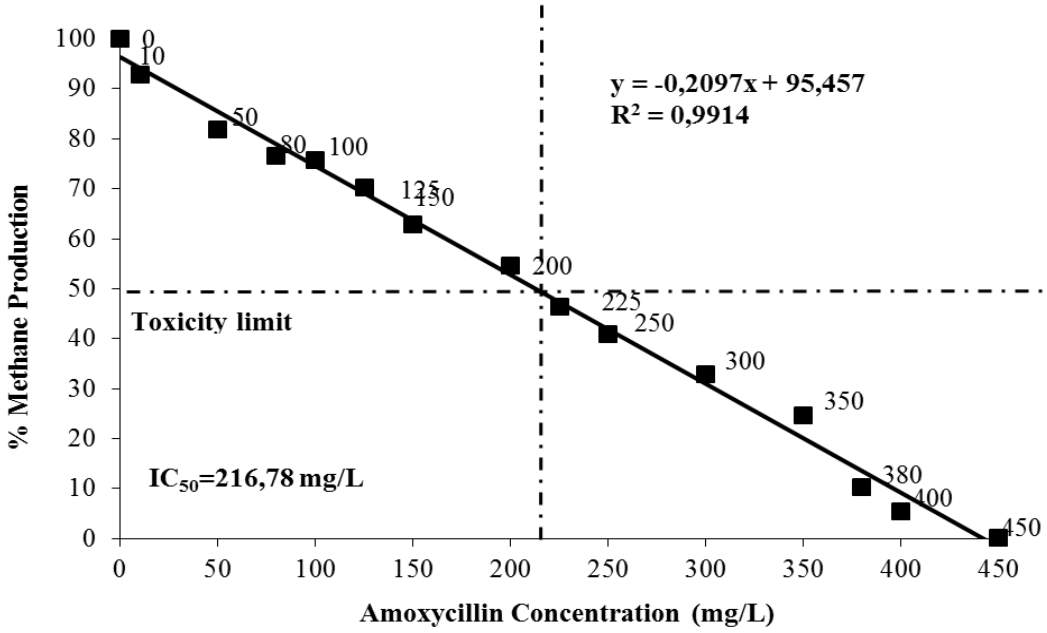

Figure 6.2 IC_{50} value for AMX (IC_{50} = 216.78 mg/L).

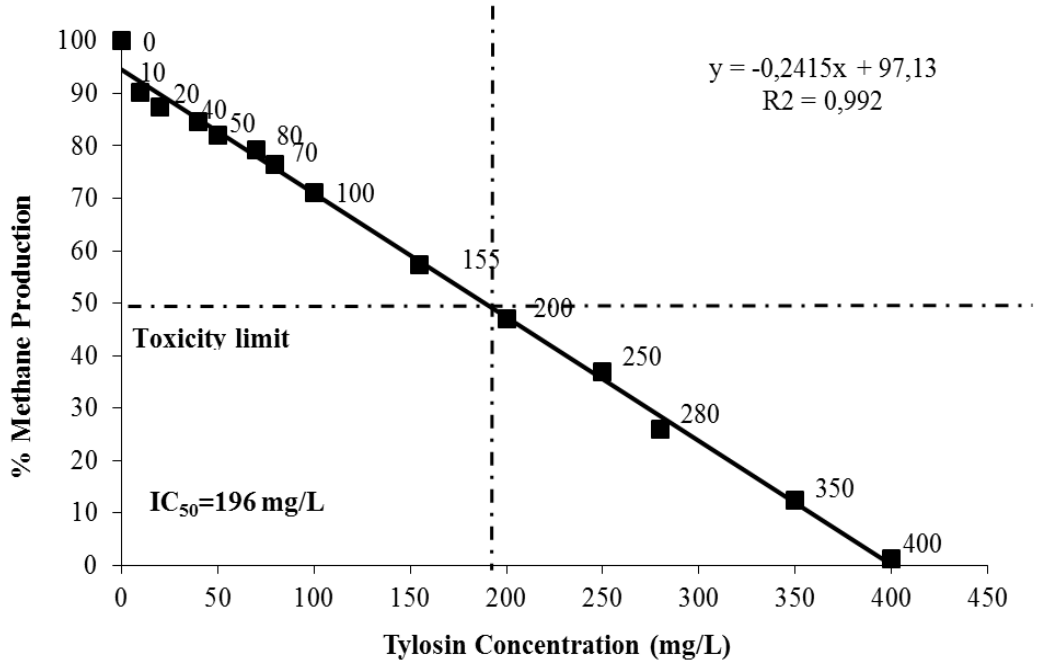

Figure 6.3 IC_{50} value for TYL (IC_{50} = 196 mg/L)

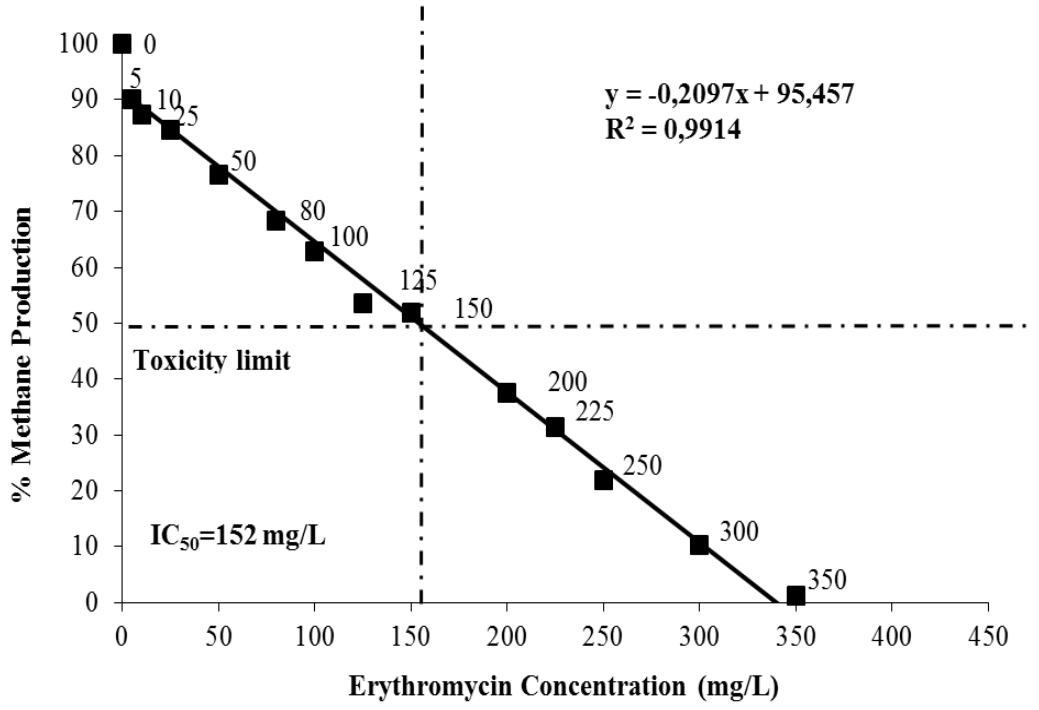

Figure 6.4 IC_{50} value for ERY (IC_{50} = 152 mg/L)

6.1.2 Specific Methanogenic Activity Results for OTC, AMX, TYL, ERY

In the second step of this study, the inhibitory effect of OTC, AMX, TYL and ERY on methane *archaea* was investigated using SMA test under batch conditions in the beginning of the study in order to determine the SMA values of the OTC, AMX, TYL and ERY (see Table 5.3, Study 2 for operational conditions).

Figure 6.5 shows the SMA values of sludge taken from batch reactor (serum bottles) during batch operation of serum bottles at increasing OTC concentrations. The SMA is an indicator of methanogenic activity of biomass without substrate limiting factor. As shown in Figure 6.5, SMA values decreased from 1.13 g COD-CH_4/g VSS d to 0.21 g COD-CH_4/g VSS d when OTC concentration increased from the 0 mg/L to 400 mg/L (approximately 90% reduce was observed in SMA). SMA was around 0.51 g COD-CH_4/g VSS d at high OTC concentration such as 150 mg/L and 200 mg/L. SMA increased 0.56 g COD-CH_4/g VSS d at an OTC concentration of 250 mg/L. This loading was tolerated by the granules, resulting in recoveries in the SMA. After this OTC concentration (250 mg/L), SMA values decreased to 0.38 g COD-CH_4/g VSS d at an OTC concentration of 300 mg/L, 0.32 g COD-CH_4/g VSS d OTC concentration 350 mg/L and 0.21 gCOD-CH_4/gVSS d at an OTC concentration of 400 mg/L. The reason of this could be explained with high OTC loading rates which decrease the activity of methanogens. Afterwards, it can be concluded that methanogenic activity decreased with increased OTC concentration. The SMA value was found to be lower (0.24 gCH_4/gVSS d) in the study performed by Cetecioglu et al., (2012) under anaerobic conditions in an anaerobic sequencing batch reactor (ASBR), compared to the present study. Similarly, the SMA value (0.48 gCH_4/gVSS d) obtained by Wollenberg et al., (2000) is lower than those of our results.

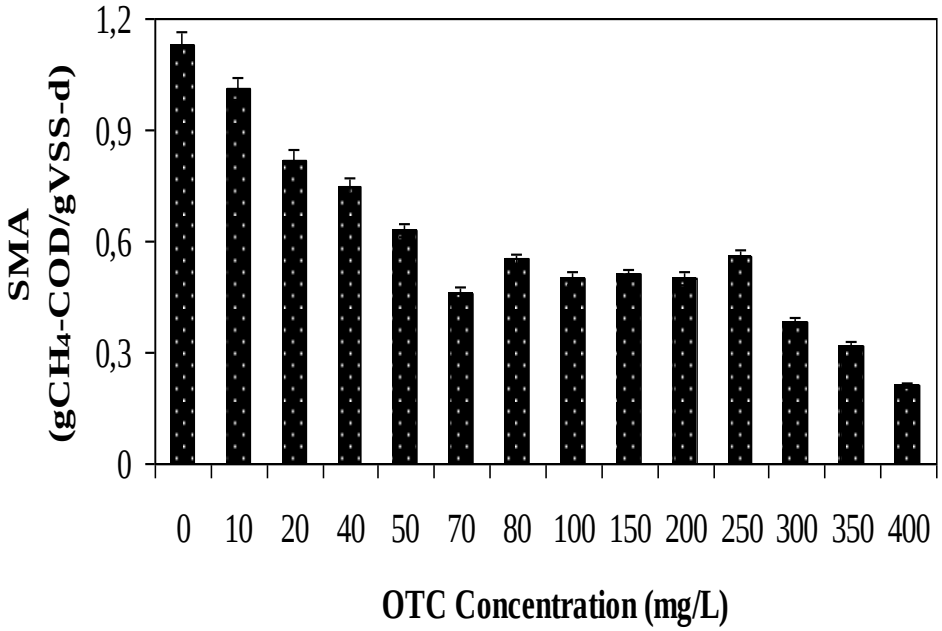

Figure 6.5 SMA values in batch reactor at different OTC concentration

The SMA points out the gas productions, based on COD, per each gram of anaerobic biomass through anaerobic operation. Figure 6.6 show the variations of SMA in serum bottles during the batch operation. As shown in Figure 5.6, SMA values decreased from 1.05 to 0.12 gCOD-CH_4/gVSS d when the AMX concentration increased from 0 mg/L to 350 mg/L in batch serum bottles. SMA was high at AMX concentration such as 10 mg/L. The maximum SMA value was calculated from the methane production through this period. This shows that methanogenic activity decreased with increased AMX concentrations. This result is comparable with those obtained by Oz et al. (2004) in an anaerobic CSTR reactor treating only AMX (SMA=0.98 gCH_4COD/gVSSd). Lallai et al. (2002) have evaluated inhibitory effects of three antibiotics on methanogen bacteria by SMA test.

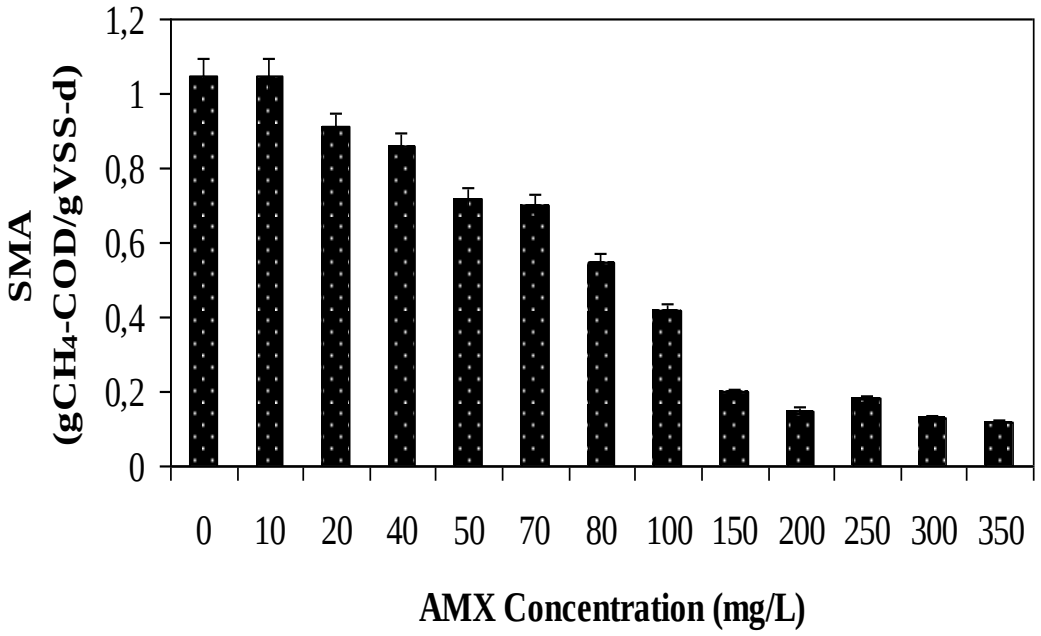

Figure 6.6 SMA values in batch reactor at different AMX concentration

Figure 6.7 shows the SMA values of sludge taken from the serum bottles during batch operation of batch reactor (serum bottles) at different TYL concentrations. The SMA is an indicator of methanogenic activity in anaerobic systems. As shown in Figure 6.7, SMA values varied between 0.87 and 0.15 g COD-CH_4/ g VSS d when TYL increased from zero to 300 mg/L. After this TYL concentration SMA values remained stable between 0.18 and 0.15 g COD-CH_4/ g VSS d at TYL concentrations varied between 150 and 300 mg/L. SMA value was 0.15 g COD-CH_4/ g VSS d at a TYL concentration of 300 mg/L. The SMA value decreased at maximum TYL concentration such as 300 mg/L. The reason of this could be explained with high TYL loading rates decrease the activity of methanogens. Shimada et al., (2006) and Shimada et al., (2008) reported that SMA values of TYL were 0.57-0.64 g-CH_4/g VSS d and 0.24-0.37 g-CH_4/g VSS d, respectively.

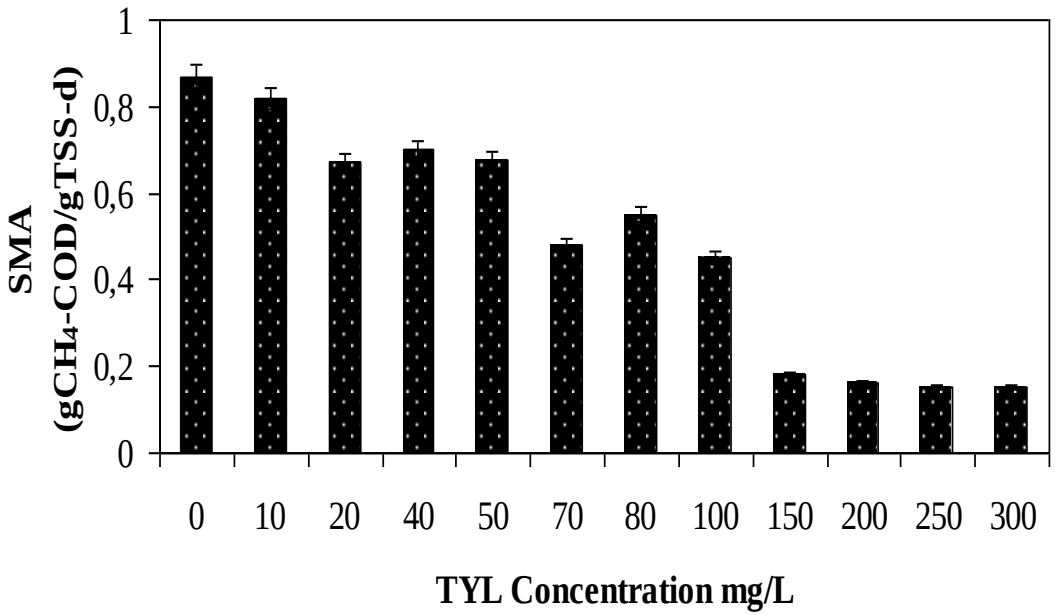

Figure 6.7 SMA values in batch reactor at different TYL concentration

The SMA is an indicator of methanogenic activity of the biomass forming granules. The SMA levels of granules measured in the serum vials are depicted in Figure 6.8. At the beginning of the ERY concentration the SMA was measured to be 1.2 gCH_4-COD/gVSS.d as seen in Figure 5.8. When ERY concentration of 10 mg/L was added the SMA activity increased to 0.85 gCH_4-COD/g-VSS.d. After increasing the ERY concentration from 50 to 250 mg/L, the SMA level decreased from 0.7 to 0.13 gCH_4-COD/g-VSS.d. The minimum SMA was achieved as 0.13 gCH_4-COD/g-VSS d at the maximum ERY concentration (250 mg/L). These results are comparable with by the studies performed Amin, (2004) in a laboratory-scale anaerobic sequencing batch reactor (ASBR) treating only glucose, mineral medium with ERY (0.13-0.23 g CH_4-COD/gVSS.d). The inhibitory effect of ERY was evaluated by monitoring biogas production and methane content of the biogas. Ince et al., (2002) indicated that acetoclastic methanogens value treatment of synthetic pharmaceutical wastewater in up flow anaerobic filter reactor operating as batch was 0.15 gCH_4/g VSS d and 2.86 gCH_4/g VSS d.

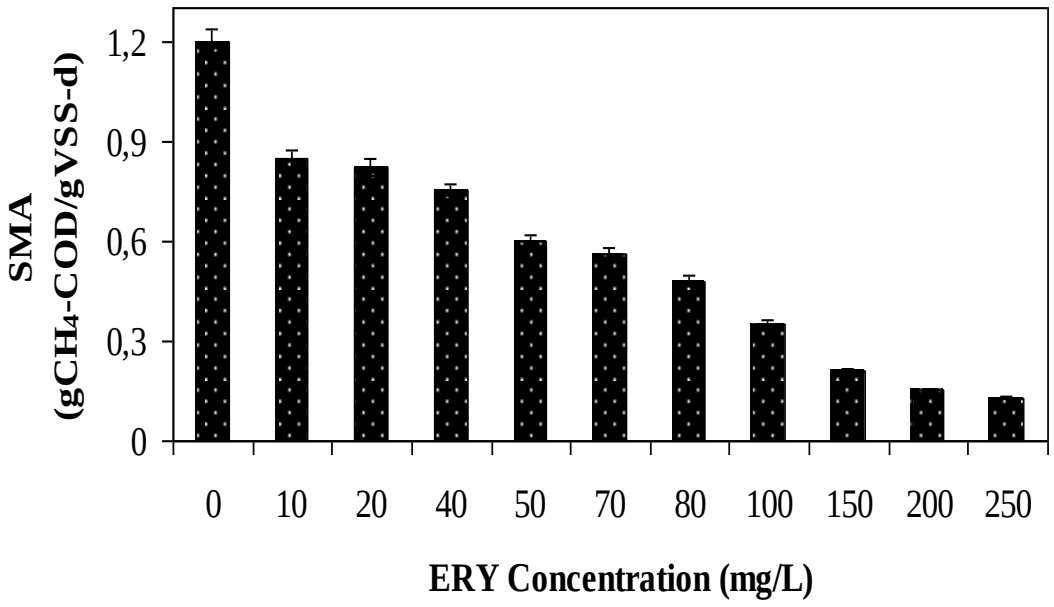

Figure 6.8 SMA values in batch reactor at different ERY concentration

6.1.3 Batch Abiotic, Biotic Test Results for OTC, AMX, TYL, ERY

The batch abiotic and biotic tests were performed at a temperature above 35 °C to keep favorable conditions for growth of the anaerobic microorganisms for which 37°C is the optimal temperature (Speece, 1996). The operating pH of each sample was measured about 7.12. The anaerobic conditions occurred in batch reactors. The ORP values during the anaerobic phases were approximately -50 mV and -242 mV. The operational conditions and the influent OTC, AMX, TYL and ERY concentrations were illustrated in Table 6.4 in the section “Materials and Methods” respectively (Study 3).

6.1.3.1 Main Mechanisms for the Removal of OTC

In order to determine the main removal mechanism of 100 mg/L OTC under anaerobic conditions, abiotic and biotic batch tests were conducted (Table 6.1). 0.88% of OTC was adsorbed by anaerobic biomass through anaerobic incubation of 28 days. The abiotic transformation rate in the abiotic experiment was found as

$0.58x10^{-3}$ mg OTC/ mg VSS d on days 22 and $0.18x10^{-2}$ mg OTC /mg VSS d on days 28, respectively. After 25 days of incubation time, the OTC concentration decreased to 99.9 mg/L in supernatant samples in the volatilization bottle tests with 100 mg/L OTC. It was found that the volatilization is not significant for OTC removal (Table 6.1). In order to determine whether OTC accumulated inside the granules, the granules were mixed in distilled water for 15 days. The OTC percentage accumulated into granular sludge was found to be not significant (Table 6.1). Batch serum bottles containing 100 mg/L OTC and anaerobic granules were incubated for 15 days at 37 ^{0}C to determine the biodegradation. These results showed that biodegradation is the main removal mechanism for OTC under anaerobic conditions while adsorption and volatilization of the OTC were found to be negligible (Table 6.1).

Table 6.1 The main removal mechanisms for removal of 100 mg/L OTC

Adsorption	
Removal efficiency with adsorption (%)	0.88 after 28 d
Abiotic transformation rate with adsorption (mg OTC/ mg VSS d)	$0.58x10^{-3}$ mg OTC/ mg VSS d on days 22 $0.18x10^{-2}$ mg OTC /mg VSS d on days 28
Volatilization	
Volatilization losses (%)	0.01 on days 15
Accumulation	
Accumulated into granular sludge (%)	0.02 on days 26
Biodegradation	
Biplogic degradation under anaerobic conditions	99.9 % on days 28

Our results were consistent with the literature studies performed by Ingerslev et al. (2001), Alvarez et al., (2010), Radjenovic et al., (2009) and Tsung-Hsien et al., (2011). In these studies they reported that OTC was mainly biodegraded throughout anaerobic digestion of pig manure, sulfamethoxazole, sulfadimethoxine, and sulfamethazine, respectively. However, Kulshrestha et al., (2004) and Santos et al.,

(2010) reported that the adsorption of some antibiotics onto the sludge can be influenced by intermolecular forces such as Van der Waals.

6.1.3.2 Main Mechanisms for the Removal of AMX

The mechanism of AMX verifies that the biodegradation, adsorption and volatilization mechanism were able to remove AMX from wastewater (Table 5.4, Study 3 for operational conditions). The abiotic test results were given in Table 6.2. 2.30 % of AMX was adsorbed by anaerobic biomass (1.50 gVSS/L) through anaerobic incubation of 15 days. The abiotic transformation rate in abiotic experiment was found as $0.15x10^{-3}$ mg AMX/mg VSS d after 15 d and $0.11x10^{-3}$ mg AMX/mg VSS d after 25 days, respectively. These results were similar with the results reported by Chen et al., (2011). Chen et al., (2011) found that the abiotic transformation rate was $0.20x10^{-3}$ mg AMX/mg VSS d after 30 days for AMX. Therefore the abiotic AMX removal was not taken into consideration. The results demonstrated in Table 6.2 show that biodegradation is the most important mechanism for removing AMX in the batch reactors (serum bottles). The results also support the fact that biodegradation and adsorption were responsible for degradation of AMX. 100 mg/L of AMX concentration was used at the beginning of the volatilization study in serum bottles. After 20 days of incubation time, 100 mg/L of AMX decreased to 99.5 mg/L AMX. The results indicated that 1.25% of AMX was removed by volatilization after 20 days of anaerobic incubation (see Table 6.2). Therefore it was concluded that AMX removal with volatilization is not significant. The AMX doses measured in the supernatant showed that 0.5 mg/L of AMX is released to the water. As a result it can be said that 0.05% of AMX was accumulated into granular sludge (Table 6.2).

Table 6.2 The main removal mechanisms for removal of 100 mg/L AMX

Adsorption	
Removal efficiency with adsorption (%)	2.3 after 25 d
Abiotic transformation rate with adsorption (mg AMX/ mg VSS d)	$0.15x10^{-3}$ mg AMX/ mg VSS d on days 15 $0.11x10^{-3}$ mg AMX /mg VSS d on days 25
Volatilization	
Volatilization losses (%)	0.01 on days 20
Accumulation	
Accumulated into granular sludge (%)	0.05 on days 24
Biodegradation	
Biplogic degradation under anaerobic conditions	99% on days 25

6.1.3.3 Main Mechanisms for the Removal of TYL

The abiotic test result is given in Table 5.3. 0.6% of TYL was adsorbed by biomass (1.35 gVSS/L) through anaerobic incubation of 26 days. The abiotic transformation rate in the abiotic experiment was found as $0.45x10^{-3}$ mgTYL/mgVSS d on day 22 and $0.17x10^{-2}$ mg TYL/mgVSS d on day 26. 100 mg/L TYL was spiked to the serum bottles at the beginning of the volatilization study. After 20 days incubation time, 100 mg/L of TYL concentration decreased to 99.9 mg/L in supernatant samples. The TYL measured in the headspace of the serum bottles was approximately 0.1 mg/L. The results indicated that 0.001% of TYL was removed by volatilization after 20 days anaerobic incubation (Table 6.3). Therefore, it was concluded that volatilization is not significant for TYL removal. In order to determine whether TYL is accumulated inside the granules, granules were mixed in distilled water for 22 days. The TYL concentrations measured in the supernatant showed that 0.1 mg/L of TYL was released into the water. As a result it can be said that 0.01% of TYL was accumulated into granular sludge. This indicated that TYL is biodegraded under anaerobic conditions and accumulation in granules is not significant for TYL removal (Table 6.3).

Table 6.3 The main removal mechanisms for removal of 100 mg/L TYL

Adsorption	
Removal efficiency with adsorption (%)	0.60 after 26 d
Abiotic transformation rate with adsorption (mg TYL/ mg VSS d)	0.45×10^{-3} mg TYL/mgVSS d on day 22 0.17×10^{-2} mg TYL/ mgVSS d on day 26
Volatilization	
Volatilization losses (%)	0.001 on days 20
Accumulation	
Accumulated into granular sludge (%)	0.01 on days 22
Biodegradation	
Biplogic degradation under anaerobic conditions	99.9 % on days 26

Batch serum bottles containing 100 mg/L TYL and anaerobic granules were incubated for 20 days at 37 ^{0}C to determine the biodegradation. 99.9% OTC removal was detected at the end of the incubation period. These results showed that anaerobic biodegradation is the main removal mechanism for TYL under anaerobic conditions while adsorption and volatilization of the TYL were found to be negligible. Based on the literature data no sorption onto the granular sludge would be expected for TYL (Miege et al., 2009 and Larsen et al., 2004). One essential point to consider is whether TYL removal from the batch reactor system was caused by adsorption or anaerobic biodegradation. Some studies on anaerobic biodegradation of TYL did not clearly state the reason for TYL disappearance (Chelliapan et al., 2010). Loke et al., (2003) reported that the loss of TYL in batch anaerobic biodegradation experiments of pig manure was caused by a combination of adsorption, abiotic and biotic transformation; however, no further details were examined. Kolz et al., (2005) also showed that TYL disappearance in batch anaerobic degradation experiments of swine manure slurries was caused by abiotic and biotic degradation, but suggested strong sorption to slurry solids to be the main removal mechanism of TYL. Consequently, the removal of TYL in batch system could be combination of adsorption to sludge, abiotic and biotic degradation.

6.1.3.4 Main Mechanisms for the Removal of ERY

The abiotic test results were given in Table 6.4. The test results for abiotic study showed that 0.74% of ERY was adsorbed by anaerobic biomass (0.9 gVSS/L) through anaerobic incubation of 25 days. The initial ERY concentration was 100 mg/L. After 25 days, ERY concentration decreased to 99.0 mg/L. The abiotic transformation rate was found as $0.13x10^{-3}$ mg ERY/mg VSS d after 25 days. The results were similar compared with TYL (see Table 6.3). Therefore abiotic removal does no an important removal mechanisms. For volatilization study the influent concentration of ERY was kept around 100 mg/L. Test bottles were incubated at 37 °C through 15 days. After 10 days, the concentration of ERY in bottles was found to be around 99 mg/L. The results of test showed that the removal of ERY by volatilization is 1.00% compared to influent ERY concentration (Table 6.4). This is not significant for ERY removal. The ERY doses measured in the supernatant showed that 0.4 mg/L of ERY is released to the water. The result showed that 0.04% of ERY was accumulated into granular sludge, which is not significant for ERY removal (see Table 6.4).

Table 6.4 The main removal mechanisms for removal of 100 mg/L ERY

Adsorption	
Removal efficiency with adsorption (%)	0.74 after 25 d
Abiotic transformation rate with adsorption (mg ERY/ mg VSS d)	0.13×10^{-3} mg ERY/mgVSS d on day 20 0.07×10^{-2} mgERY/mgVSS d on day 25
Volatilization	
Volatilization losses (%)	0.01 on days 15
Accumulation	
Accumulated into granular sludge (%)	0.04 on days 22
Biodegradation	
Biplogic degradation under anaerobic conditions	99 % on days 25

The fate of ERY in the environment is associated with both abiotic and biotic factors including volatilization, adsorption and transformation (Fatta-Kassinos et al., 2011). The low solubility and high hydrophobic of ERY limit their ability to be transported into microbial cells and thus be biodegraded. Anaerobic systems are considered as the most significant route for ERY removal. Several studies have examined the relative role of biodegradation in the fate of ERY in anaerobic sludge (Senta et al., 2011). Amin et al., (2006) showed that the ERY was removed biologically with 76% treatment efficiency under anaerobic conditions. In another study, the continuous decreases in ERY concentration were attributed to biodegradation and to adsorption (Senta et al., 2011). During the past 20 years, several different treatment technologies have been tested in efforts to remove the antibiotics. Among them, biodegradation has shown particular promise as a safe and cost-effective option (Gulkowska et al., 2008). In spite of their xenobiotic (antibiotics, hormones etc.) properties, a variety of genera of microorganisms have been isolated and characterized for their ability to utilize antibiotics in anaerobic reactor systems.

6.2 Continuous Studies for *the Sequential AMCBR/CSTR System*

6.2.1 The Removal of OTC, AMX, TYL, ERY in the Sequential AMCBR/CSTR System

6.2.1.1 Start-up Period for OTC

Start-up procedure is important in anaerobic treatment systems. A successful start-up allows the acclimation and phase separation of bacteria in the reactor. Once the biomass has been established, either as a granular particle or a floc, while the reactor operation is quite stable (Speece, 1996). The operational conditions were illustrated in Table 5.5 in the section “Material and Methods” (Study 4).

The AMCBR reactor was inoculated with granular sludge taken from PAKMAYA Yeast industry and first fed with only molasses as the carbon source in order to

determine the performance of the reactor in the absence of OTC. The HRT and flow rate were kept constant at 2.25 d and 2 L/d, respectively. The start-up period was 45 days and the influent molasses COD concentration was 3950-4010 mg/L. When the reactor continuously started to feed with wastewater which had a COD concentration of 3950-4010 mg/L, the effluent COD concentration was around 512 mg/L resulting a COD removal efficiency of 88-91%. Through the end of the start-up period about 93% COD removal efficiency was achieved. During the anaerobic phase zero dissolved oxygen was observed and the redox potential was around -370 mV. The COD variations through start-up period are shown in Figure 6.9.

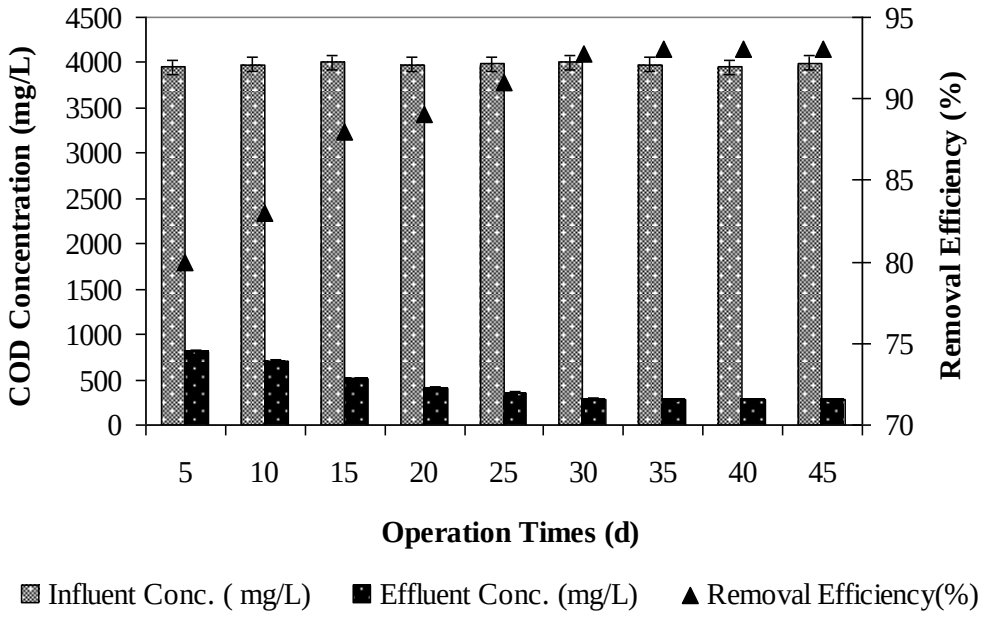

Figure 6.9 COD removal efficiencies in the AMCBR during the start-up period in AMCBR

Figure 6.10 shows the methane gas and percentages in the AMCBR during the start-up period. The methane gas production and methane percentage were approximately 3 L/d and 25% at the beginning of the start-up period (operation day between 1 and 10 days). The methane gas production and methane percentage reached 5 L/d and 42%, respectively at operation day of 25 days. The daily methane gas production and methane percentage remained stable at 6.7 L/d and 53%, respectively, after 30 days of the start-up period.

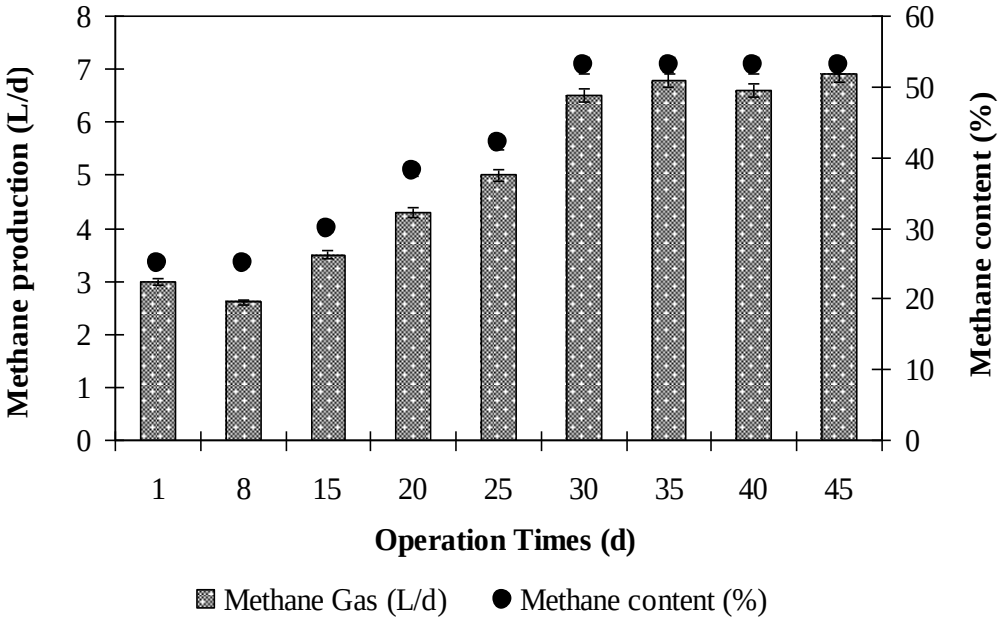

Figure 6.10 Methane gas production and percentages during the start-up period in the AMCBR

6.2.1.2 Start-up Period for AMX

The adaptation period is very important since the bacterial population used as seed is going to be exposed to the AMX in an anaerobic environment of the AMCBR reactor. In order to acclimation the partially granulated biomass in the AMCBR reactor, the anaerobic reactor was operated with synthetic wastewater through 45 days without AMX for reach to steady-state conditions. The steady state was arbitrarily considered as the variation of COD in the effluent and the variations of methane gas production and percentage less than 5% in consecutive 7 days. During the anaerobic phase the dissolved oxygen was zero and the redox potential was around -360 mV (see Table 5.6, Study 5).

Figure 6.11 illustrated the influent and effluent COD concentrations and COD removal efficiencies for 45 days of start-up period. At the beginning of the start-up period (on days between 5 and 20), the influent COD concentrations were between 3965-4000 mg/L. On the first 20 days, the COD removal efficiency varied between 80% and 91%. Later, the COD removal efficiency started to increase from 91% to 94% and reached steady-state conditions.

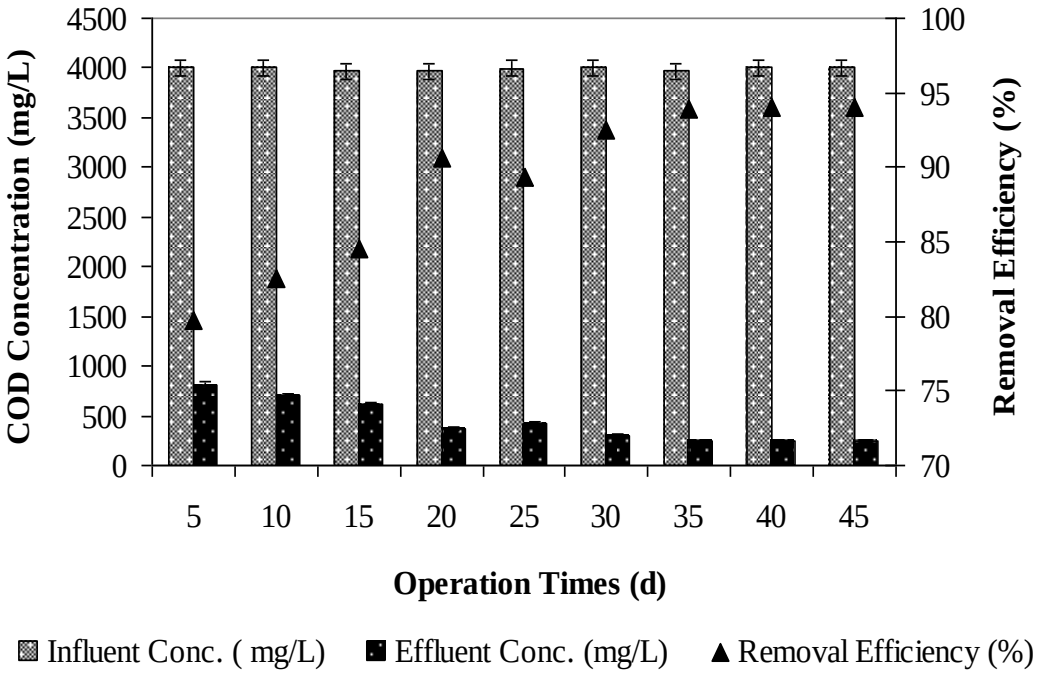

Figure 6.11 COD removal efficiencies in the AMCBR during the start-up period in the AMCBR

Figure 6.12 shows the methane gas and percentages in the AMCBR during the start-up period. At the beginning of the start-up period (on days between 5 and 10), the methane gas and percentages were 2.5 L/d and 18%, respectively. On the first 10 days, the methane gas and percentages varied between 2.5-4.2 L/d and 18-40%, respectively. Later, the methane gas and percentages started to increase from 4.2 to 6 L/d and from 40 to 55%, respectively and reached steady-state conditions.

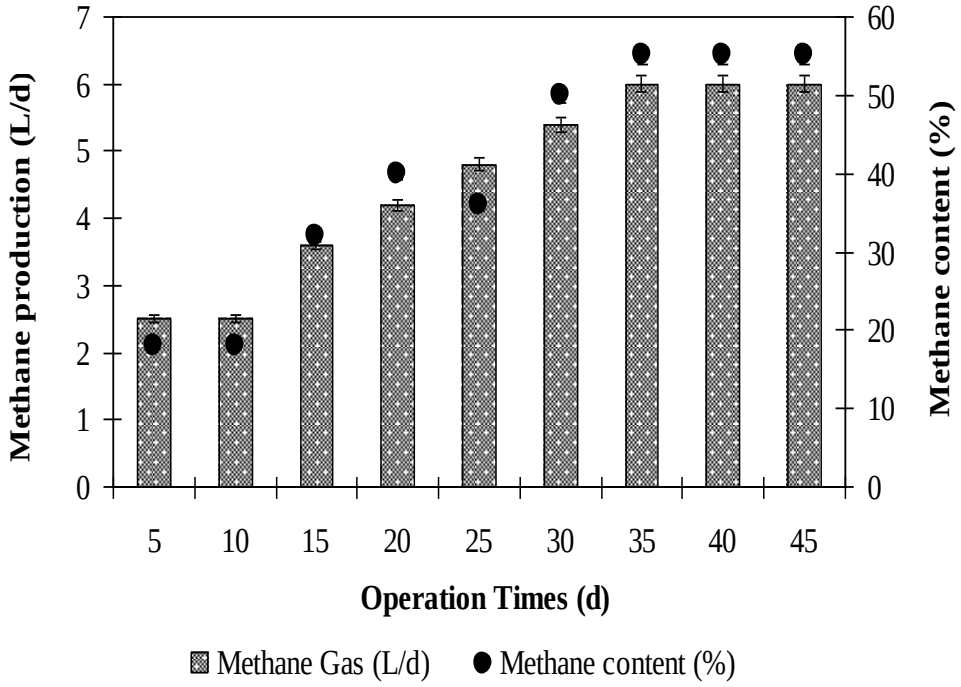

Figure 6.12 Methane gas production and content variations through start-up period in the AMCBR

6.2.1.3 Start-up Period for TYL

The start-up period was performed at a temperature above 36 °C to keep favorable conditions for growth of the anaerobic microorganisms for which 37 °C is the optimal temperature (Speece, 1996). The operating OLR of each sample was measured about 1.78 g.COD/L.d. The anaerobic conditions occurred in AMCBR reactor. The ORP values during the anaerobic phases were between -350 mV and -370 mV. The operational conditions were illustrated in Tables 5.7 in the section "Material and Methods" respectively (Study 6).

A start-up period led to a more complete biological degradation of the toxic substances such as antibiotics and a better adaptation of the biomass for the degradation of the antibiotic. The results of the start-up of the AMCBR reactor are shown in Figure 6.13 and 6.14. The AMCBR reactor was operated through 60 days without TYL to acclimate the granular sludge to the AMCBR reactor. The HRT and organic loading rate were 2.25 days and 1.78 g.COD/L.d, respectively. The COD

removal efficiency was 83% after 10 days of the operation period. The COD removal efficiency increased to 91% after 30 days of operation then the COD yields remained stable at 92% throughout 30 days after an operation period of 60 days and the effluent COD was stabilized at 302 mg/L for 2 consecutive weeks. This showed that the AMCBR had reached steady state conditions the methane gas production and percentages were between 3.2-4.2 L/d and 20-32% at the beginning of the start-up period (between 5 and 15 days), respectively (Figure 6.14). The methane gas production and the methane percentage reached 6 L/d and 50%, respectively, on day 35 and they remained stable at 7.2 L/d and 60%, respectively, throughout 25 days.

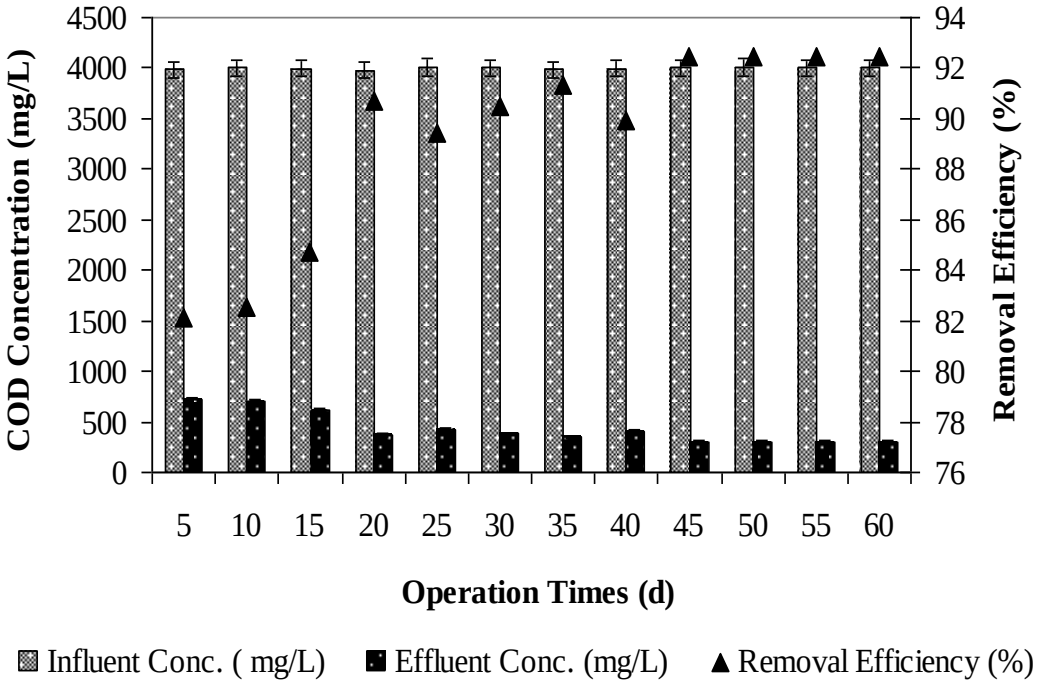

Figure 6.13 COD removal efficiencies in the AMCBR reactor during the start-up period

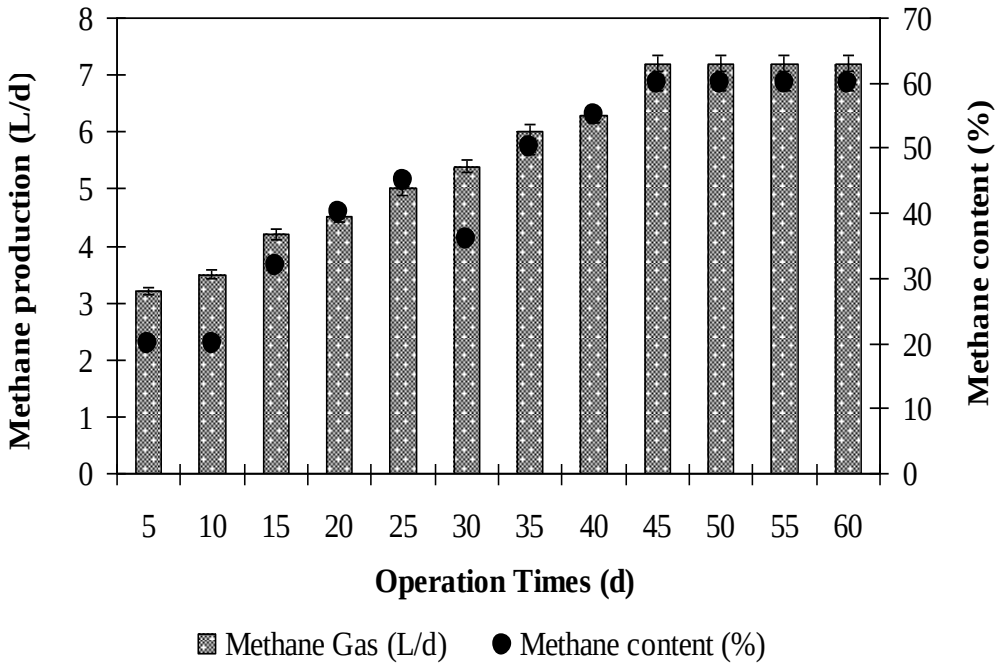

Figure 6.14 Methane gas production and percentages in the AMCBR during the start-up period

6.2.1.4 Start-up Period for ERY

Start-up procedures will depend on various factors, including wastewater composition and strength, available inoculum, reactor operating conditions, and reactor configuration. During anaerobic reactor start-up, the biomass is acclimatized to new environmental conditions, such as substrate, operating strategies, temperature and reactor configuration (Pandey et al., 2011). The operational conditions were illustrated in Table 5.8 in the section "Material and Methods" respectively for start-up period (Study 7).

The COD removal efficiency was 82% after 40 days of the operation day. The methane gas production and methane percentage were approximately 2.8 L/d and 20% at the beginning of the start-up period. The methane gas production and methane content reached 6.8 L/d, 50%, respectively, after 45 days of the operation day. The COD removal efficiencies remained stable at 91% after an operation period of 80 days. The methane gas production and content remained stable at 9.6 L/d and

56%, respectively after 75 days of the start-up period before feeding with synthetic pharmaceutical wastewater containing ERY (see Figure 6.15 and 6.16).

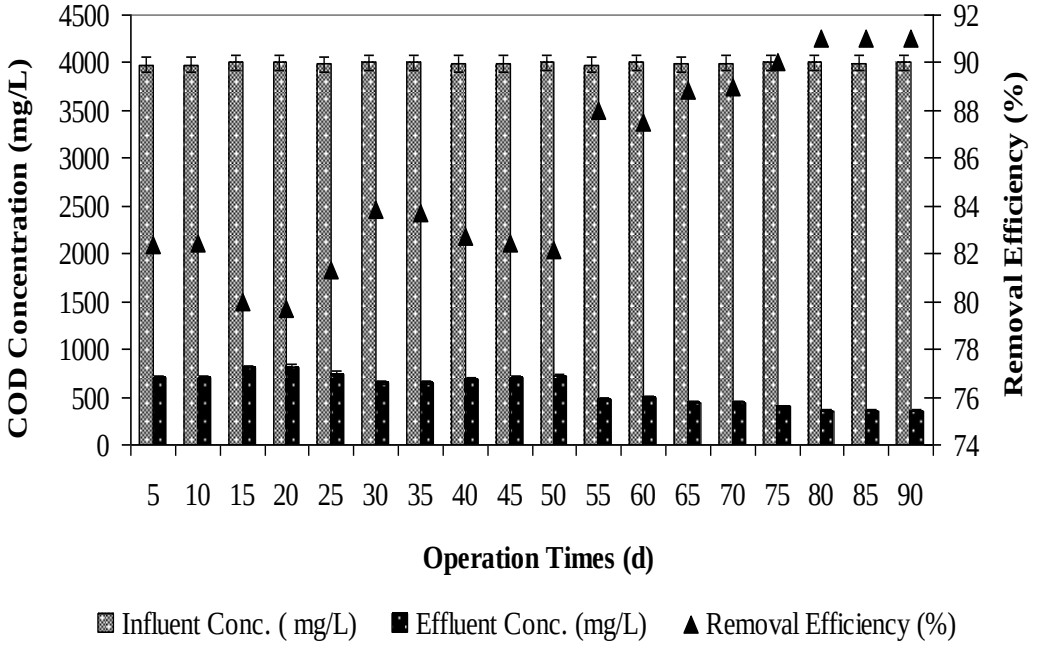

Figure 6.15 COD removal efficiencies in the AMCBR during the start-up period in the AMCBR

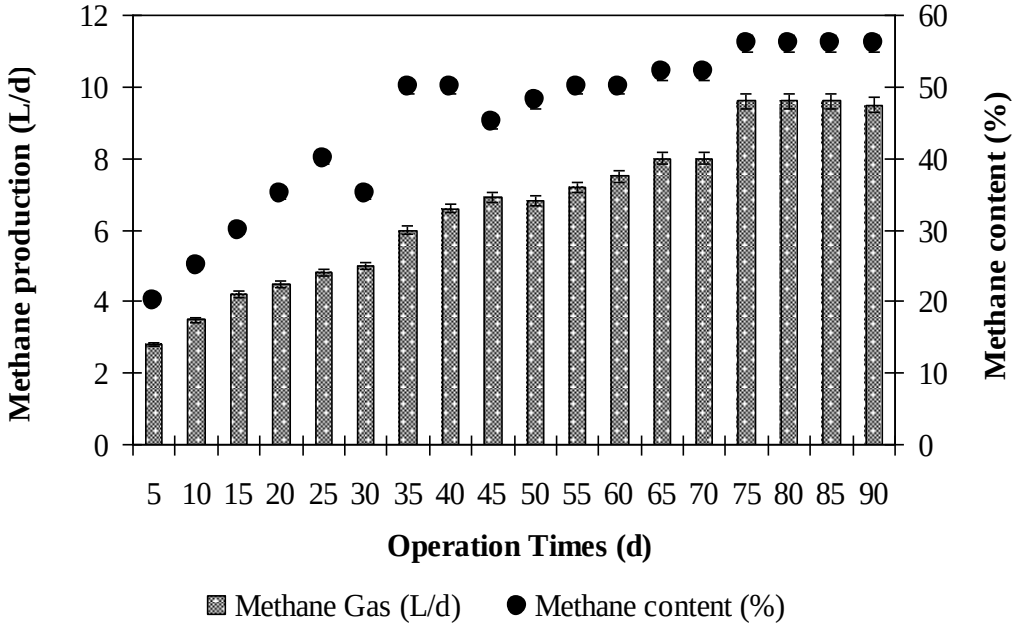

Figure 6.16 Methane gas production and percentages in the AMCBR during the start-up period

6.2.2 Effect of Increasing OTC Concentration on Performance of AMCBR Reactor

6.2.2.1 Effect of Increasing OTC Concentration on the COD Removal Efficiencies in the AMCBR Reactor

In this run, the effect of increasing OTC concentrations on COD removal efficiencies was investigated. The COD equivalents of OTC concentration are shown in Table 6.5.

Table 6.5 The COD equivalents of OTC concentration

Parameters	**Unit**	**Concentrations**
Molasses-COD concentration	mg/L	3900; 3917; 3925; 3950; 3960; 3978; 3990; 4000
OTC concentration	mg/L	50; 100; 150; 200; 250; 300; 350; 400
COD equivalent of OTC	mg/L	40; 60; 80; 90; 100; 110; 120; 140
Total COD concentration	mg/L	3940; 3977; 4005; 4040; 4060; 4088; 4110; 4140

The operation of the AMCBR with OTC introduction was started at an influent OTC concentration of 50 mg/L and an OTC loading rate of 22.22 g/m^{3}d. As shown in Figure 6.17, the COD removal efficiency was 92% at an OTC loading rate of 22.22 g/m^{3}d. The COD removal efficiency increased to 95 from 91% as the OTC loading rate was increased to 133.33 from 22.22 g/m^{3}d. The maximum COD removal efficiency was obtained as 95% in the aforementioned organic loading rate resulting in a COD concentration of 205 mg/L in the effluent among the runs applied to the AMCBR reactor (Figure 6.17). When the OTC loading rate was increased from 133.33 and 155.56 g/m^{3}d, at corresponding OTC concentration of 350 mg/L, the COD removal efficiencies decreased from 95 to 88%. No significant decreases in COD removals were obtained when the OTC loading rates increased from 155.56 to 177.78 g/m^{3}d. The COD removals (88-81%) were obtained in the aforementioned loading rates, (Figure 6.17). However, the COD removal efficiencies decreased rapidly from 88 to 81% when the OTC loading rate raised to 177.78 from 155.56 g/m^{3}d (Figure 6.17). The optimum OTC loading rate was 133.33 g/m^{3}d at an OTC

concentration of 300 mg/L for maximum COD removal while the minimum COD removal efficiency was obtained at an OTC loading rate of 177.78 g/m^3d. These results shows that OTC degrading methanogens produced methane through the utilization of OTC as co-substrate together with molasses-COD used as primary carbon and energy source.

In this study, 95% of 4088 mg/L COD was removed in the AMCBR reactor at an OTC concentration of 300 mg/L (OTC loading rate=133.33 g/m^3d, COD equivalent of OTC=110 mg/L) and a molasses-COD concentration of 3978 mg/L (total influent COD concentration of 4088 mg/L) under anaerobic conditions (see Table 6.5). A significant linear relationship was found between the COD yields and the OTC loading rates for 22.22 and 133.33 g/m^3d (ANOVA), (R^2=0.92, F=5.66, p=0.01).

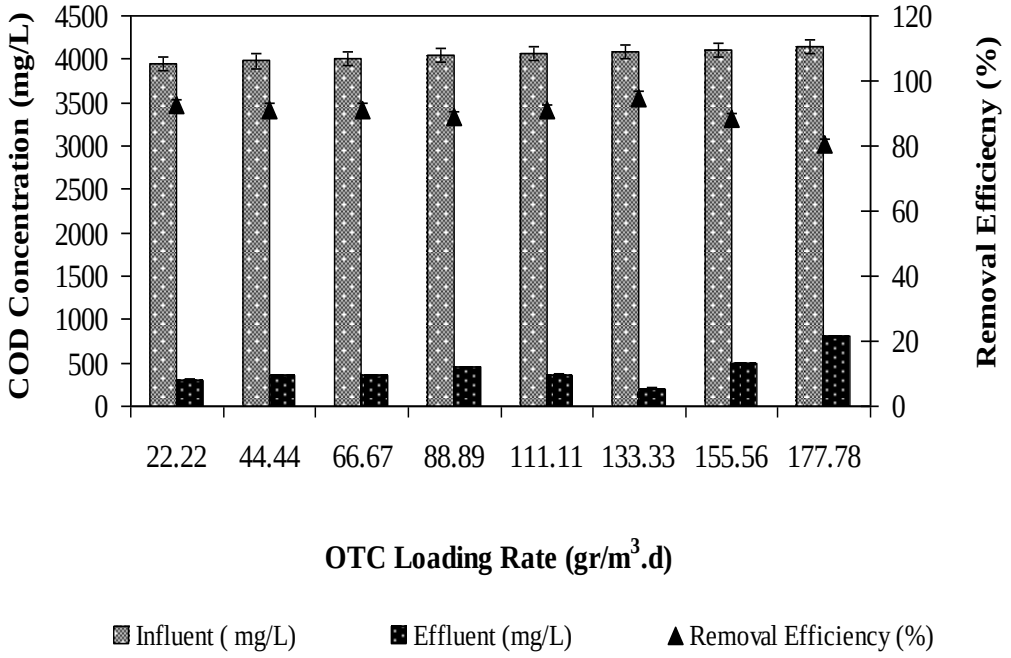

Figure 6.17 Effects of increasing OTC loading rates on COD removal efficiencies in AMCBR reactor

OTC loading rates varied between 22.22 g/m^3d and 133.33 g/m^3d could be used as carbon source by the methanogenic granular sludge resulting in high methane productions based on high COD removal under anaerobic conditions. In this study, molasses was used as the primary substrate for the reduction of OTC. Molasses-COD

is consumed as an energy source and electron donor for anaerobic antibiotic biotransformation. In other words the molasses-COD was used as a carbon and energy source by the OTC transforming methanogens while OTC was used as co-substrate by them and reduced to their metabolites.

These results are higher than the findings of Akarsubasi et al., (2005) who found a COD removal of 90% at an organic loading of 6 kg COD/m^3d. In the study performed by Fernandez et al., (2009) the COD removal efficiency decreased from 87 to 43% as the OTC hydrochloride concentrations increased from 100 to 1000 mg/L in an anoxic-anaerobic reactor. The COD yields found in these studies were lower than those in our study. The difference in COD yields could be attributed to the combining effects of anaerobic sludge which is resistant to OTC, to type of antibiotics to the antibiotic concentrations to the aerobic/anaerobic conditions and reactor configuration. On the other hand, high antibiotic doses under different oxygen conditions can affect the yields.

Similarly the COD yields obtained in recent studies including the synthetic pharmaceutical wastewater treating the OTC antibiotic were low in comparison with the COD removals in this study. In the study by Shi et al., (2011) 52-77% COD removal efficiency was observed for the anaerobic degradation of 95 mg/L of initial tetracycline (TC) concentration in swine and pig manure after 30 days degradation time, at 25 ^{0}C, at pH range of 6.7-7.4. Alvarez et al., (2010) found 57-82% and 58-83% COD removals in anaerobic conditions for OTC (250 mg/L) and chlortetracycline (CTC) (145 mg/L), after 35 days digestion time. In another study, Wu et al., (2011) reported that the C:N ratio was 9.01 by the influent OTC concentration 85 mg/L, resulting in 59-87% COD removal efficiency in an anaerobic compost system during the operation period. In our study, 97% COD removal was measured at the influent COD concentration from 3940-4140 mg/L. The yields obtained in the aforementioned studies are low in comparison to the removal performances of COD found in this study. The high COD yields in the AMCBR reactor can be explained by the granulated sludge which is resistant to the high toxic compounds and to the AMCBR reactor which is a high rate reactor. The high

removal efficiency of this reactor came from its compartmentalized structure. In this reactor acidification and methanogenesis predominate in the 1^{st}, 2^{nd}, 3^{rd} compartments.

The separation of acetogenic/methanogenic phases causes an increase in protection against toxic compounds and higher resistance to changes in environmental parameters such as pH, temperature and organic loading. The AMCBR is a high rate bioreactor with many advantages compared with the anaerobic reactors such as simple design due to no special gas or sludge separation, lower sludge generation, longer biomass retention times, lower HRT and higher stability to organic, hydraulic and toxic shock loads (Patel and Madamwar, 2001).

The COD yields found in our study agree with the COD removals reported by Nandy et al., (1998) in the treatment of herbal pharmaceutical wastewater containing mixed antibiotics in an up flow fixed bed reactor (UFFBR). The organic loading rate was 1.0 kgCOD/m^3d by the influent COD concentration from 5000 mg/L, resulting in a 96% COD removal efficiency in an UFFBR reactor during the operation time (86 days).

6.2.2.1.1 COD Subcategories in the AMCBR Treating OTC. The determination of soluble inert COD (COD_{inert}) of influent wastewater and inert microbial product (COD_{imp}) generated in the biological treatment is of considerable importance for meeting stringent discharge limits and aquatic toxicity (Ekama et al., 1986). In other words, the inert COD fractions of the wastewaters are of importance in meeting the discharge limitations as they by-pass the biological treatment system without being affected by the biochemical reactions and become the major constituent of the effluent (Ekama et al., 1986). This is important for refractory wastewater treatment, such as in the antibiotic production industry. It was reported that only the residual COD_{inert} is the key issue in the lowering of reactor performance for pharmaceutical wastewater (Sponza and Demirden, 2007, 2010). Substantial parts of the COD and OTC may be biodegradable while other parts of the COD may be inert in antibiotic industry wastewaters. The COD parameter alone used for substrate utilization cannot

give enough information about the degradation of the organic matter. Therefore, the inert fraction of COD must be determined since all design calculations need to deal with biodegradable COD (Sponza and Demirden, 2007, 2010).

Variation in COD_{inert} levels: The experiments performed with the measurements in COD_{inert} concentrations showed that the COD_{inert} in the influent of the control without OTC was measured as 25 mg/L (Table 6.6). This result showed that a part of the molasses-COD is inert even in the control reactor. In other words, the molasses in the influent contained inert fraction (Table 6.6). Table 6.6 also shows the variation of COD_{inert} in the influent and effluent of the AMCBR reactor versus OTC loading rates. When the OTC loading rates increased from 22.22 to 44.44 g/m^3d the COD_{inert} concentration began to increase up to 36 mg/L and then the COD_{inert} concentrations in the AMCBR reactor decreased from 36 to 30 mg/L at an OTC loading rate of 66.67 g/m^3d. As shown in Table 6.6, the COD_{inert} concentrations were 22, 23 and 18 mg/L at OTC loading rates of 88.89, 111.11 and 133.33 g/m^3d, respectively. The COD_{inert} concentrations increased from 29 up to 161 and 208 mg/L as the OTC loading rates increased from 155.56 and 177.78 g/m^3d, respectively, in the influent of the AMCBR depending on the increasing inert fraction of the OTC antibiotic in the influent. The effluent of the AMCBR contained 18-22 mg/L COD_{inert} at OTC loading rates of 88.89-133.33 g/m^3d, respectively (see Table 6.6).

Table 6.6 COD subcategories in AMCBR reactor

M-COD[a]	OTC[b]	COD-OTC[c]	OLR[d]	COD_{inert}[e] M-COD	COD_{inert}[f] OTC	Total COD_{inert}[g]	Total COD_{inert}[h]	Total COD_{inert}[k]	COD_{imp}[l]	COD_{imp}[m]
4000	0	0	0	25	0	25.00±1.0	5±0.8	19±0.2	0	23.99±0.5
4000	50	25	22.22	25	8.86±0.0	33.86±0.8	29±0.6	17±0.2	0	53.45±0.8
4000	100	50	44.44	25	16.92±0.3	41.92±1.5	36±0.5	13±0.2	0	49.56±0.3
4000	150	75	66.67	25	24.70±1.0	49.70±1.7	30±1.2	22±0.3	0	60.22±1.2
4000	200	100	88.89	25	32.03±0.6	57.03±1.0	22±0.5	44±0.2	0	50.45±2.0
4000	250	125	111.11	25	40.89±1.8	65.89±1.9	23±1.2	51±0.3	0	21.34±2.4
4000	300	150	133.33	25	48.72±0.9	73.72±2.0	18±2.0	57±0.1	0	15.45±1.8
4000	350	175	155.56	25	56.07±1.2	81.07±2.5	161±2.3	-	0	110.23±6.0
4000	400	200	177.78	25	64.03±2.0	89.03±3.0	208±2.5	-	0	119.56±6.8

a: Molasses-COD concentration in the influent of the AMCBR (mg/L); b: OTC concentration in the influent of the AMCBR (mg/L); c: COD equivalent of OTC concentration in the influent of the AMCBR (mg/L); d: OTC loading rate in the influent of the AMCBR (g/m^3d); e: inert COD concentration originating from molasses-COD in the influent of the AMCBR (mg/L); f: inert COD concentration originating from OTC in the influent of the AMCBR (mg/L); g: Total inert COD concentration in the influent of the AMCBR (mg/L); h: Total inert COD concentration in the effluent of the AMCBR (mg/L); k: Total inert COD removal efficiency in the effluent of the AMCBR (%); l: COD concentration originating from the inert microbial products in the influent of the AMCBR reactor (mg/L); m: COD concentration originating form the inert microbial products in the effluent of the AMCBR (mg/L)

It was found that the COD_{inert} concentrations in the effluent of the AMCBR reactor decreased by 44% and 57% compared to the influent, for OTC loading rates between 88.89 and 133.33 g/m^3d while the CODinert originating only from molasses-COD in the control reactor decreased only by 19%. This showed that the COD_{inert} is taken up by the cells of anaerobic granule bacteria together with biodegradable COD and OTC throughout hydrolytic, acidogenic and methanogenic phases of the anaerobic treatment in the AMCBR reactor at a HRT of 2.5 days as reported in previous studies (Sponza and Demirden, 2007, 2010).

The COD_{inert} yields found in this study were compared with some aerobic reactors treating antibiotics and toxic substances (Majewsky et al., 2011). The COD_{inert} concentrations produced were found to be low in aerobic activated sludge during the biodegradation of some veterinary antibiotics (OTC and CTC) compared with anaerobic conditions (Majewsky et al., 2011). No further studies were found for inert COD evaluation throughout anaerobic treatment of OTC. The maximum COD_{inert} yields in the AMCBR treating OTC were significantly higher than that anaerobic baffled and up flow anaerobic sludge blanket reactors treating 32 mg/L kemicetine (KEM) at a KEM loading rate of 52 g/m^3d and 98 mg/L sulfamerazine (SM) at a SM loading rate of 143 g/m^3d, respectively (Sponza and Demirden, 2007, 2010). This could be attributed to the structure of antibiotic and to the configuration of AMCBR since in this reactor a separation of acidogenesis and methanogenesis phases occurred. These phases result in an increase in protection against toxic materials and higher resistance to changes in environmental parameters such as pH, temperature and organic loading compared with the anaerobic baffled (ABR) and up flow anaerobic sludge blanket reactors. In the study performed by Sponza and Demirden, (2007) the COD_{inert} which originated from the SM was biodegraded by the acclimatized anaerobic bacteria in the UASB (Sponza and Demirden, 2007). In this study it was shown that the anaerobic archae acclimatized to SM and decreased the COD_{inert} ratio of this toxic antibiotic (Sponza and Demirden, 2007). Therefore the concentration of non-biodegradable inert COD_{inert} decreased.

Variation in COD_{imp} levels: Measurements of COD originating from the inert microbial products (COD_{imp}) showed that the effluent of the control AMCBR (without OTC) reactor contained 23.99 mg/L COD_{imp} (Table 6.6). The presence of the COD_{imp} in the control AMCBR reactor could be attributed to the extracellular metabolites produced from the biomass even in an AMCBR reactor treating molasses-COD under anaerobic conditions. The COD_{imp} was measured as 15.45 and 119.56 mg/L at OTC loading rates as high as 133.33 and 177.78 g/m^3d, respectively (Table 6.6). It was shown that the COD_{imp} increased at high OTC loadings due to the toxicity of high OTC concentrations since the death of the biomass produced more inert metabolites and extracellular organics. Rittman and McCarty, (2001); Aquino and Stuckey, (2004) showed that the COD_{imp} is produced during environmental stress such as high substrate concentration and in the presence of some toxicants (refractory organics and antibiotics) or due to enhanced cell lysis. The COD_{imp} concentration was at the lowest level at an OTC loading rate of 133.33 g/m^3d in which the maximum OTC removal efficiency was obtained. The COD_{imp} generated by the hydrolysis of molasses COD to more degradable soluble molasses COD concentration and by the decay of biomass is directly converted into stored material in bacterial cells when the substrate is metabolized effectively. In this study the stored COD_{imp} was subsequently used as a carbon and energy source for growth purposes. Bacteria in the anaerobic process might be able to directly utilize the OTC with COD and the stored component of COD mentioned above. Therefore the COD_{imp} productions were low in the AMCBR at high OTC removals. This agrees with the results by Kuo and Parkin, (1996). The COD_{imp} concentrations measured at the optimum OTC loadings in the AMCBR exhibited similarities with the studies performed by Sponza and Demirden, (2007, 2010) treating KEM and SM in the UASB and ABR reactors.

6.2.2.1.2 Variations of COD in Compartments of the AMCBR Reactor at Increasing OTC Loading Rates. In order to determine the variations of COD and OTC in compartments of the AMCBR reactor, samples were taken from the sampling points of each compartment of the AMCBR reactor and the COD and OTC concentrations were measured. Table 6.7 shows the variations in COD and OTC

concentrations in all compartments of the AMCBR reactor. As indicated in Table 6.7, the COD concentrations were different in three compartments, indicating that staging had been accomplished in the compartments of AMCBR. It was observed that most of the influent COD was removed in 1st compartment at OTC loading rate of 133.33 g/m^{3}d. The influent COD concentration was around 4088 mg/L and then decreased to 790 mg/L (E=81%) in the effluent of the 1st compartment at an OTC loading rate of 133.33 g/m^{3}d. The COD concentration was around 4140 mg/L in the influent of the 1st compartment at an OTC loading rate of 177.78 g/m^{3}d. Then this decreased to 1215 mg/L in the effluent of the 1st compartment result a COD removal efficiency of 71%. The COD yields decreased with increasing OTC loading rates in the 1st compartment.

The effluent COD concentrations was 400 mg/L in the 2nd compartment resulting a COD removal efficiency of 49% at OTC loading rate of 133.33 g/m^{3}d. The effluent COD concentration was measured as 910 mg/L in the effluent of the 2nd compartment, resulting in a COD removal efficiency of 25% at an OTC loading rate of 177.78 g/m^{3}d. The COD removal efficiency was 49% in the effluent of the 2nd compartment at an OTC loading rate of 133.33 g/m^{3}d. The COD removal efficiencies were between 40-49% in the 2nd compartment, respectively, at OTC loading rates between 22.22 and 133.33 g/m^{3}d. The COD removal efficiencies in this compartment varied between 25 to 32% with increasing OTC loading rates (155.56 and 177.78 g/m^{3}d). A small amount of COD yields (12-49%) were measured in 3rd compartment. The COD yield in 3rd compartment varied between 18% and 49% at OTC loading rates varying between 22.22 and 133.33 g/m^{3}d. The effluent COD concentration was 485 mg/L in the 3rd compartment while 20% COD removal efficiency was observed at an OTC loading rate of 155.56 g/m^{3}d. The COD removal efficiency was 12% in the 3rd compartment at an OTC loading rate of 177.78 g/m^{3}d. COD removal efficiencies decreased with increasing OTC loading rates in compartments and the effluent of the AMCBR reactor. The total COD removals in the effluent of the AMCBR reactor were 92% and 81% at OTC loading rates of 22.22 and 177.78 g/m^{3}d, respectively (see Figure 6.17).

Although COD was mainly removed in the 1st compartment, the 2nd and 3rd compartments contribute to increasing the COD removal efficiencies in the effluents, particularly at high OTC loading rates. Since COD concentrations are high in the effluent of the 3rd compartment and in the outlet of the AMCBR at high OTC loading rates, a final aerobic stage could contribute to degrading the remaining COD from the anaerobic stage and improving the COD removal efficiencies in sequential anaerobic/aerobic reactor systems, particularly at high OTC loading rates.

Table 6.7 Variations of COD Concentrations in Compartments of AMCBR Reactor at Increasing OTC Loading Rates

Influent		**1st Compartment**		**2nd Compartment**		**3rd Compartment**	
OTC Load. (g/m^3d)	**COD Conc. (mg/L)**	**Effluent COD (mg/L)**	**COD Yield (%)**	**Effluent COD (mg/L)**	**COD Yield (%)**	**Effluent COD (mg/L)**	**COD Yield (%)**
22.22	3940±133	610±48	85	365±40	40	300±40	18
44.44	3977±136	745±60	81	425±53	43	350±35	18
66.67	4005±90	765±71	81	464±38	39	354±30	24
88.89	4040±53	800±90	80	515±30	36	445±32	14
111.11	4060±74	810±105	80	530±45	35	365±26	31
133.33	4088±55	790±95	81	400±98	49	205±20	49
155.56	4110±40	900±100	78	610±105	32	485±35	20
177.78	4140±32	1215±120	71	910±110	25	800±90	12

6.2.2.2 Effect of OTC Loading Rate on the OTC Removal Efficiencies in the AMCBR Reactor

The effect of OTC loading rate on the OTC removal efficiencies is shown in Figure 6.18. An OTC removal efficiency of 95% was obtained at an initial OTC concentration of 50 mg/L and at an OTC loading rate of 22.22 g/m^3d. When the OTC loading rate was increased from 22.22 to 133.33 g/m^3d the OTC removal efficiency remained stable at between 95% and 99%. A maximum OTC removal efficiency of 99% was obtained at an initial OTC concentration of 300 mg/L at an OTC loading rate of 133.33 g/m^3d in the AMCBR. The effluent OTC concentration was measured as 3.0 mg/L (E=99%) at an OTC loading rate of 133.33 g/m^3d. The OTC yields were

between 97 and 98% and 97% for OTC loading rates of 44.44-66.67 g/m^{3}d and 88.89-111.11 g/m^{3}d, respectively, in the anaerobic reactor. When the OTC loading rate was increased from 133.33 g/m^{3}d to 155.56 and to 177.78 g/m^{3}d the OTC removal efficiency decreased from 99% to 79% and 77%, respectively, in the AMCBR reactor (Figure 6.18). A significant linear correlation between OTC yields and increasing OTC loading rates was not observed (ANOVA), (Figure 5.18) (R^2= 0.56, F = 13.90, p = 0.01).

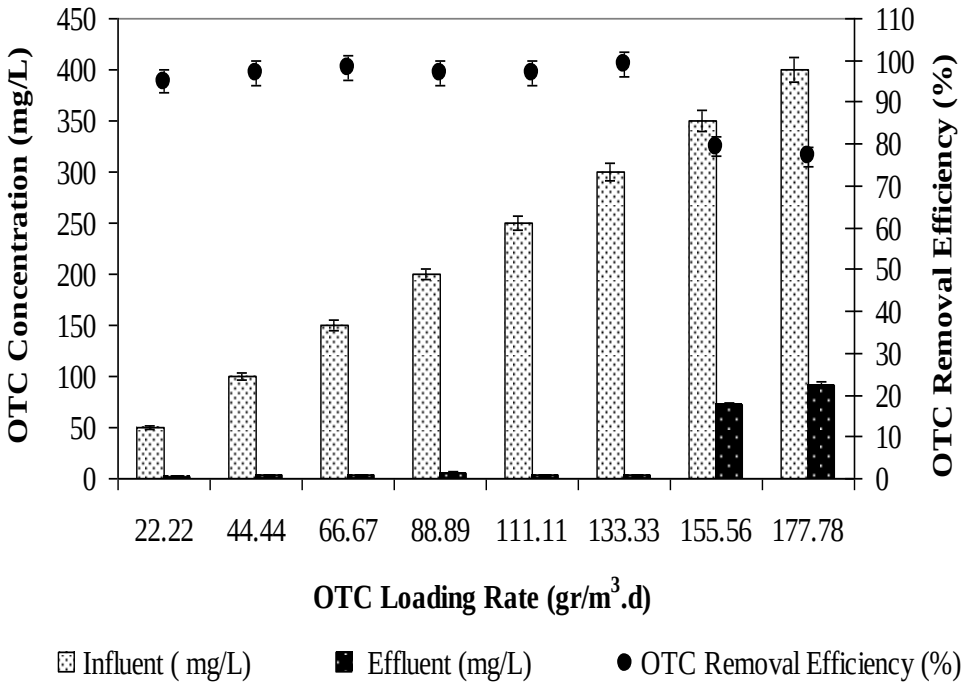

Figure 6.18 The effect of OTC loading rate on OTC removal efficiencies in AMCBR.

In this study, molasses used as the primary substrate was consumed as energy source and electron donor for anaerobic OTC biotransformation. This shows that the anaerobic granule microorganisms in AMCBR reactor acclimated to high OTC concentration. OTC at high concentrations is metabolized with the simultaneous utilization of primary substrate (molasses-COD) serving as the source of carbon and energy required for growth. Emerging compounds, such as OTC, act as secondary substrates that do not contribute to the anabolic process leading to cell growth.

In our study the OTC removal was mainly through biodegradation since the studies performed in previous section (see Table 5.4, Study 3) showed that the biodegradation is seen a major mechanism of OTC removal and contributed around 99% of the total OTC treatment in the batch reactors. The contributions of volatilization and adsorption to the OTC removal were not observed.

The OTC yields obtained in our study are high in comparison to the removal performances of OTC in the studies given below: In the study by Kim et al., (2005) 85% OTC removal efficiency was observed for the anaerobic degradation of 200 mg/L OTC concentration in wastewater after 7.4-24 hours HRT and 3-10 days SRT, at pH 7.38. In the study performed by Mohan et al., (2001) 89% OTC removal efficiency was obtained at a HRT of 1 day in an up-flow anaerobic sludge blanket (UASB) reactor at an influent OTC concentration of 200 mg/L. The yields obtained in the aforementioned studies are low in comparison to the removal performances of OTC found in this study. This could be explained by the differences in AMCBR reactor configuration by the OTC degradating anaerobic bacteria type, by the differences in OTC loading rates and by the differences in the composition of the pharmaceutical wastewater.

Similarly, in the studies performed by Sreekanth et al., (2009) and Pallavi et al., (2009) lower antibiotic removals were found than those in our study (maximum COD removals were 73%, 80% and 75% at COD loading rates of 1.25, 0.99 and 1.21 g/m^3d) in an anaerobic sludge blanket reactor treating pharmaceutical wastewater containing paracetamol and some other antibiotics.

6.2.2.3 Effect of OTC Loading Rate on the Total and Methane Gas Production in AMCBR Reactor

Biogas production was monitored through the continuous operation of the AMCBR reactor, particularly for detection the methanogenic activity. The effect of OTC loading rate on daily total gas and methane gas production and methane percentages are illustrated in Figure 6.19. The daily total gas, methane gas

productions and methane percentage were recorded as 11 L/d and 6.36 L/d and 58%, respectively at an OTC loading rate of 22.22 g/m^3d. The maximum total gas, methane gas productions and methane percentage were found about 14 L/d, 9.36 L/d and 65%, respectively at an OTC loading rate of 133.33 g/m^3d. After this loading rate, methane percentage decreased rapidly from 65% to 60%. This indicated an inhibition effect of OTC on methane *Archaea* at OTC loading rates as high as 155.56 g/m^3d. OTC loading rates varied between 22.22 g/m^3d and 155.56 g/m^3d could be used as carbon source by the methanogenic granular sludge resulting in high methane productions based on high COD removal under anaerobic conditions.

In this study, molasses was used as the primary substrate for the reduction of OTC. Molasses-COD is consumed as an energy source and electron donor for anaerobic antibiotic biotransformation. In other words the OTC was used as secondary carbon source by the anaerobic bacteria.

A significant linear relationship was found between the total and methane gas productions and the OTC loading rates (only for between 22.22-133.33 g/m^3d) (ANOVA), (R^2=0.91, F=4.80, p=0.01 (for total gas); R^2=0.90, F=5.03, p= 0.02 (for CH_4). Similarly, a linear relationship was found between the methane content and the OTC loading rates (Only for between 22.22-133.33 g/m^3d) and this relationship is significant (ANOVA), (R^2=0.88, F=6.06, p=0.01).

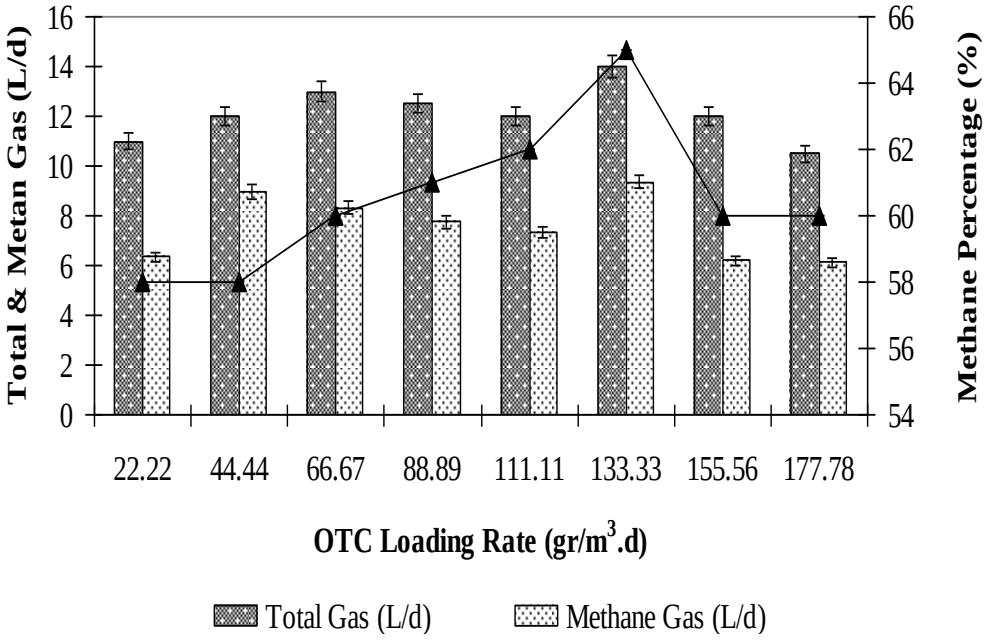

Figure 6.19 The effect of OTC loading rate on total, methane gas production and methane percentage in the AMCBR reactor

The results of this study showed that the OTC loadings affected the total volume of CH_4 produced during anaerobic degradation of pharmaceutical wastewater. In a study performed by Liu et al., (2009) the methane gas productions were found as 12, 30 and 66 L/d at OLRs of 1.04, 2.01 and 6.17 kg COD/m^3d, respectively, in an anaerobic baffled reactor (ABR). In our study methane gas productions were 6.36, 8.97, 8.32, 7.75, 7.32, 9.36, 6.20 and 6.12 L/d at OTC loading rates of 22.22, 44.44, 66.67, 88.89, 111.11, 133.33 and 177.78 g/m^3d, respectively in the AMCBR reactor. In this study the methane productions are comparable higher than that aforementioned study.

In another study, Heidari et al., (2011) reported that, 48% methane percentage and 0.12 L/d CH_4 production at an influent OTC concentration of 105 mg/L at an COD yield of 2.03 kg COD/m^3d respectively in an anaerobic sequencing batch reactor (SBR). In our study, 58-65% methane percentage and 6.36-9.36 L/d CH_4 production was measured at influent OTC concentrations varying between 50 and 300 mg/L. In a study performed by Amin et al., (2006) methane gas production and methane content were found as 5 L/d and 48%, respectively, at an OLR of 2.90 kg COD/m^3d

in an anaerobic sequencing batch reactor (SBR). The yields obtained in the aforementioned studies are low in comparison to the methane gas productions found in our study. The study performed by Alvarez et al., (2010) agree with the methane yields obtained in our study in a pig manure wastewater containing mixed antibiotics in an anaerobic degradation system. 56-60% methane content was obtained at an influent OTC concentration of 250 mg/L, during 35 days of operation time.

6.2.2.4 Determine of Intermetabolite Products of OTC under Anaerobic Conditions

Chen and Huang, (2011) reported that tetracycline's (TCs) are transformed partially or completely to its OTC and Chlortetracycline (CTC) derivatives under abiotic and biotic conditions. The metabolic products of OTC, such as isomerization products (epi-OTC) and dehydration products (α-Apo-OTC and ß-Apo-OTC) can be found in manure slurry (Arıkan et al., 2006), under anaerobic conditions (Loke et al., 2003) and abiotic conditions with low pH level (3-6.5) (Halling-Sørensen et al., 2002). In our study, α-Apo-OTC and ß-Apo-OTC were observed in the effluent of anaerobic AMCBR reactor as the intermediate metabolites of OTC. This showed that OTC is transformed to α-Apo-OTC and then α-Apo-OTC converted ß-Apo-OTC under anaerobic conditions. In our study, 4-epi-OTC was no detected in the effluent of anaerobic AMCBR reactor.

Figure 6.20 shows the HPLC chromatogram of effluent α-Apo-OTC and ß-Apo-OTCs. Peak of 300 mg/l OTC standards was obtained at a retention time of 5.32 min and at a wave length of 254 nm (see Figure 4.20). Similar peak are showed on the chromatograms at 9.92 and 15.00 min retention times in the effluent sample of the AMCBR. The presence of α-Apo-OTC and ß-Apo-OTC peak in effluent of anaerobic AMCBR indicated that the OTC converted to α-Apo-OTC and ß-Apo-OTC under anaerobic conditions. In our study, the metabolic pathway of OTC through anaerobic stage was illustrated in Figure 6.21.

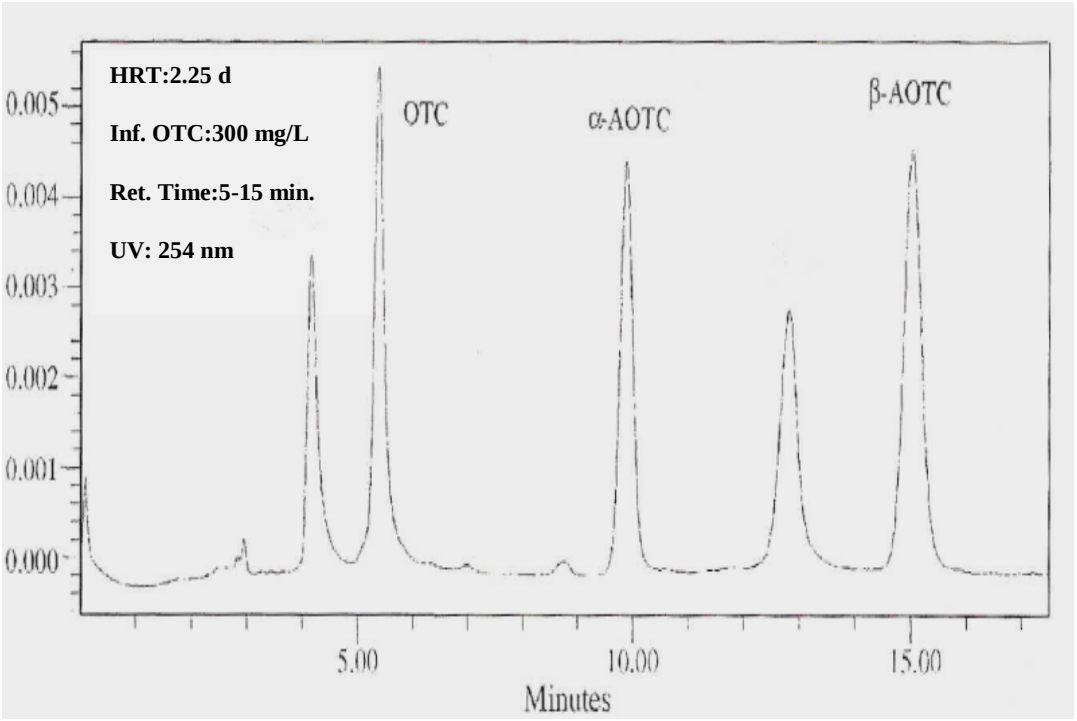

Figure 6.20 HPLC chromatograms of α-Apo-OTC and ß-Apo-OTC in the effluent of AMCBR reactor

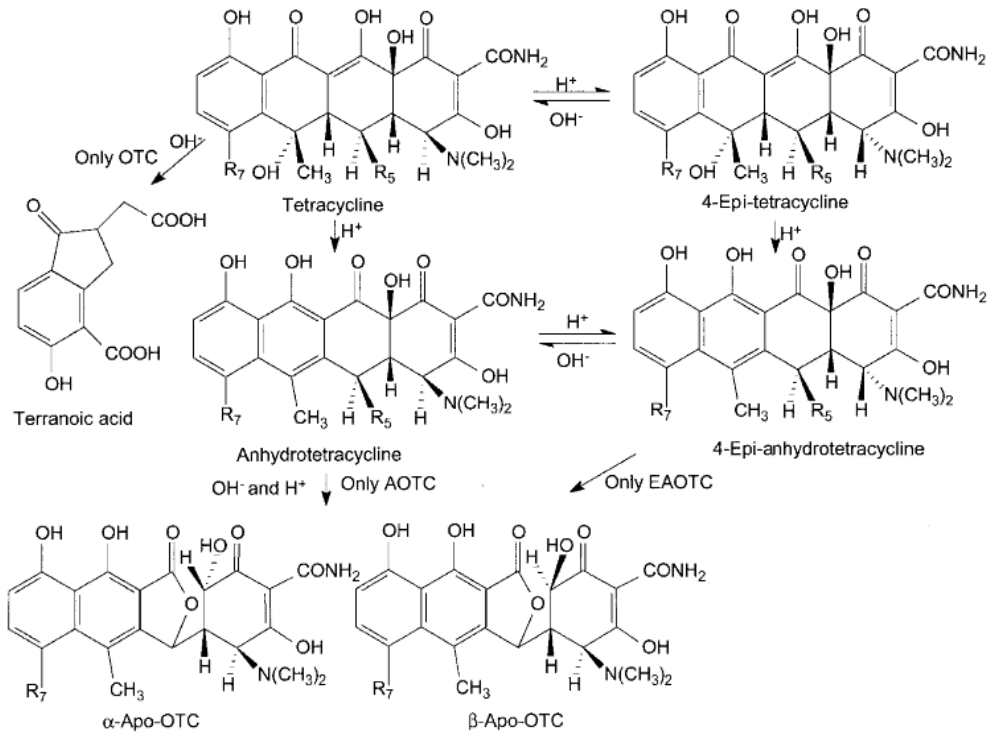

Figure 6.21 Degradation pathway of OTC in anaerobic stage.

The AMCBR was operated throughout 220 days at eight different OTC loading rates (Figure 6.22). The effluent α-Apo-OTC and ß-Apo-OTC concentrations were 22 and 25 mg/L for operation days of 1-5 then it decreased from 18 to 5 mg/L and from 20 to 8 mg/L throughout operation days of 10-30 at an OTC concentration of 50 mg/L corresponding to an OTC loading rate of 22.22 g/m^3d, respectively. The α-Apo-OTC and ß-Apo-OTC concentrations increased to 27 and 30 mg/L when the OTC loading rate was increased to 44.44 g/m^3d (OTC concentration= 100 mg/L) on days 38 then it decreased from 15 to 6 mg/L and from 18 to 10 mg/L on days between 50-55 and 56-60, respectively. The effluent α-Apo-OTC and ß-Apo-OTC concentration was recorded as 6 and 8 mg/L.

On day 70, the effluent α-Apo-OTC and ß-Apo-OTC concentrations increased to 30 and 36 mg/L and then it decreased from 20 to 9 mg/L and from 25 to 12 mg/L on days between 75-80 and 81-100, respectively, when the OTC loading rate was increased to 66.67 g/m^3d (OTC conc.=150 mg/L), respectively. The α-Apo-OTC and ß-Apo-OTC concentrations fluctuated to 36 and 37 mg/L when the OTC loading rate was increased to 88.89 g/m3d (OTC conc=200 mg/L), and 111.11 g/m^3d (OTC conc.=250 mg/L), on days 98 and 130, respectively. On days 155 the α-Apo-OTC and ß-Apo-OTC concentrations elevated to 40 and 45 mg/L, respectively.

On day 165 the α-Apo-OTC and ß-Apo-OTC levels decreased to 2 and 6 mg/L at an OTC loading rate of 133.33 g/m^3d (OTC conc.=300 mg/L). On day 175, the α-Apo-OTC and ß-Apo-OTC concentrations reached 42 and 50 mg/L and then it decreased from 30 to 20 mg/L and from 42 to 37 mg/L on days between 152-158 and 160-165, respectively, when the OTC loading rate increased to 155.56 g/m3d (OTC conc.=350 mg/L). The α-Apo-OTC and ß-Apo-OTC concentrations increased to 56 and 65 mg/L when the OTC loading rate was increased to 177.78 g/m^3d (OTC concentration=400 mg/L) on days 195 then it decreased from 45 to 35 mg/L and from 57 to 50 mg/L on days between 200-205 and 206-211, respectively.

Figure 6.23 indicates the α-Apo-OTC and ß-Apo-OTC production through increasing OTC loading rates in the AMCBR reactor. The production of α-Apo-OTC and ß-Apo-OTC were measured as 5 and 6.5 mg/L at an initial OTC concentration of 50 mg/L, respectively. As shown in Figure 6.23, when the OTC loading rate was raised, the α-Apo-OTC and ß-Apo-OTC concentration also increased. The α-Apo-OTC and ß-Apo-OTC were measured as 2 and 4 mg/L, respectively at an OTC loading rate of 133.33 g/m^3d. The concentrations of α-Apo-OTC and ß-Apo-OTC increased to 56 and 89 mg/L, respectively, at an OTC loading rate of 177.78 g/m^3d. A strong linear correlation between influent OTC loading rates and the effluent α-Apo-OTC and ß-Apo-OTC concentration was observed (R^2=0.97, F=3.86, p=0.01) (only for between 22.22-133.33 g/m^3d) α-Apo-OTC and ß-Apo-OTC concentration in the effluent increased from 5 to 35 mg/L and 6.5 to 50 mg/L when OTC loading rates in the influent increased from 22.22 to 177.78 g/m^3d.

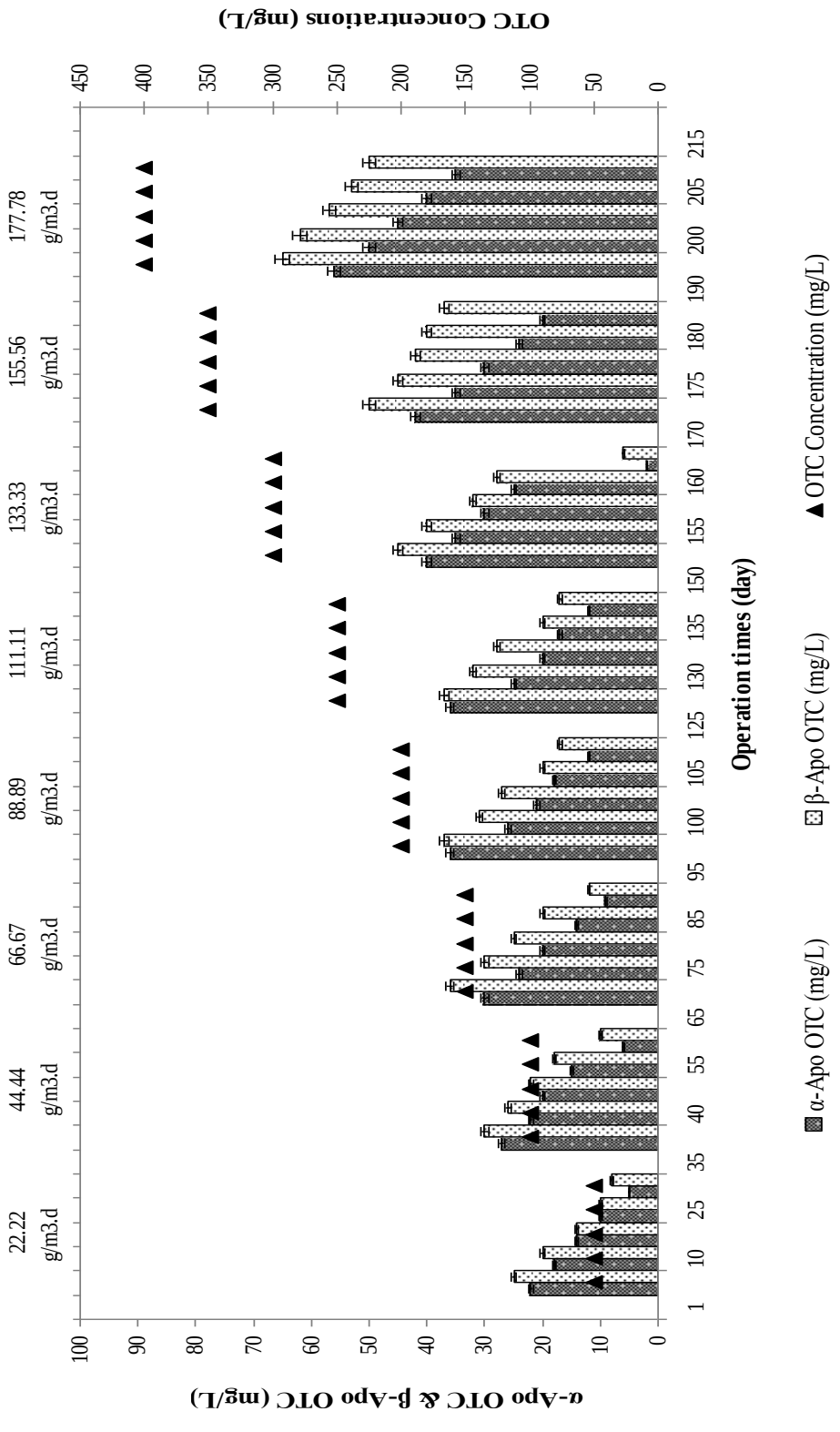

Figure 6.22 Variation of α-Apo-OTC and ß-Apo-OTC concentrations versus operation days in the AMCBR reactor

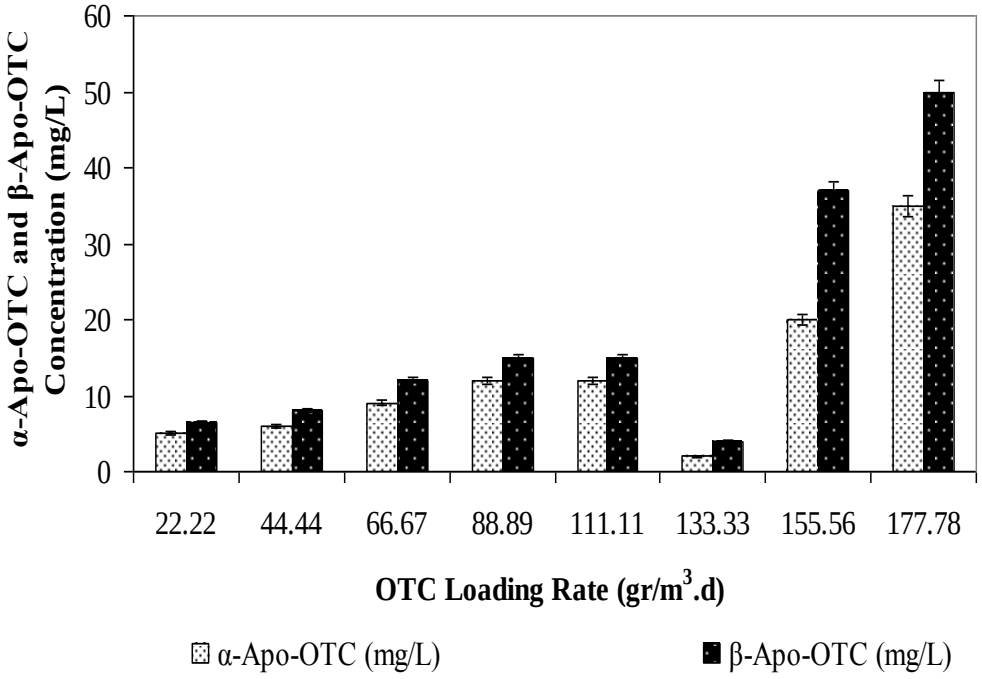

Figure 6.23 Effect of OTC loading rate on α-Apo-OTC and ß-Apo-OTC production in the AMCBR reactor

This showed that the metabolites were accumulated at high OTC loadings. These metabolites were also found in the studies performed by Arıkan et al., (2006); Arıkan et al., (2008); Loke et al., (2003). Loke et al., 2003 also found that besides α-Apo-OTC and ß-Apo-OTC, epi-OTC was produced from the anaerobic degradation of OTC. In our study, epi-OTC was no detected in the compartments and the effluent of the AMCBR reactor.

Arıkan et al., (2006) reported that OTC is transformed completely to epi-OTC. In their study, the OTC only was transformed to epi-OTC with efficiency near to 90% in the anaerobic phase. In another study, Li et al., (2008) found that only 4-epi-OTC during the anaerobic biodegradation of OTC. This could be attributed to the differences in reactor configurations, to the wastewater characteristic, to the dominancy of bacteria types and to some environmental conditions such as pH, temperature and co-metabolic interactions between substrate and OTC.

6.2.2.5 Variation of pH, Total Volatile Fatty Acids (TVFA) and Composition (H_{ac}, H_{bu}, H_{la}, H_{pr}) in Compartments of the AMCBR Reactor at Increasing OTC Loading Rates

As mentioned earlier, during the first step of the anaerobic treatment TVFAs are produced by the microorganisms in the process of hydrolysis and acidification. TVFA production at this stage depends mainly on wastewater characteristics, environmental conditions such as temperature and pH, reactor type and operating parameters such as HRT, and on the toxic compounds present in the anaerobic reactor system. In the hydrolysis step, the acidogens convert the complex organics to acetic acid (H_{ac}) and propionic acid (H_{pr}), carbon dioxide (CO_2) and hydrogen (H_2). In this study, although a decrease in the TVFA levels was observed at increasing OTC concentrations (>133.33 g/m^3d), no change of pH was detected. Figure 4.22 indicates the pH variations in the compartments of the AMCBR reactor at increasing OTC concentrations. As shown in Figure 6.24 (a), the influent and effluent pH values varied between 7.10-7.55 and 7.50-8.00 at increasing OTC concentrations. pH values did not significantly change in the compartments. The pH values varied between 7.32 and 8.00 in compartment of AMCBR at all OTC concentrations. These values were between optimum pH values as reported by Speece, (1996). The pH values were lower in the 1st compartment than all of the other compartments since TVFA in the 1st compartment was higher (Figure 6.24 (b)). In this study, although a decrease in the TVFA levels was observed at increasing OTC concentrations (>133.33 g/m^3d), no change of pH was detected.

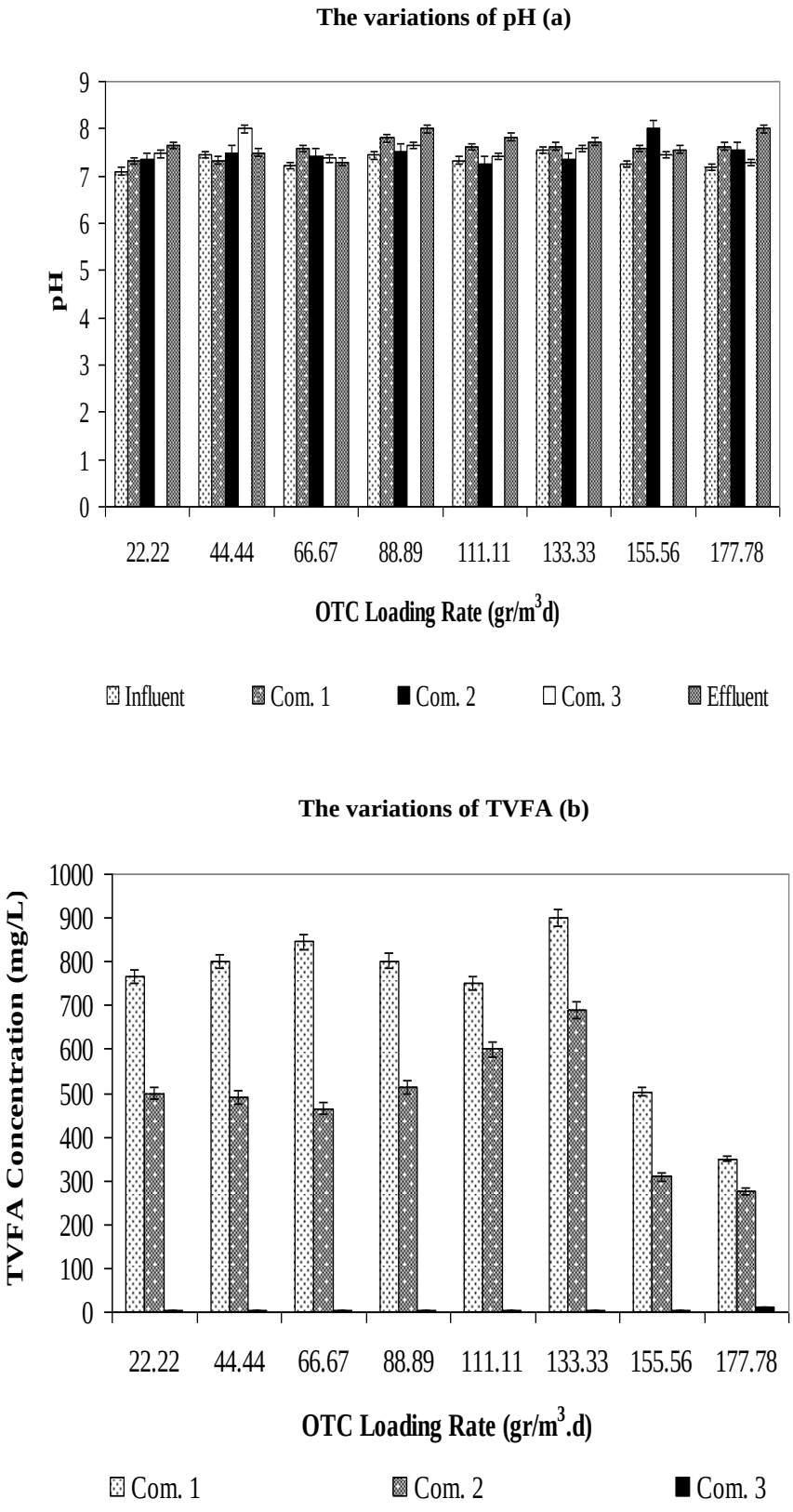

Figure 6.24 The variations of pH (a) and TVFA (b) in AMCBR at increasing OTC loading rates

The TVFA concentration in the 1st compartment was measured between 750 and 900 mg/L for the OTC loading rates between 44.44 and 133.33 g/m^{3}d, respectively. Almost 490-690 and 2 mg/L TVFA concentrations were detected in the 2nd and 3rd compartments of the AMCBR respectively, for the OTC loading rates given above. It was found that the TVFA concentrations decreased from compartment 1st to compartments 2nd and 3rd. The TVFA concentrations were measured as 276 and 350 mg/L at OTC loading rate as high as 177.78 g/m^{3}d due to inhibition effects of high OTC concentrations to acidogens in the 1st and 2nd compartments of the AMCBR. It was found that the minimum total TVFA value in the effluent was approximately 2 mg/L at OTC loading rates of 44.44 and 133.33 g/m^{3}d while the TVFA level was 10 mg/L at OTC loading 177.78 g/m^{3}d in the 3rd compartment. A significant linear relationship was found between OTC loading rates up to an OTC loading rate of 155.56 g/m^{3}d (Only for OTC loadings between 22.22 and 133.33 g/m^{3}d) and TVFA production (ANOVA), (R^2= 0.88, F =5.14, p =0.02).

As mentioned earlier, during the first step of anaerobic treatment TVFAs are produced by the microorganisms in the process of hydrolysis and acidification (Zaman, 2010). TVFA production at this stage depends mainly on wastewater characteristics, environmental conditions such as temperature and pH, reactor type and operating parameters such as HRT on the toxic compounds present in the anaerobic system (Owen et al., 1979). In the hydrolysis step, the acidogens convert the complex organics to carbon dioxide (CO_2) and hydrogen (H_2). Anaerobic degradation involves a series of biochemical reactions in the degradation of complex organic matter into CH_4 and CO_2. These reactions are often classified into hydrolysis, acidogenesis, acetogenis, and methanogenesis. TVFAs, which act as the most important intermediate products in the acidogenesis and acetogenesis steps, play a key role in the overall process. High levels of TVFAs may cause inhibition of methanogenesis and even reactor failure. Propionate and butyrate are C_3 and C_4 TVFAs, which are to be converted into acetate and H_2 in the acetogenesis stage before the final conversion into methane. Acetate would be degraded further to CH_4 and CO_2 in the terminal stage of methanogenesis (Wong et al., 2008).

6.2.2.5.1 TVFA Components. The determination of TVFA composition in the anaerobic treatment is important, since it provides significant information regarding the metabolic pathway of the process. Four major TVFAs, namely H_{ac}, H_{pr}, H_{ba} and H_{la} were produced throughout the operation of the AMCBR reactor. The other TVFAs were detected at insignificant concentrations. The intermediates produced during the anaerobic biodegradation of an organic compound are mainly $H_{ac,}$ H_{pr}, H_{ba} and H_{la} (see Table 6.8). As shown in Table 6.8, it was found that H_{pr}, H_{ba} and H_{la} were converted to H_{ac} in anaerobic conditions.

Table 6.8 Scheme of the anaerobic reactions of the main wastewater

TVFA composition	**Anaerobic reaction**
H_{ac}	$CH_3COOH \rightarrow CH_4 + CO_2$
H_{ba}	$CH_3CH_2CH_2COOH + 2H_2O \rightarrow 2CH_3COOH + 2H_2$
H_{pr}	$CH_3CH_2COOH + 2H_2O \rightarrow CH_3COOH + 3H_2 + CO_2$
H_{la}	$CH_3CHOHCOOH + H_2O \rightarrow CH_3COOH + 2H_2 + CO_2$

TVFAs are important intermediate compounds in the metabolic pathway of methane fermentation and cause microbial stress if present in high concentrations. This results in a decrease of pH, ultimately leading to failure of the digester. Therefore, the monitoring of TVFA concentrations is very important for the operation performance of an anaerobic digester. It is therefore necessary to investigate the optimum conditions and efficiencies by examining TVFA concentrations (Büyükkamacı and Filibeli, 2004). Mainly acetic, butyric and propionic acids were detected at significant concentrations in the 1st and in the 2nd compartment of the AMCBR. H_{ac}, H_{pr}, H_{ba} and H_{la} are short TVFAs formed directly from the anaerobic degradation of molasses-COD. At low OTC loading rates, Hac is considered to be the major precursor of methane (see Table 6.9). Therefore, conversion of TVFA to H_{ac} and to HCO_3 alkalinity was higher than that of H_{pr}, in the 1^{st} compartment of the AMCBR. The composition of the TVFA is also given in Table 6.8. It is seen that 305 and 485 mg/L H_{ac} was produced by acidogens at OTC loading rates 44.44 and 133.33 g/m^3d, respectively, in the 1^{st} compartment of the AMCBR. However, the Hac production decreased to 150 mg/L at OTC loading rates

higher than 133.33 g/m^{3}d in the 1st compartment of AMCBR due to the toxicity of high OTC concentrations to the acidogens.

In this study it was found that the H_{ac} concentrations decreased to 180 from 485 mg/L at an OTC loading rate of 133.33 g/m^{3}d due to the utilization of H_{ac} by the acetoclastic methanogens to form CO_2 and methane in the 2nd compartment of the AMCBR (Table 6.9). In other words, approximately 54% of 485 mg/L H_{ac} was consumed by acetoclastic methanogens in the AMCBR. The H_{pr} productions were 280 and 100 mg/L in the 1st compartment of AMCBR at OTC loading rates of 133.33 and 177.78 g/m^{3}d, respectively. This fraction of TVFA increased to 310 mg/L in the 2nd compartment of the AMCBR reactor after H_{ac} was consumed at an OTC loading rate of 133.33 g/m^{3}d (Table 6.9). It was found that both H_{pr} and H_{ba} were converted to H_{ac} at all OTC loading rates. H_{ac} was ultimately degraded and consumed by the methanogens and concentrations of it were as low as 2 mg/L in the 3rd compartment at low OTC loadings. The utilization of H_{pr} increased in the 2nd compartment at low OTC loadings. The H_{ba} reached a maximum value of 200 mg/L after Hac and Hpr were consumed by the methanogens and acetogens in the 2nd compartment. In this study the TVFA composition results were similar to those obtained by Kaparaju et al., (2009). The TVFA levels and the TVFA components decreased at high OTC and organic loadings. As mentioned in recent literature the methanogens were affected by high OTC concentration or by homo acetogenic bacteria forming methane from the acetate at high OTC loading (Arıkan et al., 2006; Arıkan et al., 2008). The production of hydrogen and CO_2 from the acetate by homo acetogenic bacteria also decreased for hydrogen-utilizing methanogens. In this study the fatty acids which had more than 3-C chain (H_{pr}, H_{ba}) with higher molecular weights probably cannot be converted into methane directly (Sentürk et al., 2010). Therefore, they are converted into methane followed by conversion into H_{ac} at high OTC loading rates.

Table 6.9 TVFA production and composition on days 50 throughout continuous operation of AMCBR reactor

Parameter	AMCBR, 1st compartment				AMCBR, 2nd compartment				AMCBR, 3rd compartment			
	OTC Loading Rate				OTC Loading Rate				OTC Loading Rate			
	44.44	111.11	133.33	177.78	44.44	111.11	133.33	177.78	44.44	111.11	133.33	177.78
TVFA[a]	800±15.2	750±9.0	900±19.6	350±7.5	490±7.6	600±8.2	690±9.6	276±2.8	2±0	2±0	2±0	10±0.3
H_{ac}[b]	305±3.1	400±5.2	485±6.3	150±1.5	120±1.0	140±2.0	180±4.3	90±2.0	2±0	2±0	2±0	10±0.2
H_{pr}[c]	240±9.1	220±8.2	280±10.2	100±7.5	300±5.5	280±9.2	310±4.5	87±0.5	0	0	0	0
H_{ba}[d]	105±7.0	38±0.7	100±5.8	56±0.8	120±1.1	180±3.6	200±5.0	80±0.8	0	0	0	0
H_{la}[e]	0	0	0	0	45±0.9	35±0.5	56±1.2	23±0.2	0	0	0	0

a: TVFA Conc. (mg/L); b: Acetic Acid Conc. (mg/L); c: Propionic Acid Conc. (mg/L); d: Butyric Acid Conc. (mg/L); e: Lactic Acid Conc. (mg/L)

6.2.2.6 Variation of Bicarbonate Alkalinity and TVFA/HCO_3 Ratio in Compartments of the AMCBR at Increasing OTC Loading Rates

The HCO_3, TVFA/HCO_3 ratio variations in all compartments of the AMCBR reactor at increasing OTC concentrations (from 50 mg/L up to 400 mg/L) were shown in Figure 6.25. Since CO_2 often exceed other weak acids in aqueous anaerobic systems with microbial activity, sufficient bicarbonate alkalinity must be present to neutralize it and is therefore of prime importance. If the acid concentrations exceed the available alkalinity, the reactor will sour, severally inhibiting microbial activity, especially the methanogens (Speece, 1996). The HCO_3 concentrations remained between 2600 and 3200 mg/L in the effluent of AMCBR at increasing OTC concentration (see Figure 6.25 (a)). The HCO_3 concentration in the 1st compartment was lower than the other compartments. This indicates the utilization of alkalinity to buffer the TVFA and CO_2 produced from the anaerobic co-metabolism of OTC, particularly at high concentrations.

Figure 6.25 (a) shows the variation of HCO_3 alkalinity versus OTC loading rates. Figure 6.25 (a) indicates that the HCO_3 levels were low (between 1046 and 1168 mg/L) in the 1st compartment for all OTC concentrations (50-400 mg/L) and OTC loadings (22.22-177.78 g/m^{3}d). However, in 3rd compartment, the HCO_3 alkalinity concentrations increased from 1827 mg/L to 2292 mg/L at an OTC concentration of 300 mg/L corresponding to OTC loading rate of 133.33 g/m^{3}d. Although the HCO_3 concentration increased as the OTC loadings increased from 22.22 up to 133.33 g/m^{3}d. A significant linear correlation between HCO_3 alkalinity and increasing OTC concentration was not observed (ANOVA), (R^2=0.57, F=11.07, p=0.02).

TVFA/HCO_3 ratio gives necessary information to determine the stability of the anaerobic reactor. The ratio of TVFA/HCO_3 is an important indicator of the acid-base equilibrium and process stability, (Lorestani et al, 2006; Sanchez et al., 2005). When this ratio is less than 0.3-0.4, the process is considered to be operating favorably without the risk of acidification. The measurement of quantity and composition of the biogas produced, in terms of methane and carbon dioxide content,

is of fundamental importance to evaluate the stability of the process, (Lorestani et al., 2006). When the process is stable the amount and composition of biogas are stable too. A decrease in biogas production contemporary to an increase in CO2 content can indicate an inhibition of the methanogenesis of the system. In fact, TVFA/HCO_3 ratio and biogas composition are strictly linked one to each other. When the TVFA/HCO_3 ratio is lower than 0.4, the reactor is stable (Behling et al, 1997). When the TVFA/HCO_3 ratio is lower than 0.8, the reactor system is moderately stable or unstable (Behling et al, 1997). As shown in Figure 6.25 (b), this ratio varied between 0.001 and 0.4 in every compartment of AMCBR at increasing OTC concentrations. These results indicated that AMCBR reactor was stable at increasing OTC concentration because the TVFA/HCO_3 ratios in the effluent and in the compartments were lower than 0.4.

Generally it was found that in the 1st compartment of the AMCBR reactor the acidogenesis is the major step of the anaerobic treatment. The 3rd compartment is the major removal step for methanogenesis. Therefore the TVFA concentrations were high while the HCO_3 alkalinities were low in the 1st compartment of AMCBR.

(a) The variations of HCO_3

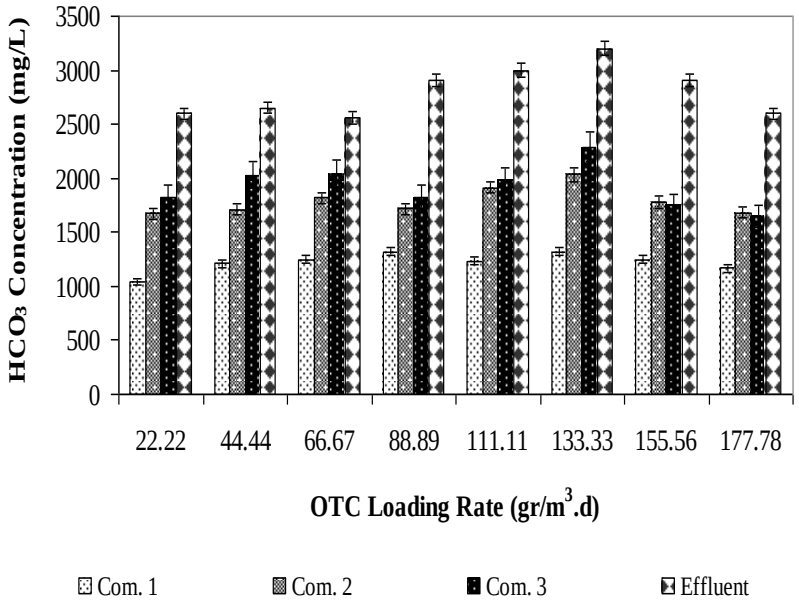

(b) TVFA/HCO_3 ratio

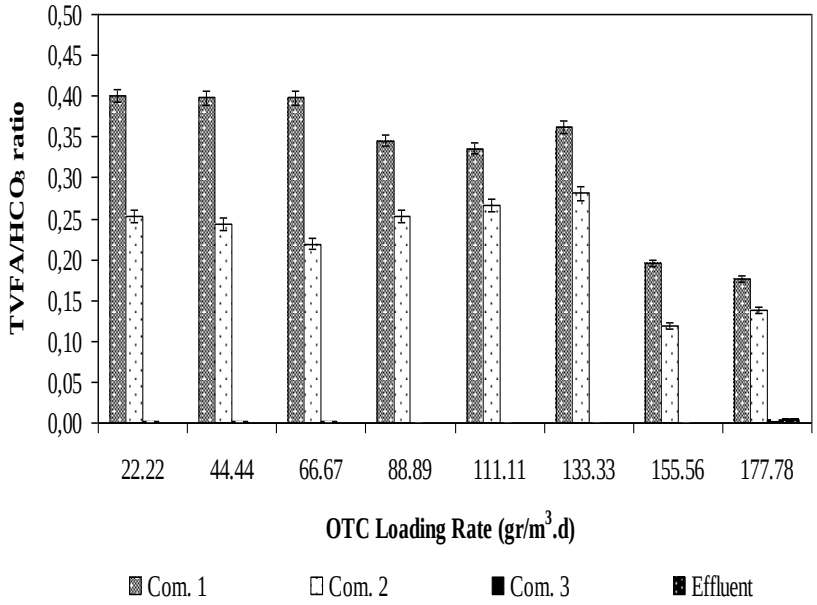

Figure 6.25 The variations of HCO_3 **(a)** and TVFA/HCO_3 ratio **(b)** in AMCBR at increasing OTC loading rates

6.2.2.7 Performance of the Aerobic CSTR Reactor

Table 6.10 shows the effect of increasing OTC loading rates on the COD and OTC removals in the aerobic CSTR reactor. The COD removal efficiencies were around 90% for OTC loading rates of 22.22, 44.44 and 66.67 g/m^3d, respectively in the CSTR. The OTC yields were 85%, 80% and 76% for the aforementioned OTC loading rates. The maximum COD and OTC removal efficiencies were 91% and 90% for OTC loading rates of 133.33 g/m^3d, respectively. The COD removal efficiencies were 76% and 65% for OTC loadings of 155.56 and 177.78 g/m^3d, respectively in the CSTR reactor. The OTC yields decreased to 70% and 65% at OTC loading rates of 155.56 and 177.78 g/m^3d, respectively. The COD and OTC removal efficiencies decreased at high OTC loading rates in the aerobic CSTR reactor. Since the effluent of the AMCBR was used as the feed in the influent of the CSTR; the COD and the OTC remaining from the AMCBR were removed in the CSTR. This means that the COD and OTC were mainly biodegraded in the AMCBR.

Table 6.10 COD and OTC yields in CSTR at eight different OTC loading rates

Parameters	**OTC Loading Rates (g/m^3d)**							
	22.22	**44.44**	**66.67**	**88.89**	**111.11**	**133.33**	**155.56**	**177.78**
COD_{inf}[a]	300	350	354	500	365	205	485	800
COD_{eff}[b]	30	35	36	75	55	18.5	97	200
R_{COD}[c]	90	90	90	85	85	91	80	75
OTC_{inf}[d]	2.5	3	3	6	3	3	70	85
OTC_{eff}[e]	0.38	0.60	0.72	1.62	0.75	0.30	21	30
R_{OTC}[f]	85	80	76	73	75	90	70	65

a: COD conc. in inf. (mg/L); b: COD conc. in efl. (mg/L); c: COD Rem. Eff. (%); d: OTC conc. inf. (mg/L)
e: OTC conc. in efl. (mg/L); f: OTC Rem. Eff. (%)

The aerobic CSTR reactor was used to remove the residual COD and OTC entering from the AMCBR reactor and mineralization of the intermediate products. Figure 6.26 shows the α-Apo-OTC and ß-Apo-OTC removal efficiencies in the aerobic CSTR reactor. α-Apo-OTC and ß-Apo-OTC produced in AMCBR reactor was mineralized in the CSTR reactor. Approximately 70-100% mineralization of α-Apo-OTC and ß-Apo-OTC was observed in aerobic phase (see Figure 6.26). α-Apo-OTC and ß-Apo-OTC removal efficiencies were 100% until an OTC loading rate of 133.33 g/m^3d in the aerobic CSTR reactor. After this OTC loading rate, α-Apo-OTC and ß-Apo-OTC removal efficiencies decreased from 80% to 75% and from 84% to 70% at OTC loading rates of 155.56 and 177.78 g/m^3d, respectively.

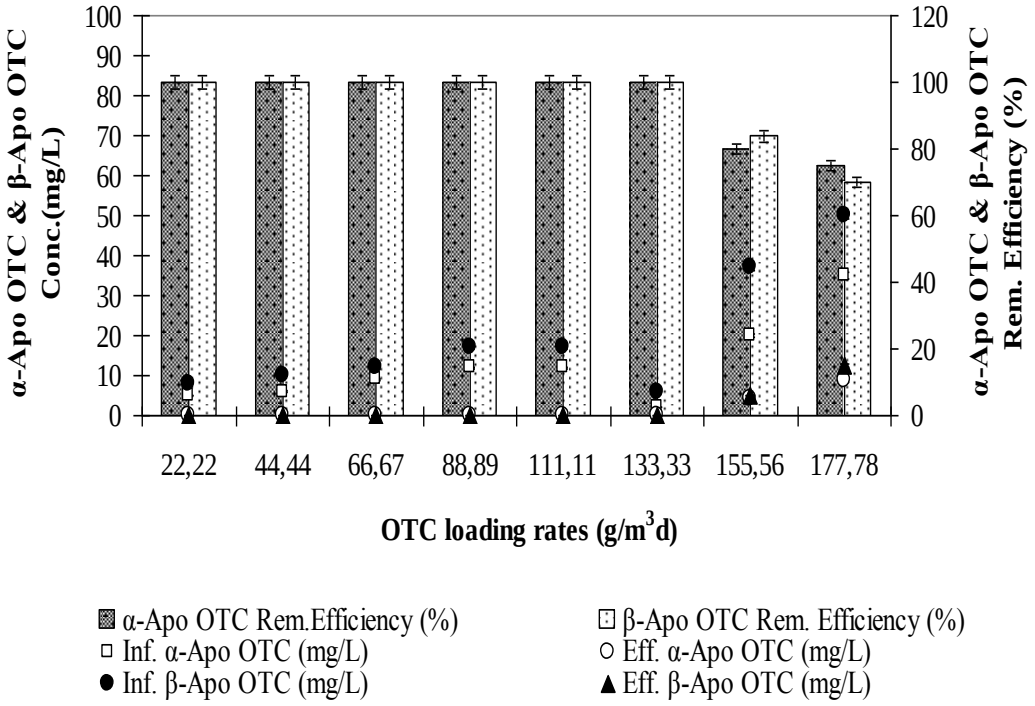

Figure 6.26 The α-Apo-OTC and ß-Apo-OTC removal efficiencies in aerobic CSTR reactor

6.2.2.8 Performance of Anaerobic/Aerobic Sequential Reactor System

Figure 6.27 shows the removal efficiencies of COD, OTC at eight studied OTC loading rates in the AMCBR/CSTR system. The COD removals in the total sequential AMCBR/CSTR system were ≥ 95% at all OTC loading rates while the OTC yields were found to be ≥ 92%. The maximum COD and OTC yields were 100% at OTC loading rates 133.33 g/m^{3}d, while the lowest COD and OTC removals were 95 and 92% at an OTC loading rates of 177.78 g/m^{3}d, respectively in the sequential AMCBR/CSTR system. 97% of the COD and 99% of the OTC were removed in the anaerobic AMCBR reactor while the remaining COD and OTC 3% of COD and 2% of OTC were biodegraded in the aerobic CSTR reactor. This showed that a significant part of the OTC could be removed with high removal efficiency in the sequential AMCBR/CSTR system.

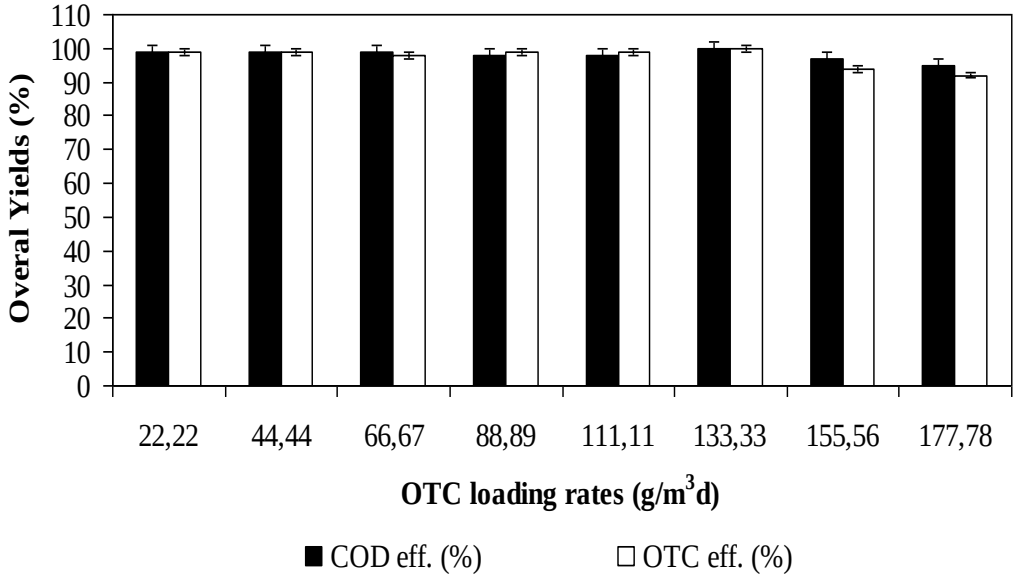

Figure 6.27 The total performance of sequential AMCBR/CSTR reactor system

In a study carried out by Zhang et al., (2012) 85% both OTC and COD yields were obtained at an influent COD and OTC concentration of 5145 and 80 mg/L, respectively, in a combined anaerobic/two-stage aerobic reactor at a HRT of 2 days. In our study the OTC and COD removal efficiencies are higher than this study although the influent OTC concentration is comparably higher than the study performed by Zhang et al., (2012). The literature survey showed that the OTC yields obtained in old studies are lower than those in our data: 65% COD and 60% antibiotic removals was obtained by Gao et al., (2012) in a sequential anaerobic baffled and aerobic film reactor system to remove pharmaceutical wastewaters containing OTC at 8500 mg/L COD and at a HRT of 2.65 days.

The biotransformation of OTC to α-Apo-OTC and ß-Apo-OTC was observed in the reductive anaerobic phase. A transformation of 48-92% of α-Apo-OTC and ß-Apo-OTC were found to be in the anaerobic AMCBR reactor (see Table 6.11). A mineralization of 70-100% of α-Apo-OTC and ß-Apo-OTC were found to be in the aerobic CSTR reactor (Table 6.11).

Table 6.11 The AMCBR, CSTR and AMCBR/CSTR system treating α-Apo-OTC and ß-Apo-OTC removal

Anaerobic AMCBR Reactor							Aerobic CSTR Reactor						Sequential AMCBR/CSTR System					
OLR	α-Apo-OTC			ß-Apo-OTC			α-Apo-OTC			ß-Apo-OTC			α-Apo-OTC			ß-Apo-OTC		
	Inf.	Eff.	Rem.	Inf.	Eff.	Rem.	Inf.	Eff.	Rem.	Inf.	Eff.	Rem.	Inf.	Eff.	Rem.	Inf.	Eff.	Rem.
22.22	0	5	77	0	8	76	5	0	100	8	0	100	0	0	100	0	0	100
44.44	0	6	80	0	10	80	6	0	100	10	0	100	0	0	100	0	0	100
66.67	0	9	84	0	12	76	9	0	100	12	0	100	0	0	100	0	0	100
88.89	0	12	82	0	17	69	12	0	100	17	0	100	0	0	100	0	0	100
111.11	0	12	85	0	17	71	12	0	100	17	0	100	0	0	100	0	0	100
133.33	0	2	92	0	6	90	2	0	100	6	0	100	0	0	100	0	0	100
155.56	0	20	67	0	37	56	20	4	80	37	6	84	4	0	100	6	0	100
177.78	0	35	60	0	50	48	35	9	74	50	15	70	9	0.2	98	15	0.5	97

OLR =OTC loading rate (g/m^{3}d); Inf. = Influent concentration (mg/L); Eff. = Effluent concentration (mg/L); Rem. = Removal efficiency (%)

6.2.3 Effect of Increasing AMX Concentration on Performance of AMCBR Reactor

6.2.3.1 Effect of Increasing AMX Concentration on the COD Removal Efficiencies in the AMCBR Reactor

In this step of the study, the effect of increasing AMX concentrations on COD removal efficiencies was investigated. The operation of the AMCBR with AMX was started at an influent AMX concentration of 50 mg/L and an AMX loading rate of 22.22 g/m^{3}d. Then the AMX concentrations were subsequently increased from 100 to 150, 200 and 250 to 300 mg/L corresponding to AMX loading rates of 44.44, 66.67, 88.89, 111.11 and 133.33 g/m^{3}d. The variations of COD with increasing AMX loading rates are shown in Figure 5.28. The COD equivalents of AMX concentration are shown in Table 6.12.

Table 6.12 The COD equivalents of AMX concentration

Parameters	Unit	Concentrations
Molasses-COD concentration	mg/L	4000; 4005; 4010; 3990; 4000; 4025
AMX concentration	mg/L	50; 100; 150; 200; 250; 300
COD equivalent of AMX	mg/L	25; 35; 40; 45; 55; 65
Total COD concentration	mg/L	4025; 4040; 4050; 4035; 4055; 4090

As shown in Figure 6.28, the COD removal efficiency was 88% at AMX loading rates varying between 22.22 and 44.44 g/m^{3}d. When the AMX loading rate was increased to 66.67 g/m^{3}d corresponding an AMX concentration of 150 mg/L the COD removal efficiency increased to 94%. The COD yield was 86% for AMX loading rate of 88.89 g/m^{3}d in the anaerobic AMCBR reactor. As shown in Figure 6.28, the COD removal efficiency was 80% at an AMX loading rate of 111.11 g/m^{3}d. When the AMX loading rate was increased from 111.11 and 133.33 g/m^{3}d, at corresponding AMX concentration of 300 mg/L, the COD removal efficiencies decreased from 80% to 66%. The effluent COD concentrations also were approximately 286 mg/L until an AMX loading rate of 66.67 g/m^{3}d. After this AMX

concentration (150 mg/L), COD removal efficiency decreased rapidly from 80% to 66%. The effluent COD concentration and removal efficiency were measured as 1456 mg/L and 66%, respectively, at a maximum AMX loading rate of 133.33 g/m^{3}d. The optimum AMX loading rate and AMX concentration were found as 66.67 g/m^{3}d and 150 mg/L, respectively, for maximum COD removal efficiency of 94%. The results obtained in this study showed that AMX could be used as carbon source together with molasses-COD with high treatment efficiencies in AMCBR reactor. A significant linear relationship was found between the COD yields and the AMX loading rates (Only for AMX loading rates between 22.22-66.67 g/m^{3}d) (ANOVA), (R^2=0.89, F=5.36, p=0.02).

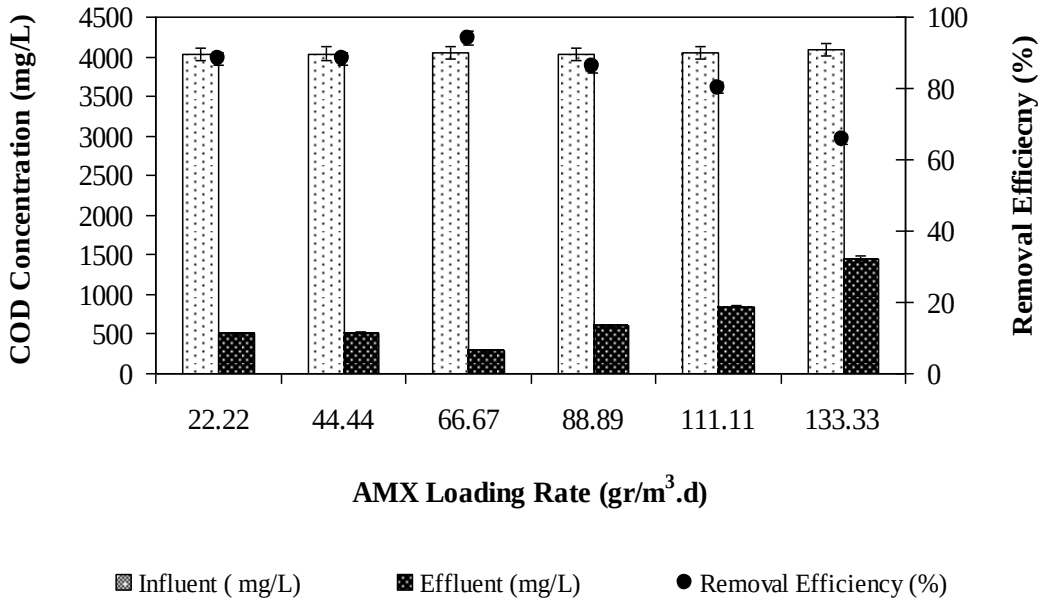

Figure 6.28 Effects of increasing AMX loading rates on COD removal efficiencies in the AMCBR

The COD yields obtained in recent studies were low in comparison with the COD removals in this study. In the study by Chen et al., (2011) 60% COD removal efficiency was obtained at a HRT of 2 days in an UASB reactor at an influent AMX concentration of 61 mg/L. In the study performed by Zhou et al., (2006), the COD (E=67%) yield was lower than those of our data (94% for COD) at a HRT of 3 days in an anaerobic contact reactor (ACR) treating 3.2 mg/L AMX. In another study, Sreekanth et al., (2009) reported that in a hybrid up flow anaerobic sludge blanket

reactor (HUASB) at an influent COD concentration of 13000-15000 mg/L (E=65-75% COD removal efficiency) at a HRT of 2 days. The above results are consistent with observations made by Akbarpour and Mehrdadi, (2011) in an UASB reactor, treating a chemical synthesis-based pharmaceutical wastewater. The COD yield was 54.6% at a HRT of 1.4 days. Results of aforementioned studies are in disagreement with a stable COD yield reported in the anaerobic reactors (UASB, ACR and HUASB) since the raw pharmaceutical wastewater contained different AMX and COD concentrations. This inconsistency is presumably attributed to the daily varying wastewater concentrations, with different AMX and COD loading rates in aforementioned studies. In our study, 94% COD removal was measured at the influent COD concentration 4050 mg/L. The yields obtained in the aforementioned studies are low in comparison to the removal performances of COD found in this study. The high COD removal efficiencies in the AMCBR reactor could be explained by the reactor configuration, operational conditions, seed properties and AMX loading rates used throughout reactor operation.

6.2.3.2 Effect of AMX Loading Rate on the AMX Removal Efficiencies in the AMCBR Reactor

In this study, AMX concentration in the synthetic pharmaceutical wastewater feed varied from 50 to 300 mg/L and Figure 6.29 shows the AMX removal efficiencies profile throughout the experimental study in the AMCBR reactor. The AMX removal efficiency of 90% was obtained at an initial AMX loading rate of 22.22 g/m^3d. When the AMX loading rate was increased from 22.22 to 66.67 g/m^3d the AMX removal efficiency remained stable between 90% and 93%. A maximum AMX removal efficiency of 93% was obtained at an initial AMX concentration of 150 mg/L at an AMX loading rate of 66.67 g/m^3d in the AMCBR. The effluent AMX concentration was measured as 10 mg/L at an AMX loading rate of 66.67 g/m^3d. The AMX yields were between 90% and 80-85% for AMX loading rates of 44.44-88.89 g/m^3d and 111.11-133.33 g/m^3d, respectively, in the AMCBR reactor. When the AMX loading rate was increased from 88.89 g/m^3d to 111.11 and to 133.33 g/m^3d the AMX removal efficiency decreased from 90% to 85% and 80%, respectively, in the

AMCBR reactor (Figure 6.29). The results obtained in this study showed that AMX could be used as co-substrate together with molasses-COD with high removal efficiencies in AMCBR reactor. A significant linear correlation between AMX yields and increasing AMX loading rate (only for AMX loading rates between 22.22-66.67 g/m^{3}d) was observed (ANOVA), (Figure 6.29) (R^2= 0.91, F=4.86, p=0.01).

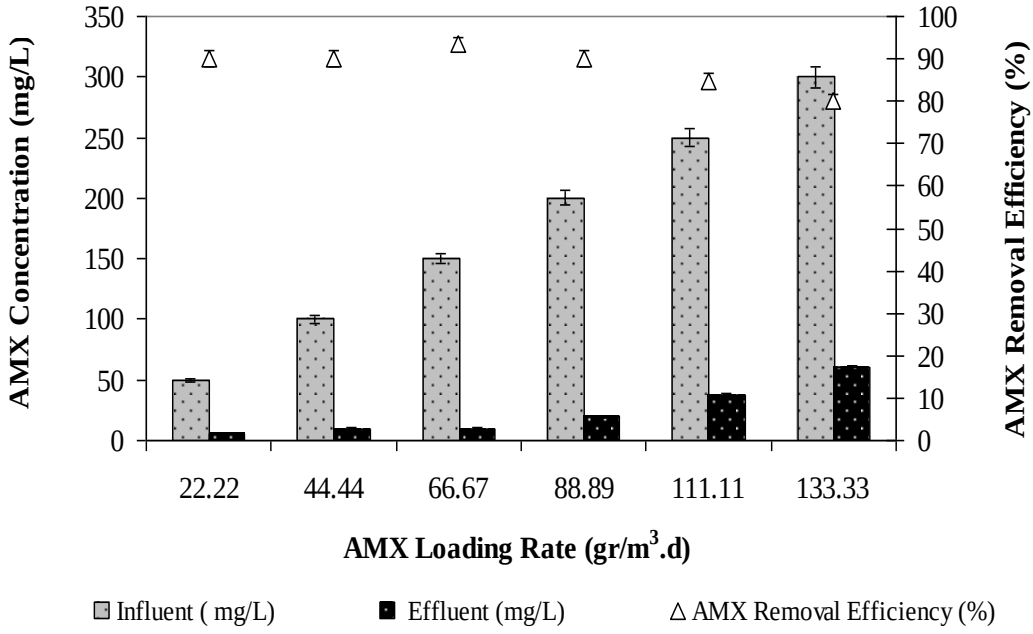

Figure 6.29 The effect of AMX loading rate on AMX removal efficiencies in the AMCBR reactor

The recent literature on the anaerobic AMX treatment showed that the yields obtained in some high rate anaerobic reactors are lower than the AMX removals found in our study: In a study performed by Chen et al., (2011) 34% AMX removal efficiencies were obtained at a HRT of 2 days in an UASB reactor at an influent AMX concentration of 61 mg/L. In the study performed by Zhou et al., (2006), the AMX (40%) yields were lower than those of our data (93% for AMX) at a HRT of 3 days in an anaerobic contact reactor treating 3.2 mg/L AMX.

Similarly, in the studies performed by Zhou et al., (2006) lower antibiotic removals were found than those in our study. Zhou et al., (2006) reported that when HRT of an anaerobic baffled reactor treating pharmaceutical wastewater containing antibiotics (Ampicillin and Aureomycin) was extended from 1.25 to 2.5 days, the

COD removal efficiency increased from 77% to 85%. They also observed that the antibiotic removal efficiencies increased from 16 to 42% for Ampicillin and 26 to 31% for Aureomycin. Deng et al., (2012) achieved that the AMX removal was found to be lower (82%) under anaerobic conditions at an influent AMX concentration of 78 mg/L at a HRT of 1.56 days.

Similarly Pallavi et al., (2009) reported that lower AMX yields 65% than those found in our study at a HRT of 1.95 days and at an influent AMX concentration of 89 mg/L. The yields obtained in the aforementioned studies are low in comparison to the removal performances of AMX found in our study. In other words; in our study, the high AMX yields in the AMCBR could be due to the reactor configuration, operational conditions, seed properties and AMX loading rates used throughout reactor operation.

6.2.3.3 Effect of AMX Loading Rate on the Biogas Production and CH_4 Content in the AMCBR Reactor

The effect of organic loading rate on biogas composition can be used as a direct indicator of the vitality of the anaerobic degradation. Biogas composition was monitored in the anaerobic AMCBR reactor throughout the operation, mainly for the assessment of methanogenic activity. Figure 6.30 illustrates the methane productivity and showed that the reactor had relatively higher levels of methane content (around 50-55%) during the period of low AMX loading rates (22.22-66.67 g/m^3d), but this was reduced to 48% when the AMX loading rates was increased to 111.11-133.33 g/m^3d. The decrease in methane content of biogas is generally observed when the rate of acid formation exceeds the rate of break down to methane at high loading rates (Ince et al. 2002; Kim and Aga, 2007). The total, methane gas productions and methane contents were approximately 8-12 L/d, 4.2-6.5 L/d and 48-55%, respectively, for AMX loadings varying between 22.22 and 133.33 g/m^3d. The maximum total, methane gas productions and methane content were found as 12 L/d and 6.5 L/d and 55%, respectively, at an AMX loading rates of 66.67 g/m^3d. A significant linear relationship was found between the biogas productions and the

AMX loading rates (22.22-66.67 g/m^3d) (ANOVA), (R^2=0.95, F=3.96, p=0.02) (for total gas). (R^2=0.91, F=4.80, p=0.01 (for methane gas). Similarly, a linear relationship was found between the methane content and the AMX loading rates (Only for AMX loading rates between 22.22-133.33 g/m^3d) and this relationship is significant (ANOVA), (R^2=0.90, F=5.06, p=0.02). High AMX concentrations cause a greater inhibitory effect on one or more of the major metabolic bacterial groups in the AMCBR reactor. Lallai et al., (2002) also reported an increase in the accumulation of volatile fatty acids and a decrease in gas production upon the application of increasing amounts of antibiotic to methane reactor.

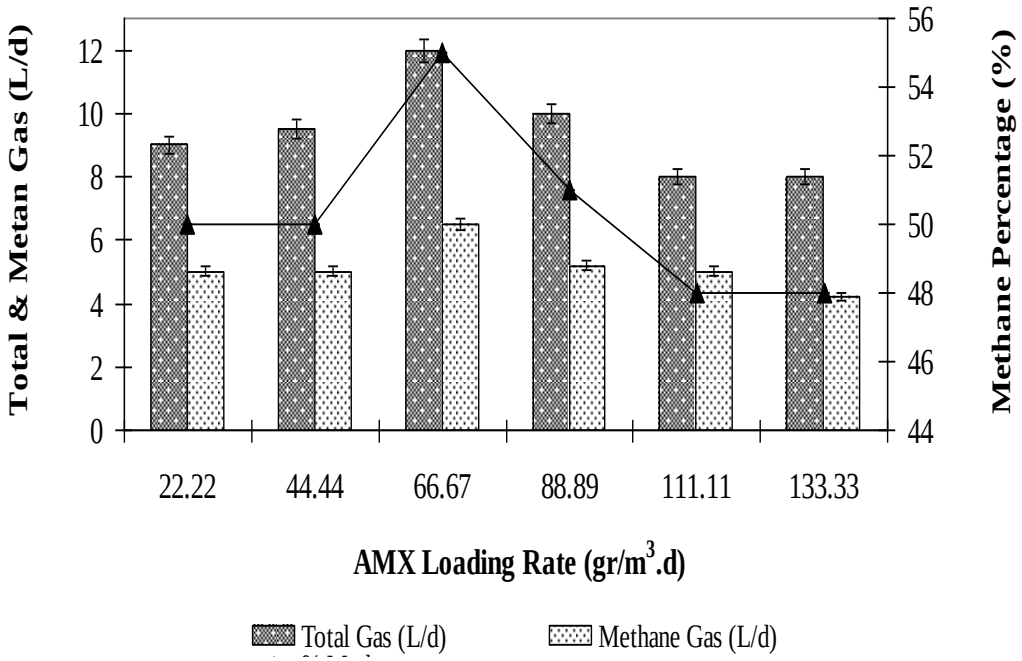

Figure 6.30 The effect of AMX loading rate on total, methane gas production and methane content in the AMCBR reactor

In this study, the methane yield can be a useful parameter to assess the performance of the AMCBR. As the treatment of wastewater is directly related to the amount of methane produced, the amount of methane generated per kg of COD stabilized is taken to be an indicator of AMX and COD stabilization degree. Figure 6.31 shows the variations of methane yields versus AMX loading rates. The methane yields decreased from 0.34 to 0.09 $m^3CH_4/kgCOD_{removed}$, when the AMX loading

rates were increased 22.22 to 133.33 g/m^3d. A significant linear relationship was found between the methane yields and the AMX loading rates (only between 22.22 and 66.67 g/m^3d) (ANOVA), (R^2=0.93, F=5.06, p=0.01).

Lower methane yields (0.26-0.34 $m^3CH_4/kgCOD_{removed}$) were obtained in a study performed by Nandy and Kaul, (2001) throughout anaerobic treatment of fermentation-based herbal pharmaceutical wastewaters containing 48 mg/L AMX at a HRT of 2 days. Similarly, a lower methane yield value (0.19 $m^3CH_4/kgCOD_{removed}$) was obtained in the anaerobic treatment of chemical synthesis-based pharmaceutical wastewater at a HRT of 1.98 days (Ince et al., 2002). The lower methane yields in the studies mentioned above could be due to the configuration of the anaerobic reactor, type of anaerobic microorganism, to the biomass concentration and to the operational conditions.

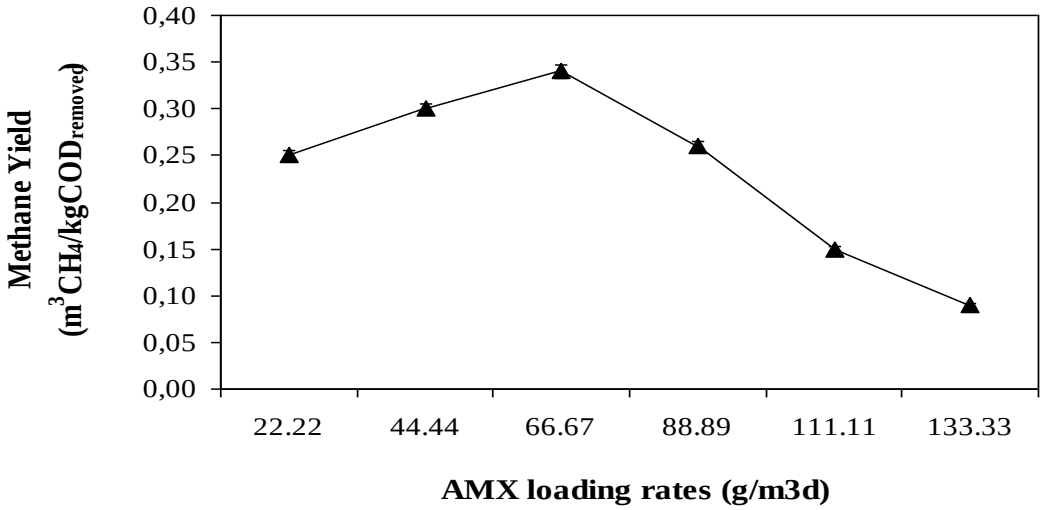

Figure 6.31 Variations of methane yields versus AMX loading rates in the AMCBR reactor.

6.2.3.4 Variations of pH, TVFA, HCO_3 Alk., TVFA/HCO_3 Alk. Ratio in the AMCBR at Increasing AMX Loading Rates

Microbial groups involved in anaerobic degradation have a specific pH region for optimal growth. The desired pH for anaerobic treatment is between 6.6-7.6 (Rittman and McCarty, 2001). Figure 6.32 shows the pH, TVFA, HCO_3 Alk., TVFA/HCO_3 Alk. ratio variation in compartments of the AMCBR at increasing AMX loading rates. As shown in Figure 6.32 (a), the pH values in the effluent and in the all compartments of AMCBR varied between 6.7 and 7.5. The pH values varied between 6.7 and 7.5 in compartment of AMCBR at all AMX concentrations. These values were between optimum pH values for anaerobic treatment as reported by Speece (1996). The pH values were lowers in 1st compartment than that the other compartments since TVFA in the 1st compartment is raised. The pH values were around 6.9 and 7.3 in the initial compartment at AMX loading rates of 22.22 and 133.33 g/m^{3}d, respectively.

The high TVFA concentrations in the anaerobic processes cause the inhibition of methanogenesis. Under anaerobic conditions of overloading and in the presence of inhibitors, methanogenic activity cannot remove hydrogen and volatile organic acids as quickly as they are produced. The result is the accumulation of acids and the decrease of pH to levels that also inhibit the hydrolysis or acidogenesis phase. It has also been shown that even when reactor pH is optimal, the accumulation of TVFAs may contribute to a reduced rate of hydrolysis of the solid organic substrate. Organic acids such H_{ac}, H_{pr}, H_{bu} and H_{la} are central to evaluating the performance of anaerobic degradation. The total TVFA concentration of the AMCBR reactor is shown in Figure 6.32 (b) and indicates a low concentration of TVFA (average 5 mg/L) was present in the AMCBR reactor effluent when operated at AMX loading rates in the range 22.22 to 111.11 g/m^{3}d. The TVFA concentration in the 1st compartment was measured between 408 and 605 mg/L (see Figure 6.32 (b)) for the AMX loading rates between 22.22 and 133.33 g/m^{3}d, respectively. Almost 256-512 and 5-25 mg/L TVFA concentrations were detected in the 2nd and 3rd compartments of the AMCBR respectively, for the AMX loading rates between 22.22 and 133.33

g/m^{3}d, respectively. It was found that the TVFA concentrations decreased from compartment 1st to compartments 2nd and 3rd. The TVFA concentrations were measured as 256 and 408 mg/L at AMX loading rate as high as 133.33 g/m^{3}d due to inhibition effects of high AMX concentrations to acidogens in the 1st and 2nd compartments of the AMCBR. It was found that the minimum TVFA value in the effluent was approximately 5 mg/L at AMX loading rates of 22.22 and 111.11 g/m^{3}d while the TVFA level was 15 mg/L at OTC loading 133.33 g/m^{3}d in the 3rd compartment. At high organic loading rates (OLRs), the relatively complex pharmaceutical wastewater caused pre-acidification resulting in accumulation of COD (as TVFA), which did not subsequently convert to methane, resulting in an accumulation of TVFA. In another word, short contact times between the substrate and biomass could have been favour the activity of acidogens, leading to a low conversion of substrate to methane by the biomass flocs, and substantial amounts of TVFAs being washed through the reactor into the effluent. According to previous studies, higher OLRs generally provide the optimum conditions for acid-forming bacteria and greatly affected TVFA production (Penoud et al., 1997; Elefsiniotis and Oldham, 1994).

The HCO_3 concentrations remained between 2800 and 3300 mg/L in the effluent of AMCBR at increasing AMX loading rates (see Figure 6.32 (c)). The HCO_3 alk. concentration in the 1st compartment was lower than the other compartments. This indicates the utilization of alkalinity to buffer the TVFA and CO_2 produced from the anaerobic co-metabolism of AMX, particularly at high concentrations. Figure 5.32 (c) indicates a low concentration of HCO_3 from 2050 mg/L down to 2330 mg/L was present in the 1st compartment when the AMCBR was operated at AMX loading rates in the range 22.22-133.33 g/m^{3}d. However, in 3rd compartment, the HCO_3 alkalinity concentrations increased to 3092 mg/L at an AMX loading rate 66.67 g/m^{3}d. The AMX loading rates increased from 22.22 to 44.44 g/m^{3}d the HCO_3 alkalinity concentrations increased from 3027 to 3092 mg/L at an AMX loading rate of 66.67 g/m^{3}d in 3rd compartment. As shown in Figure 6.32 (c), the HCO_3 alkalinity concentrations were 2323-2900, 2235-3000 and 2330-3300 mg/L at an AMX loading rates of 88.89, 111.11 and 133.33 g/m^{3}d, respectively in the effluent and all

compartment. A significant linear correlation between HCO_3 and increasing AMX loading rate was not observed (ANOVA), (R^2=0.63, F=12.06, p=0.02).

The TVFA/HCO_3 ratio gives necessary information to determine the stability of the anaerobic AMCBR reactor. If the TVFA/HCO_3 ratio is lower than 0.4, the reactor is stable or unstable as reported by Behling et al., (1997). As shown in Figure 6.32 (d), this ratio varied between 0.01 and 0.27 in compartments and the effluent of AMCBR at increasing AMX loading rates (22.22-133.33 g/m^3d). These results indicated that the AMCBR reactor treating AMX was operated under stable conditions at increasing AMX loading rates.

(a) Variations of pH

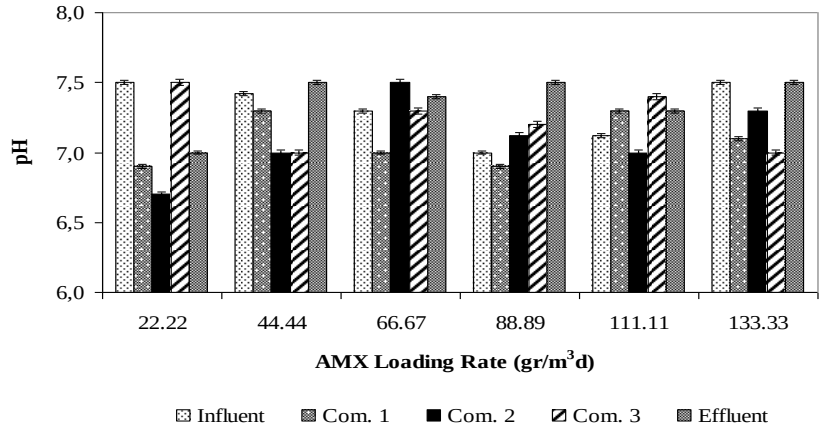

(b) Variations of TVFA

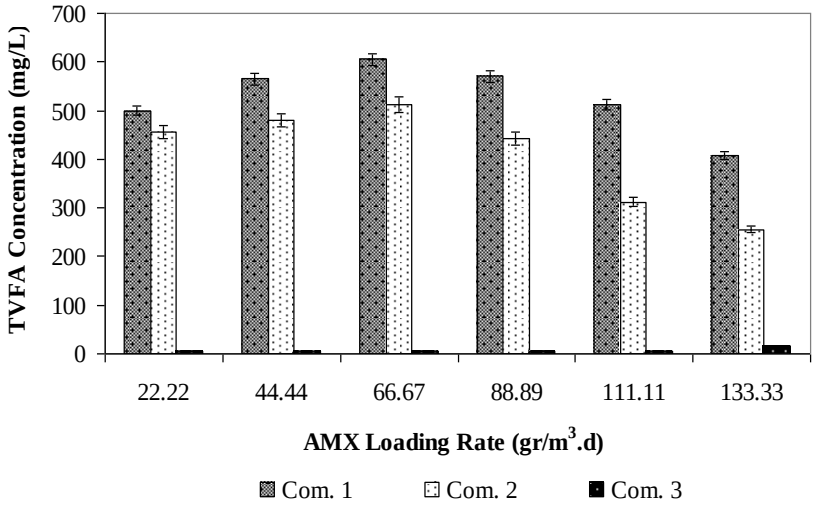

(c) Variations of HCO_3 Alk.

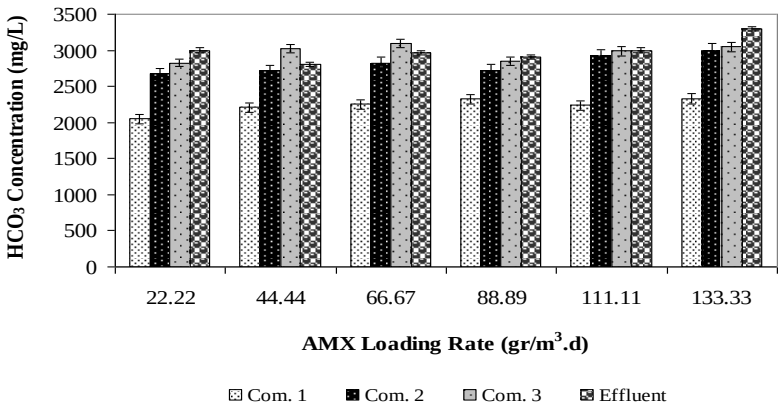

(d) Variations of TVFA/HCO_3 Alk. ratio

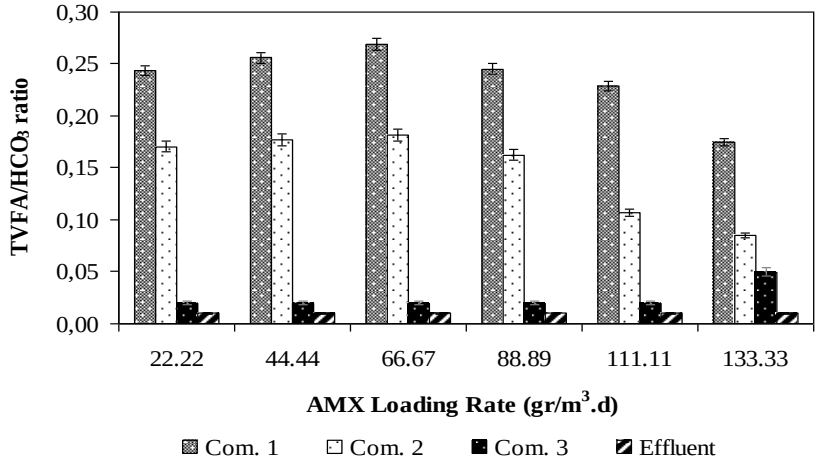

Figure 6.32 Variations of pH (a); TVFA (b); HCO_3 Alk. (c); and TVFA/HCO_3 Alk. ratio (d) in AMCBR at increasing AMX loading rates

6.2.3.5 Effect of AMX Loading Rate on the COD and AMX Removal Efficiencies in the CSTR Reactor

Figure 6.33 and 6.34 shows the effect of increasing AMX loading rate on the COD and AMX removals in the aerobic CSTR reactor. The COD removal efficiencies were around 80% for AMX loading rates of 22.22, 44.44 and 88.89 g/m^3d, respectively in the CSTR. As shown in Figure 6.33, the COD removal efficiency was 80% at an AMX loading rates of 22.22-44.44 g/m^3d. The COD yields were between 80 and 74% for AMX loading rates of 88.89–111.11 g/m^3d, respectively, in the CSTR reactor. The COD removal efficiency remained

approximately 88% until an AMX loading rate of 66.67 g/m^{3}d corresponding an AMX concentration of 150 mg/L. The effluent COD concentrations also were approximately 38 mg/L until an AMX loading rate of 66.67 g/m^{3}d. After this AMX concentration, COD removal efficiency decreased rapidly from 80% to 70%. The effluent COD concentration and removal efficiency were measured as 240 mg/L and 70%, respectively, at a maximum AMX loading rate of 133.33 g/m^{3}d. The optimum AMX loading rate was found as 66.67 g/m^{3}d for maximum COD removal efficiency of 88%.

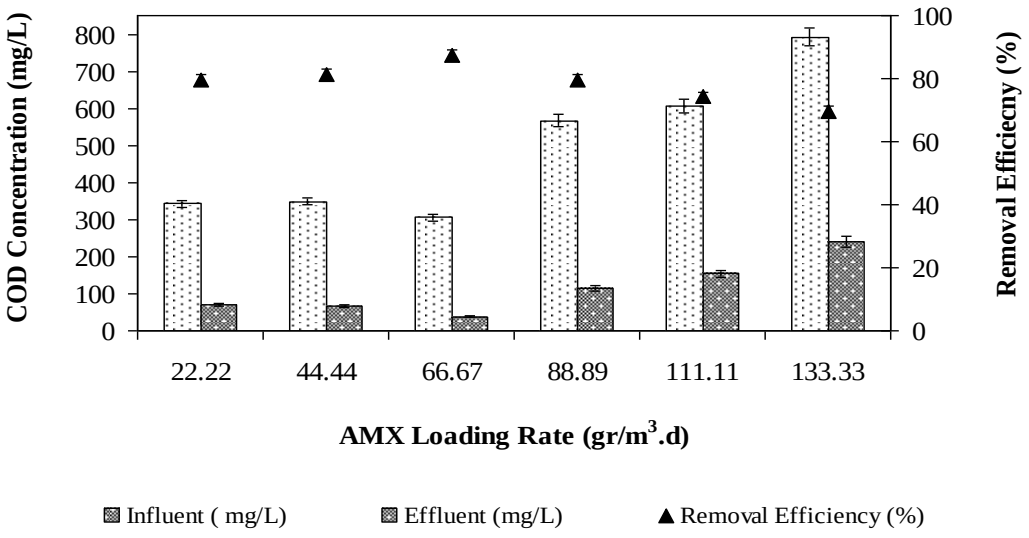

Figure 6.33 COD removal in the aerobic CSTR reactor at increasing AMX loading rates

The AMX removal efficiency of 80% was obtained at an AMX loading rate of 22.22 g/m^{3}d. When the AMX loading rate was increased from 22.22 to 66.67 g/m^{3}d the AMX removal efficiency remained stable between 80% and 90%. A maximum AMX removal efficiency of 90% was obtained at an AMX loading rate of 66.67 g/m^{3}d in the aerobic CSTR reactor. The effluent AMX concentration was measured as 0.8 mg/L at an AMX loading rate of 66.67 g/m^{3}d. The AMX yield was 76% for AMX loading rates of 44.44 g/m^{3}d in the aerobic CSTR reactor. When the AMX loading rate was increased from 88.89 g/m^{3}d to 111.11 and to 133.33 g/m^{3}d the AMX removal efficiency decreased from 79% to 76% and 64%, respectively, in the aerobic CSTR reactor (Figure 6.34). The COD yields obtained in our study are high in comparison to the removal performances of COD in the studies given below: The

COD removals were found to be lower (60%) in the study performed by Chen et al. (2008) under aerobic conditions treating the 78 mg/L AMX in an up flow anaerobic sludge blanket reactor, compared to the present study. Similarly, the COD removal efficiencies (38-62%) obtained by Lapara et al., (2001) are lower than those of our results.

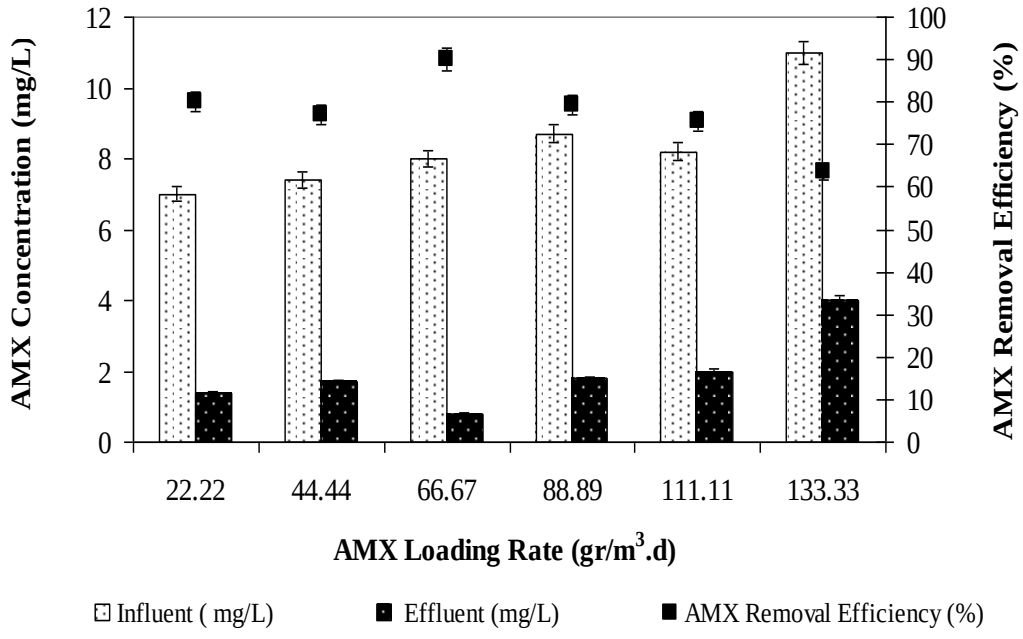

Figure 6.34 AMX removals in the aerobic CSTR reactor at increasing AMX loading rates

6.2.3.6 Treatment Efficiencies of Anaerobic/Aerobic Sequential Reactor System

Figure 6.35 shows the overall COD and AMX removal efficiencies in anaerobic/aerobic sequential reactor system. The maximum COD and the AMX removal efficiency in sequential AMCBR/CSTR reactor system were measured as 98% and 100% at an AMX loading rates of 66.67 g/m^{3}d, respectively. The COD and AMX removal efficiencies were 98% and 97% at minimum AMX loading rates of 22.22-44.44 g/m^{3}d in overall reactor system, respectively. Total COD and AMX removal efficiencies decreased from 96% to 94% and from 99% and 98% as the AMX loading rates increased from 111.11 to 133.33 g/m^{3}d in sequential AMCBR/ CSTR reactor system. The COD and AMX removal efficiencies were above 94% and 97%, respectively, at all AMX loading rates in sequential AMCBR/CSTR reactor

system. In a study carried out by Chen et al., (2011) 87% both AMX and COD yields were obtained at an influent COD and AMX concentration of 3690 and 105 mg/L, respectively, in a combined anaerobic/micro-aerobic two-stage aerobic process at a HRT of 1.98 days. In our study the AMX and COD removal efficiencies are higher than this study although the influent AMX concentration is comparably higher than the study performed by Chen et al., (2011).

The literature survey showed that the AMX yields obtained in old studies are lower than those in our data: 50% COD and antibiotic removals was obtained by Fox and Venkatasubbiah, (1996) in a combined anaerobic baffled and aerobic attached-film reactor to remove pharmaceutical wastewaters containing antibiotic and sulfate at 4000 mg/L COD and at a HRT of 1 day. Similarly, Buitron et al., (2003) found 96% COD yield in a sequencing batch bio filter operating under anaerobic and aerobic conditions to treat pharmaceutical wastewater with an influent COD of 28-72 g/L.

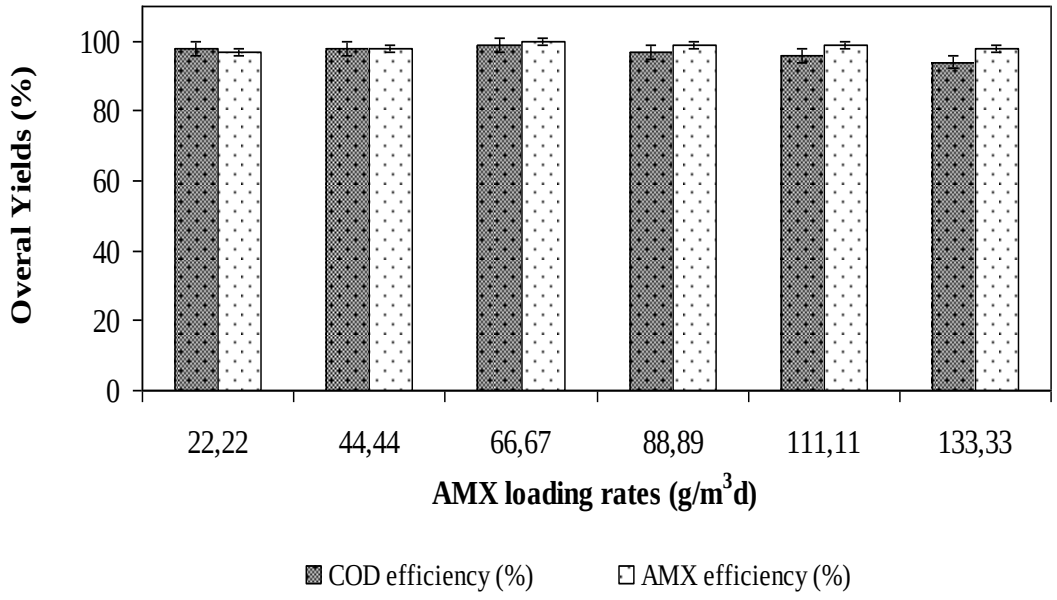

Figure 6.35 AMX and COD removal in the sequential AMCBR/CSTR reactor at increasing AMX loading rates

6.2.4 Effect of Increasing TYL Concentration on the Performance of AMCBR Reactor

6.2.4.1 Effect of Increasing TYL Concentration on the COD Removal Efficiencies in the AMCBR Reactor

In this step, the effect of increasing TYL concentrations on COD removal efficiencies was investigated. The COD equivalents of TYL concentration are shown in Table 6.13.

Table 6.13 The COD equivalents of TYL concentration

Parameters	**Unit**	**Concentrations**
Molasses-COD concentration	mg/L	3900; 3905; 3917; 3986; 4000; 4100
TYL concentration	mg/L	50; 100; 150; 200; 250; 300
COD equivalent of OTC	mg/L	25; 35; 40; 65; 75; 100
Total COD concentration	mg/L	3925; 4005; 3957; 4051; 4075; 4200

The operation of the AMCBR reactor was started with an influent TYL concentration of 50 mg/L corresponding to a TYL loading rate of 22.22 gTYL/m^3d. Then the TYL concentrations were subsequently increased from 100 to 150, 200, and 250 and to 300 mg/L corresponding to TYL loading rates increasing from 44.44 to 66.67, 88.89, 111.11 and 133.33 gTYL/m^3d, respectively. Figure 6.36 shows the variations of COD concentrations and the COD removal efficiencies in AMCBR reactor with increasing TYL loading rates. As shown in Figure 6.36, the COD removal efficiency was 96% at a TYL loading rate of 22.22 g/m^3d. The effluent COD concentration was 400 mg/L resulting a COD removal efficiency of 90% at a TYL loading rate of 44.44 g/m^3d.

The COD removal efficiency remained around 90% until a TYL loading rate of 88.89 g/m^3d (for TYL was loading rates at between 44.44 and 88.89 g/m^3d corresponding TYL concentrations varying between 100-200 mg/L). After this TYL loading rate (88.89 g/m^3d) the COD removal efficiency decreased from 90% to 79%

and 75% corresponding to TYL loading rates of 111.11 and 133.33 g/m^{3}d. In this study, molasses was used as the primary substrate for the reduction of TYL. Molasses-COD is consumed as an energy source and electron donor for anaerobic antibiotic biotransformation. In other words the molasses-COD was used as a carbon and energy source by the TYL transforming methanogens while TYL was used as co-substrate by them and reduced to their metabolites.

These results are higher than the findings of Akarsubaşı et al., (2005) which they found a COD removal of 90% at an organic loading rate of 6 g/m^{3}d. The maximum COD removal efficiency was obtained as 96% in the aforementioned organic loading rate resulting in a COD concentration of 50 mg/L in the effluent among the runs applied to the AMCBR reactor. In our study a significant linear relationship was found between the COD yields for the TYL loading rates at between 88.89 and 133.33 g/m^{3}d (ANOVA), (R^2=0.90, F=4.96, p=0.02).

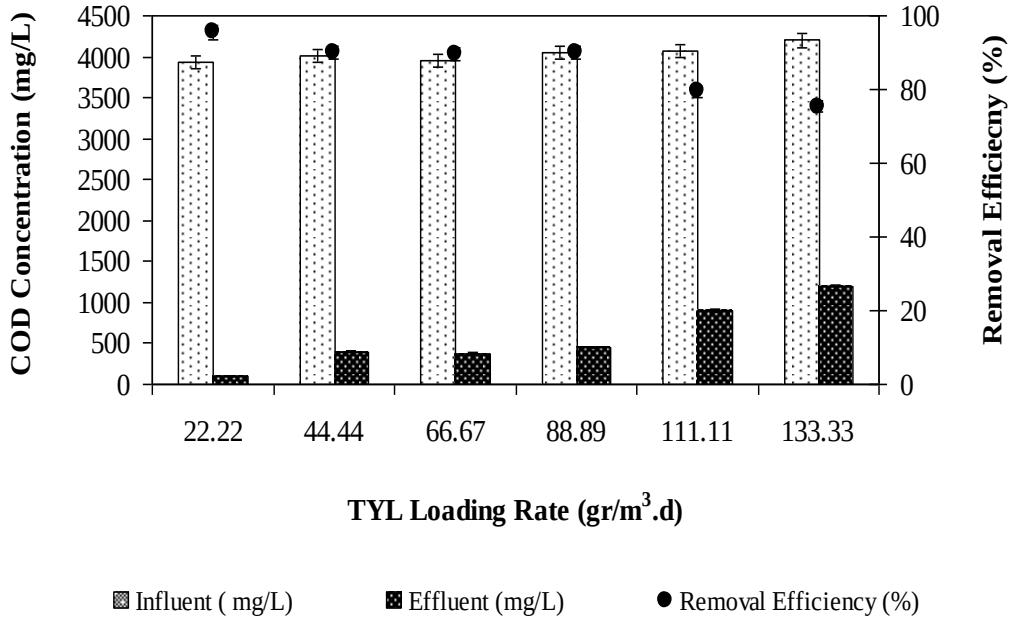

Figure 6.36 Effects of increasing TYL loading rates on COD removal efficiencies in the AMCBR

The COD yields obtained in recent studies were low in comparison with the COD removals in this study. In the study by Chelliapan et al., (2011) 70-75% COD removal efficiencies were obtained at a HRT of 2-4 days in an up-flow anaerobic stage reactor (UASR) at influent OLRs of (0.43-1.86 kgCOD/m^3d). In the study performed by Chelliapan et al., (2006), 70% COD removal efficiency was obtained at OLR of 1.88 kgCOD/m^3d in an UASR reactor treating 100-800 mg/L TYL. In our study, 75-96% COD removal was measured for the influent TYL concentration varying between 50 and 300 mg/L. Öktem et al., (2008) has conducted a study on the performance of a lab-scale hybrid UASB reactor, treating a chemical synthesis-based pharmaceutical wastewater. At an OLR of 8 kgCOD/m^3d, COD reduction of 72% was achieved in the reactor system. The yields obtained in the aforementioned studies are low in comparison to the removal performances of COD found in this study.

A similar study was also reported by Chelliapan et al., (2011) when treating pharmaceutical wastewater containing TYL (100-400 mg/L) in an UASR reactor. 93% COD removal efficiency was obtained in an UASR reactor at an organic loading rate of 7.5 kg COD/m^3d, corresponding to the influent COD concentration of 7500 mg/L, during 280 days of operation time. In another study, Shimada et al., (2008) 96% COD removal efficiency reported in an ASBR at a HRT of 1.67 days at an influent TYL concentration of 1.67 mg/L.

In the study performed by Shimada et al., (2011), the COD (E=98%) yield was higher than those of our data (96% for COD) at a HRT of 1.67 days in an anaerobic sequencing batch reactor (ASBR) treating 1.67 mg/L TYL. This could be attributed to the antibiotic concentrations to the anaerobic conditions and reactor configuration. A similar study was also reported by Shimada et al., (2006). 95% COD removal efficiency was obtained at an OLR of 3.5 kgCOD/m^3d in the ASBR reactor treating 1 mg/L TYL.

6.2.4.2 Effect of TYL Loading Rate on the TYL Removal Efficiencies in the AMCBR Reactor

The effect of TYL loading rate on the TYL removal efficiencies in AMCBR was shown in Figure 6.37. A TYL removal efficiency of 94% was obtained at an initial TYL concentration of 50 mg/L, corresponding to a TYL loading rate of 22.22 g/m^{3}d. After this TYL loading rate, the TYL removal efficiencies remained constant as 85%. This can be explained with the acclimation of methane *Archaea* bacteria to TYL. TYL removal efficiency was measured as 85% even at maximum TYL loading rates. The effluent TYL concentration was 50 mg/L at maximum TYL loading rate of 133.33 g/m^{3}d. The TYL yields were between 85% and 83% for TYL loading rates of 44.44, 88.89, 111.11 and 133.33 g/m^{3}d, respectively, in the AMCBR reactor (see Figure 6.37). A significant linear correlation between TYL yields and increasing TYL loading rate was not observed (ANOVA), (R^2=0.61, F=8.76, p=0.01). The HPLC chromatograms of TYL were illustrated in Figure 6.38 for the effluent samples of the AMCBR at initial TYL concentrations of 50 and 150 mg/L, respectively. The recent literature on the anaerobic TYL treatment showed that the yields obtained in some high rate anaerobic reactors are lower than the TYL removals found in our study with AMCBR: In a study performed by Chelliapan et al., (2011) 75% TYL removal efficiencies were obtained at an organic loading rate of 7.5 kgCOD/m^{3}d in an UASR reactor at influent TYL concentrations varying between 100 and 400 mg/L. In the study performed by Shimada et al., (2011), the TYL yields (54%) were lower than those of our data (94% for TYL) at a HRT of 1.67 days in an ASBR treating 1.67 mg/L TYL. The yields obtained in the aforementioned studies are low in comparison to the removal performances of TYL found in this study. The reason of high TYL yields in our study could be attributed to the granulated sludge which is resistant to the high toxic compounds and to the AMCBR reactor which is a high rate reactor. The high removal efficiency of this reactor came from its compartmentalized structure. In another study was also reported by Chelliapan et al., (2011) 95% TYL removal efficiencies were obtained at an organic loading rate of 3.5 kgCOD/m^{3}d in an UASR reactor at influent TYL concentrations varying between 10

and 200 mg/L. The yield obtained in the aforementioned study is high in comparison to the removal performances of TYL found in our study.

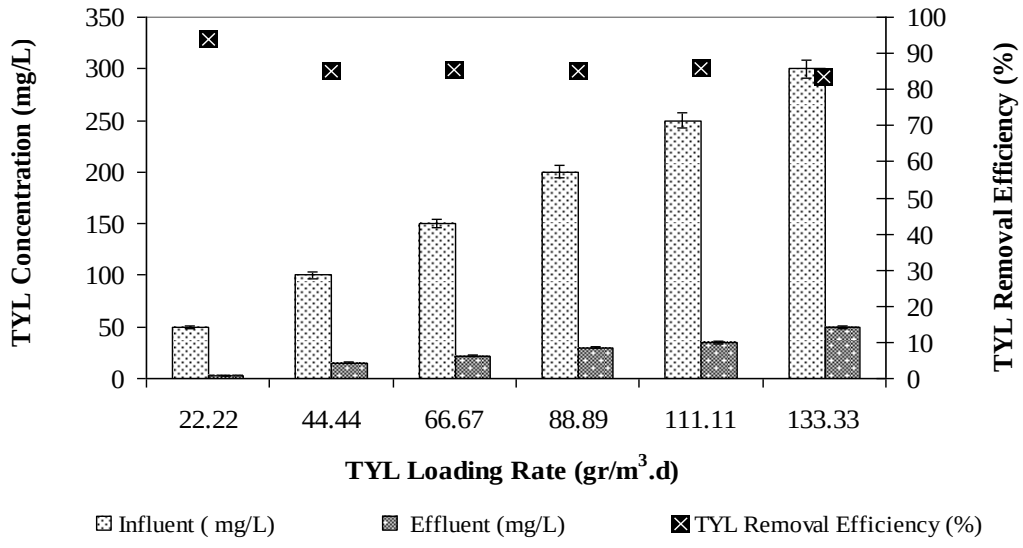

Figure 6.37 The effect of TYL loading rate on TYL removal efficiencies in the AMCBR reactor

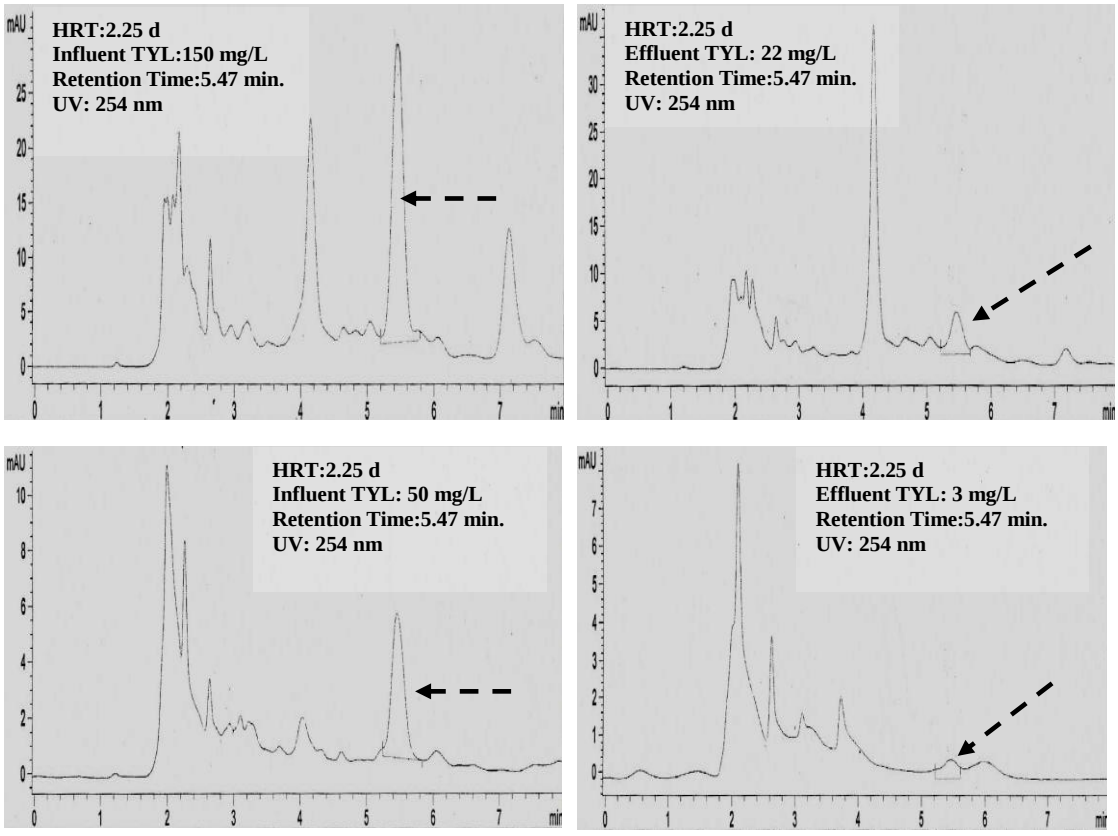

Figure 6.38 HPLC chromatograms of TYL in the influent and effluent of AMCBR reactor

6.2.4.3 Effects of Increasing TYL Loading Rates on the Total and Methane Gas Production in the AMCBR Reactor

The total and methane gas production rates and methane percentages in AMCBR reactor are shown in Figure 6.39. The daily total gas, methane gas productions and methane percentages were approximately 13-15 L/d, 7-9 L/d and 60%, respectively, for TYL loadings varying between 22.22 and 133.33 g/m^{3}d. The maximum total gas, methane gas productions and methane percentage were found as 15 L/d and 9.4 L/d and 60%, respectively, at TYL loading rates of 22.22 and 44.44 g/m^{3}d. After these loading rates, the daily total gas, methane gas productions and methane percentage decreased. Total gas, methane gas productions and methane percentage were found as 13.8 L/d, 7 L/d and 52% at maximum TYL loading rate of 133.33 g/m^{3}d. This indicated an inhibition effect of TYL on methane *Archaea* at aforementioned TYL loading rates. A significant linear relationship was not found between the biogas productions and the TYL loading rates (ANOVA), (R^2=0.50, F=9.76, p=0.02).

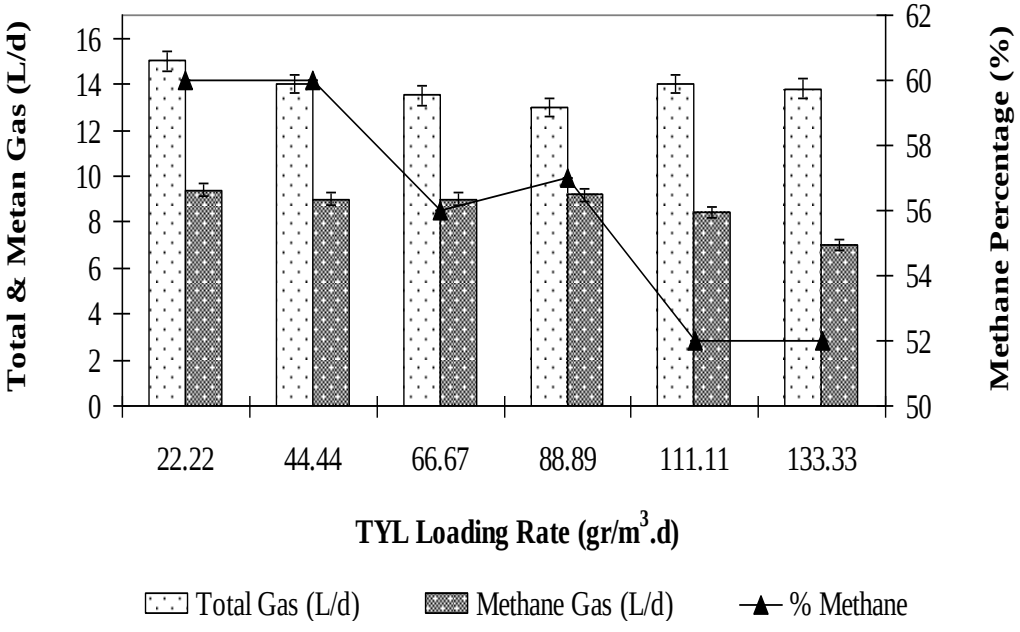

Figure 6.39 The effect of TYL loading rate on total, methane gas production and methane content in the AMCBR reactor

The results of this study showed that the TYL loadings affected the total and methane gas produced during anaerobic degradation of pharmaceutical wastewater. In a study performed by Chelliapan et al., (2006) 3.4 L/d methane gas production was found at OLRs varying at between 0.43 and 1.86 kg COD/m^3d, at an influent TYL=20-200 mg/L and a HRT=4 days in an UASR reactor. Shimada et al., (2011) reported that, 2.6 L/d biogas production at an influent TYL concentration of 167 mg/L at HRT of 1.67 days and at an OLR of 3.5 kg COD/m^3d in an ASBR reactor. In another study, in a study performed by Amin et al., (2006) methane gas production and percentage were found as 5 L/d and 48%, respectively at an OLR of 2.90 kg COD/m^3d in an ASBR. In our study, 60% methane percentage and 9.4 L/d CH_4 production was measured at influent TYL concentrations varying between 50 and 300 mg/L in an AMCBR reactor. The yields obtained in the aforementioned studies are low in comparison to the methane gas productions found in our study.

A similar study was also reported by Chelliapan et al., (2011) when treating pharmaceutical wastewater containing TYL in an anaerobic UASR reactor. 60% methane content was obtained at an influent TYL concentration of 100 mg/L, during 106 days of operation time. In our study, similar yields were observed with the study performed by Chelliapan et al., (2011).

The methane yield can be a useful parameter to assess the performance of an anaerobic reactor. Figure 6.40 shows the variations of methane yields versus TYL loading rates. The lower values of methane yield in all the compartments of the AMCBR, but particularly in 1st compartment, were most likely caused by methanogenic populations were partially inhibited by TYL.

The methane yields decreased from 0.28 to 0.12 $m^3CH_4/kgCOD_{removed}$, when the TYL loading rates were increased from 22.22 to 133.33 g/m^3d, respectively in the 1st compartment of AMCBR reactor. The methane yields in 2nd compartment of the reactor system decreased from 0.33 to 0.16 $m^3CH_4/kgCOD_{removed}$ when the TYL loading rates were increased 22.22 to 133.33 g/m^3d. 3rd compartment (0.16-0.35 $m^3CH_4/kgCOD_{removed}$) and effluent (0.17-0.37 $m^3CH_4/kgCOD_{removed}$) exhibited a

relatively constant level of methane yield for all the TYL loading rates studied. A significant linear relationship was found between the methane yields and the TYL loading rates for TYL loading rates of 22.22 and 133.33 g/m^{3}d (ANOVA), (R^2=0.88, F=6.12, p=0.02).

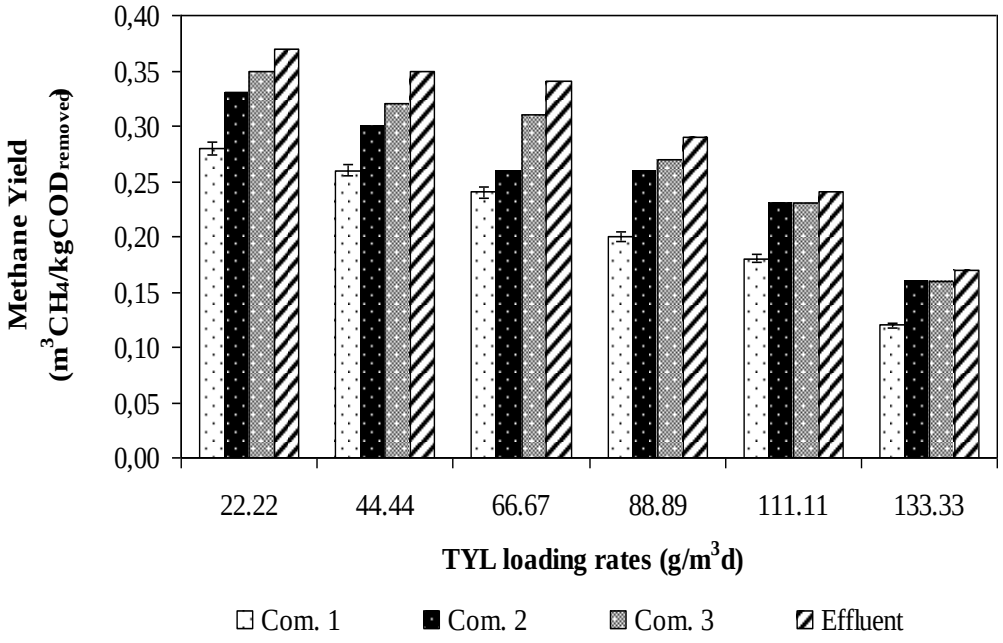

Figure 6.40 Variations of CH_4 yields versus TYL loading rates in all compartment of the AMCBR

The methane yields obtained in our study are similar in comparison to the yield performances of methane in the studies given below: In the study by Nandy and Kaul, (2001), 0.26-0.34 $m^3CH_4/kgCOD_{removed}$ methane yields was observed for the anaerobic degradation of 200 mg/L TYL in herbal pharmaceutical wastewater after 2 days HRT. In the study performed by Mohan et al., (2001) 0.20 $m^3CH_4/kgCOD_{removed}$ methane yields was obtained at a HRT of 1.98 days in anaerobic treatment of chemical synthesis-based pharmaceutical wastewater. A similar study was also reported by Chelliapan et al., (2006) when treating pharmaceutical wastewater containing 20- 200 mg/L TYL in an UASR. 0.10-0.40 $m^3CH_4/kgCOD_{removed}$ methane yields were obtained during 106 days of operation time. The yields obtained in the aforementioned studies are similar in comparison to the yield performances of methane found in this study.

6.2.4.4 Variation of pH, Total Volatile Fatty Acids (TVFA) and Composition (H_{ac}, H_{bu}, H_{la}, H_{pr}) in Compartments of the AMCBR Reactor at Increasing TYL Loading Rates

The pH is an essential factor to control during anaerobic degradation. The methane-producing microorganisms have optimum growth in the pH range between 6.6 and 7.6 (Rittman and McCarty, 2001), although stability may be achieved in the formation of methane over a wider pH range (6.0-8.0). pH values below 6.0 and above 8.3 should be avoided, as they can inhibit the methane-forming microorganism (Chernicharo, 2007). Figure 6.41 shows the pH variation in compartments of the AMCBR at increasing TYL loading rates. As shown in Figure 5.41, the pH values in the effluent and in the all compartments of AMCBR varied between 7.10 and 7.52. The pH values were lower in the 1st compartment than all of the other compartments since TVFA in the 1st compartment was higher (Figure 6.42). When the TYL loading rates was increased from 22.22 to 133.33 g/m^{3}d in the AMCBR reactor, the pH in the 1st compartment dropped from 7.36 to 7.10 due to the increased acidogenic activity. The pH profile of the AMCBR reactor system with average pH in 1st compartment was 7.24; while the pH in 2nd compartment was measured as 7.48. The pH in 3rd compartment was measured as 7.45. As shown in Figure 6.41, the pH values in the effluent of AMCBR varied between 7.40 and 7.55. In theory, the pH in 1st compartment should be lower than in compartments 2nd, 3rd, and effluent due to horizontal separation of acidogenesis and methanogenesis in a high rate reactor namely AMCBR (Nachaiyasit and Stuckey, 1997b).

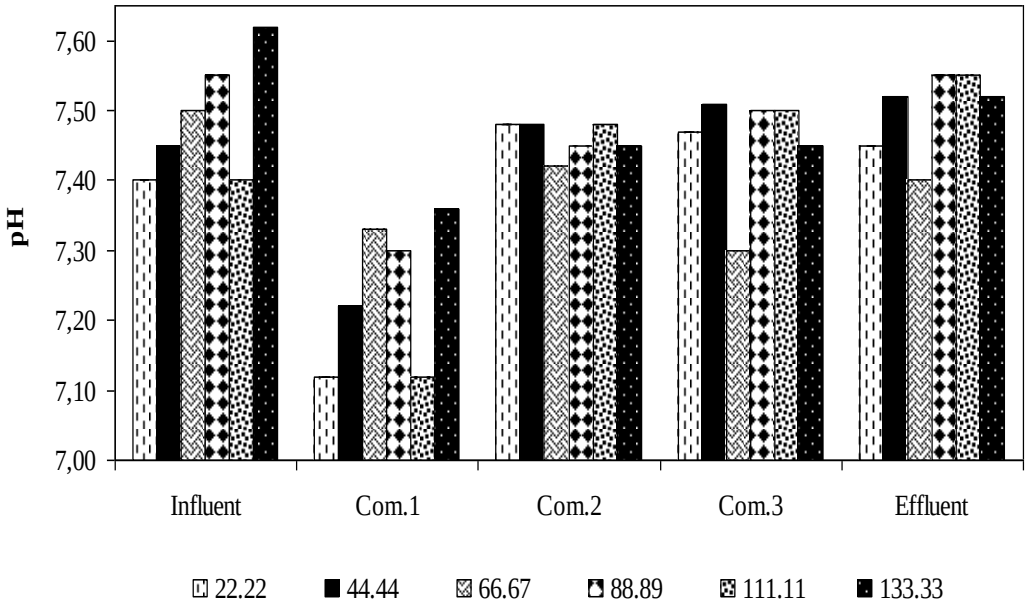

Figure 6.41 Variations of pH in the AMCBR reactor at increasing TYL loading rates

The total TVFA concentration of the AMCBR reactor is shown in Figure 6.42 and indicates a low concentration of TVFA (average 7 mg/L) in the AMCBR reactor effluent when operated at TYL loading rates in the range 22.22 to 111.11 g/m^{3}d. The TVFA concentration in the 1st compartment was measured between 500 and 950 mg/L (see Figure 6.42) for the TYL loading rates between 22.22 and 133.33 g/m^{3}d, respectively. Almost 250-690 and 7-18 mg/L TVFA concentrations were detected in the 2nd and 3rd compartments of the AMCBR respectively, for the TYL loading rates between 22.22 and 133.33 g/m^{3}d, respectively. It was found that the TVFA concentrations decreased from compartment 1st to compartments 2nd and 3rd. The TVFA concentrations were measured as 250 and 500 mg/L at TYL loading rate as high as 133.33 g/m^{3}d due to inhibition effects of high TYL concentrations to acidogens in the 1st and 2nd compartments of the AMCBR.

It was found that the minimum TVFA value in the effluent was approximately 2 mg/L at TYL loading rates of 22.22 and 111.11 g/m^{3}d while the TVFA level was 7 mg/L at OTC loading 133.33 g/m^{3}d in the 3rd compartment (see Figure 6.42). A strong linear correlation between TVFA concentrations and TYL loading rates was observed in the 1st and 2nd compartments for TYL loading rates of 22.22 and 133.33

g/m^{3}d (ANOVA) (R^2=0.96; F=3.89, p=0.01). At high organic loading rates (OLRs), the relatively complex pharmaceutical wastewater caused pre-acidification resulting in accumulation of COD-TVFA, which did not subsequently convert to methane, resulting in an accumulation of TVFA.

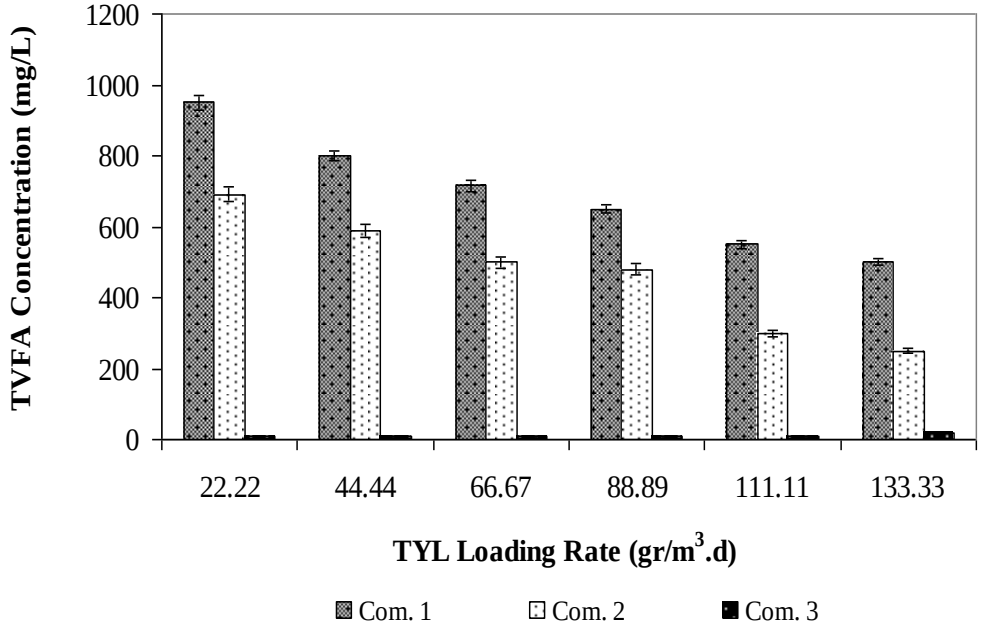

Figure 6.42 Variations of TVFA concentration in the AMCBR reactor at increasing TYL loading rates

The results of this study showed that the TYL loadings affected the TVFA production during anaerobic degradation of pharmaceutical wastewater. In a study performed by Shimada et al., (2011) 8.9-3400 mg/L TVFA concentrations were obtained at a HRT of 1.67 days in an ASBR reactor at influent TYL concentrations varying between 1.67 and 167 mg/L. In the study performed by Chelliapan et al., (2006), the TVFA concentrations (100-800 mg/L) were lower than those of our results (950 mg/L) at a HRT of 4 days in an anaerobic UASR reactor treating 20-200 mg/L TYL.

In a study performed by Chelliapan et al., (2011) TVFA productions were 550-1050 mg/L, 350-750 mg/L, 200-570 mg/L and 40-400 mg/L for 1st, 2nd, 3rd and 4th compartments, in an anaerobic UASR reactor respectively. In our study TVFA productions were 500-950 mg/L, 250-690 mg/L, 7-18 mg/L and 2-7 mg/L in an 1st,

2^{nd}, 3^{rd} compartments and effluent of AMCBR reactor for TYL loading rates of 22.22 and 133.33 g/m^3d. In this study the TVFA productions are comparable higher than that aforementioned study.

6.2.4.4.1 Variation of TVFA Components (H_{ac}, H_{pr}, H_{bu}, H_{la} and H_{pr}/H_{ac} ratios in the AMCBR at Increasing TYL Loading Rates. The H_{ac} concentrations lower than 800 mg/L and the ratio of H_{pr}/H_{ac} lower than 1.4 is two indicators for successful methane production (Hill et al., 1987). Table 6.14 and Figure 6.43 shows all the result H_{pr}/H_{ac} is lower than 1.4 that means the system is successful for produce methane. As shown in Figure 6.43, this ratio varied between 0.66-0.95 and 0.65-0.84, respectively in 1^{st} and 2^{nd} compartments of AMCBR reactor at increasing TYL loading rates (from 22.22 to 133.33 g/m^3d). The H_{pr}/H_{ac} ratios were found as 0.66, 0.68, 0.72, 0.95, 0.66 and 0.82 respectively, at TYL loading rates of 22.22-133.33 g/m^3d in 1^{st} compartment of AMCBR reactor. As shown in Figure 5.43, this ratio varied between 0.82, 0.65, 0.75, 0.84, 0.71, 0.66 and 0.66 respectively in 2^{nd} compartments of AMCBR reactor at increasing TYL loading rates (from 22.22 to 133.33 g/m^3d). The AMCBR reactor system was successful if check from ratio between H_{pr} to H_{ac}. It was ratio between H_{pr} to H_{ac} lower than 1.4.

As the TYL loading rates were increased from 22.22, 44.44, 66.67, 88.89, 111.11 to 133.33 g/m^3d H_{ac} concentrations decreased from 450, 380, 285, 200, 150 to 110 mg/L, respectively in the 1^{st} compartment (Table 6.14). The concentrations of H_{pr} also decreased from 300, 260, 205, 190 to 100, 90 mg/L respectively. The concentrations of H_{bu} were obtained as 150, 120, 105, 85, 65 and 50 mg/L, respectively, at TYL loading rates of 22.22-133.33 g/m^3d (Table 6.14). As the TYL loading rates were increased from 22.22, 44.44, 66.67, 88.89, 111.11 to 133.33 g/m^3d H_{la} concentrations decreased from 50, 30, 20, 10, 10 to 10 mg/L, respectively in the 1^{st} compartment (Table 6.14).

As shown in Table 6.14, the H_{ac} concentrations were decreased from 245, 189, 120, 108, 45 to 30 mg/L at TYL loading rates of 22.22, 44.44, 66.67, 88.89, 111.11 to 133.33 g/m^3d, respectively in the 2^{nd} compartment. Similarly, the concentrations

of H_{pr} also decreased from 160, 141, 101, 77, 30 to 20 mg/L, respectively, when 22.22, 44.44, 66.67, 88.89, 111.11 to 133.33 g/m^{3}d TYL were added to the AMCBR reactor. The H_{bu} concentrations were found as 82, 65, 52, 46, 20 and 13 mg/L, respectively, at TYL loading rates of 22.22, 44.44, 66.67, 88.89, 111.11 to 133.33 g/m^{3}d, respectively in the 2nd compartment of AMCBR reactor (see Table 6.14). As the TYL loading rates were increased from 22.22, 44.44, 66.67, 88.89, 111.11 to 133.33 g/m^{3}d H_{la} concentrations decreased from 31, 24, 20, 13, 7 to 4 mg/L, respectively in the 2nd compartment (Table 6.14).

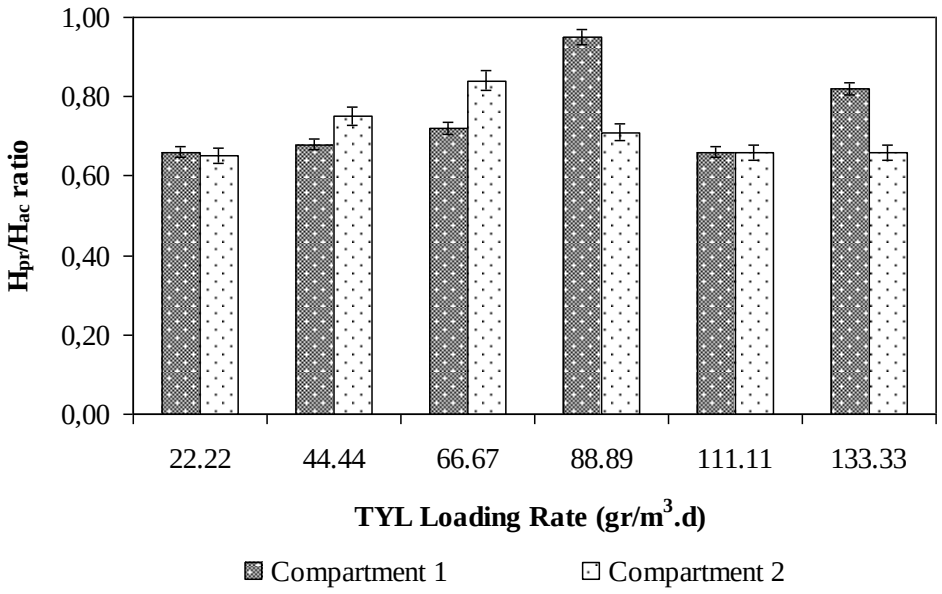

Figure 6.43 Variations of H_{pr}/H_{ac} ratio in the AMCBR reactor at increasing TYL loading rates

Table 6.14 Variations of TVFA composition (H_{ac}, H_{pr}, H_{bu}, H_{la}) and H_{pr}/H_{ac} ratio in the AMCBR reactor at increasing TYL loading rates

Parameter	AMCBR, 1st compartment						AMCBR, 2nd compartment					
	TYL Loading Rate						TYL Loading Rate					
	22.22	44.44	66.67	88.89	111.11	133.33	22.22	44.44	66.67	88.89	111.11	133.33
H_{ac} (mg/L)	450	380	285	200	150	110	245	189	120	108	45	30
H_{pr} (mg/L)	300	260	205	190	100	90	160	141	101	77	30	20
H_{bu} (mg/L)	150	120	105	85	65	50	82	65	52	46	20	13
H_{la} (mg/L)	50	30	20	10	10	10	31	24	20	13	7	4
H_{pr}/H_{ac} ratio	0.66	0.68	0.72	0.95	0.66	0.82	0.65	0.75	0.84	0.71	0.66	0.66

6.2.4.4.2 Effects of Increasing TYL doses on TVFA Composition, Production Rates, Activity and Acidification Degrees in the AMCBR Reactor. In order to determine the effects of increasing TYL loading rates on acidogens, on TVFA concentrations, and on the TVFA composition, the TVFA productions rates, activity, inhibition of acidogens, and the acidification degrees were monitored in every TYL loading rates during all compartments of the AMCBR reactor (see Table 6.15). The methane percentages of total gas decreased from 60% to 52% as the TYL loading rates increased from 50 to 300 mg/L while the TVFA concentrations reduced from 950 to 500 mg/L in 1st compartment of AMCBR reactor. The TVFA concentrations decreased from 690 to 250 mg/L in 2nd compartment of AMCBR reactor. By elevating the TYL loading rates the acidification degree decreased from 37.57%, 25.84%, 22.09%, 19.56%, 15.61% to 14.02%, indicating the inhibition of acidogens in 1st compartment of AMCBR reactor. As the TYL loading rates increased from 22.22, 44.44, 66.67, 88.89, 111.11 to 133.33 g/m^3d the acidification degree decreased from 27.30%, 23.35%, 19.78%, 18.98%, 11.86% to 9.85%, respectively, in 2nd compartment of AMCBR reactor.

The activity of acidogens decreased from 77%, 52%, 47%, 43%, 39% to 36%, respectively, at TYL loading rates increased from 22.22, 44.44, 66.67, 88.89, 111.11 to 133.33 g/m^3d in 1st compartment. Similarly, the activity of acidogens decreased from 61%, 43%, 40%, 38%, 24% to 20%, respectively. As the TYL loading rates increased from 22.22, 44.44, 66.67, 88.89, 111.11 to 133.33 g/m^3d the inhibition of acidogens increased from 13%, 41%, 50%, 60%, 65% to 70%, respectively, in 1st compartment of AMCBR reactor. The inhibition of acidogens were found as 11%, 34%, 43%, 53%, 55% and 60%, respectively, at a TYL loading rates of 22.22, 44.44, 66.67, 88.89, 111.11 to 133.33 g/m^3d in the 2nd compartment.

The TVFA composition mainly consisted of H_{ac} and H_{pr} as depicted in Table 5.15. Increases in TYL loading rates resulted in decreases in H_{ac} percentages of TVFA while H_{pr} fractions of TVFA increased. The TVFA consisted of 47.36% H_{ac} in the samples with TYL (22.22 g/m^3d) while the H_{ac} percentage decreased to 22.00% at a TYL loading rate of 133.33 g/m^3d in 1st compartment of AMCBR reactor. The H_{pr} percentages of TVFA decreased from 30%, 32.5%, 28.67%, 29.23% to 18.20% and 18%, respectively, at a TYL loading rates of 22.22, 44.44, 66.67, 88.89, 111.11 to 133.33 g/m^3d in 1st compartment. The H_{ac} percentages of TVFA were 35.40%, 32.07%, 23.84%, 22.50%, 14.06% to 11.50% respectively, at a TYL loading rates of 22.22, 44.44, 66.67, 88.89, 111.11 to 133.33 g/m^3d in 2nd compartment of AMCBR reactor (see Table 6.15). Similarly, the H_{pr} percentages of TVFA also decreased from 23.24%, 23.96%, 20.05%, 15.88%, 9.72% to 8.00%, respectively. The increase in H_{pr} fraction of TVFA also could be interpreted as an important indication of acidogenesis inhibition as reported by Dinopoulou et al., (1988). It can be concluded that inhibition in acidogens causes a decrease in TVFA production rates and methane percentages of total gas at increasing TYL loading rates in AMBCR reactor.

Table 6.15 Effects of Increasing TYL Doses on TVFA Composition, Production Rates, Activity, and Inhibition of Acidogens and on Acidification Degrees in the AMCBR reactor

Parameter		**AMCBR 1st Compartment**									**AMCBR 2nd Compartment**							
TYL (g/m^3d)	Methane (%)	**TVFA (mg/L)**	TVFA composition (%)				TPR (mg/L.h)	AA (%)	IA (%)	AD (%)	**TVFA (mg/L)**	TVFA composition (%)				TPR (mg/L.h)	AA (%)	IA (%)	AD (%)
			H_{ac}	H_{pr}	H_{bu}	H_{la}						H_{ac}	H_{pr}	H_{bu}	H_{la}				
22.22	60	**950**	47.36	30.00	12.35	5.80	36.17	77	13	37.57	**690**	35.40	23.24	11.87	4.51	28.75	61	11	27.30
44.44	60	**800**	47.50	32.50	15.00	3.75	32.67	52	41	25.84	**590**	32.07	23.96	11.06	4.09	24.60	43	34	23.35
66.67	56	**715**	38.86	28.67	14.68	2.80	25.36	47	50	22.09	**500**	23.84	20.05	10.27	3.72	21.00	40	43	19.78
88.89	57	**650**	31.00	29.23	13.01	1.54	19.61	43	60	19.56	**480**	22.50	15.88	9.61	2.75	20.00	38	53	18.98
111.11	52	**550**	27.30	18.20	11.82	1.82	17.30	39	65	15.61	**300**	14.06	9.72	6.45	1.72	12.5	24	55	11.86
133.33	52	**500**	22.00	18.00	10.00	2.00	16.81	36	70	14.02	**250**	11.50	8.00	5.00	1.56	10.42	20	60	9.85

TPR: TVFA production rate; AA: Activity of acidogens; IA: Inhibition of acidogens; AD: Acidification degree

6.2.4.5 Variation of Bicarbonate Alkalinity (HCO_3) and TVFA/HCO_3 Ratio in Compartments of the AMCBR at Increasing TYL Loading Rates

The HCO_3 concentrations remained between 3645 and 3978 mg/L in the effluent of AMCBR at increasing TYL loading rates (22.22-133.33 g/m^3d) (see Figure 6.44). The HCO_3 concentration in the 1st compartment was lower than the other compartments. This indicates the utilization of alkalinity to buffer the TVFA and CO_2 produced from the anaerobic co-metabolism of TYL, particularly at high concentrations. Figure 6.44 indicates a low concentration of HCO_3 from 3895 mg/L down to 2050 mg/L was present in the 1st compartment when the AMCBR was operated at TYL loading rates in the range 22.22-133.33 g/m^3d. However, in 3rd compartment, the HCO_3 concentrations between 3960 and 4012 mg/L at increasing TYL loading rates of 22.22-133.33 g/m^3d. The TYL loading rates increased from 22.22 to 66.67 g/m^3d the HCO_3 alkalinity concentrations increased from 3960 to 3985 mg/L in 3rd compartment.

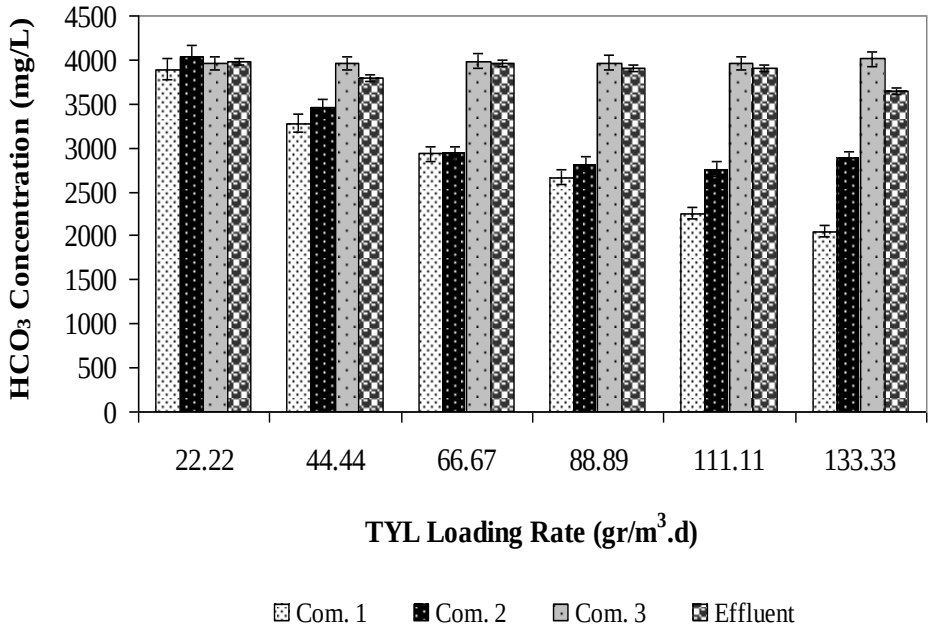

Figure 6.44 Variations of HCO_3 concentration in the AMCBR reactor at increasing TYL loading rates

The stability of an anaerobic reactor can be evaluated by the TVFA/HCO_3 ratio (Khanal, 2008). Barampouti et al., (2005), suggest that the ideal ratio of TVFA/HCO_3 is in the range of 0.1 to 0.3 to avoid the acidification of the anaerobic reactor. A value above 0.4 is an indicator of instability. The TVFA/HCO_3 ratios for this study are shown in Figure 6.45. As shown in Figure 6.45, this ratio varied between 0.01 and 0.24 in compartments and the effluent of AMCBR at increasing TYL loading rates (22.22-133.33 g/m^3d). These results indicated that the AMCBR reactor treating TYL was operated under stable conditions at increasing TYL loading rates. This suggests that the TVFA concentrations in the anaerobic reactor are linked to the easily assimilated organic matter by microorganisms and to methane production.

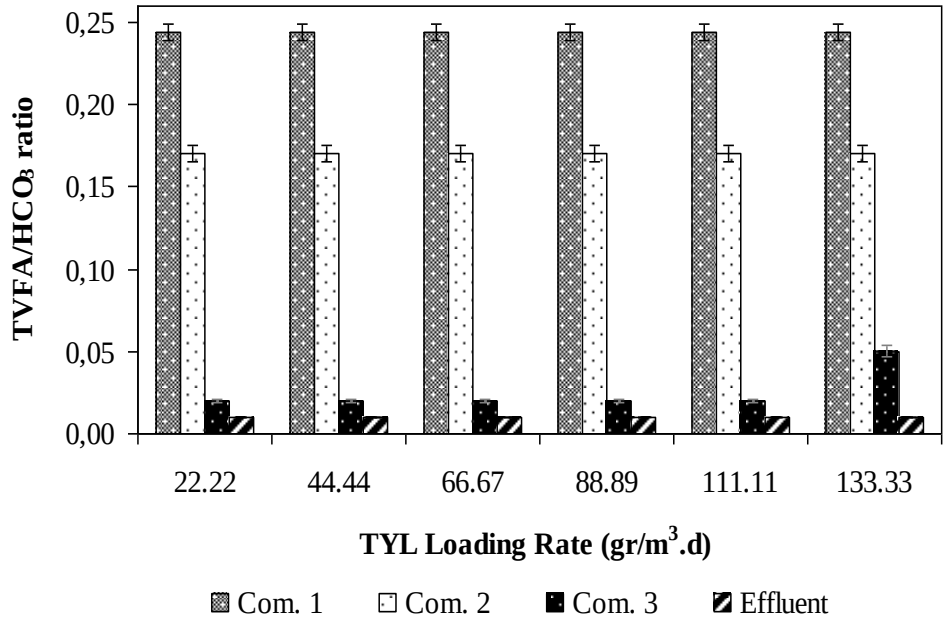

Figure 6.45 Variations of TVFA/HCO_3 ratio in the AMCBR reactor at increasing TYL loading rates

6.2.4.6 Effect of TYL Loading Rate on the COD and TYL Removal Efficiencies in the CSTR Reactor

Figure 6.46 and 6.47 shows the effect of increasing TYL loading rates on the COD and TYL yields in the aerobic CSTR reactor. The COD removal efficiencies were around 80% for TYL loading rates of 22.22, 44.44 and 88.89 g/m^3d,

respectively in the CSTR. As shown in Figure 6.46, the COD removal efficiency was 86% at a TYL loading rate of 22.22 g/m^{3}d. The COD yields were between 75 and 62% for TYL loading rates of 44.44-133.33 g/m^{3}d, respectively, in the CSTR reactor. The COD removal efficiency remained approximately 67% until a TYL loading rate of 88.89 g/m^{3}d corresponding a TYL concentration of 200 mg/L. After this TYL concentration, COD removal efficiency decreased rapidly from 67% to 62%. The effluent COD concentration and removal efficiency were measured as 455 mg/L and 62%, respectively, at a maximum TYL loading rate of 133.33 g/m^{3}d. The optimum TYL loading rate was found as 22.22 g/m^{3}d for maximum COD removal efficiency of 86%.

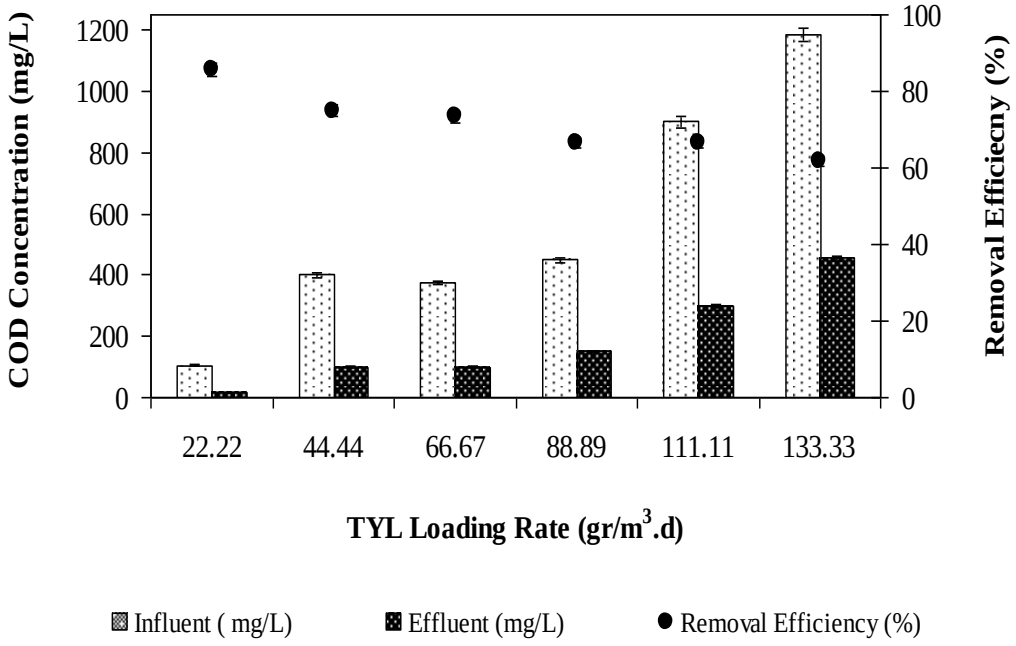

Figure 6.46 COD removal in the aerobic CSTR reactor at increasing TYL loading rates

The TYL removal efficiency of 67% was obtained at a TYL loading rate of 22.22 g/m^{3}d. When the TYL loading rate was increased from 22.22 to 66.67 g/m^{3}d the TYL removal efficiency decreased from 67% to 55%. A maximum TYL removal efficiency of 67% was obtained at a TYL loading rate of 22.22 g/m^{3}d in the aerobic CSTR reactor. The effluent TYL concentration was measured as 1.0 mg/L at a TYL loading rate of 22.22 g/m^{3}d. The TYL yield was 67% for TYL loading rate of 44.44

g/m^{3}d in the aerobic CSTR reactor. When the TYL loading rate was increased from 88.89 g/m^{3}d to 111.11 and to 133.33 g/m^{3}d the TYL removal efficiency decreased from 50% to 43% and 40%, respectively, in the aerobic CSTR reactor (Figure 6.47).

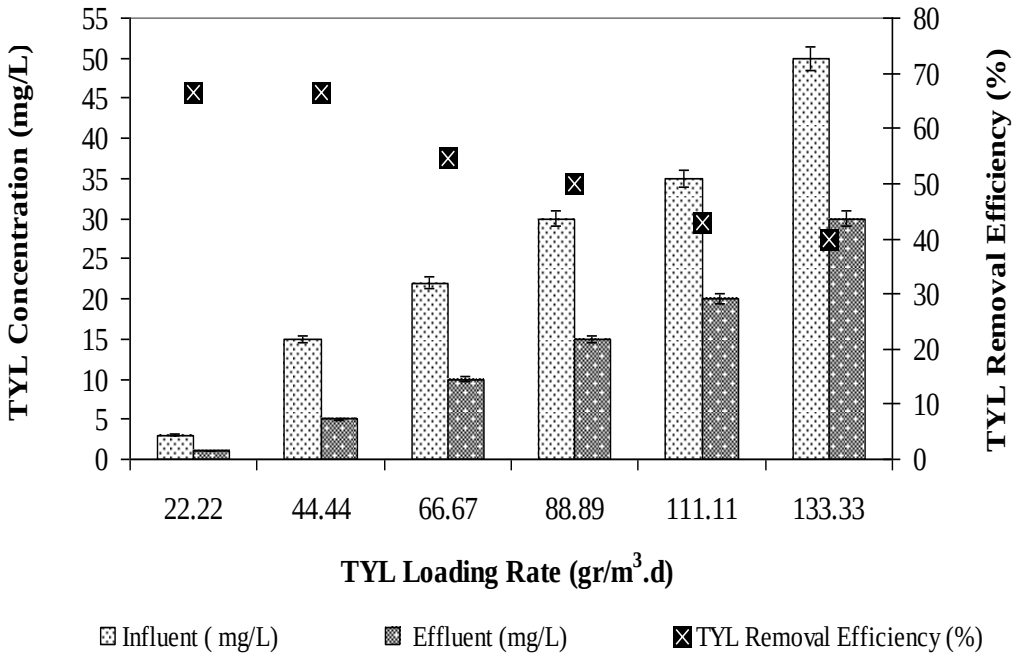

Figure 6.47 TYL removals in the aerobic CSTR reactor at increasing TYL loading rates

6.2.4.7 Treatment Efficiencies of Anaerobic/Aerobic Sequential Reactor System

Figure 6.48 shows the overall COD and TYL removal efficiencies in anaerobic/aerobic sequential reactor system. The maximum COD and the TYL removal efficiency in sequential AMCBR/CSTR reactor system were measured as 99% and 98% at a TYL loading rate of 22.22 g/m^{3}d, respectively. The TYL removal efficiencies were 98% and 95% at minimum TYL loading rates of 22.22-44.44 g/m^{3}d in overall reactor system, respectively. Total COD and TYL removal efficiencies decreased from 93% to 92% and from 90% and 89% as the TYL loading rates increased from 111.11 to 133.33 g/m^{3}d in sequential AMCBR/ CSTR reactor system.

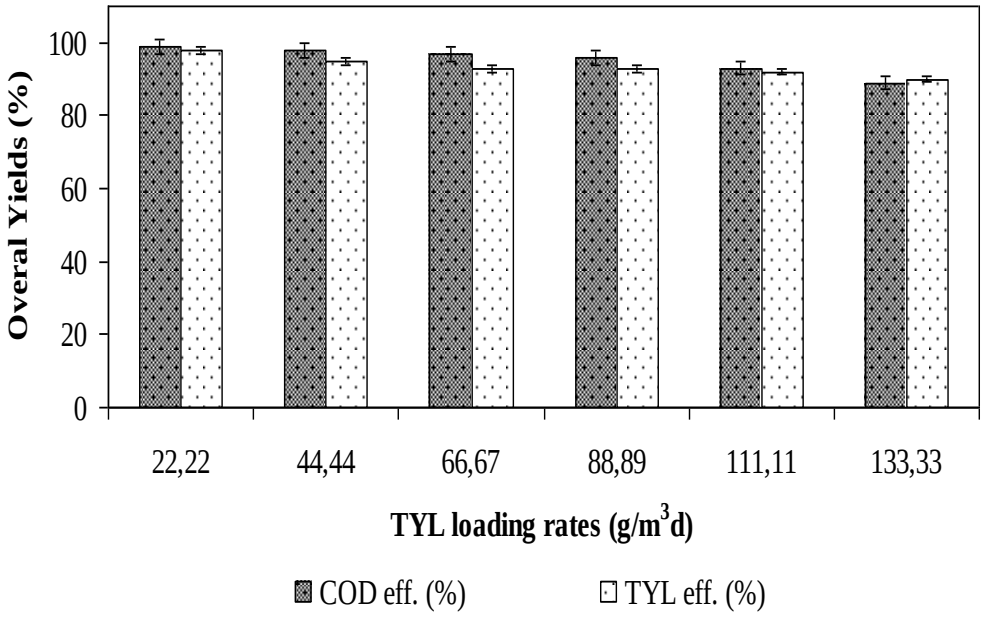

Figure 6.48 TYL and COD removal in the sequential AMCBR/CSTR reactor at increasing TYL loading rates

6.2.5 Effect of Increasing ERY Concentration on Performance of AMCBR Reactor

6.2.5.1 Effects of Increasing ERY loading rates on the COD Removal Efficiencies in the AMCBR Reactor

The COD was monitored as an indicator parameter of the pharmaceutical wastewater organic strength. The variations in COD concentrations of the pharmaceutical wastewaters collected at the top of the lab-scale anaerobic AMCBR reactor are given in Figure 6.49. In this run, the effect of increasing ERY concentrations on COD removal efficiencies was investigated. The operation of the AMCBR with ERY was started at an influent ERY concentration of 50 mg/L and an ERY loading rate of 22.22 g/m^{3}d. Then the ERY concentrations were subsequently increased from 100 to 150, 200 and 250 to 300 mg/L corresponding to ERY loading rates of 44.44, 66.67, 88.89, 111.11 and 133.33 g/m^{3}d. The COD equivalents of ERY concentration are shown in Table 6.16.

Table 6.16 The COD equivalents of ERY concentrations

Parameters	Unit	Concentrations
Molasses-COD concentration	mg/L	4000
ERY concentration	mg/L	50; 100; 150; 200; 250; 300
COD equivalent of ERY	mg/L	20; 40; 60; 80; 100; 120
Total COD concentration	mg/L	4020; 4040; 4060; 4080; 4100; 4120

Figure 6.49 shows the variations of COD concentrations and the COD removal efficiencies in AMCBR reactor with increasing ERY loading rates. As shown in Figure 6.49, the COD removal efficiency was 95% at an ERY loading rates of 22.22 and 44.44 g/m^{3}d. The effluent COD concentrations were 205 and 210 mg/L resulting a COD removal efficiency of 95% at an ERY loading rates of 22.22 and 44.44 g/m^{3}d.

The COD removal efficiency decreased from 95 to 80% as the ERY loading rate was increased from 22.22 to 133.33 g/m^{3}d. The maximum COD removal efficiency was obtained as 95% in the aforementioned organic loading rates resulting in a COD concentration of 205 and 250 mg/L in the effluent among the runs applied to the AMCBR reactor (Figure 6.49). The COD yield remained around 85% until an ERY loading rate of 66.67 g/m^{3}d. After this ERY loading rate, the COD removal efficiency decreased from 89% to 80% and 79% corresponding to ERY loading rates of 88.89, 111.11 and 133.33 g/m^{3}d.

The optimum ERY loading rates was 22.22 and 44.44 g/m^{3}d at ERY concentrations of 50 and 100 mg/L for maximum COD yield while the minimum COD removal efficiency was obtained at an ERY loading rate of 133.33 g/m^{3}d. These results shows that ERY degrading methanogens produced methane through the utilization of ERY as co-substrate together with molasses-COD used as primary carbon and energy source. In this study, molasses was used as the primary substrate for the reduction of ERY. Molasses-COD is consumed as an energy source and electron donor for anaerobic antibiotic biotransformation. In our study a significant linear relationship was found between the COD yields for the ERY loading rates at between 22.22 and 44.44 g/m^{3}d (ANOVA), (R^2=0.89, F=4.71, p=0.01).

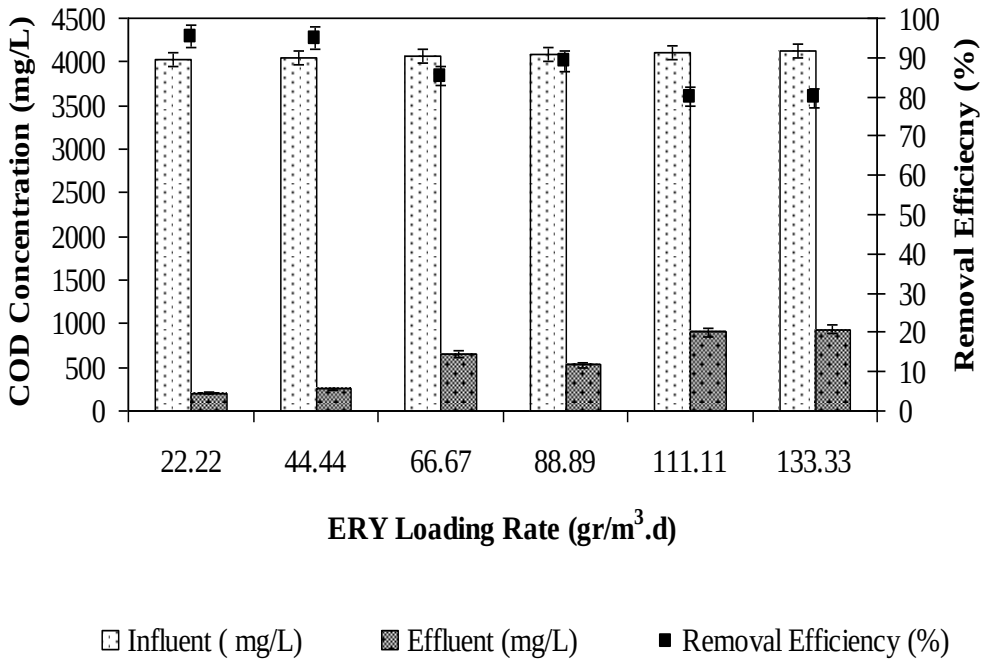

Figure 6.49 Effects of increasing ERY loading rates on COD removal efficiencies in the AMCBR reactor

The COD yields obtained in recent studies were low in comparison with the COD removals in this study. In the study by Rodriguez-Martinez et al., (2005) 70-85% COD removal efficiencies were obtained at a HRT of 2 days in an UASB reactor at influent OLRs of (1.5-2.09 kgCOD/m^3d). In the study performed by Chelliapan et al., (2006), 70% COD removal efficiency was obtained at OLR of 1.88 kgCOD/m^3d in the UASR reactor treating TYL concentrations of 100 and 800 mg/L. In our study, 79-95% COD removal was measured for the influent ERY concentration varying between 50 and 300 mg/L. In other study carried out by Öktem et al., (2008), the COD yields were (72-90%), also, higher than those of our data (79-95%) in a fixed-film reactor treating ERY at concentrations varying between 50 and 200 mg/L. The yields obtained in the aforementioned studies are low in comparison to the removal performances of COD found in this study.

In the study performed by Nandy and Kaul, (2001), the COD (E=80-98%) yield was higher than those of our data (E=79-95%) at a HRT of 1.5 days in an anaerobic hybrid reactor comprising of trickling filter treating 90 mg/L ERY. This could be

attributed to the antibiotic concentrations to the anaerobic conditions and reactor configuration. A similar study was also reported by Amin et al., (2006). 99% COD removal efficiency was obtained at OLR of 2.9 kgCOD/m^3d in the ASBR reactor treating 1-200 mg/L ERY.

6.2.5.1.1 Variations of COD in Compartments of the AMCBR at Increasing ERY Loading Rates. In order to determine the variations of COD and ERY in compartments of the AMCBR reactor, samples were taken from the sampling points of each compartment of the AMCBR reactor and the COD and ERY concentrations were measured. Table 6.17 shows the variations in COD and ERY concentrations in all compartments of the AMCBR reactor. As indicated in Table 6.17, the COD concentrations were different in three compartments, indicating that staging had been accomplished in the compartments of AMCBR. It was observed that most of the influent COD was removed in 1st compartment at ERY loading rates of 22.22 and 44.44 g/m^3d. The influent COD concentration was between 4020-4040 mg/L and then decreased to 550 and 646 mg/L (E=86%) in the effluent of the 1st compartment at an OTC loading rates of 22.22 and 44.44 g/m^3d. The COD concentration was around 4100-4120 mg/L in the influent of the 1st compartment at an ERY loading rates of 111.11 and 133.33 g/m^3d. Then this decreased to 1200 and 1300 mg/L in the effluent of the 1st compartment results COD removal efficiency of 71% and 68%, respectively. The COD yields decreased with increasing ERY loading rates in the 1st compartment.

The effluent COD concentrations were 365 and 425 mg/L in the 2nd compartment results COD removal efficiency of 34% at ERY loading rates of 22.22 and 44.44 g/m^3d. The effluent COD concentration was measured as 1000 mg/L in the effluent of the 2nd compartment, resulting in COD removal efficiency of 17% and 25% at an ERY loading rates of 111.11 and 133.33 g/m^3d. The COD removal efficiencies were between 21-24% in the 2nd compartment, respectively, at ERY loading rates between 66.67 and 88.89 g/m^3d. A small amount of COD yields (5-49%) were measured in 3rd compartment. The effluent COD concentrations were 205 and 250 mg/L in the 3rd compartment while 41% COD removal efficiency was observed at ERY loading rates

of 22.22 and 44.44 g/m^{3}d. The COD removal efficiencies were 5% and 12% in the 3rd compartment at ERY loading rates of 111.11 and 133.33 g/m^{3}d. COD removal efficiencies decreased with increasing ERY loading rates in compartments and the effluent of the AMCBR reactor. The total COD removals in the effluent of the AMCBR reactor were 95% and 79% at OTC loading rates of 22.22 and 133.33 g/m^{3}d, respectively (Figure 6.49).

Table 6.17 Variations of COD Concentrations in Compartments of AMCBR Reactor at Increasing ERY Loading Rates

Influent		**1st Compartment**		**2nd Compartment**		**3rd Compartment**	
ERY Loading (g/m^{3}d)	**COD Conc. (mg/L)**	**Eff. COD (mg/L)**	**COD Yield (%)**	**Eff. COD (mg/L)**	**COD Yield (%)**	**Eff. COD (mg/L)**	**COD Yield (%)**
22.22	4020±63	550	86	365±40	34	205±20	44
44.44	4040±50	646	86	425±50	34	250±25	41
66.67	4060±65	965	76	764±36	21	650±32	15
88.89	4080±70	850	79	650±32	24	525±40	19
111.11	4100±90	1200	71	1000±74	17	900±75	10
133.33	4120±103	1300	68	1000±82	23	950±90	5

6.2.5.2 Effect of ERY Loading Rate on the ERY Removal Efficiencies in the AMCBR Reactor

The effects of increasing ERY loading rate on the ERY removal efficiencies are shown in Figure 6.50 in AMCBR reactor. A maximum ERY removal efficiency of 95% was obtained at initial ERY concentrations of 50-100 mg/L at an ERY loading rates of 22.22 and 44.44 g/m^{3}d. This can be explained with the acclimation of methane *Archaea* bacteria to ERY. The ERY removal efficiency decreased from 95% to 90%, respectively, at an ERY loading rates of 44.44 to 66.67 g/m^{3}d in the AMCBR reactor. When the ERY loading rates was increased from 66.67 g/m^{3}d to 88.89 g/m^{3}d the ERY removal efficiency decreased from 90% to 87%, respectively in the AMCBR reactor. As the ERY loading rates increased from 88.89 to 111.11 g/m^{3}d the ERY yield decreased from 87% to 80%, respectively, in AMCBR reactor.

The ERY yield was found as 80% and 75%, respectively, at an ERY loading rates of 111.11 to 133.33 g/m^{3}d in AMCBR reactor (see Figure 6.50).

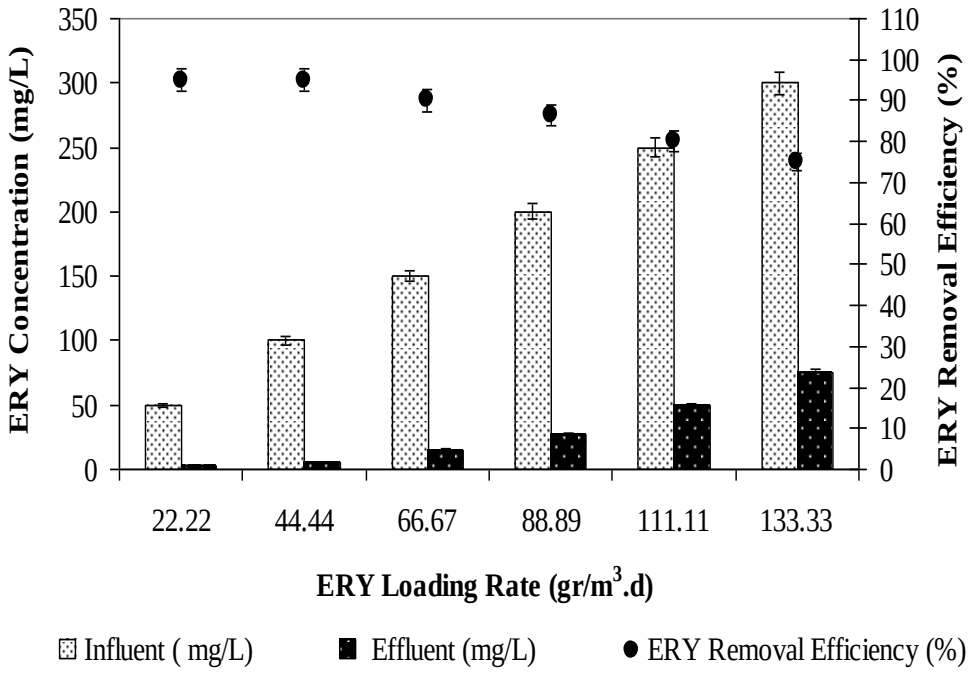

Figure 6.50 Effects of increasing ERY loading rates on ERY removal efficiencies in the AMCBR

The HPLC chromatograms of ERY were illustrated in Figure 6.51 for the effluent samples of the AMCBR at initial ERY concentration of 100 mg/L. Figure 6.51 shows the HPLC chromatogram of ERY standard of 100 mg/L (a), and anaerobic AMCBR reactor effluent (b). A peak of ERY standard of 100 mg/L was obtained at a retention time of 1.24 min and at a wave length of 287 nm (sees Figure 6.51 (a)). Similar peak are showed on the chromatograms at the same wave length in the effluent sample of AMCBR reactor (see Fig. 6.51 (b)). In our study, molasses used as the primary substrate was consumed as energy source and electron donor for ERY biotransformation. This shows that the anaerobic granule sludge in AMCBR reactor acclimated to different ERY concentrations. ERY at different concentrations is metabolized with the simultaneous utilization of primary substrate serving as the source of carbon and energy required for growth.

In our study the ERY removal was mainly through biodegradation since the studies performed in previous section (see Table 5.4-Study 3) showed that the biodegradation is seen a major mechanism of ERY removal and contributed around 99.9% of the total ERY removal in the batch reactors. The contributions of volatilization and adsorption to the ERY removal were not observed.

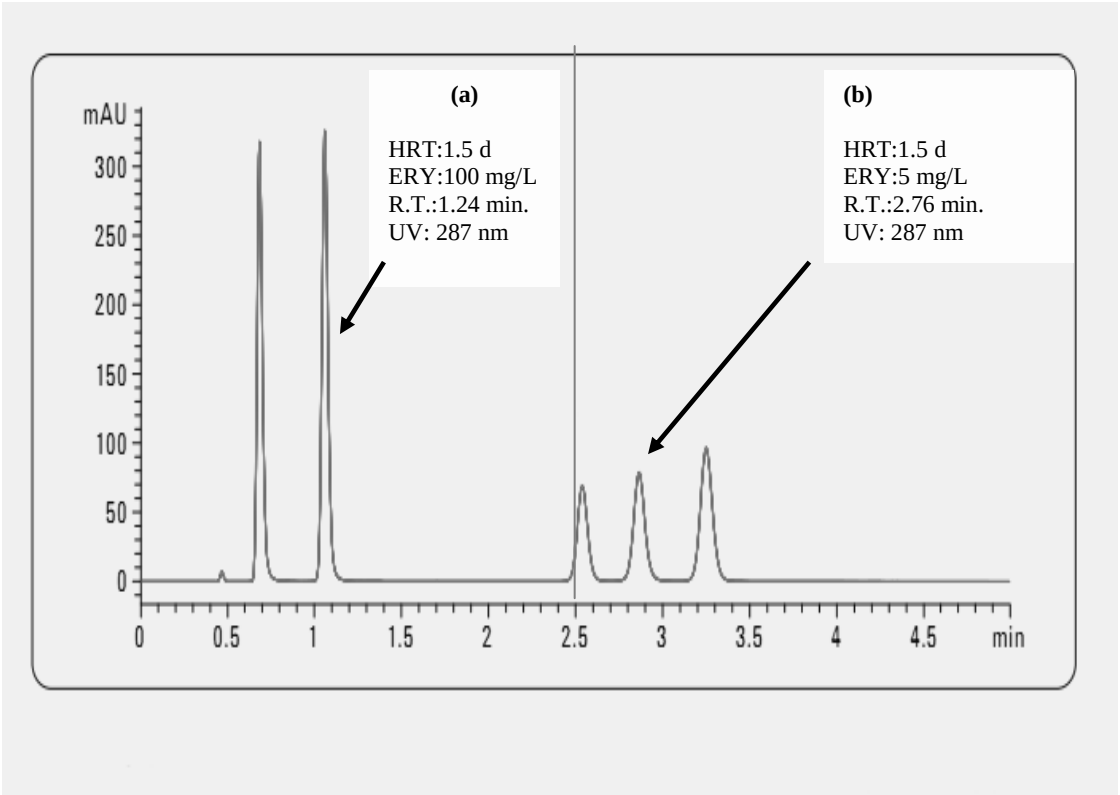

Figure 6.51 HPLC chromatograms of ERY in the influent and effluent of AMCBR reactor

The ERY yields obtained in our study are high in comparison to the removal performances of ERY in the studies given below: In a study performed by Kim et al., (2008) 85% azithromycin removal efficiency was observed for the anaerobic degradation of 100 mg/L azithromycin concentration in pharmaceutical wastewater after 2.4 days HRT and 10-20 days SRT, at pH 7.46. In the study performed by Shimada et al., (2011), the ERY yields (80%-86%) were lower than those of our data (75%-95%) at a OLRs 1.9 and 5.8 kgCOD/m^3d in an ASBR treating 90 mg/L ERY. In a study performed by Busetti and Heitz, (2011) 90%, ERY removal was obtained in synthetic pharmaceutical wastewater containing 100 mg/L mix antibiotic solution in an anaerobic conditions at a HRT of 2 days. In our study removal efficiencies of ERY was higher than those in the study performed by Busetti and Heitz, (2011). The

ERY removal was found to be lower (E=85%) in the study performed by Jessick et al., (2011) under anaerobic conditions at 80 mg/L ERY concentration, compared to the our study.

The yields obtained in the aforementioned studies are low in comparison to the removal performances of ERY found in our study. The reason of high ERY yields in our study could be explained by the granulated sludge which is resistant to the high toxic compounds and to the AMCBR reactor which is a high rate reactor. The high removal efficiency of this reactor came from its compartmentalized structure.

6.2.5.3 Effects of Increasing ERY Loading Rates on the Total and Methane Gas Production in the AMCBR Reactor

The total and methane gas production rates and methane contents in AMCBR reactor are shown in Figure 6.52. The daily total gas, methane gas productions and methane contents were approximately 7-12 L/d, 3-7.5 L/d and 45%-62%, respectively, for ERY loadings varying between 22.22 and 133.33 g/m^3d. The maximum total and methane gas productions and methane contents were found as 12 L/d and 7.5 L/d and 62%, respectively, at TYL loading rates of 22.22 and 44.44 g/m^3d. After these loading rates, the daily total gas, methane gas productions and methane percentage decreased. Total gas, methane gas productions and methane percentage were found as 7 L/d, 3 L/d and 45% at maximum ERY loading rate of 133.33 g/m^3d. This indicated an inhibition effect of ERY on methane *Archaea* at aforementioned ERY loading rates. The low rate of methane formation and methanogenic activity is attributed to the inhibitory effects of the pharmaceutical wastewater including antibiotic.

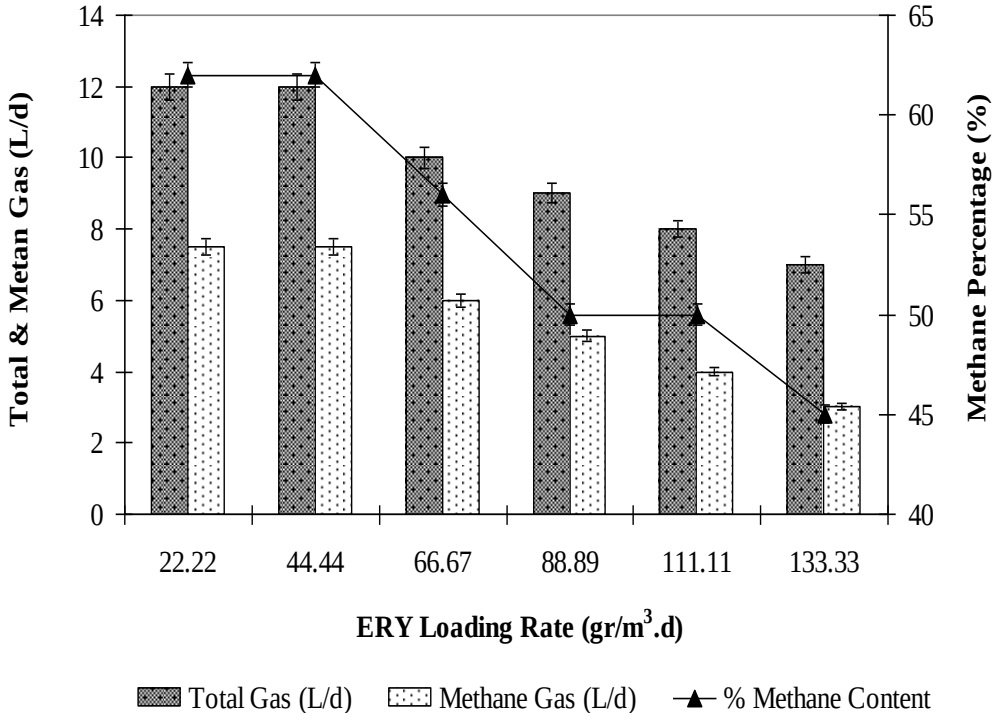

Figure 6.52 Effects of increasing ERY loading rates on the gas production, methane content in the AMCBR reactor.

In a study performed by Liu et al., (2011) 7.49 L/d methane gas production was found at OLRs varying at between 1.23 and 2.16 kg COD/m^3d, at an influent ERY=50-200 mg/L and a HRT=2 days in a full-scale UASB reactor. Shimada et al., 2011 reported that, 2.6 L/d biogas production at an influent TYL concentration of 167 mg/L at HRT of 1.67 days and at an OLR of 3.5 kg COD/m^3d in an ASBR reactor. In another study, in a study performed by Amin et al., (2006) methane gas production and percentage were found as 5 L/d and 48%, respectively at an OLR of 2.90 kg COD/m^3d in an ASBR. In our study, 62% methane percentage and 7.5 L/d CH_4 production was measured at influent ERY concentrations varying between 50 and 300 mg/L in an AMCBR reactor. The yields obtained in the aforementioned studies are low in comparison to the methane gas productions found in our study. This could be explained by the macrolide antibiotics (ERY, TYL, etc.) were inhibited methane production and content in anaerobic reactors. The degree of inhibition depended upon the antibiotic concentration.

The methane yield can be useful parameter to assess the performance of an anaerobic reactor Figure 6.53 shows the variations of methane yields versus ERY loading rates. The methane yields decreased from 0.36 to 0.12 $m^3CH_4/kgCOD_{removed}$, when the ERY loading rates were increased 22.22 to 133.33 g/m3d. As the ERY loading rates were increased from 44.44 to 66.67 g/m^3d methane yield decreased from 0.36 to 0.30 $m^3CH_4/kgCOD_{removed}$, respectively, in the AMCBR reactor (Figure 6.53). The methane yield was obtained as 0.25 and 0.21 $m^3CH_4/kgCOD_{removed}$, respectively, at ERY loading rates of 88.89-111.11 g/m^3d. As the TYL loading rates were increased from 111.11 to 133.33 g/m3d methane yield decreased from 0.21 to 0.12 $m^3CH_4/kgCOD_{removed}$, respectively in the AMCBR reactor (see Figure 6.53).

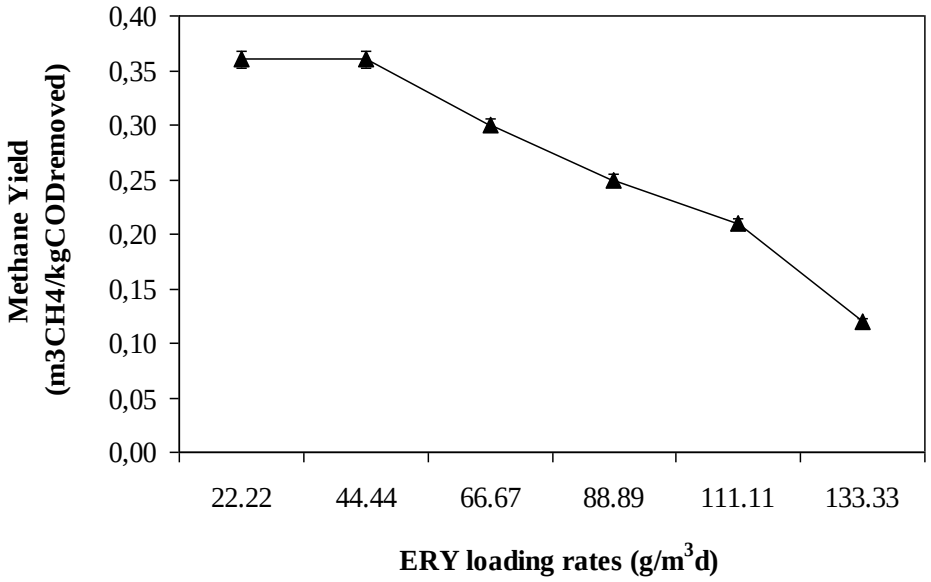

Figure 6.53 Effects of increasing ERY loading rates on the gas production, methane content in the AMCBR reactor

The methane yields obtained in our study are similar in comparison to the yield performances of methane in the studies given below: In the study by Nandy and Kaul, (2001), 0.26-0.34 $m^3CH_4/kgCOD_{removed}$ methane yields was observed for the anaerobic degradation of 200 mg/L TYL in herbal pharmaceutical wastewater after 2 days HRT. A similar study was also reported by Chelliapan et al., (2006) when treating pharmaceutical wastewater containing 20-200 mg/L TYL in an UASR. 0.10-0.40 $m^3CH_4/kgCOD_{removed}$ methane yields were obtained during 106 days of

operation time. Similarly, a lower methane yield value (0.20 $m^3CH_4/kgCOD_{removed}$) was obtained in the anaerobic treatment of chemical synthesis-based pharmaceutical wastewater at a HRT of 1.98 days (Ince et al., 2002). The lower methane yields in the studies mentioned above could be due to the configuration of the anaerobic reactor, type of anaerobic microorganism, to the biomass concentration and to the operational conditions.

6.2.5.4 Variation of pH, TVFA and Composition (H_{ac}, H_{bu}, H_{la}, H_{pr}) in Compartments of the AMCBR Reactor at Increasing ERY Loading Rates

In an anaerobic system, pH places an important role, which may affect the activity of the mixed microorganisms. The increase in the pH may be due to the accumulation of HCO_3 or decrease the pH due to the formation of volatile fatty acids. There by reducing the activity of the anaerobes. Optimum pH for anaerobic activity is in the range between 6.5 and 8.0 (Speece, 1996). The pH value is considered as one of the important factors affecting the behavior and fate of antibiotics in an environment (Rubert and Pedersen, 2006; Shaojun et al., 2008).

Figure 6.54 shows the pH variation in compartments of the AMCBR at increasing ERY loading rates. As shown in Figure 6.54, the pH values in the effluent and in the all compartments of AMCBR varied between 7.12 and 7.60. The pH values were lower in the 1st compartment than all of the other compartments since TVFA in the 1st compartment was higher (Figure 6.55). When the ERY loading rates was increased from 22.22 to 133.33 g/m^3d in the AMCBR reactor, the pH in the 1st compartment dropped from 7.36 to 7.12 due to the increased acidogenic activity. The pH profile of the AMCBR reactor system with average pH in 1st compartment was 7.24; while the pH in 2nd compartment was measured as 7.48. The pH in 3rd compartment was measured as 7.45. As shown in Figure 6.54, the pH values in the effluent of AMCBR varied between 7.40 and 7.55. In theory, the pH in 1st compartment should be lower than in compartments 2nd, 3rd, and effluent due to horizontal separation of acidogenesis and methanogenesis in a high rate reactor namely AMCBR (Nachaiyasit and Stuckey, 1997b).

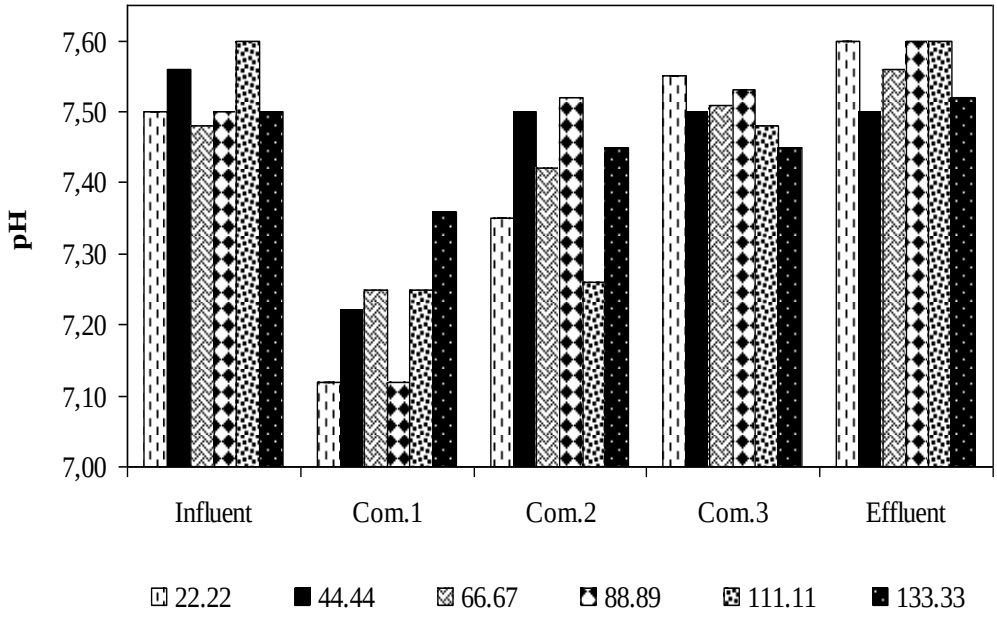

Figure 6.54 Variations of pH in the AMCBR reactor at increasing ERY loading rates

The TVFA concentration in each compartment of the AMCBR reactor is shown in Figure 6.55 and indicates a low concentration of TVFA (average 2 mg/L) in the AMCBR reactor effluent when operated at ERY loading rates in the range 22.22 to 111.11 g/m^{3}d. The TVFA concentration in the 1st compartment was measured between 500 and 900 mg/L (see Figure 6.55) for the ERY loading rates between 22.22 and 133.33 g/m^{3}d, respectively. Almost 350-700 and 15-22 mg/L TVFA concentrations were detected in the 2nd and 3rd compartments of the AMCBR for the ERY loading rates between 22.22 and 133.33 g/m^{3}d, respectively. It was found that the TVFA concentrations decreased from compartment 1st to compartments 2nd and 3rd. The TVFA concentrations were measured as 350 and 500 mg/L at ERY loading rate as high as 133.33 g/m^{3}d due to inhibition effects of high ERY concentrations to acidogens in the 1st and 2nd compartments of the AMCBR reactor. The minimum TVFA concentration in the effluent of the AMCBR reactor was measured between 0-2 mg/L for the ERY loading rates between 22.22 and 133.33 g/m^{3}d, respectively (see Figure 6.55). A strong linear correlation between TVFA concentrations and ERY loading rates was observed in the 1st and 2^{n}d compartments for TYL loading rates of 22.22 and 133.33 g/m^{3}d (ANOVA) (R^2=0.95; F=3.85, p=0.01).

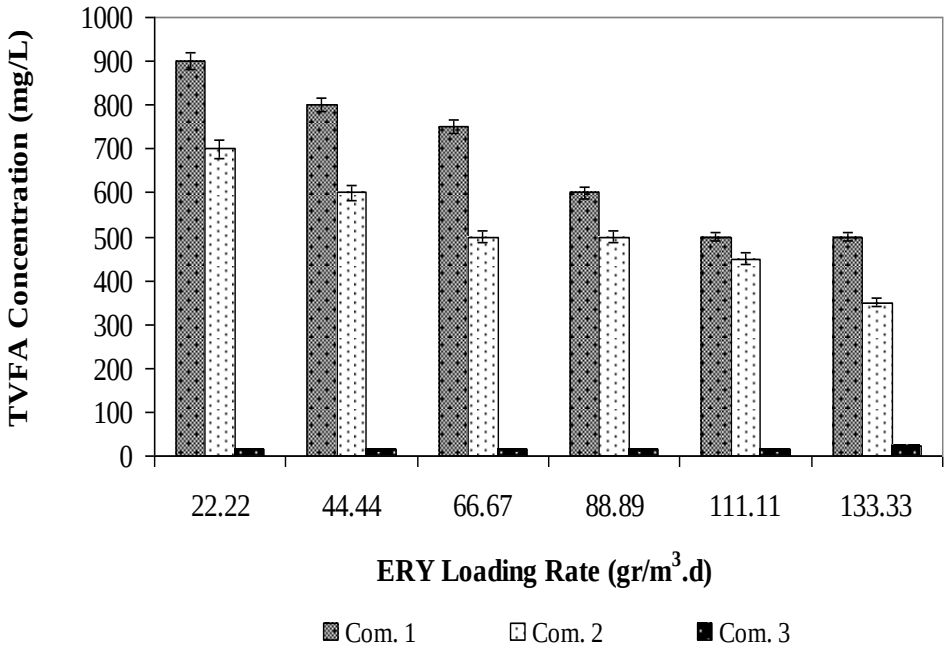

Figure 6.55 Variations of TVFA concentration in the AMCBR at increasing ERY loading rates

The results of this study showed that the TYL loadings affected the TVFA production during anaerobic degradation of pharmaceutical wastewater. In a study performed by Shimada et al., (2011) 8.9-3400 mg/L TVFA concentrations were obtained at a HRT of 1.67 days in an ASBR reactor at influent TYL concentrations varying between 1.67 and 167 mg/L. In the study performed by Chelliapan et al., (2006), the TVFA concentrations (100-800 mg/L) were lower than those of our results (950 mg/L) at a HRT of 4 days in an anaerobic UASR reactor treating 20-200 mg/L TYL.

6.2.5.4.1 Variation of TVFA Components (H_{ac}, H_{pr}, H_{bu}, H_{la} and H_{pr}/H_{ac}) Ratios in the AMCBR at Increasing ERY Loading Rates. The H_{ac} concentrations lower than 800 mg/L and the ratio of H_{pr}/H_{ac} lower than 1.4 is two indicators for successful methane production (Hill et al., 1987). Table 6.18 and Figure 6.56 show all the result H_{pr}/H_{ac} is lower than 1.4 that means the system (AMCBR) is successful for produce methane. As shown in Figure 6.56, this ratio varied between 0.71-0.87 and 0.52-0.85, respectively in 1st and 2nd compartments of AMCBR reactor at increasing ERY

loading rates (from 22.22 to 133.33 g/m^{3}d). The H_{pr}/H_{ac} ratios were found as 0.78, 0.77, 0.85, 0.87, 0.71 and 0.83 respectively, at TYL loading rates of 22.22-133.33 g/m^{3}d in 1st compartment of AMCBR reactor. As shown in Figure 5.56, this ratio varied between 0.75, 0.80, 0.85, 0.85, 0.52, and 0.72 respectively in 2nd compartments of AMCBR reactor at increasing TYL loading rates (from 22.22 to 133.33 g/m^{3}d). The AMCBR reactor system was successful if check from ratio between H_{pr} to H_{ac}. It was ratio between H_{pr} to H_{ac} lower than 1.4.

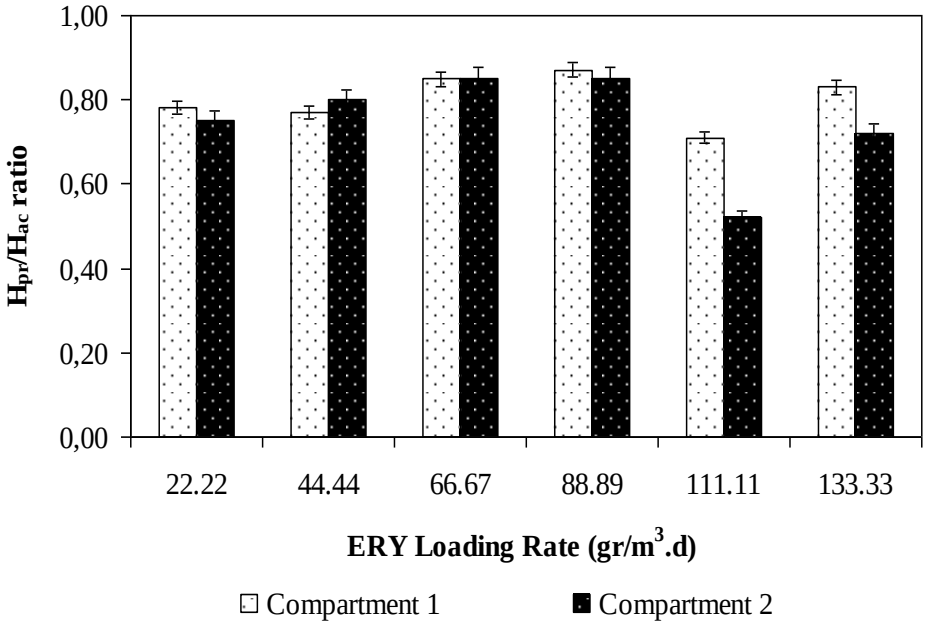

Figure 6.56 Variations of H_{pr}/H_{ac} ratio in the AMCBR reactor at increasing ERY loading rates

As the ERY loading rates were increased from 22.22, 44.44, 66.67, 88.89, 111.11 to 133.33 g/m^{3}d H_{ac} concentrations decreased from 400, 360, 300, 230, 170 to 120 mg/L, respectively in the 1st compartment (Table 6.18). The concentrations of H_{pr} also decreased from 310, 280, 255, 200, 120 to 100 mg/L respectively. The concentrations of H_{bu} were obtained as 140, 130, 105, 100, 80 and 70 mg/L, respectively; at ERY loading rates of 22.22-133.33 g/m^{3}d (see Table 5.18). As the ERY loading rates were increased from 22.22, 44.44, 66.67, 88.89, 111.11 to 133.33 g/m^{3}d H_{la} concentrations decreased from 40, 30, 30, 20, 20 to 20 mg/L, respectively in the 1st compartment (Table 6.18).

As shown in Table 6.18, the H_{ac} concentrations were decreased from 345, 200, 110, 100, 50 to 32 mg/L at ERY loading rates of 22.22, 44.44, 66.67, 88.89, 111.11 to 133.33 g/m^3d, respectively in the 2nd compartment. Similarly, the concentrations of H_{pr} also decreased from 260, 160, 94, 85, 26 to 23 mg/L, respectively, when 22.22, 44.44, 66.67, 88.89, 111.11 to 133.33 g/m^3d ERY were added to the AMCBR reactor. The H_{bu} concentrations were found as 70, 100, 60, 50, 30 and 20 mg/L, respectively, at ERY loading rates of 22.22, 44.44, 66.67, 88.89, 111.11 to 133.33 g/m^3d, respectively in the 2nd compartment of AMCBR reactor (see Table 6.18). As the ERY loading rates were increased from 22.22, 44.44, 66.67, 88.89, 111.11 to 133.33 g/m^3d H_{la} concentrations decreased from 25, 40, 30, 20, 10 to 5 mg/L, respectively in the 2nd compartment (Table 6.18).

Table 6.18 Variations of TVFA composition (H_{ac}, H_{pr}, H_{bu}, H_{la}) and H_{pr}/H_{ac} ratio in the AMCBR reactor at increasing ERY loading rates

Parameter	AMCBR, 1st compartment						AMCBR, 2nd compartment					
	ERY Loading Rate						ERY Loading Rate					
	22.22	44.44	66.67	88.89	111.11	133.33	22.22	44.44	66.67	88.89	111.11	133.33
TVFA (mg/L)	900	800	750	600	500	500	700	600	500	500	450	350
H_{ac} (mg/L)	400	360	300	230	170	120	345	200	110	100	50	32
H_{pr} (mg/L)	310	280	255	200	120	100	260	160	94	85	26	23
H_{bu} (mg/L)	140	130	105	100	80	70	70	100	60	50	30	20
H_{la} (mg/L)	40	30	30	20	20	20	25	40	30	20	10	5
H_{pr}/H_{ac} ratio	0.78	0.77	0.85	0.87	0.71	0.83	0.75	0.80	0.85	0.85	0.52	0.72

6.2.5.5 Variation of HCO_3 and TVFA/HCO_3 Ratio in Compartments of the AMCBR Reactor at Increasing ERY Loading Rates

The HCO_3 concentrations remained between 3856 and 4012 mg/L in the effluent of AMCBR reactor at increasing ERY loading rates (22.22-133.33 g/m^3d) (see Figure 6.57). The HCO_3 concentration in the 1st compartment was lower than the other compartments. This indicates the utilization of alkalinity to buffer the TVFA and CO_2 produced from the anaerobic co-metabolism of ERY, particularly at high concentrations. Figure 6.57 indicates a low concentration of HCO_3 from 3800 mg/L down to 2000 mg/L was present in the 1st compartment when the AMCBR was operated at ERY loading rates in the range 22.22-133.33 g/m^3d. However, in 3rd compartment, the HCO_3 concentrations between 3960 and 4005 mg/L at increasing ERY loading rates of 22.22-133.33 g/m^3d. The ERY loading rates increased from 22.22 to 66.67 g/m^3d the HCO_3 alkalinity concentrations increased from 3960 to 3985 mg/L in 3rd compartment. Similarly, the concentrations of HCO_3 alkalinity also increased from 3985 to 3900 mg/L, respectively, when 66.67 to 88.89 g/m^3d ERY were added to the AMCBR reactor.

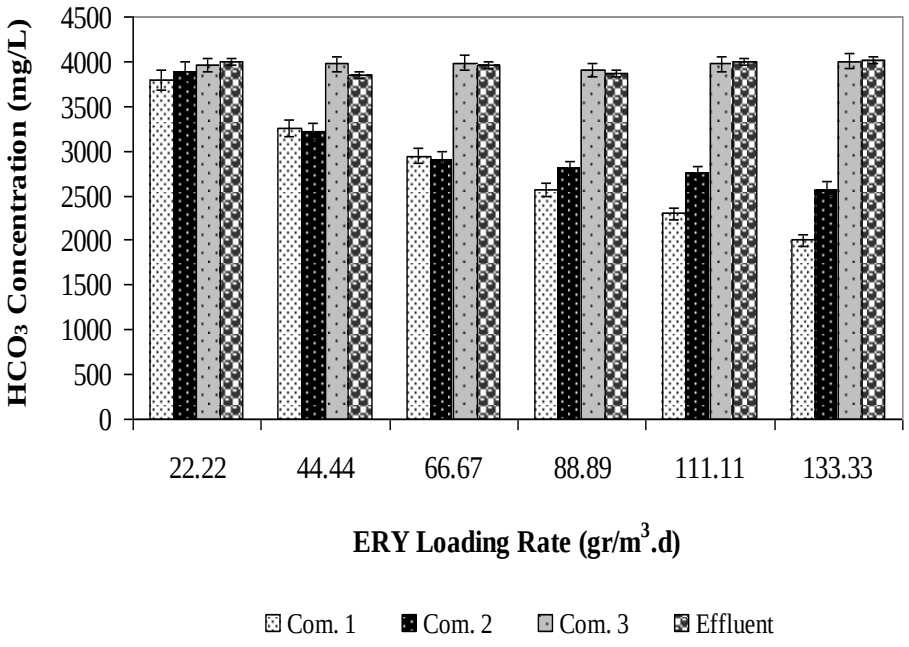

Figure 6.57 Variations of HCO_3 concentration in AMCBR at increasing ERY loading rates

The stability of an anaerobic reactor can be evaluated by the TVFA/HCO_3 ratio (Khanal, 2008). Barampouti et al., (2005), suggest that the ideal ratio of TVFA/HCO_3 is in the range of 0.1 to 0.3 to avoid the acidification of the anaerobic reactor. A value above 0.4 is an indicator of instability. The TVFA/HCO_3 ratios for this study are shown in Figure 6.58. As shown in Figure 5.58, this ratio varied between 0.01 and 0.25 in compartments and the effluent of AMCBR at increasing ERY loading rates (22.22-133.33 g/m^3d). These results indicated that the AMCBR reactor treating ERY was operated under stable conditions at increasing ERY loading rates. This suggests that the TVFA concentrations in the anaerobic reactor are linked to the easily assimilated organic matter by microorganisms and to methane production.

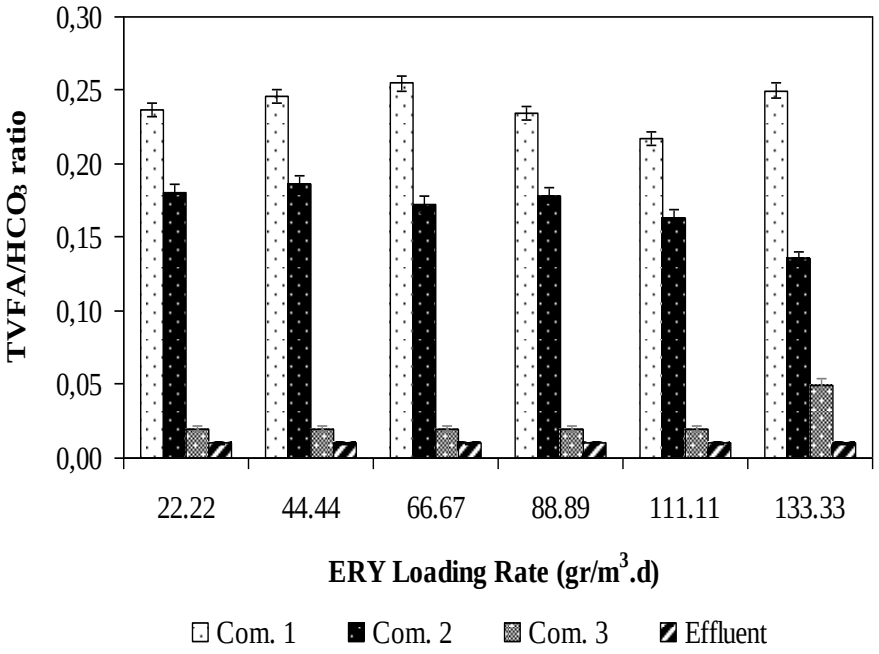

Figure 6.58 Variations of TVFA/HCO_3 ratio in the AMCBR at increasing ERY loading rates

6.2.5.6 Effect of ERY Loading Rate on the COD and ERY Removal Efficiencies in the CSTR Reactor

Figure 6.59 and 6.60 shows the effect of increasing ERY loading rates on the COD and ERY yields in the aerobic CSTR reactor. As shown in Figure 6.59, the COD removal efficiency was 90% at an ERY loading rate of 22.22 g/m^3d. The COD

yields were between 80 and 63% for ERY loading rates of 44.44-133.33 g/m^{3}d, respectively, in the CSTR reactor. The COD removal efficiency remained approximately 71% until an ERY loading rate of 88.89 g/m^{3}d. After this ERY loading rate, COD removal efficiency decreased rapidly from 71% to 63%. The effluent COD concentration and removal efficiency were measured as 350 mg/L and 63%, respectively, at a maximum ERY loading rate of 133.33 g/m^{3}d. The optimum ERY loading rate was found as 22.22 g/m^{3}d for maximum COD removal efficiency of 90%.

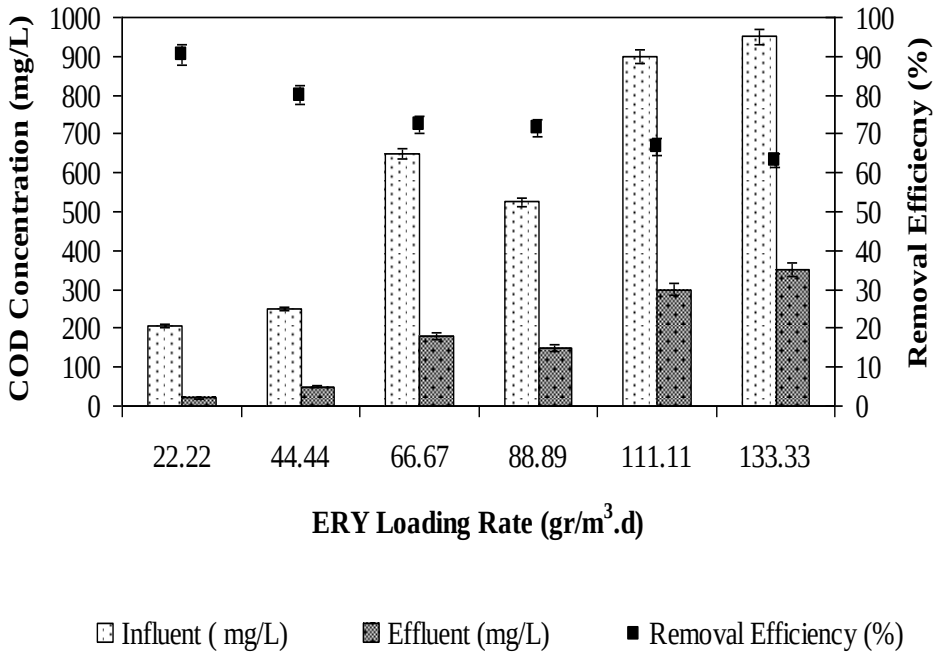

Figure 6.59 COD removal in the aerobic CSTR reactor at increasing ERY loading rates

The ERY removal efficiency of 80% was obtained at an ERY loading rate of 22.22 g/m^{3}d. When the ERY loading rate was increased from 22.22 and 44.44 to 66.67 g/m^{3}d the ERY removal efficiency decreased from 80% and 73% to 73%, respectively. A maximum ERY removal efficiency of 80% was obtained at an ERY loading rate of 22.22 g/m^{3}d in the aerobic CSTR reactor. The effluent ERY concentration was measured as 0.5 mg/L at an ERY loading rate of 22.22 g/m^{3}d. The ERY yield was 73% for ERY loading rates of 44.44 and 66.67 g/m^{3}d in the aerobic CSTR reactor. When the ERY loading rate was increased from 88.89 g/m^{3}d to

111.11 and to 133.33 g/m^{3}d the TYL removal efficiency decreased from 67% to 50% and 50%, respectively, in the aerobic CSTR reactor (Figure 6.60).

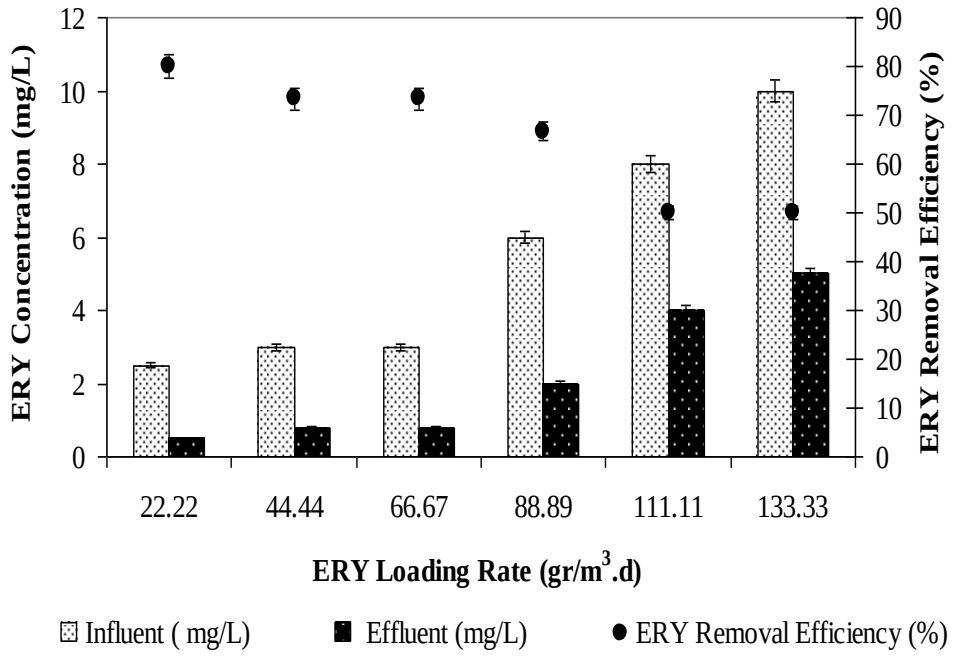

Figure 6.60 TYL removals in the aerobic CSTR reactor at increasing ERY loading rates

6.2.5.7 Treatment Efficiencies of Anaerobic/Aerobic Sequential Reactor System

Figure 6.61 shows the overall COD and ERY removal efficiencies in the anaerobic/aerobic sequential reactor system. The maximum COD and the ERY removal efficiency in sequential AMCBR/CSTR reactor system were measured as 99% and 99% at an ERY loading rate of 22.22 g/m^{3}d, respectively. Total COD and ERY removal efficiencies decreased from 93% to 95% and from 92% and 94% as the ERY loading rates increased from 111.11 to 133.33 g/m^{3}d in the sequential AMCBR/ CSTR reactor system.

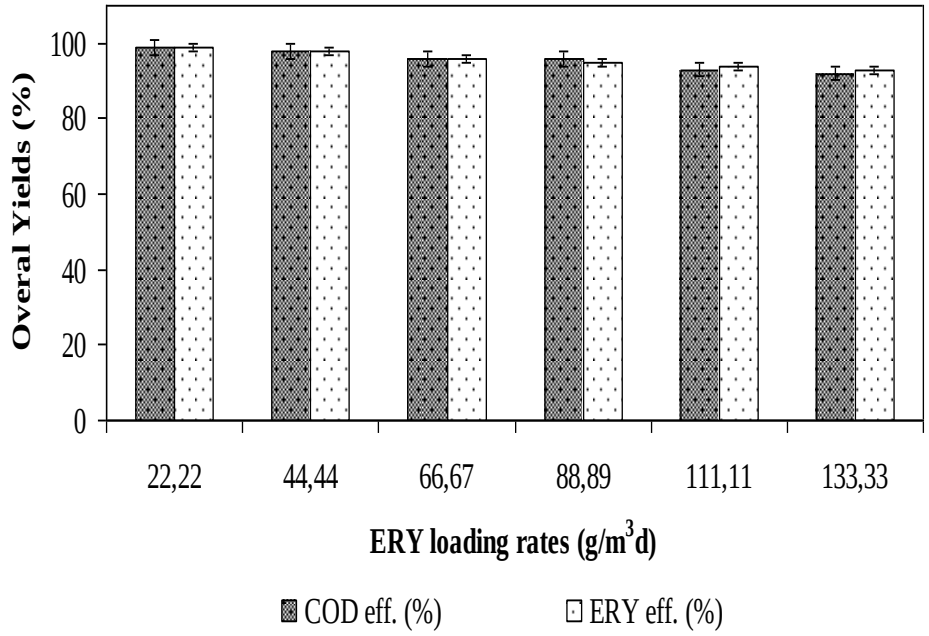

Figure 6.61 ERY and COD removal in the sequential AMCBR/CSTR reactor at increasing ERY loading rates

6.2.6 Effect of Hydraulic Retention Time (HRT) on Performance of AMCBR Reactor

6.2.6.1 Effects of HRTs on the COD and OTC Removal Efficiencies in the AMCBR Reactor

The effect of HRT on the COD and OTC yields are shown in Figure 6.62. In this study the HRT were decreased from 5.5, 4.5, 2.25, 1.5, 1.13 to 0.9 days. This corresponds to the increasing OLR loadings step by step from 0.74 to 0.89, 1.80, 2.70, 3.60 and 4.52 kgCOD/m^3d. The influent OTC concentration was kept constant as 100 mg/L. 100 mg/L OTC gives an additional COD concentration to total COD (4062 mg/L) thought continuous operation. As shown in Figure 6.62, 92% COD removal efficiency was obtained at HRTs of 5.5 and 4.5 days in the AMCBR reactor. When the HRT was decreased from 2.25 to 1.13 days, the COD removal efficiency decreased from 88% to 70%, respectively. The COD removal efficiency was 68% at a HRT of 0.9 day.

The maximum COD and OTC (E=92% and E=95%) removal efficiencies were observed at HRTs varying between 4.5 and 5.5 days. In our study, molasses was used as the primary substrate for the reduction of OTC. The primary substrate (molasses) is consumed as an energy source and electron donor for anaerobic antibiotic biodegradation. In other words the OTC was used as secondary carbon and energy source by the anaerobic bacteria.

These removal efficiencies were higher that those obtained by Öktem et al., (2008). Öktem et al., (2008) investigated the performance of an anaerobic sludge blanket reactor treated a chemical synthesis–based pharmaceutical wastewater at two HRTs (1 and 3 days). The COD removal efficiency increased from 58% to 78% when the HRT was increased from 1 to 3 days. Similarly, the maximum COD removal efficiency obtained by Akunna and Clark, (2000) was low (88%) at a HRT of 4 days in an anaerobic baffled reactor treating a pharmaceutical wastewater.

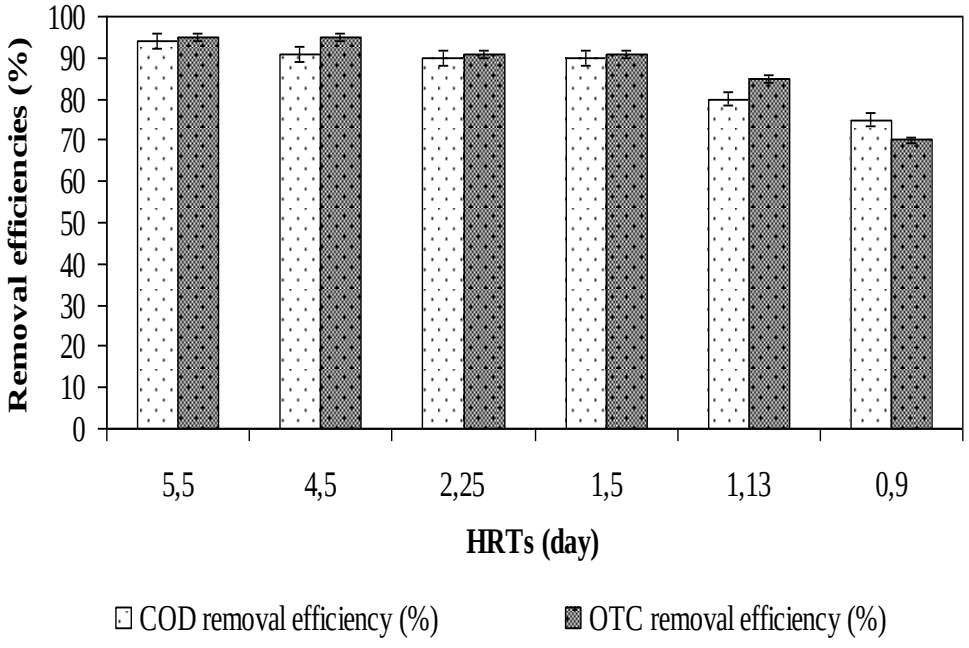

Figure 6.62 The effect of HRTs on the COD and OTC removal efficiencies in AMCBR reactor

6.2.6.2 Effect of HRTs on the Total and the Methane Gas Productions in the AMCBR Reactor

The variations of the total, methane gas productions and methane percentage in AMCBR are shown for all HRTs in Figure 6.63. From this figure, it can be seen that the daily gas productions and methane percentage decreased whenever HRT was decreased. The methane gas productions in the AMCBR were obtained as 7 and 6.8 L/d while the HRTs were 5.5 and 4.5 days, respectively (see Figure 6.63). The total gas productions and the methane percentage remained around 13 L/d and 60%, respectively, for the HRTs mentioned above. The methane gas production remained the same as is in high HRTs (5.6 L/d) while the total gas production decreased slightly (from 13 to 12 L/d) as the HRT decreased from 4.5 to 2.25 days. The decrease in HRT from 2.25 to 1.5 days slightly decreased the volumetric total and methane gas productions (11 and 5 L/d, respectively) while the methane gas percentage was recorded as 48% (Figure 6.63).

At low HRTs the granulated bacteria could not have enough time to metabolize the 100 mg/L OTC. Therefore the methane gas production dropped to 4 and 3.8 L/day as well as the total gas production decreased at HRTs 1.13 and 0.9 days, respectively. The methane percentage also decreased to 48 and 40% for the aforementioned HRTs. The decline of methane percentage could be attributed to the inhibition of activity of methanogens. On the other hand sulfate-reducing bacteria can out compete with methanogens for molasses-COD since hydrogen sulfide production can be predominant over methane gas production at lower HRTs. In those cases, organic carbon is oxidized to CO_2 with a contaminant reduction of sulfate to H_2S resulting in a limitation of methane gas production as reported by Malina et al., (1992); Ince et al., (2002) and Kim et al., (2007). In this study, the H_2S concentration in the gas was measured as 190 ppm at short HRTs such as 1.13 and 0.9 days.

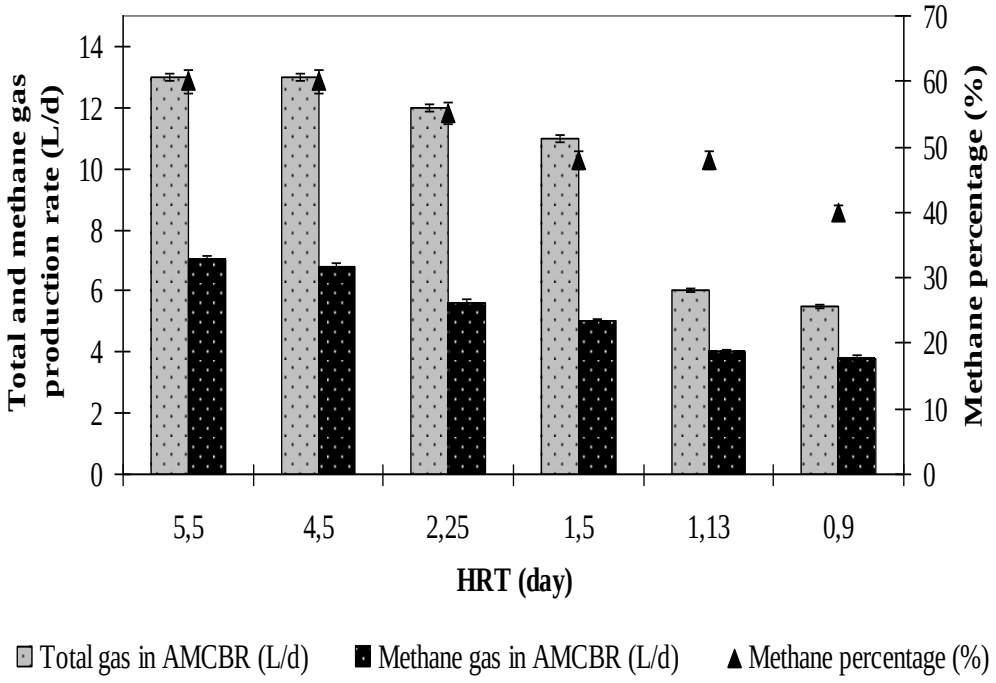

Figure 6.63 The effect of HRTs on total, methane gas production and methane percentage in AMCBR reactor

The optimum HRTs for maximum methane gas productions (60%) varied between 4.5 and 5.5 days. A strong linear correlation between COD removal and methane percentage was observed only for HRTs between 4.5 and 5.5 days (R^2=0.98, F=1.99, p=0.03). Similarly, a strong linear correlation between COD removal and methane gas production was observed only for HRTs between 4.5 and 5.5 days (R^2=0.95, F=3.48 p=0.02). In this study, the methane yield ($m^3CH_4/kgCOD_{removed}$) can be a useful parameter to assess the performance of AMCBR. As the treatment of wastewater is directly related to the amount of methane produced per kg of COD stabilized is taken to be an indicator of OTC and COD stabilization degree. Figure 6.64 show the variations of methane yields versus HRTs. It was observed that the methane yields decreased from 0.31 to 0.10 $m^3CH_4/kgCOD_{removed}$, when the HRT were increased from 5.5 days to 0.9 day in AMCBR reactor. A linear correlation between COD removal and methane yield only for HRTs between 4.5 and 5.5 days (R^2=0.92, F=4.19, p=0.01).

The methane yield results obtained in this study are higher than those obtained by Uyanık et al., (2002). Uyanık et al., (2002) found that the methane yield was 0.15 $m^3CH_4/kgCOD_{removed}$ at an OLR of 0.62 $kgCOD/m^3d$ in the anaerobic baffled reactor (ABR) treated industrial wastewater.

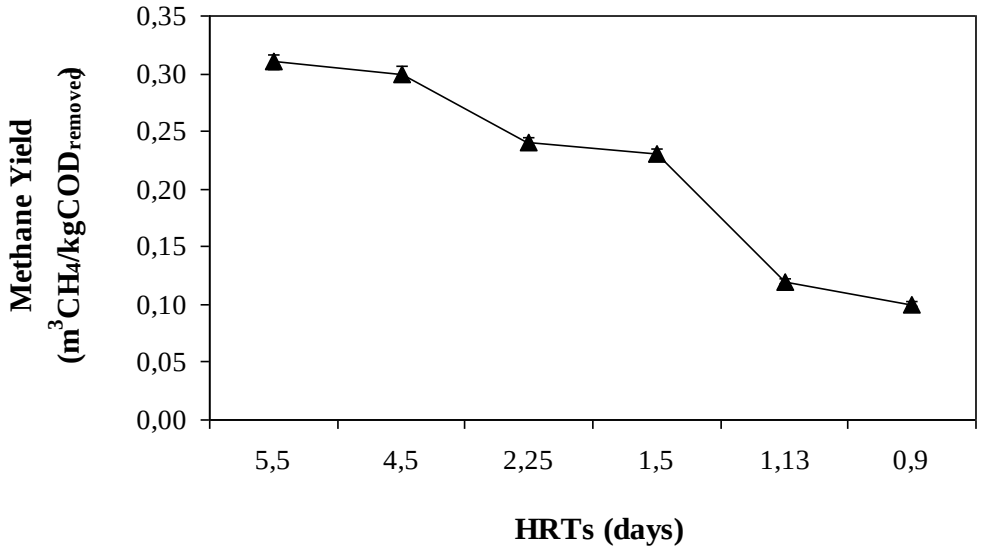

Figure 6.64 Variations of methane yields versus HRTs in the AMCBR reactor

6.2.6.3 Effects of HRTs on pH, TVFA, HCO_3 Alk. and TVFA/HCO_3 Alk. Ratio Variations in Compartments of the AMCBR Reactor

Figure 6.65 shows the variations of pH, TVFA, HCO_3 Alk. and TVFA/HCO_3 ratio in compartments of AMCBR reactor at decreasing HRTs. As shown in Figure 6.65 (a), the influent pH values remained stable at between 7.1 and 7.6 through continuous operation. The pH values varied between 7.4 and 7.85 in the effluent of AMCBR at HRTs varied between 5.5 and 0.9 days. These values are between optimum pH values of 6.5 and 8.3 reported by Speece, (1996). From Figure 6.65 (a) shows that the pH values in the 1st compartment were lower than the other two compartments. The possible reason of the decreases of pH in the 1st compartment can be explained by the increasing of TVFA levels (see Figure 6.65 (b)). TVFA concentrations in 1st compartment increased from 600 mg/L to 900 mg/L as the HRT

decreased from 5.5 to 0.9 days. However pH values were between optimum values, approximately, 7.2 in the 1st compartment at all HRTs, because of sodium bicarbonate concentration in the feed water. pH values varied between 7.2 and 7.6 in the 2nd and 3rd compartments at all HRTs. pH values in the effluent were around 7.4 at all HRTs. TVFA concentrations decreased in 2nd and 3rd compartment and effluent at all HRTs. This caused rising of pH values in the 2nd and 3rd compartments. When HRT was decreased from 5.5 to 0.9 days, the TVFA concentrations in 1st, 2nd and 3rd compartments were 900, 590 and 65 mg/l as HRT decreased from 5.5 to 0.9 day. Our studies exhibit similar results with the studies performed by Angenent et al., (2001) in AMBR reactor at a HRT of 3 hour. In this study, TVFA concentration was high in the 1st compartment than other compartments. TVFA concentrations were found as 1859 mg/l in the 1st compartment, 1388 mg/L in the 2nd compartment, 774 mg/L in the 3rd compartment, 432 mg/L in the 4th compartment and 353 mg/L in final compartment at shock OLR of 50 kgCOD/m^3d at HRT of 3 hours.

The HCO_3 Alk. in the feed was required to buffer the media to provide the favorable conditions for conversion of substrate to methane (Speece, 1996). Figure 6.65 (c) shows HCO_3 concentration in the compartments and effluent of AMCBR at different HRTs. HCO_3 concentrations in the feed wastewater were around 2500-3000 mg/L at all HRT. HCO_3 concentration in the 1st compartment was lower than the other compartments due to higher TVFA. HCO_3 concentration in the 1st compartment decreased from 3000 mg/L to 2700 mg/L with increasing of TVFA concentration from 600 mg/L to 900 mg/L as the HRT decreased from 5.5 days to 0.9 day. HCO_3 concentrations in the 2nd and 3rd compartment varied between 2800-3000 mg/L until a HRT of 1.5 days. HCO_3 concentration was around 2900 mg/L in compartments 2nd and 3rd at lower HRTs such as 0.9 day. This caused high TVFA concentration in compartments of AMCBR at lower HRTs. The effluent HCO_3 concentrations were between 2600-2900 mg/L at all HRTs. Figure 6.65 (d) showed the TVFA/HCO_3 ratios in the compartments and in the effluent of AMCBR. This ratio changed between 0.20 and 0.33 in 1st compartment, between 0.11 and 0.22 in 2nd compartment and between 0.04 and 0.08 in 3rd compartment and between 0.00 and 0.03 in the effluent of AMCBR at all HRTs. TVFA/ HCO_3 ratios were lower than 0.4

in the compartments and in the effluent of AMCBR at all HRTs. This shows the stability of the AMBR reactor as reported by Behling et al., (1997).

(a) The variations of pH

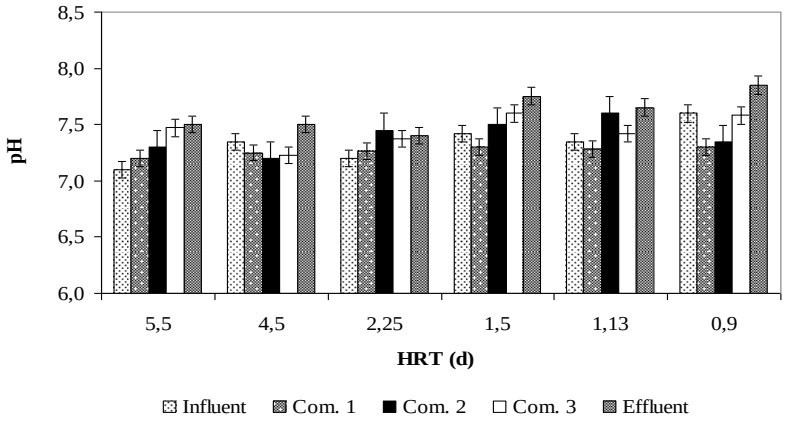

(b) The variations TVFA

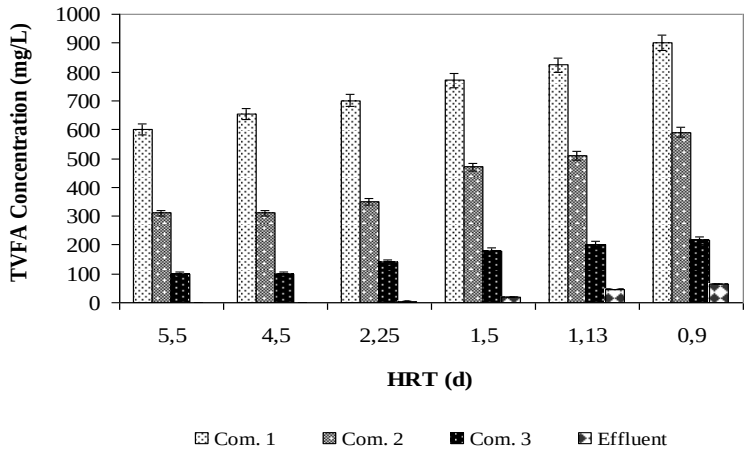

(c) The variations HCO_3 Alk.

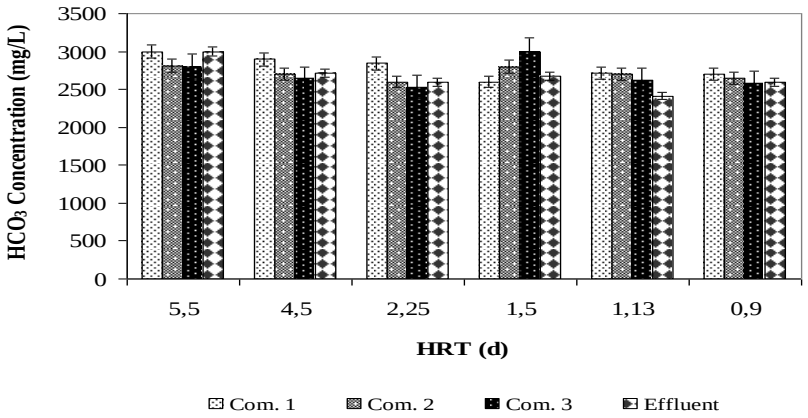

(d) The variations TVFA/HCO_3 ratio

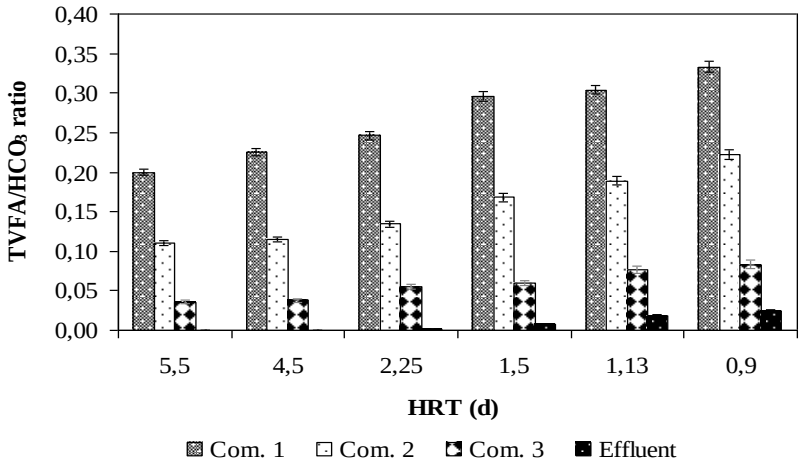

Figure 6.65 The variations of pH **(a)**, TVFA **(b)**, HCO_3 Alk. **(c)** TVFA/HCO_3 ratio **(d)** in compartments of AMCBR at decreasing HRTs.

6.2.6.4 Effects of HRTs on the COD and OTC Removal Efficiencies in the CSTR Reactor

Table 6.19 shows the effect of decreasing HRT on the COD and OTC removals in the aerobic reactor. The COD removal efficiencies were around 85%, 83%, and 82% for HRTs of 10.97, 9.00 and 4.50 days, respectively in the CSTR reactor. The OTC yields were 80, 80 and 75% for the aforementioned HRTs. The COD and OTC yields decreased to 75-65% and 69-65% at HRTs of 2.25 and 1.80 days, respectively. The COD and OTC removal efficiencies decreased at low HRTs in the aerobic reactor. Since the effluent of the AMCBR was used as the feed in the influent of the CSTR the COD and the OTC remaining from the AMCBR were removed in the CSTR. In the CSTR the rest of the COD and OTC which could not be biodegraded in the AMCBR were low. This means that the COD and OTC were mainly biodegraded in the AMCBR.

Table 6.19 COD and OTC yields in CSTR at six different HRTs

Parameters	**HRT (day)**					
	10.97	**9.0**	**4.5**	**3.0**	**2.25**	**1.80**
COD concentration in influent (mg/L)	300	300	300	300	300	300
COD concentration in effluent (mg/L)	45	51	54	60	75	105
COD Removal efficiency (%)	85	83	82	80	75	65
OTC concentration in influent (mg/L)	2.5	2.5	2.5	2.5	2.5	2.5
OTCconcentration in effluent (mg/L)	0.50	0.5	0.63	0.73	0.78	1.00
OTC Removal efficiency (%)	80	80	75	71	69	65

6.2.6.5 Performance of Anaerobic AMCBR /Aerobic CSTR Sequential Reactor System

Figure 6.66 shows the removal efficiencies of COD, OTC at six studied HRTs in the AMCBR/CSTR system. The COD and OTC removals in the total sequential total system were ≥ 90% as the HRTs decreasing from 16.47 to 2.70 days. The maximum COD and OTC yields were 99% and 99%, respectively, for the HRTs given above while the lowest COD and OTC yields were 94% and 90%, respectively at a HRT of 2.70 days, in the sequential AMCBR/CSTR system. 94% of the COD was removed in the anaerobic reactor while the remaining COD (5% of COD) was biodegraded in the aerobic reactor at HRTs between 6.75 and 16.47 days. This showed that a significant part of the OTC could be removed with high removal efficiency in the sequential AMCBR/CSTR system.

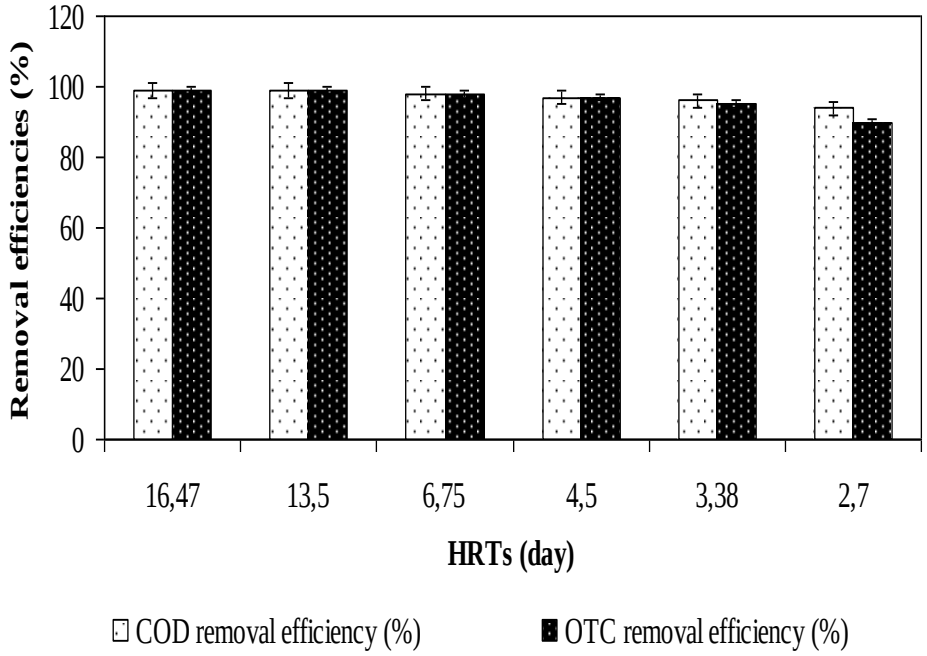

Figure 6.66 COD and OTC removal efficiencies in the sequential AMCBR/CSTR system

6.2.6.6 Effects of HRTs on the COD and AMX Removal Efficiencies in the AMCBR Reactor

When the HRT of the AMCBR was decreased from 5.5 to 4.5, 2.25 and 1.5 days, no significant changes occurred in the effluent water quality (Figure 6.67). The influent COD and AMX concentrations were 4000 mg/L and 150 mg/L, respectively, in the AMCBR reactor. The influent AMX concentration was kept constant as 150 mg/L. 150 mg/L AMX gives an additional COD concentration to total COD (4040 mg/L) thought continuous operation.

93% COD and 94% AMX maximum removal efficiencies were obtained at HRTs of 4.5 and 5.5 days. These were the maximum COD and AMX yields obtained in the AMCBR. The COD and AMX removal efficiencies at 2.25 days HRT were around 90% and 92%, respectively, after which point there was a slightly decrease at 1.5 days HRT only for COD yield (91%) while the AMX yield remained as the same (94%), and the yields were reduced further (COD and AMX yields decreased to 70 and 84%) at a HRT of 1.13 days (see Figure 6.67). The yields decreased to around

70% at a HRT of 0.9 day. This indicates that COD and AMX removal efficiencies became less efficient and more variable with the HRT reduction from 1.5 days to 1.13 and to 0.9 days. ANOVAs test statistics showed that a significant linear relationship between COD, AMX yields and HRTs varying between 1.5 and 5.5 days was not observed (R^2=0.39, p=0.05, F=8.67) while the linear relationship between yields and low HRTs (0.9 and 1.13 days HRT) (R^2=0.83, p=0.05, F=2.78) was significant. Although the AMCBR with a high granulated sludge concentration of 89 mg/L exhibited a successful anaerobic treatment for AMX and COD at high HRTs between 1.5 and 5.5 days, these yields decreased at HRT as low as 0.9 and 1.13 days. In this study it was found that decreasing the HRT from 5.5 days to 1.5 days do not to have a significant effect on COD and AMX removals since the granulated sludge used in this study with high microorganism content and high activity increase the reactor performance. The low AMX and COD yields in the AMCBR at lower HRTs like 0.9 and 1.13 days the granulated sludge does not have sufficient time available for mineralization of COD and AMX and their metabolites. Under these conditions the mass transfer (COD and AMX) into the granules from the AMCBR is not sufficient to remove most of the substrate. Therefore, there was an increase in the effluent COD concentration. Another possible reason for the drop in treatment efficiency (to 70%) in this study at HRTs 0.9 and 1.13 days may be the partial inhibition of granulated biomass by AMX may resulted in lower methanogenic activity to such an extent that the TVFAs were not well metabolised, resulting in the increasing effluent COD and AMX concentrations. Moreover, the difference in COD and AMX removal efficiencies of 13% and 24% (differences between HRTs 5.5, 1.13 and 0.9 days) may be due to more recalcitrant molecules in the AMX needing longer time for bacterial degradation in the anaerobic biomass resulting in toxicities in the AMCBR. However, the minimal effect on reactor performance confirms that the AMCBR was efficient at HRTs as low as 1.5 days and, therefore, a short HRT was not responsible for the drop in treatment efficiency (less than 2 and 4% for AMX and COD yields) while HRTs as low as 0.9 and 1.13 days decrease significantly the AMCBR performance.

In consequence, it appears that the performance of the AMCBR becomes virtually independent of 1.5-5.5 days HRT. For HRT lower than 1.5 days the performance of the AMCBR is dependent the decreasing HRT. When the HRT was decreased, the increasing acidogenic activity usually results in lower pH values; reduced methanogenic activity; increased COD, AMX and TVFA in the effluent of the AMCBR. Even though it was expected that the AMCBR would be stable at short HRTs, it was not able to withstand the short HRT, probably due to the complexity of synthetic pharmaceutical wastewater which contained AMX. In general, longer HRT can help the kinetics of degradation, i.e. more complex organics like recalcitrants. Simply have longer to be degraded. Nandy and Kaul, (2001) have demonstrated that substrate removal efficiency increases with increase in HRT in anaerobic treatment of herbal-based pharmaceutical wastewater using fixed-bed reactor. Zhou et al., (2006) reported that when HRT of an anaerobic baffled reactor treating pharmaceutical wastewater containing antibiotics (Ampicillin and Aureomycin) was extended from 1.25 to 2.5 days, the COD removal efficiency increased from 77 to 85%. They also observed that the antibiotic removal efficiencies increased from 16 to 42% for Ampicillin and 26 to 31% for Aureomycin.

The recent literature on the anaerobic AMX treatment showed that the yields obtained in some high rate anaerobic reactors are lower than the AMCBR removals found in this study: In a study performed by Chen et al., (2011) 60% COD and 34 % AMX removal efficiencies were obtained at a HRT of 2 days in an up-flow anaerobic sludge blanket reactor at an influent AMX concentration of 61 mg/L. In the study performed by Zhou et al., (2006), the COD (67%) and AMX (40%) yields were lower than those of our data (90% and 92% for COD and AMX, respectively) at a HRT of 3 days in an anaerobic contact reactor treating 3.2 mg/L AMX.

The results obtained in this study are considerably higher than the data obtained by Sreekanth et al., (2009) in a hybrid up flow anaerobic sludge blanket reactor at an influent COD concentration of 13000-15000 mg/L (E=65-75% COD removal efficiency) at a HRT of 2 days. The above results are consistent with observations made by Akbarpour and Mehrdadi, (2011) in an up-flow anaerobic sludge blanket

reactor, treating a chemical synthesis-based pharmaceutical wastewater. The COD yield was 54.6% at a HRT of 1.4 days. In our study, the high AMX yields in the AMCBR could be due to the reactor configuration, operational conditions, seed properties and HRTs used throughout reactor operation.

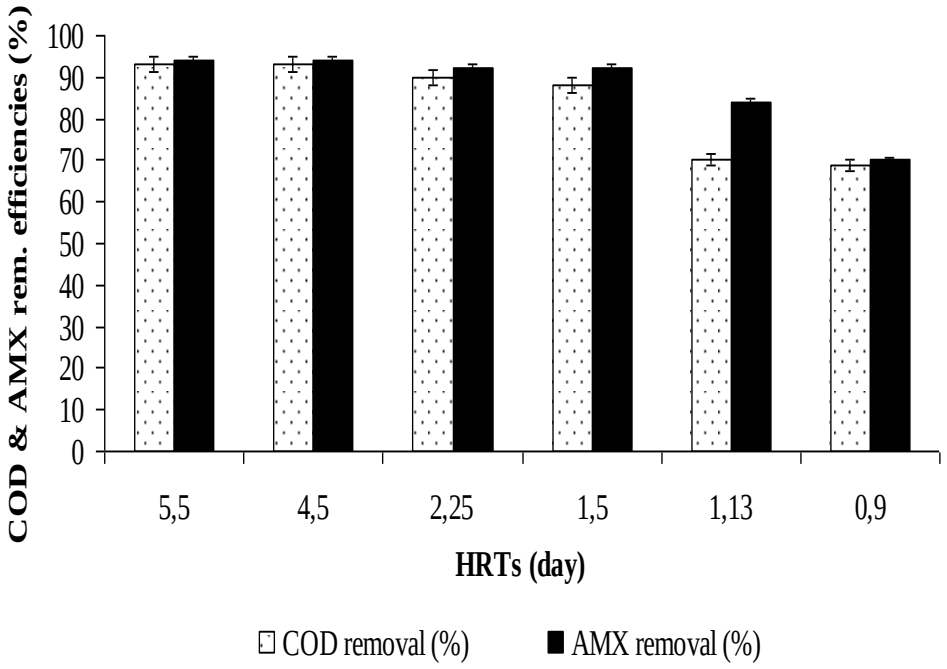

Figure 6.67 COD and AMX removal efficiencies versus HRTs for AMCBR reactor

6.2.6.6.1 Variation of AMX versus Operation Time in the AMCBR. After the start-up period, the AMCBR was operated throughout 189 days with 150 mg/L AMX at six different HRTs (Figure 6.68). The effluent AMX concentration was 12 mg/L for operation days of 1-15 then it decreased to 9 mg/L for 21-36 days resulting in AMX yield of 94% at a HRT of 5.5 days. The AMX yields remained as 94% on days 65-74 (the effluent AMX concentration was recorded as 9 mg/L) when the HRT was decreased to 4.5 days following the slightly decrease on days 37-48 (88%) and 50-64 (90%). On days between 99 and 103, the AMX yield slightly decreased to 92% at a HRT of 2.25 days following the slightly decrease on days between 75-87 (80%) and 90-98 (85%), respectively. The effluent AMX concentration was measured as 9 mg/L on days between 65 and 74. This showed that granulated anaerobic biomass in the AMCBR quickly acclimated to the AMX at long HRTs. The AMX yields remained as 92% and decreased to 84 % on days 128 and 152 as the HRTs decreased to 1.5

and 1.13 days, respectively following the decrease on days between 104-110 and 134-145, respectively (see Figure 6.68). The effluent AMX concentrations were 12 and 24 mg/L for the HRTs given above. The AMCBR reactor recovered quickly and reached steady-state conditions for the HRTs varying between 1.5 and 5.5 days. The AMX concentration remained relatively constant in the reactor effluent throughout the experiment for the HRTs given above. The minimal effect of the AMX antibiotic on overall AMCBR reactor performance confirms that the bacteria were adapted to AMX at 1.5 and 5.5 days HRTs (Figure 6.68). In other words, at HRT_s varying between 1.5 and 5.5 days the AMX have a relatively minor influence on the yield of the AMCBR and do not inhibit substantially the activity of methanogenic granular sludge microorganisms. On days between 175 and 189 the AMX yield decreased to 70% with an effluent AMX concentration of 45 mg/L at a HRT of 0.9 day following a decrease of AMX yield (59-62%) on days 165-172. The lower AMX removal efficiency resulted from the short HRT was probably due to the incomplete degradation of the AMX at the shorter contact times (Figure 6.68).

The studies performed with the anaerobic treatability of AMX showed that the yields obtained in the present study were higher than the other studies: The AMX removal was found to be lower (82%) in the study performed by Deng et al. (2012) under anaerobic conditions at an influent AMX concentration of 78 mg/L at a HRT of 1.56 days. Similarly, the AMX removal efficiencies obtained by Chen et al. (2011) are lower than our data. 47% AMX yield was obtained at a HRT of 1.7 days in an up-flow anaerobic sludge blanket reactor at an influent AMX concentration of 61 mg/L. Similarly Pallavi et al. (2009) reported lower AMX yields 65% than those found in our study at a HRT of 1.95 days and at an influent AMX concentration of 89 mg/L.

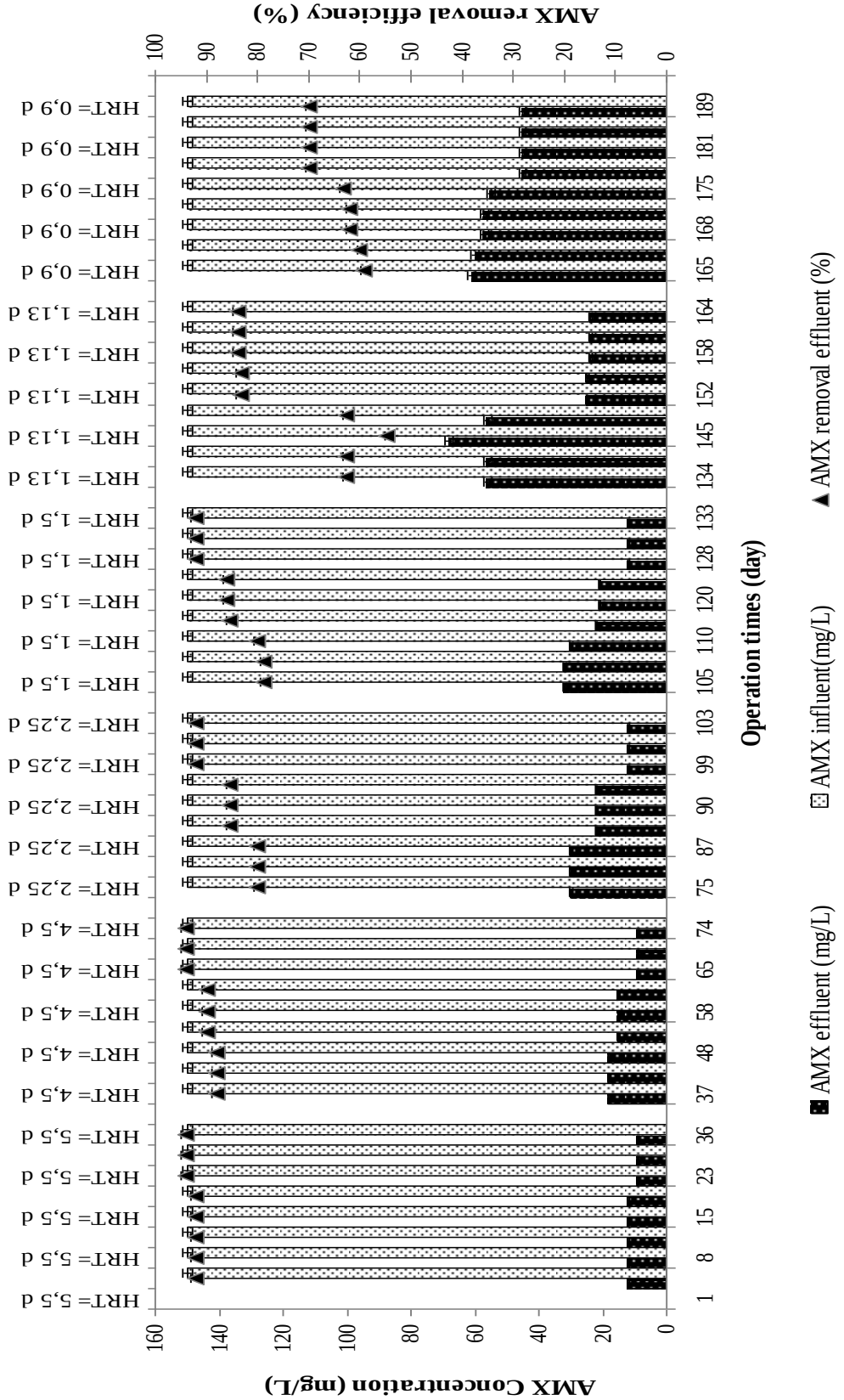

Figure 6.68 Variation of AMX concentrations and yields versus operation days in the AMCBR reactor

6.2.6.7 Effects of HRT on the Gas productions, Methane Content and TVFA in the AMCBR Reactor

The methane gas productions in the AMCBR were obtained as 6.19 and 6.18 L /d while the HRTs were 5.5 and 4.5 days, respectively (Figure 6.69). The total gas productions and the methane percentage remained around 12.00 L/d and 55%, respectively, for the HRTs mentioned above. The methane gas production remained the same as is in high HRTs (5.99 L/d) while the total gas production decreased slightly (from 12.10 L/d to 11.80 L/d) as the HRT decreased from 4.5 to 2.25 days. It is important to note that the decrease in HRT to half did not significantly affect the methane volume. The decrease in HRT from 2.25 to 1.5 days slightly decreased the volumetric total and methane gas productions (10.00 and 5.00 L/d, respectively) while the methane gas percentage was recorded as 45% (Figure 6.69). At low HRTs the granulated bacteria could not have enough time to metabolize the 150 mg/L AMX. Therefore both the methane gas content which dropped to 6.00 and 5.28 L/day as well as total gas production decreased at HRTs 1.13 and 0.9 days. The methane percentage also decreased to 42% and 33% for aforementioned HRTs. The decrease in methane content of biogas is generally observed when the rate of acid formation exceeds the rate of break down to methane at short HRTs (Ince et al., 2002; Kim et al., 2007).

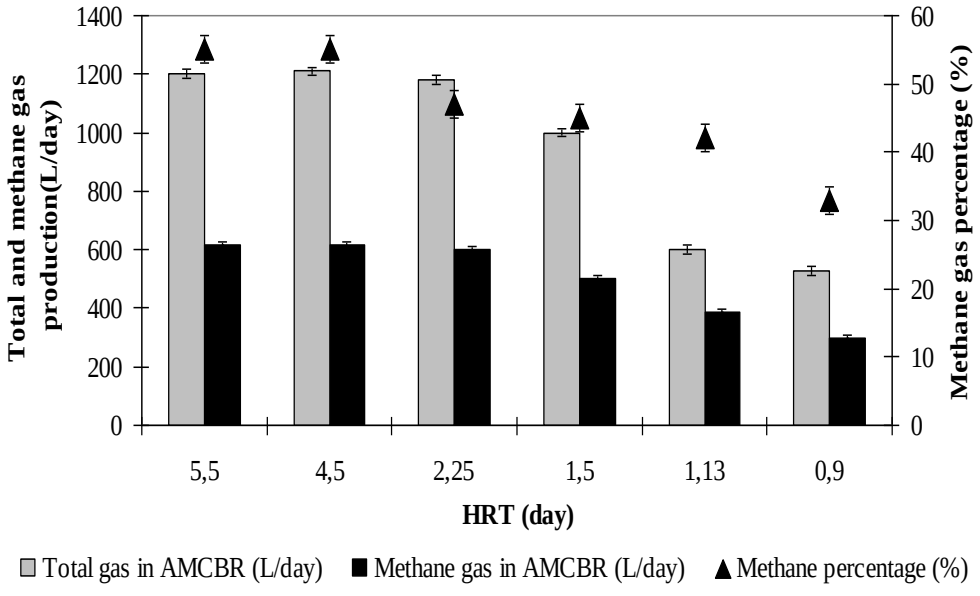

Figure 6.69 Biogas productions and methane content in the AMCBR reactor

In this study, the methane yield can be a useful parameter to assess the performance of the AMCBR. Figure 6.70 show the variations of methane yields versus HRTs. It was observed that that the methane yield decreased with decreasing of the HRTs. The methane yields decreased from 0.40 to 0.05 $m^3CH_4/kgCOD_{removed}$, when the HRTs were decreased 5.5 to 0.9 days. Lower methane yields (0.26-0.34 $m^3CH_4/kgCOD_{removed}$) were obtained in a study performed by Nandy and Kaul (2001) throughout anaerobic treatment of fermentation-based herbal pharmaceutical wastewaters containing 48 mg/L AMX at a HRT of 2 days. Similarly, a lower methane yield value (0.19 $m^3CH_4/kgCOD_{removed}$) was obtained in the anaerobic treatment of chemical synthesis-based pharmaceutical wastewater at a HRT of 1.98 days (Ince et al., 2002).The lower methane yields in the studies mentioned above could be due to the configuration of the anaerobic AMCBR reactor, type of anaerobic microorganism, to the biomass concentration and to the operational conditions.

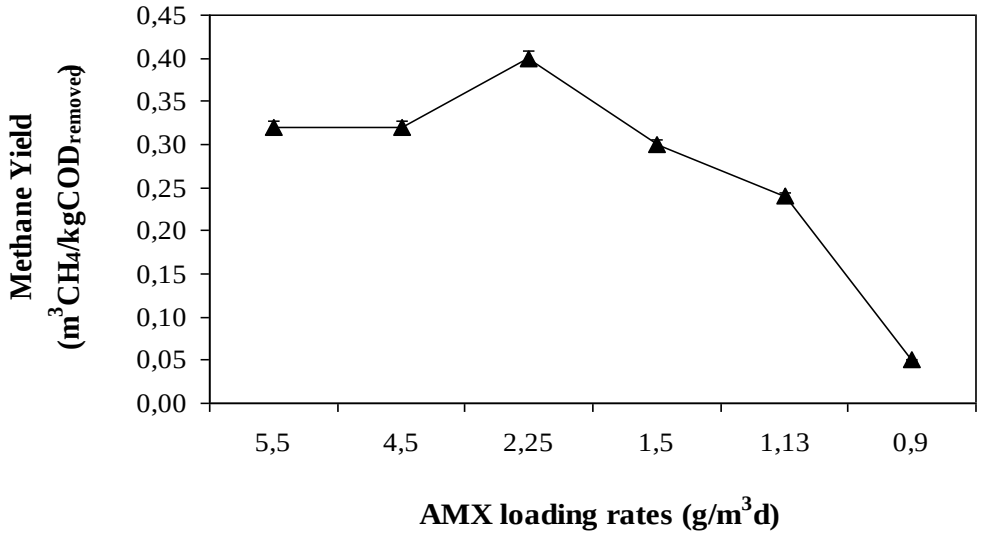

Figure 6.70 Variations of methane yields versus HRTs in AMCBR reactor.

Another reason for decrease in methane content of the gas at low HRTs may be high carbon dioxide content resulting from TVFA accumulation. At high HRTs such as 4.5 and 5.5 days the TVFA concentrations were found to be low in all compartments compared to the short HRTs (Figure 6.71). The TVFA concentrations were around 253, 110 and 90 mg/L in the 1st, 2nd and 3rd compartments while it was

zero in the effluent of the AMCBR for the aforementioned high HRTs. The TVFA levels increased to 300-370, 200-270 and 120-180 mg/L at HRTs of 2.25 and 1.5 days, respectively while the TVFA concentrations were recorded as 3 and 19 mg/L in the effluent of the AMCBR (Figure 6.71). In anaerobic compartmentalized AMCBR, the 1st compartment is referred to as ‘‘acid fermentation’’ and involves the production of TVFA, while the second and third compartments are referred to as ‘‘methane fermentation’’ because the TVFA are converted to methane and CO_2 production (Azbar and Speece, 2001). The maximum TVFA concentrations were measured as 550, 400 and 78 mg/L in the 1st, 2nd compartments and in the effluent. From the results of this study it can be concluded that the TVFAs could not be effectively transformed to methane by the sensitive methane *archae* since low HRTs like 1.13 and 0.9 days did not allow enough time for this group of slowly growing bacteria. Although acidogenic bacteria could more rapidly complete the acidogenic phase, methanogenic bacteria could not produce methane at the same rate with decreasing HRT. These lead to TVFA accumulation in the 1st, 2nd compartments. On the other hand at low HRTs the granulated anaerobic bacteria could not easily use the AMX as co-substrate and some toxic metabolites decrease the number of viable methane bacteria, inhibits the methanogenic activity resulting in TVFA accumulation in the AMCBR.

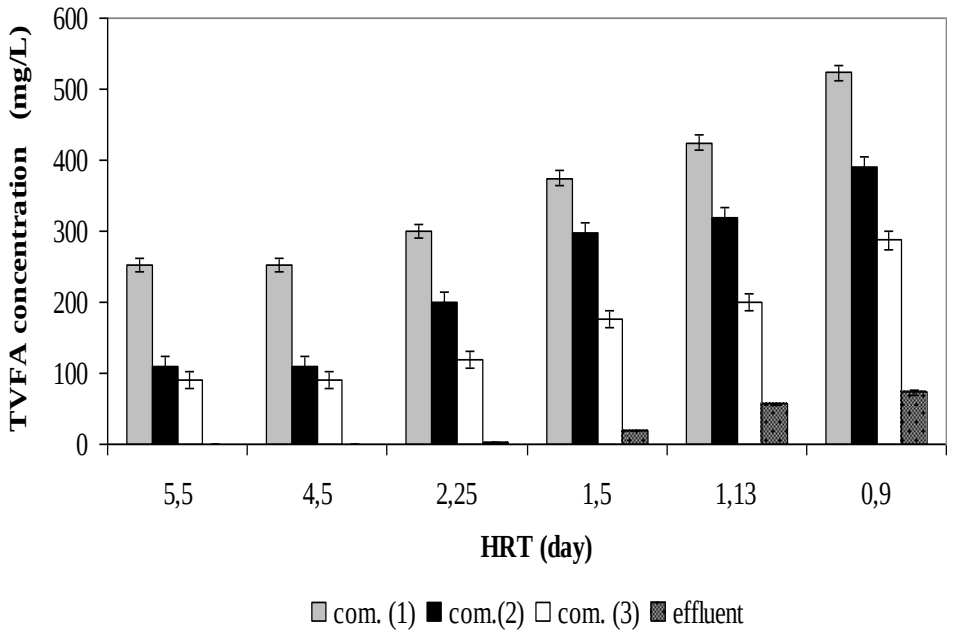

Figure 6.71 TVFA variations in the AMCBR reactor

6.2.6.8 Effects of HRTs on the COD and AMX Removal Efficiencies in the CSTR Reactor

Table 6.20 shows the effect of decreasing HRT on the COD and AMX removals in the aerobic reactor. The COD removal efficiencies were around 83% for HRTs of 10.97, 9.0 and 4.5 days, respectively in the CSTR. The AMX yields were 83%, 80% and 75% for the aforementioned HRTs. The COD and AMX yields decreased to 76-65% and 70-65% at HRTs of 2.25 and 1.80 days, respectively. The COD and AMX removal efficiencies decreased at low HRTs in the aerobic reactor. Since the effluent of the AMCBR was used as the feed in the influent of the CSTR the COD and the AMX remaining from the AMCBR were removed in the CSTR. In the CSTR the rest of the COD and AMX which could not be biodegraded in the AMCBR were low. This means that the COD and AMX were mainly biodegraded in the AMCBR. From 4000 mg/L of COD and 150 mg/L AMX in the influent of the AMCBR 3675 mg/L of COD and 141 mg/L AMX were removed in the anaerobic reactor while the rest of the 325 mg/L COD and 9 mg/L AMX were biodegraded in the CSTR reactor with 83% yields at HRTs of 9.0 and 10.97 days. The COD removals were found to be lower (60%) in the study performed by Chen et al., (2008) under aerobic conditions treating the 78 mg/L AMX in an up flow anaerobic sludge blanket reactor, compared to the present study. Similarly, the COD removal efficiencies (38-62%) obtained by Lapara et al., (2001) are lower than those of our results.

Table 6.20 COD and AMX yields in the CSTR reactor at six different HRTs

Parameters	**HRT (day)**					
	10.97	**9.0**	**4.5**	**3.0**	**2.25**	**1.80**
COD concentration in influent (mg/L)	325	325	325	325	325	325
COD concentration in effluent (mg/L)	55	52	52	65	78	114
COD Removal efficiency (%)	83	83	83	80	76	65
AMX concentration in influent (mg/L)	9	9	9	9	9	9
AMX concentration in effluent (mg/L)	1.50	1.50	1.80	2.25	2.7	3.15
AMX Removal efficiency (%)	83	83	80	75	70	65

6.2.6.9 Performance of Anaerobic AMCBR /Aerobic CSTR Sequential Reactor System

Figure 6.72 shows the removal efficiencies of COD, AMX at six studied HRTs in the AMCBR/CSTR system. The COD and AMX removals in the total sequential total system were > 95% as the HRTs decreasing from 16.47 to 13.50, 6.75 days. The maximum COD and AMX yields were 99% and 99%, respectively, for the HRTs given above while the lowest COD and AMX yields were 94% at a HRT of 2.7 days, in the sequential AMCBR/CSTR system. 90% of the COD and AMX were removed in the anaerobic reactor while the remaining COD and AMX (5% of COD and AMX) were biodegraded in the aerobic reactor at HRTs between 6.75 and 16.47 days. This showed that a significant part of the AMX could be removed with high removal efficiency in the sequential AMCBR/CSTR system. In a study carried out by Chen et al., (2011) 87% both AMX and COD yields were obtained at an influent COD and AMX concentration of 3690 and 105 mg/L, respectively, in a combined anaerobic/micro-aerobic two-stage aerobic process at a HRT of 1.98 day. In our study the AMX and COD removal efficiencies are higher than this study although the influent AMX concentration is comparably higher than the study performed by Chen et al., (2011).

The literature survey showed that the AMX yields obtained in old studies are lower than those in our data: 50% COD and antibiotic removals was obtained by Fox and Venkatasubbiah, (1996) in a combined anaerobic baffled and aerobic attached-film reactor to remove pharmaceutical wastewaters containing antibiotic and sulfate at 4000 mg/L COD and at a HRT of 1 day. Similarly, Buitron et al., (2003) found 96% COD yield in a sequencing batch bio filter operating under anaerobic and aerobic conditions to treat pharmaceutical wastewater with an influent COD of 28-72 g/L.

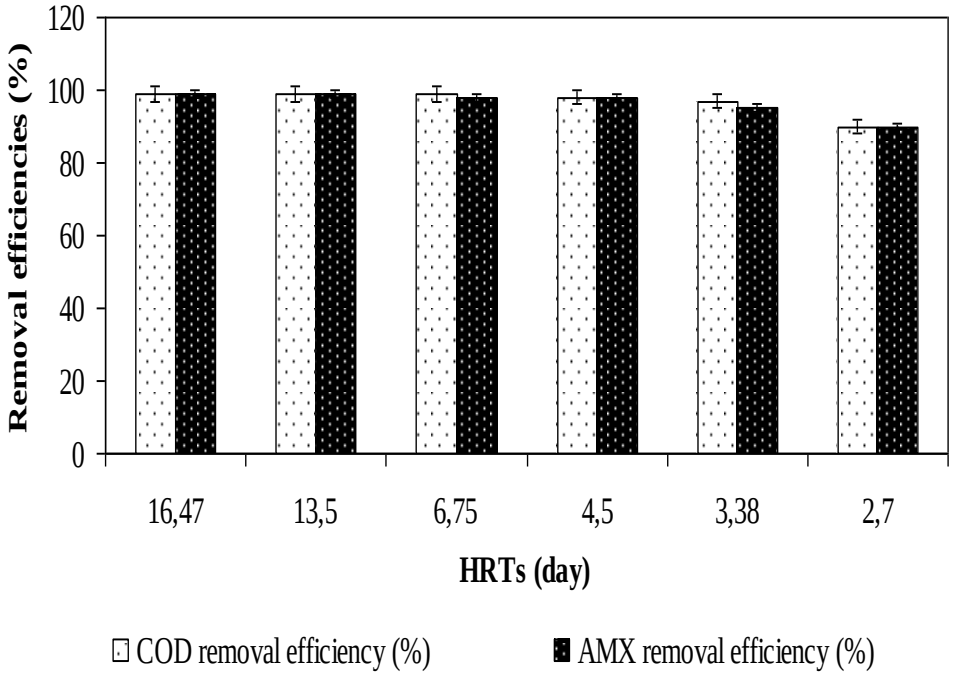

Figure 6.72 COD and AMX removal efficiencies in the sequential AMCBR/CSTR system

6.2.6.10 Influence of HRTs on the COD and TYL Removal Efficiencies in the AMCBR Reactor

This part of the research studies the effect of different HRTs on the system performance. The influent TYL concentration was kept constant as 100 mg/L. The reactor was fed with molasses and TYL containing 3940, 3945, 3955, 4015, 4025, 4035 mg COD/L at six different HRTs of 5.5, 4.5, 2.25, 1.5, 1.13 and 0.9 days coinciding with organic loading rates of 0.71, 0.87, 1.75, 2.67, 3.57 and 4.48 g.COD/L.d, respectively (see Table 5.21, Study 14 for operational conditions). In order to study the influence of HRT on reactor performance, the reactor was operated on six different HRTs (5.5, 4.5, 2.25, 1.5, 1.13, 0.9 days). Figure 6.73 present the results obtained at 5.5, 4.5, 2.25, 1.5 days and 1.13, 0.9 days HRTs respectively in the AMCBR reactor.

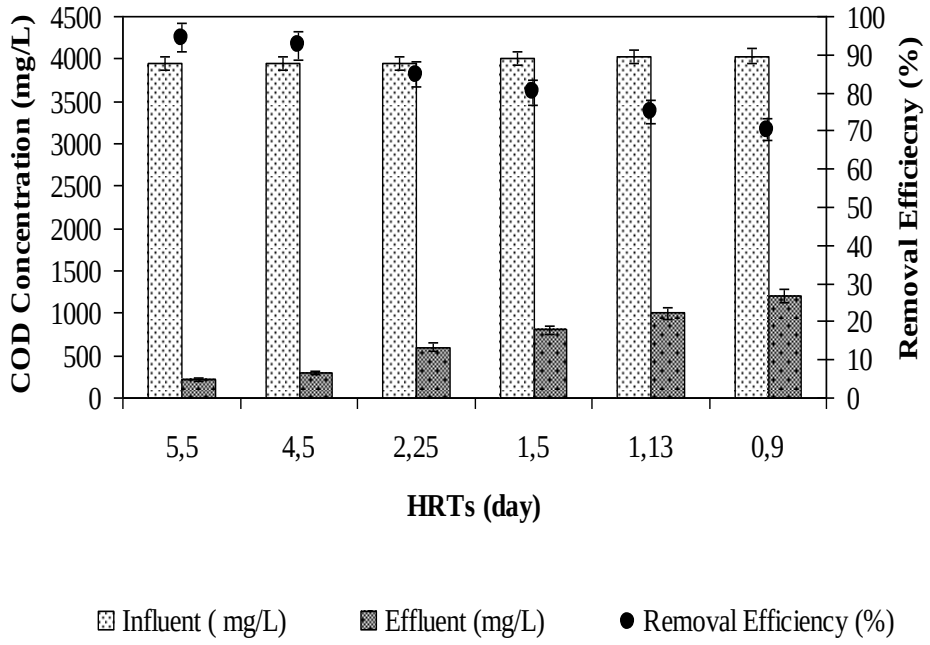

Figure 6.73 The effect of HRTs on the COD removal efficiencies in the AMCBR reactor

As shown in Figure 6.74, the COD removal efficiency was 94% at a HRT of 5.5 day in the AMCBR reactor. The effluent COD concentration was 300 mg/L resulting a COD removal efficiency of 92% at a HRT of 4.5 days. The COD removal efficiency remained around 85% until a HRT of 2.25 days in the AMCBR reactor. After this HRT (2.25 days) the COD removal efficiency decreased from 80% to 75% and 70% corresponding to HRTs of 1.5, 1.13 and 0.9 days. The maximum COD (E=94%) removal efficiency was observed at HRT of 5.5 days. The minimum COD (E=70%) yield was found at HRT of 0.9 day. ANOVAs test statistics showed that a significant linear relationship between COD yields and HRTs varying between 4.5 and 5.5 days was not observed (R^2=0.42, F=7.82, p=0.04) while the linear relationship between yields and low HRTs (0.9 and 2.25 days) (R^2=0.85, F=3.86, p=0.04) was significant. In our study, molasses was used as the primary substrate for the treatment of TYL. The primary substrate is consumed as an energy source and electron donor for anaerobic antibiotic biodegradation.

The recent literature on the anaerobic TYL reduction showed that the removal efficiencies obtained in some high rate anaerobic reactors are lower than the AMCBR reactor removals found in this study: In a study performed by Chelliapan et al., (2010) reported that when HRT of an anaerobic UASR reactor treating pharmaceutical wastewater containing TYL was extended from 2 to 4 days, the COD removal efficiency increased from 70 to 75%. Chelliapan et al., (2011) investigated the performance of an UASR reactor treated a pharmaceutical wastewater containing macrolide antibiotic TYL at four HRTs (1, 2, 3 and 4 days). The COD removal efficiency increased from 76%, 80% to 90% when the HRT was increased from 1, 2, 3 to 4 days. The COD yields found in these studies were lower than those in our study (E=75%-94%). The difference in COD yields could be attributed to the reactor configuration, operational conditions, seed properties and HRTs used throughout reactor operation.

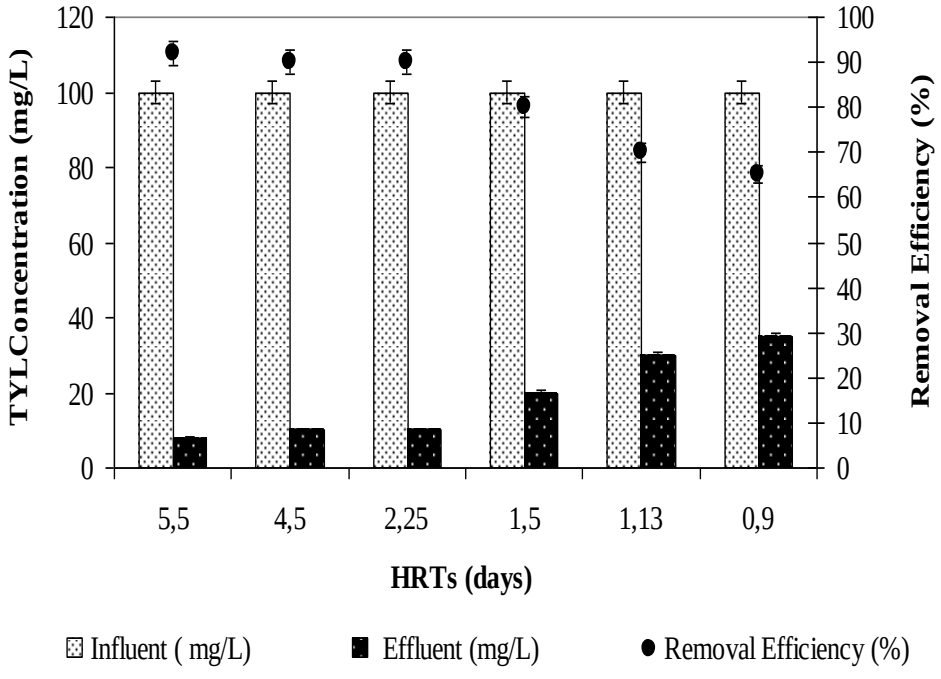

Figure 6.74 The effect of HRTs on the TYL removal efficiencies in the AMCBR reactor

6.2.6.11 Influence of HRTs on the Total and the Methane Gas Productions in the AMCBR Reactor

Biogas production was monitored through the operation of the AMCBR reactor, particularly for detection the methanogenic activity. The variations of the total, methane gas productions and methane percentage in AMCBR are shown for all HRTs in Figure 6.75. From this figure, it can be seen that the biogas productions and methane percentage decreased whenever HRT was decreased. The methane gas productions in the AMCBR were obtained as 10 L/d and 8 L/d while the HRTs were 5.5 and 4.5 days, respectively (see Figure 6.75). The total gas productions and the methane percentage remained around 16 L/d and 62%, respectively, for the HRTs mentioned above. The methane gas production remained the same as is in high HRTs (8 L/d) while the total gas production decreased slightly (from 16 to 12 L/d) as the HRT decreased from 4.5 to 2.25 days. The decrease in HRT from 2.25 to 1.5 days slightly decreased the total and methane gas productions (6 and 5 L/d, respectively) while the methane gas percentage was recorded as 45% and 40%, respectively in the AMCBR reactor (Figure 6.75). At low HRTs the granulated bacteria could not have enough time to metabolize the 100 mg/L TYL. Therefore the methane gas production dropped to 5 and 4 L/d as well as the total gas production decreased at HRTs 1.13 and 0.9 days, respectively (see Figure 6.75). The methane percentage also decreased to 40 and 30% for the aforementioned HRTs. The decline of methane percentage could be attributed to the inhibition of activity of methanogens. The optimum HRTs for maximum methane gas productions (62%) varied between 4.5 and 5.5 days. A strong linear correlation between COD removal and methane content was observed only for HRTs between 4.5 and 5.5 days (R^2=0.92, F=3.99, p=0.02). Similarly, a strong linear correlation between COD removal and methane gas production was observed only for HRTs between 4.5 and 5.5 days (R^2=0.90, F=4.48 p=0.02).

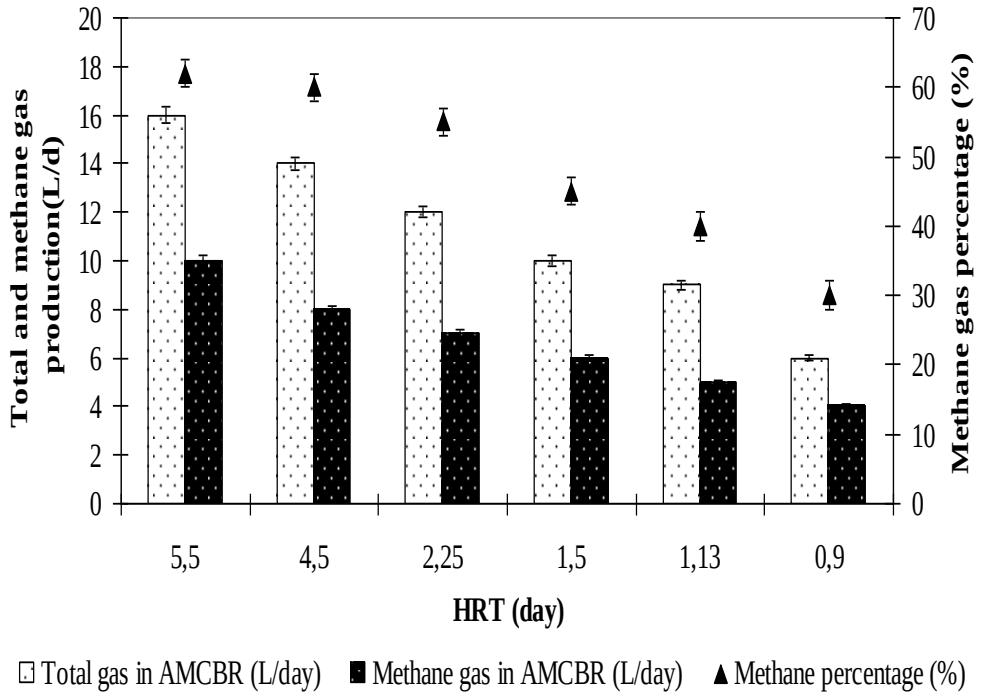

Figure 6.75 The effect of HRTs on total, methane gas production and methane percentage in the AMCBR reactor

The results of this study showed that the TYL loadings affected the total and methane gas produced during anaerobic degradation of pharmaceutical wastewater. In a study performed by Chelliapan et al., (2006) 3.4 L/d methane gas production was found at OLRs varying at between 0.43 and 1.86 kg COD/m^3d, at an influent TYL=20-200 mg/L and a HRT=4 d in an UASR reactor. Shimada et al., (2011) reported that, 2.6 L/d biogas production at an influent TYL concentration of 167 mg/L at HRT of 1.67 day and at an OLR of 3.5 kg COD/m^3d in an ASBR reactor. In our study, 62% methane content and 10 L/d CH_4 production was measured at influent TYL concentrations varying between 50 and 300 mg/L in the AMCBR reactor. The yields obtained in the aforementioned studies are low in comparison to the methane gas productions found in our study.

Figure 6.76 shown the variations of methane yields versus decreasing HRTs. It was observed that the methane yield decreased partly with decreasing HRTs. The methane yield was 0.33 m^3CH_4/kg $COD_{removed}$ at HRT of 5.5 days. The methane yield decreased from 0.33 to 0.12 m^3CH_4/kg $COD_{removed}$ as HRT decreased from 5.5

to 0.9 days. A linear correlation between COD removal and methane yield only for HRTs between 4.5 and 5.5 days (R^2=0.90, F=5.09, p=0.02).

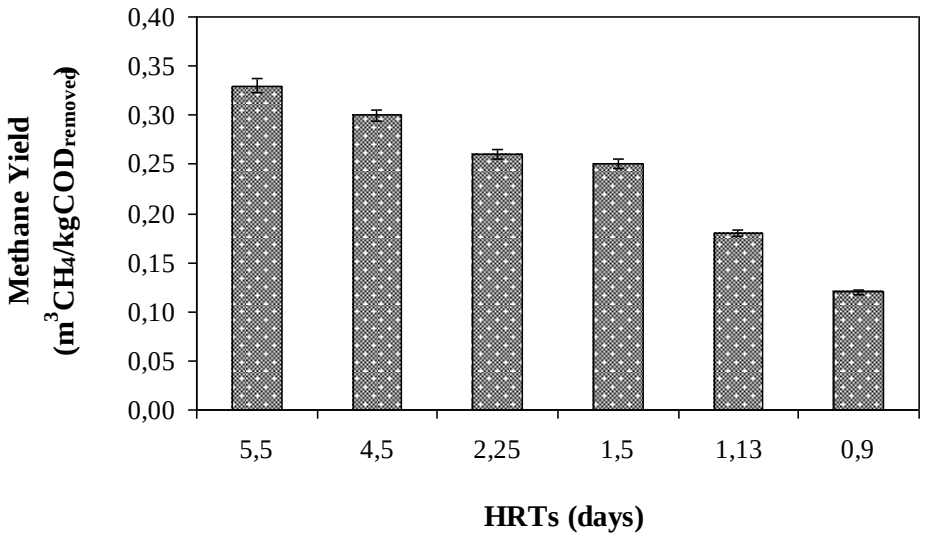

Figure 6.76 Variations of methane yields versus HRTs in the AMCBR reactor.

In the study by Nandy and Kaul, (2001), 0.26-0.34 $m^3CH_4/kgCOD_{removed}$ methane yields was observed for the anaerobic degradation of 200 mg/L TYL in herbal pharmaceutical wastewater after 2 days HRT. In the study performed by Mohan et al., (2001) 0.20 $m^3CH_4/kgCOD_{removed}$ methane yields was obtained at a HRT of 1.98 days in anaerobic treatment of chemical synthesis-based pharmaceutical wastewater. A similar study was also reported by Chelliapan et al., (2006) when treating pharmaceutical wastewater containing 20- 200 mg/L TYL in an UASR. 0.10-0.40 $m^3CH_4/kgCOD_{removed}$ methane yields were obtained during 106 days of operation time. The yields obtained in the aforementioned studies are similar in comparison to the yield performances of methane found in this study.

6.2.6.12 Effects of HRTs on pH, TVFA, HCO_3 Alk. and TVFA/HCO_3 Alk. Ratio Variations in Compartments of the AMCBR Reactor

As shown in Figure 6.77, the influent pH values remained stable at between 7.12 and 7.50 under the anaerobic condition. The pH values varied between 7.50 and 7.75

in the effluent of AMCBR at HRTs varied between 5.5 and 0.9 days. These values are between optimum pH values of 6.5 and 8.3 reported by Speece, (1996). From Figure 6.77 shows that the pH values in the 1st compartment were lower than the all of the other compartments. The possible reason of the decreases of pH in the 1st compartment can be explained by the increasing of TVFA levels (see Figure 6.78). When the HRTs were decreased from 5.5 to 0.9 days in the AMCBR reactor, the pH in the 1st compartment dropped from 7.35 to 7.15 due to the increased acidogenic activity. The pH profile of the AMCBR reactor system with average pH in 1st compartment was 7.23; while the pH in 2nd compartment was measured as 7.49. The pH in 3rd compartment was measured as 7.47. As shown in Figure 6.77, the pH values in the effluent of AMCBR varied between 7.50 and 7.75.

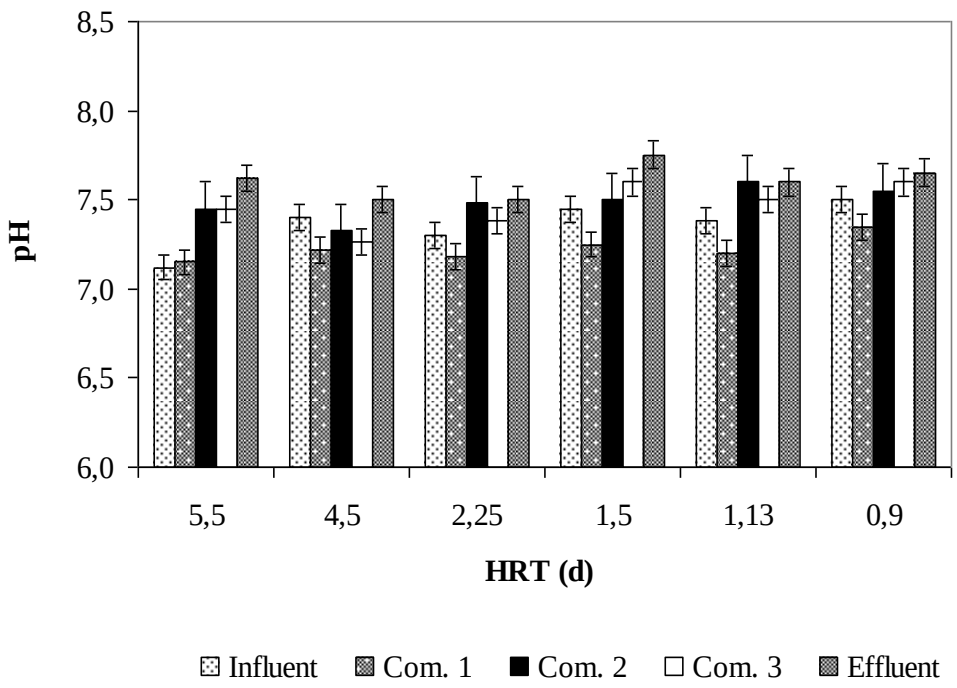

Figure 6.77 shows the variations of pH in compartments of AMCBR reactor at decreasing HRTs.

Figure 6.78 shows the variations of TVFA concentrations in compartments of AMCBR reactor at decreasing HRTs. At high HRTs such as 4.5 and 5.5 days the TVFA concentrations were found to be low in all compartments compared to the short HRTs (Figure 6.78). The TVFA concentrations were around 400, 250 and 100 mg/L in the 1st, 2nd and 3rd compartments while it was 5 mg/L in the effluent of the

AMCBR for the aforementioned high HRTs. The TVFA levels in 1st compartment increased from 400 mg/L to 900 mg/L as the HRTs decreased from 5.5 to 0.9 days. It was found that the minimum TVFA value in the effluent was approximately 5 mg/L at HRTs of 5.5 and 4.5 days in 1st compartment of AMCBR reactor (see Figure 6.78). The TVFA concentrations were found as 250, 700, 800 and 900 mg/L respectively, at HRTs of 2.25, 1.5, 1.13 and 0.9 days, respectively in 1st compartment of AMCBR reactor. As shown in Figure 6.78, TVFA levels varied between 250, 250, 450, 500, 590 and 650 mg/L respectively in 2nd compartments of AMCBR reactor at decreasing HRTs (from 5.5 to 0.9 days). As the HRTs were decreased from 5.5, 4.5, 2.25, 1.5, 1.13 to 0.9 days TVFA concentrations increased from 100, 100, 120, 150, 200 to 250 mg/L, respectively in the 3rd compartment (Figure 6.78). The TVFA concentrations were recorded as 5 and 65 mg/L in the effluent of the AMCBR reactor (Figure 6.78).

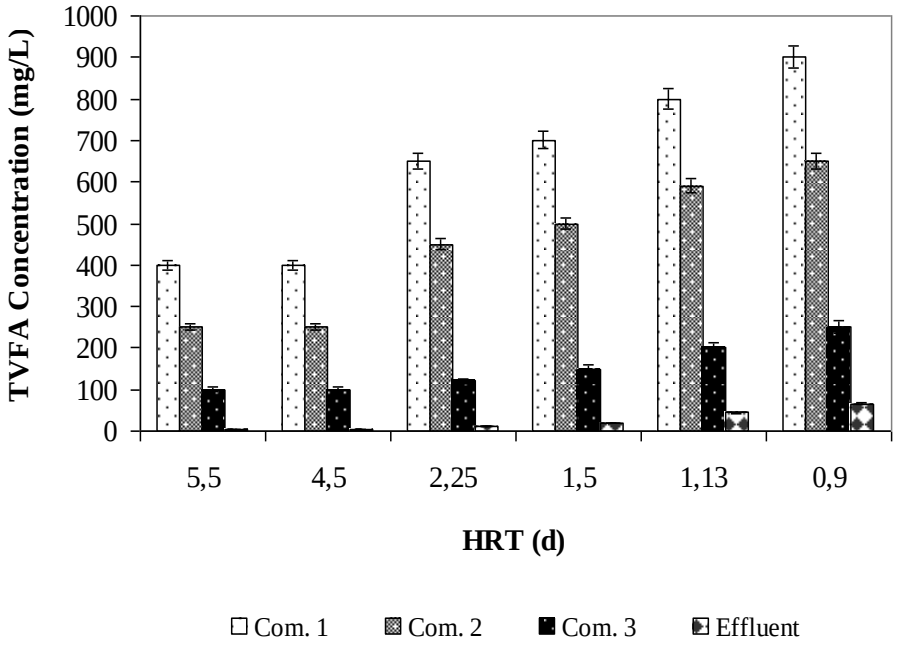

Figure 6.78 The variations of TVFA concentrations in compartments of AMCBR reactor

The results of this study showed that the TYL loadings affected the TVFA production during anaerobic degradation of pharmaceutical wastewater. In a study performed by Shimada et al., (2011) 8.9-3400 mg/L TVFA concentrations were obtained at a HRT of 1.67 days in an ASBR reactor at influent TYL concentrations

varying between 1.67 and 167 mg/L. In the study performed by Chelliapan et al., (2006), the TVFA concentrations (100-800 mg/L) were lower than those of our results (950 mg/L) at a HRT of 4 days in an anaerobic UASR reactor treating 20-200 mg/L TYL.

In a study performed by Chelliapan et al., (2011) TVFA productions were 550-1050 mg/L, 350-750 mg/L, 200-570 mg/L and 40-400 mg/L for 1^{st}, 2^{nd}, 3^{rd} and 4^{th} compartments, in an anaerobic UASR reactor respectively. In our study TVFA productions were 500-950 mg/L, 250-690 mg/L, 7-18 mg/L and 2-7 mg/L in an 1^{st}, 2^{nd}, 3^{rd} compartments and effluent of AMCBR reactor for TYL loading rates of 22.22 and 133.33 g/m^3d. In this study the TVFA productions are comparable higher than that aforementioned study.

Figure 6.79 shows HCO_3 concentration in the compartments and effluent of AMCBR at different HRTs. The HCO_3 concentration in the 1^{st} compartment decreased from 2600 mg/L to 2185 mg/L with increasing of TVFA concentration from 400 mg/L to 900 mg/L as the HRT decreased from 5.5 to 0.9 days. The HCO_3 concentrations remained between 2300 and 2500 mg/L in the 2^{nd} compartment of AMCBR at decreasing HRTs (5.5-0.9 days) (see Figure 6.79). The HRTs decreased from 5.5 to 0.9 days the HCO_3 concentrations decreased from 2600 to 2125 mg/L in 3^{rd} compartment.

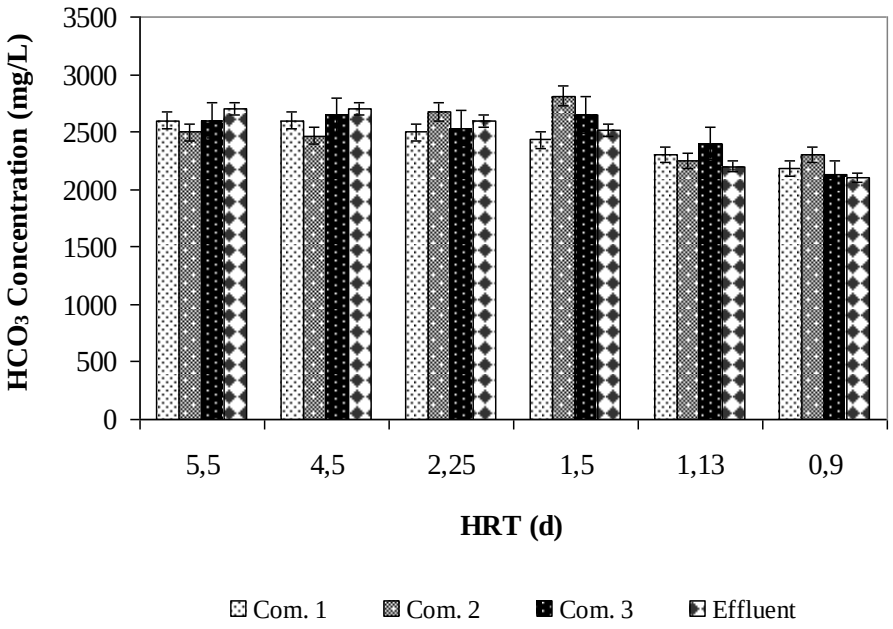

Figure 6.79 Variations of HCO_3 concentration in compartments of AMCBR at decreasing HRTs

Barampouti et al., (2005), suggest that the ideal ratio of TVFA/HCO_3 is in the range of 0.1 to 0.3 to avoid the acidification of the anaerobic reactor. A value above 0.4 is an indicator of instability. TVFA/ HCO_3 ratios were lower than 0.4 in the compartments and in the effluent of AMCBR at all HRTs. This shows the stability of the AMBR reactor as reported by Behling et al., (1997). Figure 6.80 showed the TVFA/HCO_3 ratios in the compartments and in the effluent of AMCBR. This ratio changed between 0.15 and 0.38 in the 1st compartment, between 0.10 and 0.28 in the 2nd compartment, between 0.04 and 0.12 in the 3rd compartment. This ratio changed between 0.01 and 0.03 in the effluent of AMCBR reactor at all HRTs (5.5, 4.5, 2.25, 1.5, 1.13 and 0.9 days).

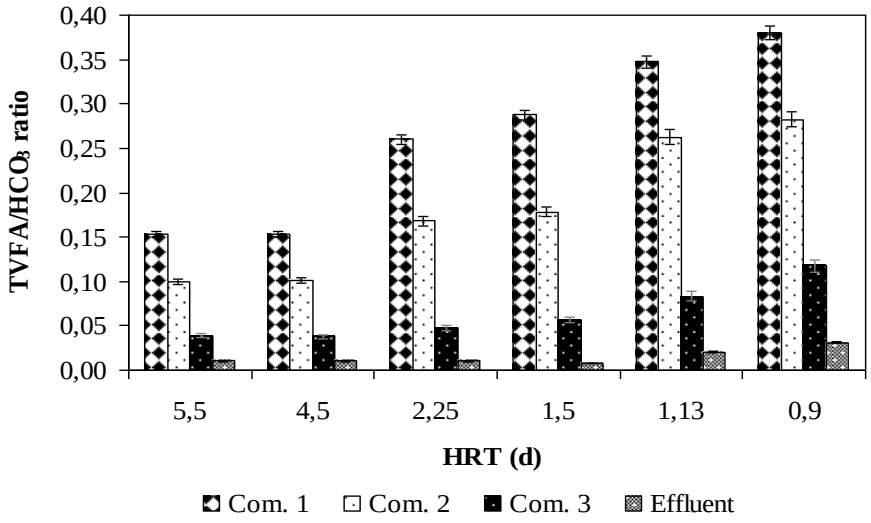

Figure 6.80 The variations of TVFA/HCO_3 ratio in compartments of AMCBR at decreasing HRTs.

6.2.6.13 Effects of HRTs on the COD and TYL Removal Efficiencies in the CSTR Reactor

Table 6.21 shows the effect of decreasing HRT on the COD and TYL removals in the aerobic reactor. The COD removal efficiencies were around 86% and 85% for HRTs of 10.97 and 9.0 days, respectively in the aerobic CSTR reactor. The COD yields were 82% and 80% for HRTs of 4.5 and 3.0 days, respectively. The COD yields decreased from 75% to 66% at HRTs of 2.25 and 1.80 days, respectively (see Table 6.21). The COD concentrations were increased from 30, 45, 108, 160, 250 to 408 mg/L at HRTs of 10.97, 9.0, 4.50, 3.0, 2.25 to 1.8 days, respectively in the effluent of the CSTR reactor.

As shown in Table 6.21, the TYL yields were increased from 1.2, 1.5, 2.0, 5.8, 9.6 to 12.95 mg/L at HRTs of 10.97, 9.0, 4.50, 3.0, 2.25 to 1.8 days respectively in the effluent of the CSTR reactor. The TYL removal efficiencies were around 85% for HRTs of 10.97, and 9.0 days, respectively in the aerobic CSTR reactor (see Table 6.21). The TYL yields were 80% and 71% for HRTs of 4.5 and 3.0 days, respectively. The TYL removal efficiencies decreased from 68% to 63% at HRTs of 2.25 and 1.8 days, respectively. The COD and TYL removal efficiencies decreased at

low HRTs in the aerobic reactor. Since the effluent of the AMCBR was used as the feed in the influent of the CSTR the COD and the TYL remaining from the AMCBR were removed in the CSTR.

The COD removals were found to be lower (average 65%) in the study performed by Chelliapan et al., (2010) under aerobic conditions treating the 200 mg/L TYL in an aerobic Porous Membrane Activated Sludge Reactor (APMASR), compared to the our study (E=66-86%, influent TYL concentration 100 mg/L). The difference in COD yields could be explained by the APMASR and AMCBR reactor configuration, operational conditions and TYL concentrations used throughout reactor operation.

Table 6.21 COD and TYL yields in the CSTR reactor at six different HRTs

Parameters	**HRT (day)**					
	10.97	**9**	**4.50**	**3**	**2.25**	**1.8**
COD concentration in influent (mg/L)	225	225	225	225	225	225
COD concentration in effluent (mg/L)	31.50	34	41	45	56.30	77
COD Removal efficiency (%)	86	85	82	80	75	66
TYL concentration in influent (mg/L)	8	8	8	8	8	8
TYL concentration in effluent (mg/L)	1.2	1.2	1.6	2.32	2.56	2.96
TYL Removal efficiency (%)	85	85	80	71	68	63

6.2.6.14 Performance of Anaerobic AMCBR /Aerobic CSTR Sequential Reactor System

Generally, an anaerobic process is applied to remove high concentrations of organic matter followed by an aerobic treatment to oxidise the residual organic matter. Given that influent COD is very high, effluent from anaerobic reactor can still have residual COD (Chelliapan et al., 2010). Consequently, direct discharge of effluent from anaerobic reactor is not permitted, and pre-treatment of anaerobic reactor effluent with an aerobic reactor is necessary. The effluent from AMCBR was further subjected to aerobic treatment (CSTR) to remove the residual COD.

Figure 6.81 shows the removal efficiencies of COD, TYL at six studied HRTs in the AMCBR/CSTR system. The COD and TYL removals in the sequential AMCBR/CSTR system were ≥ 95% as the HRTs decreasing from 16.97 to 9.0, 6.75 days. The maximum COD and TYL yields were 99% and 99%, respectively, for the HRTs given above while the minimum COD and TYL removal efficiencies were 90% and 87%, respectively, at a HRT of 2.70 days, in the sequential AMCBR/CSTR system.

The literature survey showed that the TYL and COD yields obtained in recent studies are lower than those in our data: In a study carried out by Chelliapan et al., (2010) 90% and 97% COD and TYL yields were obtained at an influent COD and TYL concentration of 7000 and 200 mg/L, respectively, in a combined anaerobic UASR/aerobic APMASR reactor system at a HRT of 4.00 day. In our study the TYL and COD removal efficiencies are higher than this study although the influent TYL concentration is comparably higher than the study performed by Chelliapan et al., (2010). Similarly, Buitron et al., (2003) found 96% COD yield in a sequencing batch bio filter (SBB) operating under anaerobic and aerobic conditions in one tank to treat pharmaceutical wastewater with an influent OLR of 4.6-5.7 kg COD/m^3.d, at HRT 8-24 hours.

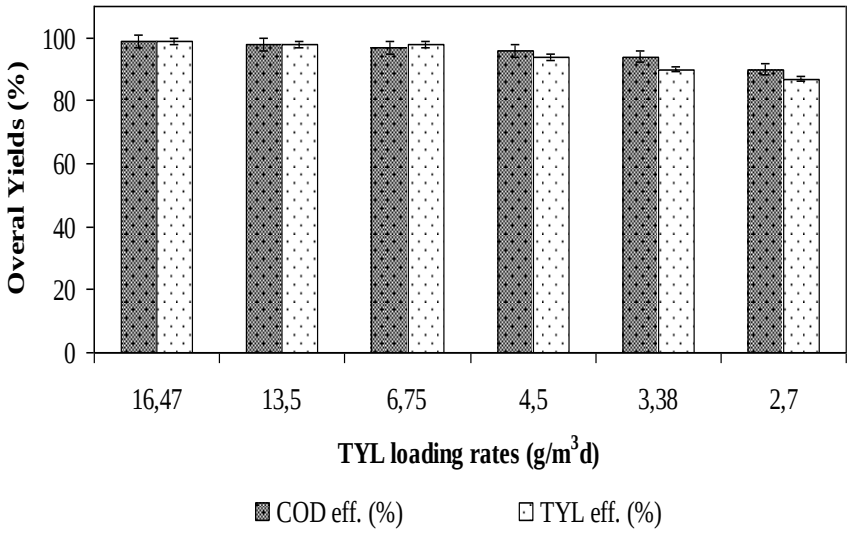

Figure 6.81 COD and TYL removal efficiencies in sequential AMCBR/CSTR system

6.2.6.15 Influence of HRTs on the COD and ERY Removal Efficiencies in the AMCBR Reactor

In this part of the experiments the effects of HRT to operating parameters such as pH, COD, ERY and TVFA, HCO_3 concentrations were investigated in the AMCBR reactor system. Figure 6.82 shows the COD removal efficiencies of anaerobic AMCBR reactor. The COD removal efficiency in this reactor system was 90% until a HRT of 5.5 days. After that COD removal efficiency of the reactor decreased from 90% to 88% when the HRT were decreased from 5.5 to 4.5 days in the AMCBR reactor. For maximum COD removal efficiency (E=94.52%) the optimum HRT was found as 5.5 days. As shown in Figure 6.82, the COD removal efficiency was 78% at HRT of 2.25 and 1.5 days in the AMCBR reactor. After the HRT of 1.5 days the COD removal efficiency decreased from 69% to 65% corresponding to HRTs of 1.13 and 0.9 days. The minimum COD yield (E=65%) was found at HRT of 0.9 day. Decreases in HRTs caused decreases in COD removal efficiencies. The reason for low COD removal efficiency was the accumulation of intermetabolite products in AMCBR reactor. ANOVAs test statistics showed that a significant linear relationship between COD yields and HRTs varying between 4.5 and 5.5 days was not observed (R^2=0.38, F=8.63, p=0.05) while the linear relationship between yields and low HRTs (0.9 and 1.5 days) (R^2=0.88, F=4.36, p=0.03) was significant.

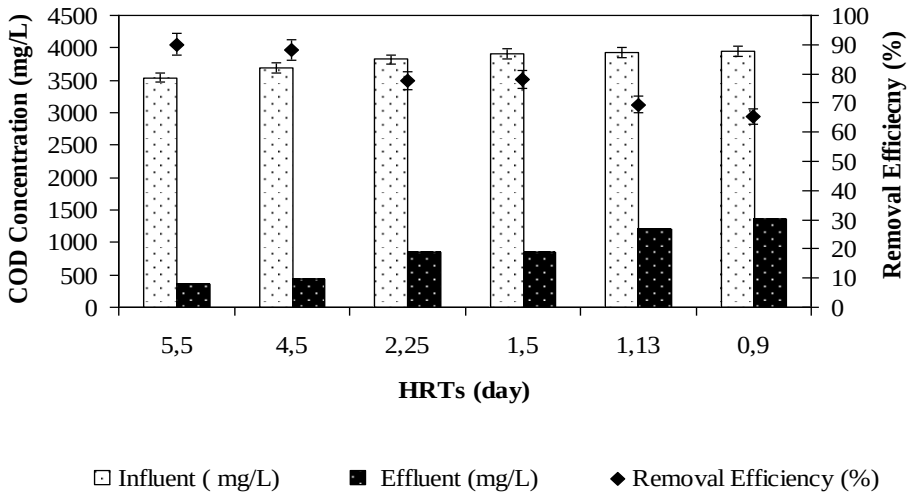

Figure 6.82 The effect of HRTs on the COD removal efficiencies in AMCBR reactor

In the study by Rodriguez-Martinez et al., (2005) 70-85% COD removal efficiencies were obtained at a HRT of 2 days in an UASB reactor at OLRs of (1.5-2.09 kgCOD/m^3d). In a study performed by Chelliapan et al., (2010) reported that when HRT of an anaerobic UASR reactor treating pharmaceutical wastewater containing TYL was extended from 2 to 4 days, the COD removal efficiency increased from 70 to 75%. In our study, 65-90% COD removal was measured for the influent ERY concentration varying between 50 and 300 mg/L. In other study carried out by Öktem et al., (2008), the COD yields were (72-90%), also, the same those of our data (65-90%) in a fixed-film reactor treating ERY at concentrations varying between 50 and 200 mg/L. The yields obtained in the aforementioned studies are low in comparison to the removal performances of COD found in this study.

In the study performed by Nandy and Kaul, (2001), the COD (E=80-98%) yield was higher than those of our data (E=79-95%) at a HRT of 1.5 days in an anaerobic hybrid reactor comprising of trickling filter treating 90 mg/L ERY. This could be attributed to the antibiotic concentrations to the anaerobic conditions and reactor configuration. A similar study was also reported by Amin et al., (2006). 99% COD removal efficiency was obtained at HRT of 2.5 days in an ASBR reactor treating 1-200 mg/L ERY.

Variations of percent ERY removal from the synthetic pharmaceutical wastewater with the feed ERY constant (100 mg/L) at different HRTs (5.5, 4.5, 2.25, 1.5, 1.13 and 0.9 days) and variable feed COD concentration of 3540, 3690, 3820, 3900, 3930, 3940 mg/L are depicted in Figure 6.83. A maximum ERY removal efficiency of 95% was obtained at a HRT of 5.5, 4.5 and 2.25 days in the AMCBR reactor. The ERY reduction at 1.5 and 1.13 days HRT were around 80% in the AMCBR reactor. After this HRT (1.13 days) the ERY yields decreased from 80% to 60% corresponding to HRT of 0.9 day (see Figure 6.83). This indicates that ERY removal efficiencies became less efficient and more variable with the HRT reduction from 1.5 days to 1.13 and to 0.9 days. A significant linear relationship between ERY yields and HRTs varying between 2.25, 4.5 and 5.5 days was not observed (R^2=0.41, F=8.21, p=0.04)

while the linear relationship between yields and low HRTs (0.9 and 1.13 days) (R^2=0.90, F=3.65, p=0.02) was significant.

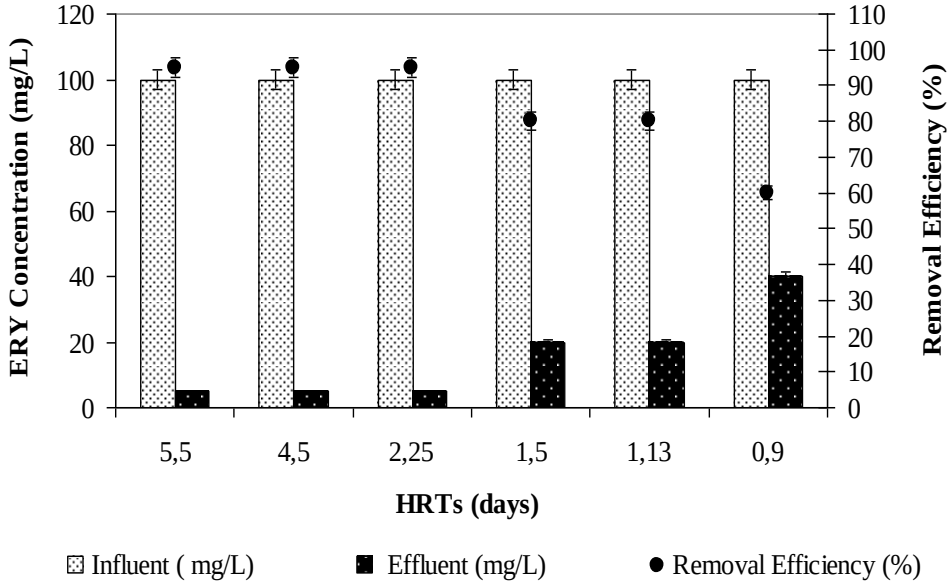

Figure 6.83 The effect of HRTs on the ERY removal efficiencies in AMCBR reactor

The ERY yields obtained in our study are high in comparison to the removal performances of ERY in the studies given below: In a study performed by Kim et al., (2008) 85% azithromycin removal efficiency was observed for the anaerobic degradation of 100 mg/L azithromycin concentration in pharmaceutical wastewater after 2.4 day HRT, at pH 7.46. In the study performed by Shimada et al. (2010), the ERY yields (80%-86%) were lower than those of our data (75%-95%) at a OLRs 1.9 and 5.8 kgCOD/m^3.d in ASBR treating 90 mg/L ERY. In a study performed by Busetti and Heitz, (2011) 90%, ERY removal was obtained in synthetic pharmaceutical wastewater containing 100 mg/L mix antibiotic solution in an anaerobic conditions at a HRT of 2 days. In our study removal efficiencies of ERY was higher than those in the study performed by Busetti and Heitz, (2011). The ERY removal was found to be lower (E=85%) in the study performed by Jessick et al., (2011) under anaerobic conditions at 80 mg/L ERY concentration, compared to the our study.

The yields obtained in the aforementioned studies are low in comparison to the removal performances of ERY found in our study (E=88%-99%). The reason of high ERY yields in our study could be explained by the granulated sludge which is resistant to the high toxic compounds and to the AMCBR reactor which is a high rate reactor. The high removal efficiency of this reactor came from its compartmentalized structure.

6.2.6.16 Influence *of HRTs on the Total and the Methane Gas Productions in the AMCBR Reactor*

From Figure 6.84, it can be seen that the total and methane gas, methane percentage production decreased whenever HRTs was decreased. The methane gas productions in the AMCBR were obtained as 9 L/d while the HRTs were 5.5, 4.5 and 2.25 days, respectively (see Figure 6.84). The total gas productions and the methane percentage remained around 14 L/d and 58%, respectively, for the HRTs mentioned above. The optimum HRTs for maximum methane gas productions (58%) varied between 2.25, 4.5 and 5.5 days. The decrease in HRT from 2.25 to 1.5 days rapidly decreased the methane gas productions (9 and 5 L/d, respectively) while the methane gas percentage was recorded as 58% and 50%, respectively in the AMCBR reactor (Figure 6.84). As shown in Figure 4.63, the total, methane gas concentration and methane content were 6 L/d, 3 L/d and 35% at a HRT of 1.13 days, respectively in the AMCBR reactor. At low HRTs the granulated bacteria could not have enough time to metabolize the 100 mg/L ERY. Percent methane content and methane production were 20% and 1 L/d at a HRT of 0.9 day in this reactor system. The minimum methane gas production (20%) was found at HRT of 0.9 day.

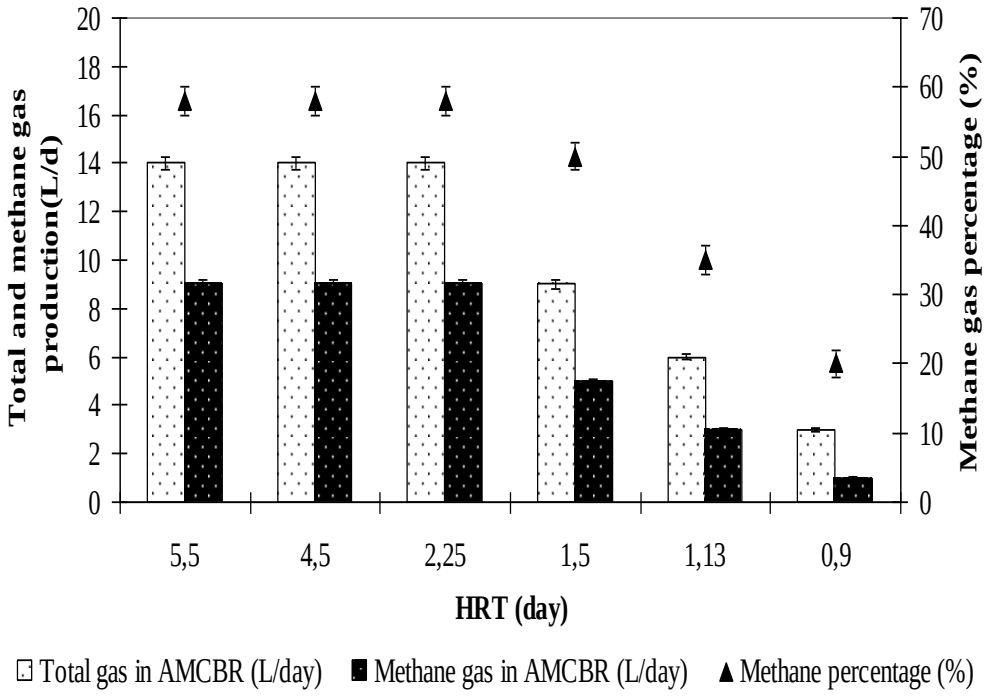

Figure 6.84 The effect of HRTs on total, methane gas production and methane percentage in the AMCBR reactor

The results of this study showed that the ERY loading affected the total and methane gas produced during anaerobic degradation of pharmaceutical wastewater. In a study performed by Liu et al., (2011) 7.49 L/d methane gas production was found at OLRs varying at between 1.23 and 2.16 kg COD/m^3d, at an influent ERY concentration varied between 50 and 200 mg/L and a HRT of 2 day in a full-scale UASB reactor. Shimada et al., 2011 reported that, 2.6 L/d biogas production at an influent TYL concentration of 167 mg/L at HRT of 1.67 day and at an OLR of 3.5 kg COD/m^3d in an ASBR reactor. In another study, in a study performed by Amin et al., (2006) methane gas production and percentage were found as 5 L/d and 48%, respectively at an OLR of 2.90 kg COD/m^3d in an ASBR. In our study, 58% methane percentage and 9 L/d CH_4 production was measured at influent ERY concentrations varying between 50 and 300 mg/L in an AMCBR reactor. The yields obtained in the aforementioned studies are low in comparison to the methane gas productions found in our study. This could be explained by the macrolide antibiotics (ERY, TYL, etc.) were inhibited methane production and content in anaerobic reactors. The degree of inhibition depended upon the antibiotic concentration.

Figure 6.85 show the variations of methane yields versus decreasing HRTs. It was observed that the methane yield decreased partly with decreasing HRTs. The methane yield was 0.31 m3 CH4/kg COD removed at HRT of 4.5 and 5.5 days. The methane yield decreased from 0.31 to 0.10 $m^3CH_4/kgCOD_{removed}$ as HRT decreased from 5.5 to 0.9 days. A linear correlation between COD removal and methane yield only for HRTs between 2.25 and 4.5 days (R^2=0.85, F=5.48, p=0.02).

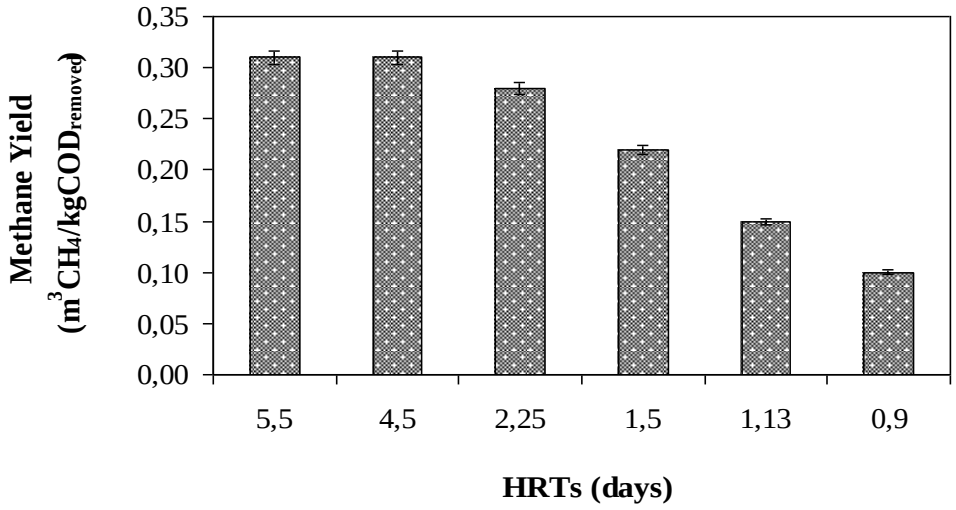

Figure 6.85 Variations of methane yields versus HRTs in AMCBR reactor.

The methane yields obtained in our study are similar in comparison to the yield performances of methane in the studies given below:

In the study by Nandy and Kaul, (2001), 0.26-0.34 $m^3CH_4/kgCOD_{removed}$ methane yields was observed for the anaerobic degradation of 200 mg/L TYL in herbal pharmaceutical wastewater after 2 day HRT. A similar study was also reported by Chelliapan et al., (2006) when treating pharmaceutical wastewater containing 20-200 mg/L TYL in an UASR. 0.10-0.40 $m^3CH_4/kgCOD_{removed}$ methane yields were obtained during 106 days of operation time. Similarly, a lower methane yield value (0.20 $m^3CH_4/kgCOD_{removed}$) was obtained in the anaerobic treatment of chemical synthesis-based pharmaceutical wastewater at a HRT of 1.98 days (Ince et al., 2002). The lower methane yields in the studies mentioned above could be due to the

configuration of the anaerobic reactor, type of anaerobic microorganism, to the biomass concentration and to the operational conditions.

6.2.6.17 Effects of HRTs on pH, TVFA, HCO_3 Alk. and TVFA/HCO_3 Alk. Ratio Variations in Compartments of the AMCBR Reactor

As shown in Figure 6.86 (a), the influent pH values remained stable at between 7.32 and 7.50 under the anaerobic condition. The pH values varied between 7.48 and 7.65 in the effluent of AMCBR at HRTs varied between 5.5 and 0.9 days. From Figure 6.86 (a) shows that the pH values in the 1st compartment were lower than the all of the other compartments. When the HRTs were decreased from 5.5 to 0.9 days in the AMCBR reactor, the pH in the 1st compartment dropped from 7.00 to 7.40 due to the increased acidogenic activity. The pH in 2nd compartment was measured as 7.35 and 7.60. As shown in Figure 6.86 (a), the pH values in the 3rd compartment of AMCBR reactor varied between 7.40 and 7.56.

Figure 6.86 (b) shows the variations of TVFA concentrations in compartments of AMCBR reactor at decreasing HRTs. At high HRTs such as 4.5 and 5.5 days the TVFA concentrations were found to be low in all compartments compared to the short HRTs (Figure 6.86 (b)). The TVFA concentrations were around 600, 400 and 150 mg/L in the 1st, 2nd and 3rd compartments while it was 10 mg/L in the effluent of the AMCBR for the aforementioned high HRTs. The TVFA levels in 1st compartment increased from 600 mg/L to 1125 mg/L as the HRTs decreased from 5.5 to 0.9 days. It was found that the minimum TVFA value in the effluent was approximately 10 mg/L at HRTs of 5.5 and 4.5 days in 1st compartment of AMCBR reactor (see Figure 6.86 (b)). The TVFA concentrations were found as 800, 856, 1030 and 1125 mg/L respectively, at HRTs of 2.25, 1.5, 1.13 and 0.9 days, respectively in 1st compartment of AMCBR reactor. As shown in Figure 4.65 (b), TVFA concentrations varied between 400, 400, 550, 580, 620 and 900 mg/L respectively in 2nd compartments of AMCBR reactor at decreasing HRTs (from 5.5 to 0.9 days). As the HRTs were decreased from 5.5, 4.5, 2.25, 1.5, 1.13 to 0.9 days TVFA concentrations increased from 150, 150, 170, 190, 250 to 485 mg/L,

respectively in the 3rd compartment (Figure 6.86 (b)). The TVFA concentrations were recorded as 10, 10, 18, 26, 58 and 76 mg/L in the effluent of the AMCBR reactor at decreasing HRTs (from 5.5 to 0.9 days). Figure 6.86 (c) shows HCO_3 concentration in the compartments and effluent of AMCBR at different HRTs. The HCO_3 concentration in the 1st compartment decreased from 2700 mg/L to 2200 mg/L with increasing of TVFA concentration from 600 mg/L to 1125 mg/L as the HRT decreased from 5.5 to 0.9 days. The HCO_3 concentrations remained between 2200 and 2850 mg/L in the 2nd compartment of AMCBR at decreasing HRTs (5.5-0.9 days) (see Figure 6.86 (c)). The HRTs decreased from 5.5 to 0.9 days the HCO_3 concentrations decreased from 2800 to 2145 mg/L in the 3rd compartment.

Barampouti et al., (2005), suggest that the ideal ratio of TVFA/HCO_3 is in the range of 0.1 to 0.3 to avoid the acidification of the anaerobic reactor. Figure 6.86 (d) showed the TVFA/HCO_3 ratios in the compartments and in the effluent of AMCBR. This ratio changed between 0.22 and 0.40 in the 1st compartment, between 0.14 and 0.40 in the 2nd compartment, between 0.05 and 0.23 in the 3rd compartment. This ratio changed between 0.01 and 0.04 in the effluent of AMCBR reactor at all HRTs (5.5, 4.5, 2.25, 1.5, 1.13 and 0.9 days).

(a) The variations of pH

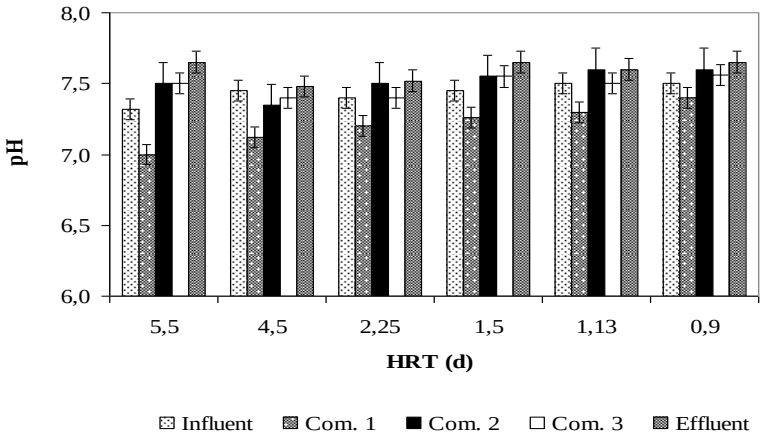

(b) The variations TVFA

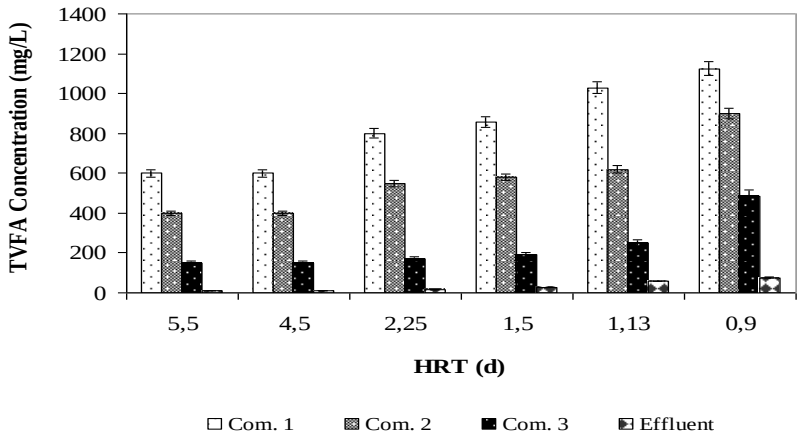

(c) The variations HCO_3 Alk.

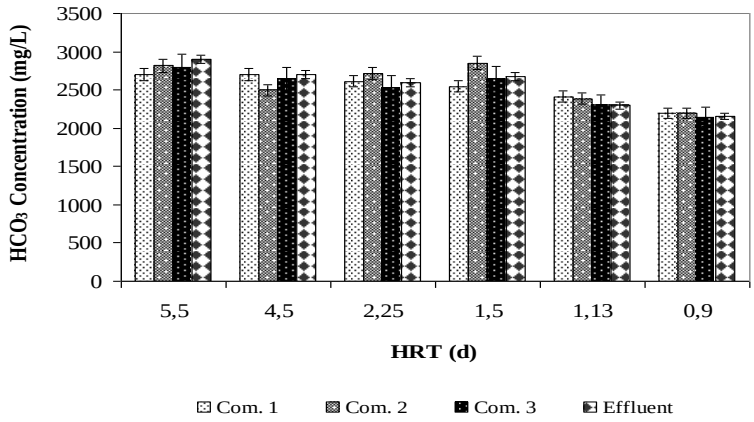

(d) The variations TVFA/HCO_3 ratio

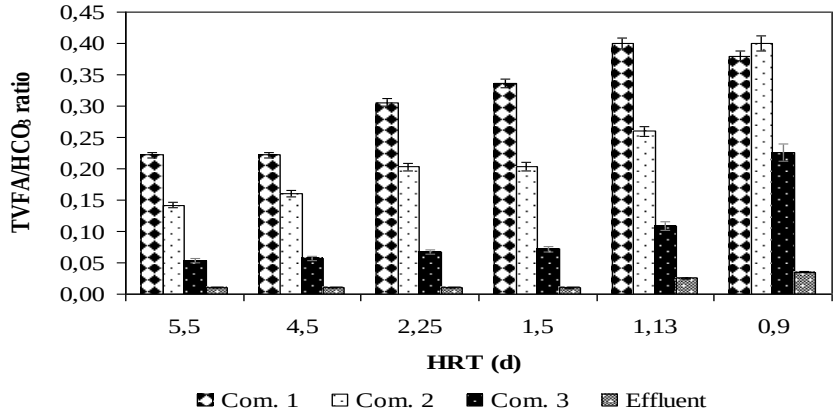

Figure 6.86 The variations of pH **(a)**, TVFA **(b)**, HCO_3 Alk. **(c)** TVFA/HCO_3 ratio **(d)** in the compartments of AMCBR at decreasing HRTs.

6.2.6.18 Effects of HRTs on the COD and ERY Removal Efficiencies in the Aerobic CSTR Reactor

Table 6.22 shows the effect of decreasing HRT on the COD and ERY removals in the CSTR reactor. The COD removal efficiencies were around 82% for HRTs of 10.97 and 9.0, 4.5 days, respectively in the aerobic CSTR reactor. The COD yields were 82% and 78% for HRTs of 4.5 and 3.0 days, respectively. The COD yields decreased from 75% to 70% at HRTs of 2.25 and 1.80 days, respectively (see Table 6.22). The COD concentrations were increased from 68.40, 72.54, 108, 176, 250 to 360 mg/L at HRTs of 10.97, 9.0, 4.50, 3.0, 2.25 to 1.80 days, respectively in the effluent of the CSTR reactor.

As shown in Table 6.22, the ERY yields were increased from 0.70, 0.70, 0.70, 4.00, 4.80 to 12.00 mg/L at HRTs of 10.97, 9.0, 4.50, 3.0, 2.25 to 1.80 days respectively in the effluent of the CSTR reactor. The ERY removal efficiencies were around 86% for HRTs of 10.97 and 9.0, 4.50 days, respectively in the aerobic CSTR reactor (see Table 6.22). The ERY yields were 86% and 80% for HRTs of 4.5 and 3.0 days, respectively. The ERY removal efficiencies decreased from 76% to 70% at HRTs of 2.25 and 1.80 days, respectively. The COD and ERY removal efficiencies decreased at low HRTs in the aerobic reactor.

Table 6.22 COD and ERY yields in the CSTR at six different HRTs

Parameters	**HRT (day)**					
	10.97	**9.0**	**4.5**	**3.0**	**2.25**	**1.80**
COD concentration in influent (mg/L)	377	377	377	377	377	377
COD concentration in effluent (mg/L)	68	68	68	83	94	113
COD Removal efficiency (%)	82	82	82	78	75	70
ERY concentration in influent (mg/L)	5	5	5	5	5	5
ERY concentration in effluent (mg/L)	0.70	0.70	0.70	1.00	1.20	1.50
ERY Removal efficiency (%)	86	86	86	80	76	70

6.2.6.19 Performance of Anaerobic AMCBR /Aerobic CSTR Sequential Reactor System

Figure 6.83 shows the removal efficiencies of COD, ERY at six studied HRTs in the sequential AMCBR/CSTR system. The COD and ERY removals in the sequential AMCBR/CSTR system were ≥ 95% as the HRTs decreasing from 16.47, 13.50 to 6.75 days. The maximum COD and ERY yields were 98% and 99%, respectively, for the HRTs given above while the minimum COD and ERY removal efficiencies were 91% and 88%, respectively, at a HRT of 2.70 days, in the sequential AMCBR/CSTR system.

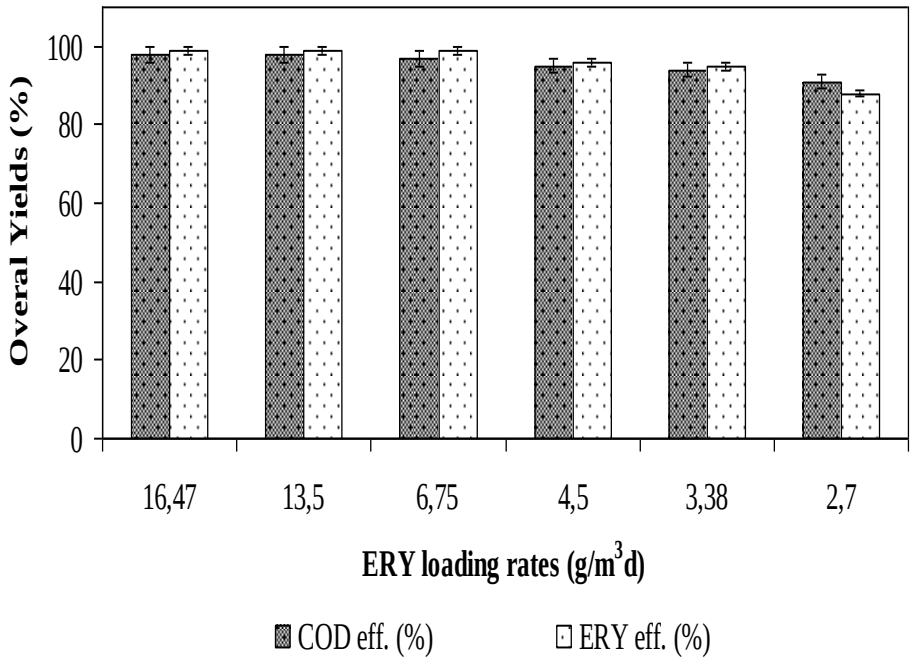

Figure 6.83 COD and ERY removal efficiencies in the sequential AMCBR/CSTR system

6.3 Continuous Studies for *the Sequential Anaerobic Buoyant Filter Reactor (ABFR)/Aerobic CSTR System*

6.3.1 The Removal of OTC, AMX, TYL, ERY in the Sequential Anaerobic ABFR/Aerobic CSTR System

6.3.1.1 Start-up Period for OTC

Start-up is often considered to be the most unstable and difficult phase in anaerobic degradation. Therefore, the main objective of this study is to observe and to evaluate the start-up performance of ABFR using synthetic wastewater at various organic loading rates. The performance of ABFR was evaluated based on the COD yields and methane gas productions. The ABFR was operated through 65 days without OTC to acclimate the granular sludge to the ABFR. The operational conditions were illustrated in Table 5.26 in the section "Material and Methods" (Study 17).

During the start-up period, the ABFR reactor was fed with molasses mineral medium containing mineral salts, sodium thioglycollate, $NaHCO_3$ having a COD concentration of 3990-4100 mg/L and organic loading rate of 0.66-0.68 g.COD/L.d. The start-up phase took about 9 weeks with no OTC addition. During the anaerobic phase zero dissolved oxygen was observed and the redox potential was around -370 mV. The COD variations through start-up period are shown in Figure 6.84.

As shown in Figure 6.84, the effluent COD concentrations were between 1200 and 1600 mg/L for operation days of 5-10 then it decreased from 1200 to 900 mg/L for 15 days resulting in a COD yield of 78% in the ABFR reactor. On days between 25, 35, 45, 55 and 65 days, the COD removal efficiencies slightly increased from 80% to 81%, 82% and to 90% at a HRT of 6 days, respectively in the effluent of the ABFR reactor. The effluent COD concentrations decreased from 800 to 400 mg/L at operation days between 45 and 50 days, respectively in the ABFR reactor. The COD yields remained as 90% on days between 50 and 65 (the effluent COD concentration

was recorded as 400 mg/L) and this COD removal efficiency was the maximum COD yield obtained in the start-up period.

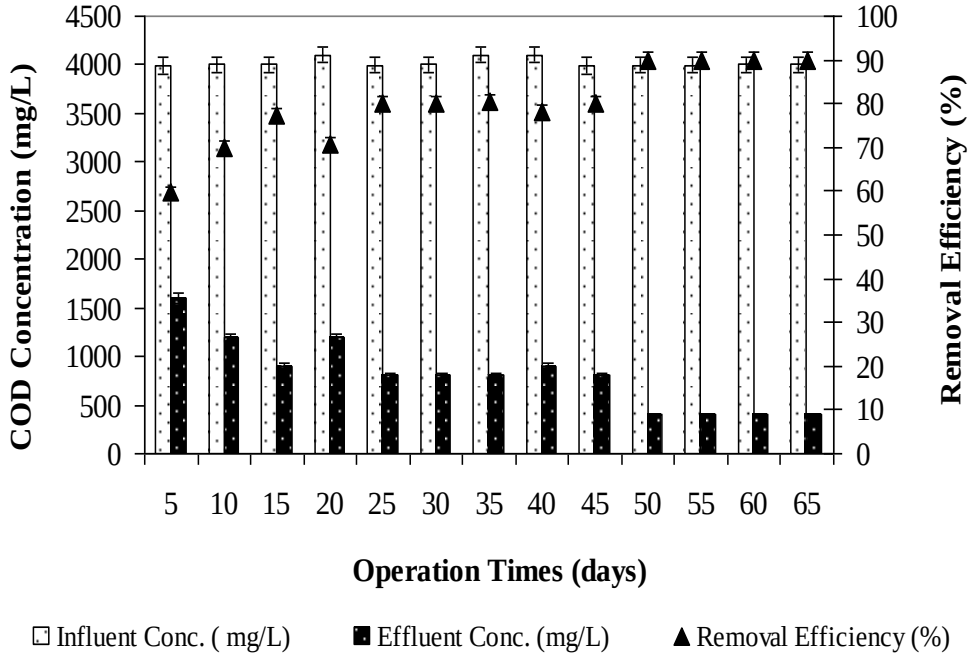

Figure 6.84 COD removal efficiencies in the ABFR during the start-up period in the ABFR reactor

Figure 6.85 shows the methane gas and methane percentages in the ABFR reactor during the start-up period. The methane gas production and methane percentage were approximately 3 L/d and 20% at the beginning of the start-up period (for operation days between 1 and 10 days). The methane gas production and methane percentage reached 5 L/d and 40%, respectively, at operation day of 25 days. The daily methane gas production and methane percentage remained stable at 7.1 L/d and 50%, respectively, after 45 days of the start-up period until 65 days of continuous operation, indicating the steady-state conditions of the ABFR reactor system.

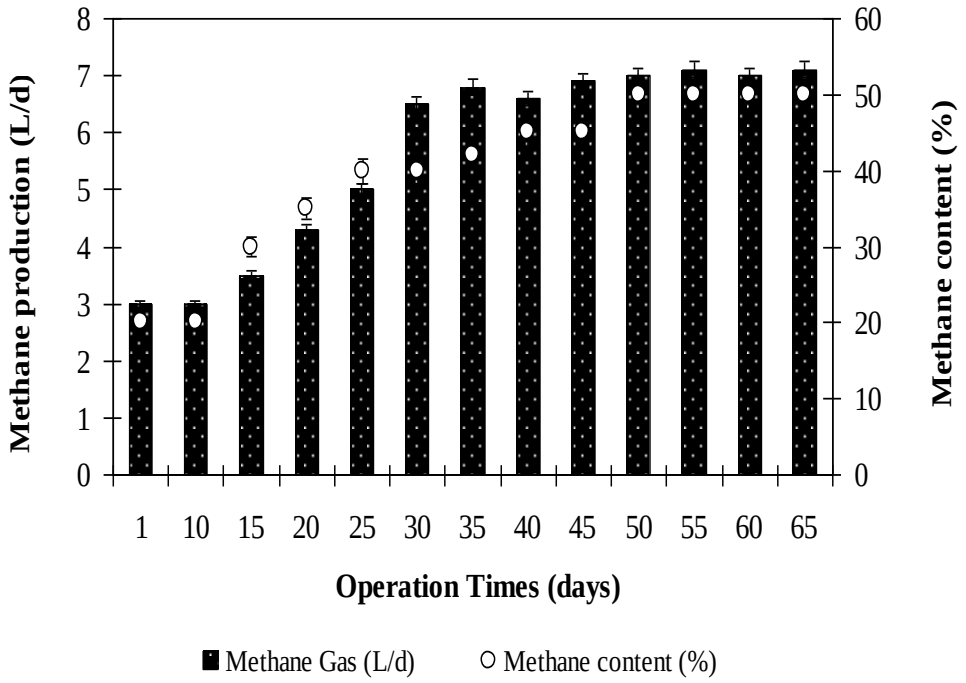

Figure 6.85 Methane gas production and percentages in the ABFR during the start-up period in the ABFR reactor

6.3.1.2 Start-up Period for AMX

The reactor start-up is very important as it has an impact on continuous and efficient operation without any system failure. During the initial startup of the reactor, the synthetic pharmaceutical wastewater was fed continuously with a HRT of 6 days. The anaerobic ABFR reactor was operated with synthetic pharmaceutical wastewater through 50 days without AMX to reach to steady-state conditions. The steady state was arbitrarily considered as the variation of COD in the effluent and the variations of methane gas production and percentage less than 5% in consecutive 7 days. During the anaerobic phase the dissolved oxygen was zero and the redox potential was around -360 mV (see Table 5.27, Study 18 for operational conditions).

Figure 6.86 illustrated the influent and effluent COD concentrations and COD removal efficiencies for 50 days of the start-up period. At the beginning of the start-up period (on days between 5 and 20), the influent COD concentrations were between 4000-4200 mg/L. On days between 5 and 20 days, the COD removal

efficiency varied between 80 and 88%. The COD removals increased from 88 to 90% on day 25 in the ABFR reactor, (see Figure 6.86). Later, the COD removal efficiency started to increase from 90% to 95% on day 35 and reached steady-state conditions (on days between 35 and 50).

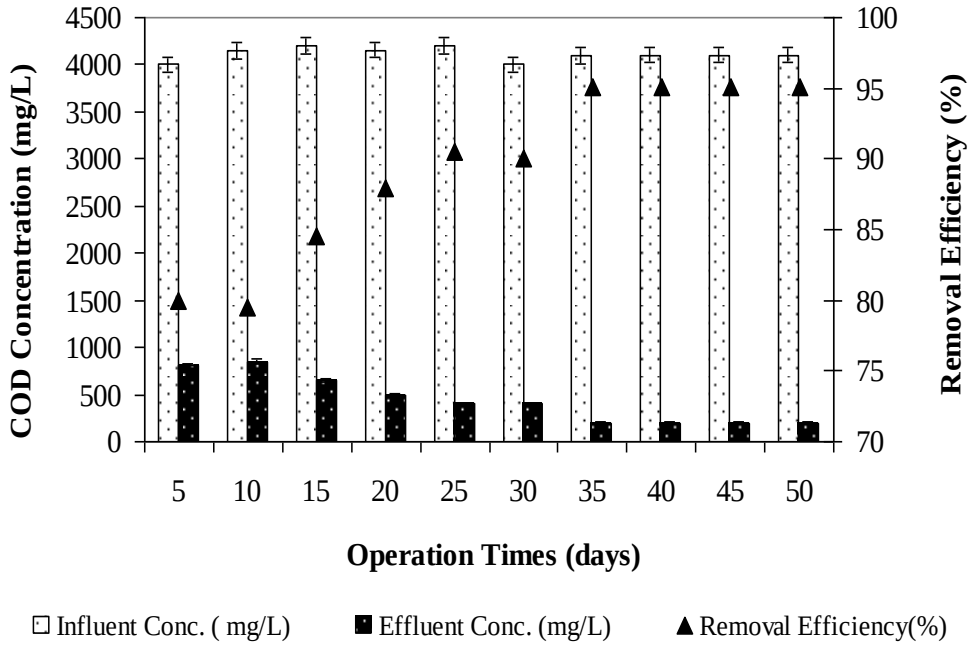

Figure 6.86 COD removal efficiencies in the ABFR during the start-up period in the ABFR reactor

Figure 6.87 shows the methane gas and methane percentages in the anaerobic ABFR reactor during the start-up period. At the beginning of the start-up period (on days between 1 and 15), the methane gas and methane percentages were 4 L/d and 25%, respectively. On days 20, 25 and 30 days, the methane percentages increased to 41%, 48% and 51%, respectively, in the anaerobic ABFR reactor. Later, the methane gas and methane percentages started to increase from 6.5 to 7.5 L/d and from 51% to 56%, respectively, on day 35 and remained the same between days 35 and 50. This showed that the ABFR reactor reached steady-state conditions.

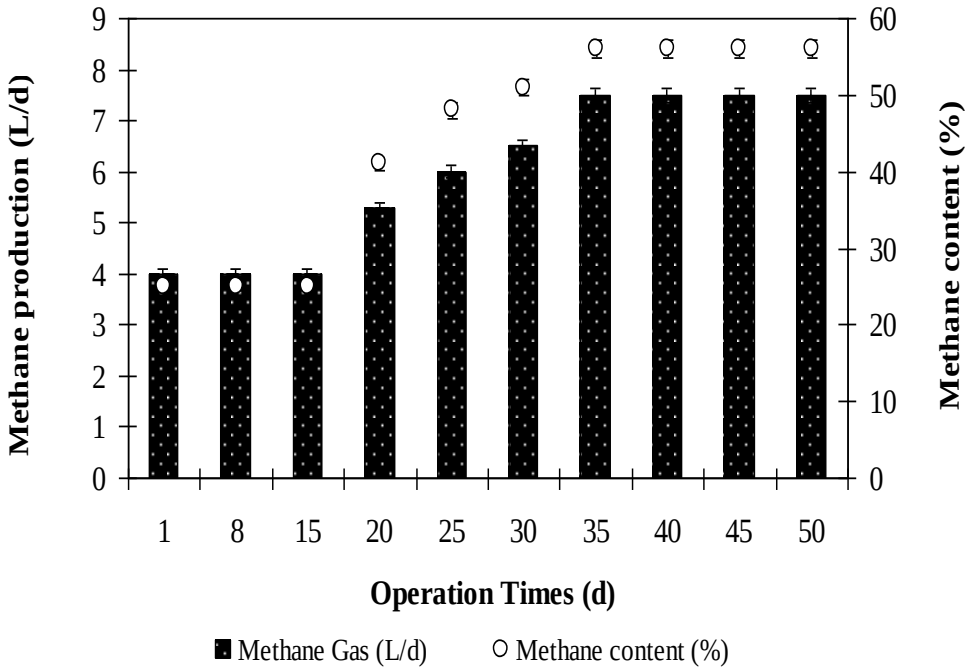

Figure 6.87 Methane gas production and content variations through start-up period in the ABFR reactor

6.3.1.3 Start-up Period for TYL

The start-up period was performed at a temperature above 36±2 °C to keep favorable conditions for growth of the anaerobic microorganisms for which 37°C is the optimal temperature for anaerobic conditions (Speece, 1996). The anaerobic conditions occurred in the ABFR reactor. The ORP values during the anaerobic phases were between -350 and -370 mV. The operational conditions were illustrated in Tables 5.28 in the section "Material and Methods" respectively (Study 19).

A start-up period led to a more complete biological degradation of the toxic substances such as antibiotics and a better adaptation of the biomass for the degradation of the antibiotics. The results of the start-up of the ABFR reactor are shown in Figures 6.88 and 6.89. The ABFR reactor was operated through 70 days without TYL to acclimate the granular sludge to the ABFR reactor. The HRT and organic loading rate were adjusted as 6 days and 0.65±1 g.COD/L.d, respectively. The COD removal efficiency was 65% after 10 days of the operation period. The

COD removal efficiency increased to 75% after 30 days of operation days. On days 35 and 45 days, the COD yields increased from 80% to 82%, respectively, in the anaerobic ABFR reactor. The COD removal efficiency increased to 90% after 50 days of operation then the COD yields remained stable at 96% throughout 20 days after an operation period of 70 days and the effluent COD was stabilized at 150 mg/L for 2 consecutive weeks. This showed that the ABFR had reached steady state conditions.

The methane gas production and methane percentages were between 3-4 L/d and 18-26% at the beginning of the start-up period (between days 5 and 15), respectively (Figure 6.89). The methane gas production and the methane percentage reached 6 L/d and 50%, respectively, on day 35 and the methane gas production and percentages remained stable at 8.6 L/d and 60%, respectively, in the ABFR reactor. On days between 35 and 50 days, the methane gas production and the methane percentage increased from 6 L/d to 6.5 L/d and from 50% to 55%, respectively in the effluent of the ABFR reactor. The methane gas production and the methane content remained stable at 8.6 L/d and 60% at operation days between 55 and 70 days, respectively, in the ABFR reactor.

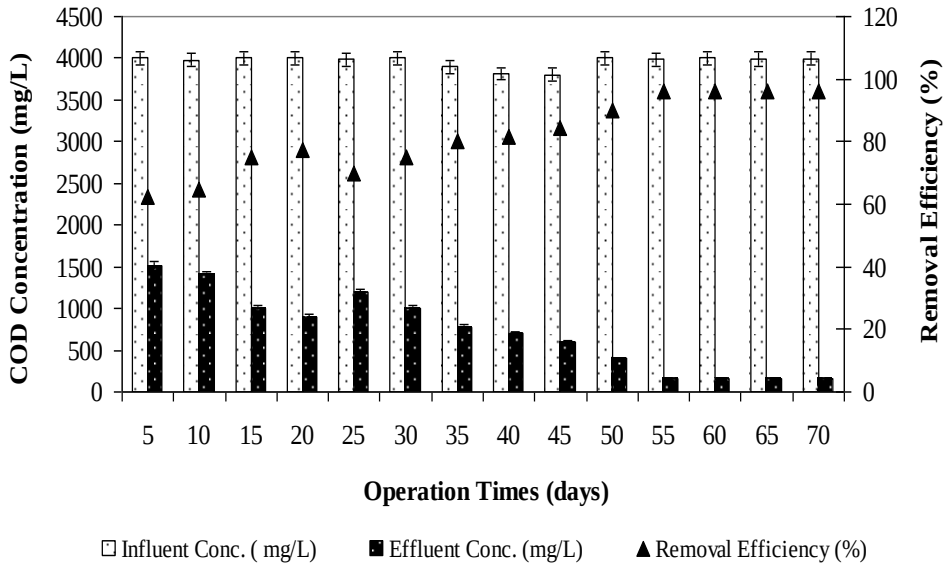

Figure 6.88 COD removal efficiencies in the ABFR during the start-up period in the ABFR reactor

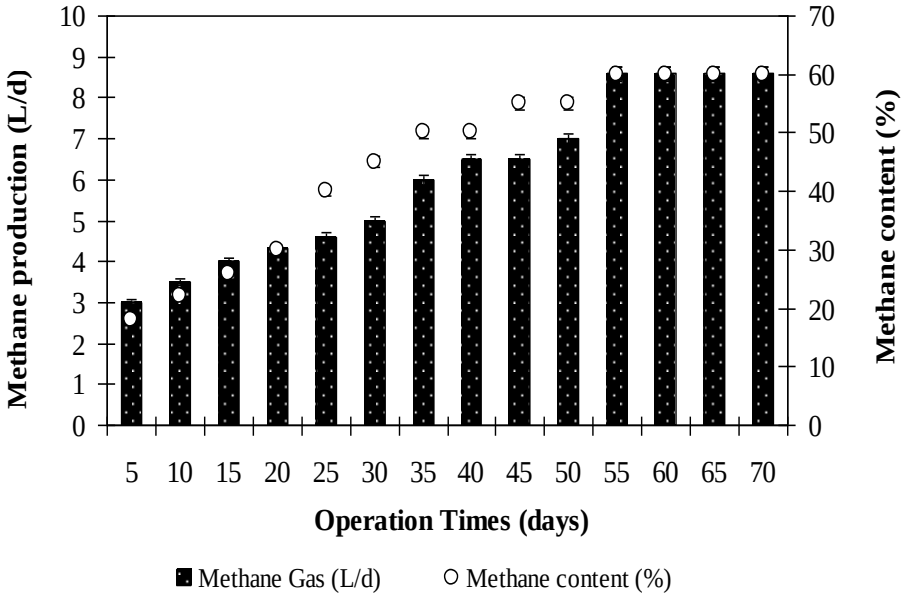

Figure 6.89 Methane gas production and percentages in the ABFR during the start-up period in the ABFR reactor

6.3.1.4 Start-up Period for ERY

Start-up procedures will depend on various factors, including wastewater composition and strength, available inoculum, reactor operating conditions, and reactor configuration. During anaerobic reactor start-up, the biomass is acclimatized to new environmental conditions, such as substrate, operating strategies, temperature and reactor configuration (Pandey et al., 2011). The operational conditions were illustrated in Table 5.29 in the section "Material and Methods" respectively for start-up period Study 20.

On days 5, 20 and 35, the COD removal efficiencies slightly increased from 78% to 80% and to 81% at an HRT of 6 days, respectively, in the effluent of the ABFR reactor (Figure 6.90). The effluent COD concentrations in the ABFR reactor decreased from 650 to 560 mg/L at operation days of 40 to 50 days, respectively. The COD yields were between 85% and 87% at operation days of 40 and 50, respectively, in the ABFR reactor. The COD removal efficiency was 89% after 55 days of the operation period. The COD yields were between 89% and 90% at operation days of 60 and 65, respectively, in the ABFR reactor (see Figure 6.90). The

COD yield remained as 90% on days between 70 and 90 while the effluent COD concentration was recorded as 200 mg/L.

Figure 6.91 shows the methane gas and methane percentages in the anaerobic ABFR reactor during the start-up period. At the beginning of the start-up period (on days between 5 and 20), the methane gas and methane percentages were 3, 3.5, 4.5, 6 L/d and 20%, 25%, 30%, 35%, respectively. On days 30, 40, 50 and 60 the methane percentages were 40%, 50%, 51% and 52%, respectively in the anaerobic ABFR reactor. The methane gas and methane percentages increased from 8 to 10 L/d and from 54% to 62%, respectively and reached steady-state conditions on days between 70 and 90.

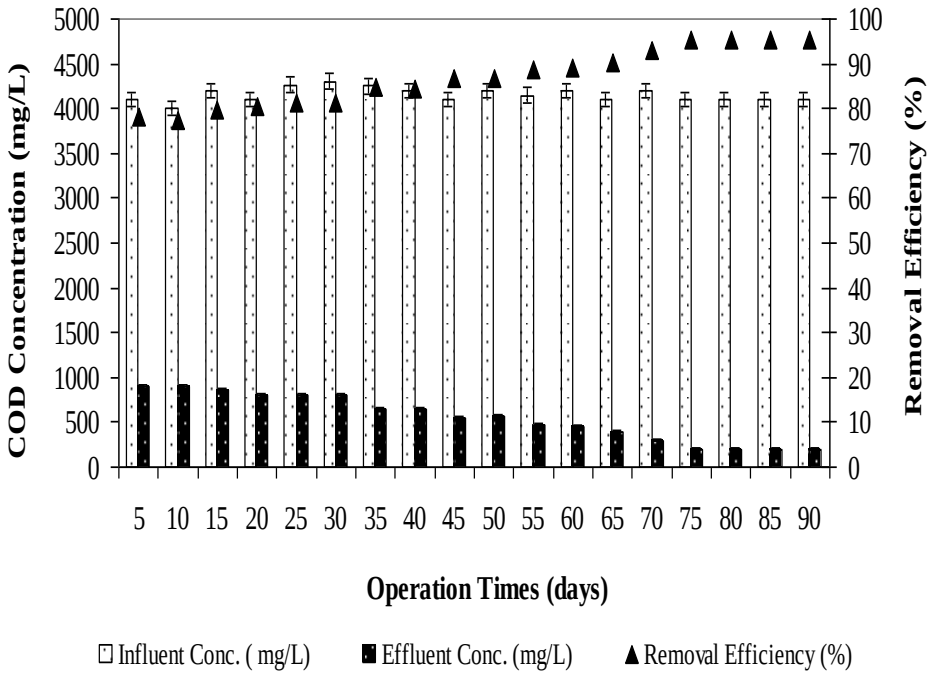

Figure 6.90 COD removal efficiencies in the ABFR during the start-up period in the ABFR reactor

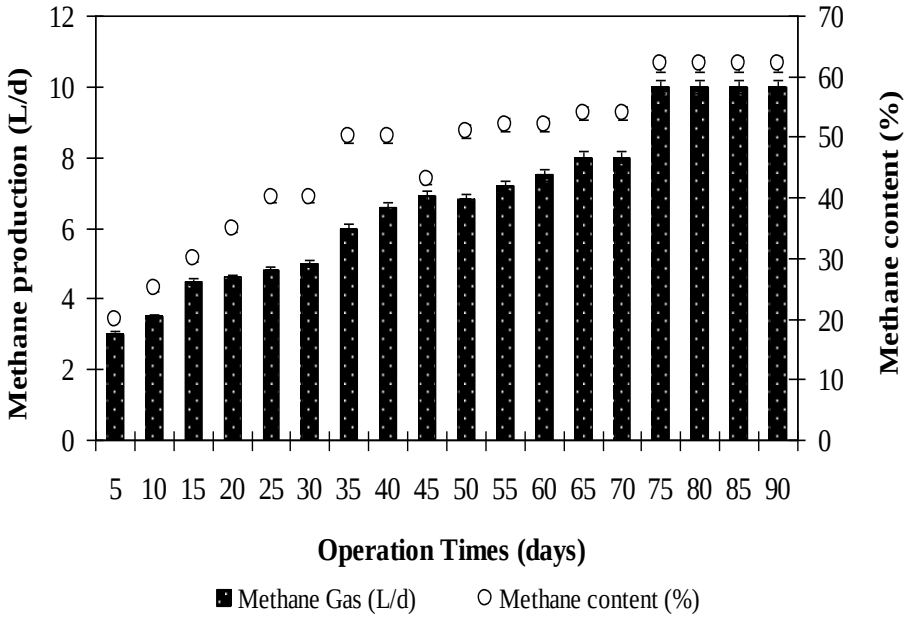

Figure 6.91 Methane gas production and percentages in the ABFR during the start-up period in the ABFR reactor

6.3.2 Effect of Increasing OTC Concentration on the Performance of ABFR

6.3.2.1 Effect of Increasing OTC Concentration on the Performance of ABFR

In this step, the effect of increasing OTC loading rates on COD removal efficiencies was investigated. The reactor was operated continuously for 183 days. Increasing OTC loading rates were applied to the anaerobic ABFR reactor system. The COD equivalents of OTC concentration are shown in Table 6.23.

Table 6.23 The COD equivalents of OTC concentration

Parameters	**Unit**	**Concentrations**
Molasses-COD concentration	mg/L	3900; 3950;3975; 3990; 4060
OTC concentration	mg/L	50; 100; 150; 200; 250
COD equivalent of OTC	mg/L	25; 50; 75; 100; 125
Total COD concentration	mg/L	3925; 4000; 4050; 4090; 4185

The influent COD concentrations were 3925, 4000, 4050, 4090 and 4185 mg/L. The influent, effluent concentrations and removal efficiencies of COD are also

shown in Figure 6.92. The operation of the ABFR reactor with OTC introduction was started at an influent OTC loading rate of 8.33 g/m^{3}d. As shown in Figure 6.92, the COD removal efficiency was 94% at an OTC loading rate of 8.33 g/m^{3}d in the ABFR reactor. The effluent COD concentration was 400 mg/L resulting a COD removal efficiency of 91% at an OTC loading rate of 16.67 g/m^{3}d. The COD yield remained around 83% until an OTC loading rate of 25.00 g/m^{3}d in the ABFR reactor. After this OTC loading rate (25.00 g/m^{3}d) the COD removal efficiencies decreased from 80% to 75% corresponding to OTC loading rates of 33.33 and 41.67 g/m^{3}d. For maximum COD removal efficiency of 94% the optimum OTC loading rate and OTC concentration were found as 8.33 g/m^{3}d and 50 mg/L, respectively, in the influent of the ABFR reactor (see Figure 6.92). The minimum COD (E=75%) yield was found at OTC loading rate of 41.67 g/m^{3}d. In our study, molasses was used as the primary substrate for the treatment of OTC. The primary substrate is consumed as an energy source and electron donor for anaerobic biodegradation while OTC was used as co-substrate by the anaerobic *archae* throughout anaerobic degradation. A significant linear relationship was found between the COD yields and the OTC loading rates varying between 16.67 and 41.67 g/m^{3}d (ANOVA), (R^2=0.97, F=7.05, p=0.02).

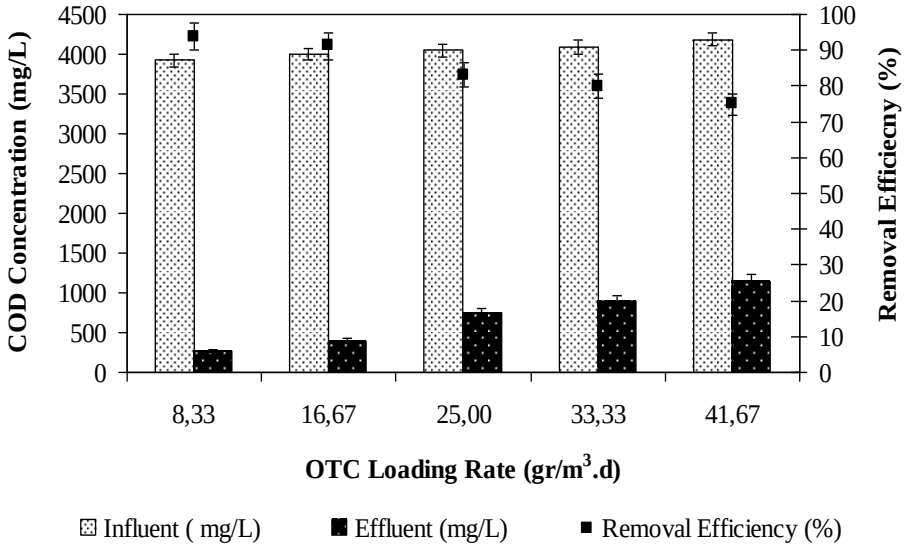

Figure 6.92 Effects of increasing OTC loading rates on COD removal efficiencies in the ABFR reactor

The COD yields obtained in recent studies including the synthetic pharmaceutical wastewater treating the OTC antibiotic were low in comparison with the COD removals in this study. In the study by Shi et al., (2011) 52-77% COD removal efficiency was observed for the anaerobic degradation of 95 mg/L initial tetracycline (TC) concentration in swine and pig manure after 30 days degradation time, at 25 ^{0}C, at pH range of 6.7-7.4. Alvarez et al., (2010) 57-82% COD removals found that under anaerobic conditions for 250 mg/L OTC after 35 days. In our study, 94% COD yield was measured at influent COD concentrations varying between 3925 and 4185 mg/L. The yields obtained in the aforementioned studies are low in comparison to the removal performances of COD found in our study. The difference in COD yields could be attributed to the combining effects of anaerobic sludge which is resistant to OTC used in this study, to the differences in antibiotic concentrations to the anaerobic conditions and to the reactor configurations.

The COD yields found in our study agree with the COD yields reported by Nandy et al., (1998) in the treatment of herbal pharmaceutical wastewater containing mixed antibiotics in an up-flow fixed bed reactor (UFFBR). The organic loading rate was 1.0 kgCOD/m^{3}d with an influent COD concentration of 5000 mg/L, resulting in a COD removal efficiency of 96% in an UFFBR reactor during the operation time (86 day). This could be attributed to the similarities in COD concentrations to the operational conditions, and to the similarities in ABFR and UFFBR reactor configurations.

The high COD yields in the ABFR reactor can be explained by the granulated sludge which is resistant to the high toxic organic compounds and to the ABFR reactor configuration which is a high rate reactor. The ABFR reactor is a high-rate two-phase anaerobic reactor designed for the treatment of complex wastewater. The high removal efficiency of this reactor came from its two-phase (lover and upper region) structure. In this reactor acidogenesis and methanogenesis phases are predominate in the lover (1st, 2nd, 3rd sampling points, see Figure 5.4 in the section "Material and Methods") and upper (4th, 5th sampling points, see Figure 5.4) regions of the ABFR reactor, respectively. The ABFR has many advantages compared with

the other anaerobic reactors such as lower sludge generation, lower HRT and higher stability to organic, hydraulic and toxic shock loads (Haridas et al., 2005) (see Table 6.24).

Table 6.24 The comparison of the ABFR reactor with the other high-rate anaerobic reactor designs (Haridas et al., 2005)

Aspect	**UASB**	**Fixed film**	**Fluidized bed**	**ABFR**
Biomass retention	Depends on settle ability	Only biofilm forming microbes are retained	Only biofilm forming microbes are retained	Retains sludge irrespective of settle ability or ability to form biofilm
Solids retention	Limited capacity of sludge bed to retain solids lead to sludge washout	Solids can be captured, but leads to bed choking	No capacity to retain solids	High capacity to retain solids, irrespective of its settle ability
Mixing of solids and gas transfer	Limited by liquid up-flow velocity and gas production rate	Poor mixing and very limited gas transfer	Good mixing but not independent of liquid velocity	Any degree of mixing can be provided irrespective of liquid velocity

6.3.2.1.1 Performance of the ABFR Reactor Versus Sampling Points. As shown in Table 6.25, the effluent COD concentration was 850 mg/L at an OTC loading rate of 8.33 g/m^{3}d in the 1st sampling point (valve 1) of the ABFR reactor (see Figure 5.4 in the section "Material and Methods"). The COD concentration was measured as 612 mg/L at the same OTC loading, in the 2nd sampling point (valve 2) of the ABFR reactor (see Figure 5.4 in the section "Material and Methods")). The COD level decreased to 485 mg/L at an OTC loading rate of 8.33 g/m^{3}d in the 3rd sampling point of the ABFR reactor while the COD concentration in 4th sampling point of the ABFR reactor was measured as 335 mg/L. This showed that the COD concentrations decreased from sampling point 1st to the sampling point 5th throughout height of the ABFR reactor between five sampling points, indicating that staging had been accomplished in the compartments of ABFR reactor. The COD concentration was measured as 300 mg/L in the 5th sampling point (effluent) of the ABFR reactor (see Figure 5.4 in the section "Material and Methods"). The 1st, 2nd and 3rd sampling

points characterize the lover region (mostly acidogenesis phase) while the 4th and 5th sampling points indicate the upper region (methanogenesis phase) of the anaerobic ABFR reactor. The COD yields in the lower region of the ABFR reactor , in 1st sampling point, between sampling points 1st-2nd and 2nd-3rd were 78%, 28% and 21%, respectively, at an OTC loading rate of 8.33 g/m3d. The COD yield in the upper level of the ABFR reactor in 4th sampling point and in the sampling points between 4th and 5th were 31% and 10%, respectively. The total COD removal in the lower region of the ABFR reactor was (3925-485/3925) 88% while the total COD yield in the upper region of the ABFR reactor was calculated as (485-300/485) 38% at an OTC loading rate of 8.33 g/m3d. The total COD yield between influent and effluent (3925-300/3925) of the ABFR reactor system was 92%.

The effluent COD concentration was 950 mg/L at an OTC loading rate of 16.67 g/m3d in the 1st sampling point of the ABFR reactor. The COD concentration was found as 805 mg/L in the 2nd sampling point, at the same OTC loading (Table 6.25). The COD value decreased to 600 mg/L at the same OTC loading in the 3rd sampling point while the COD concentration in the 4th sampling point was measured as 425 mg/L. The COD value was measured as 400 mg/L in the 5th sampling point (see Table 6.25). As illustrated in Table 4.27, the COD yields in the lower region of the ABFR reactor in the 1st,sampling point, between sampling points 1st-2nd and 2nd-3rd were 76%, 15% and 25%, respectively, at an OTC loading rate of 16.67 g/m3d. The COD yield in the upper region of the ABFR reactor in 4th sampling and in the sampling points between 4th and 5th were 29% and 6%, respectively. The total COD removal in the lower region of the ABFR reactor was (4000-600/4000) 85% while the total COD yield in the upper region of the ABFR reactor was calculated as (600-400/600) 33% at an OTC loading rate of 16.67 g/m3d. The total yield between influent and effluent (4000-400/4000) of the ABFR reactor system was 90%.

At an OTC loading rate of 25.00 g/m3d the COD concentration was 1123 mg/L in the 1st sampling point of the ABFR reactor. The COD concentration was determinated as 965 mg/L in the 2nd sampling point, at an OTC loading rate of 25.00 g/m3d (Table 6.25). The COD value was determinated as 850 mg/L at the same OTC

loading in the 3rd sampling point. The COD concentrations in the 4th and 5th sampling points of the ABFR reactor were found as 814 and 750 mg/L, respectively, at an OTC loading rate of 25.00 g/m^{3}d (see Table 6.25). At the same OTC loading the COD yields in the lower region of the ABFR reactor in the 1st sampling point and between sampling points 1st-2nd and 2nd-3rd were 72%, 14% and 12%, respectively. The COD removal efficiencies in the upper region of the ABFR reactor in sampling 4th and in the sampling points between 4th and 5th were 4% and 8%, respectively. The total COD yields in the lower and upper region of the ABFR reactor was calculated as (4050-850/4050) 79% and (850-750/850) 12% at an OTC loading rate of 25.00 g/m^{3}d. The total yield between influent and effluent (4050-750/4050) of the ABFR reactor system was 82%.

As shown in Table 6.25, the effluent COD concentration was 1242 mg/L at an OTC loading rate of 33.33 g/m^{3}d in the 1st sampling point of the ABFR reactor (see Table 6.25). The COD concentration was measured as 1093 mg/L at the same OTC loading, in the 2nd sampling point of the ABFR reactor (Table 6.25). The COD level decreased to 1000 mg/L at an OTC loading rate of 33.33 g/m^{3}d in the 3rd sampling point. The COD concentration in 4th sampling point of the ABFR reactor was measured as 950 mg/L. The COD concentration was found as 900 mg/L in the 5th sampling point of the ABFR reactor (see Table 6.25). At an OTC loading rate of 33.33 g/m^{3}d the COD yields in the lower level of the ABFR reactor in sampling point 1st, between sampling points 1st-2nd and 2nd-3rd were 70%, 12% and 9%, respectively. The COD yield in the upper level of the ABFR reactor in sampling 4th and in the sampling points between 4th and 5th were 5% and 5%, respectively. The total COD removal efficiency in the lower level of the ABFR reactor was (4090-1000/4090) 76% while the total COD yield in the upper level of the ABFR reactor was calculated as (1000-900/1000) 10% at an OTC loading rate of 33.33 g/m^{3}d. The total yield between influent and effluent (4090-900/4090) of the ABFR reactor system was 78%.

The COD value was measured as 1351 mg/L at an OTC loading rate of 41.67 g/m^{3}d in the 1st sampling point of the ABFR reactor. The COD value was measured as 1268 mg/L in the 2nd sampling point, at an OTC loading rate of 41.67 g/m^{3}d (Table 4.27). The COD value was obtained as 1200 mg/L in the 3rd sampling point, at the same OTC loading (Table 6.25). The COD value decreased to 1100 mg/L at the same OTC loading in the 4th sampling point of the ABFR reactor. The COD value in the 5th sampling point was measured as 1000 mg/L (see Table 6.25). As shown in Table 6.25, the COD yields in the lower part of the ABFR reactor in the sampling point 1st, between sampling points 1st-2nd and 2nd-3rd were 68%, 6% and 5%, respectively, at an OTC loading rate of 41.67 g/m^{3}d. The COD yields were 8% and 9%, respectively in the upper part of the ABFR reactor in4th sampling and in the sampling points between 4th and 5th. The total COD yield in the lower part of the ABFR reactor was (4185-1200/4185) 71%. The total COD yield in the upper part of the ABFR reactor was calculated as (1200-1000/1200) 17% at an OTC loading rate of 41.67 g/m^{3}d. The total yield between influent and effluent (4185-1000/4185) of the ABFR reactor system was 76%.

The effluent COD removal profile across the anaerobic ABFR reactor system followed the Sampling point 1st > Sampling point 2nd > Sampling point 3rd > Sampling point 4th > Sampling point 5th. Most of the COD removal in the anaerobic ABFR reactor system occurred in the 1st sampling point following the lower yields occurring in the subsequent sampling points (2nd, 3rd, 4th, 5th):

The COD removal efficiencies were 78%, 76%, 72%, 70% and 68% in the 1st sampling point for the OTC loading rates of 8.33, 16.67, 25.00, 33.33, 41.67 g/m^{3}d, respectively. The COD yields were 28%, 15%, 14%, 12% and 6% at OTC loading rates of 8.33, 16.67, 25.00, 33.33, 41.67 g/m^{3}d, respectively, in the 2nd sampling point of the anaerobic ABFR reactor (see Table 6.25). Similarly, the COD yields decreased from 21% to 25%, 12%, 9% to 5%, respectively in the 3rd sampling point, at the same OTC loading rates (Table 6.25). The COD removal efficiencies were 31%, 29%, 4%, 5% and 8% in the 4th sampling point for the same OTC loading rates, respectively. As the OTC loading rates were increased from 8.33, 16.67, 25.00, 33.33

to 41.67 g/m^{3}d the COD yields decreased in the 5th sampling point (effluent) of the ABFR reactor (see Table 6.25).

As a result the COD mainly removed (68%-78%) in the lower part of the ABFR reactor throughout sampling point 1st while small amounts of COD removals (6%-28%, 5%-21%, 4%-31%, 5%-10%) occurred in the subsequent sampling points namely 2nd, 3rd, 4th and 5th, respectively at all OTC loading rates (8.33, 16.67, 25.00, 33.33 and 41.67 g/m^{3}d). Aciogenesis takes place in the 1st, 2nd, 3rd sampling points in the lower part of the ABFR while methanogenesis occurred in the sampling points, 4th and 5th, in the upper part of the anaerobic ABFR reactor.

It is important to note that as the OTC loading rates increased from 8.33 to 16.67, 25.00, 33.33 and to 41.67 g/m^{3}d the COD concentrations in the 1st sampling point increased from 850, 950, 1123, 1242 to 1351 mg/L, respectively resulting in COD yields of 78%, 76%, 72%, 70%, 68%, respectively. The COD concentrations in the 2nd sampling point increased from 612 to 805, 965, 1093 and to 1268 mg/L, respectively resulting in COD yields of 28%, 15%, 14%, 12% and 6%. As the OTC loading rates were increased from 8.33 to 16.67, 25.00, 33.33 and 41.67 g/m^{3}d the COD concentrations were measured as 485, 600, 850, 1000 and 1200 mg/L, respectively, in the 3rd sampling point of the ABFR reactor resulting in COD yields of 21%, 25%, 12%, 9% and 5% (see Table 6.25). At the same OTC loading rates, the COD concentrations in the 4th sampling point increased from 335 to 425, 814, 950 and to 1100 mg/L, respectively. Similarly, the COD concentrations in the 5th sampling point of the ABFR reactor increased from 300 to 400, 750, 900 and to 1000 mg/L, respectively resulting in COD yields of 10%, 6%, 8%, 5% and 9%, respectively.

Table 6.25 Variations of COD Concentrations and COD Yields in Sampling Points of ABFR Reactor at Increasing OTC

Influent			**LOVER REGION**						**UPPER REGION**			
OTC Loading rate (g/m^3d)	**OTC Conc. (mg/L)**	**COD Conc. (mg/L)**	**Effluent COD (mg/L)**			**COD Yield (%)**			**Effluent COD (mg/L)**		**COD Yield (%)**	
			1st sampling point	2nd Sampling point	3rd Sampling point	**1st sampling point**	2nd Sampling point	3rd Sampling point	4th Sampling point	**5th sampling point**	4th Sampling point	**5th sampling point**
8.33	50	3925±120	**850±48**	612±43	485±38	**78**	28	21	335±40	**300±36**	31	**10**
16.67	100	4000±108	**950±60**	805±60	600±60	**76**	15	25	425±51	**400±21**	29	**6**
25.00	150	4050±92	**1123±71**	965±70	850±50	**72**	14	12	814±52	**750±34**	4	**8**
33.33	200	4090±68	**1242±90**	1093±90	1000±73	**70**	12	9	950±75	**900±56**	5	**5**
41.67	250	4185±96	**1351±105**	1268±102	1200±98	**68**	6	5	1100±65	**1000±72**	8	**9**

6.3.2.2 Effect of OTC Loading Rate on the OTC Removal Efficiencies in the ABFR Reactor

In this part of the experiments the OTC removal efficiencies in the ABFR reactor under the same operating conditions were monitored. The influence of different OTC loading rates (8.33, 16.67, 25.00, 33.33, 41.67 g/m^3d) on the OTC removal efficiencies in ABFR reactor was shown in Figure 6.93. The effluent OTC concentration was 5 mg/L in the ABFR reactor resulting in an OTC removal efficiency of 90% at an OTC loading rate of 8.33 g/m^3d. As shown in Figure 6.93, the OTC removal efficiency was 85% (effluent OTC concentration=15 mg/L) at an OTC loading rate of 16.67 g/m^3d in the ABFR reactor. The effluent OTC concentration was 25 mg/L resulting in an OTC removal efficiency of 83% at an OTC loading rate of 25.00 g/m^3d. The effluent OTC concentrations were 50 and 62 mg/L in the ABFR reactor at OTC loading rates of 33.33 and 41.67 g/m^3d, respectively. For maximum OTC removal efficiency of 90% the optimum OTC loading rate and OTC concentration were 8.33 g/m^3d and 50 mg/L, respectively, in the effluent of the ABFR reactor (Figure 6.93). The minimum COD (E=75%) yield was found at OTC loading rates of 33.33 and 41.67 g/m^3d. A significant linear relationship was found between the OTC yields and the OTC loading rates for 8.33, 16.67, 25.00 and 33.33 g/m^3d (ANOVA), (R^2=0.93, F=11.46, p=0.01).

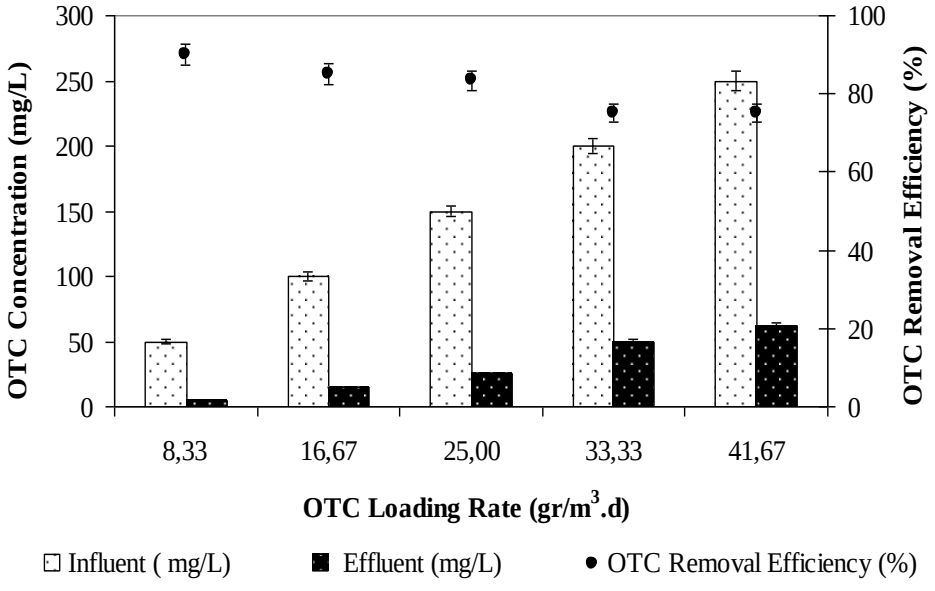

Figure 6.93 The effect of OTC loading rate on OTC removal efficiencies in the ABFR reactor.

The HPLC chromatogram of OTC was illustrated in Figure 6.94 (a-b) for the influent and effluent samples of the ABFR reactor. A peak was obtained for the influent OTC concentration of 50 mg/L at a retention time of 5.28 min and at a wave length of 254 nm (Figure 6.94(a)). Similarly, a peak was measured for the effluent OTC concentration of 5 mg/L at a retention time of 7.12 min and at a wave length of 254 nm (Figure 6.94(b)). This indicates that 50 mg/L OTC is co-metabolized by the anaerobic granules with a removal efficiency of 90% with a simultaneous utilization of the primary substrate and OTC by the archae for growth requirement.

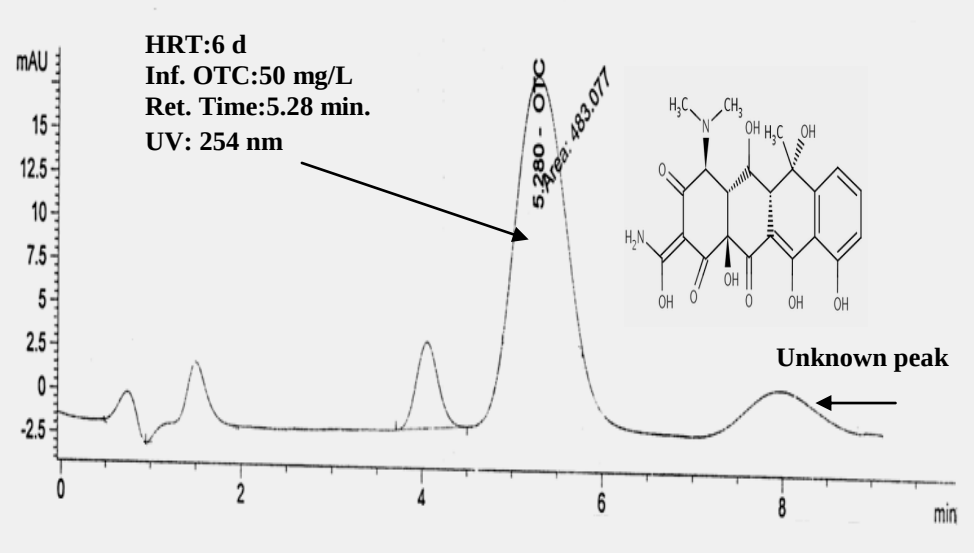

Figure 6.94 (a) HPLC chromatograms of OTC (50 mg/L) in the influent of the ABFR reactor system

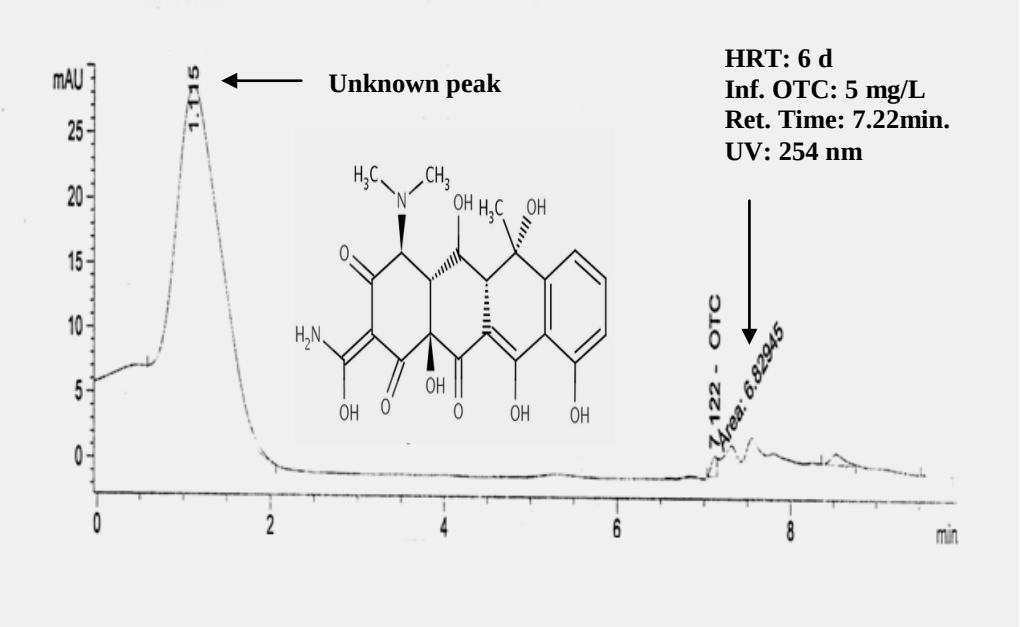

Figure 6.94 (b) HPLC chromatograms of OTC (5 mg/L) in the effluent of the ABFR reactor system

The OTC yields obtained in our study are high in comparison to the removal performances of OTC in the studies given below: In the study by Kim et al. (2005) 85% OTC removal efficiency was observed for the anaerobic degradation of 200 mg/L OTC in an anaerobic batch reactor (ABR) after 7.4-24 h HRTs and 3-10 days SRTs, at pH 7.38. This could be explained by the differences in the anaerobic reactor type by the OTC degradating anaerobic bacteria type, by the differences in OTC concentrations and by the differences in the composition of the wastewater.

6.3.2.3 Effect of OTC Loading Rate on the Total and Methane Gas Production in the ABFR Reactor

Figure 6.95 illustrates the variation of biogas production and methane contents in the ABFR reactor system. From this figure, it can be seen that the biogas production and methane contents decreased whenever OTC loading rates were increased. The daily total gas, methane gas productions and methane content were recorded as 12.30 L/d and 9.12 L/d and 65%, respectively at an OTC loading rate of 8.33 g/m^{3}d. The maximum total gas, methane gas productions and methane content were found in this OTC loading rate (see Figure 6.95). After this loading rate, the methane percentage

decreased from 65% to 60% at an OTC loading rate of 16.67 g/m^{3}d in the ABFR reactor. As the OTC loading rates were increased from 16.67 to 25.00 g/m^{3}d, methane contents decreased from 60% to 50%, respectively (Figure 6.95). The total gas, methane gas productions were measured as 10.08 L/d and 7.65 L/d, at an OTC loading rate of 25.00 g/m^{3}d, respectively (see Figure 6.95). When the OTC loading rates were increased from 33.33 to 41.67 g/m^{3}d, the daily total gas and methane gas productions from 9.21 L/d, to 6.20 L/d and from 7.12 L/d, to 5.14 L/d, respectively in the ABFR system. The methane content also remained constant as 40% for the aforementioned OTC loadings.

A significant linear relationship was found between the total and methane gas productions and the OTC loading rates (between 8.33-16.67-25.00 and 33.33 g/m^{3}d) (ANOVA), (R^2=0.99, F=6.68, p=0.02 (for total gas); R^2=0.92, F=11.14, p= 0.05 (for CH_4). Similarly, a linear relationship was found between the methane content and the OTC loading rates (between 8.33-16.67-25.00 and 33.33 g/m^{3}d) and this relationship is significant (ANOVA), (R^2=0.98, F=9.34, p=0.01).

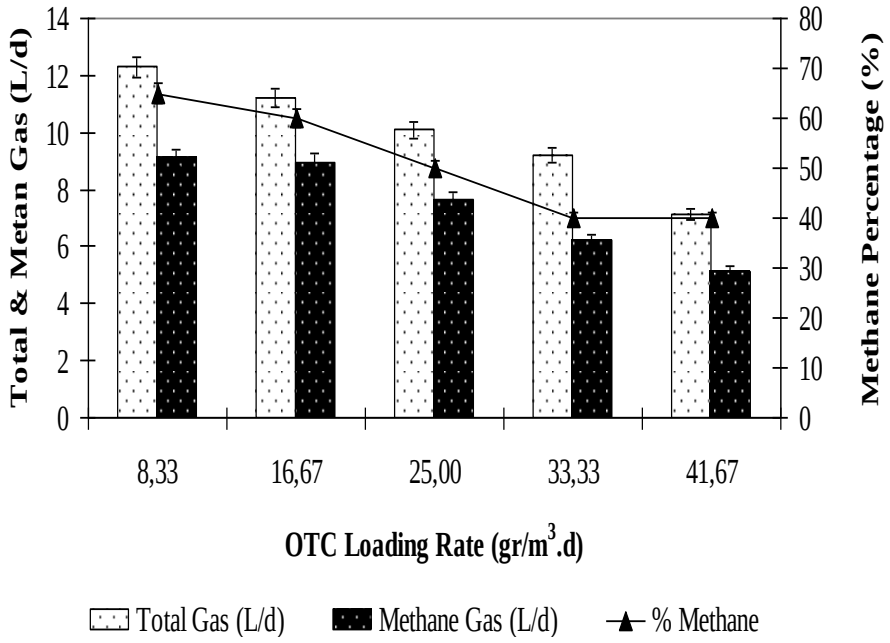

Figure 6.95 The effect of OTC loading rate on total, methane gas production and methane percentage in the ABFR reactor

The results of this study showed that the OTC loadings affected the total volume of CH_4 produced during anaerobic degradation of the synthetic pharmaceutical wastewater used in this study.

In a study performed by Liu et al., (2009) the methane gas productions were found as 12, 30 and 66 L/d at OLRs of 1.04, 2.01 and 6.17 kg COD/m^3d, respectively, in an anaerobic baffled reactor (ABR) treating pharmaceutical wastewater. In our study the methane gas productions were 9.12, 8.97, 7.65, 6.20 and 5.14 L/d at OTC loading rates of 8.33, 16.67, 25.00, 33.33 and 41.67 g/m^3d, respectively in the ABFR reactor. In OUR study the methane productions are comparable higher than that aforementioned study.

Heidari et al., (2011) reported 48% methane percentage and 0.12 L/d CH_4 production at an influent OTC concentration of 105 mg/L at a COD load of 2.03 kg COD/m^3d in an anaerobic sequencing batch reactor (SBR). In our study, 58-65% methane percentage and 6.36-9.36 L/d CH_4 production was measured at influent OTC concentrations varying between 50 and 300 mg/L.

The methane yield can be a useful parameter to assess the performance of the ABFR. Figure 6.96 shows the variations of methane yields versus OTC loading rates. The methane yields decreased from 0.31 to 0.10 $m^3CH_4/kgCOD_{removed}$, when the OTC loading rates were increased 8.33 to 41.67 g/m^3d. A significant linear relationship was found between the methane yields and the OTC loading rates (between 8.33, 16.67, 25.00, 33.33 and 41.67 g/m^3d) (ANOVA), (R^2=0.99, F=9.06, p=0.001).

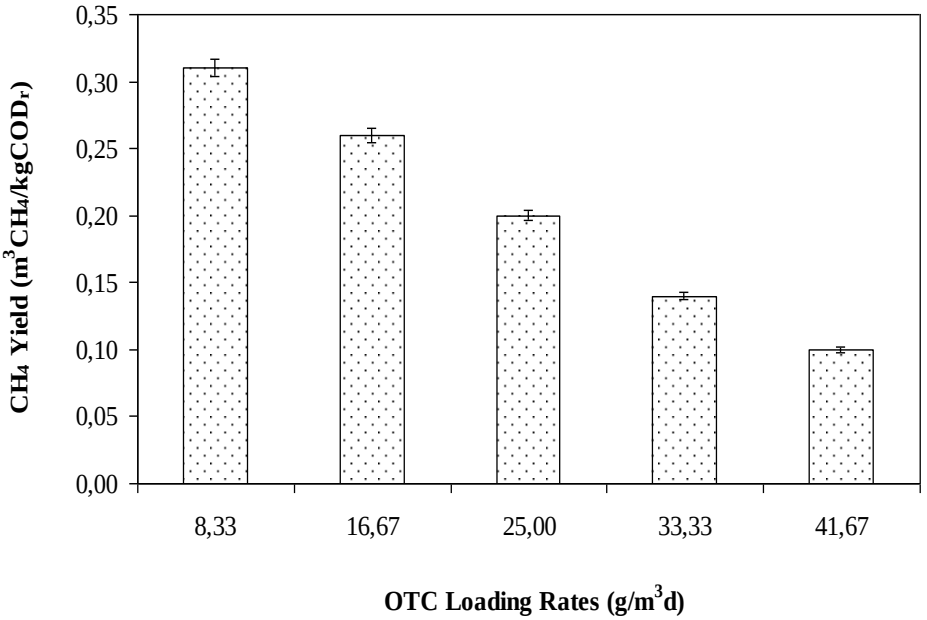

Figure 6.96 Variations of methane yields versus OTC loading rates in the anaerobic ABFR reactor

6.3.2.4 Variation of pH, TVFA and Composition (H_{ac}, H_{bu}, H_{la}, H_{pr}) in Compartments of the ABFR Reactor at Increasing OTC Loading Rates

The pH plays a major role in the anaerobic degradation. It influences the activity of the microorganisms which they are active within certain and narrow pH ranges. Althoughout anaerobic degradation occur in the pH range of 6.00 to 8.30, however, methanogenes have a optimum pH value between 7.00 and 8.00 while acidogenes have a lower optimum pH range (3-6) (Speece, 1996). If the pH of waste is outside the optimum range and if the buffering capacity of the system is not sufficient, the anaerobic process could be inhibited (Dlamini, 2009). Figure 6.97 shows the pH variation in sampling points of the ABFR reactor at increasing OTC loading rates. The pH values in the all sampling points of the ABFR reactor varied between 6.80 and 7.61. The pH values were lower in the 1st sampling point than all of the other sampling points since TVFA in the 1st sampling point was higher (see Figure 6.98). When the OTC loading rates was increased from 8.33 to 41.67 g/m^{3}d in the ABFR reactor, the pH in the 1st sampling point slightly dropped from 7.00 to 6.90 due to the increased acidogenic activity. The pH profile of the ABFR reactor system with

average pH in the 1st sampling point was measured as 6.96, at OTC loading rates of 8.33, 16.67, 25.00, 33.33 and 41.67 g/m^{3}d. As the OTC loading rates were increased from 8.33, 16.67, 25.00, 33.33 to 41.67 g/m^{3}d, the pH values decreased slightly from 7.32, 7.42, 7.26, 7.20 to 7.18, respectively in 2nd sampling point (Figure 6.97). As shown in Figure 4.55, the pH values in the 3rd and 4th sampling points of the ABFR reactor varied between 7.30-7.40-7.38-7.30-7.32 and 7.40-7.50-7.40-7.40-7.45 at OTC loading rates of 8.33, 16.67, 25.00, 33.33 and 41.67 g/m^{3}d, respectively. The effluent pH values varied between 7.55, 7.61, 7.55, 7.55 and 7.60 at OTC loading rates of 8.33, 16.67, 25.00, 33.33 to 41.67 g/m^{3}d, respectively in the 5th sampling point (valve 5) of ABFR reactor.

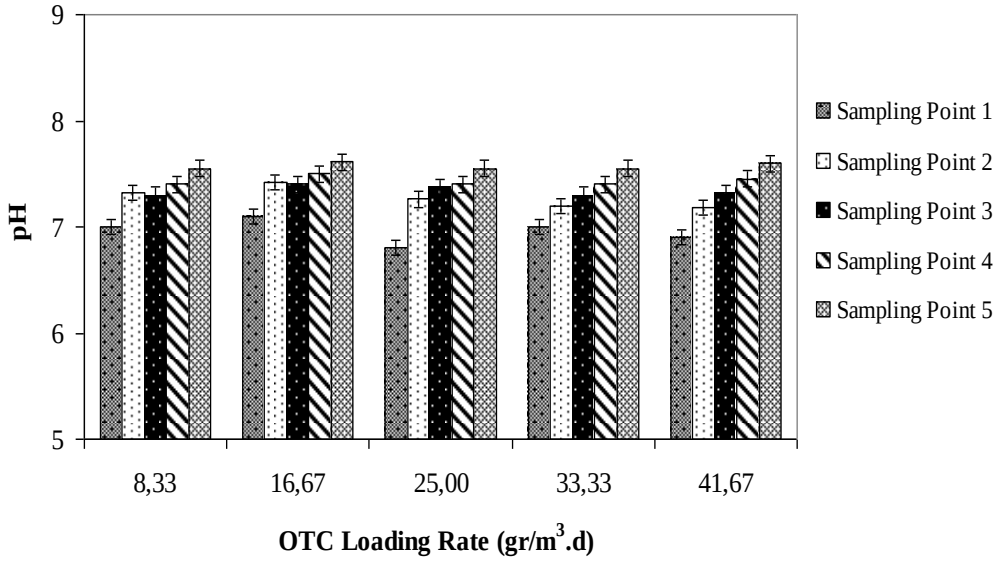

Figure 6.97 The variations of pH in the ABFR reactor at increasing OTC loading rates.

Organic matter is converted into organic TVFAs (mainly acetic (H_{ac}), propionic (H_{pr}), butyric (H_{ba}), and lactic (H_{la}) acids) during acidogenesis. In the acetogenesis step, TVFA longer than two carbons are converted to H_{ac}, CO_2, and H_2, which in turn, become CH_4 through methanogenesis (Speece, 1996). These process steps must be well balanced to prevent TVFA accumulation and thus to avoid a sudden drop in system pH, which may lead to complete failure of the conversion process (Switzembaum et al., 1990; Ahring et al., 1995; Tay and Zhang, 2000; Lahav et al., 2002a; Steyer et al., 2006).

The concentration of TVFA was used as an indication of activity of acidogens. Figure 6.98 shows the variations of TVFA concentrations in the all sampling points of the ABFR reactor at increasing OTC loading rates. The TVFA concentrations in the 1st sampling point decreased from 1062, 900, 845, 750 to 650 mg/L for the OTC loading rates increasing from 8.33, 16.67, 25.00, 33.33 and 41.67 g/m^3d, respectively. The TVFA profile demonstrated that acidogenesis were the main biochemical activities occurring in the 1st compartments (Baloch and Akunna, 2003; Krishna et al. 2009).

As shown in Figure 6.98, the effluent TVFA concentrations decreased from 750, 690, 512, 450 to 287 mg/L at OTC loading rates of 8.33, 16.67, 25.00, 33.33 to 41.67 g/m^3d, respectively in the 2nd sampling point (valve 2) of the ABFR reactor. When the OTC loading rates were increased from 8.33, 16.67, 25.00, 33.33 to 41.67 g/m^3d the TVFA concentrations decreased from 500 to 386, 245, 230 to 200 mg/L, respectively in the 3rd sampling point (valve 5) of the ABFR reactor (Figure 6.98). The effluent TVFA concentrations decreased to 142, 112, 98, 86 and 65 mg/L as the OTC loading rates increased from 8.33, 16.67, 25.00, 33.33 to 41.67 g/m^3d, respectively in the 4th sampling point. Almost 3 and 12 mg/L TVFA concentrations were detected in the 5th sampling point of the ABFR respectively, for the OTC loading rates given above. The anaerobic reactor stability, as evidenced by lower TVFA concentration, is one of the sensitive parameters in anaerobic reactors (Patel and Madamwar, 1998). It was found that the TVFA concentrations decreased from sampling point 1st to sampling points 2nd, 3rd, 4th and to 5th. The TVFA concentrations were low (287 and 600 mg/L) at OTC loading rate as high as 41.67 g/m^3d due to inhibition effects of high OTC concentrations on acidogens in the 1st and 2nd sampling points of the ABFR reactor. A significant linear relationship was found between OTC loadings 8.33, 16.67, 25.00 and 33.33, 41.67 g/m^3d and TVFA productions (ANOVA), (R^2= 0.98, F = 12.28, p = 0.002) (for 1st sampling point); (R^2= 0.97, F = 11.61, p = 0.002) (for 2nd sampling point); (R^2= 0.89, F = 23.10, p = 0.02) (for 3rd sampling point); (R^2= 0.97, F = 10.88, p = 0.002) (for 4th sampling point); (R^2= 0.75, F = 18.89, p = 0.06) (for 5th sampling point).

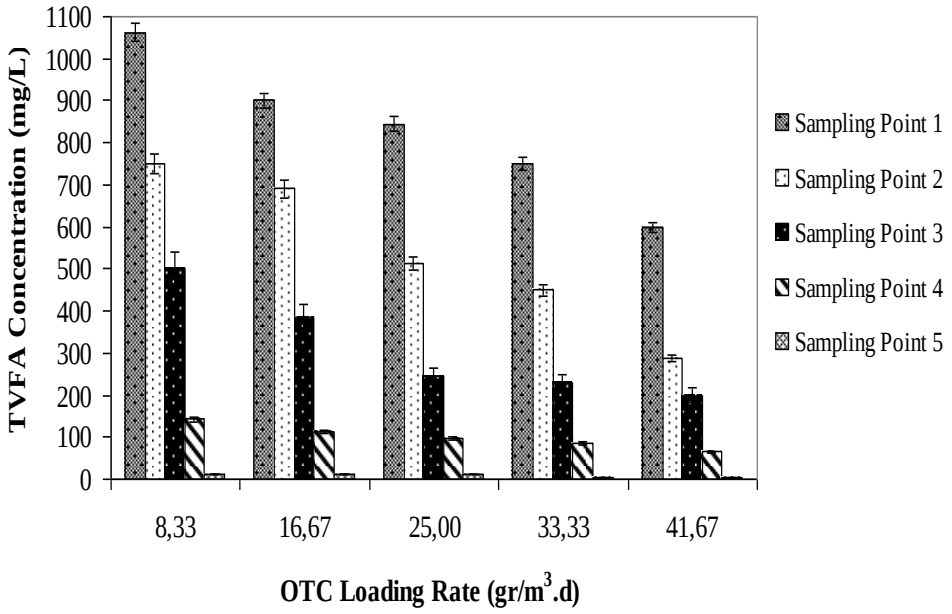

Figure 6.98 The variations of TVFA in the ABFR reactor at increasing OTC loading rates.

In this study, molasses was used as the primary substrate for the reduction of OTC. Primary substrate is consumed as an energy source for anaerobic biotransformation and is converted to CH_4, TVFA and CO_2. Because the TVFA converted to CH_4, its accumulations were important for the performance of anaerobic bacteria in the ABFR reactor. Lower TVFA formation in the upper region of the anaerobic ABFR reactor could be explained by the advantages of immobilized anaerobic microorganism culture. Immobilization provides high cell concentrations, eliminates cell washout problems at low HRTs, provides favorable micro-environmental conditions (that is, cell–cell contact, nutrient–product gradients, pH gradients) for cells, resulting in better performance of the reactor system (Krishna et al. 2009).

6.3.2.4.1 TVFA Components. The determination of TVFA composition in the anaerobic treatment is important, since it provides significant information regarding the metabolic pathway of the process. Four major TVFAs, namely H_{ac}, H_{pr}, H_{ba} and H_{la} were produced throughout the operation of the ABFR reactor (Table 4.28 and Figure 4.57). The other TVFAs were detected at insignificant concentrations. H_{ac}, H_{pr} and H_{ba} were detected at significant concentrations in the 1st and 2nd sampling points

of the ABFR reactor (Table 6.26 and Figure 6.99). H_{ac}, H_{pr}, H_{ba} and H_{la} are short TVFAs formed directly from the anaerobic degradation of molasses-COD. The H_{ac} concentrations lower than 800 mg/L and the ratio of H_{pr}/H_{ac} lower than 1.4 is an indicator for successful methane production (Hill et al., 1987). All the H_{pr}/H_{ac} ratios are lower than 1.4 that means the system is successful for produce methane. The H_{pr}/H_{ac} ratios were found as 0.60, 0.53, 0.51, 0.79 and 0.63 respectively, at OTC loading rates of 8.33-16.67-25.00-33.33-41.67 g/m^{3}d in the 1st sampling point of the ABFR reactor. As shown in Figure 6.99, this ratio varied between 0.61, 0.54, 0.52, 0.51 and 0.75 respectively in 2nd sampling point of ABFR reactor at increasing OTC loading rates (from 8.33, 16.67, 25.00, 33.33 to 41.67 g/m^{3}d). The ratios of H_{pr}/H_{ac} were obtained as 0.74, 0.68, 0.80, 0.76 and 0.63, respectively, at OTC loading rates of 8.33-16.67-25.00-33.33-41.67 g/m^{3}d in the 3rd sampling point of ABFR reactor (Table 6.26). As the OTC loading rates were increased from 8.33, 16.67, 25.00, 33.33 to 41.67 g/m^{3}d the H_{pr}/H_{ac} ratio decreased from 0.40 to 0.30, 0.33, 0.30 and to 0.23, respectively in the 4th sampling point (Table 6.26). In this study it was found that all the H_{pr}/H_{ac} ratios are lower than 1.4. This means that the anaerobic reactor system is stable for produce methane. As shown in Figure 6.99, this ratio varied between 0.00 and 0.40 in the 5th sampling point of the ABFR reactor at increasing OTC loading rates (from 8.33 to 41.67 g/m^{3}d respectively).

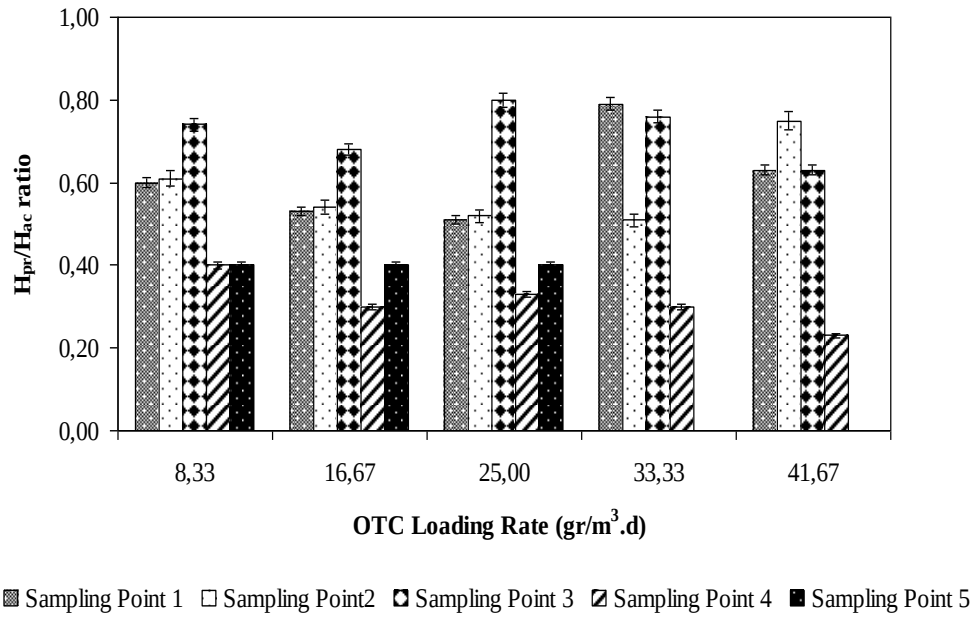

Figure 6.99 Variations of H_{pr}/H_{ac} ratio in the ABFR at increasing OTC loading rates

As the OTC loading rates were increased from 8.33, 16.67, 25.00, 33.33 to 41.67 g/m^{3}d the H_{ac} concentrations decreased from 530, 400, 430, 380 to 310 mg/L, respectively in the 1st sampling point (Table 6.26). The concentrations of H_{pr} also decreased from 320, 210, 220, 300 to 196 mg/L respectively. The concentrations of H_{bu} were measured as 110, 135, 100, 56 and 63 mg/L, respectively, at OTC loading rates of 8.33-16.67-25.00-33.33-41.67 g/m^{3}d, respectively (Table 6.26). As the OTC loading rates were increased from 8.33, 16.67, 25.00, 33.33 to 41.67 g/m^{3}d the H_{la} concentrations decreased from 102, 96, 85, 10 to 12 mg/L, respectively in the 1st sampling point of the ABFR reactor (see Table 6.26).

The H_{ac} concentrations decreased from 415, 356, 300, 212 to 128 mg/L at OTC loading rates of 8.33, 16.67, 25.00, 33.33 to 41.67 g/m^{3}d, respectively in the 2nd sampling point. Similarly, the concentrations of H_{pr} also decreased from 254, to 192, 156, 108 and to 96 mg/L, respectively, when 8.33, 16.67, 25.00, 33.33 to 41.67 g/m^{3}d OTC loading were administered to the ABFR reactor in the 2nd sampling point (Table 6.26). The H_{bu} concentrations were 48, 100, 50, 62 and 48 mg/L, respectively, at OTC loading rates of 8.33, 16.67, 25.00, 33.33 to 41.67 g/m^{3}d respectively in the 2nd sampling point of the ABFR reactor (see Table 6.26). As the OTC loading rates were increased from 8.33, 16.67, 25.00, 33.33 to 41.67 g/m^{3}d the H_{la} concentrations decreased from 26, 0, 0, 7 to 0 mg/L, respectively, in the 2nd sampling point (Table 6.26).

The H_{ac} concentrations decreased from 200, 156, 108, 103 to 100 mg/L, as the OTC loading rates increased from 8.33, 16.67, 25.00, 33.33 to 41.67 g/m^{3}d, respectively, in the 3rd sampling point. As the OTC loading rates increased from 8.33, 16.67, 25.00, 33.33 to 41.67 g/m^{3}d the H_{bu} concentrations were measured as 76, 58, 32, 41 and 24 mg/L, respectively, in the 3rd sampling point of the ABFR reactor. The H_{la} concentrations were 42, 12, 10, 0 and 0 mg/L at OTC loading rates of 8.33, 16.67, 25.00, 33.33 and 41.67 g/m^{3}d, respectively, in the 3rd sampling point (Table 6.26).

The H_{ac} concentrations were measured as 90, 76, 54, 50 and 43 mg/L, at OTC loading rates of 8.33, 16.67, 25.00, 33.33 and 41.67 g/m^3d, respectively in the 4^{th} sampling point (Table 6.26). When the OTC loading rates were increased from 8.33, 16.67 to 25.00, 33.33 and to 41.67 g/m^3d, the H_{pr} concentrations were determined as 35, 23, 18, 15 and10 mg/L, respectively in the 4^{th} sampling point of ABFR reactor system. Similarly, the H_{bu} concentrations also were found as 7, 10, 12, 10, 7 mg/L respectivelyfor the aforementioned OLRs. The H_{la} concentrations were found as 5, 0, 7, 5 and 0 mg/L, respectively, at OTC loading rates of 8.33, 16.67, 25.00, 33.33 and 41.67 g/m^3d in the 4^{th} sampling point (Table 6.26).

As shown in Table 6.26, the H_{ac} concentrations were found as 5, 5, 5 and 0, 0 mg/L, respectively, at OTC loading rates of 8.33, 16.67, 25.00, 33.33 and 41.67 g/m^3d in the 5^{th} sampling point of the ABFR reactor. The H_{pr} concentrations were obtained as 2, 2, 2, 0 and 0 mg/L, at OTC loading rates of 8.33, 16.67, 25.00, 33.33 and 41.67 g/m^3d, respectively in the 5^{th} sampling point (Table 6.26). Similarly, the H_{bu} and H_{la} concentrations were also found as zero mg/L at all OTC loading rates in the 5^{th} sampling point of the ABFR reactor.

Among the TVFAs, H_{ac} has been reported as a precursor in methane production, resulting in 70% of total methane production in anaerobic reactors (Chen, 2010). H_{ac} is converted into CO_2 and CH_4 by acetotrophic methanogens, and all other TVFA have to be converted to H_{ac} before methane production (McCarty and Mosey 1991). It is generally believed that methane generated from H_{ac} is the most sensitive anaerobic phase; therefore, this step is always considered as a rate limitation step in anaerobic degradation (Pavlostathis and Giraldo-Gomez, 1991). A lot of studies reported that H_{ac} is an easy degraded substrate (McCarty and Mosey, 1991). H_{pr} is a common intermediate fermentation product in anaerobic degradation (Wang et al.,2009). It inhibits methanogenesis in anaerobic degradation (Hyun et al. 1998, Wang et al., 2009). H_{bu} is often examined simultaneously with H_{ac} and H_{pr} during anaerobic degradation (Vavilin and Lokshina, 1996, Wang et al., 2009). H_{bu} could be an intermediate product from the anaerobic degradation of carbonaceous substrates of (Vavilin and Lokshina, 1996). H_{la} is often viewed as an undesigned terminal

fermentation product (Wang et al., 2009). The rate of TVFA conversion to methane usually follows the order of $H_{ac} > H_{pr} > H_{bu} > H_{la}$ (Ren et al., 2003).

In this study, the maximum H_{ac} concentration was obtained as 530 mg/L at an OTC loading rate of 8.33 g/m^3d in the 1st sampling point of the ABFR reactor. The maximum H_{pr} concentration was found as 320 mg/L in the 1st sampling point, at the same OTC loading (Table 6.26). As illustrated in Table 6.26, the maximum H_{bu} concentration was measured as 135 mg/L in the same sampling point, at an OTC loading rate of 8.33 g/m^3d. Similarly, the maximum H_{la} concentration was determinated as 102 mg/L at the same OTC loading in the 1st sampling point of the ABFR reactor system.

The TVFA component (H_{ac}, H_{pr}, H_{bu} and H_{la}) profile across the anaerobic ABFR reactor system followed the Sampling point 1st > Sampling point 2nd > Sampling point 3rd > Sampling point 4th > Sampling point 5th.

Table 6.26 Variations of TVFA concentrations, TVFA components and ratio Concentrations in Sampling Points of the ABFR Reactor at Increasing OTC

OTC Loading rate (g/m^3d)	ABFR Reactor		TVFA composition					
			TVFA (mg/L)	H_{ac} (mg/L)	H_{pr} (mg/L)	H_{bu} (mg/L)	H_{la} (mg/L)	H_{pr}/H_{ac} ratio
8.33	1st Sampling point	LOWER REGION	1062±48.00	530±21.45	320±11.00	110±5.65	102±5.00	0.60
16.67			900±41.57	400±15.46	210±10.00	135±7.00	96±4.50	0.53
25.00			845±37.65	430±17.21	220±8.65	100±5.00	85±4.00	0.51
33.33			750±37.00	380±14.58	300±10.00	56±3.00	10±0.42	0.79
41.67			600±29.65	310±10.56	196±8.76	63±3.12	12±0.45	0.63
8.33	2nd Sampling point		750±37.00	415±12.00	254±10.00	48±2.54	26±1.52	0.61
16.67			690±34.00	356±15.00	192±9.75	100±4.87	0	0.54
25.00			512±25.12	300±11.24	156±8.86	50±2.00	0	0.52
33.33			450±22.00	212±10.00	108±5.54	62±3.00	7±0.35	0.51
41.67			287±14.35	128±8.76	96±6.00	48±3.12	0	0.75
8.33	3rd Sampling point		500±20.24	200±10.00	147±7.00	76±4.12	42±2.14	0.74
16.67			386±18.45	156±9.00	106±5.61	58±3.00	12±0.45	0.68
25.00			245±11.23	108±5.63	86±4.20	32±1.00	10±0.42	0.80
33.33			230±12.00	103±5.78	78±4.12	41±2.18	0	0.76
41.67			200±10.00	100±4.98	63±3.00	24±1.00	0	0.63
8.33	4th Sampling point	UPPER REGION	142±7.10	90±5.00	35±1.12	7±0.35	5±0.25	0.40
16.67			112±5.60	76±4.00	23±1.00	10±0.42	0	0.30
25.00			98±5.10	54±3.00	18±0.72	12±0.45	7±0.35	0.33
33.33			86±4.20	50±3.00	15±0.63	10±0.42	5±0.25	0.30
41.67			65±3.00	43±1.56	10±0.60	7±0.35	0	0.23
8.33	5th Sampling point		12±0.40	5±0.25	2±0.10	0	0	0.40
16.67			12±0.40	5±0.25	2±0.10	0	0	0.40
25.00			12±0.40	5±0.25	2±0.10	0	0	0.40
33.33			3±0.00	0	0	0	0	0.00
41.67			3±0.00	0	0	0	0	0.00

6.3.2.5 Variation of Bicarbonate Alkalinity (HCO_3) and TVFA/HCO_3 Ratio in Compartments of the ABFR Reactor at Increasing OTC Loading Rates

HCO_3 Alkalinity is a measure of the capacity of a solution to neutralize acids and is primarily due to the salts of weak acids (Sawyer et al., 2002). Anaerobic reactors operate optimally at neutral pH conditions in which HCO_3 is the primary constituent; therefore HCO_3 alkalinity is significant (Dlamini, 2009). The HCO_3 Alkalinity, TVFA/HCO_3 ratio variations in all compartments of the ABFR reactor at increasing OTC concentrations (from 50, 100, 150, 200 up to 250 mg/L) were shown in Figures 6.100 and 6.101. The HCO_3 concentrations were 2612, 2600, 2456, 2100 and 1876 mg/L in the 1st sampling point of the ABFR reactor at increasing OTC loading rates of 8.33, 16.67, 25.00, 33.33 and 41.67 g/m^3d, respectively (see Figure 6.100). The HCO_3 concentration in the 1st sampling point was lower than the other sampling points. This indicates the utilization of alkalinity to buffer the TVFA and CO_2 produced from the anaerobic co-metabolism of OTC during anaerobic treatment of molasses-COD in the ABFR reactor. The HCO_3 concentrations were 2600, 2712, 2500, 2212 and 2000 mg/L, at OTC loading rates of 8.33, 16.67, 25.00, 33.33 and 41.67 g/m^3d, respectively, in the 2nd sampling point **(**Figure 6.100**)**. When the OTC loading rates were increased from 8.33, 16.67, 25.00, 33.33 to 41.67 g/m^3d, the HCO_3 concentrations were determined as 2745, 2800, 2617, 2365 and 2300 mg/L, respectively in the 3rd sampling point of the ABFR reactor system. Similarly, the HCO_3 concentrations were 2875, 2875, 2745, 2400, 2415 mg/L for the aforementioned OTC loadings in the 4th sampling point. The HCO_3 concentrations were measured as 2900, 2950, 2800, 2500 and 2512 mg/L, respectively, at OTC loading rates of 8.33, 16.67, 25.00, 33.33 and 41.67 g/m^3d in the 5th sampling point. A significant linear correlation between HCO_3 alkalinity and increasing OTC loadings was observed (ANOVA), (R^2=0.91, F=10.33, p=0.01) (for 1st sampling point).A significant linear relationship was found between OTC loadings 8.33, 16.67, 25.00 and 33.33, 41.67 g/m^3d and HCO_3 alkalinity (ANOVA), (R^2= 0.84, F = 16.20, p = 0.03) (for 2nd sampling point); (R^2= 0.88, F = 21.05, p = 0.02) (for 3rd sampling point); (R^2= 0.86, F = 17.84, p = 0.02) (for 4th sampling point); (R^2= 0.82, F = 13.94, p = 0.02) (for 5th sampling point).

The HCO_3 alkalinity were between 1876 and 2612 mg/L in the 1st sampling point for the OTC loading rates of 8.33, 16.67, 25.00, 33.33, 41.67 g/m^3d. The HCO_3 alkalinities were between 2000 and 2600 mg/L at the same OTC loadings, in the 2nd sampling point (see Figure 6.100). Similarly, the HCO_3 alkalinity was measured between 2300 and 2800 mg/L in the 3rd sampling point, at the same OTC loading rates (Figure 6.100). The HCO_3 alkalinities were 2400 and 2875 mg/L in the 4th sampling point for the same OTC loadings. The maximum HCO_3 alkalinity production were 2500, 2512, 2800, 2900 and 2950 mg/L at OTC loading rates of 8.33, 16.67, 25.00, 33.33 and 41.67 g/m^3d, respectively in the 5th sampling point of the ABFR reactor. The HCO_3 alkalinity production profile across the ABFR reactor system followed the Sampling point 1st < Sampling point 2nd < Sampling point 3rd < Sampling point 4th < Sampling point 5th.

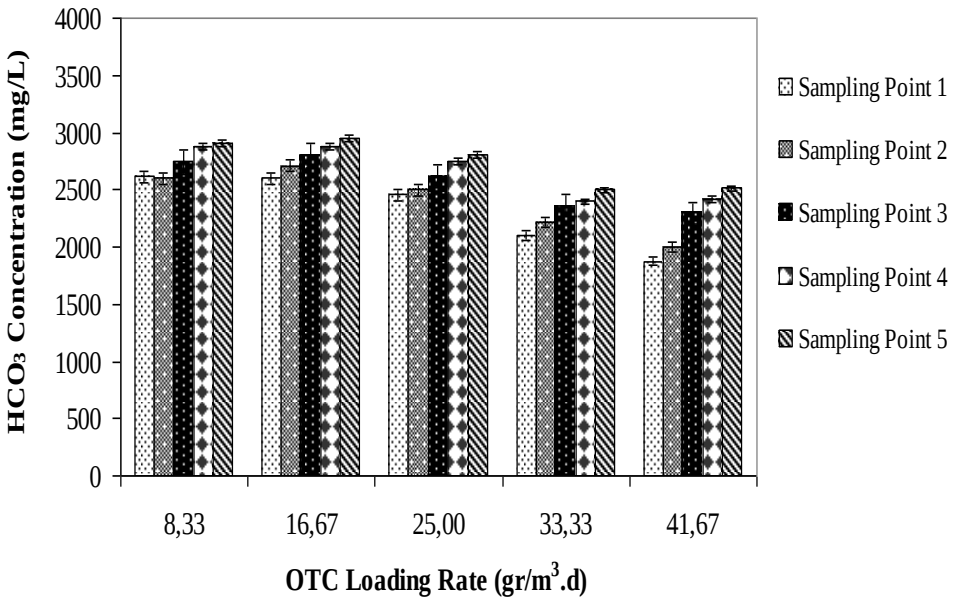

Figure 6.100 The concentrations of HCO_3 in ABFR reactor at increasing OTC loading rates

TVFA/HCO_3 ratio gives necessary information to determine the stability of the anaerobic reactor. The ratio of TVFA/HCO_3 is an important indicator of the acid-base equilibrium and process stability, (Lorestani et al, 2006; Sanchez et al., 2005). If the TVFA/HCO_3 ratio is lower than 0.4, the reactor is stable or unstable as reported by Behling et al. (1997). The TVFA/HCO_3 ratios were found as 0.41, 0.35, 0.34, 0.36 and 0.32 respectively, at OTC loading rates of 8.33-16.67-25.00-33.33-41.67 g/m^3d in the1st sampling point of the ABFR reactor. As shown in Figure 6.101, these ratios

were 0.29, 0.25, 0.20, 0.20 and 0.14 in 2nd sampling point of the ABFR reactor at increasing OTC loading rates (from 8.33, 16.67, 25.00, 33.33 to 41.67 g/m^{3}d, respectively). The ratios of TVFA/HCO_3 were obtained as 0.20, 0.13, 0.10, 0.10 and 0.10, respectively, at OTC loading rates of 8.33-16.67-25.00-33.33-41.67 g/m^{3}d, respectively, in the 3rd sampling point of ABFR reactor (Figure 6.101). As the OTC loading rates were increased from 8.33, 16.67, 25.00, 33.33 to 41.67 g/m^{3}d the TVFA/HCO_3 ratio was measured as 0.01 in the 4th and 5th sampling points (Figure 6.101). These results indicated that ABFR reactor was stable at increasing OTC concentration because the TVFA/HCO_3 ratios in the effluent and in the compartments were lower than 0.4.

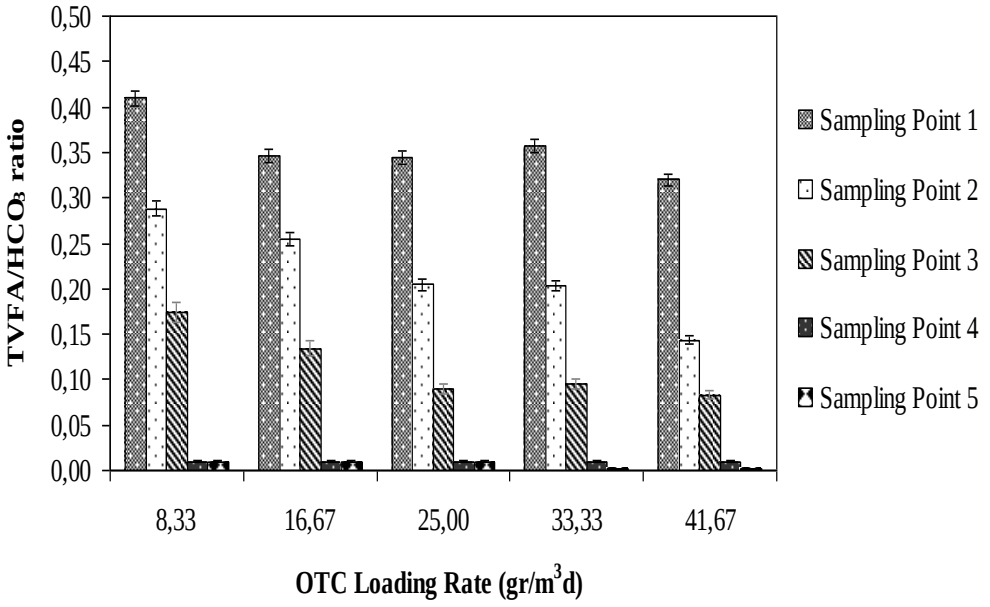

Figure 6.101 The variations of TVFA/HCO_3 ratio in ABFR at increasing OTC loading rates

6.3.2.6 Effect of OTC Loading Rate on the COD and OTC Removal Efficiencies in the CSTR Reactor

Figures 6.102 and 6.103 showed the effect of increasing OTC loading rates on the COD and OTC removals in the aerobic CSTR reactor. The COD concentrations increased from 30, 75, 185, 265 to 305 mg/L at OTC loading rates of 8.33, 16.67, 25.00, 33.33 to 41.67 g/m^{3}d, respectively in the effluent of the aerobic CSTR reactor

(see Figure 6.102). The COD removal efficiencies were around 90% for OTC loading rate of 8.33 g/m^{3}d in the CSTR reactor. As shown in Figure 4.60, the COD removal efficiencies decreased to 81% and 78% at OTC loading rates of 16.67 and 25.00 g/m^{3}d. The COD yields were around 71% at OTC loading of 33.33 and 41.67 g/m^{3}d in the effluent of the CSTR reactor.

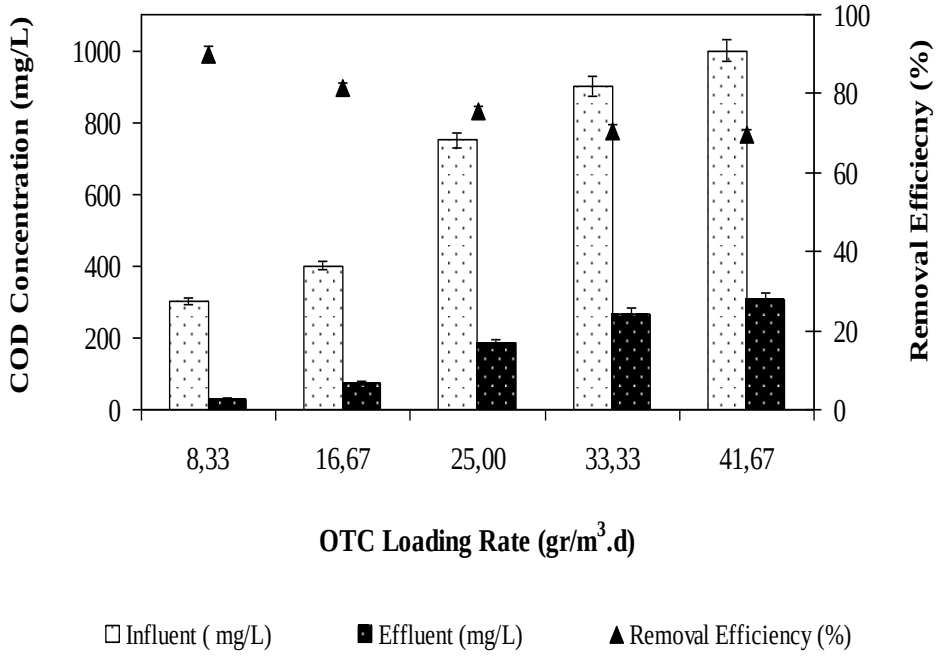

Figure 6.102 COD removal in the aerobic CSTR reactor at increasing OTC loading rates

As shown in Figure 6.103, the OTC yields decreased from 90% to 80%, 72%, 72% and to 60% at OTC loading rates of 8.33, 16.67, 25.00, 33.33 to 41.67 g/m^{3}d, respectively, in the effluent of the CSTR reactor. The OTC removal efficiency was around 90% for OTC loading rate of 8.33 g/m^{3}d (see Figure 6.103). The OTC yields were 80% and 72% for OTC loading rates of 16.67 and 25.00 g/m^{3}d, respectively, in the effluent of the CSTR reactor. The OTC removal efficiencies decreased from 72% to 60% at OTC loading rates of 33.33 and 41.67 g/m^{3}d, respectively. The COD and OTC removal efficiencies decreased at high OTC loading rates in the aerobic reactor.

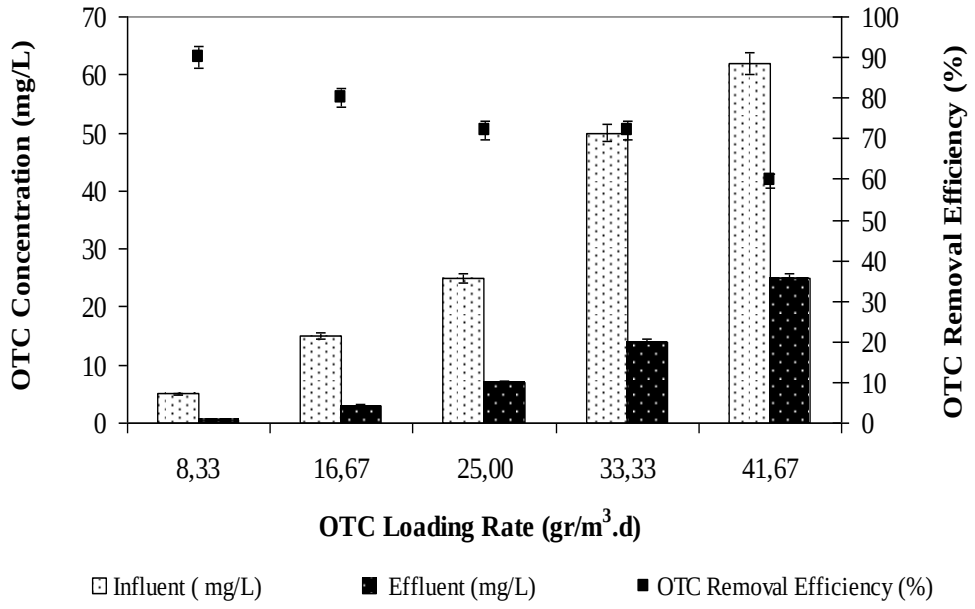

Figure 6.103 OTC removals in the aerobic CSTR reactor at increasing OTC loading rates

6.3.2.7 Treatment Efficiencies of Anaerobic/Aerobic Sequential Reactor System

Figure 6.104 shows the removal efficiencies of COD and OTC at five studied OTC loading rates in the ABFR/CSTR system. The COD removals in the total sequential ABFR/CSTR system were ≥ 92% at all OTC loading rates while the OTC yields were found to be ≥ 90% for all OTC loading rates. The maximum COD and OTC yields were 99% at an OTC loading rate of 8.33 g/m^{3}d, while the lowest COD and OTC removals were 93% and 90% at an OTC loading rate of 41.67 g/m^{3}d, respectively, in the sequential ABFR/CSTR system. 97% of the COD and 99% of the OTC were removed in the anaerobic ABFR reactor while the remaining COD (3%**)** and OTC (2%) were biodegraded in the aerobic CSTR reactor. In other words, the COD and OTC were mainly removed in the anaerobic ABFR reactor. This showed that a significant part of the OTC could be removed with high removal efficiency in the sequential ABFR/CSTR reactor system (see Figure 6.104). In a study performed by Zhang et al. (2012) 85% OTC and COD yields were obtained at influent COD and OTC concentration of 5145 and 80 mg/L, respectively, in a combined anaerobic/two-staged aerobic reactor at a HRT of 2 d. In our study the OTC and COD removal efficiencies are higher than this study although the influent OTC concentration is comparably higher than the study performed by Zhang et al. (2012).

The literature survey showed that the OTC yields obtained in other studies are lower than those in our data: 65% COD and 60% antibiotic removals was obtained by Gao et al. (2012) in a sequential anaerobic baffled and aerobic film reactor system to remove the pharmaceutical wastewaters containing 100 mg/L OTC and 8500 mg/L COD at a HRT of 2.65 d. This could be attributed to the differences in COD and OTC concentrations in the wastewater, to the reactor configurations (sequential anaerobic baffled and aerobic film reactor system and sequential ABFR/CSTR reactor system) and to the dominated anaerobic bacteria.

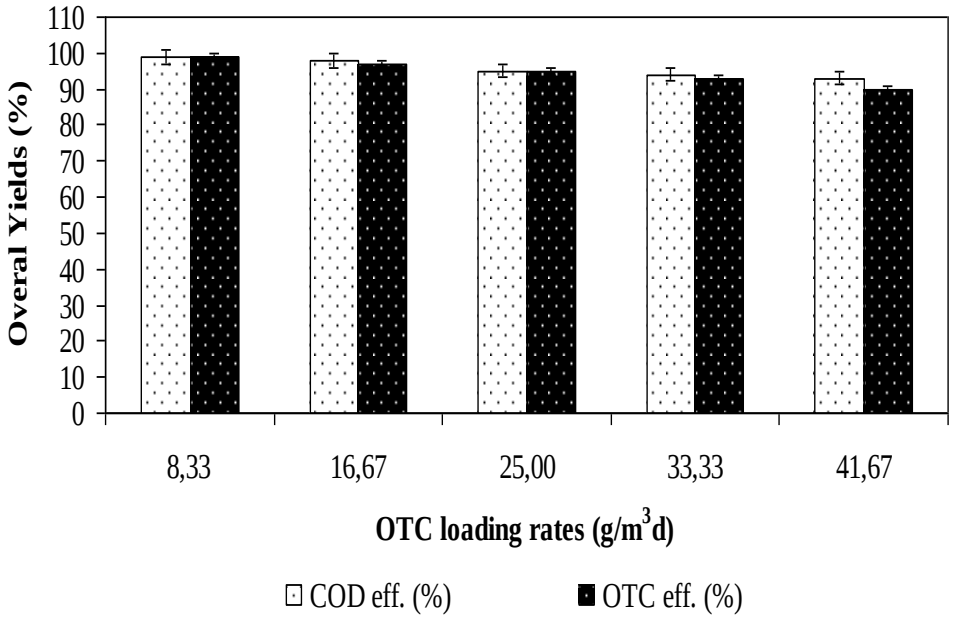

Figure 6.104 OTC and COD removal in the sequential ABFR/CSTR reactor at increasing OTC loading rates

6.3.3 Effect of Increasing AMX Concentration on the Performance of ABFR

6.3.3.1 Effect of Increasing AMX Concentration on the Performance of ABFR

The ABFR reactor was operated continuously for 156 days. The COD equivalents of AMX concentration are shown in Table 6.27.

Table 6.27 The COD equivalents of AMX concentration

Parameters	**Unit**	**Concentrations**
Molasses-COD concentration	mg/L	4000; 4100; 4010; 4200
AMX concentration	mg/L	50; 100; 150; 200
COD equivalent of AMX	mg/L	25; 35; 40; 45
Total COD concentration	mg/L	4025; 4135; 4050; 4245

Figure 6.105 illustrated the influent, effluent COD concentrations and COD removal efficiency of the ABFR reactor during the experimental period. The operation of the ABFR reactor with AMX was started at an influent AMX concentration of 50 mg/L and an AMX loading rate of 8.33 g/m^{3}d. Then the AMX concentrations were subsequently increased from 100 to 150, 200 mg/L corresponding to AMX loading rates of 16.67, 25.00, 33.33 g/m^{3}d.

As shown in Figure 6.105, the effluent COD concentrations increased from 604 to , 630, 810 and to 1254 mg/L at AMX loading rates of 8.33, 16.67, 25.00 to 33.33 g/m^{3}d, respectively, in the effluent of the ABFR reactor. The COD removal efficiency was 85% at AMX loading rates varying between 8.33 and 16.67 g/m^{3}d. When the AMX loading rate was increased to 25.00 g/m^{3}d, the COD removal efficiency decreased to 80%. After this AMX concentration (150 mg/L), the COD removal efficiency decreased rapidly from 80% to 70% (see Figure 6.105). The effluent COD concentration and COD removal efficiency were measured as 1254 mg/L and 70%, respectively, at a maximum AMX loading rate of 33.33 g/m^{3}d, in the anaerobic ABFR reactor (see Figure 6.105). For maximum COD removal efficiency of 85% the optimum AMX loading rates were found as 8.33 and 16.67 g/m^{3}d, respectively, in the effluent of the ABFR reactor (see Figure 6.105). The minimum COD (E=70%) yield was found at an AMX loading rate of 33.33 g/m^{3}d.The results obtained in this study showed that AMX could be used as co-substrate together with molasses-COD with high treatment efficiencies in the ABFR reactor. A significant linear relationship was found between the COD yields and the AMX loading rates (AMX loading rates between 8.33-16.67-25.00-33.33 g/m^{3}d) (ANOVA), (R^2=0.85, F=10.81, p=0.08).

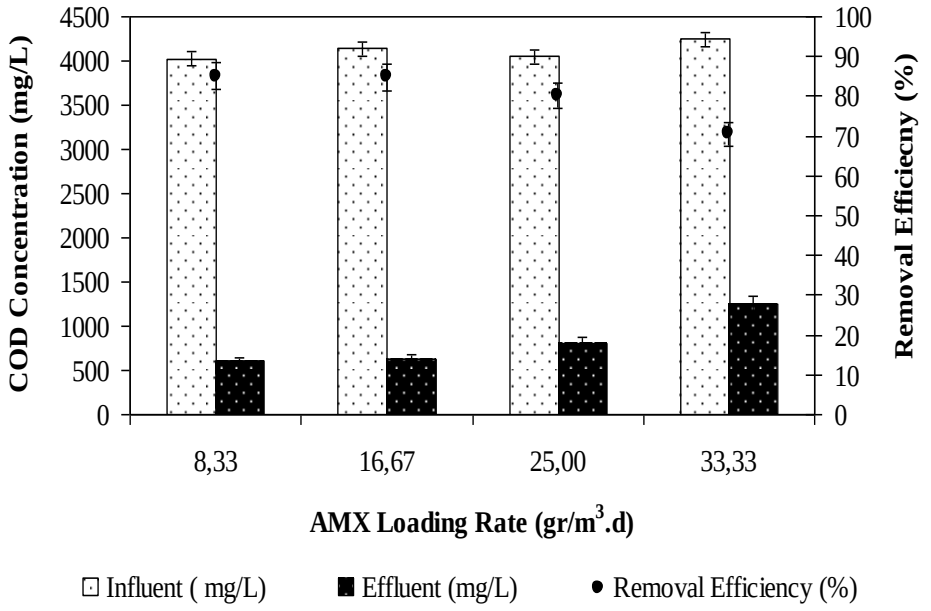

Figure 6.105 Effects of increasing AMX loading rates on COD removal efficiencies in the ABFR reactor

The COD yields obtained in recent studies were low in comparison with the COD removals in this study. In the study by Chen et al. (2011) 60% COD removal efficiency was obtained at a HRT of 2 days in an UASB reactor at an influent AMX concentration of 61 mg/L. In another study, Sreekanth et al. (2009) reported 65-75% COD removal efficiency in a hybrid up flow anaerobic sludge blanket reactor (HUASB) at influent COD concentration varying between 13000 and 15000 mg/L at a HRT of 2 days. The above results are consistent with observations made by Akbarpour and Mehrdadi, (2011) in an UASB reactor, treating a chemical synthesis-based pharmaceutical wastewater. The COD yield was 54.6% at a HRT of 1.4 days. This inconsistency is presumably attributed to the daily varying wastewater concentrations, with different AMX and COD loading rates in the aforementioned studies. In our study, 85% COD removal was measured at influent COD concentrations varying between 4025 and 4135 mg/L. The yields obtained in the aforementioned studies are low in comparison to the removal performances of COD found in this study. The high COD removal efficiencies in the ABFR reactor could be explained by the reactor configuration, operational conditions and AMX concentrations used throughout reactor operation.

6.3.3.1.1 Variations of COD in Sampling Points of the ABFR Reactor at Increasing AMX Loading Rates. The effluent COD concentration was 1050 mg/L at an AMX loading rate of 8.33 g/m^{3}d in the 1st sampling point. The COD concentration was measured as 984 mg/L at the same AMX loading, in the 2nd sampling point of the ABFR reactor. The COD level decreased to 885 mg/L at an AMX loading rate of 8.33 g/m^{3}d in the 3rd sampling point while the COD level in 4th sampling point was measured as 765 mg/L (Table 6.28). The COD concentration was measured as 604 mg/L in the 5th sampling point (effluent) of the ABFR reactor (see Table 6.28). The COD yields in the lower region of the reactor in sampling point 1st, between sampling points 1st-2nd and 2nd-3rd were 74%, 6% and 10%, respectively, at an AMX loading rate of 8.33 g/m^{3}d. The COD yield in the upper region of the reactor in sampling 4th and in the sampling points between 4th and 5th were 14% and 21%, respectively. The total COD removal in the lower region of the ABFR reactor was (4025-825/4025) 78% while the total COD yield in the upper region of the ABFR reactor was calculated as (885-604/885) 32% at an AMX loading rate of 8.33 g/m^{3}d. The total yield between influent and effluent (4025-604/4025) of the ABFR reactor system was 85%.

The COD concentration was 1375 mg/L at an AMX loading rate of 16.67 g/m^{3}d in the 1st sampling point of the anaerobic reactor. The COD concentration was found as 1200 mg/L in the 2nd sampling point, at the same AMX loading (Table 6.28). The COD value decreased to 1000 mg/L at the same AMX loading in the 3rd sampling point. The COD concentration in the 4th sampling point was found as 825 mg/L. The COD value was measured as 630 mg/L in the 5th sampling point (see Table 6.28). As shown in Table 4.30, the COD yields in the lower region of the ABFR reactor in the sampling point 1st, between sampling points 1st-2nd and 2nd-3rd were 68%, 13% and 17%, respectively, at the same AMX loading. The COD yield in the upper region of the anaerobic reactor in the sampling points 4th and 5th were 18% and 24%, respectively. The total COD yield in the lower level of the anaerobic reactor was (4135-1000/4135) 76% while the total COD yield in the upper level of the anaerobic reactor was calculated as (1000-630/1000) 37% at an AMX loading rate of 16.67

g/m^{3}d. The total yield between influent and effluent (4025-604/4025) of the ABFR reactor system was 85%.

At an AMX loading rate of 25 g/m^{3}d the COD concentrations were between 1685, 1487 and 1245 mg/L, respectively in the lower region (1st-2nd -3rd sampling points) of the ABFR reactor. The COD concentrations were determinated as 1014 and 810 mg/L in the upper region (4th and 5th sampling point) of the ABFR reactor, at an OTC loading rate of 25 g/m^{3}d (Table 6.28). At the same AMX loading the COD yields in the lower region of the ABFR reactor in the sampling point 1st, between sampling points 1st-2nd and 2nd-3rd were 58%, 12% and 16%, respectively. The COD removal efficiency in the upper region of the ABFR reactor in sampling 4th and in the sampling points between 4th and 5th were 19% and 20%, respectively. The total COD yields in the lower and upper region of the ABFR reactor was calculated as (4050-1245/4050) 69% and (1245-810/1245) 35% at an AMX loading rate of 25 g/m^{3}d. The total COD yield (4050-810/4050) of the ABFR reactor system was 80%.

As the COD concentration was 1772 mg/L at an AMX loading rate of 33.33 g/m^{3}d in the 1st sampling point of the ABFR reactor. The COD value was measured as 1542 mg/L in the 2nd sampling point, at an AMX loading rate of 33.33 g/m^{3}d (Table 6.28). The COD value was obtained as 1460 mg/L in the 3rd sampling point, at the same AMX loading (Table 6.28). The COD value decreased to 1357 mg/L at the same AMX loading in the 4th sampling point of the ABFR reactor. The COD value in the 5th sampling point was found as 1254 mg/L (see Table 6.28). As shown in Table 4.30, the COD yields in the lower part (between sampling points 1st-2nd and 2nd-3rd) of the ABFR reactor were 57%, 13% and 5%, respectively, at an AMX loading rate of 33.33 g/m^{3}d. The COD yields were 7% and 8%, respectively in the upper part of the ABFR reactor in sampling 4th and in the sampling points between 4th and 5th. The total COD yield in the lower part of the ABFR reactor was (4245-1460/4245) 66%. The total COD yield in the upper part of the ABFR reactor was calculated as (1460-1254/1460) 14% at an OTC loading rate of 33.33 g/m^{3}d. The total COD yield (4245-1254/4245) of the ABFR reactor system was 70%.

Table 6.28 Variations of COD Concentrations and COD yields in Sampling Points of ABFR Reactor at Increasing AMX Loading Rates

Influent		**LOVER REGION**						**UPPER REGION**			
AMX Loading rate (g/m^3d)	**COD Conc. (mg/L)**	**Effluent COD (mg/L)**			**COD Yield (%)**			**Effluent COD (mg/L)**		**COD Yield (%)**	
		1st Sampling point	**2nd Sampling point**	3rd Sampling point	1st Sampling point	**2nd Sampling point**	3rd Sampling point	4th Sampling point	**5th Sampling point**	4th Sampling point	**5th Sampling point**
8.33	4025±132	1050±50	**984±43**	885±41	74	**6**	10	765±36	**604±30**	14	**21**
16.67	4135±126	1375±65	**1200±54**	1000±45	68	**13**	17	825±41	**630±28**	18	**24**
25.00	4050±105	1685±80	**1487±72**	1245±58	58	**12**	16	1014±50	**810±26**	19	**20**
33.33	4245±156	1772±86	**1542±74**	1460±65	57	**13**	5	1357±60	**1254±48**	7	**8**

6.3.3.2 Effect of AMX Loading Rate on the AMX Removal Efficiencies in the ABFR Reactor

Variations of AMX removal efficiencies during operation with different feed concentrations are depicted in Figure 6.106. Initially the ABFR reactor was fed with the synthetic pharmaceutical wastewater at concentration of 50, 100, 150 and 200 mg/L.

As shown in Figure 6.106 the AMX removal efficiency of 85% was obtained at AMX loading rates of 8.33 and 16.67 g/m^3d. When the AMX loading rates was increased from 16.67 to 25.00 g/m^3d the AMX removal efficiency decreased from 85% to 73% at an AMX concentration of 150 mg/L at an AMX loading rate of 25.00 g/m^3d in the effluent of the ABFR reactor. The effluent AMX concentration was measured as 40 mg/L at an AMX loading rate of 25.00 g/m^3d. When the AMX loading rate was increased from 25.00 g/m^3d to 33.33 g/m^3d the AMX removal efficiency decreased from 73% to 70%, respectively, in the ABFR reactor (Figure 6.106). The best performance was observed with an AMX loading rates of 8.33 and 16.67 g/m^3d (E=85%) (see Figure 6.106). The relatively poor performance observed at AMX loading rates of 33.33 g/m^3d (E=70%) was attributed principally to the instability created by the sudden doubling of the influent loading rate. The results obtained in this study showed that AMX could be used as co-substrate together with molasses-COD with high removal efficiencies in ABFR reactor. A significant linear correlation between AMX yields and increasing AMX loading rate (AMX loading rates between 8.33-16.67-25.00-33.33 g/m^3d) was observed (ANOVA), (Figure 6.106) (R^2= 0.88, F = 14.10, p = 0.05).

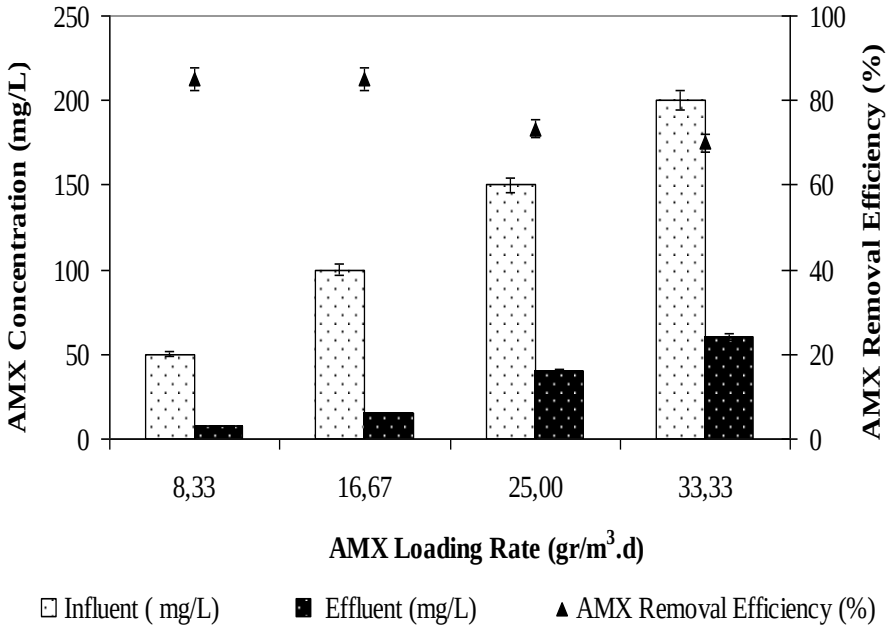

Figure 6.106 The effect of AMX loading rate on AMX removal efficiencies in the ABFR reactor

The recent literature on the anaerobic AMX treatment showed that the yields obtained in some high rate anaerobic reactors are lower than the AMX removals found in our study: In a study performed by Chen et al. (2011) 34% AMX removal efficiencies were obtained at a HRT of 2 days in an UASB reactor at an influent AMX concentration of 61 mg/L. Pallavi et al. (2009) reported that lower AMX yields 65% than those found in our study at a HRT of 1.95 days and at an influent AMX concentration of 89 mg/L. The yields obtained in the aforementioned studies are low in comparison to the removal performances of AMX found in our study.

6.3.3.2.1 Determine of Intermetabolite Products of AMX Under Anaerobic Conditions. The metabolic products of AMX, such as amoxicilloic acid and AMX-diketopiperazine-2, 5 can be found in aquatic environment (Lamm et al. 2009, Valvo et al. 1998). In our study, AMX-diketopiperazine-2, 5 was observed in the effluent of anaerobic ABFR reactor as the intermediate metabolite of AMX. This showed that AMX is transformed to amoxicilloic acid and then amoxicilloic acid converted AMX-diketopiperazine-2, 5 under anaerobic conditions. In our study, amoxicilloic acid was no detected in the effluent of anaerobic ABFR reactor system. The

suggested degradation pathway of AMX in an aqueous medium (Figure 6.107) starts with the opening of the four-membered β-Lactam ring by hydrolysis and yields the intermediate amoxicilloic acid, which contains an extra free carboxylic acid group. Subsequently, this intermediate rapidly forms a more stable six-membered ring product, the AMX-diketopiperazine-2,5 (Nagele and Moritz, 2005; Lamm et al. 2009).

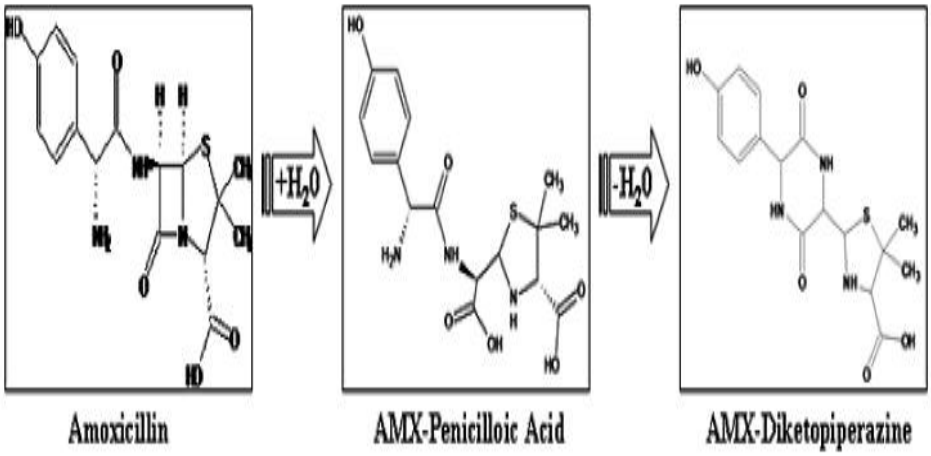

Figure 6.107 Suggested degradation pathway of AMX in aqueous medium (Lamm et al., 2009)

Typical chromatograms of AMX and AMX-diketopiperazine-2, 5 standard solutions and formulation samples are shown in Figure 6.108. Figure 6.108 shows the HPLC chromatogram of effluent AMX and AMX-diketopiperazine-2, 5. Peak of 7.5 mg/L AMX standards was obtained at a retention time of 6.50 min and at a wave length of 210 nm (see Figure 6.108). A peak is showed on the HPLC chromatograms at 8.42 min retention time in the effluent sample of the ABFR reactor. The presence of AMX-diketopiperazine-2,5 peak in effluent of anaerobic ABFR indicated that the AMX converted to AMX-diketopiperazine-2,5 under anaerobic conditions.

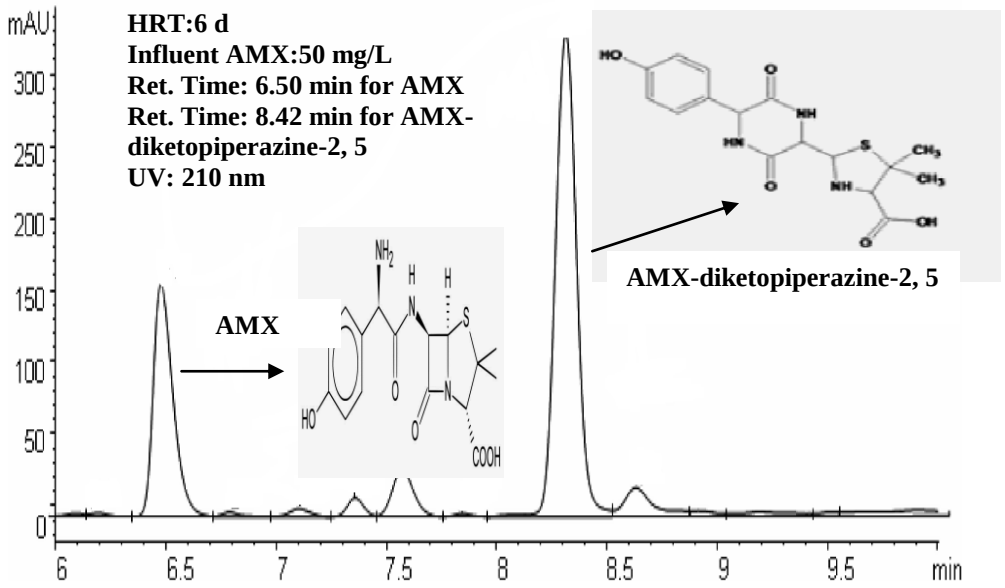

Figure 6.108 HPLC chromatograms of AMX and AMX-diketopiperazine-2, 5 in the effluent of ABFR reactor at AMX loading rate of 22.22 g/m^{3}d

The ABFR reactor was operated throughout 150 days at four different AMX loading rates (Figure 6.109). The effluent AMX-diketopiperazine-2, 5 concentrations was 30 mg/L for operation days of 1-5 then it decreased from 21 to 7 mg/L throughout operation days of 10-20 at an AMX concentration of 50 mg/L corresponding to an AMX loading rate of 8.33 g/m^{3}d, respectively. The AMX-diketopiperazine-2, 5 concentration increased to 32 mg/L when the AMX loading rate was increased to 16.67 g/m^{3}d (AMX conc.=100 mg/L) on days 25 then it decreased from 18 to 8 mg/L on days between 50 and 60 days, respectively (see Figure 6.109). AMX-diketopiperazine-2,5 concentrations was recorded as 6 and 8 mg/L. On day 70, the effluent AMX-diketopiperazine-2,5 concentration increased to 40 mg/L and then it decreased from 32 to 15 mg/L on days between 75 and 100, respectively, when the AMX loading rate was increased to 25.00 g/m^{3}d (AMX concentration=150 mg/L), respectively (Figure 6.109).The AMX-diketopiperazine-2, 5 concentration increased to 45 mg/L when the AMX loading rate was increased to 33.33 g/m^{3}d (AMX concentration=200 mg/L on days 110, respectively. On days between 120 and 150 the AMX-diketopiperazine-2,5 concentrations decreased from 33 to 18 mg/L, respectively (see Figure 6.109).

As shown in Figure 6.110 the AMX-diketopiperazine-2,5 productions of 7.00 mg/L was obtained at AMX loading rates of 8.33 g/m^{3}d. The effluent AMX-diketopiperazine-2, 5 productions was measured as 8 mg/L at an AMX loading rate of 16.67 g/m^{3}d. When the AMX loading rate was increased from 16.67 g/m^{3}d to 25.00 g/m^{3}d the AMX-diketopiperazine-2,5 productions decreased from 8 to 15 mg/L, respectively, in the ABFR reactor (Figure 6.110). As shown in Figure 4.68 the AMX-diketopiperazine-2,5 productions of 18 mg/L was obtained at AMX loading rate of 33.33 g/m^{3}d in the effluent of the ABFR reactor.

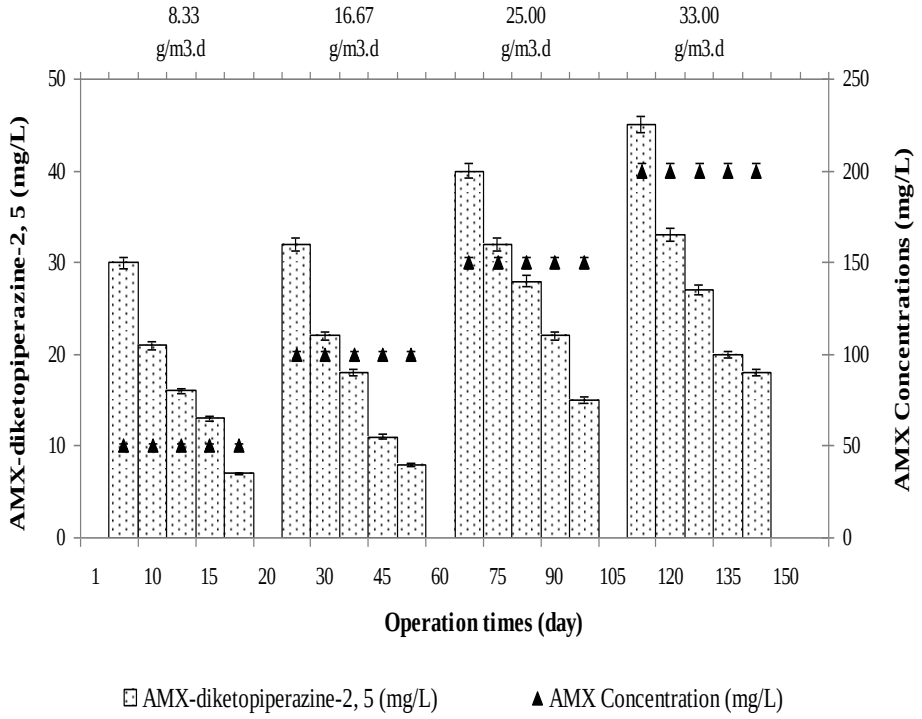

Figure 6.109 Variation of AMX-diketopiperazine-2, 5 concentrations versus operation days in the ABFR reactor

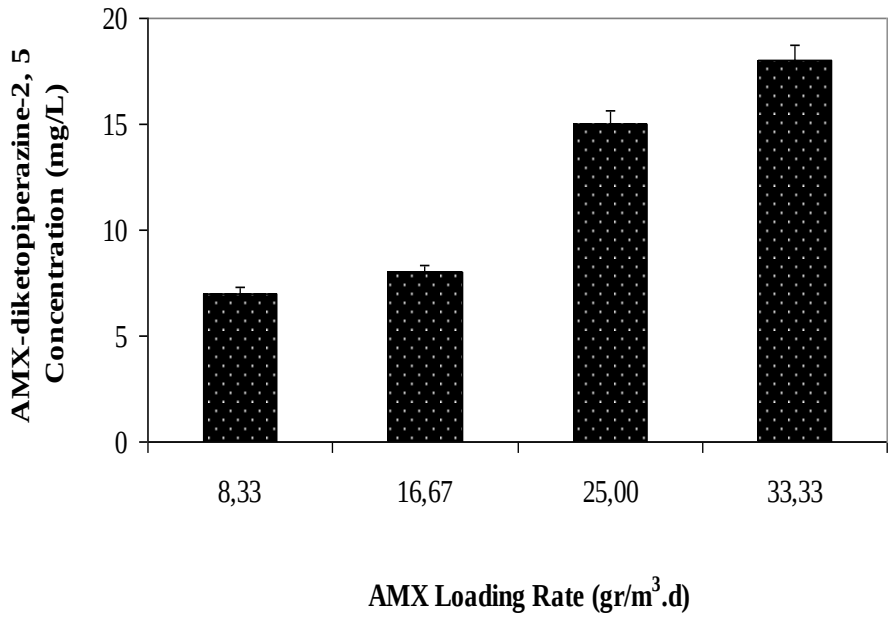

Figure 6.110 Effect of AMX loading rate on AMX-diketopiperazine-2, 5 productions in the ABFR reactor

This showed that the metabolites were accumulated at high AMX loadings. These metabolites were also found in the studies performed by De Baere et al. (2005); Lamm et al., (2009); Valvo et al., (1998). Lamm et al., 2009 also found that besides amoxicilloic acid and AMX-diketopiperazine-2, 5 was produced from the wastewater samples of AMX. In our study, amoxicilloic acid was no detected in the sampling points and the effluent of the ABFR reactor. Valvo et al. 1998 also found similar AMX metabolites. This could be attributed to the differences wastewater characteristic, to the dominancy of bacteria types and to some environmental conditions such as pH, temperature and co-metabolic interactions between substrate and AMX. De Baere et al., (2005) described a prolonged presence of the amoxicilloic acid in food samples, consequently, the occurrence of AMX-diketopiperazine-2,5 as a penicillin drug degradation product, in food and water consumed by human, has a potential to cause an allergic drug reactions. Thus, there is an enormous importance to trace the presence of AMX-diketopiperazine-2,5 in the environment and especially in various water resources and food.

6.3.3.3 Effect of AMX Loading Rate on the Biogas Production and CH_4 Content in the ABFR Reactor

ABFR system investigated in terms of simultaneously biogas production and methane content in wastewater at four different AMX loading rates (8.33, 16.67, 25.00, 33.33 g/m^3d). Figure 6.111 show the behavior of biogas production and methane contents of the ABFR reactor system. During the whole experiments the total gas, methane gas productions and methane content of ABFR reactor averaged at 10.21, 6.57 L/d and 47%, respectively, which demonstrate that ABFR performance well in biogas productions and methane content. The maximum total gas, methane gas productions and methane content were found about 11.42 L/d, 8.12 L/d and 58%, respectively at AMX loading rates of 8.33 and 16.67g/m^3d (see Figure 4.69). As the AMX loading rates were increased from 16.67 to 25.00 g/m^3d, methane contents decreased from 58% to 40%, respectively (Figure 6.111). The total gas, methane gas productions were obtained as 9.00 L/d and 5.68 L/d, at an AMX loading rate of 25.00 g/m^3d, respectively (see Figure 6.111). When the AMX loading rates were increased from 25.00 to 33.33 g/m^3d, the daily total gas, methane gas productions and methane content were determined as 9.00 L/d, 4.35 L/d and 30%, respectively in the ABFR system at an AMX loading rate of 33.33 g/m^3d. The decrease in methane content of biogas is generally observed when the rate of acid formation exceeds the rate of break down to methane at high loading rates (Kim et al., 2007). A significant linear relationship was found between the biogas productions and the AMX loading rates (8.33, 16.67, 25.00, 33.33 g/m^3d) (ANOVA), (R^2=0.80, F=8.00, p=0.01) (for total gas). (R^2=0.90, F=17.64, p=0.05 (for methane gas). Similarly, a linear relationship was found between the methane content and the AMX loading rates (8.33, 16.67, 25.00, 33.33 g/m^3d) and this relationship is significant (ANOVA), (R^2=0.89, F=17.70, p=0.05). Lallai et al., (2002) also reported an increase in the accumulation of TVFA and a decrease in gas production upon the application of increasing amounts of antibiotic to methane reactor.

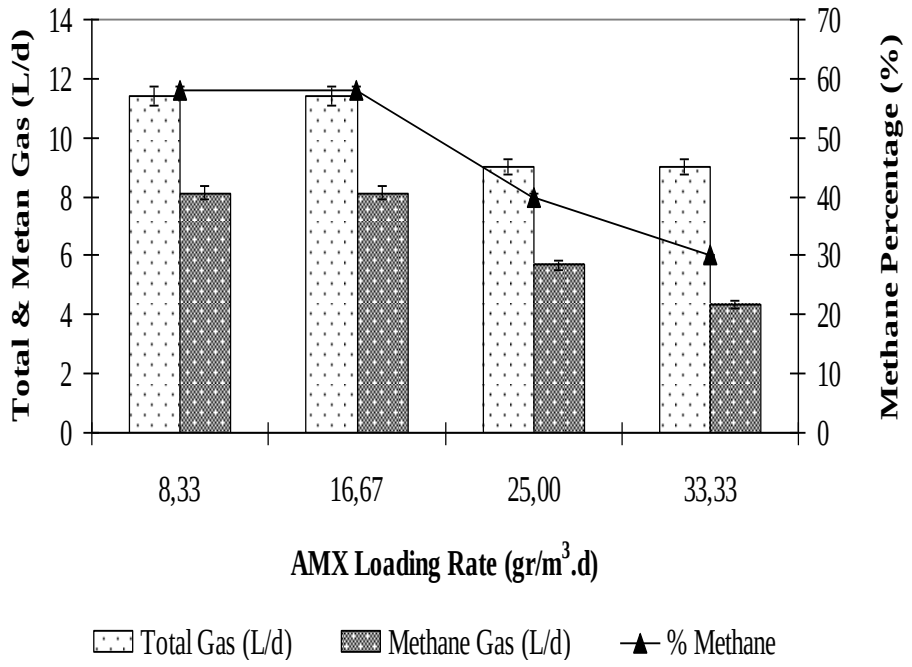

Figure 6.111 The effect of AMX loading rate on total, methane gas production and methane content in the ABFR reactor

In this study, the methane yield can be a useful parameter to assess the performance of the ABFR reactor. Figure 6.112 shows the variations of methane yields versus AMX loading rates. The methane yields decreased from 0.32 to 0.18 $m^3CH_4/kgCOD_{removed}$, when the AMX loading rates were increased from 8.33, 16.67, 25.00 to 33.33 g/m^3d. A significant linear relationship was found between the methane yields and the AMX loading rates (8.33, 16.67, 25.00, 33.33 g/m^3d) (ANOVA), (R^2=0.90, F=17.65, p=0.05).

Lower methane yields (0.26-0.34 $m^3CH_4/kgCOD_{removed}$) were obtained in a study performed by Nandy and Kaul, (2001) throughout anaerobic treatment of fermentation-based herbal pharmaceutical wastewaters containing 48 mg/L AMX at a HRT of 2 days. The lower methane yields in the studies mentioned above could be due to the configuration of the anaerobic reactor, type of anaerobic microorganism, to the biomass concentration and to the operational conditions.

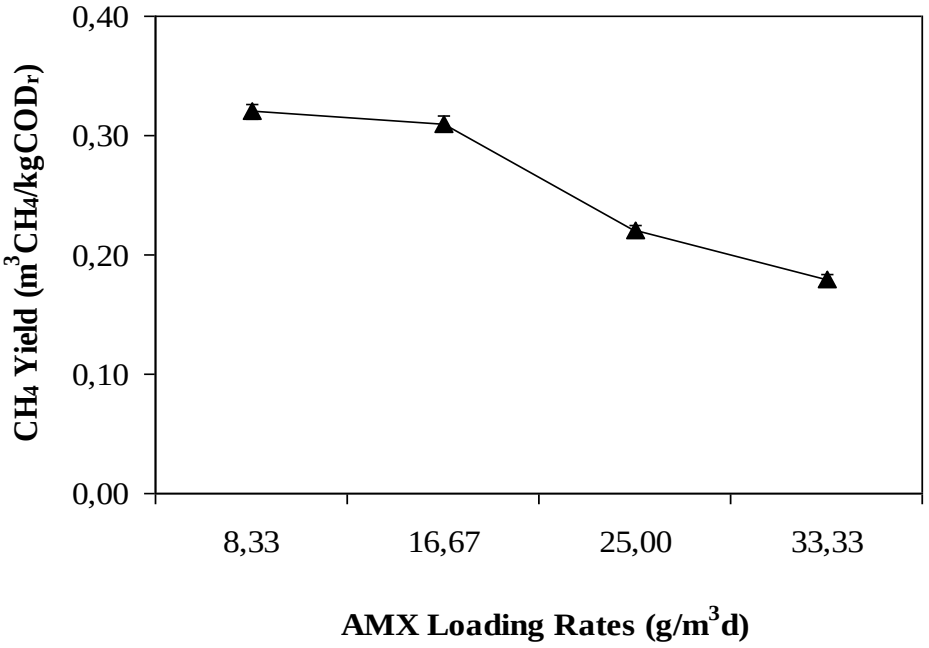

Figure 6.112 Variations of methane yields versus AMX loading rates in the ABFR reactor

6.3.3.4 Variations of pH, TVFA, HCO_3 Alk., TVFA/HCO_3 Alk. Ratio in ABFR at Increasing AMX Loading Rates

The pH profiles for the ABFR reactor at 8.33, 16.67, 25 and 33.33 g/m^{3}d AMX loading rates are shown in Figure 6.113 (a). Sudden drop in the pH in the 1st sampling point is quite noticeable. It gradually increases as wastewater moves towards the later sampling points. The AMX loading rates were increased from 8.33, 16.67, 25 to 33.33 g/m^{3}d pH values decreased from 7.12, 7.00, 6.92 to 6.85, respectively in the 1st sampling point. Similarly AMX loading rates were increased from 8.33, 16.67, 25 to 33.33 g/m^{3}d pH values varying between 7.23, 7.31, 7.26 and 7.28, respectively in the 2nd sampling point of the ABFR reactor (Figure 6.113 (a)). As shown in Figure 6.113 (a), the pH values in the 3rd and 4th sampling points of the ABFR reactor varied between 7.41-7.45-7.32-7.30 and 7.45-7.51-7.40-7.30 at AMX loading rates of 8.33, 16.67, 25 and 33.33 g/m^{3}d, respectively. As shown in Figure 6.113 (a), the effluent pH values decreased from 7.56, 7.55, 7.52 to 7.45 at AMX loadings from 8.33, 16.67, 25 to 33.33 g/m^{3}d, respectively in the 5th sampling point (valve 5) of the ABFR reactor. The pH values increased the ABFR reactor (near

effluent point) due to the degradation of TVFA in the later sampling points (Baloch and Akunna, 2003).

Figure 6.113 (b) shows the TVFA concentrations in sampling points of the ABFR reactor at increasing AMX loading rates. The TVFA concentrations in the 1st sampling point were decreased from 981, 833, 825 to 760 mg/L for the AMX loading rates increased from 8.33, 16.67, 25 to 33.33 g/m^{3}d, respectively. The TVFA profile demonstrated that hydrolysis and acidogenesis were the main biochemical activities occurring in the 1st and 2nd sampling points (Akunna and Clark, 2000; Baloch and Akunna, 2003). The high TVFA concentrations in the anaerobic processes cause the inhibition of methanogenesis.

As shown in Figure 6.113 (b), the TVFA concentrations were decreased from 703, 685, 612 to 546 mg/L at AMX loading rates of 8.33, 16.67, 25.00 to 33.33 g/m^{3}d, respectively in the 2nd sampling point of the ABFR reactor. The AMX loading rates were increased from 8.33, 16.67, 25 to 33.33 g/m^{3}d TVFA concentrations decreased from 512, 486, 345 to 300 mg/L, respectively in the 3rd sampling point of the ABFR reactor (see Figure 6.113 (b)). The effluent TVFA concentrations were measured 205, 120, 96 and 75 mg/L at AMX loading rates of 8.33, 16.67, 25 and 33.33 g/m^{3}d, respectively in the 4th sampling point. Almost 48, 18, 5 and 5 mg/L TVFA concentrations were detected in the 5th sampling point, respectively, for the AMX loading rates given above. The ABFR reactor stability, as evidenced by lower TVFA concentration, is one of the sensitive parameters in anaerobic reactors (Haridas et al. 2005). The TVFA concentration decreased in the ABFR reactor towards upper region. The methanogenesis also appears to be dominant in the last sampling points (4th and 5th). These observations suggest that the ABFR reactor system promoted a systematic selection in the different sampling points in such a manner as to bring out phase separation. Wang et al. (2009) while treating high strength wastewater using ABFR also reported that the TVFA concentration increased longitudinally down the reactor from sampling point 4th. A significant linear relationship was found between AMX loadings 8.33, 16.67, 25 and 33.33 g/m^{3}d and TVFA productions (ANOVA), (R^2= 0.86, F = 12.28, p = 0.07) (for 1st sampling point); (R^2=0.95, F=38.54, p=0.03)

(for 2nd sampling point); (R^2= 0.93, F = 26.08, p = 0.04) (for 3rd sampling point); (R^2=0.88, F=14.88, p=0.06) (for 4th and 5th sampling points).

Adequate HCO_3 alkalinity, or buffer capacity, is necessary to maintain a stable pH in the digester for optimal biological activity (Ağdağ, 2004). An HCO_3 alkalinity varying between 1000 and 5000 mg/L, was recommended for anaerobic treatment depending on COD and TVFA produced (Ağdağ, 2004). Traditionally, the total alkalinity in an anaerobic reactor includes all the HCO_3 alkalinity and approximately 80% of the TVFA (Anderson and Yang, 1992). When the system is in balance, the methanogens could be inactivated by unfavorable environmental conditions, e.g., pH drop, accumulation of TVFA, intermetabolites and toxicity of pollutants due to their toxic properties (Kuai et al., 1998).

The HCO_3 alkalinity concentrations remained between 2500, 2730, 2612 and 2300 mg/L in the 1st sampling point of ABFR at increasing AMX loading rates (see Figure 6.113 (c)). The HCO_3 alkalinity concentration in the 1st sampling point was lower than the other sampling points. The HCO_3 concentrations were obtained as 2800, 2740, 2546 and 2547 mg/L, at AMX loading rates of 8.33, 16.67, 25.00 and 33.33 g/m^3d, respectively in the 2nd sampling point **(**Figure 6.113 (c)**)**. When the AMX loading rates were increased from 8.33, 16.67, 25 to 33.33 g/m^3d, the HCO_3 alkalinity concentrations were determined as 2865, 2900, 2745 and 2500 mg/L, respectively in the 3rd sampling point of the ABFR reactor. Similarly, the HCO_3 alkalinity concentrations also were found as 2960, 2875, 2800, 2685 mg/L respectively in the 4th sampling point. The HCO_3 concentrations were obtained as 3100, 3000, 2950 and 2900 mg/L, respectively, at AMX loading rates of 8.33, 16.67, 25.00 and 33.33 g/m^3d in the 5th sampling point (see Figure 6.113 (c)). A significant linear correlation between HCO_3 alkalinity and increasing AMX loading rate was not observed (ANOVA), (R^2=0.27, F=0.69, p=0.49) (for 1st sampling point). A significant linear relationship was found between AMX loadings 8.33, 16.67, 25.00 and 33.33 g/m^3d and HCO_3 alkalinity (ANOVA), (R^2= 0.90, F=14.33, p=0.06) (for 2nd sampling point); (R^2= 0.80, F = 7.77, p = 0.11) (for 3rd sampling point); (R^2=0.96, F=56.31, p=0.02) (for 4th and 5th sampling points). Methane-producing *archaea* are

active within the pH range of 6.8 to 7.2 (Novaes, 1986). With decreasing pH, methane-producing *archaea* become more inhibited whilst the fermentative bacteria become more active, even at pH 4.5 and produce more TVFA. These acids can overcome the wastewater HCO_3 alkalinity and depress its pH, causing inhibition of the methanogens. The buffering capacity or HCO_3 alkalinity of a biological system is shown by its degree of resistance to changes in pH. HCO_3 alkalinity in the anaerobic digester is derived from the degradation of organic-nitrogen compounds, such as amino acids and proteins, and the production of CO2 from the degradation of organic compounds (McInerney, 1988). HCO_3 alkalinity is important for process stability as it serves to neutralize the organic acids produced during organic biodegradation.

One of the criteria for judging digester stability is the TVFA/ HCO_3 alkalinity ratio. There are three critical values for this: < 0.4 digester should be stable; 0.4–0.8 some instability will occur; > 0.8 significant instability (Callaghan et al. 2002). The TVFA/HCO_3 alkalinity ratios were found as 0.39, 0.31, 0.32 and 0.33 respectively, at AMX loading rates of 8.33-16.67-25.00-33.33 g/m^3d in 1st sampling point of the ABFR reactor. As shown in Figure 6.113 (d), TVFA/HCO_3 alkalinity ratio varied between 0.25, 0.25, 0.24 and 0.21 respectively in 2nd sampling point of the ABFR reactor at increasing AMX loading rates (from 8.33, 16.67, 25.00 to 33.33 g/m^3d). The ratios of TVFA/HCO_3 alkalinity were obtained as 0.17, 0.17, 0.12 and 0.11, respectively, at AMX loading rates of 8.33-16.67-25.00-33.33 g/m^3d in the 3rd sampling point of the ABFR reactor (Figure 6.113 (d)). As the AMX loading rates were increased from 8.33, 16.67, 25.00 to 33.33 g/m^3d TVFA/HCO_3 alkalinity ratio were obtained as 0.07, 0.04, 0.03 and 0.03, respectively in the 4th sampling point (Figure 6.113 (d)). TVFA/HCO_3 alkalinity ratio varied between 0.02, 0.01, 0.002 and 0.002 respectively in 5th sampling point of the ABFR reactor at increasing AMX loading rates (from 8.33, 16.67, 25.00 to 33.33 g/m^3d). The TVFA/HCO_3 ratios of the ABFR reactor system in all sampling points were 0.002 and 0.39, which were much lower than 0.4 and showing high stability.

(a) Variations of pH

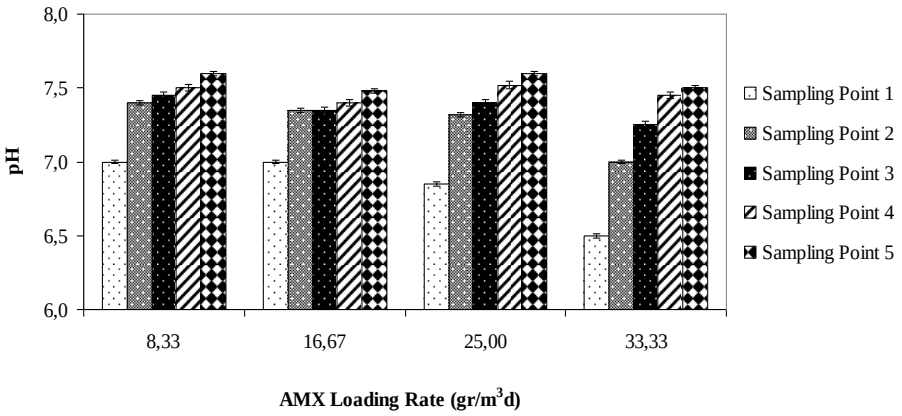

(b) Variations of TVFA

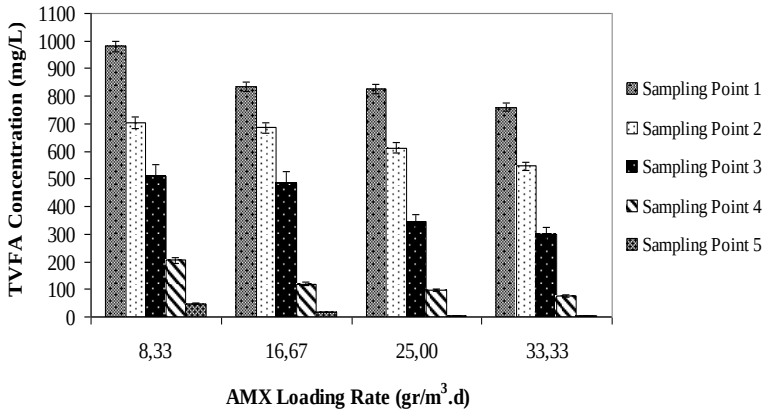

(c) Variations of HCO_3 Alk.

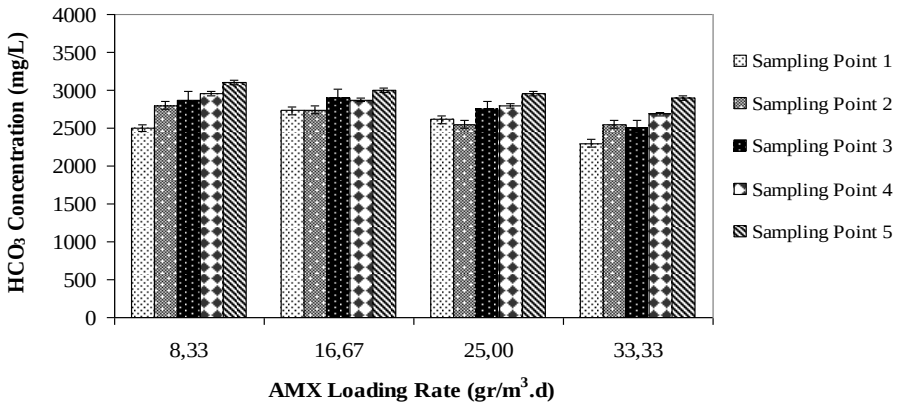

(d) Variations of $TVFA/HCO_3$ Alk. ratio

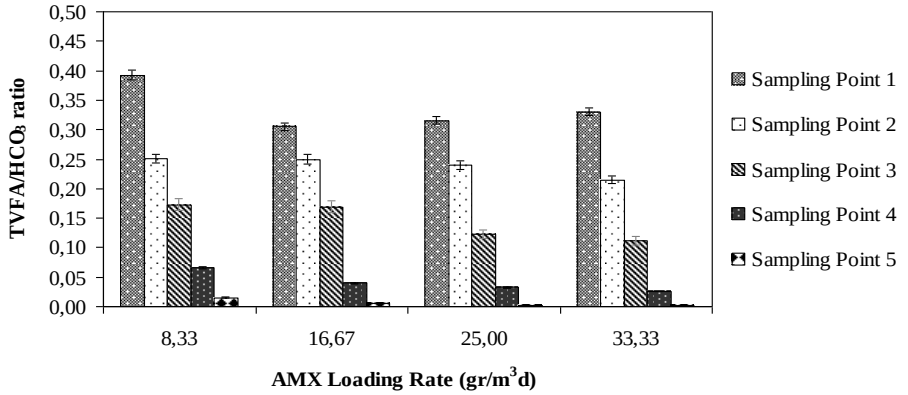

Figure 6.113 Variations of pH (a); TVFA (b); HCO_3 Alk. (c); and $TVFA/HCO_3$ Alk. ratio (d) in ABFR at increasing AMX loading rates

6.3.3.5 Effect of AMX Loading Rate on the COD, AMX Removal Efficiencies in the CSTR Reactor

Figures 6.114 and 6.115 illustrate the effect of increasing AMX loading rate on the COD and AMX concentrations and yields in the CSTR reactor. The COD removal efficiencies were around 86% for AMX loading rates of 8.33 and 16.67 g/m^3d, respectively in the CSTR reactor. As shown in Figure 6.114, the COD removal efficiency was 72% at an AMX loading rate of 25.00 g/m^3d. The COD removal efficiency remained approximately 69% until an AMX loading rate of 33.33 g/m^3d corresponding an AMX concentration of 200 mg/L. The COD concentrations were increased from 85, 90, 230 to 386 mg/L at AMX loading rates of 8.33, 16.67, 25.00 to 33.33 g/m^3d, respectively in the effluent of the aerobic CSTR reactor system (see Figure 6.114). The optimum AMX loading rates were found as 8.33 and 16.67 g/m^3d, respectively, for maximum COD removal efficiency of 86% in the effluent of the CSTR reactor (see Figure 6.114). The minimum COD (E=69%) yield was found at an AMX loading rate of 33.33 g/m^3d.

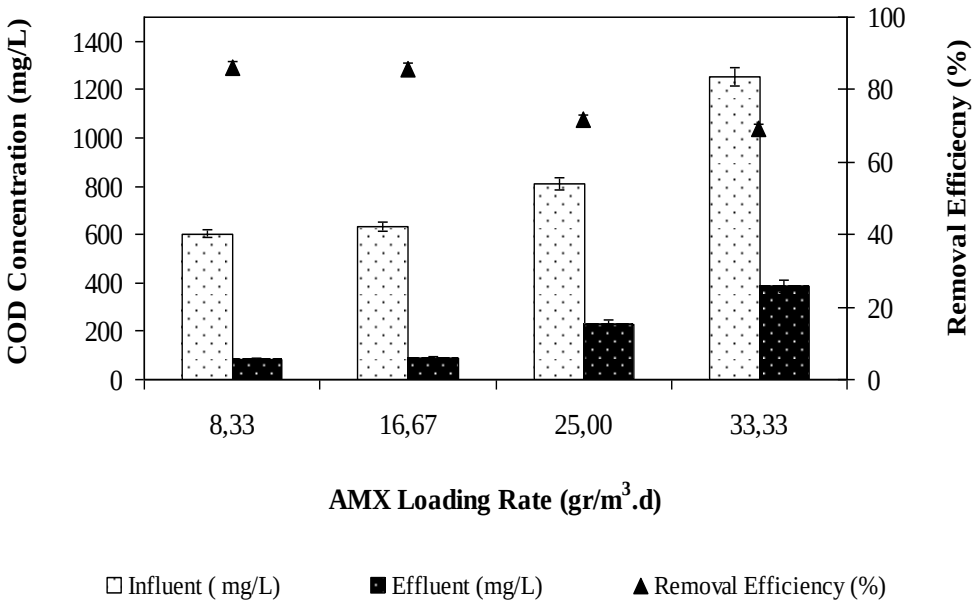

Figure 6.114 COD removal in the aerobic CSTR reactor at increasing AMX loading rates

As shown in Figure 6.115, the AMX yields were decreased from 80%, 80%, 70% to 60% at AMX loading rates of 8.33, 16.67, 25 to 33.33 g/m^{3}d respectively in the effluent of the CSTR reactor. The AMX removal efficiency was around 80% for AMX loading rates of 8.33 and 16.67 g/m^{3}d (see Figure 6.115). The AMX yields were 70% and 60% for AMX loading rates of 25 and 33.33 g/m^{3}d, respectively in the effluent of the CSTR reactor. The COD yields obtained in our study are high in comparison to the removal performances of COD in the studies given below: The COD removals were found to be lower (60%) in the study performed by Chen et al., (2008) under aerobic conditions treating the 78 mg/L AMX in an up flow anaerobic sludge blanket reactor, compared to the present study.

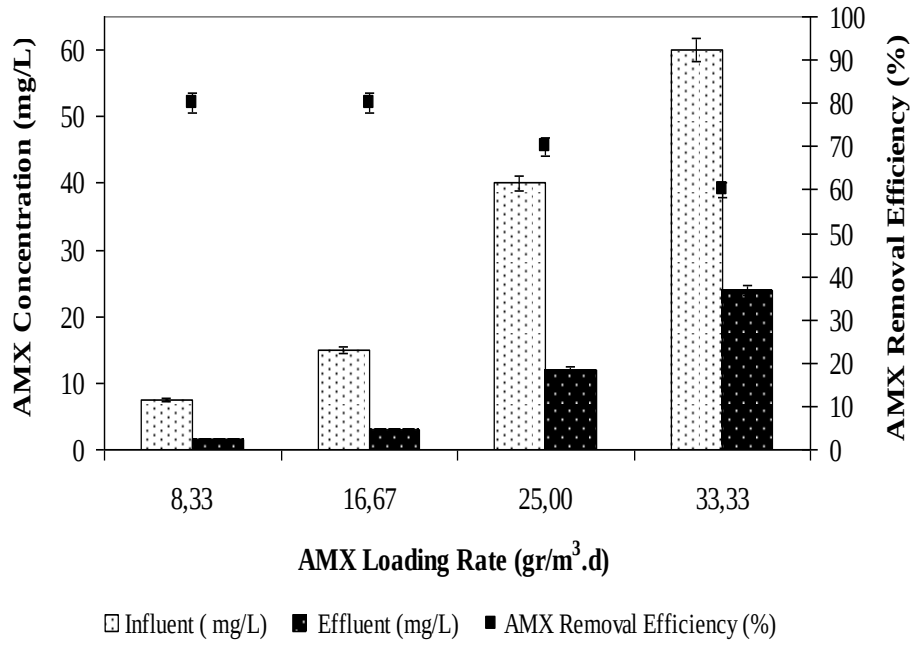

Figure 6.115 AMX removals in the aerobic CSTR reactor at increasing AMX loading rates

6.3.3.6 Treatment Efficiencies of Anaerobic/Aerobic Sequential Reactor System

Figure 6.116 shows the overall COD and AMX removal efficiencies in anaerobic/aerobic sequential reactor system. The maximum COD and the AMX removal efficiency in sequential ABFR/CSTR reactor system were measured as 98% and 97% at AMX loading rates of 8.33 and 16.67 g/m^{3}d, respectively. The COD and AMX removal efficiencies were 98% and 97% at minimum AMX loading rates of 8.33-16.67 g/m^{3}d in overall reactor system, respectively (see Figure 6.116). Total COD and AMX removal efficiencies decreased from 92% to 88% and from 94% and 91% as the AMX loading rates increased from 25.00 to 33.33 g/m^{3}d in sequential ABFR/CSTR reactor system (see Figure 6.116). The minimum COD and the AMX removal efficiency in sequential ABFR/CSTR reactor system were measured as 91% and 88% at an AMX loading rate of 33.33 g/m^{3}d, respectively (see Figure 6.116). In a study carried out by Chen et al. (2011) 87% both AMX and COD yields were obtained at an influent COD and AMX concentration of 3690 and 105 mg/L, respectively, in a combined anaerobic/micro-aerobic two-stage aerobic process at a HRT of 1.98 day. In our study the AMX and COD removal efficiencies are higher

than this study although the influent AMX concentration is comparably higher than the study performed by Chen et al. (2011).

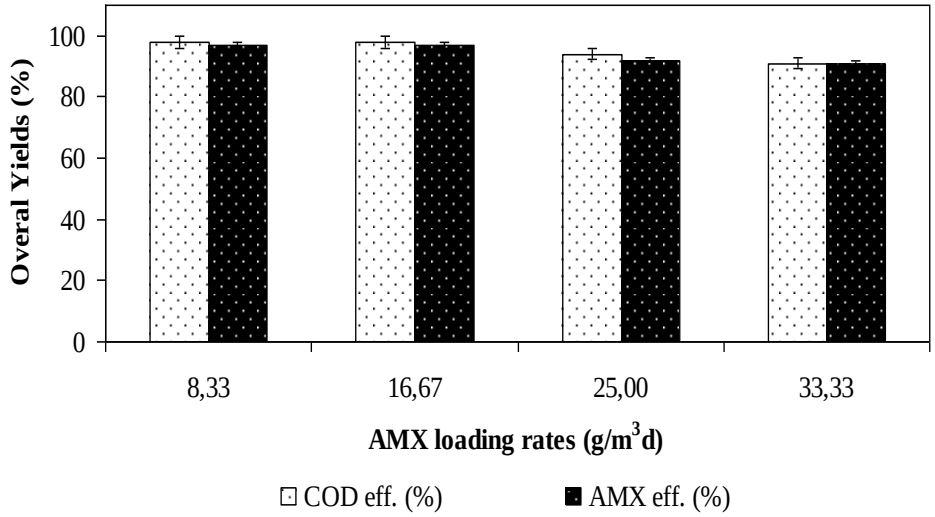

Figure 6.116 AMX and COD removal in the sequential ABFR/CSTR reactor at increasing AMX loading rates

6.3.4 Effect of Increasing TYL Concentration on the Performance of ABFR

6.3.4.1 Effect of Increasing TYL Concentration on the COD Removal Efficiencies in the ABFR Reactor

The performance of anaerobic ABFR reactor system has been evaluated for the following operational conditions:

1. Variation in influent COD concentration ranging from 3925, 4140, 3988 to 4391 mg/L
2. Different TYL loading rates (8.33, 16.67, 25.00, 33.33 g/m^3d).

The performance of ABFR reactor was evaluated by estimating percent COD removal efficiency (E_{COD}) calculated using Eq. (6.1). C_O represents the initial COD concentration (mg/L) in the feed and C_S denotes COD concentration (mg/L) in the reactor outlet:

$$E_{COD} = \frac{C_{Ö} - C_S}{C_{Ö}} \times 100 \qquad \text{Eq. (6.1)}$$

The results in Figure 6.117 show the concentration of different COD fractions and removal efficiencies at the treatment of synthetic pharmaceutical wastewater in the ABFR reactor system. As shown in Figure 6.117, the effluent COD concentrations were increased from 410, 300, 1200 to 1400 mg/L at TYL loading rates of 8.33, 16.67, 25 to 33.33 g/m^{3}d, respectively in the effluent of the ABFR reactor. As shown in Figure 6.117, the COD removal efficiency was 90% at a TYL loading rate of 8.33 g/m^{3}d. The effluent COD concentration was 300 mg/L resulting a COD removal efficiency of 93% at a TYL loading rate of 16.67 g/m^{3}d. After this TYL loading rate (16.67 g/m^3.d) the COD removal efficiency rapidly decreased from 93% to 70% corresponding to TYL loading rate of 25 g/m^{3}d. The COD removal efficiency remained around 68% until a TYL loading rate of 33.33 g/m^{3}d. The maximum COD reduction of 93% the TYL loading rate and TYL concentration were found as 16.67 g/m^{3}d and 100 mg/L, respectively, in the effluent of the ABFR reactor (see Figure 6.117). The minimum COD (E=68%) yield was found at TYL loading rate of 33.33 g/m^{3}d. In our study a significant linear relationship was not found between the COD yields for the TYL loading rates at between 8.33 and 33.33 g/m^{3}d (ANOVA), (R^2=0.76, F=6.48, p=0.1).

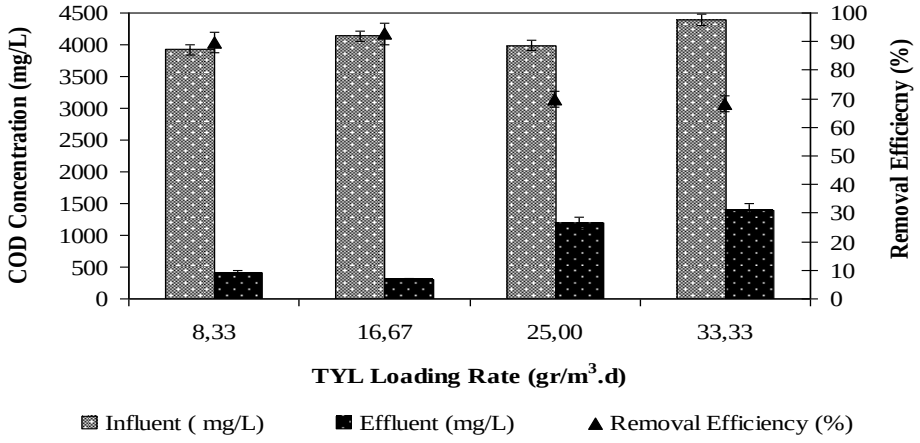

Figure 6.117 Effects of increasing TYL loading rates on COD removal efficiencies in the ABFR reactor

The COD yields obtained in recent studies were low in comparison with the COD removals in this study. In the study by Chelliapan et al., (2011) 70-75% COD removal efficiencies were obtained at a HRT of 2-4 days in an up-flow anaerobic stage reactor (UASR) at influent OLRs of (0.43-1.86 kgCOD/m^3d). In the study performed by Chelliapan et al., (2006), 70% COD removal efficiency was obtained at OLR of 1.88 kgCOD/m^3d in an UASR reactor treating 100-800 mg/L TYL. In our study, 68-93% COD removal was measured for the influent TYL concentration varying between 50 and 200 mg/L. The yields obtained in the aforementioned studies are low in comparison to the removal performances of COD found in this study.

6.3.4.2 Effect of TYL Loading Rate on the TYL Removal Efficiencies in the ABFR Reactor

The effect of TYL loading rate on the TYL yields in ABFR reactor was shown in Figure 6.118. A TYL yield of 82% was obtained at a TYL loading rate of 8.33 g/m^3d (effluent TYL concentration=9 mg/L). After this TYL loading rate, the TYL removal efficiency was found as 92% in the ABFR reactor at a TYL loading rate of 16.67 g/m3d (effluent TYL concentration=8.5 mg/L). As shown in Figure 6.118, the TYL removal efficiency remained around 80% until TYL loading rates of 25.00 and 33.33 g/m^3d. The effluent TYL concentrations varied between 30 and 40 mg/L in the ABFR reactor at TYL loading rates of 25.00 and 33.33 g/m^3d. For maximum TYL removal efficiency of 92% the optimum OTC loading rate was found as 16.67 g/m^3d in the effluent of the ABFR reactor (Figure 6.118). The minimum TYL (E=80%) yield was found at TYL loading rates of 25.00 and 33.33 g/m^3d. A significant linear correlation between TYL yields and increasing TYL loading rate was not observed (ANOVA), (R^2= 0.61, F = 8.76, p = 0.01).

The HPLC chromatograms of TYL were illustrated in Figure 6.119 for the effluent samples of the ABFR at initial TYL concentrations of 50 and 100 mg/L, respectively. Figure 6.119 (a-b) shows the HPLC chromatogram of TYL standard of 50 and 100 mg/L and anaerobic ABFR reactor effluent. A peak of TYL standard of 50 and 100 mg/L was obtained at retention times of 2.92 and 3.10 min and at a wave

length of 254 nm (see Figure 6.119 (a-b)). Similar peak are showed on the chromatograms at the same wave length in the effluent sample (TYL conc.=9 and 8.5 mg/L) of ABFR reactor (see Figure 6.119 (a-b)). This shows that the anaerobic granule sludge in ABFR reactor acclimated to different TYL concentrations. TYL at different concentrations is metabolized with the simultaneous utilization of primary substrate serving as the source of carbon and energy required for growth.

The recent literature on the anaerobic TYL treatment showed that the yields obtained in some high rate anaerobic reactors are lower than the TYL removals found in our study with ABFR: In a study performed by Chelliapan et al., (2011) 75% TYL removal efficiencies were obtained at an organic loading rate of 7.5 kgCOD/m^3.d in an UASR reactor at influent TYL concentrations varying between 100 and 400 mg/L. The yields obtained in the aforementioned studies are low in comparison to the removal performances of TYL found in this study. The differences of TYL yields could be explained by the ABFR reactor which is a high rate reactor for our study.

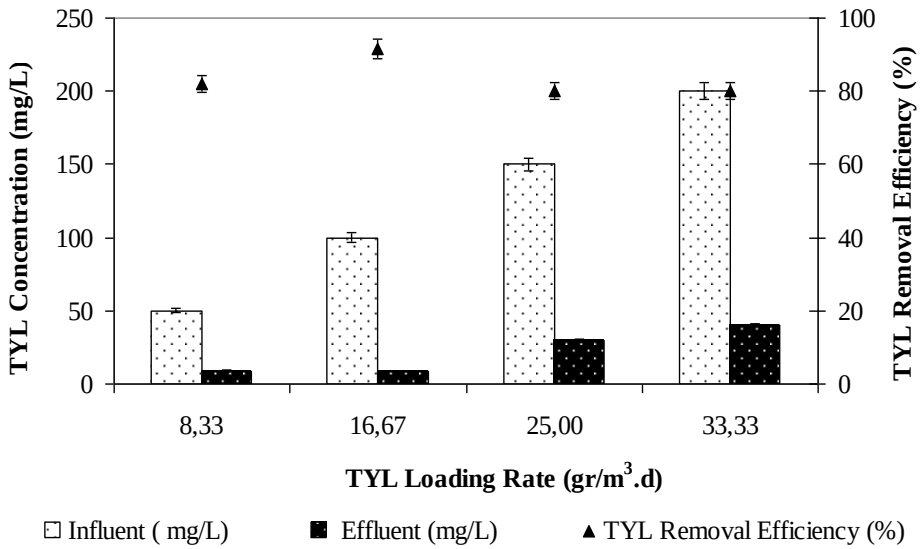

Figure 6.118 The effect of TYL loading rate on TYL removal efficiencies in the ABFR reactor

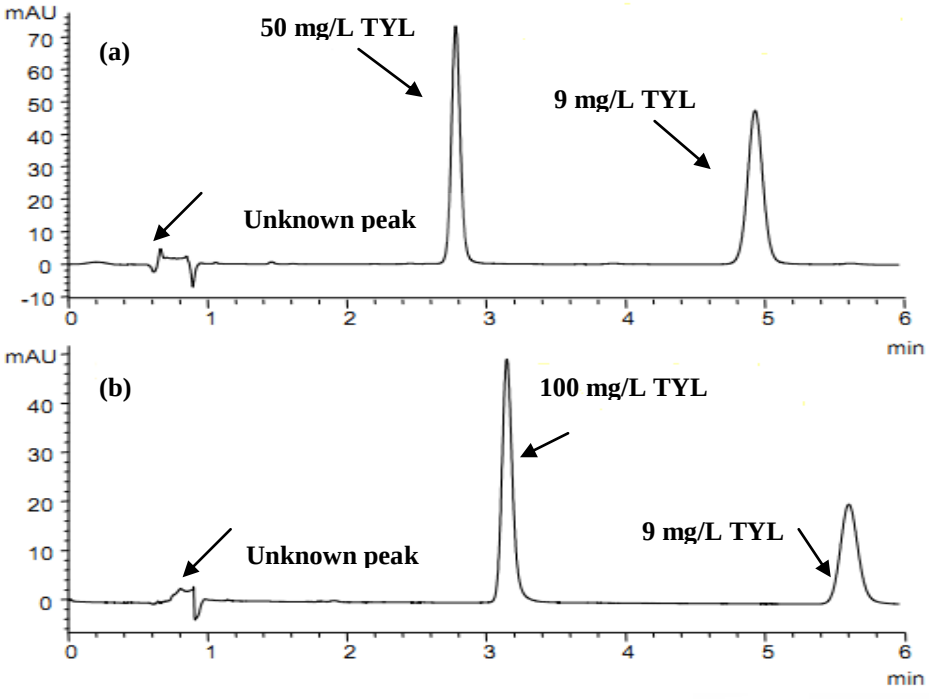

Figure 6.119 HPLC chromatograms of TYL in the influent and effluent of ABFR reactor

6.3.4.3 Effects of Increasing TYL Loading Rates on the Total and Methane Gas Production in the ABFR Reactor

The total and methane gas production rates and methane percentages in AMCBR reactor are shown in Figure 6.120. The total gas, methane gas productions and methane contents were approximately 2.5-4.20 L/d, 1.2-2.5 L/d and 48%-60%, respectively, for TYL loadings varying between 8.33 and 33.33 g/m^{3}d. The maximum total gas, methane gas productions and methane content were found as 4.50 L/d and 2.50 L/d and 60%, respectively, at TYL loading rate of 16.67 g/m^{3}d. After this loading rate, the total gas, methane gas productions and methane percentage decreased. Total gas, methane gas productions and methane percentage were found as 2.5 L/d, 1.2 L/d and 48% at maximum TYL loading rate of 33.33 g/m^{3}d. This indicated an inhibition effect of TYL on methane *Archaea* at TYL loading rate of 33.33 g/m^{3}d. A significant linear relationship was not found between the biogas productions and the TYL loading rates (ANOVA), (R^2=0.50, F=9.76, p=0.02).

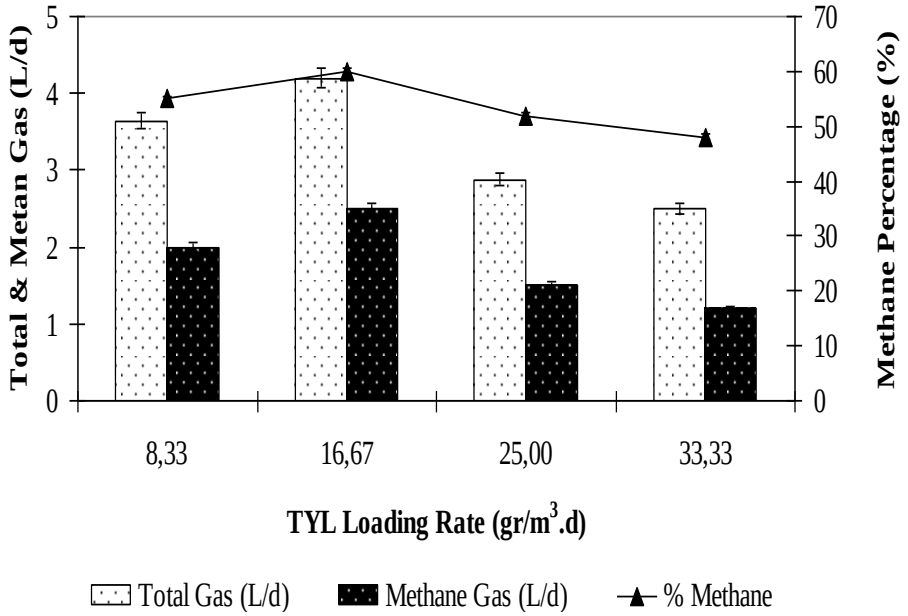

Figure 6.120 The effect of TYL loading rate on total, methane gas production and methane content in the ABFR reactor

The results of this study showed that the OTC loadings affected the total and methane gas produced during anaerobic degradation of pharmaceutical wastewater. Shimada et al., 2011 reported that, 2.6 L/d biogas production at an influent TYL concentration of 167 mg/L at HRT of 1.67 day and at an OLR of 3.5 kg COD/m^3d in an ASBR reactor. In another study, in a study performed by Amin et al., (2006) methane gas production and percentage were found as 5 L/d and 48%, respectively at an OLR of 2.90 kg COD/m^3d in an ASBR. In our study, 60% methane percentage and 2.5 L/d CH_4 production was measured at influent TYL concentrations varying between 50 and 200 mg/L in an ABFR reactor. The yields obtained in the aforementioned studies are low in comparison to the methane gas productions found in our study.

Figure 6.121 shows the variations of methane yields versus TYL loading rates. The methane yields increased from 0.28 to 0.33 $m^3CH_4/kgCOD_{removed}$, when the TYL loading rates were increased from 8.33 to 16.67 g/m^3d, respectively in the ABFR reactor. The methane yields in the ABFR reactor system decreased from 0.27 to 0.20 $m^3CH_4/kgCOD_{removed}$ when the TYL loading rates were increased 25.00 to 33.33

g/m^{3}d. A significant linear relationship was found between the methane yields and the TYL loading rates for TYL loading rates of 8.33 and 133.33 g/m^{3}d (ANOVA), (R^2=0.88, F=6.12, p=0.02). Chelliapan et al., (2006) found that when treating pharmaceutical wastewater containing 20- 200 mg/L TYL in an UASR. 0.10-0.40 $m^3CH_4/kgCOD_{removed}$ methane yields were obtained during 106 days of operation time. The yields obtained in the aforementioned study are similar in comparison to the yield performances of methane found in this study.

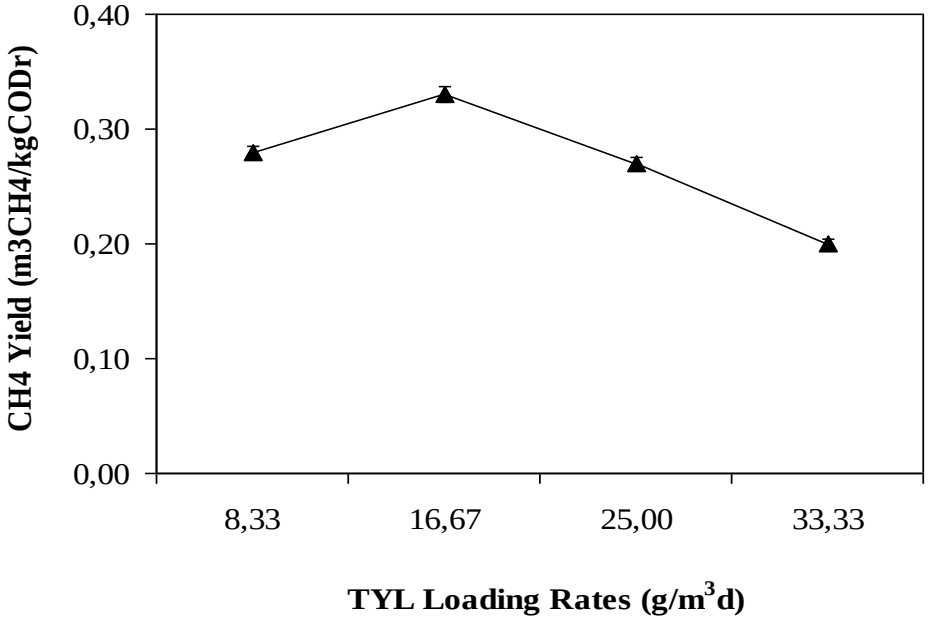

Figure 6.121 Variations of CH_4 yields versus TYL loading rates in all compartment of the ABFR reactor

6.3.4.4 Variation of pH, TVFA and Composition (H_{ac}, H_{bu}, H_{la}, H_{pr}) in Compartments of the AMCBR Reactor at Increasing TYL Loading Rates

The pH is an important factor for keeping functional anaerobic degradation. A typical pH is in the range of 6.5-7.6 (Chen, 2010). Figure 6.122 shows the pH variation in sampling points of the AMCBR at increasing TYL loading rates. As shown in Figure 4.37, the pH values in the effluent (5th sampling point) and in the all sampling points of AMCBR varied between 6.50 and 7.60. The pH values were lower in the 1st sampling point than all of the other sampling points since TVFA in the 1st sampling point was higher (Figure 6.123). When the TYL loading rates was

increased from 8.33 to 33.33 g/m^{3}d in the AMCBR reactor, the pH in the 1st sampling point dropped from 7.00 to 6.50 due to the increased acidogenic activity. As the TYL loading rates were increased from 8.33, 16.67, 25.00 to 33.33 g/m3d, pH values decreased from 7.40, 7.35, 7.32 to 7.00, respectively in 2nd sampling point (Figure 6.122). The pH values in the 3rd sampling point of the ABFR reactor varied between 7.45, 7.35, 7.40 and 7.25 at the same OTC loadings, respectively. As shown in Figure 6.122, the pH values were found as 7.50, 7.40, 7.52 and 7.45, respectively, in the 4th sampling point of the ABFR reactor at OTC loading rates of 8.33, 16.67, 25.00 and 33.33 g/m3d. The effluent pH values varied between 7.60, 7.48, 7.60 and 7.50 at OTC loading rates of 8.33, 16.67, 25.00 and 33.33 g/m^{3}d, respectively in the 5th sampling point of ABFR reactor.

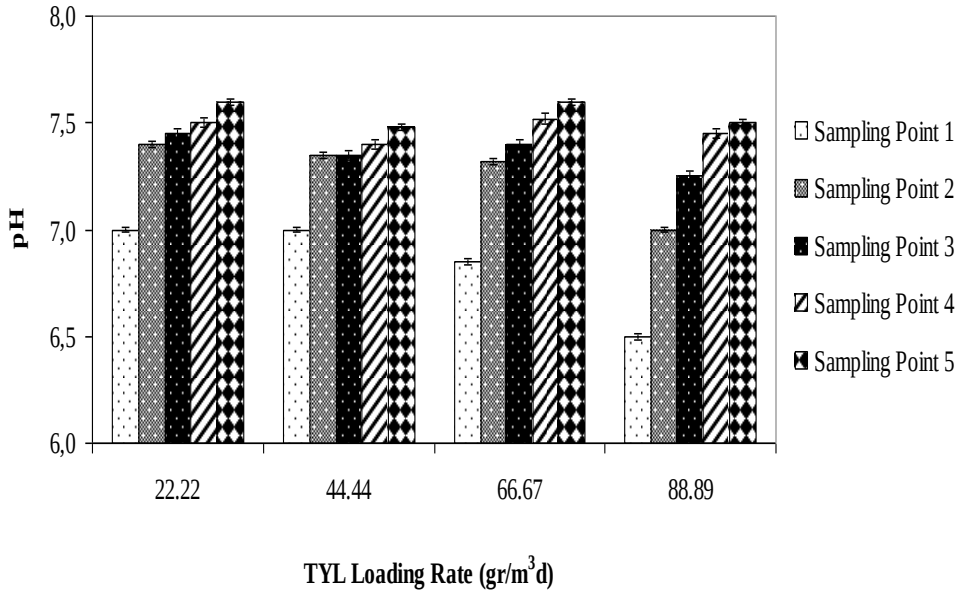

Figure 6.122 Variations of pH in the ABFR reactor at increasing TYL loading rates

A stable reactor operation for various types of reactor designs, substrates used and operational conditions during the start-up period has been widely reported in many studies. In this study, the parameters used were volatile fatty acids, alkalinity, pH, biogas production and COD removal efficiency, methane yield to indicate the stability of the reactor (Suleiman et al., 2010). As TVFA are potential inhibitors to the anaerobic process, their determination is important in the control of anaerobic

wastewater treatment processes. Figure 6.123 shows the TVFA production in the different sampling points. The TVFA production in the 1st sampling point was significantly greater than that in sampling points at TYL loadings. The TVFA profile (Figure 6.123) demonstrated that hydrolysis and acidogenesis were the main biochemical activities occurring in the 1st and 2nd sampling points. The reason for the fall in TVFA concentration in the 3rd sampling point and its rise in the 4th sampling point were not clear. However, methanogenesis appeared to be dominant thereafter (5th sampling point).

The TVFA concentrations in the 1st sampling point decreased from 1100, 1000, 986 to 812 mg/L for the TYL loading rates increasing from 8.33, 16.67, 25.00 to 33.33 g/m^{3}d, respectively. As shown in Figure 6.123, the TVFA concentrations decreased from 900, 765, 542 to 346 mg/L at the same TYL loadings, respectively in the 2nd sampling point of the ABFR reactor. The TYL loading rates were increased from 8.33, 16.67, 25.00 to 33.33 g/m^{3}d the TVFA concentrations varying between 600, 384, 274 and 200 mg/L, respectively in the 3rd sampling point of the ABFR reactor (Figure 6.123). The effluent TVFA concentrations were measured as 210, 155, 100 and 85 mg/L at the same OTC loadings, respectively in the 4th sampling point. As shown in Figure 6.123, TVFA concentrations were detected as 70, 40, 20, 20 mg/L in the 5th sampling point of the ABFR respectively, for the OTC loading rates given above. It was found that the TVFA concentrations decreased from sampling point 1st to sampling points 2nd, 3rd and 4th, 5th. The TVFA concentrations were measured as 346 and 812 mg/L at TYL loading rate as high as 33.33 g/m^{3}d due to inhibition effects of high TYL concentrations to acidogens in the 1st and 2nd sampling points of the ABFR reactor system. A strong linear correlation between TVFA concentrations and TYL loading rates was observed in the 1st and 2nd compartments for TYL loading rates of 8.33 and 133.33 g/m^{3}d (ANOVA) (R^2=0.96; F=3.89, p=0.01).

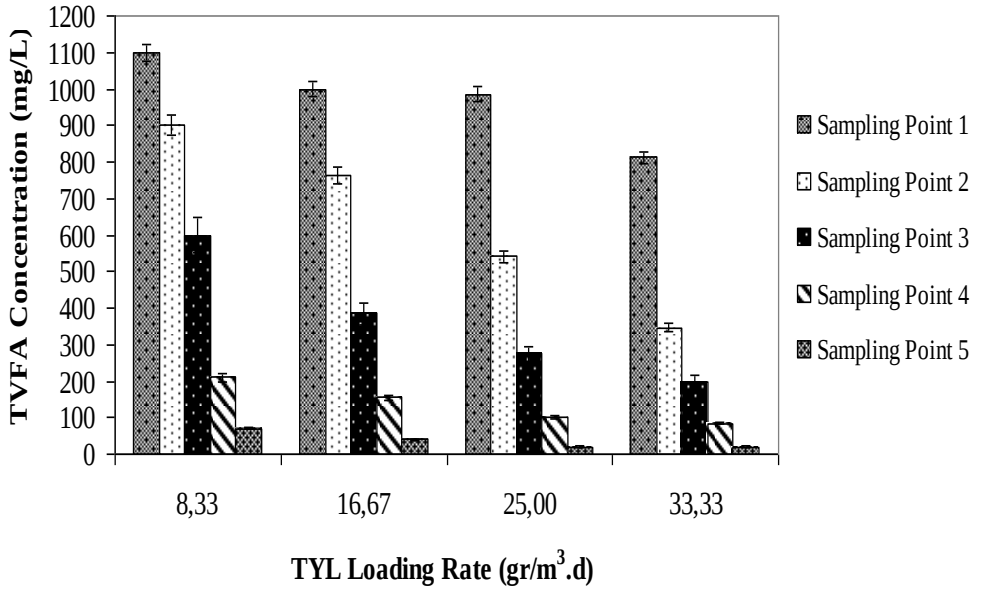

Figure 6.123 Variations of TVFA concentration in the ABFR reactor at increasing TYL loading rates

The results of this study showed that the TYL loadings affected the TVFA production during anaerobic degradation of pharmaceutical wastewater. In a study performed by Chelliapan et al. (2011) TVFA productions were 550-1050 mg/L, 350-750 mg/L, 200-570 mg/L and 40-400 mg/L for 1st, 2nd, 3rd and 4th compartments, in an anaerobic UASR reactor respectively. In our study TVFA productions were 812-1100 mg/L, 346-900 mg/L, 200-600 mg/L, 85-210 mg/L and 20-70 mg/L in the 1st, 2nd, 3rd, 4th, 5th sampling points of the ABFR reactor for TYL loading rates of 8.33 and 33.33 g/m^{3}d. In this study the TVFA productions are comparable higher than that aforementioned study.

6.3.4.5 Variation of HCO_3 and TVFA/HCO_3 Ratio in Compartments of the ABFR Reactor at Increasing TYL Loading Rates

HCO_3 alkalinity measurements were used in evaluating the buffering capacity of the wastewater. The HCO_3 alkalinity in all sampling point s of the ABFR reactor at increasing TYL concentrations (from 50, 100 and 150 up to 200 mg/L) was shown in Figure 6.124. The HCO_3 alkalinity concentrations remained between 2300, 2400,

2512 and 2100 mg/L in the 1st sampling point of ABFR at increasing TYL loading rates (see Figure 6.124). The HCO_3 alkalinity concentration in the 1st sampling point was lower than the other sampling points. The HCO_3 alkalinity concentrations were found as 2750, 2800, 2600 and 2500 mg/L, at TYL loading rates of 8.33, 16.67, 25.00 and 33.33 g/m^3d, respectively in the 2nd sampling point **(**Figure 6.124**)**. When the TYL loading rates were increased from 8.33, 16.67, 25 to 33.33 g/m^3d, the HCO_3 alkalinity concentrations were determined as 2795, 2900, 2800 and 2400 mg/L, respectively in the 3rd sampling point of the ABFR reactor. Similarly, the HCO_3 alkalinity concentrations also were found as 2875, 2900, 2800, 2765 mg/L respectively in the 4th sampling point. The HCO_3 concentrations were determined as 3100, 3200, 3150 and 3000 mg/L, respectively, at the same TYL loading rates in the 5th sampling point (see Figure 6.124). A significant linear correlation between HCO_3 alkalinity and increasing AMX loading rate was not observed (ANOVA), (R^2=0.27, F=0.69, p=0.49) (for 1st sampling point).A significant linear relationship was found between AMX loadings 8.33, 16.67, 25 and 33.33 g/m^3d and HCO_3 alkalinity (ANOVA), (R^2= 0.90, F = 14.33, p = 0.06) (for 2nd sampling point); (R^2= 0.80, F = 7.77, p = 0.11) (for 3rd sampling point); (R^2= 0.96, F = 56.31, p = 0.02) (for 4th and 5th sampling points).

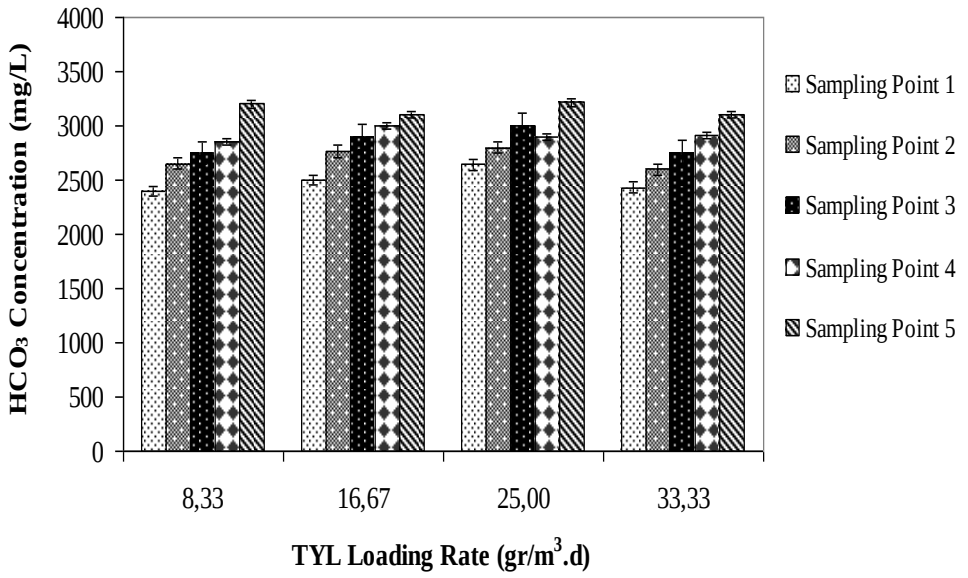

Figure 6.124 Variations of HCO_3 concentration in the ABFR at increasing TYL loading rates

In this study the stability was assessed based on total volatile fatty acids-to-alkalinity ratio (TVFA/HCO_3). The TVFA/Talk ratio remained below the threshold of 0.4 for optimum performance (Rincon et al. 2009).The TVFA/HCO_3 ratios for this study are shown in Figure 6.125. The TVFA/HCO_3 alkalinity ratios were found as 0.40, 0.40, 0.39 and 0.39 respectively, at TYL loading rates of 8.33-16.67-25-33.33 g/m^3d in 1st sampling point of the ABFR reactor. TVFA/HCO_3 alkalinity ratio varied between 0.33, 0.27, 0.21 and 0.14 respectively in 2nd sampling point of the ABFR reactor at the same TYL loadings. The ratios of TVFA/HCO_3 were obtained as 0.21, 0.13, 0.10 and 0.07, respectively, at TYL loading rates of 8.33-16.67-25-33.33 g/m^3d in the 3rd sampling point (6.125). As the TYL loading rates were increased from 8.33, 16.67, 25 to 33.33 g/m^3d TVFA/HCO_3 alkalinity ratio were obtained as 0.07, 0.05, 0.03 and 0.03, respectively in the 4th sampling point (Figure 6.125). TVFA/HCO_3 alkalinity ratio varied between 0.02, 0.01, 0.01 and 0.01 respectively in 5th sampling point of the ABFR reactor at the same TYL loadings. The TVFA/HCO_3 ratios of the ABFR reactor system in all sampling points were 0.01 and 0.40 which were much lower than 0.4 and showing high stability.

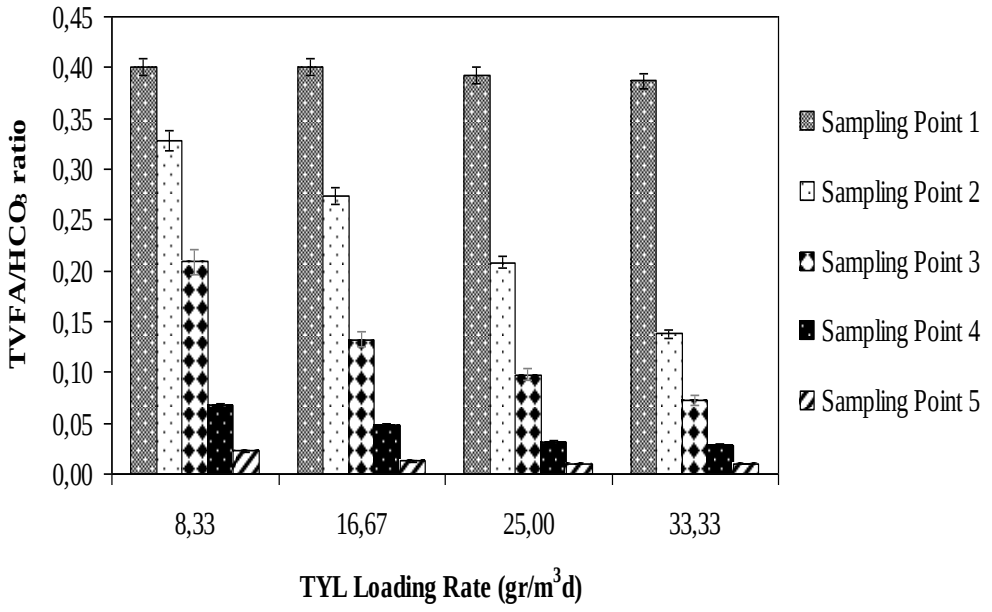

Figure 6.125 Variations of TVFA/HCO_3 ratio in the ABFR at increasing TYL loading rates

6.3.4.6 *Effect of TYL Loading Rate on the COD, TYL Removal Efficiencies in the CSTR Reactor*

Figures 6.126 and 6.127 illustrate the effect of increasing TYL loading rate on the COD and TYL concentrations and removal efficiencies in the CSTR reactor. The COD removal efficiency was around 80% for TYL loading rate of 8.33 g/m^{3}d in the CSTR reactor. As shown in Figure 6.126, the COD removal efficiency was 85% at a TYL loading rate of 16.67 g/m^{3}d. The COD removal efficiency remained approximately 78% until an AMX loading rate of 25. The COD yield was found as 64% at a TYL loading rate of 33.33 g/m^{3}d in the ABFR reactor system. The COD concentrations were increased from 45, 260 to 500 mg/L at TYL loading rates of 8.33, 16.67, 25 and 33.33 g/m^{3}d, respectively in the effluent of the aerobic CSTR reactor system (see Figure 6.126). The optimum TYL loading rate was found as 16.67 g/m^{3}d, respectively, for maximum COD removal efficiency of 85% in the effluent of the CSTR reactor (see Figure 6.126). The minimum COD (E=64%) yield was found at an AMX loading rate of 33.33 g/m^{3}d.

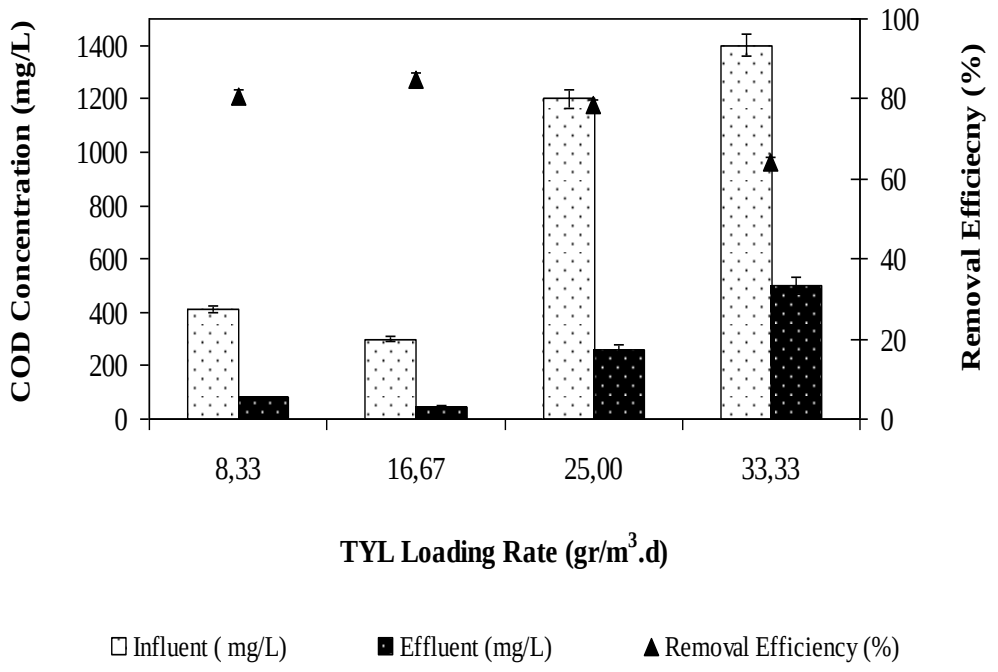

Figure 6.126 COD removal in the aerobic CSTR reactor at increasing TYL loading rates

The TYL removal efficiency was around 70% for TYL loading rate of 8.33 g/m^{3}d (see Figure 6.127). As shown in Figure 6.127, the TYL yields were decreased from 76%, 67% to 67% at AMX loading rates of 16.67, 25 to 33.33 g/m^{3}d respectively in the effluent of the CSTR reactor. The TYL removal efficiency was around 76% for TYL loading rate of 16.67 g/m^{3}d (see Figure 6.127). The TYL yields were 67% for TYL loading rates of 25 and 33.33 g/m^{3}d, respectively in the effluent of the CSTR reactor. The COD yields obtained in our study are high in comparison to the removal performances of COD in the studies given below: The COD removals were found to be lower (average 65%) in the study performed by Chelliapan et al., (2010) under aerobic conditions treating the 200 mg/L TYL in an aerobic Porous Membrane Activated Sludge Reactor (APMASR), compared to the our study (E=66-86%, influent TYL concentration 100 mg/L). The difference in COD yields could be explained by the APMASR and AMCBR reactor configuration, operational conditions and TYL concentrations used throughout reactor operation.

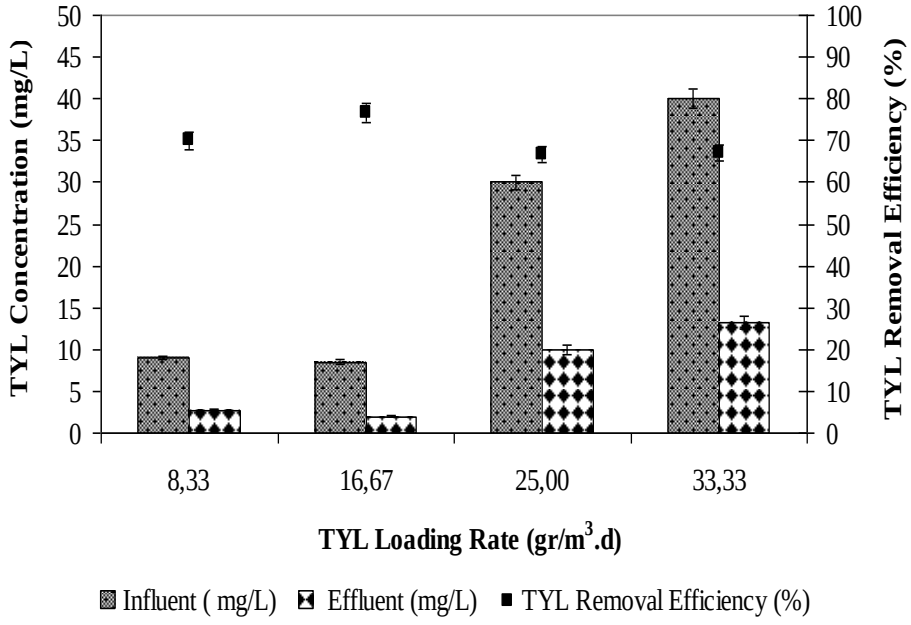

Figure 6.127 TYL removals in the aerobic CSTR reactor at increasing TYL loading rates

6.3.4.7 *Treatment Efficiencies of Anaerobic/Aerobic Sequential Reactor System*

Generally, an anaerobic process is applied to remove high concentrations of organic matter followed by an aerobic treatment to oxidise the residual organic

matter. Given that influent COD is very high, effluent from anaerobic reactor can still have residual COD (Chelliapan et al., 2010). The effluent from AMCBR was further subjected to aerobic treatment (CSTR) to remove the residual COD. Figure 6.128 shows the overall COD and TYL removal efficiencies in anaerobic/aerobic sequential reactor system. The COD and TYL removal efficiencies were 98% and 95% at minimum TYL loading rate of 8.33 g/m^{3}d in overall reactor system, respectively (see Figure 6.128). The maximum COD and the TYL removal efficiency in sequential ABFR/CSTR reactor system were measured as 99% and 98% at TYL loading rate of 16.67 g/m^{3}d, respectively. Total COD and TYL removal efficiencies decreased from 93% to 89% and from 93% and 93% as the TYL loading rates increased from 25.00 to 33.33 g/m^{3}d in sequential ABFR/CSTR reactor system (see Figure 6.128). The minimum COD and the TYL removal efficiency in sequential ABFR/CSTR reactor system were measured as 89% and 93% at a TYL loading rate of 33.33 g/m^{3}d, respectively (see Figure 6.128). The literature survey showed that the TYL and COD yields obtained in recent studies are lower than those in our data: In a study carried out by Chelliapan et al., (2010) 90% and 97% COD and TYL yields were obtained at an influent COD and TYL concentration of 7000 and 200 mg/L, respectively, in a combined anaerobic UASR/aerobic APMASR reactor system at a HRT of 4 days. In our study the TYL and COD removal efficiencies are higher than this study although the influent TYL concentration is comparably higher than the study performed by Chelliapan et al., (2010).

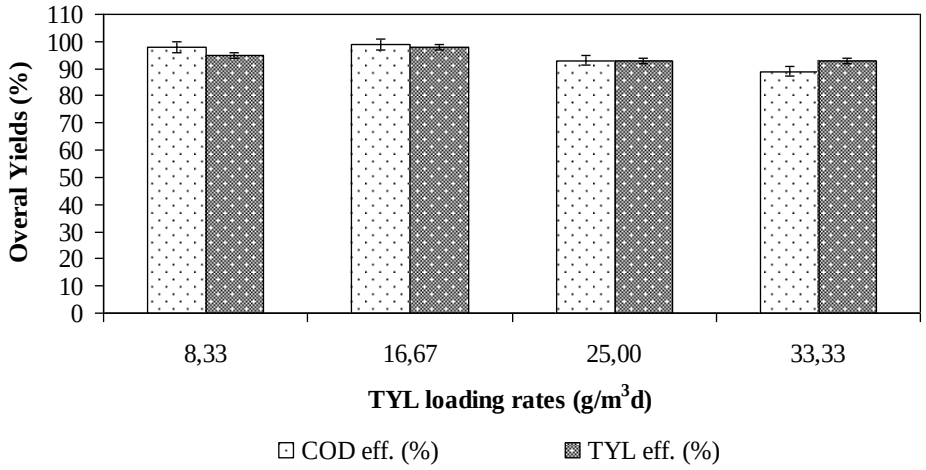

Figure 6.128 TYL and COD removal in the sequential ABFR/CSTR reactor at increasing TYL loading rates

6.3.5 Effect of Increasing ERY Concentration on the Performance of ABFR

6.3.5.1 Effect of Increasing ERY Concentration on the COD Removal Efficiencies in the ABFR Reactor

The anaerobic treatability performance of ABFR reactor was evaluated by analyzing the influent and effluent of COD in the ABFR reactor. The COD was monitored as an indicator parameter of the pharmaceutical wastewater organic strength. In this run, the effect of increasing ERY concentrations on COD removal efficiencies was investigated. The operation of the AMCBR with ERY was started at an influent ERY concentration of 50 mg/L. Then the ERY concentrations were subsequently increased from 100 to 150, 200 mg/L corresponding to ERY loading rates of 16.67, 25.00 and 33.33 g/m^3d. The COD equivalents of ERY concentration are shown in Table 6.29.

Table 6.29 The COD equivalents of ERY concentration

Parameters	**Unit**	**Concentrations**
Molasses-COD concentration	mg/L	4100
ERY concentration	mg/L	50; 100; 150; 200
COD equivalent of ERY	mg/L	20; 40; 60; 80
Total COD concentration	mg/L	4120; 4140; 4160; 4180

The results in Figure 6.130 show the concentration of different COD fractions and removal efficiencies at the treatment of synthetic pharmaceutical wastewater in the ABFR reactor system. As shown in Figure 6.130, the effluent COD concentrations were increased from 350, 350, 900 to 1250 mg/L at ERY loading rates of 8.33, 16.67, 25.00 to 33.33 g/m^3d, respectively in the effluent of the ABFR reactor. As shown in Figure 6.130, the COD removal efficiency was 92% at an ERY loading rates of 8.33 and 16.67 g/m^3d. The effluent COD concentration was 350 mg/L resulting a COD removal efficiency of 92% at ERY loading rates of 8.33 and 16.67 g/m^3d in the ABFR reactor system. The COD removal efficiency decreased from 92 to 78% as the ERY loading rate was increased from 16.67 to 25.00 g/m^3d. As shown in Figure 6.130, the COD removal efficiency was 70% at an ERY loading rate of

33.33 g/m^{3}d. The maximum COD reduction of 92% the ERY loading rates were found as 8.33 and 16.67 g/m^{3}d, respectively, in the effluent of the ABFR reactor (see Figure 6.130). The minimum COD (E=70%) yield was found at ERY loading rate of 33.33 g/m^{3}d. The optimum ERY loading rates was 8.33 and 16.67 g/m^{3}d at ERY concentrations of 50 and 100 mg/L for maximum COD yield while the minimum COD removal efficiency was obtained at an ERY loading rate of 33.33 g/m^{3}d. In our study a significant linear relationship was found between the COD yields for the ERY loading rates at between 8.33 and 16.67 g/m^{3}d (ANOVA), (R^2=0.89, F=4.71, p=0.01).

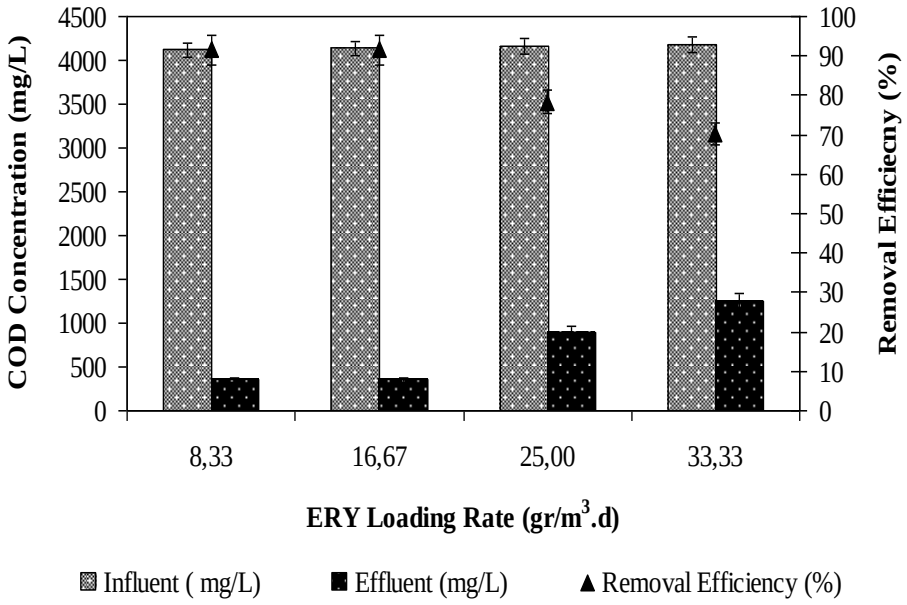

Figure 6.130 Effects of increasing ERY loading rates on COD removal efficiencies in the ABFR reactor

The COD yields obtained in recent studies were low in comparison with the COD removals in this study. In the study by Rodriguez-Martinez et al., (2005) 70-85% COD removal efficiencies were obtained at a HRT of 2 days in an UASB reactor at influent OLRs of (1.5-2.09 kgCOD/m^{3}d). In the study performed by Chelliapan et al., (2006), 70% COD removal efficiency was obtained at OLR of 1.88 kgCOD/m^{3}d in an UASR reactor treating 100-800 mg/L TYL. In our study, 70-92% COD removal was measured for the influent ERY concentration varying between 50 and

200 mg/L. The yields obtained in the aforementioned studies are low in comparison to the removal performances of COD found in this study.

6.3.5.2 Effect of ERY Loading Rate on the ERY Removal Efficiencies in the ABFR Reactor

The effects of increasing ERY loading rate on the ERY removal efficiencies are shown in Figure 6.131 in the ABFR reactor. A maximum ERY removal efficiency of 90% was obtained at initial ERY loading rates of 8.33 and 16.67 g/m^{3}d. This can be explained with the acclimation of methanogenic bacteria to ERY. The ERY removal efficiency decreased from 90% to 73%, respectively, at an ERY loading rates of 16.67 to 25.00 g/m^{3}d in the ABFR reactor. When the ERY loading rates was increased from 25.00 g/m^{3}d to 33.33 g/m^{3}d the ERY removal efficiency decreased from 73% to 60%, respectively in the ABFR reactor. For maximum ERY removal efficiency of 90% the optimum ERY loading rates were found as 8.33 and 16.67 g/m^{3}d in the effluent of the ABFR reactor (Figure 6.131). The minimum ERY (E=60%) yield was found at ERY loading rate of 33.33 g/m^{3}d.

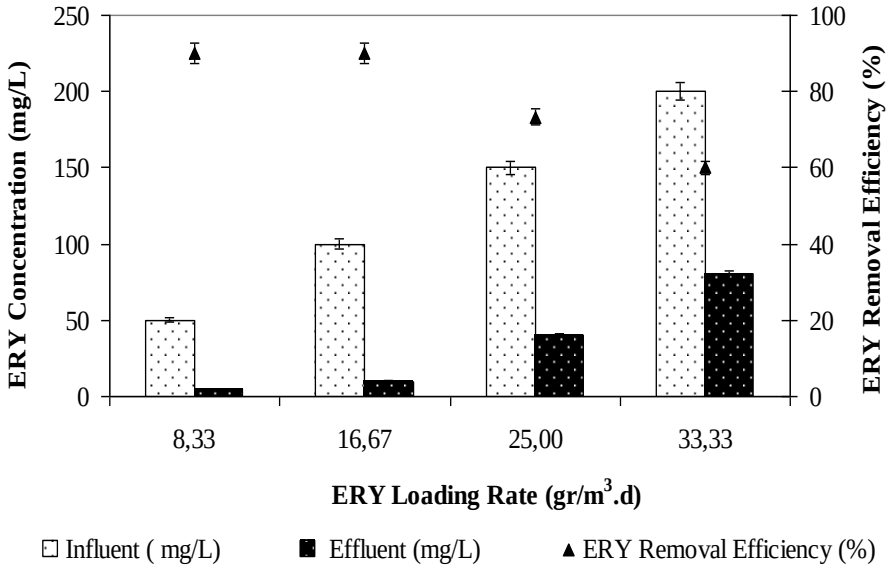

Figure 6.131 Effects of increasing ERY loading rates on ERY removal efficiencies in the ABFR reactor

The HPLC chromatograms of ERY were illustrated in Figure 6.132 for the effluent samples of the ABFR at initial ERY concentration of 100 mg/L. Figure 4.44 shows the HPLC chromatogram of ERY standard of 100 mg/L (a), and anaerobic ABFR reactor effluent (b). A peak of ERY standard of 100 mg/L was obtained at a retention time of 1.24 min and at a wave length of 287 nm (See Figure 6.132 (a)). A peak is showed on the chromatogram at the same wave length in the effluent sample of ABFR reactor (See Fig. 6.132 (b)). This shows that the anaerobic granule sludge in the ABFR reactor acclimated to different ERY concentrations. ERY at different concentrations is metabolized with the simultaneous utilization of primary substrate serving as the source of carbon and energy required for growth.

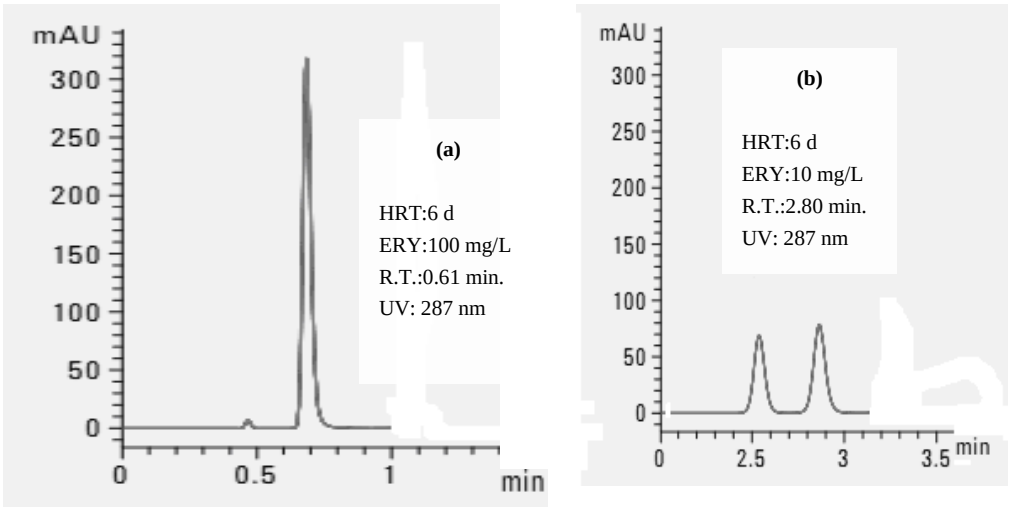

Figure 6.132 HPLC chromatograms of ERY in the influent and effluent of ABFR reactor

The ERY yields obtained in our study are high in comparison to the removal performances of ERY in the studies given below: In the study performed by Shimada et al. (2011), the ERY yields (80%-86%) were lower than those of our data (75%-95%) at a OLRs 1.9 and 5.8 kgCOD/m^3.d in the ASBR treating 90 mg/L ERY. In a study performed by Busetti and Heitz, (2011) 90%, ERY removal was obtained in synthetic pharmaceutical wastewater containing 100 mg/L mix antibiotic solution in an anaerobic conditions at a HRT of 2 days. In our study removal efficiencies of ERY was higher than those in the study performed by Busetti and Heitz, (2011). The yields obtained in the aforementioned studies are low in comparison to the removal performances of ERY found in our study. The reason of high ERY yields in our

study could be explained by the granulated sludge which is resistant to the high toxic compounds and to the AMCBR reactor which is a high rate reactor.

6.3.5.3 Effects of Increasing ERY Loading Rates on the Total and Methane Gas Production in the ABFR Reactor

Figure 6.133 show the behavior of biogas production and methane contents of the ABFR reactor system. The daily total gas, methane gas productions and methane contents were approximately 2.33-3.64 L/d, 1.12-2.00 L/d and 48%-55%, respectively, for ERY loadings varying between 8.33, 16.67, 25 and 33.33 g/m^{3}d. The maximum total and methane gas productions and methane contents were found as 3.64 L/d and 2.00 L/d and 55%, respectively, at ERY loading rates of 8.33 and 16.67 g/m^{3}d. After these loading rates, the daily total gas, methane gas productions and methane percentage decreased. The total gas, methane gas productions were obtained as 3.20 L/d and 1.60 L/d, 50% at an OTC loading rate of 25 g/m^{3}d, respectively (see Figure 6.133). When the OTC loading rates were increased from 25 to 33.33 g/m^{3}d, the daily total gas, methane gas productions and methane content were measured as 2.33 L/d, 1.12 L/d and 48%, respectively in the ABFR system. The low rate of methane formation and methanogenic activity is attributed to the inhibitory effects of the pharmaceutical wastewater including antibiotic.

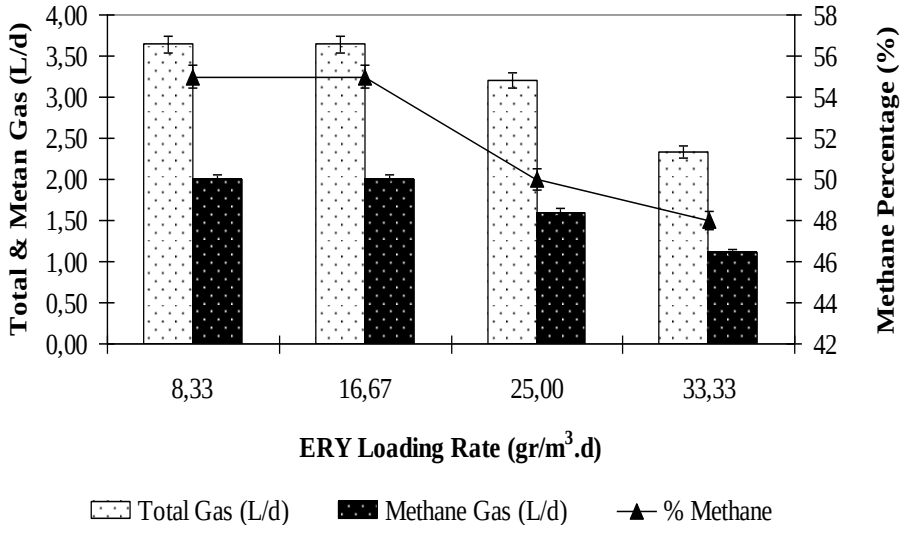

Figure 6.133 Effects of increasing ERY loading rates on the gas production, methane content in the ABFR reactor.

In a study performed by Liu et al., (2011) 7.49 L/d methane gas production was found at OLRs varying at between 1.23 and 2.16 kg COD/m^3d, at an influent ERY=50-200 mg/L and a HRT=2 days in a full-scale UASB reactor. In another study, in a study performed by Amin et al., (2006) methane gas production and percentage were found as 5 L/d and 48%, respectively at an OLR of 2.90 kg COD/m^3d in an ASBR. In our study, 55% methane content and 2.00 L/d CH_4 production was measured at influent ERY concentration varying between 50 and 100 mg/L in an AMCBR reactor. The yields obtained in the aforementioned studies are low in comparison to the methane gas productions found in our study. This could be explained by the macrolide antibiotics (ERY, TYL, etc.) were inhibited methane production and content in anaerobic reactors. The methane yield can be useful parameter to assess the performance of an anaerobic reactor Figure 6.134 shows the variations of methane yields versus ERY loading rates. The methane yields decreased from 0.27 to 0.19 $m^3CH_4/kgCOD_{removed}$, when the ERY loading rates were increased from 8.33, 16.67, 25 to 33.33 g/m^3d. The methane yield was obtained as 0.27 and 0.26 $m^3CH_4/kgCOD_{removed}$, respectively, at ERY loading rates of 8.33 and 16.67 g/m^3d. As the ERY loading rates were increased from 25.00 to 33.33 g/m^3d methane yield decreased from 0.25 to 0.19 $m^3CH_4/kgCOD_{removed}$, respectively in the AMCBR reactor (Figure 6.134). A significant linear relationship was found between the methane yields and the ERY loading rates for ERY loading rates of 8.33 and 133.33 g/m^3d (ANOVA), (R^2=0.88, F=6.12, p=0.02).

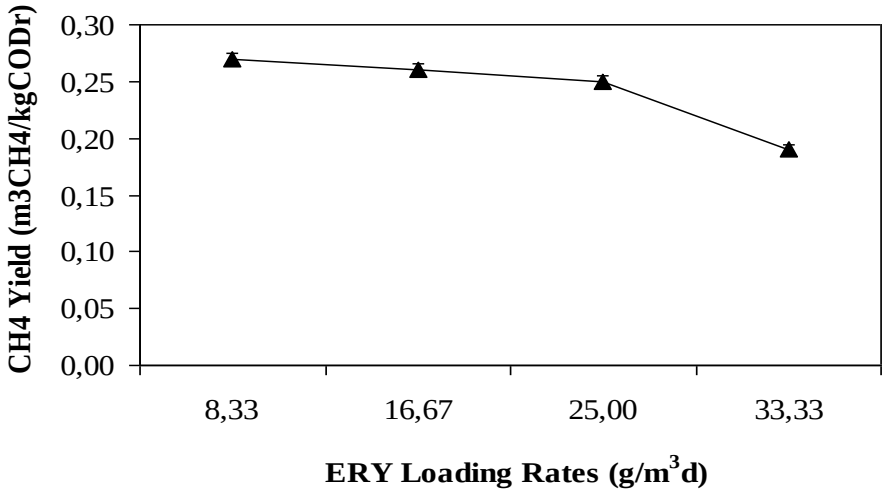

Figure 6.134 Effects of increasing ERY loading rates on the gas production, methane content in the ABFR reactor

The methane yields obtained in our study are similar in comparison to the yield performances of methane in the studies given below: In the study by Nandy and Kaul, (2001), 0.26-0.34 $m^3CH_4/kgCOD_{removed}$ methane yields was observed for the anaerobic degradation of 200 mg/L TYL in herbal pharmaceutical wastewater after 2 day HRT. Similarly, a lower methane yield value (0.20 $m^3CH_4/kgCOD_{removed}$) was obtained in the anaerobic treatment of chemical synthesis-based pharmaceutical wastewater at a HRT of 1.98 days (Ince et al., 2002). The lower methane yields in the studies mentioned above could be due to the type of anaerobic microorganism and to the operational conditions.

6.3.5.4 Variation of pH, TVFA in Compartments of the ABFR Reactor at Increasing ERY Loading Rates

Optimum pH for anaerobic activity is in the range between 6.5 and 8.0 (Speece, 1996). The pH value is considered as one of the important factors affecting the behavior and fate of antibiotics in an environment (Rubert and Pedersen, 2006; Shaojun et al., 2008). Figure 6.135 shows the pH variation in sampling points of the AMCBR at increasing ERY loading rates. The pH values were lower in the 1st sampling point than all of the other sampling points. The ERY loading rates was increased from 8.33 to 33.33 g/m^3d in the AMCBR reactor, the pH in the 1st sampling point dropped from 7.00 to 7.21 due to the increased acidogenic activity. As the ERY loading rates were increased from 8.33, 16.67, 25 to 33.33 g/m^3d, pH values were found as 7.32, 7.45, 7.55 and 7.20, respectively in 2nd sampling point (Figure 6.135). The pH values in the 3rd sampling point of the ABFR reactor varied between 7.45, 7.50, 7.45 and 7.30 at the same ERY loadings, respectively. As shown in Figure 6.135, the pH values were found as 7.50, 7.55, 7.55 and 7.50, respectively, in the 4th sampling point of the ABFR reactor at OTC loading rates of 8.33, 16.67, 25 and 33.33 g/m^3d. The effluent pH values varied between 7.60, 7.65, 7.60 and 7.65 at ERY loading rates of 8.33, 16.67, 25 and 33.33 g/m^3d, respectively in the 5th sampling point of ABFR reactor. In theory, the pH in 1st compartment should be lower than in compartments 2nd, 3rd, and effluent due to horizontal separation of

acidogenesis and methanogenesis in a high rate reactor namely ABFR (Nachaiyasit and Stuckey, 1997).

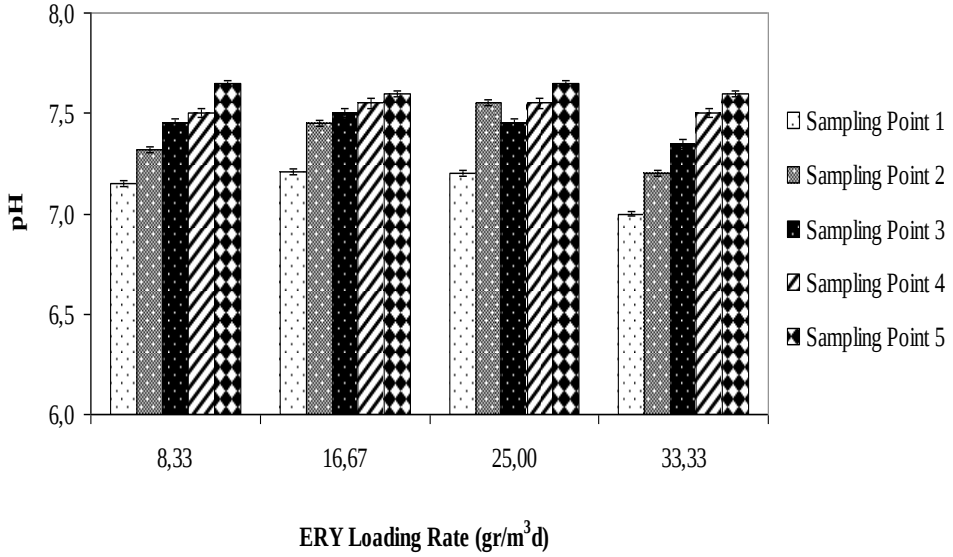

Figure 6.135 Variations of pH in the ABFR reactor at increasing ERY loading rates

Figure 6.136 shows the variations of TVFA concentrations in the all sampling points of the ABFR reactor at increasing ERY loading rates. The TVFA concentrations in the 1st sampling point decreased from 1060, 950, 875 to 705 mg/L for the ERY loading rates increasing from 8.33, 16.67, 25 to 33.33 g/m^{3}d, respectively. The TVFA concentrations decreased from 850, 654, 500 to 305 mg/L at the same ERY loadings, respectively in the 2nd sampling point of the ABFR reactor. The ERY loading rates were increased from 8.33, 16.67, 25 to 33.33 g/m^{3}d the TVFA concentrations varying between 462, 614, 250 and 186 mg/L, respectively in the 3rd sampling point of the ABFR reactor (Figure 6.136). As shown in Figure 6.136, the effluent TVFA concentrations were measured as 200, 150, 125, 98 mg/L at the same ERY loadings, respectively in the 4th sampling point. As shown in Figure 6.136, TVFA concentrations were detected as 85, 50, 30, 30 mg/L in the 5th sampling point of the ABFR respectively, for the ERY loading rates given above. The minimum TVFA concentration in the effluent of the ABFR reactor was measured between 30-85 mg/L for the ERY loading rates between 8.33 and 33.33 g/m^{3}d, respectively (see Figure 6.136). A strong linear correlation between TVFA

concentrations and ERY loading rates was observed in the 1st and 2nd compartments for ERY loading rates of 8.33 and 133.33 g/m^{3}d (ANOVA) (R^2=0.95; F=3.85, p=0.01).

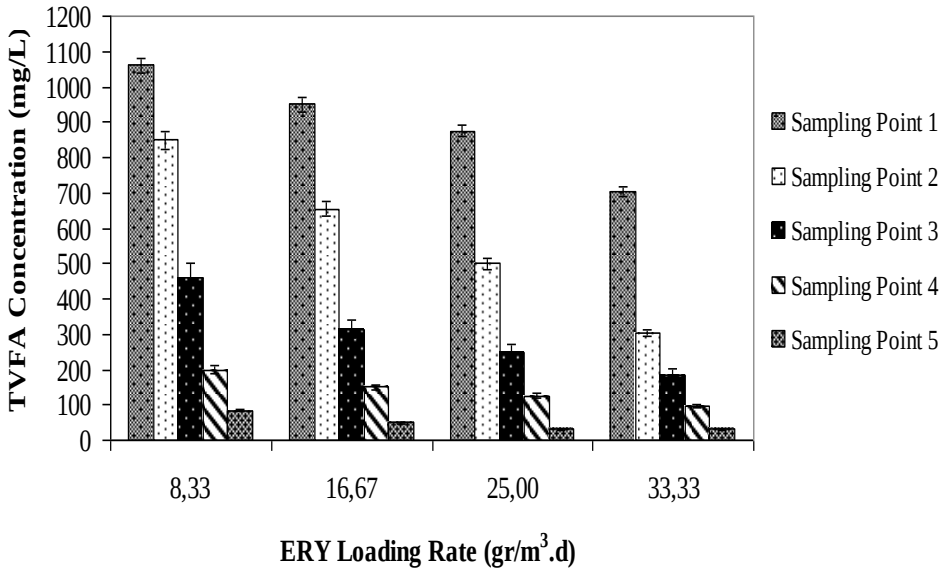

Figure 6.136 Variations of TVFA concentration in the ABFR reactor at increasing ERY loading rates

The results of this study showed that the ERY loadings affected the TVFA production during anaerobic degradation of pharmaceutical wastewater. In a study performed by Shimada et al., (2011) 8.9-340 mg/L TVFA concentrations were obtained at a HRT of 1.67 days in an ASBR reactor at influent TYL concentrations varying between 1.67 and 167 mg/L. In our study TVFA productions were 705-1060 mg/L, 305-850 mg/L, 186-462 mg/L, 98-200 mg/L and 30-85 mg/L in an 1st, 2nd, 3rd, 4th and 5th sampling points of the AMCBR reactor for ERY loading rates of 8.33 and 33.33 g/m^{3}d. In this study the TVFA productions are comparable higher than those aforementioned studies.

6.3.5.5 Variation of HCO_3 and TVFA/HCO_3 Ratio in Compartments of the ABFR Reactor at Increasing ERY Loading Rates

The HCO_3 alkalinity in all sampling point s of the ABFR reactor at increasing TYL concentrations (from 50, 100 and 150 up to 200 mg/L) was shown in Figure 6.137. The HCO_3 alkalinity concentrations remained between 2400, 2500, 2642 and 2430 mg/L in the 1st sampling point of ABFR at increasing ERY loading rates (see Figure 6.137). The HCO_3 alkalinity concentration in the 1st sampling point was lower than the other sampling points. The HCO_3 alkalinity concentrations were found as 2654, 2765, 2800 and 2600 mg/L, at TYL loading rates of 8.33, 16.67, 25.00 and 33.33 g/m^3d, respectively in the 2nd sampling point (Figure 6.137). When the ERY loading rates were increased from 8.33, 16.67, 25.00 to 33.33 g/m^3d, the HCO_3 alkalinity concentrations were observed as 2750, 2900, 3000 and 2752 mg/L, respectively in the 3rd sampling point of the ABFR reactor. Similarly, the HCO_3 alkalinity concentrations also were found as 2850, 3000, 2900, 2915 mg/L respectively in the 4th sampling point. The HCO_3 concentrations were determined as 3200, 3100, 3215 and 3100 mg/L, respectively, at the same TYL loading rates in the 5th sampling point (see Figure 6.137). A significant linear correlation between HCO_3 alkalinity and increasing AMX loading rate was not observed (ANOVA), (R^2=0.27, F=0.69, p=0.49) (for 1st sampling point).A significant linear relationship was found between ERY loadings 8.33, 16.67, 25 and 33.33 g/m^3d and HCO_3 alkalinity (ANOVA), (R^2= 0.90, F = 14.33, p = 0.06) (for 2nd sampling point); (R^2= 0.80, F = 7.77, p = 0.11) (for 3rd sampling point); (R^2= 0.96, F = 56.31, p = 0.02) (for 4th and 5th sampling points).

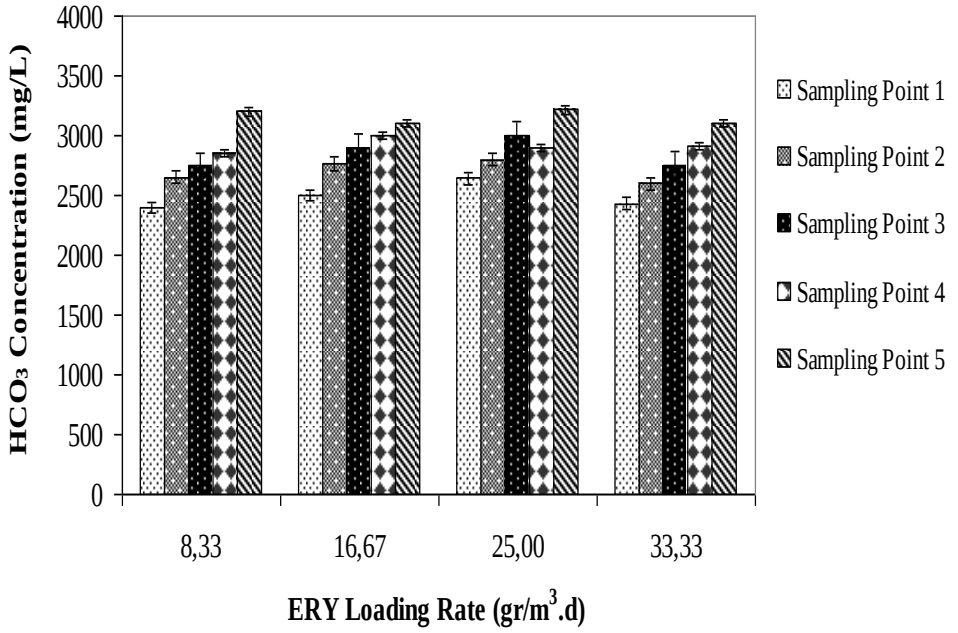

Figure 6.137 Variations of HCO_3 concentration in the ABFR at increasing ERY loading rates

Another stability parameter for anaerobic reactor is the ratio of TVFA to HCO_3 alkalinity, which should be less than 0.3 to 0.4 (Rincon et al., 2009). The TVFA/ HCO_3 ratio remained below the threshold of 0.4 for optimum performance (Rincon et al., 2009). The TVFA/HCO_3 alkalinity ratios were found as 0.40, 0.40, 0.33 and 0.29 respectively, at the same ERY loadings in 1st sampling point of the ABFR reactor. As shown in Figure 6.138, TVFA/HCO_3 alkalinity ratio varied between 0.32, 0.24, 0.18 and 0.12 respectively in 2nd sampling point of the ABFR reactor at increasing AMX loading rates. The ratios of TVFA/HCO_3 alkalinity were obtained as 0.20, 0.10, 0.10 and 0.10, respectively, at ERY loading rates of 8.33-16.67-25.00-33.33 g/m^{3}d in the 3rd sampling point of the ABFR reactor (Figure 6.138). TVFA/HCO_3 alkalinity ratios were obtained as 0.10, 0.05, 0.04 and 0.03, respectively in the 4th sampling point (Figure 6.138). TVFA/HCO_3 alkalinity ratio varied between 0.03, 0.02, 0.01 and 0.01 respectively in 5th sampling point of the ABFR reactor at the same ERY loadings. The TVFA/HCO_3 ratios of the ABFR reactor system in all sampling points were 0.01 and 0.40, which were much lower than 0.4 and showing high stability.

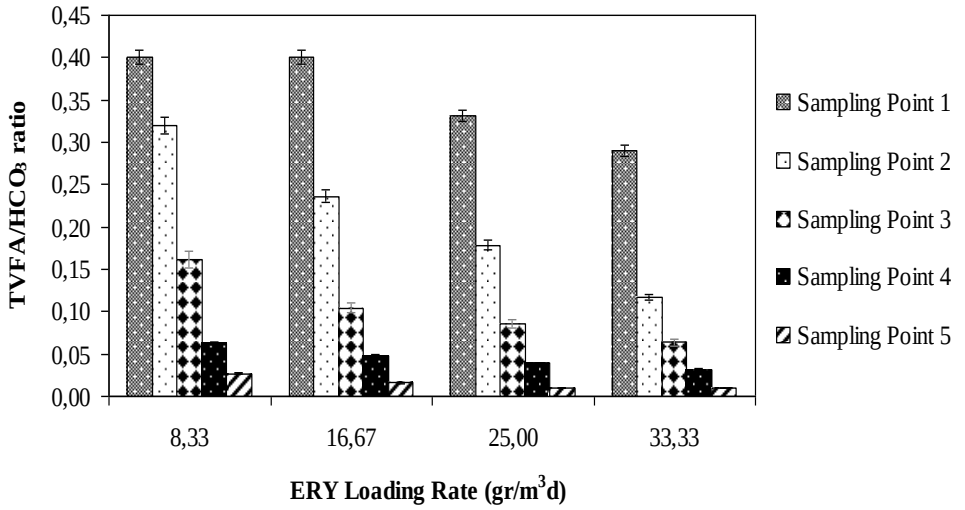

Figure 6.138 Variations of TVFA/HCO_3 ratio in the ABFR at increasing ERY loading rates

6.3.5.6 Effect of ERY Loading Rate on the COD, ERY Removal Efficiencies in the CSTR Reactor

Figures 6.139 and 6.140 illustrate the effect of increasing ERY loading rate on the COD and AMX concentrations and removal efficiencies in the CSTR reactor. The COD removal efficiency was around 83% for ERY loading rates of 8.33 and 16.67 g/m^3d in the CSTR reactor. As shown in Figure 6.139, the COD removal efficiency was 72% at an ERY loading rate of 25 g/m^3d. The COD removal efficiency remained approximately 60% until an ERY loading rate of 33.33 g/m^3d. The effluent COD concentrations were increased from 60, 60, 250 to 500 mg/L at AMX loading rates of 8.33, 16.67, 25 and 33.33 g/m^3d, respectively in the effluent of the aerobic CSTR reactor system (see Figure 6.139). The optimum ERY loadings were found as 8.33 and 16.67 g/m^3d, respectively, for maximum COD removal efficiency of 83% in the effluent of the CSTR reactor (see Figure 6.139). The minimum COD (E=60%) yield was found at an ERY loading rate of 33.33 g/m^3d.

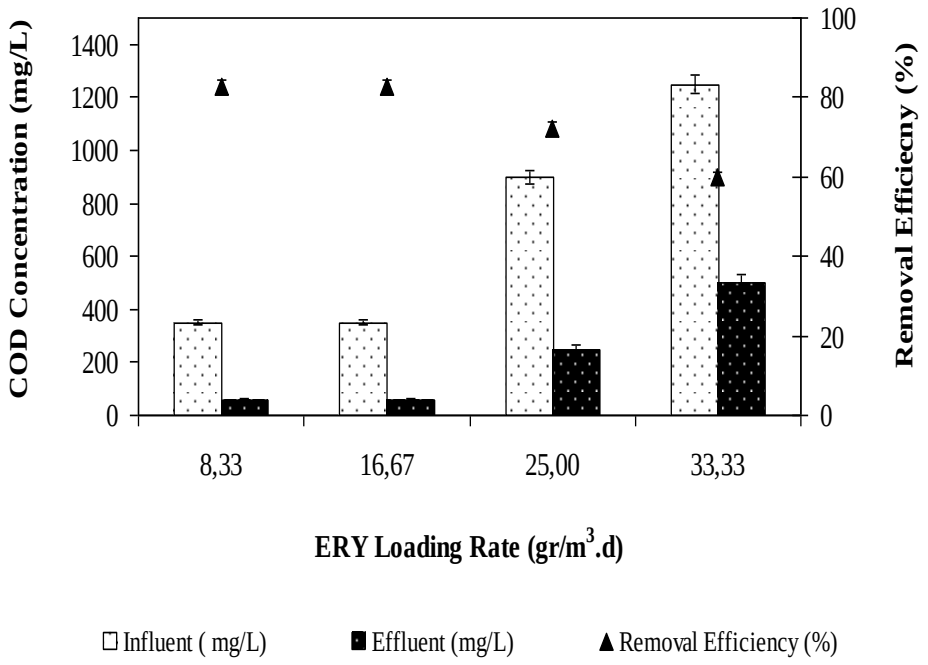

Figure 6.139 COD removal in the aerobic CSTR reactor at increasing ERY loading rates

The ERY removal efficiency was around 70% for ERY loading rates of 8.33 and 16.67 g/m^{3}d (see Figure 6.140). As shown in Figure 6.140, the ERY yields were decreased from 70%, 65% to 60% at ERY loading rates of 16.67, 25 to 33.33 g/m^{3}d respectively in the effluent of the CSTR reactor. The maximum ERY removal efficiency was around 70% for ERY loadings 8.33 and 16.67 g/m^{3}d (see Figure 6.140). The minimum ERY yield was found as 60% for ERY loading rate of 33.33 g/m^{3}d, respectively in the effluent of the CSTR reactor.

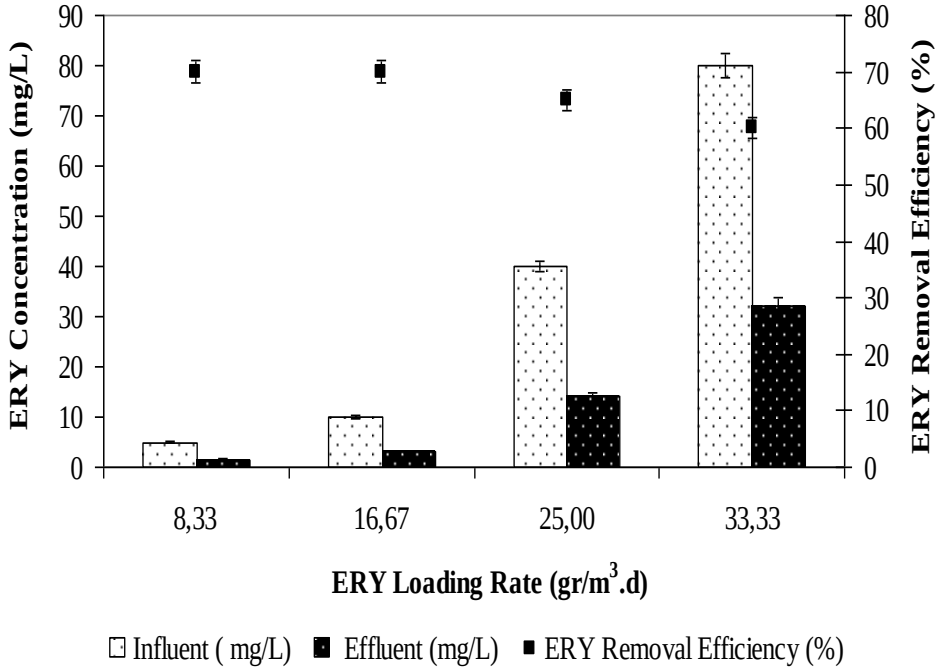

Figure 6.140 ERY removals in the aerobic CSTR reactor at increasing ERY loading rates

6.3.5.7 Treatment Efficiencies of Anaerobic/Aerobic Sequential Reactor System

The effluent from ABFR was further subjected to aerobic treatment (CSTR) to remove the residual COD. Figure 6.141 shows the overall COD and ERY removal efficiencies in anaerobic/aerobic sequential reactor system. The COD and ERY removal efficiencies were 99% and 97% at minimum ERY loading rates of 8.33 and 16.67 g/m^{3}d in overall reactor system, respectively (see Figure 6.141). The maximum COD and the ERY removal efficiency in the sequential ABFR/CSTR reactor system were measured as 99% and 97% at ERY loading rates of 8.33 and 16.67 g/m^{3}d, respectively. Total COD and ERY removal efficiencies decreased from 94% to 88% and from 91% and 84% as the ERY loading rates increased from 25 to 33.33 g/m^{3}d in sequential ABFR/CSTR reactor system (see Figure 6.141). The minimum COD and the ERY removal efficiency in sequential ABFR/CSTR reactor system were measured as 88% and 84% at an ERY loading rate of 33.33 g/m^{3}d, respectively (see Figure 6.141).

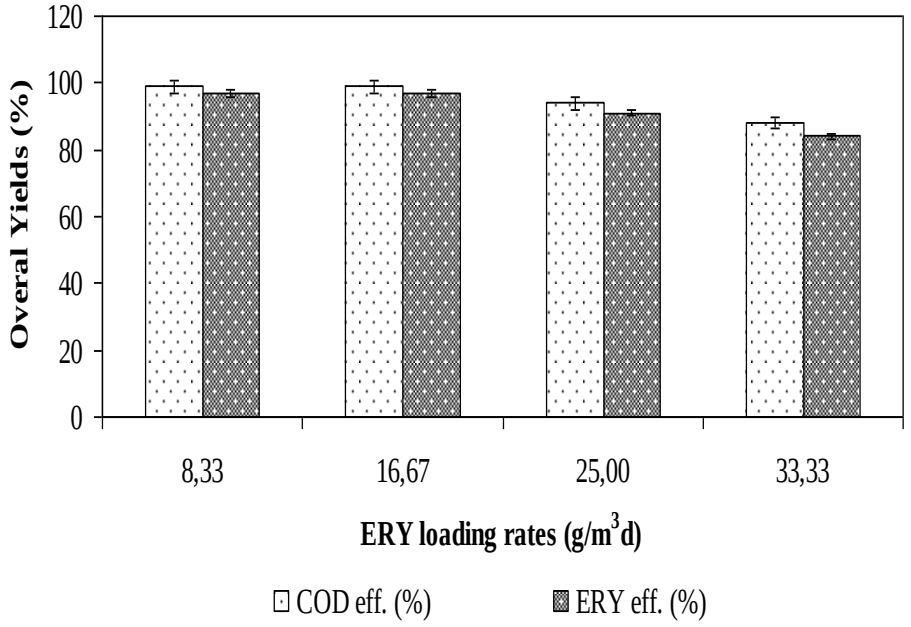

Figure 6.141 ERY and COD removal in the sequential ABFR/CSTR reactor at increasing ERY loading rates

6.3.6 Properties of the Filter Carrier (Polystyrene Ball) in the ABFR Reactor

In this step of the study, the properties of the filter (biofilm) carriers were investigated. The internal diameter and length of the filter bed were 2.6 cm and 43 cm, respectively (see Figure 6.142 b). This filter bed has holes through which liquid can flow between the upper and lower chambers of the anaerobic ABFR reactor. The filter bed is made from polystyrene balls with a porosity of 42.2%, void ratio of 0.73 and filter depth of 12.5 cm (see Figure 6.142 c). It forms a floating granular filter-‘‘Buoyant Filter’’. Biofilm were formed on the carrier particles (polystyrene balls) in the anaerobic ABFR reactor system as schematically depicted in Section 5.2.2 (Material and Methods, see Figure 5.4). The physical properties of the polystyrene balls are shown in Table 6.30 while the picture of these polystyrene balls is given Figure 6.142.

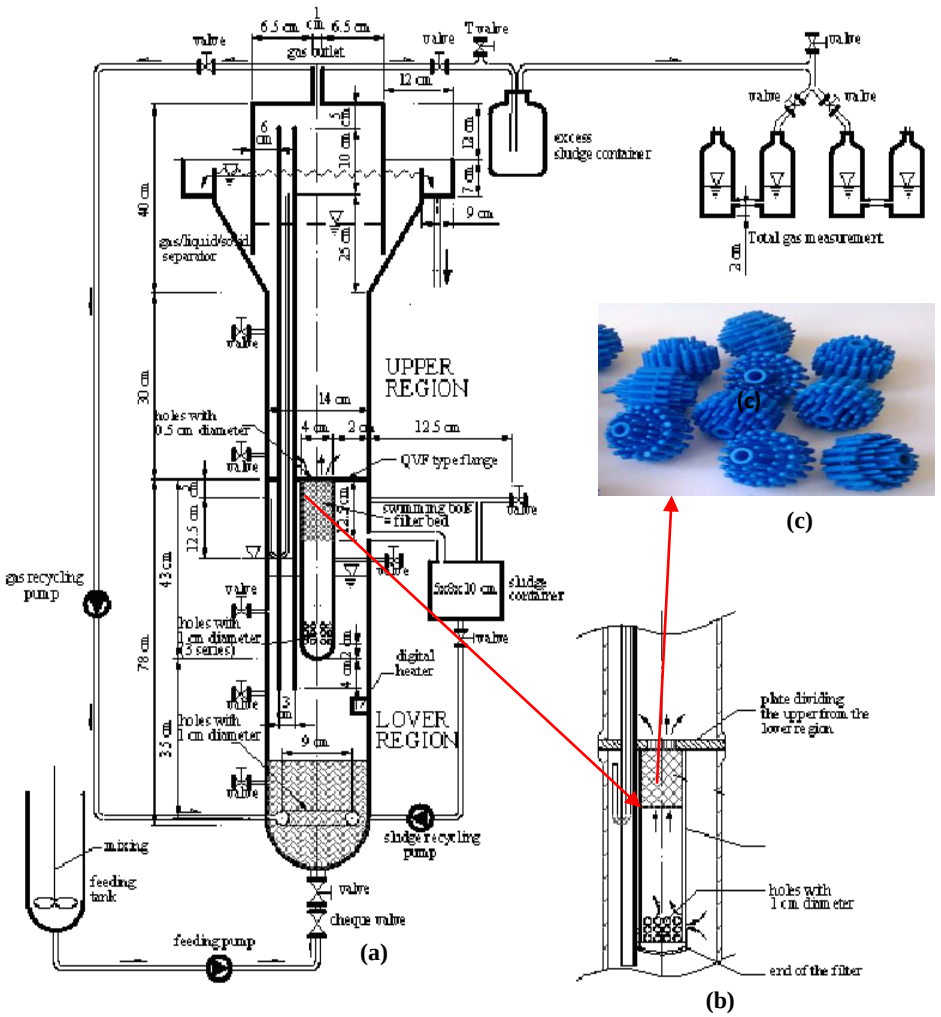

Figure 6.142 **(a)** Experimental ABFR reactor configuration **(b)** filter module inside of ABFR reactor and **(c)** Filter (biofilm) carrier (polystyrene ball).

Table 6.30 Physical properties of the polystyrene balls in the start-up period before addition to the filter bed in the ABFR reactor

Properties	**Unit**	**Values**
Internal diameter for filter carrier	**cm**	1.00
Outer diameter for filter carrier	**cm**	1.50
Total diameter for filter carrier	**cm**	2.50
Density	**g/cm^3**	1.05
Structure	-	100% plastic material

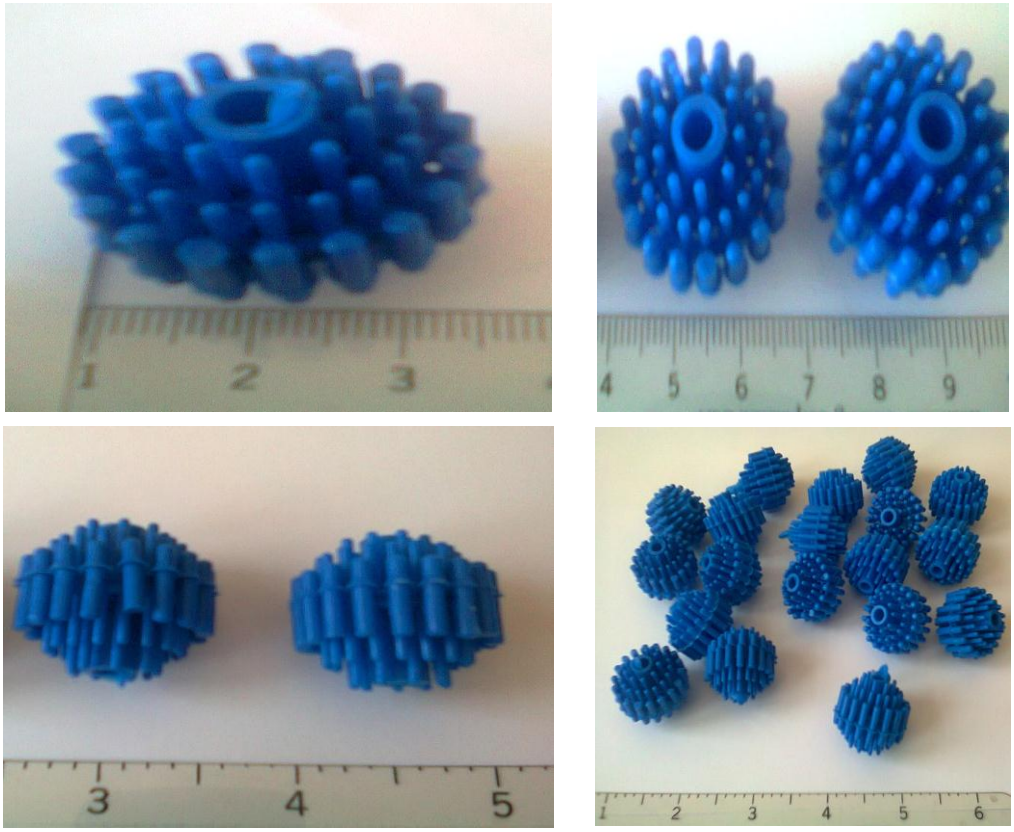

Figure 6.143 Photos of the polystyrene balls in the start-up period before adding to the filter bed in the ABFR reactor

6.3.6.1 Measurements of Volatile Suspended Solids (VSS) Concentrations in the Filter Bed in the ABFR Reactor

Volatile Suspended solids measurements were carried out in order to determine the VSS contents of the biomass developed surrounding on the polystyrene balls and in the sludge which is suspended in the filter bed in the anaerobic ABFR reactor. In the other words the total VSS concentrations in the ABFR reactor is the equal to the biomass located on the polystyrene balls and to the suspended VSS concentrations fluidized in the filter bed.

6.3.6.1.1 Measurements of Volatile Suspended Solids (VSS) Content in the Surrounding of Polystyrene Ball Carrier. Suspended solids measurements were carried out in order to determine the VSS contents on the biofilm developed on the polystyrene balls as carriers. The biofilm developed on the carriers and the liquid

inside the anaerobic ABFR reactor (see Table 6.31). The VSS content of the biofilm (biomass) were calculated averaging the results from polystyrene ball taken randomly from inside (1 times per month) the anaerobic ABFR reactor according to the procedure described in “Material and Methods”.

Table 6.31 The VSS contents of the biofilm on the carrier and the liquid inside the ABFR reactor

Operation Time	**VSS (mg/L)**		Biofilm Thickness (mm)
	Originated from biomass on the total polystyrene balls	Originated from fluidized stream	
T=0 (start-up)	0	7000	0
T=1.5 year (steady state)	30000	25000	2
Total	**55000**		

6.3.6.1.2 Estimation of the of Attached Biomass on the Polystyrene Balls in the Filter Bed of the ABFR Reactor and Comparison of the Tentative and Theoretical VSS Concentrations in the Polystyrene Balls. Figure 6.144 illustrated the VSS concentrations for 30-50 days of the start-up period. At the start-up period (on days between 30 and 50), the VSS concentrations were zero mg/L. After the start-up period, the AMCBR was operated throughout 550 days (1.5 year) at six different HRTs (Figure 6.144). The VSS concentration was 700 mg/L for operation days of 100, respectively. On days between 110 and 160, the VSS concentration was 850 mg/L, respectively on the polystyrene balls in the ABFR reactor. The VSS concentrations were between 1102 and 1300 mg/L for operation times of 200-260 days, respectively, on the polystyrene balls in the ABFR reactor. When the VSS concentrations were increased from 1400, 1486, 1512 mg/L, respectively, at 360, 410, 460 days on the polystyrene balls in the ABFR reactor (Figure 6.144). The result of the measurement, performed on the steady state conditions, gave the following results: VSS=1720 mg/L which is a relatively high for an anaerobic ABFR reactor on the 1 polystyrene ball on days 550 (see Eq. 6.2). The VSS concentration on the total polystyrene balls (32 numbers) in the anaerobic ABFR reactor was 55000 mg/L on days 550.

$$VSS_{biofilm} = 1720 \frac{mg}{polystyrene\ ball} \times 32\ polystyrene\ balls = 55000\ mg \quad \text{Eq. (6.2)}$$

Where:

"1720 mg/polystyrene ball" is measurement of biomass on the biocarrier (steady state conditions) and "32 polystyrene balls" is estimated number of polystyrene balls in the ABFR reactor.

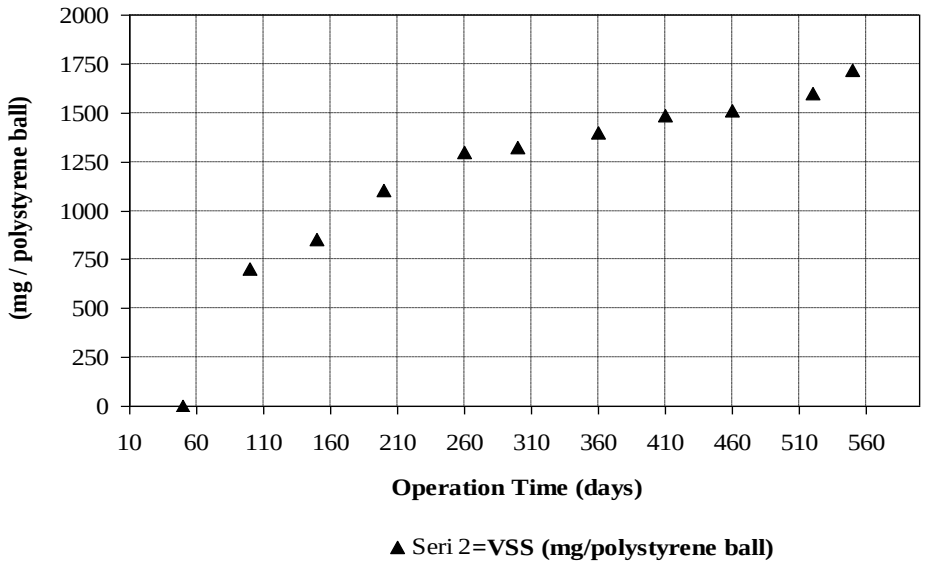

Figure 6.144 Biomass attached on the polystyrene ball carrier in the ABFR reactor (filtered 0.45 μm).

The comparison of the empty polystyrene ball and coated with biomass polystyrene ball are shown below in Figure 6.145 and Table 6.32. As it can be seen the growth of the biofilm was quite irregular among the polystyrene ball carrier a lower thickness of the biofilm on some polystyrene balls.

Table 6.32 Comparison of the empty polystyrene ball and coated with biomass polystyrene ball in the ABFR reactor

Properties	**empty polystyrene ball**	**coated with biomass polystyrene ball**
Total diameter (cm)	2.50	3.00
Density (g/cm^3)	1.05	1.20
Structure	100% plastic material	

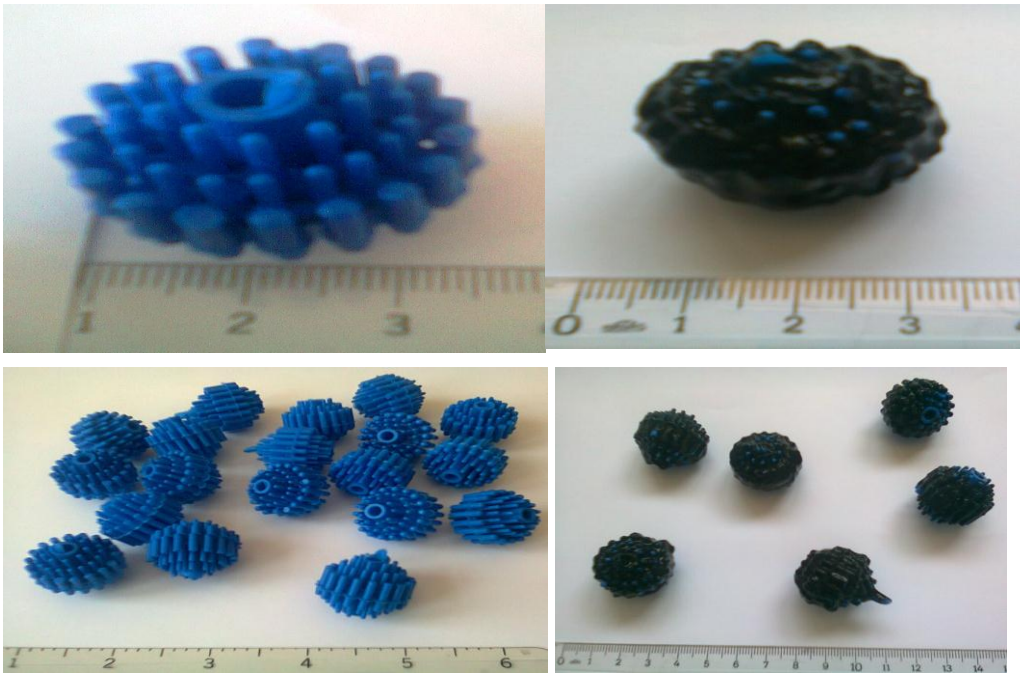

Figure 6.145 Comparison of the biocarrier before starting the anaerobic ABFR reactor (left) and after steady-state condition (right)

6.4 Continuous Studies for real raw pharmaceutical wastewater

6.4.1 Effect of Increasing OTC and AMX Loadings on Performance of AMCBR

6.4.1.1 Effect of Increasing OTC and AMX Loadings on the COD Removal Efficiencies in the AMCBR Reactor

In this part of study, the effect of increasing OTC and AMX concentrations on COD removal efficiencies was investigated. The COD equivalents of OTC and AMX and concentration are shown in Table 6.33 and 6.34.

Table 6.33 The COD equivalents of OTC concentration

Parameters	Unit	Concentrations
Molasses-COD concentration	mg/L	15102
OTC *and AMX* concentration	mg/L	65
COD equivalent of OTC and AMX	mg/L	33
Total COD concentration	mg/L	15135

As the OTC and AMX loading rates were increased from 14.44, 28.89 to 43.33 g/m^{3}d effluent COD concentrations increased from 2065, 3027 to 4644 mg/L, respectively in the AMCBR reactor system (Table 6.34). As shown in Table 6.34, the COD removal efficiency was 85% at an OTC and AMX loading rate of 14.44 g/m^{3}d. The effluent COD concentration was 3027 mg/L resulting a COD removal efficiency of 80% at OTC and AMX loading rate of 28.89 g/m^{3}d. After this OTC and AMX loading rate (28.89 g/m^3.d) the COD removal efficiency rapidly decreased from 80% to 72% corresponding to OTC and AMX loading rate of 43.33 g/m^{3}d. The maximum COD removal efficiency of 85% the OTC and AMX loading rate and OTC and AMX concentration were found as 14.44 g/m^{3}d and 50 mg/L, respectively, in the effluent of the AMCBR reactor (see Table 6.34). The minimum COD (E=72%) removal efficiency was found at OTC and AMX loading rate of 43.33 g/m^{3}d.

In our study a significant linear relationship was not found between the COD yields for the OTC and AMX loading rates at between 14.44 and 43.33 g/m^{3}d (ANOVA), (R^2=0.76, F=6.48, p=0.1).These results shows that OTC and AMX degrading methanogens produced methane through the utilization of OTC as co-substrate together with molasses-COD used as primary carbon and energy source.

Table 6.34 COD and OTC-AMX yields in the AMCBR at three different OTC and AMX loading

Parameter	**AMCBR reactor**		
	OTC-AMX loading (g/m^{3}d)		
	14.44	**28.89**	**43.33**
Influent COD concentration (mg/L)	15135	15135	15135
Effluent COD concentration (mg/L)	2065	3027	4644
COD removal efficiency (%)	86	80	69
Influent OTC and AMX concentration (mg/L)	65	65	65
Effluent OTC and AMX concentration (mg/L)	7.80	12.35	21.25
OTC-AMX removal efficiency (%)	88	82	68

6.4.1.2 Effect of OTC and AMX Loading Rate on the Total and Methane Gas Production in the AMCBR Reactor

The total and methane gas production rates and methane percentages in AMCBR reactor are shown in Figure 6.146. The total gas, methane gas productions and methane contents were approximately 2.5-3.08 L/d, 1.0-1.6 L/d and 40%-52%, respectively, for OTC and AMX loadings varying between 14.44 and 43.33 g/m^3d. The maximum total gas, methane gas productions and methane content were found as 3.08 L/d and 1.6 L/d and 52%, respectively, at OTC and AMX loading rate of 14.44 g/m^3d. After this loading rate, the total gas, methane gas productions and methane percentage decreased. A significant linear relationship was found between the total and methane gas productions and the OTC and AMX loading rates (only for between 14.44-43.33 g/m^3d) (ANOVA), (R^2=0.91, F=4.80, p=0.01 (for total gas); R^2=0.90, F=5.03, p=0.02 (for CH_4). Similarly, a linear relationship was found between the methane content and the OTC and AMX loading rates (Only for between 14.44-43.33 g/m^3d) and this relationship is significant (ANOVA), (R^2=0.88, F=6.06, p=0.01).

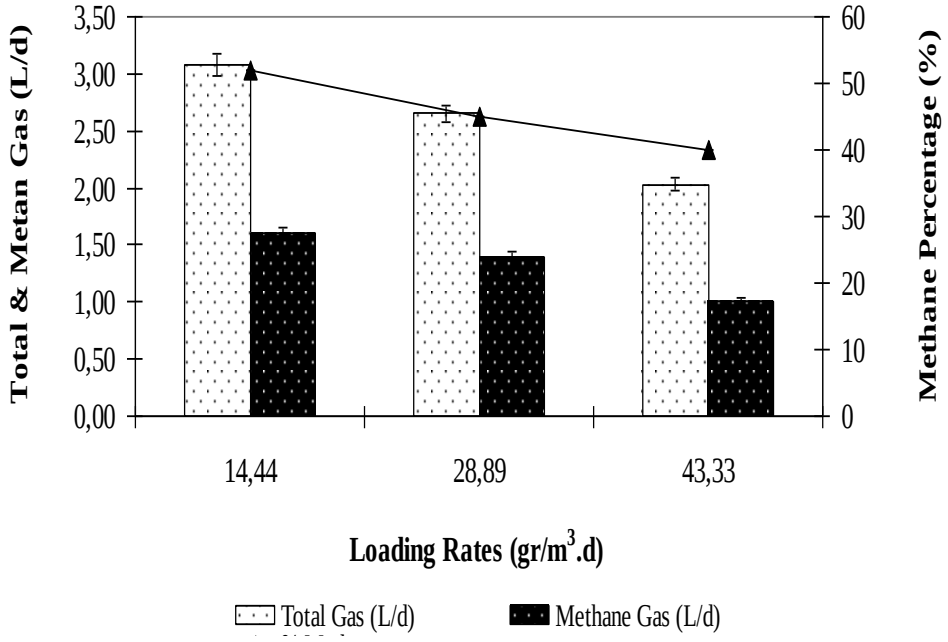

Figure 6.146 The effect of OTC and AMX loading rate on total, methane gas production and methane percentage in the AMCBR reactor

6.4.1.3 Variations of pH, TVFA, HCO_3 Alk., TVFA/HCO_3 Alk. Ratio in the AMCBR at Increasing OTC and AMX Loading Rates

Figure 6.147 shows the pH, TVFA, HCO_3 Alk., TVFA/HCO_3 Alk. ratio variation in compartments of the AMCBR at increasing OTC loading rates. As shown in Figure 6.147 (a), the OTC and AMX loading rates were increased from 14.44 to 43.33 g/m^3d in the AMCBR reactor, the pH in the 1st compartment dropped from 7.18 to 6.87 due to the increased acidogenic activity. As the OTC and AMX loading rates were increased from 14.44, 28.89 to 43.33 g/m3d, pH values decreased from 7.50, 7.45 to 7.30, respectively in 2nd compartment (Figure 6.147(a)). The pH values in the 3rd compartment of the AMCBR reactor varied between 7.55, 7.45 and 7.50 at the same OTC and AMX loadings, respectively. As shown in Figure 6.147, the pH values were found as 7.57, 7.60 and 7.55, respectively, in the effluent of the AMCBR reactor at OTC and AMX loading rates of 14.44, 28.89 and 43.33 g/m3d.

Figure 6.147 (b) shows the TVFA production in the different compartments. The TVFA concentrations in the 1st compartment decreased from 945, 800 to 750 mg/L for the OTC loading rates increasing from 14.44, 28.89 to 43.33 g/m^3d, respectively. As shown in Figure 6.147, the TVFA concentrations decreased from 500, 412 to 325 mg/L at the same OTC and AMX loadings, respectively in the 2nd compartment of the AMCBR reactor. The OTC and AMX loading rates were increased from 14.44, 28.89 to 43.33 g/m^3d the TVFA concentrations varying between 100, 55 and 20 mg/L, respectively in the 3rd compartment of the AMCBR reactor (Figure 6.147(b)). The TVFA concentrations were measured as 40, 15 and 5 mg/L at the same OTC loadings, respectively in the effluent of the AMCBR reactor. A significant linear relationship was found between OTC and AMX loading rates 14.44 and 43.33 g/m^3d and TVFA production (ANOVA), (R^2= 0.88, F=5.14, p=0.02). A strong linear correlation between TVFA concentrations and OTC loading rates was observed in the 1st and 2nd compartments for OTC and AMX loading rates of 14.44 and 43.33 g/m^3d (ANOVA) (R^2=0.96; F=3.89, p=0.01).

The HCO_3, TVFA/HCO_3 ratio variations in all compartments of the AMCBR reactor at increasing OTC and AMX loadings (from 14.44 up to 43.33 g/m^3d) were shown in Figure 6.147. The HCO_3 alkalinity concentrations remained between 2000, 2100 and 2300 mg/L in the 1st compartment of AMCBR at increasing OTC and AMX loading rates (see Figure 6.147 (c)). The HCO_3 alkalinity concentration in the 1st compartment was lower than the other compartments. The HCO_3 alkalinity concentrations were found as 2350, 2500 and 2600 mg/L, at OTC and AMX loading rates of 14.44, 28.89 and 43.33g/m^3d, respectively in the 2nd compartment **(**Figure 6.147 (c)**)**. When the OTC and AMX loading rates were increased from 14.44, 28.89 to 43.33g/m^3d, the HCO_3 alkalinity concentrations were determined as 2565, 2700 and 2600 mg/L, respectively in the 3rd compartment of the AMCBR reactor. Similarly, the HCO_3 alkalinity concentrations also were found as 2800, 2900, 2970 mg/L respectively in the effluent. A significant linear correlation between HCO_3 alkalinity and increasing OTC and AMX loading rate was not observed (ANOVA), (R^2=0.27, F=0.69, p=0.49) (for 1st sampling point).A significant linear relationship was found between OTC and AMX loadings 14.44, 28.89 to 43.33 g/m^3d and HCO_3 alkalinity (ANOVA), (R^2= 0.90, F = 14.33, p = 0.06) (for 2nd sampling point); (R^2= 0.80, F = 7.77, p = 0.11) (for 3rd sampling point); (R^2= 0.96, F = 56.31, p = 0.02) (for 4th and 5th sampling points).

TVFA/HCO_3 ratio gives necessary information to determine the stability of the anaerobic reactor. When the TVFA/HCO_3 ratio is lower than 0.4, the reactor is stable (Behling et al, 1997). When the TVFA/ HCO_3 ratio is lower than 0.8, the reactor system is moderately stable or unstable (Behling et al, 1997). As shown in Figure 6.147 (d), this ratio varied between 0.002 and 0.39 in every compartment of AMCBR at increasing OTC and AMX loadings. These results indicated that AMCBR reactor was stable at increasing OTC and AMX loading because the TVFA/HCO_3 ratios in the effluent and in the compartments were lower than 0.4.

(a) Variations of pH

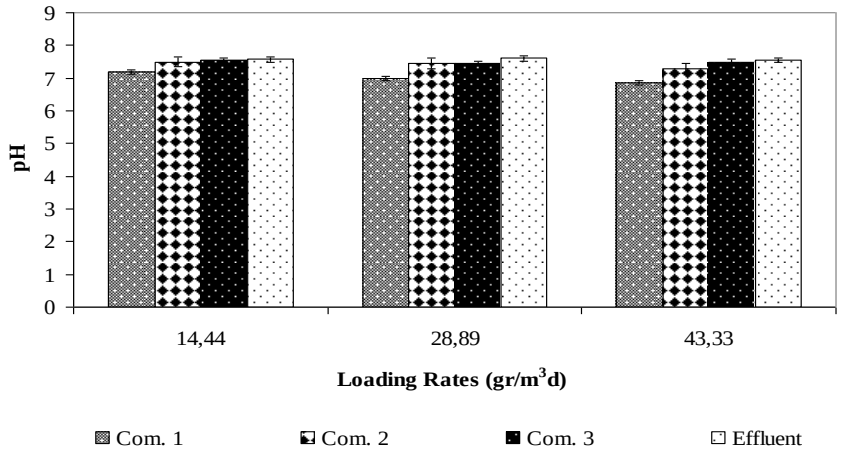

(b) Variations of TVFA

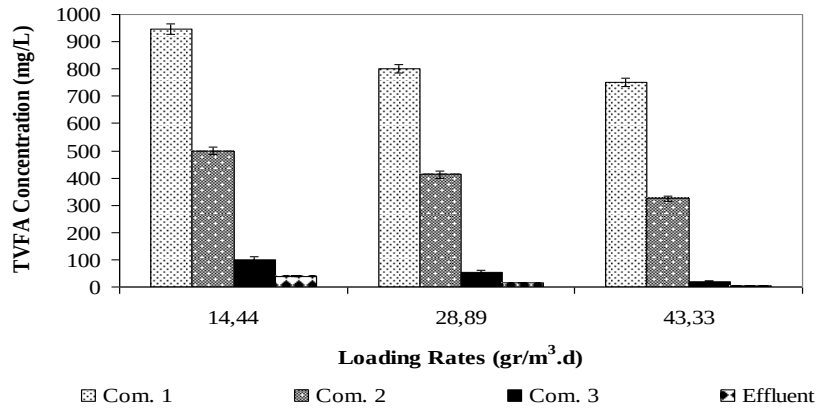

(c) Variations of HCO_3 Alk.

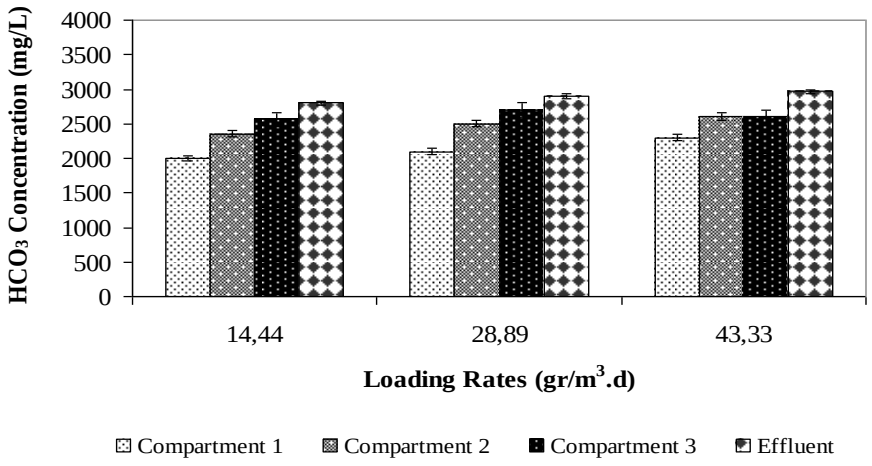

(d) Variations of $TVFA/HCO_3$ Alk. ratio

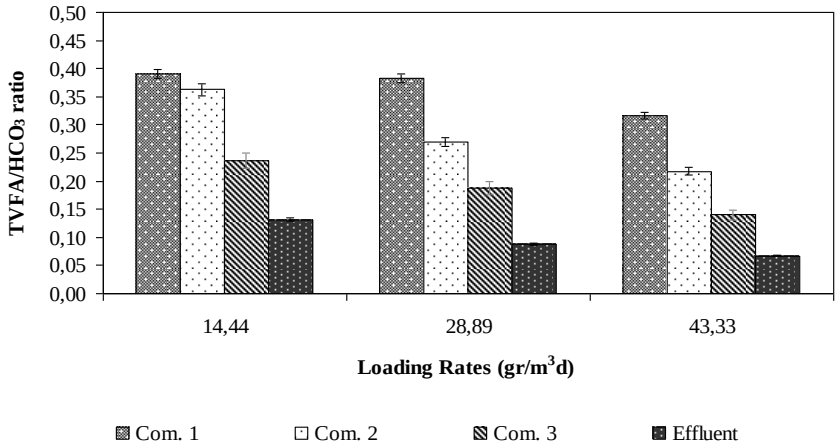

Figure 6.147 Variations of pH (a); TVFA (b); HCO_3 Alk. (c); and $TVFA/HCO_3$ Alk. ratio (d) in AMCBR at increasing OTC and AMX loading rates

6.4.2 Effect of Increasing AMX Concentration on Performance of ABFR

6.4.2.1 Effect of Increasing AMX Concentration on the COD Removal Efficiencies in the ABFR Reactor

The ABFR reactor was operated continuously for 56 days. Table 6.35 illustrated the influent, effluent COD, OTC and AMX concentrations and COD, OTC and AMX removal efficiency of ABFR reactor during the experiment period. The operation of the ABFR reactor with OTC and AMX was started at an influent OTC and AMX concentration of 65 mg/L and an AMX loading rate of 8.33 g/m^3d. The COD equivalents of OTC and AMX concentration are shown in Table 6.35.

Table 6.35 The COD equivalents of OTC and AMX concentration

Parameters	Unit	Concentrations
Molasses-COD concentration	mg/L	15102
OTC and AMX concentration	mg/L	65
COD equivalent of AMX	mg/L	33
Total COD concentration	mg/L	15135

As shown in Table 6.36, the effluent COD concentrations were increased from 2753, 4268 to 5639 mg/L at OTC and AMX loading rates of 5.42, 10.83, 16.25 g/m^{3}d, respectively in the effluent of the ABFR reactor. The COD removal efficiency was 80% at OTC loading rate of 5.42 g/m^{3}d. When the AMX loading rate was increased to 10.83 g/m^{3}d, the COD removal efficiency decreased to 72%. After this OTC and AMX concentration (65 mg/L), COD removal efficiency decreased rapidly from 72% to 66% (see Table 6.36). The effluent COD concentration and removal efficiency were measured as 5639 mg/L and 66%, respectively, at a maximum OTC and AMX loading rate of 16.25 g/m^{3}d, in the anaerobic ABFR reactor (see Table 6.36). The optimum OTC and AMX loading rates were found as 5.42 g/m^{3}d, respectively, for maximum COD removal efficiency of 80% in the effluent of the ABFR reactor (see Table 6.36). The minimum COD (E=66%) yield was found at an OTC and AMX loading rate of 16.25 g/m^{3}d.The results obtained in this study showed that OTC and AMX could be used as carbon source together with molasses-COD with high treatment efficiencies in the ABFR reactor.

A significant linear relationship was found between the COD yields and the OTC and AMX loading rates (OTC and AMX loading rates between 5.42, 10.83, 16.25 g/m^{3}d) (ANOVA), (R^2=0.85, F=10.81, p=0.08).

Table 6.36 COD and AMX yields in ABFR reactor at three different AMX loading rates

Parameter	**ABFR reactor**		
	OTC-AMX loading (g/m^3.d)		
	5.42	**10.83**	**16.25**
Influent COD concentration (mg/L)	15135	15135	15135
Effluent COD concentration (mg/L)	2753	4268	5639
COD removal efficiency (%)	82	72	63
Influent AMX concentration (mg/L)	65	65	65
Effluent AMX concentration (mg/L)	9.50	16.25	25.50
AMX removal efficiency (%)	85	75	61

6.4.2.2 Effect of OTC and AMX Loading Rate on the Biogas Production and CH_4 Content in the ABFR Reactor

Figure 6.148 show the behavior of biogas production and methane contents of the ABFR reactor system. The maximum total gas, methane gas productions and methane content were found about 3.42 L/d, 1.71 L/d and 50%, respectively at OTC and AMX loading rates of 5.42 g/m^{3}d (see Figure 6.148). As the OTC and AMX loading rates were increased from 10.83 to 16.25 g/m^{3}d, methane contents decreased from 44% to 38%, respectively (Figure 6.148). The total gas, methane gas productions were obtained as 2.46 L/d and 1.08 L/d, at an OTC and AMX loading rate of 10.83 g/m^{3}d, respectively (see Figure 6.148). When the OTC and AMX loading rates were increased from 10.83 to 16.25 g/m^{3}d, the daily total gas, methane gas productions and methane content were determined as 2.45 L/d, 0.93 L/d and 38%, respectively in the ABFR system at an OTC and AMX loading rate of 16.25 g/m^{3}d. The decrease in methane content of biogas is generally observed when the rate of acid formation exceeds the rate of break down to methane at high loading rates (Kim et al., 2007).

A significant linear relationship was found between the biogas productions and the OTC and AMX loading rates (5.42, 10.83, 16.25 g/m^{3}d) (ANOVA), (R^2=0.80, F=8.00, p=0.01) (for total gas). (R^2=0.90, F=17.64, p=0.05 (for methane gas). Similarly, a linear relationship was found between the methane content and the OTC and AMX loading rates (5.42, 10.83, 16.25 g/m^{3}d) and this relationship is significant (ANOVA), (R^2=0.89, F=17.70, p=0.05).

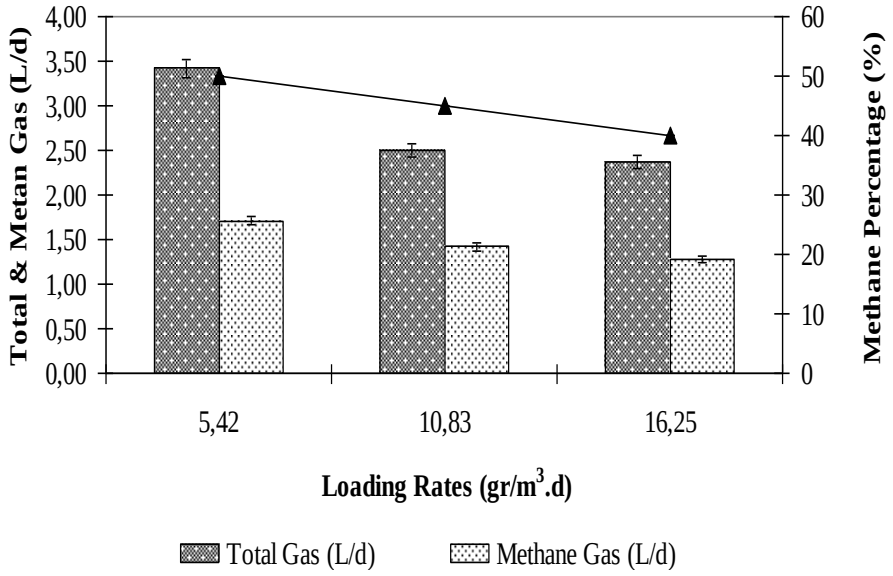

Figure 6.148 The effect of AMX loading rate on total, methane gas production and methane content in the ABFR reactor

6.4.2.3 Variations of pH, TVFA, HCO_3 Alk., TVFA/HCO_3 Alk. Ratio in the ABFR at Increasing OTC and AMX Loading Rates

The pH profiles for the ABFR reactor at 8.33, 10.83 and 14.17 g/m^{3}d AMX loading rates are shown in Figure 6.149 (a). The AMX loading rates were increased from 5.42, 10.83 to 16.25 g/m^{3}d pH values decreased from 7.25, 7.10 to 6.80, respectively in the 1st sampling point. Similarly AMX loading rates were increased from 5.42, 10.83 to 16.25 g/m^{3}d pH values varying between 7.33, 7.41 and 7.38, respectively in the 2nd sampling point of the ABFR reactor (Figure 6.149 (a)). As shown in Figure 6.149 (a), the pH values in the 3rd and 4th sampling points of the ABFR reactor varied between 7.40-7.43-7.52 and 7.45-7.51-7.50 at AMX loading rates of 5.42, 10.83 to 16.25 g/m^{3}d, respectively. As shown in Figure 6.149 (a), the effluent pH values decreased from 7.56, 7.60 to 7.55 at AMX loadings from 5.42, 10.83 to 16.25 g/m^{3}d, respectively in the 5th sampling point of the ABFR reactor. Figure 6.149 (b) shows the TVFA concentrations in sampling points of the ABFR reactor at increasing AMX loading rates. The TVFA concentrations in the 1st sampling point were decreased from 820, 815 to 762 mg/L for the AMX loading rates increased from 5.42, 10.83 to 16.25 g/m^{3}d, respectively. The TVFA profile

demonstrated that hydrolysis and acidogenesis were the main biochemical activities occurring in the 1st and 2nd sampling points (Baloch and Akunna, 2003). The high TVFA concentrations in the anaerobic processes cause the inhibition of methanogenesis.

As shown in Figure 6.149 (b), the TVFA concentrations were decreased from 876, 683 to 576 mg/L at AMX loading rates of 8.33, 10.83 to 14.17 g/m^{3}d, respectively in the 2nd sampling point of the ABFR reactor. The AMX loading rates were increased from 5.42, 10.83 to 16.25 g/m^{3}d TVFA concentrations decreased from 662, 546 to 417 mg/L, respectively in the 3rd sampling point of the ABFR reactor (see Figure 6.149 (b)). The effluent TVFA concentrations were measured 387, 265 and 208 mg/L at AMX loading rates of 5.42, 10.83 and 16.25 g/m^{3}d, respectively in the 4th sampling point. Almost 110, 80 and 12 mg/L TVFA concentrations were detected in the 5th sampling point, respectively, for the AMX loading rates given above. The ABFR reactor stability, as evidenced by lower TVFA concentration, is one of the sensitive parameters in anaerobic reactors (Haridas et al. 2005). A significant linear relationship was found between AMX loadings 6.42, 10.83, 16.25 g/m^{3}d and TVFA productions (ANOVA), (R^2= 0.86, F = 12.28, p = 0.07) (for 1st sampling point); (R^2= 0.95, F = 38.54, p = 0.03) (for 2nd sampling point); (R^2= 0.93, F = 26.08, p = 0.04) (for 3rd sampling point); (R^2= 0.88, F = 14.88, p = 0.06) (for 4th and 5th sampling points).

An HCO_3 varying between 1000 and 5000 mg/L, was recommended for anaerobic treatment depending on COD and TVFA produced (Agdag, 2004). The HCO_3 concentrations remained between 2100, 2130 and 2412 mg/L in the 1st sampling point of ABFR at increasing AMX loading rates (see Figure 6.149 (c)). The HCO_3 concentration in the 1st sampling point was lower than the other sampling points. The HCO_3 concentrations were obtained as 2400, 2540 and 2650 mg/L, at AMX loading rates of 5.42, 10.83 and 16.25 g/m^{3}d, respectively in the 2nd sampling point **(**Figure 6.149 (c)**)**. When the AMX loading rates were increased from 5.42, 10.83 to 16.25 g/m^{3}d, the HCO_3 alkalinity concentrations were determined as 2615, 2700 and 2785 mg/L, respectively in the 3rd sampling point of the ABFR reactor. Similarly, the

HCO_3 concentrations also were found as 2800, 2905, 2985 mg/L respectively in the 4th sampling point. The HCO_3 concentrations were obtained as 2950, 3000 and 3100 mg/L, respectively, at AMX loading rates of 5.42, 10.83 and 16.25 g/m^{3}d in the 5th sampling point (see Figure 6.149 (c)). A significant linear correlation between HCO_3 alkalinity and increasing AMX loading rate was not observed (ANOVA), (R^2=0.27, F=0.69, p=0.49) (for 1st sampling point).A significant linear relationship was found between AMX loadings 5.42, 10.83, 16.25 g/m^{3}d and HCO_3 (ANOVA), (R^2= 0.90, F = 14.33, p = 0.06) (for 2nd sampling point); (R^2= 0.80, F = 7.77, p = 0.11) (for 3rd sampling point); (R^2= 0.96, F = 56.31, p = 0.02) (for 4th and 5th sampling points). The TVFA/HCO_3 alkalinity ratios were found as 0.39, 0.38 and 0.32 respectively, at AMX loading rates of 5.42, 10.83 and 16.25 g/m^{3}d in 1st sampling point of the ABFR. As shown in Figure 6.149 (d), TVFA/HCO_3 ratio varied between 0.36, 0.27 and 0.22 respectively in 2nd sampling point of the ABFR reactor at increasing AMX loading rates. The ratios of TVFA/HCO_3 were obtained as 0.24, 0.19 and 0.14, respectively, at AMX loading rates of 5.42, 10.83 and 16.25 g/m^{3}d in the 3rd sampling point of the ABFR reactor (Figure 6.149 (d)). As the AMX loading rates were increased from 5.42, 10.83 to 16.25 g/m^{3}d TVFA/HCO_3 ratio were obtained as 0.13, 0.09 and 0.07, respectively in the 4th sampling point. TVFA/HCO_3 ratio varied between 0.04, 0.03 and 0.004 respectively in the 5th sampling point The TVFA/HCO_3 ratios of the ABFR system in all sampling points were 0.004 and 0.39, which were much lower than 0.4 and showing high stability.

(a) Variations of pH

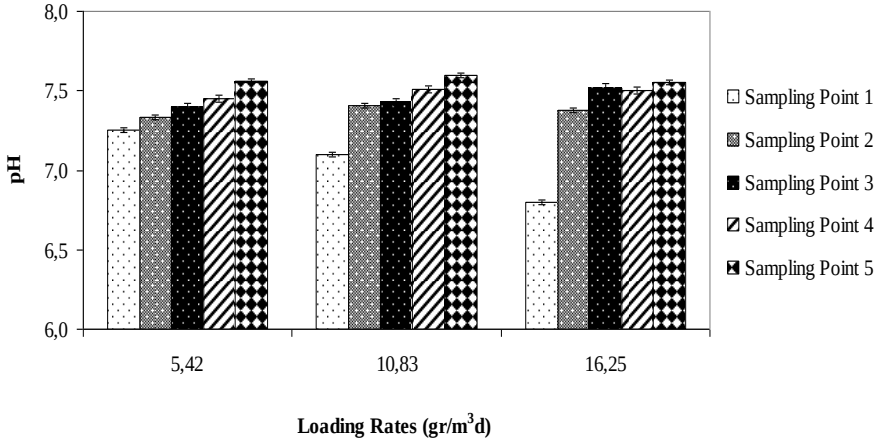

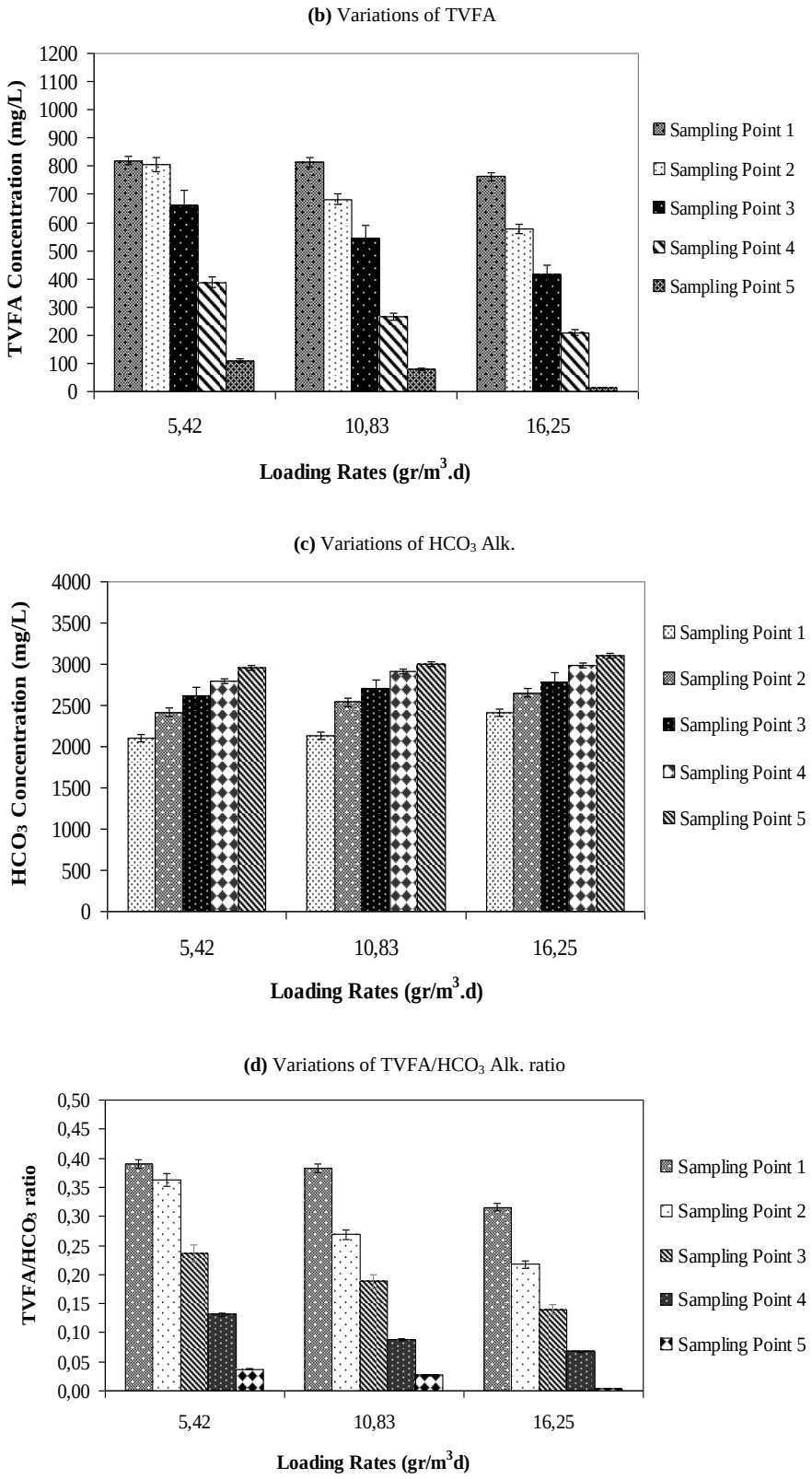

Figure 6.149 Variations of pH (a); TVFA (b); HCO_3 Alk. (c); and TVFA/HCO_3 Alk. ratio (d) in ABFR at increasing AMX loading rate

6.5 Acute Toxicity Evaluation in the Sequential AMCBR/CSTR System

Acute toxicity evaluation is an important parameter in wastewater quality monitoring as it provides an overview of the response of test organisms to all the compounds (antibiotics, drugs etc.) in the industrial wastewater (El-Deeb Ghazy and Fayed, 2011). The main objectives of this part of study include:

1. Determining of the acute toxicity of the influent of the anaerobic AMCBR reactor using Daphnia *magna* and *Vibrio fischeri (*LCK 491; strain NRRL-B-11177).

2. Determining of the acute toxicity of the effluents of the sequential treatment steps (anaerobic AMCBR and aerobic CSTR reactor) to evaluate their performances, separately.

6.5.1 Acute Toxicity Evaluation of Increasing OTC Concentrations in the Sequential AMCBR/CSTR Reactor System with Daphnia magna

Antibiotics are assessed for their acute toxicity by traditional standard tests according to established guidelines (e.g. OECD, EPA, ISO) using established laboratory organisms such as algae, water flea and other invertebrates and fish. Acute toxicities in the influent and effluents of the AMCBR and CSTR reactors were determined by acute toxicity test using *Daphnia magna*. Results were expressed as mortality percentage of the *Daphnids*. Acute toxicity was estimated in terms of EC_{50} defined as the concentration of the toxicant causing 50% reduction in activity of the water flea. The effective concentrations caused 50% mortality in *Daphnia magna* cells in synthetic pharmaceutical wastewater samples were monitored based on COD concentrations. The EC_{50} values were calculated by taking into consideration the dilution ratios based on COD. The EC_{50} values and the acute toxicity removals found in the influent, effluent of the AMCBR reactor and effluent of the CSTR reactor were given in Figures 6.150 (a-b-c), 6.151 (a-b-c) and 6.152 (a-b-c) for 50, 300 and 400 mg/L OTC concentrations, respectively.

The test samples containing initial OTC concentrations varying between 50 and 400 mg/L were diluted at 1/1, 1/2, 1/4, 1/8 and 1/16 ratios before and after anaerobic and aerobic degradation experiments. The young 10 *Daphnids* were added to each test vessel at the initiation time (t=0 hour). After 24 hour of exposure, the EC_{50} values of increasing OTC concentrations were calculated based on COD. As seen in Table 6.37 and Figure 6.150 (a-b-c) the initial EC_{50} values were obtained as 263, 242 and 197 mg/L at OTC loading rates of 22.22 g/m^3d (OTC concentration=50 mg/L), 133.33 g/m^3d (OTC concentration=300 mg/L) and 177.78 g/m^3d (OTC concentration 400 mg/L), respectively, in the influent of the AMCBR reactor. As the OTC loading rates were increased from 22.22 to 44.44 g/m^3d, the EC_{50} values decreased from 263 to 261 mg/L, respectively, in the influent of the AMCBR reactor (see Table 6.37; Figure 6.150 (a-b-c)). The EC_{50} values of OTC also decreased from 261 to 258 mg/L respectively, as the OTC loading was increased from 44.44 to 66.67 g/m^3d. Similarly, the EC_{50} values decreased from 254 to 250 mg/L, as the OTC loading was increased from 88.89 to 111.11 g/m^3d. As seen in Table 6.37 the initial EC_{50} value was obtained as 242 mg/L at an OTC loading rate of 133.33 g/m^3d, respectively, in the influent of the AMCBR reactor. The EC_{50} values were recorded as 213 and 197 mg/L, as the OTC loading rate was increased from 155.56 to 177.78 g/m^3d, respectively (see Table 6.37; Figure 6.150 (a-b-c)). The results indicated that the synthetic pharmaceutical wastewater have adverse effects on survival of the *Daphnia magna*. The reason for the decrease in EC_{50} values could be attributed to the inhibitory effect of the high OTC concentration on the anaerobic bacteria through degradation of OTC resulting a loss of anaerobic bacteria activities in the AMCBR reactor.

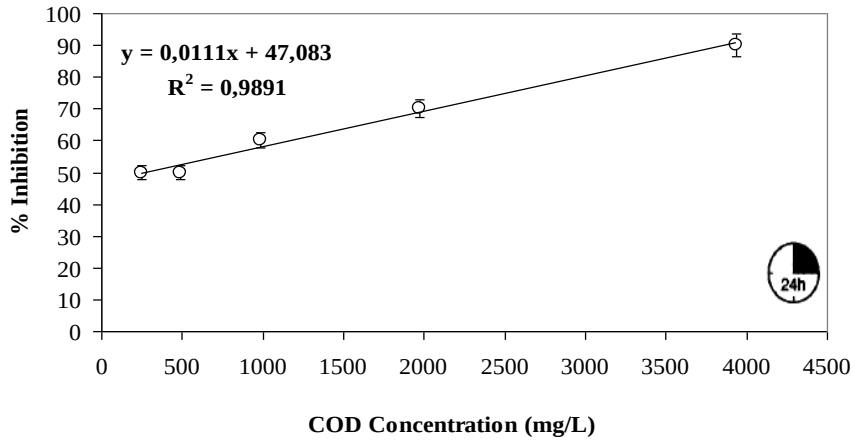

(a)

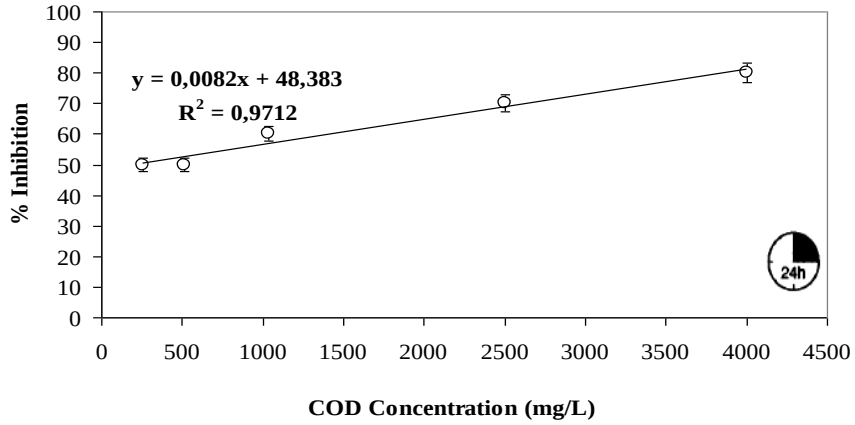

(b)

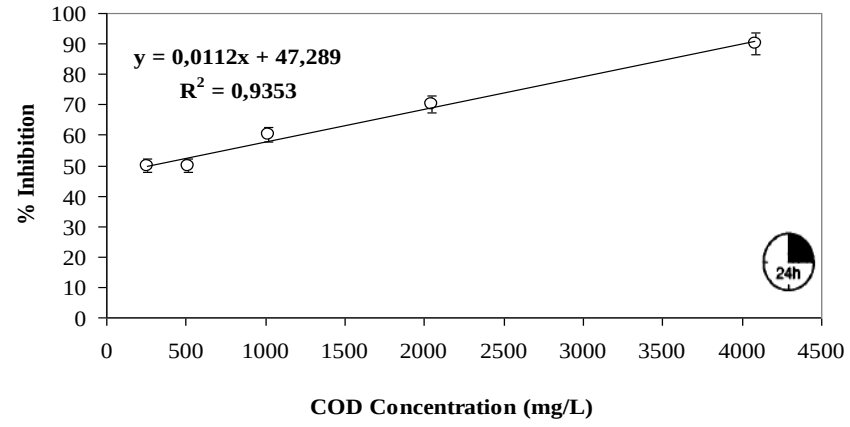

(c)

Figure 6.150 Variations of acute toxicity percentages (inhibition) and EC_{50} values in the influent of the AMCBR reactor for **(a)** OTC concentration 50 mg/L, EC_{50}=263 mg/L; **(b)** OTC concentration 300 mg/L, EC_{50}=242 mg/L and **(c)** OTC concentration 400 mg/L, EC_{50}=197 mg/L (HRT=2.25 days; SRT=94-101 days)

Table 6.37 Variations of acute toxicity values in the influent and effluents of the AMCBR, CSTR and sequential AMCBR/CSTR system (HRT=2.25 days, SRT=94-101 days for AMCBR reactor and HRT=4.5 days, SRT=20 days for CSTR reactor)

OTC Concentration (mg/L)	**AMCBR reactor**		**CSTR reactor**	**Acute Toxicity Removal in the reactor system**		
	***EC_{50} value in the influent of the AMCBR (mg/L)**	***EC_{50} value in the effluent of the AMCBR (mg/L)**	***EC_{50} value in the effluent of the CSTR (mg/L)**	**AMCBR reactor (%)**	**CSTR reactor (%)**	**AMCBR/CSTR reactor (%)**
50	263	665	2186	60	70	88
100	261	660	2176	60	70	88
150	258	600	1875	57	68	86
200	254	586	1860	56	64	85
250	250	580	1389	56	62	82
300	242	563	1210	53	54	80
350	213	453	944	53	52	77
400	197	410	820	52	52	76

* EC_{50} values were calculated based on COD (mg/L).

The acute toxicity removal efficiencies decreased from 60%, 60%, 57%, 56% and 56% to 53%, 53%, 52%, respectively, as the OTC concentrations were increased from 50 to 100, 150, 200, 250, 300, 350, 400 mg/L, respectively, in the effluent of the AMCBR reactor. The EC_{50} values increased from 263 to 665 mg/L, in the effluent of the AMCBR reactor at an OTC loading rate of 22.22 g/m^3d (see Table 6.37; Figure 6.151 (a)). The acute toxicity removal efficiency in the effluent of the AMCBR reactor was 60% at this OTC loading. The EC_{50} values increased from 242 to 563 mg/L in the effluent of the AMCBR reactor at an OTC loading rate of 133.33 g/m^3d (see Figure 6.151 (b)). The acute toxicity yield in the effluent of the AMCBR was 53% at this OTC loading. After 133.33 g/m^3d OTC loading the EC_{50} values increased from 197 to 410 mg/L, in the AMCBR reactor, at an OTC loading rate of 177.78 g/m^3d (Table 6.37; Figure 6.151 (c)). The acute toxicity removal efficiency was 52% in the effluent of the AMCBR reactor at an OTC loading rate of 177.78 g/m^3d. The acute toxicity yields decreased from 60% to 57%, in the effluent of the AMCBR reactor at OTC loading rates of 44.44 and 66.67 g/m^3d (Table 6.37). The EC_{50} values decreased from 600 to 580 mg/L at OTC loading rates of 66.67 and

111.11 g/m^{3}d were resulting in an acute toxicity removal of 57% and 56%, respectively**.** The maximum acute toxicity removal was 88% at OTC loadings of 22.22 and 44.44 g/m^{3}d in the effluent of the AMCBR reactor. This showed that the OTC was biodegraded in the AMCBR reactor at the aforementioned OTC loading. On the other hand the OTC was breakdown to non-toxic or less toxic metabolite products (α-Apo OTC and β-Apo OTC) during the anaerobic biodegradation of OTC in the AMCBR reactor. The results for OTC metabolites namely α-Apo OTC and β-Apo OTC was illustrated in the section "Result and Discussions".

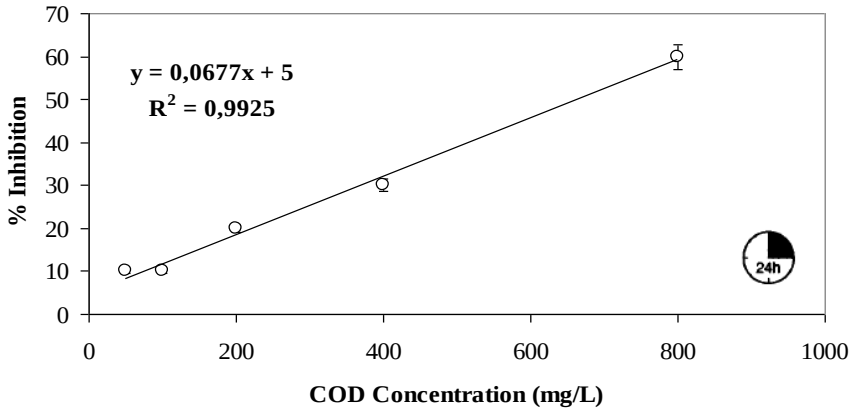

(a)

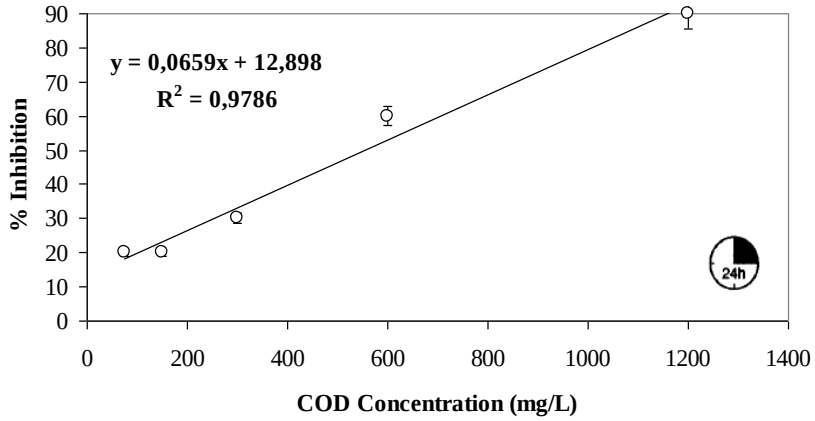

(b)

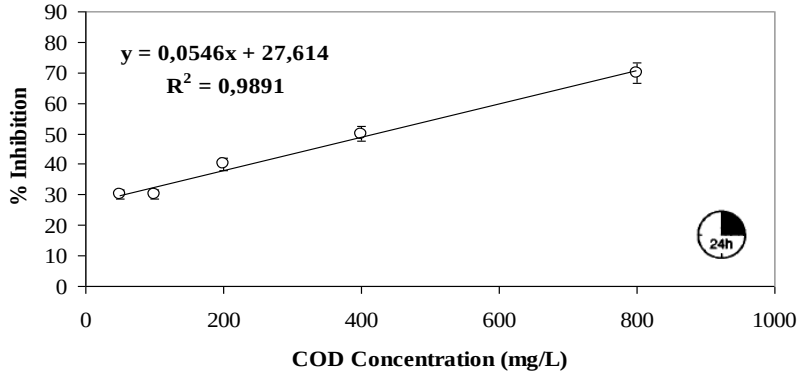

(c)

Figure 6.151 Variations of acute toxicity percentages (inhibition) and EC_{50} values in the effluent of the AMCBR reactor for **(a)** OTC concentration 50 mg/L, EC_{50}=665 mg/L; **(b)** OTC concentration 300 mg/L, EC_{50}=563 mg/L and **(c)** OTC concentration 400 mg/L, EC_{50}=410 mg/L (HRT=2.25 days; SRT=94-101 days)

After anaerobic step the EC_{50} values increased from 665 to 2186 mg/L, in the effluent of the aerobic CSTR reactor at an OTC loading rate of 22.22 g/m^3d (Table 6.37; Figure 6.152 (a)). 70% acute toxicity removal was found after aerobic conditions, in the effluent of the aerobic CSTR reactor at OTC loading rates of 22.22 and 44.444 g/m^3d. The maximum acute toxicity yields (70%) were obtained at the aforementioned OTC loading rates in the aerobic CSTR reactor. The EC_{50} value was found as 1210 mg/L, at an OTC loading rate of 133.33 g/m^3d, in the effluent of the CSTR reactor (see Figure 6.152 (b)). The acute toxicity yield in the effluent of the CSTR reactor was 54% at this OTC loading. At an influent OTC loading rate of 177.78 g/m^3d, the EC_{50} value increased from 410 mg/L to 820 mg/L in the effluent of the aerobic CSTR reactor (Table 6.37; Figure 6.152 (c)). The acute toxicity removal efficiency was 52% in the aerobic CSTR reactor.

The total acute toxicity removal in the effluent of the sequential AMCBR/CSTR reactor system was 88% for 22.22 and 44.44 g/m^3d OTC loading rates (see Table 6.37). The maximum acute toxicity reduction in the effluent of the sequential AMCBR/CSTR reactor system was 88% for the OTC loading rates given above (see Table 6.37). The results of the acute toxicity showed that the acute toxicity of OTC was removed in both anaerobic and aerobic sequential. Water flea (*Daphnia magna*)

acute toxicity test results demonstrated that the sequential anaerobic AMCBR/aerobic CSTR reactor system eliminated the inhibitory effect of the synthetic pharmaceutical wastewater containing OTC on *Daphnia magna* in anaerobic and aerobic effluents.

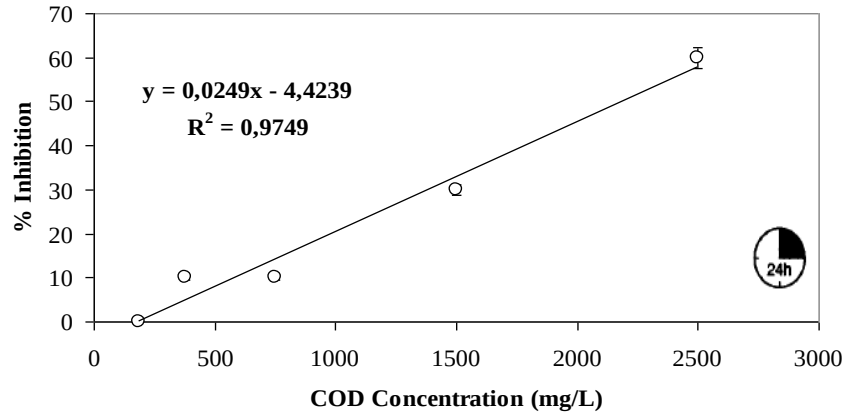

(a)

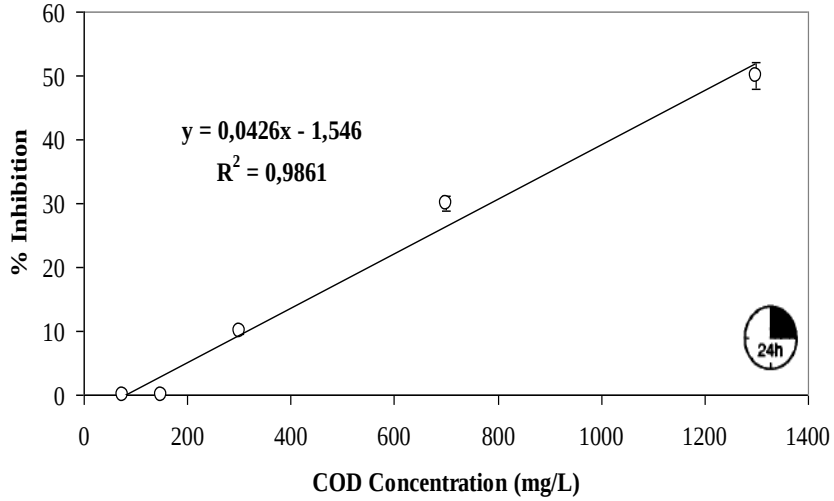

(b)

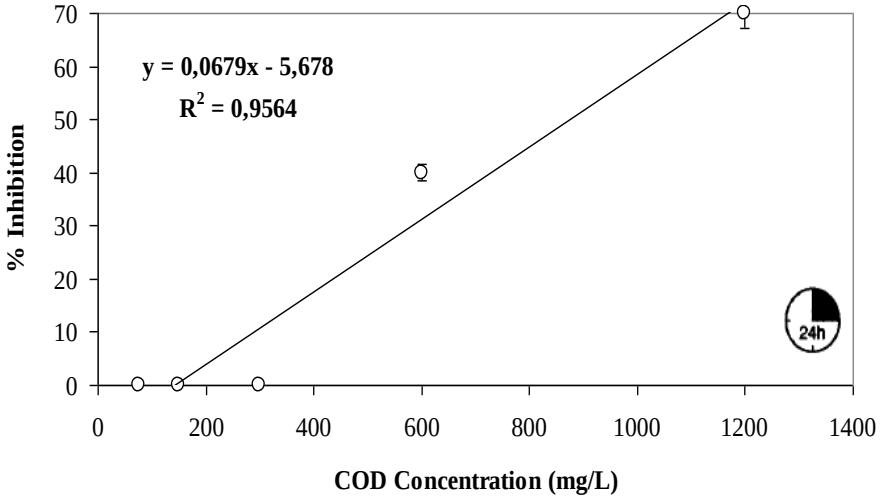

(c)

Figure 6.152 Variations of acute toxicity percentages (inhibition) and EC_{50} values in the effluent of the CSTR reactor for **(a)** OTC concentration 50 mg/L, EC_{50}=2186 mg/L; **(b)** OTC concentration 300 mg/L, EC_{50}=1210 mg/L and **(c)** OTC concentration 400 mg/L, EC_{50}=820 mg/L (HRT=4.5 days; SRT=20 days)

The acute and chronic toxicities of 8 antibiotics namely; metronidazole (1-1000 mg/L), olaquindox (0.10-1000 mg/L), oxolinic acid (0.31-20 mg/L), OTC (1-100 mg/L), streptomycin (20-160 mg/L), sulfadiazine (9.40-150 mg/L), tiamulin (24-71 mg/L) and tylosin (50-160 mg/L) used both therapeutically and as growth promoters in intensive farming were investigated on the water flea crustacean *Daphnia magna* by Wollenberger et al., (2000). The EC_{50} values for metronidazole, olaquindox, oxolinic acid, OTC, streptomycin, sulfadiazine, and tiamulin and tylosin antibiotics were 500, 250, 60, 300, 947, 127, 81, 483 mg/L, respectively in an anaerobic reactor effluent. In our study, the EC_{50} values were between 410 and 665 mg/L, at OTC concentrations varying between 50 and 400 mg/L in the effluent of the AMCBR reactor system. The EC_{50} values for OTC obtained in the aforementioned study are low in comparison to the EC_{50} values found in our study. The low EC_{50} values found at high OTC concentrations could be attributed to their detrimental (inhibiting or lethal) effect on the *Daphnia magna* cells. This showed that the acute toxicity of the wastewater containing OTC was more reduced in the effluent of the anaerobic reactor compared to the anaerobic reactor used by Wollenberg et al. (2000). Furthermore the *Daphnia magna* used in our study seems to be more resistant to the

OTC concentrations since the wastewater characterization, reactor type and differences in operational conditions could affect the sensitivity of *Daphnids*.

Kim et al., (2007) investigated the acute toxicity effects of 30 mg/L OTC on three different trophic levels. The effective concentration cause 50% mortality (EC_{50}) on *Vibrio fischeri*, *Daphnia magna* and *Pseudokirchneriella subcapitata* were 35.99, 36.56 and 0.17 mg/L, respectively. The EC_{50} values obtained in the aforementioned study are low in comparison to the EC_{50} values found in our study (EC_{50}=410-665 mg/L). The differences between trophic levels [*Vibrio fischeri* (Bacteria), *Daphnia magna* (Water flea) and *Pseudokirchneriella subcapitata* (Bacteria)] can affect the acute toxicity tests results with different responses to OTC. Furthermore, the differences in operational conditions and the differences in the anaerobic reactor system configurations can affect the acute toxicity removals.

The algal toxicity of OTC used both therapeutically and as growth promoters in fish farming was investigated on the freshwater cyanobacteria *Microcystis aeruginosa*, the freshwater green algae *Selenastrum capricornutum* and the marine cryptophycean *Rhodomonas salina* by Holten Lutzhøft et al. (1999). The EC_{50} values of 1-100 mg/L OTC on *Microcystis aeruginosa*, *Selenastrum capricornutum* and *Rhodomonas salina* were 0.21 mg/L, 4.50 mg/L and 1.60 mg/L, respectively. The EC_{50} values obtained in the aforementioned study are low in the comparison to the EC_{50} values found in our study with *Daphnia magna*. The direct comparison of sensitivity of different organisms to OTC showed that the *Microcystis aeruginosa*, *Selenastrum capricornutum* and *Rhodomonas salina* are significantly more sensitive to OTC than the *Daphnia magna* (Holten Lutzhøft et al., 1999).

Isidori et al., (2005) investigated the acute toxicity effects of 100 mg/L OTC on six different trophic levels. The EC_{50} values of *Vibrio fischeri* (luminescent bacterium), *Brachionus calyciflorus* (rotifer), *Thamnocephalus platyurus (crustacean anostraca)*, *Daphnia magna* and *Ceriodaphnia dubia* (crustacean cladocera), *Danio rerio* (teleostei, cyprinidae) were 64.50, 34.21, 25.00, 22.64, 18.65 and 10.23 mg/L, respectively. Uyaguari et al., (2009) investigated the acute toxicity effects of 100

mg/L OTC on three different trophic levels. The EC_{50} values of *Palaemonetes pugio*, *Aeromonas hydrophila* and *Vibrio alginolyticus* were 683.30, 610.85 and 664.40 mg/L, respectively.

6.5.2 Acute Toxicity Evaluation of Increasing AMX Concentrations in the Sequential AMCBR/CSTR Reactor System with Daphnia magna

The EC_{50} values and the acute toxicity removals found in the influent, effluent of the anaerobic AMCBR reactor and effluent of the aerobic CSTR reactor were given in Figures 6.153 (a-b-c), 6.154 (a-b-c) and 6.155 (a-b-c) for 22.22, 66.67 and 111.11 g/m^3d AMX loading rates, respectively.

The test samples containing initial AMX concentrations varying between 50, 100, 150, 200 and 250 mg/L were diluted at 1/1, 1/2, 1/4, 1/8 and 1/16 ratios before and after anaerobic and aerobic biodegradation experiments. The young 10 *Daphnids* were added to each test vessel at the initiation time (t=0 hour). After 24 hour of exposure, the EC_{50} values of AMX were calculated based on COD concentrations. As seen in Table 6.38 and Figure 6.153 (a-b-c) the initial EC_{50} values were obtained as 510, 376 and 318 mg/L at AMX loading rates of 22.22 g/m^3d, 66.67 and 111.11 g/m^3d, respectively, in the influent of the AMCBR reactor. As the AMX loading rates were increased from 22.22 to 44.44 g/m^3d, the EC_{50} values decreased from 510 to 410 mg/L, respectively, in the influent of the AMCBR reactor (see Table 6.38; Figure 6.153 (a-b-c)). The EC_{50} values of AMX also decreased from 376 to 330 mg/L respectively, as the AMX loading rate was increased from 44.44 to 66.67 g/m^3d. Similarly, the EC_{50} values decreased from 330 to 318 mg/L, as the AMX loading rate was increased from 88.89 to 111.11 g/m^3d. The reason for the decrease in EC_{50} values at high AMX concentrations could be attributed to the inhibitory effect of the high AMX concentration on the *Daphnia magna* resulting mortalities in *Daphnia magna* in the influent of the AMCBR reactor.

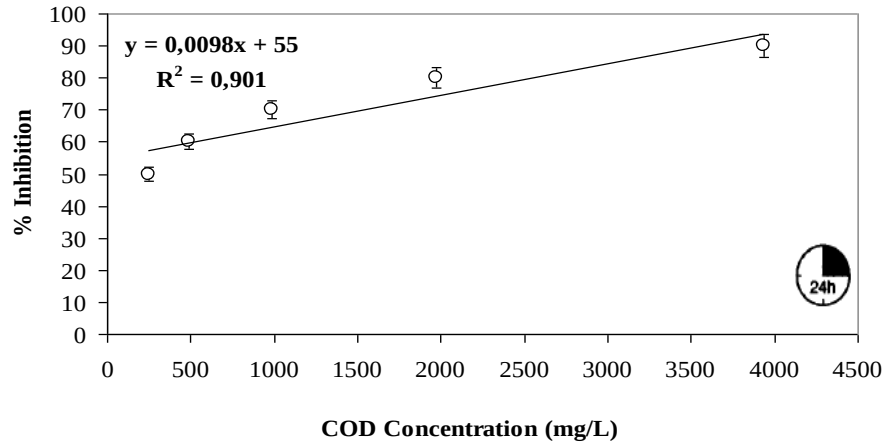

(a)

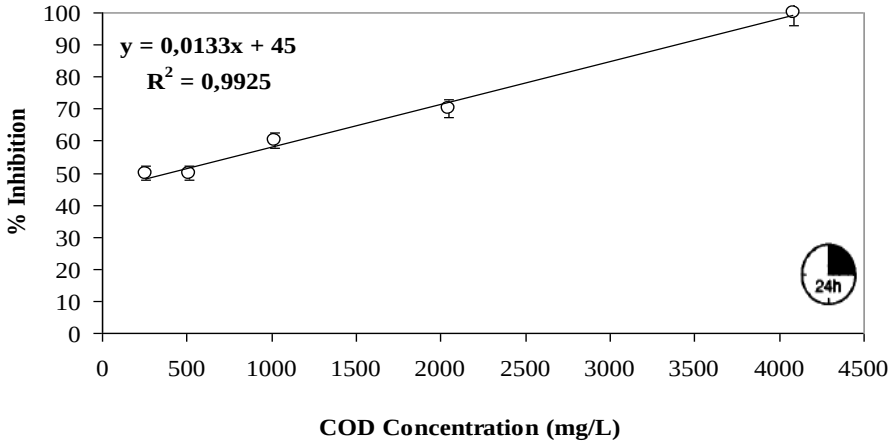

(b)

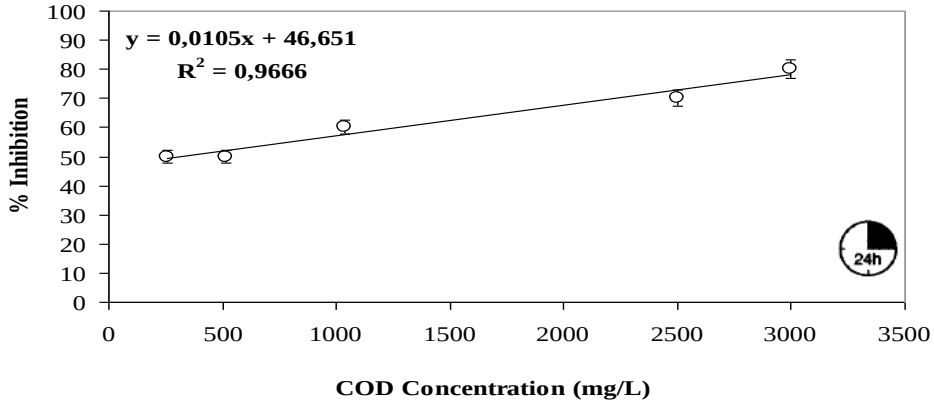

(c)

Figure 6.153 Variations of acute toxicity percentages and EC_{50} values in the influent of the AMCBR reactor for **(a)** AMX loading rate 22.22 g/m^{3}d, EC_{50}= 510 mg/L; **(b)** AMX loading rate 66.67 g/m^{3}d, EC_{50}=376 mg/L and **(c)** AMX loading rate 111.11 g/m^{3}d, EC_{50}= 318 mg/L (HRT=4.5 days; SRT=49-95 days)

Table 6.38 Variations of acute toxicity values in the influent and effluents of the AMCBR, CSTR and sequential AMCBR/CSTR system (HRT=4.5 days, SRT=49-95 days for AMCBR reactor and HRT=9 days, SRT=20 days for CSTR reactor)

AMX Concentration (mg/L)	**AMX Loadings (g/m^3d)**	**AMCBR reactor**		**CSTR reactor**	**Acute Toxicity Removal in the reactor system**		
		***EC_{50} value in the influent of the AMCBR (mg/L)**	***EC_{50} value in the effluent of the AMCBR (mg/L)**	***EC_{50} value in the effluent of the CSTR (mg/L)**	**AMCBR reactor (%)**	**CSTR reactor (%)**	**AMCBR/CSTR reactor (%)**
50	**22.22**	510	764	3225	33	76	84
100	**44.44**	410	720	3120	43	77	87
150	**66.67**	376	701	2938	46	76	86
200	**88.89**	330	586	1927	44	70	82
250	**111.11**	318	472	1217	33	61	74

* EC_{50} values were calculated based on COD (mg/L).

The acute toxicity removal efficiencies were 33% and 43%, at AMX loadings of 22.22 and 44.44 g/m^3d, respectively, in the effluent of the AMCBR reactor. The acute toxicity removal efficiencies decreased from 46% to 44% and to 43% as the AMX loadings were increased from 66.67, 88.89 to 111.11 g/m^3d, respectively, in the effluent of the AMCBR reactor. The EC_{50} values increased from 510 to 764 mg/L, in the effluent of the AMCBR reactor at an AMX loading rate of 22.22 g/m^3d (see Table 6.38; Figure 6.154 (a)). The EC_{50} values increased from 376 to 701 mg/L in the effluent of the AMCBR reactor at an AMX loading rate of 66.67 g/m^3d (see Figure 6.154 (b)). The acute toxicity yield in the effluent of the AMCBR reactor was 46% at this AMX loading.

The EC_{50} values increased from 318 to 472 mg/L in the effluent of the AMCBR reactor at an AMX loading rate of 111.11 g/m^3d (Table 6.38; Figure 6.154 (c)). The acute toxicity removal efficiency was 33% in the effluent of the AMCBR reactor at this AMX loading rate. The AMX was biodegraded to non-toxic or less toxic metabolite products during the anaerobic biodegradation of AMX in the anaerobic AMCBR reactor (see "Result and Discussions"). The maximum acute toxicity

removal was 87% at AMX loading rates of 44.44 and 66.67 g/m^3d corresponding to EC_{50} values of 764 mg/L and 701 mg/L, respectively in the effluent of the anaerobic AMCBR reactor.

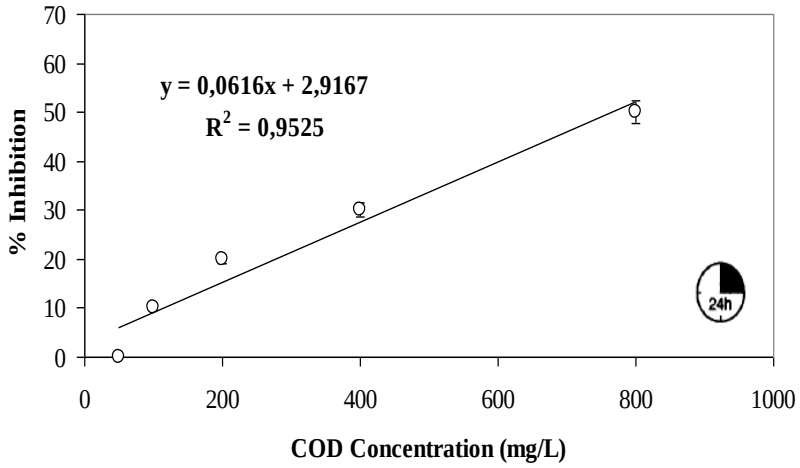

(a)

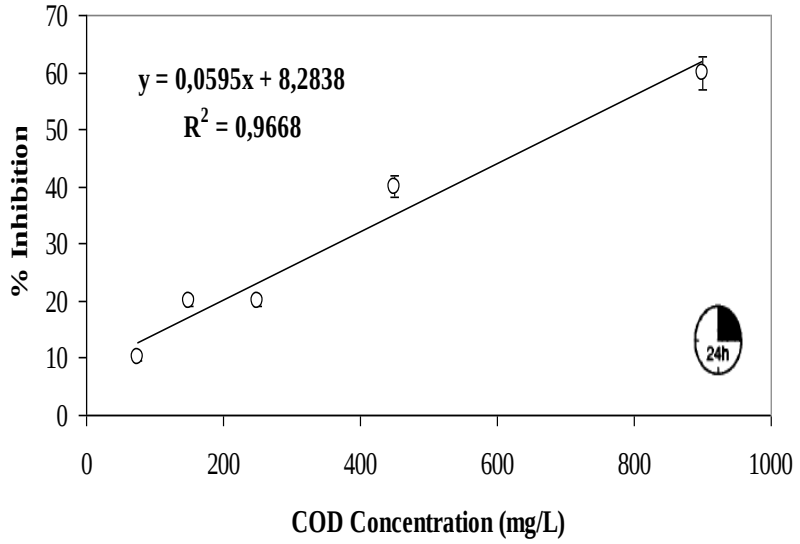

(b)

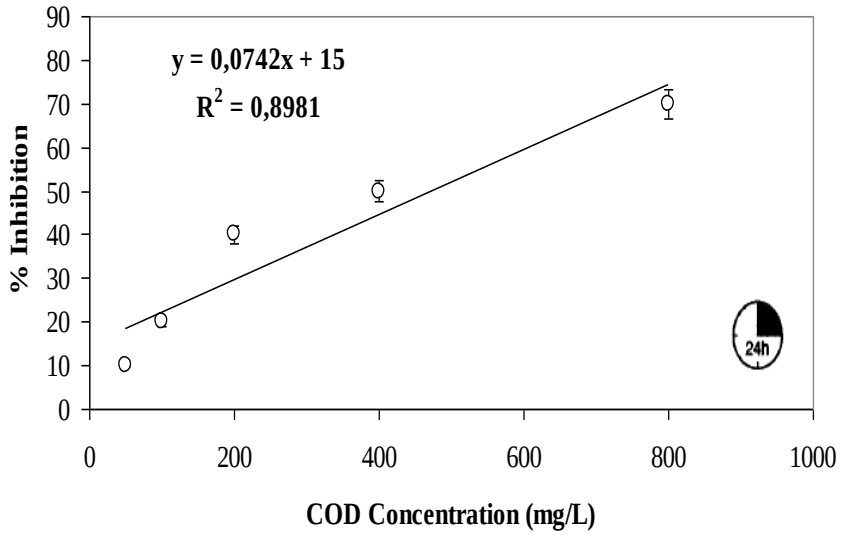

(c)

Figure 6.154 Variations of acute toxicity percentages and EC_{50} values in the effluent of the AMCBR reactor for **(a)** AMX loading rate 22.22 g/m^{3}d, EC_{50}=764 mg/L; **(b)** AMX loading rate 66.67 g/m^{3}d, EC_{50}=701 mg/L and **(c)** AMX loading rate 111.11 g/m^{3}d, EC_{50}=478 mg/L (HRT=4.5 days; SRT=49-95 days)

After anaerobic treatment the EC_{50} values increased from 764 to 3225 mg/L, in the effluent of the aerobic CSTR reactor at an AMX loading rate of 22.22 g/m^{3}d (Table 6.38; Figure 6.155 (a)). 76% acute toxicity reduction was found after aerobic conditions, in the effluent of the aerobic CSTR reactor at an AMX loading rate of 22.22 g/m^{3}d. The EC_{50} value was found as 2938 mg/L, at an AMX loading rate of 66.67 g/m^{3}d, in the effluent of the CSTR reactor (see Figure 6.155 (b)). The acute toxicity yield in the effluent of the CSTR reactor was 76% at this AMX loading. At an influent AMX loading rate of 111.11 g/m^{3}d, the EC_{50} value increased from 472 mg/L to 1217 mg/L in the effluent of the aerobic CSTR reactor (Table 6.38; Figure 6.155 (c)). The acute toxicity removal efficiency was 61% in the aerobic CSTR reactor.

The maximum acute toxicity yields were 87% and 77% in the effluents of the anaerobic AMCBR and aerobic CSTR reactors, respectively at AMX loading rate of 44.44 g/m^{3}d. The maximum acute toxicity removal efficiency in the effluent of the

sequential AMCBR/CSTR reactor system was 87% for 44.44 g/m^{3}d AMX loading rate (see Table 6.38). *Daphnia magna* acute toxicity test results demonstrated that the sequential AMCBR/CSTR system eliminated the inhibitory effect of the synthetic pharmaceutical wastewater containing AMX on *Daphnia magna* in anaerobic and aerobic effluents.

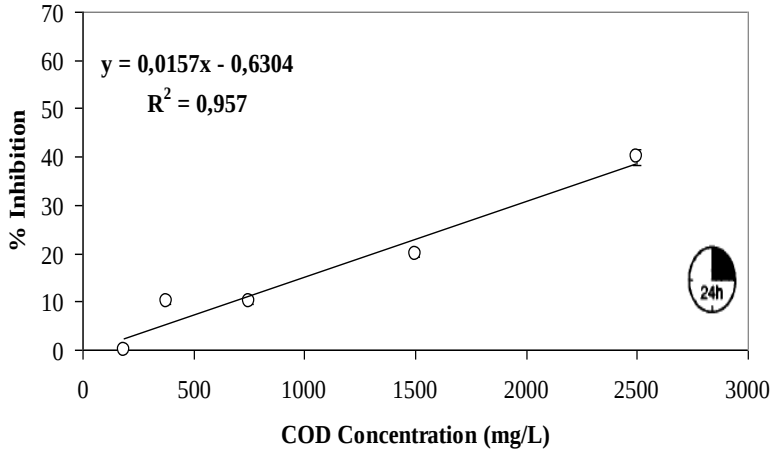

(a)

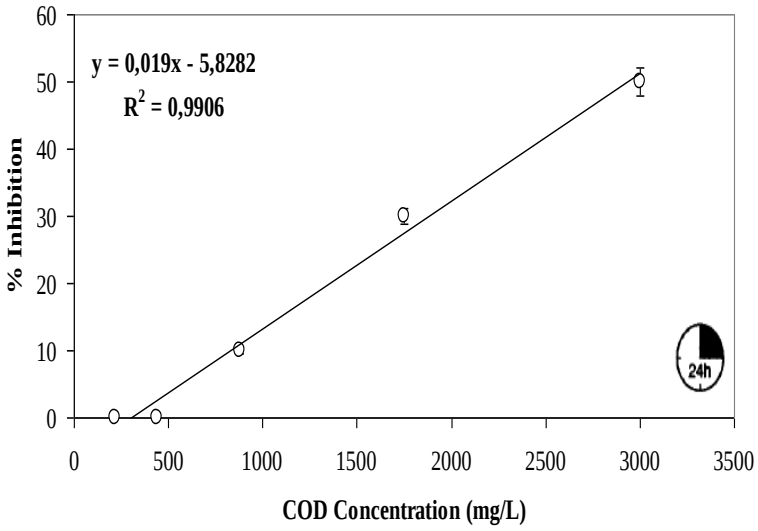

(b)

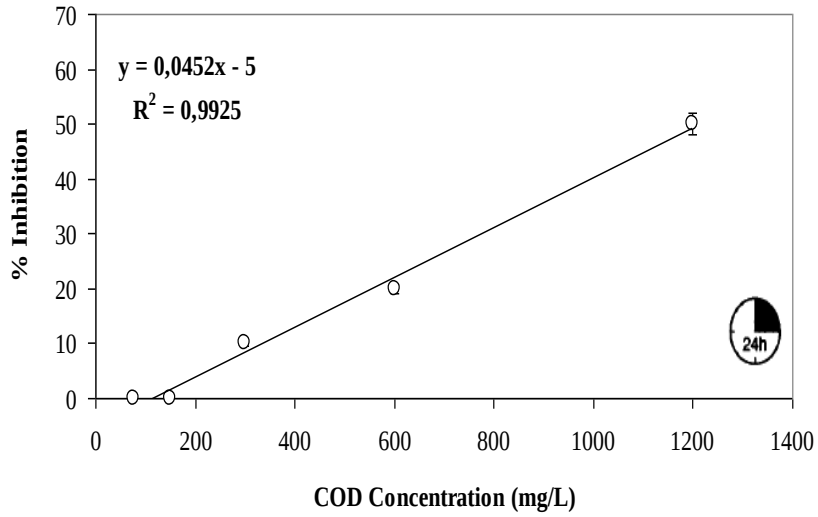

(c)

Figure 6.155 Variations of acute toxicity percentages and EC_{50} values in the effluent of the CSTR reactor for **(a)** AMX loading rate 22.22 g/m^{3}d, EC_{50}=3225 mg/L; **(b)** AMX loading rate 66.67 g/m^{3}d, EC_{50}=2938 mg/L and **(c)** AMX loading rate 111.11 g/m^{3}d, EC_{50}=1217 mg/L (HRT=9 days; SRT=20 days)

The studies performed in recent literature showed that the β-lactam antibiotics exhibited acute toxicity to different test organisms in wastewaters. For example Andreozzi et al., (2004) found that micro-algal species (EC_{50}=100 mg/L for *P. subcapitata* and EC_{50}=2 mg/L for *S. leopolensis*) are sensitive to AMX in pharmaceutical wastewaters. Holten Lützhoft et al., (1999) found a weak acute toxicity of 34 mg/L AMX to *M. aeruginosa* in 72-hour (EC_{50}=0.0037 mg/L). Park and Choi, (2008) investigated the acute toxicity of AMX to different trophic levels. The EC_{50} values for *Daphnia magna* and *O. latipes* were 42.1 mg/L and 80.8 mg/L, respectively. The EC_{50} value of AMX was found as 0.0037 and 250 mg/L to algae *M. Aeruginosa* and *S. Capricornutum*, respectively (Kim and Aga, 2007). Liu et al., (2012) investigated the acute toxicity effects of 0.08-1.00 mg/L AMX on *M. aeruginosa.* The EC_{50} on *M. aeruginosa* was 0.07 and 1 mg/L, respectively. The EC_{50} values obtained in the aforementioned study are low in comparison to the EC_{50} values found in our study (EC_{50}=410-665 mg/L). The differences between trophic levels [*Daphnia magna* (Water flea) *P. subcapitata, S. leopolensis* (micro-algae), *O.*

latipes (rice fish), and *M. aeruginosa* (cyanobacteria)] can affect the EC_{50} values with different responses to AMX.

6.5.3 Acute Toxicity Evaluation of Increasing TYL Concentrations in the Sequential AMCBR/CSTR Reactor System with Daphnia magna

Daphnia magna is one of the most important water flea species employed in acute toxicity testing through the world (APHA, AWWA, WEF, 2005). In this study, the acute toxicity of the effluent of the anaerobic AMCBR and aerobic CSTR reactors were determined by acute toxicity test using water flea *Daphnia magna*. Table 6.39 shows the EC_{50} values and the acute toxicity removals in samples taken from the influent of synthetic pharmaceutical wastewater containing TYL concentration of 50, 100, 150, 200, 250, 300 mg/L, from the effluent of the anaerobic AMCBR and aerobic CSTR reactors through continuous operation at HRT=2.25 days, SRT=71-117 days for AMCBR reactor and HRT=4.5 days, SRT=20 days for CSTR reactor. The EC_{50} values and the acute toxicity reductions found in the influent, effluent of the AMCBR reactor and effluent of the CSTR reactor were given in Figures 6.156 (a-b-c), 6.157 (a-b-c) and 6.158 (a-b-c) for 50, 200 and 300 mg/L TYL concentrations, respectively.

The initial EC_{50} values were obtained as 329, 275 and 205 mg/L at TYL concentrations of 50, 200 and 300 mg/L, respectively, in the influent of the AMCBR reactor. As the TYL concentrations were increased from 50 to 100 mg/L, the EC_{50} values decreased from 329 to 315 mg/L, respectively, in the influent of the AMCBR reactor (see Table 6.39; Figure 6.156 (a-b-c)). The EC_{50} values of TYL also decreased from 315 to 305 mg/L respectively, as the TYL concentration was increased from 100 to 150 mg/L. The EC_{50} values decreased from 275 to 205 mg/L, as the TYL concentration was increased from 200 to 300 g/m^3d.

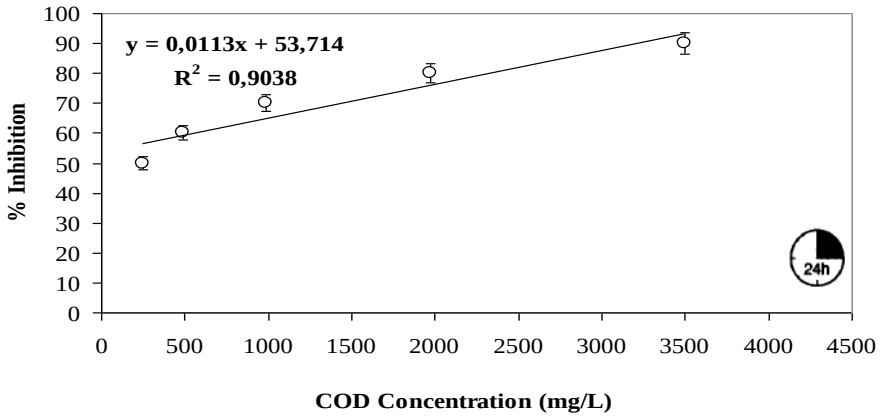

(a)

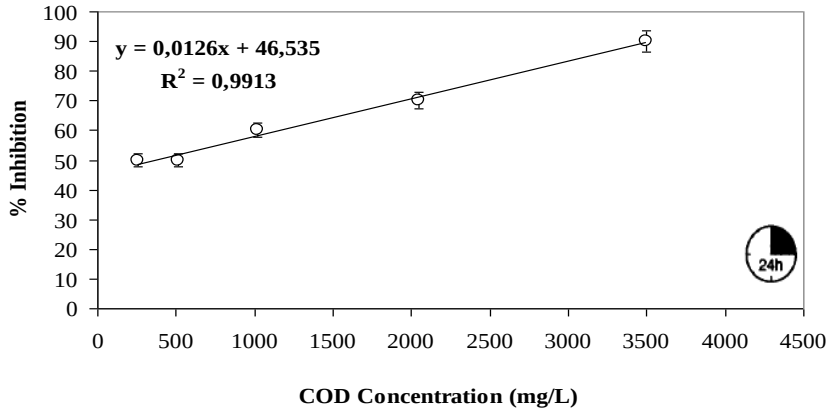

(b)

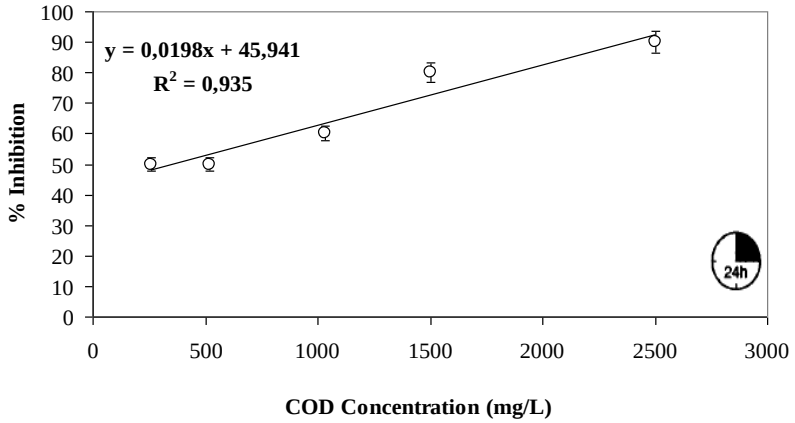

(c)

Figure 6.156 Variations of acute toxicity percentages and EC_{50} values in the influent of the AMCBR reactor for **(a)** TYL concentration 50 mg/L, EC_{50}= 329 mg/L; **(b)** TYL concentration 200 mg/L, EC_{50}=275 mg/L and **(c)** TYL concentration 300 mg/L, EC_{50}= 205 mg/L (HRT=2.25 days; SRT=71-117 days)

Table 6.39 Variations of acute toxicity values in the influent and effluents of the AMCBR, CSTR and sequential system (HRT=2.25 days, SRT=71-117 days for AMCBR reactor and HRT=4.5 days, SRT=20 days for CSTR reactor)

TYL Conc. (mg/L)	**AMCBR reactor**		**CSTR reactor**	**Acute Toxicity Removal in the reactor system**		
	***EC_{50} value in the inf. (mg/L)**	***EC_{50} value in the eff. (mg/L)**	***EC_{50} value in the eff. (mg/L)**	**AMCBR reactor (%)**	**CSTR reactor (%)**	**AMCBR/CSTR reactor (%)**
50	329	658	2632	50	75	87
100	315	618	2400	49	74	88
150	305	600	2374	49	74	88
200	275	509	1833	46	72	85
250	250	455	1517	45	70	84
300	205	360	1216	43	69	83

* EC_{50} values were calculated based on COD (mg/L).

The acute toxicity yields were 50% and 49%, respectively at TYL concentrations of 50 and 150 mg/L in the effluent of the AMCBR reactor. The acute toxicity yields decreased from 50%, 49%, 49%, 46%, 45% to 43%, respectively, as the TYL concentrations were increased from 50, 100, 150, 200, 250 to 300 mg/L, respectively, in the effluent of the AMCBR reactor. The EC_{50} values increased from 329 to 658 mg/L, in the effluent of the AMCBR reactor at a TYL concentration of 50 mg/L (see Table 6.39; Figure 6.157 (a)). The EC_{50} values increased from 275 to 509 mg/L in the effluent of the AMCBR reactor at a TYL concentration of 200 mg/L (see Figure 6.157 (b)). The acute toxicity yield in the effluent of the AMCBR reactor was 46% at this TYL concentration. The EC_{50} values increased from 250 to 455 mg/L, in the AMCBR reactor, at a TYL concentration of 250 mg/L (Table 6.39; Figure 6.157(c)). The acute toxicity removal efficiency was 45% in the effluent of the AMCBR reactor at a TYL concentration of 250 mg/L. The EC_{50} values increased from 205 to 360 mg/L, in the AMCBR reactor, at a TYL concentration of 300 mg/L (Table 6.39; Figure 6.157 (c)). The acute toxicity removal efficiency was 43% in the effluent of the AMCBR reactor at a TYL concentration of 300 mg/L.

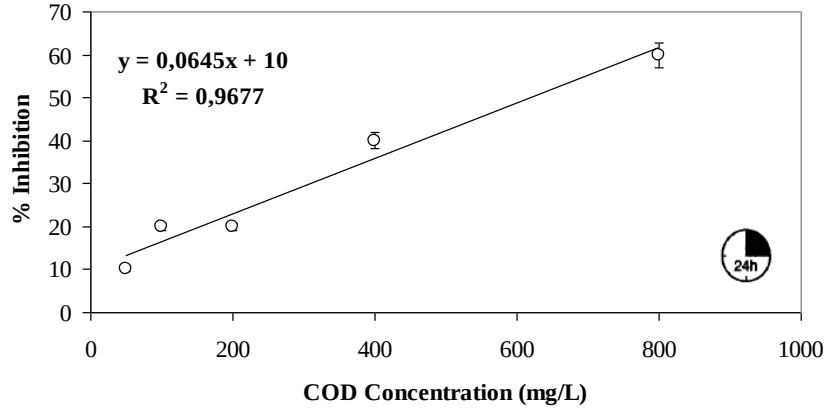

(a)

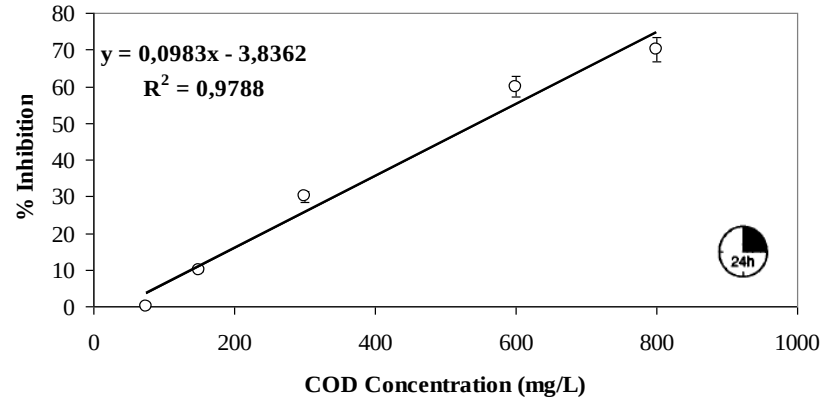

(b)

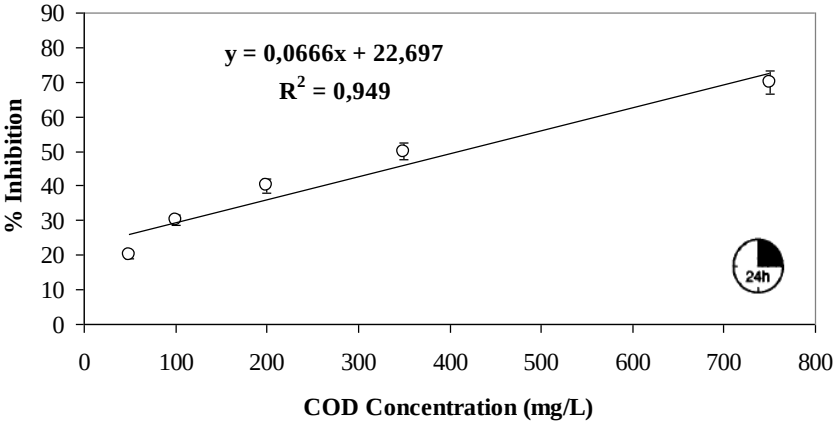

(c)

Figure 6.157 Variations of acute toxicity percentages and EC_{50} values in the effluent of the AMCBR reactor for **(a)** TYL concentration 50 mg/L, EC_{50}=658 mg/L; **(b)** TYL concentration 200 mg/L, EC_{50}=509 mg/L and **(c)** TYL concentration 300 mg/L, EC_{50}=360 mg/L (HRT=2.25 days; SRT=71-117 days)

After anaerobic step the EC_{50} values increased from 658 to 2632 mg/L, in the effluent of the aerobic CSTR reactor at a TYL concentration of 50 mg/L (Table 6.39; Figure 6.158 (a)). 75% acute toxicity reduction was found after aerobic step, in the effluent of the aerobic CSTR reactor at TYL concentration of 50 mg/L. The EC_{50} value was found as 1833 mg/L, at a TYL concentration of 200 mg/L, in the effluent of the CSTR reactor (see Figure 6.158 (b)). The acute toxicity yield in the effluent of the CSTR reactor was 72% at this TYL concentration. At an influent TYL concentration of 300 mg/L, the EC_{50} value increased from 360 mg/L to 1216 mg/L in the effluent of the aerobic CSTR reactor (Table 6.39; Figure 6.158 (c)). The acute toxicity removal efficiency was 69% in the aerobic CSTR reactor.

The maximum acute toxicity reduction in the effluent of the sequential anaerobic AMCBR/ aerobic CSTR reactor system was 88% for 100 and 150 mg/L TYL concentrations (Table 6.39). The minimum acute toxicity reduction in the effluent of the sequential AMCBR/CSTR reactor system was 83% for 300 mg/L TYL concentration (see Table 6.39). The results of the acute toxicity showed that the acute toxicity of TYL was removed in both anaerobic and aerobic sequential. *Daphnia magna* acute toxicity test results demonstrated that the sequential system eliminated the inhibitory effect of the synthetic wastewater containing TYL on *Daphnia magna* in anaerobic AMCBR and aerobic CSTR effluents.

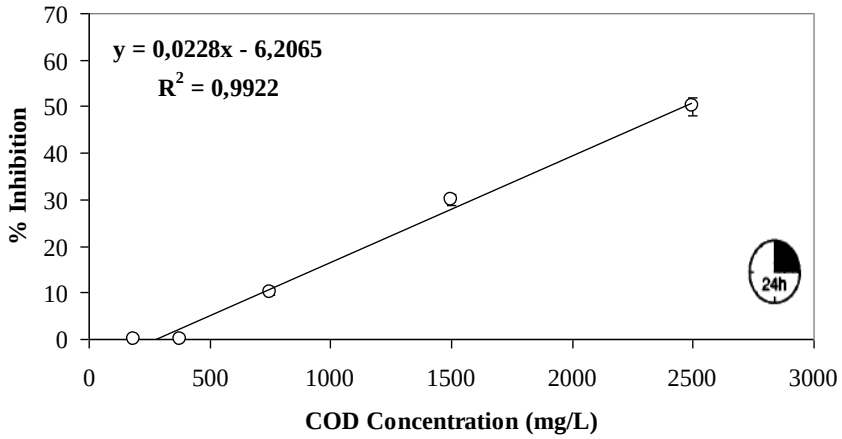

(a)

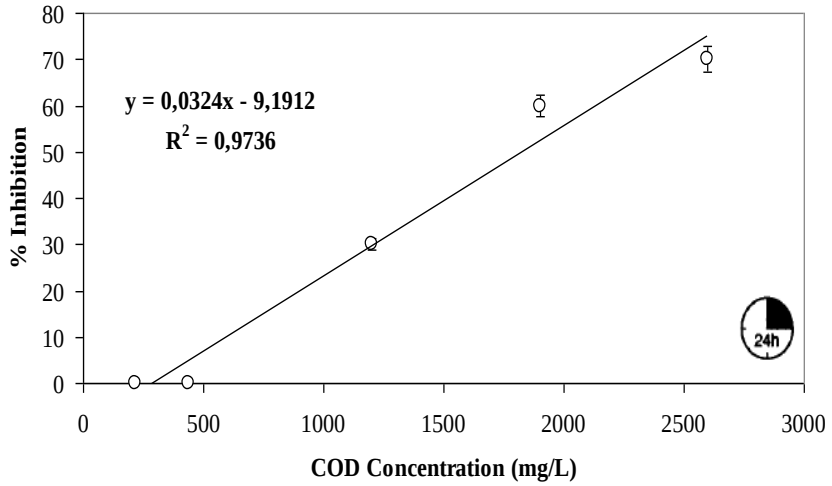

(b)

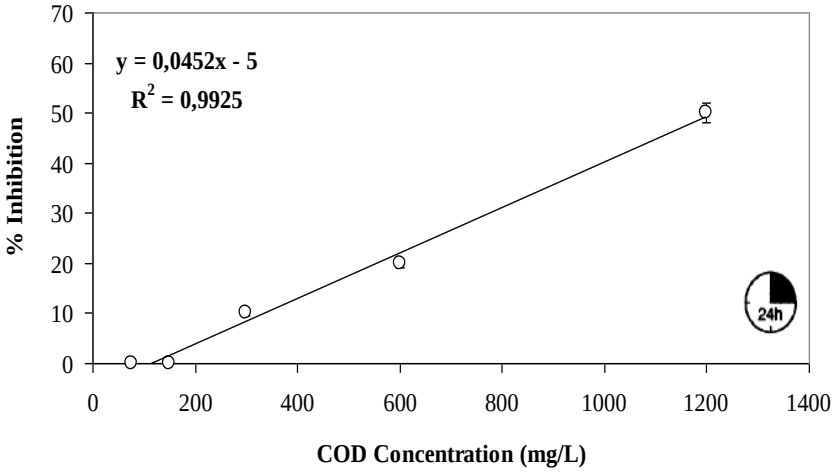

(c)

Figure 6.158 Variations of acute toxicity percentages and EC_{50} values in the effluent of the CSTR reactor for **(a)** TYL concentration 50 mg/L, EC_{50}= 2632 mg/L; **(b)** TYL concentration 200 mg/L, EC_{50}=1833 mg/L and **(c)** TYL concentration 300 mg/L, EC_{50}= 1216 mg/L (HRT=4.5 days, SRT=20 days)

The acute toxicity of TYL (50-160 mg/L) was investigated on water flea *Daphnia magna* by Wollenberger et al., (2000). The EC_{50} value for TYL varied between 56 and 483 mg/L under anaerobic conditions in this study performed by Wollenberger et al., (2000). In our study, the EC_{50} values were between 410 and 620 mg/L, at TYL concentrations varying between 50 and 300 mg/L in the effluent of the AMCBR reactor system. The EC_{50} values for TYL obtained in the aforementioned study are

low in comparison to the EC_{50} values found in our study. The low EC_{50} values found at high TYL concentrations could be explained by TYL inhibitions or lethal effect of high TYL concentrations on *Daphnia magna* cells.

Zaldivar and Baraibar, (2011) investigated the acute toxicity effect of 100 mg/L TYL on *Daphnia magna*. The effective concentration cause 50% mortality (EC_{50}) on *Daphnia magna* was 568 mg/L. The EC_{50} values obtained in the aforementioned study are low in comparison to the EC_{50} values found in our study (EC_{50}=617-2400 mg/L). The differences in operational conditions and the differences in the TYL concentrations can affect the EC_{50} values.

The acute toxicity of TYL on the freshwater green alga *Selenastrum capricornutum* was investigated by Liguoro et al., (2003). The EC_{50} value of 0.1-5 mg/L TYL on *Selenastrum capricornutum* was calculated as 0.95 mg/L. The EC_{50} values obtained in the aforementioned study are low in the comparison to the EC_{50} values found in our study with *Daphnia magna*. The direct comparison of sensitivity of different organisms to TYL showed that the *Selenastrum capricornutum* is significantly more sensitive to TYL than the *Daphnia magna*.

6.5.4 Acute Toxicity Evaluation of Increasing ERY Concentrations in the Sequential AMCBR/CSTR Reactor System with Daphnia magna

The water flea *Daphnia magna* is the most commonly used water flea in toxicological tests in wastewater treatment, due to short doubling time, high sensitivity, and simplicity; therefore, it was used as an indicator in this study (APHA, AWWA, WEF, 2005). Table 6.40 shows the EC_{50} values and the acute toxicity removals in samples taken from the influent synthetic pharmaceutical wastewater containing ERY of 50, 100, 150, 200, 250, 300 mg/L from the effluent of the anaerobic AMCBR and aerobic CSTR reactors through continuous operation at HRT=1.5 days, SRT=85-106 days for AMCBR reactor and HRT=3 days, SRT=20 days for CSTR reactor. The EC_{50} values and the acute toxicity yields found in the influent, effluent of the AMCBR reactor and effluent of the CSTR reactor were given

in Figures 6.159 (a-b-c), 6.160 (a-b-c) and 6.161 (a-b-c) for 50, 200 and 300 mg/L ERY concentrations, respectively.

The initial EC_{50} values were obtained as 329, 275 and 205 mg/L at ERY concentrations of 50, 200 and 300 mg/L, respectively, in the influent of the AMCBR reactor. As the ERY concentrations were increased from 50 to 100 mg/L, the EC_{50} values decreased from 329 to 315 mg/L, respectively, in the influent of the AMCBR reactor (see Table 6.40; Figure 6.159 (a-b-c)). The EC_{50} values of ERY also decreased from 315 to 305 mg/L respectively, as the ERY concentration was increased from 100 to 150 mg/L. Similarly, the EC_{50} values decreased from 275 to 205 mg/L, as the ERY concentration was increased from 200 to 300 mg/L.

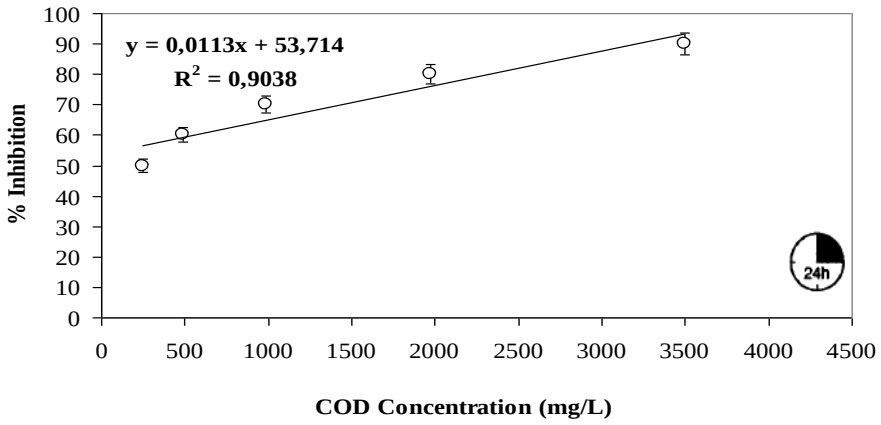

(a)

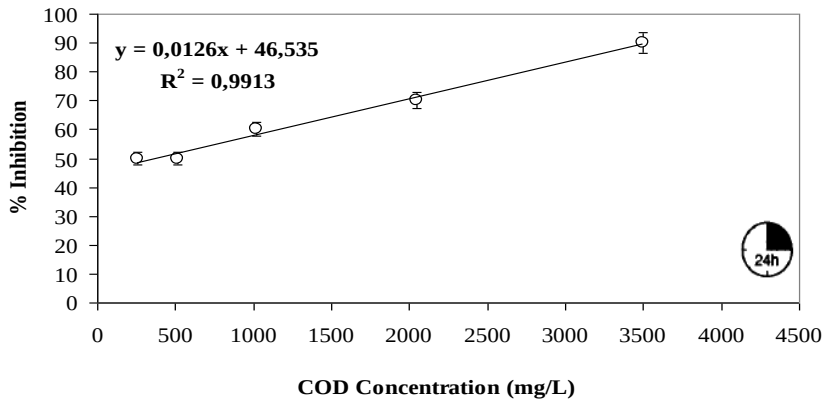

(b)

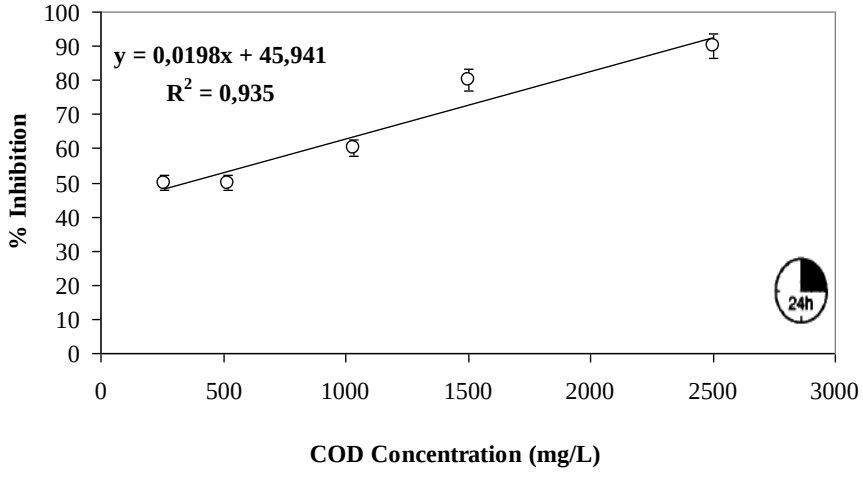

(c)

Figure 6.159 Variations of acute toxicity percentages and EC_{50} values in the influent of the AMCBR reactor for **(a)** ERY concentration 50 mg/L, EC_{50}=329 mg/L; **(b)** ERY concentration 200 mg/L, EC_{50}=275 mg/L and **(c)** ERY concentration 300 mg/L, EC_{50}=205 mg/L (HRT=1.5 days, SRT=85-106 days).

Table 6.40 Variations of acute toxicity values in the influent and effluents of the AMCBR, CSTR and sequential AMCBR/CSTR system (HRT=1.5 days, SRT=85-106 days for AMCBR reactor and HRT=3.0 days, SRT=20 days for CSTR reactor)

ERY Conc. (mg/L)	**AMCBR reactor**		**CSTR reactor**	**Acute Toxicity Removal in the reactor system**		
	***EC_{50} value in the inf. (mg/L)**	***EC_{50} value in the eff. (mg/L)**	***EC_{50} value in the effluent (mg/L)**	**AMCBR reactor (%)**	**CSTR reactor (%)**	**AMCBR /CSTR reactor (%)**
50	329	658	2632	50	75	87
100	315	618	2400	49	74	88
150	305	600	2374	49	74	88
200	275	509	1833	46	72	85
250	250	455	1517	45	70	84
300	205	360	1216	43	69	83

* EC_{50} values were calculated based on COD (mg/L).

The acute toxicity yields were 50% and 49%, respectively at the ERY concentrations of 50 and 150 mg/L in the effluent of the AMCBR reactor. The acute toxicity yields decreased from 50%, 49%, 49%, 46%, 45% to 43%, respectively, as the ERY concentrations were increased from 50, 100, 150, 200, 250 to 300 mg/L, respectively, in the effluent of the AMCBR reactor. The EC_{50} values increased from 329 to 658 mg/L, in the effluent of the AMCBR reactor at an ERY concentration of 50 mg/L (see Table 6.40; Figure 6.160 (a)). The EC_{50} values increased from 275 to 509 mg/L in the effluent of the AMCBR reactor at an ERY concentration of 200 mg/L (see Figure 6.160 (b)). The acute toxicity yield in the effluent of the AMCBR was 46% at this ERY concentration. The EC_{50} values increased from 205 to 360 mg/L, in the AMCBR reactor, at an ERY concentration of 300 mg/L (Table 6.40; Figure 6.160 (c)). The acute toxicity removal efficiency was 43% in the effluent of the AMCBR reactor at an ERY concentration of 300 mg/L.

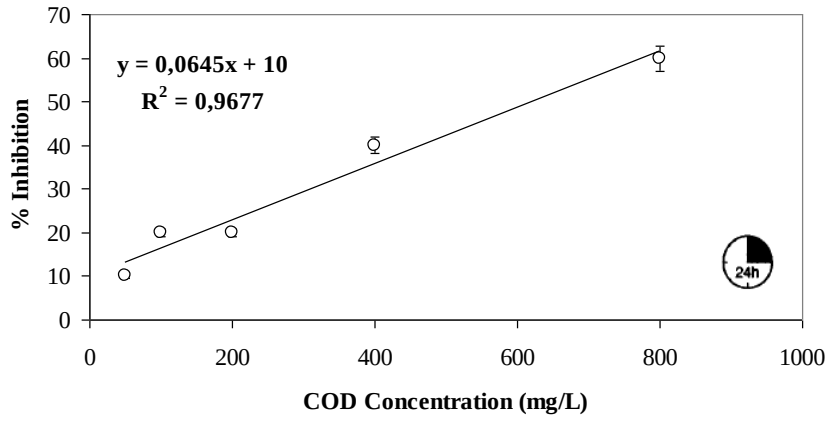

(a)

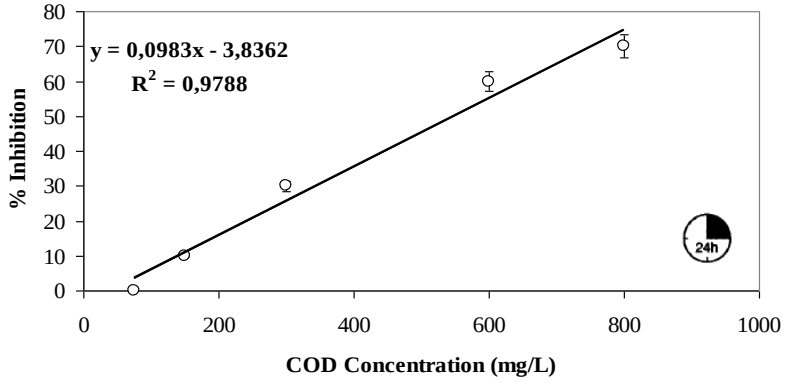

(b)

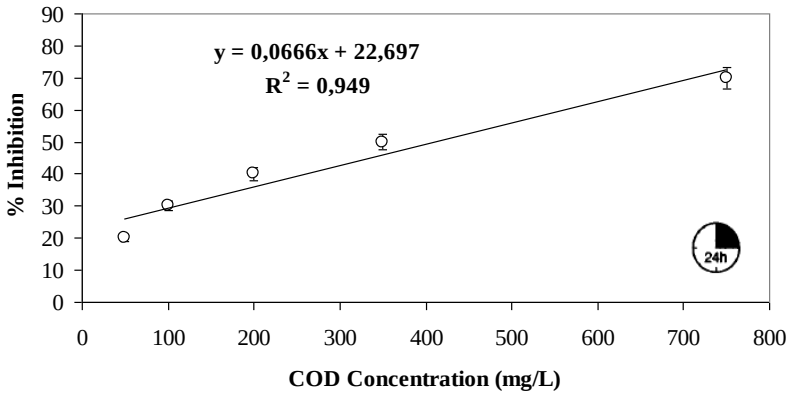

(c)

Figure 6.160 Variations of acute toxicity percentages and EC_{50} values in the effluent of the AMCBR reactor for **(a)** ERY concentration 50 mg/L, EC_{50}=658 mg/L; **(b)** ERY concentration 200 mg/L, EC_{50}=509 mg/L and **(c)** ERY concentration 300 mg/L, EC_{50}=360 mg/L (HRT=1.5 days; SRT=85-106 days)

After anaerobic step the EC_{50} values increased from 658 to 2632 mg/L, in the effluent of the aerobic CSTR reactor at an ERY concentration of 50 mg/L (Table 6.40; Figure 6.161 (a)). 75% acute toxicity reduction was found after aerobic step, in the effluent of the aerobic CSTR reactor at A ERY concentration of 50 mg/L. The EC_{50} value was found as 1833 mg/L, at an ERY concentration of 200 mg/L, in the effluent of the aerobic CSTR reactor (see Figure 6.161 (b)). The acute toxicity yield in the effluent of the aerobic CSTR reactor was 72% at this ERY concentration. At an influent ERY concentration of 300 mg/L, the EC_{50} value increased from 360 mg/L to 1216 mg/L in the effluent of the aerobic CSTR reactor (Table 6.40; Figure 6.161 (c)). The acute toxicity removal efficiency was 69% in the aerobic CSTR reactor.

The maximum acute toxicity reduction in the sequential AMCBR/CSTR reactor system effluent was 88% for 100 and 150 mg/L ERY concentrations (see Table 6.40). The minimum acute toxicity reduction in the sequential AMCBR/CSTR reactor system effluent was 83% for 300 mg/L ERY concentration (see Table 6.40). The results of the acute toxicity showed that the acute toxicity of ERY was removed in both anaerobic and aerobic effluents. Water flea acute toxicity test results demonstrated that the sequential anaerobic AMCBR/aerobic CSTR reactor system

eliminated the inhibitory effect of the synthetic pharmaceutical wastewater containing ERY on *Daphnia magna* (water flea) in all reactor system effluents.

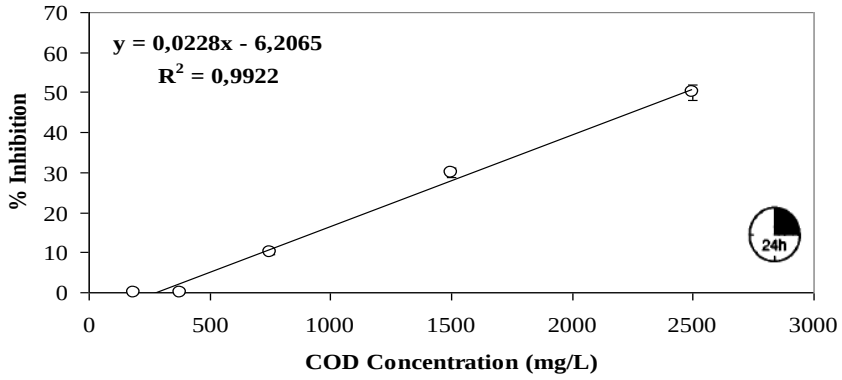

(a)

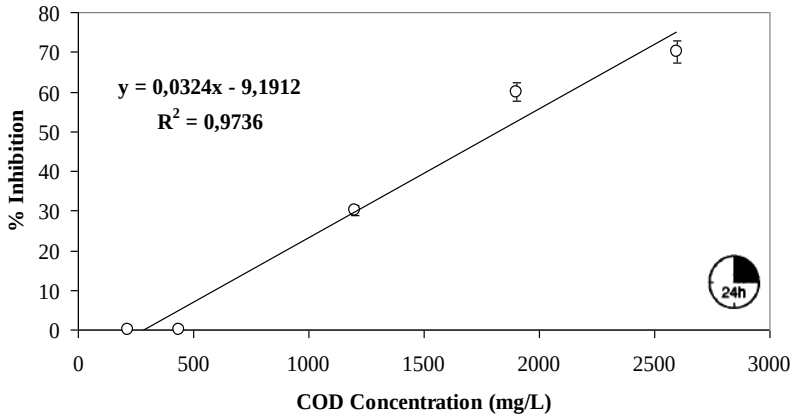

(b)

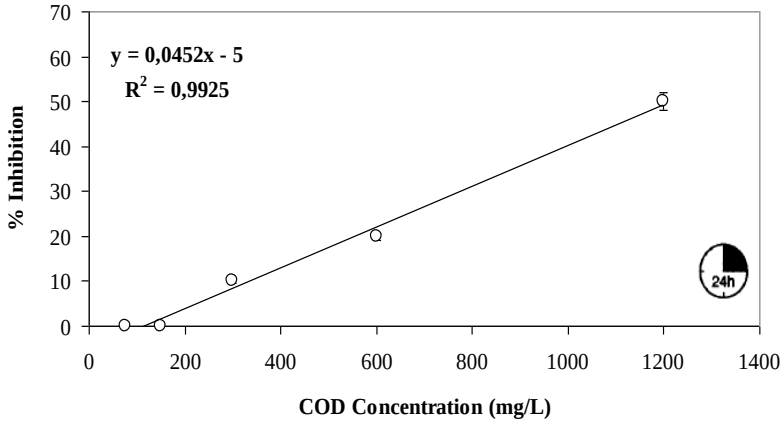

(c)

Figure 6.161 Variations of acute toxicity percentages and EC_{50} values in the effluent of the CSTR reactor for **(a)** ERY concentration 50 mg/L, EC_{50}=2632 mg/L; **(b)** ERY concentration 200 mg/L, EC_{50}=1833 mg/L and **(c)** ERY concentration 300 mg/L, EC_{50}=1216 mg/L (HRT=1.5 days; SRT=20 days)

Flaherty and Dodson, (2005) investigated the acute toxicity effects of 0.1-10 mg/L ERY on *Daphnia magna*. The EC_{50} values of *Daphnia magna* were between 3.5 and 5 mg/L. In another study, Halling-Sørensen, 2001 investigated the acute toxicity effects of 100 mg/L ERY to different species. The EC_{50} values of *Daphnia magna, Microcystis Aeruginosa, Selenastrium Capricarnitum* were found as 54.7, 13.8 and 34 mg/L. Christensen et al., (2006) investigated the acute toxicity of macrolide antibiotic used in aquaculture. They found a strong acute toxicity with *Daphnia magna* in 24 hour. The EC_{50} value was recorded as 41 mg/L. The EC_{50} values obtained in the aforementioned study are low in comparison to the EC_{50} values found in our study (EC_{50}=410-620 mg/L). The differences between trophic levels [*Microcystis Aeruginosa* (cynobacteria), *Daphnia magna* (Water flea) and *Selenastrium Capricarnitum* (green alga)] can affect the acute toxicity tests results with different responses to ERY.

6.5.5 Acute Toxicity Evaluation of Increasing OTC Concentrations in the Sequential AMCBR/CSTR Reactor System with Vibrio fischeri

Microtox acute toxicity assay was performed in order to determine the acute toxicity of OTC through anaerobic/aerobic sequential system. Acute toxicity test to the procedure described in "Material and Methods" was carried out in the influent, and effluents of anaerobic/aerobic system. Acute toxicity of the sequential AMCBR/CSTR reactor system was determined by Microtox test using bacteria *Vibrio fischeri* (NRRL-B-11177; LCK 491). Table 6.41 shows the EC_{50} values and acute toxicity yields obtained from the acute toxicity test. The EC_{50} values and the inhibition percentages found in the influent, effluent of the AMCBR and effluent of the CSTR were given in Figures 6.162, 6.163 and 6.164 (a-b-c) for 50, 150 and 250 mg/L OTC concentrations, respectively. All synthetic pharmaceutical wastewater samples were serially diluted in 2% NaCI (w/v) and each assay was performed at pH=7.0 and a temperature of 15 °C. NaCl (2%) was used as the control. After 30 min. of exposure time, the EC_{50} values of OTC were calculated.

The initial EC_{50} values increased from 208 to 520 mg/L from the influent of the anaerobic AMCBR reactor to the effluent of the AMCBR reactor at 50 mg/L OTC concentration (Table 6.41; Figures 6.162 (a) and 6.163 (a)). At the same OTC concentration the EC_{50} value in the effluent of the CSTR reactor increased to 2013 mg/L (Figures 6.164 (a)). This showed that acute toxicity decreased from the influent of the AMCBR reactor to the effluent of the CSTR reactor. The acute toxicity removal efficiencies increased from 60% to 74% and to 90% from the influent of the AMCBR reactor to the effluent of the CSTR reactor and to the sequential AMCBR/CSTR reactor system at a 50 mg/L OTC concentration (see Table 6.41).

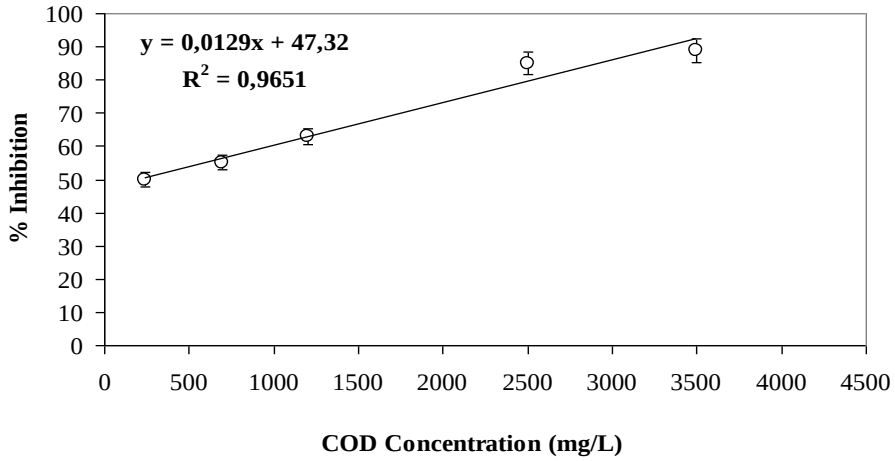

(a)

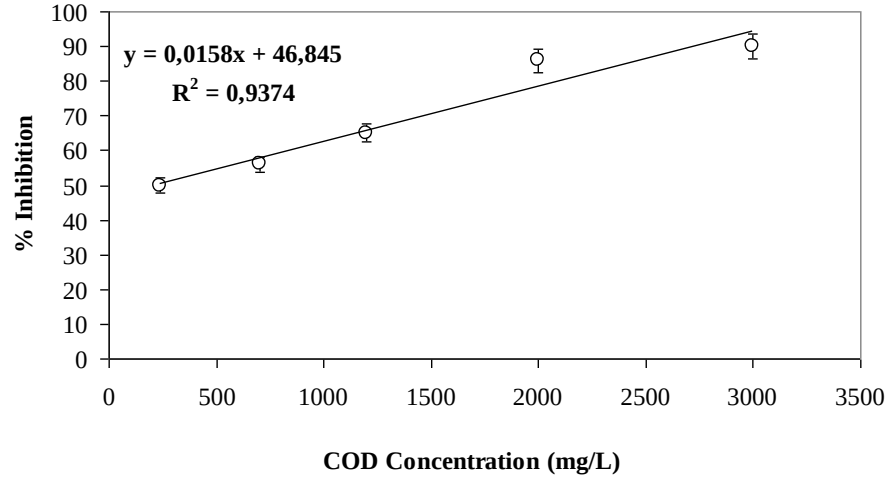

(b)

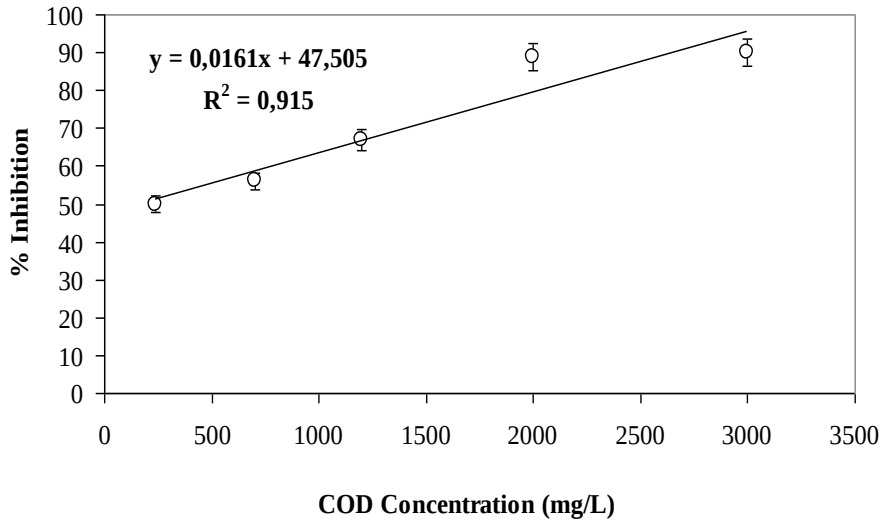

(c)

Figure 6.162 Variations of acute toxicity inhibitions and EC_{50} values in the influent of the AMCBR reactor for **(a)** OTC concentration 50 mg/L, EC_{50}=208 mg/L; **(b)** OTC concentration 150 mg/L, EC_{50}=199 mg/L; **(c)** OTC concentration 250 mg/L, EC_{50}=155 mg/L (HRT=2.25 days; SRT=94-101 days).

Table 6.41 Variations of acute toxicity values and yields in the influent and effluents of the AMCBR, CSTR and sequential AMCBR/CSTR system (HRT=2.25 days, SRT=94-101 days for AMCBR reactor and HRT=4.5 days, SRT=20 days for CSTR reactor)

OTC Conc. (mg/L)	**AMCBR reactor**		**CSTR reactor**	**Acute Toxicity Removal in the reactor system**		
	***EC_{50} value in the inf. (mg/L)**	***EC_{50} value in the effl. (mg/L)**	***EC_{50} value in the eff. (mg/L)**	**AMCBR reactor (%)**	**CSTR reactor (%)**	**AMCBR/CSTR reactor (%)**
50	208	520	2013	60	74	90
100	202	482	1683	58	72	88
150	199	456	1658	56	72	88
200	172	382	1229	55	69	86
250	155	345	1033	55	66	85

* EC_{50} values were calculated based on COD (mg/L).

The EC_{50} values increased from 199 to 456 mg/L from the influent of the anaerobic AMCBR reactor to the effluent of the AMCBR reactor at 150 mg/L OTC concentration (Figures 6.162 (b) and 6.163 (b)). The EC_{50} value in the effluent of the CSTR reactor increased to 1658 mg/L at a 150 mg/L OTC concentration (Figure 6.164 (b)). The acute toxicity removal efficiencies increased from 56% to 72% and to 88% from the influent of the AMCBR reactor to the effluent of the CSTR reactor and to the sequential AMCBR/CSTR reactor system (Table 6.41**).** At 250 mg/L OTC concentration the EC_{50} values increased from 155 to 345 mg/L from the influent of the AMCBR reactor to the effluent of the AMCBR reactor (Figures 6.162 (c) and 6.163 (c)). At the same OTC concentration the EC_{50} value in the effluent of the CSTR reactor increased to 1033 mg/L (Figures 6.164 (c)). This showed that acute toxicity decreased from the influent of the AMCBR reactor to the effluent of the CSTR reactor. The acute toxicity removal efficiencies increased from 55% to 66% and to 85% from the influent of the AMCBR reactor to the effluent of the CSTR in the sequential AMCBR/CSTR reactor system.

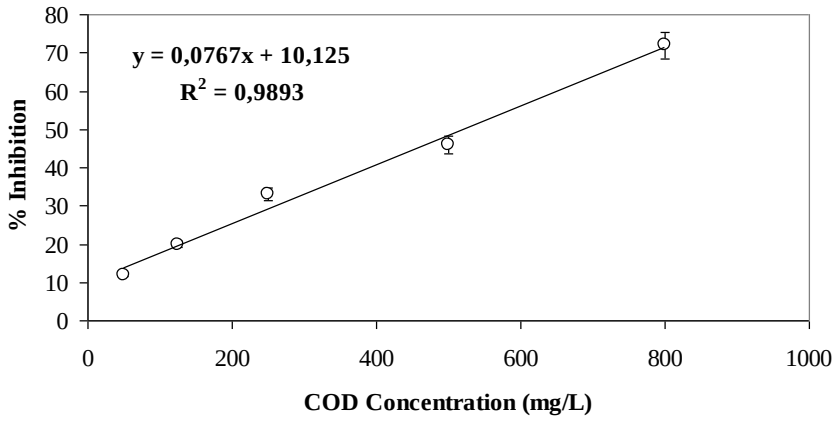

(a)

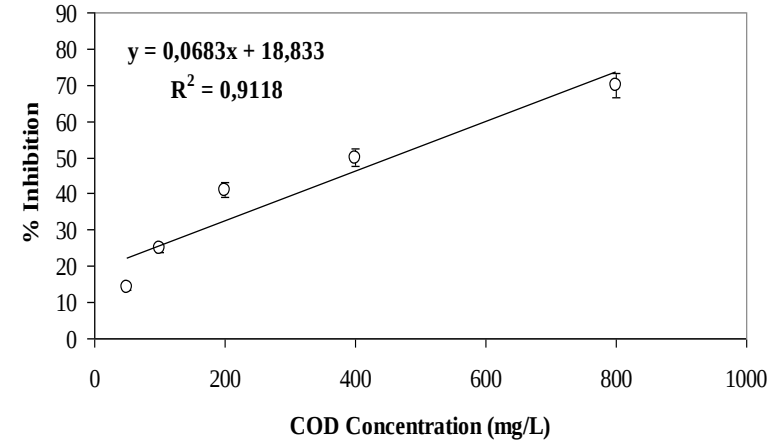

(b)

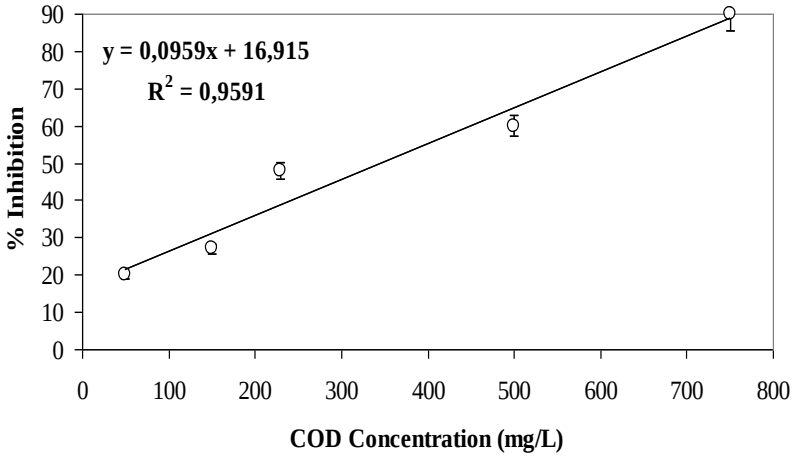

(c)

Figure 6.163 Variations of acute toxicity inhibitions, EC_{50} values in the effluent of the AMCBR for (a) OTC concentration 50 mg/L, EC_{50}= 520 mg/L; (b) OTC concentration 150 mg/L, EC_{50}=456 mg/L and (c) OTC concentration 250 mg/L, EC_{50}= 345 mg/L (HRT=2.25 days, SRT=94-101 days)

As the OTC concentrations increased from 50 to 100, 150, 200 and to 250 mg/L the EC_{50} values in the influent of the AMCBR reactor decreased from 208 to 202, 199, 172 and to 155 mg/L. Similarly, as the OTC concentrations increased from 50 up to 250 mg/L the EC_{50} values decreased from 520 mg/L to 345 mg/L in the effluent of the AMCBR reactor. The OTC concentrations increased from 50 up to 250 mg/L the EC_{50} values decreased from 2013 mg/L to 1033 mg/L in the effluent of

the CSTR reactor. Low EC_{50} values indicated the sensitivity of the *Vibrio fischeri* to the synthetic pharmaceutical wastewater at high OTC concentrations. High EC_{50} values show the resistance of Microtox to the synthetic pharmaceutical wastewater containing low OTC concentrations. The acute toxicity removals increased from the AMCBR effluent to the CSTR effluent. The acute toxicity removals decreased at all reactor system as the ERY concentration increased from 50 to 250 mg/L. The maximum acute toxicity removal in the sequential AMCBR/CSTR reactor system effluent was 90% for 50 mg/L OTC concentration (see Table 6.64). The minimum acute toxicity removal in the sequential AMCBR/CSTR reactor system effluent was 85% for 250 mg/L OTC concentration (see Table 6.64). Bioluminescence bacteria (*Vibrio fischeri*) acute toxicity test results demonstrated that the sequential anaerobic AMCBR/aerobic CSTR reactor system eliminated the inhibitory effect of the synthetic pharmaceutical wastewater containing OTC towards anaerobic AMCBR and aerobic CSTR reactor effluents.

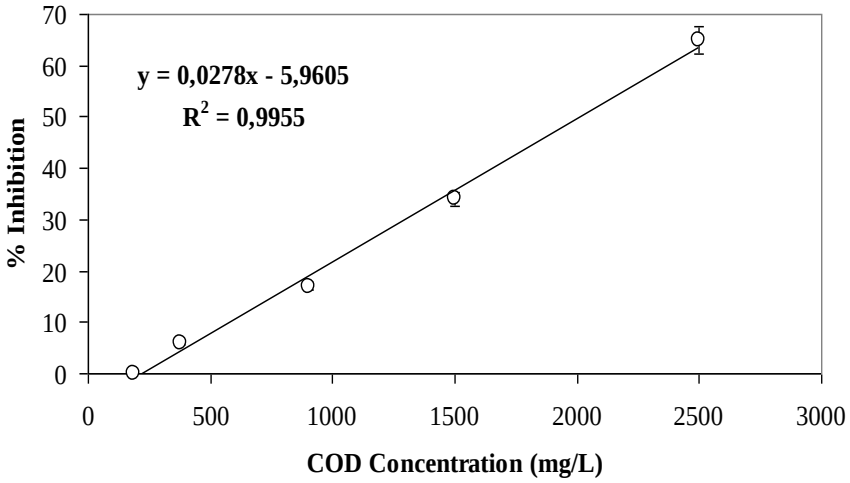

(a)

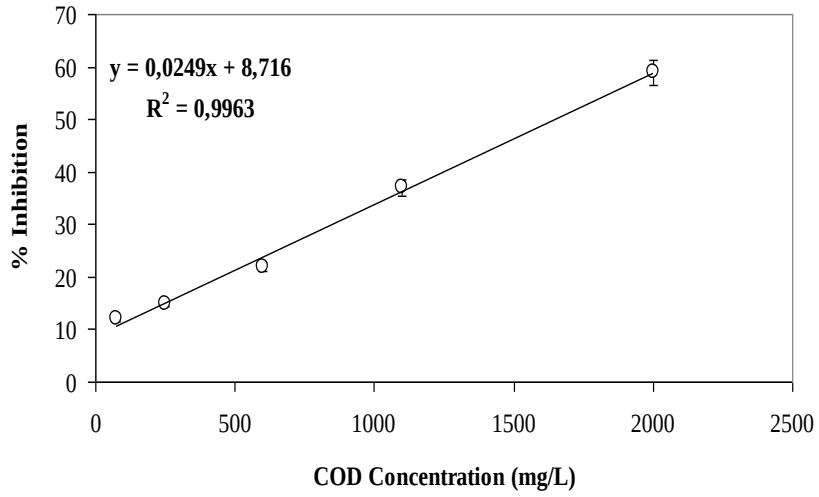

(b)

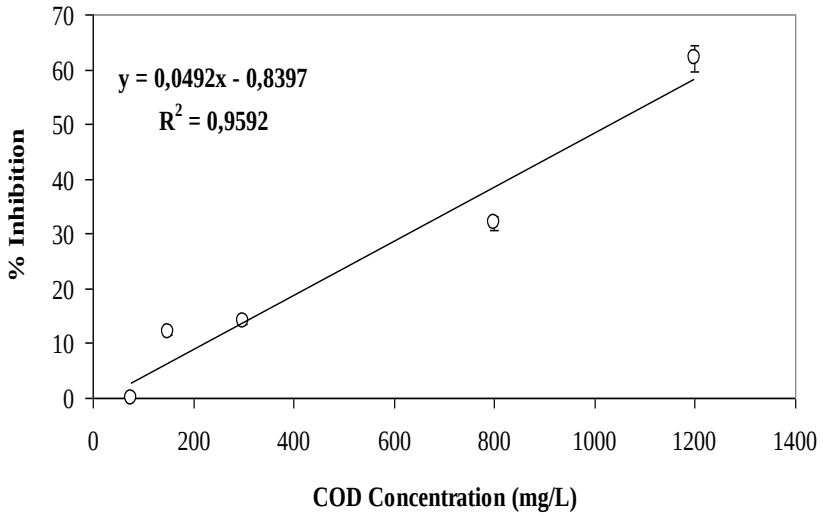

(c)

Figure 6.164 Variations of acute toxicity inhibitions and EC_{50} values in the effluent of the CSTR reactor for **(a)** OTC concentration 50 mg/L, EC_{50}= 2013 mg/L; **(b)** OTC concentration 150 mg/L, EC_{50}=1658 mg/L and **(c)** OTC concentration 250 mg/L, EC_{50}= 1033 mg/L (HRT=4.5 days, SRT=20 days)

Kim et al., (2008) investigated the acute toxicity effects of 30 mg/L OTC on three different trophic levels. The effective concentration cause 50% mortality on *Vibrio fischeri*, *Daphnia magna* and *Pseudokirchneriella subcapitata* were 35.99, 36.56 and

0.17 mg/L, respectively. The acute toxicities of OTC (50 mg/L) used therapeutically in aquaculture were investigated on different trophic levels by Zhang et al., (2012). The EC_{50} values of *Vibrio fischeri* (bioluminescence bacteria) and *Scenedesmus obliquus* (green alga) were 21.06 and 231.66 mg/L.

In another study performed by Backhaus and Grimme, (1999) the effects of OTC on *Vibrio fischeri* (bioluminescence bacteria) were investigated. The EC_{50} level for *Vibrio fischeri* was 25 mg/L. The acute toxicity effects of OTC used therapeutically in aquaculture in Italy were investigated on the *Vibrio fischeri* (strain NRRL-B-11177; LCK 491) by Lalumera et al., (2004). The EC_{50} values on *Vibrio fischeri* (strain NRRL-B-11177; LCK 491) varied between 121 and 139 mg/L The acute toxicities of 2 antibiotics namely; Chloramphenicole (20 mg/L) and OTC (50 mg/L) in pharmaceutical wastewater were investigated on the *Vibrio fischeri* (bioluminescence bacteria) by Fernandez et al. (2009). The EC_{50} values for Chloramphenicole and OTC antibiotics were 420 and 94 mg/L, respectively in an anaerobic ammonium oxidation process effluent. The EC_{50} values obtained in the aforementioned study are low in comparison to the EC_{50} values found in our study. The differences between trophic levels [*Vibrio fischeri* (bioluminescence bacteria), *Daphnia magna* (Water flea), *Pseudokirchneriella subcapitata* (bacteria) and *Scenedesmus obliquus* (green alga)] can affect the acute toxicity tests results with different responses to OTC. The low EC_{50} values found at high OTC concentrations could be attributed to their lethal effect on the *Vibrio fischeri*.

6.5.6 Acute Toxicity Evaluation of Increasing AMX Concentrations in the Sequential AMCBR/CSTR Reactor System with Vibrio fischeri

In this study, typical acute toxicity test was selected, acute toxicity based on the *Vibrio fischeri* (LCK 491; strain NRRL-B-11177) test and a simple assessment method based on acute toxicity test was explored. With this method, the removal performance of acute toxicity during anaerobic and aerobic pharmaceutical wastewater treatment processes was evaluated respectively. The acute toxicity values were evaluated in terms of Microtox test using *Vibrio fischeri* (LCK 491; strain

NRRL-B-11177) and the results were represented in the form of EC_{50} (effective concentration-the concentration responsible for a 50% reduction in the light output by *Vibrio fischeri*).

Acute toxicity values of antibiotics on *Vibrio fischeri* (LCK 491; strain NRRL-B-11177) after 30 min of exposure, expressed as EC_{50} values, are listed in Table 6.42. The EC_{50} values increased from 323 to 664 mg/L from the influent of the anaerobic AMCBR reactor to the effluent of the AMCBR reactor at 22.22 g/m^3d AMX loading (Figures 6.165 (a) and 6.166 (a)). At the same AMX loading, the EC_{50} value in the effluent of the CSTR reactor increased to 2647 mg/L (Figure 6.167 (a)). This showed that acute toxicity decreased from the influent of the AMCBR reactor to the effluent of the CSTR reactor. The acute toxicity removal efficiencies increased from 51% to 75% and to 88% from the influent of the AMCBR reactor to the effluent of the CSTR reactor in the sequential AMCBR/CSTR reactor system at a 22.22 g/m^3d AMX loading (see Table 6.42). The decrease in EC_{50} values could be explained by the inhibitory effect of the high AMX loading on the *Vibrio fischeri* (LCK 491; strain NRRL-B-11177). The results of the study showed that as the AMX loading rates increased from 22.22, 44.44, 66.67 to 88.89, 111.11 g/m^3d, respectively, the acute toxicity decreased.

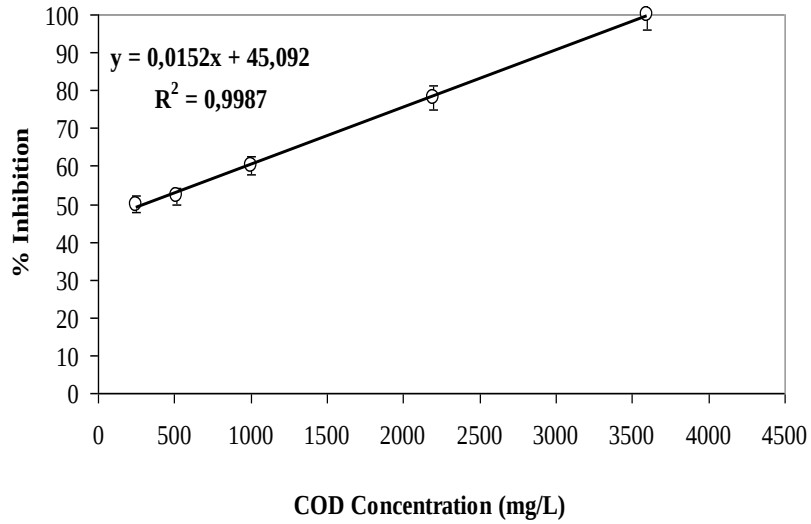

(a)

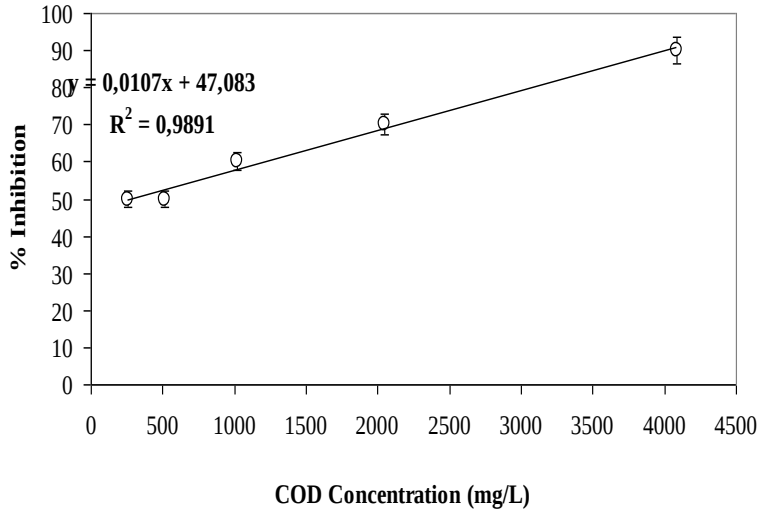

b)

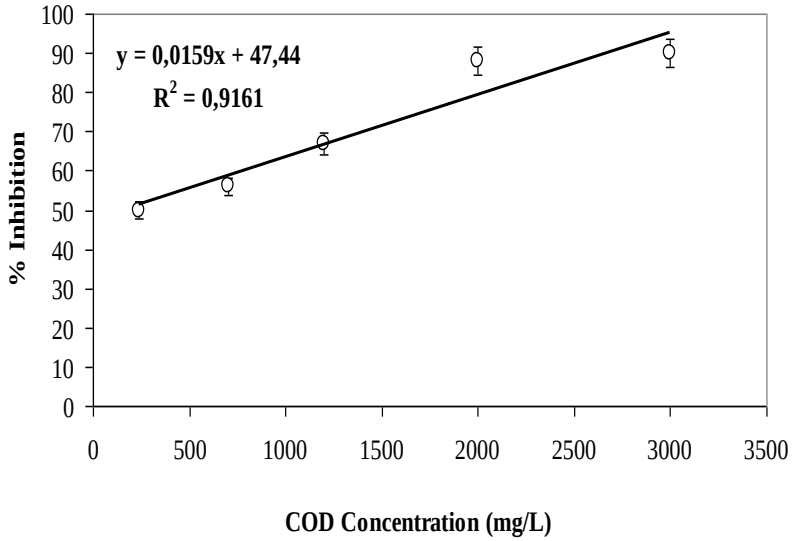

(c)

Figure 6.165 Variations of acute toxicity percentages and EC_{50} values in the influent of the AMCBR reactor for **(a)** AMX loading 22.22 g/m^{3}d, EC_{50}= 323 mg/L; **(b)** AMX loading 66.67 g/m^{3}d, EC_{50}=273 mg/L and **(c)** AMX loading 111.11 g/m^{3}d, EC_{50}= 161 mg/L (HRT=4.5 days; SRT=49-95 days)

Table 6.42 Variations of acute toxicity values in the influent and effluents of the AMCBR, CSTR and sequential AMCBR/CSTR system (HRT=4.5 days, SRT=49-95 days for AMCBR reactor and HRT=9.0 days, SRT=20 days for CSTR reactor)

AMX Conc. (mg/L)	**AMX Loading (g/m^3d)**	**AMCBR reactor**		**CSTR reactor**	**Acute Toxicity Removal in the reactor system**		
		***EC_{50} value in the inf. (mg/L)**	***EC_{50} value in the eff. (mg/L)**	***EC_{50} value in the eff. (mg/L)**	**AMCBR reactor (%)**	**CSTR reactor (%)**	**AMCBR /CSTR reactor (%)**
50	**22.22**	323	664	2647	51	75	88
100	**44.44**	302	604	2323	50	74	87
150	**66.67**	273	543	2172	50	75	87
200	**88.89**	200	385	1333	48	71	85
250	**111.11**	161	310	1033	48	70	84

* EC_{50} values were calculated based on COD (mg/L).

The EC_{50} values increased from 273 to 543 mg/L from the influent of the anaerobic AMCBR reactor to the effluent of the AMCBR reactor at 66.67 g/m^3d AMX loading (Figures 6.165 (b) and 6.166 (b)). The EC_{50} value in the effluent of the CSTR reactor increased to 2172 mg/L at a 66.67 g/m^3d AMX loading (Figure 6.167 (b)). The acute toxicity removal efficiencies increased from 50% to 75% and to 87% from the influent of the AMCBR reactor to the effluent of the CSTR reactor in the sequential AMCBR/CSTR reactor system (Table 6.42). At 111.11 g/m^3d AMX loading the EC_{50} values increased from 161 to 310 mg/L from the influent of the AMCBR reactor to the effluent of the AMCBR reactor (Figures 6.165 (c) and 6.166 (c)). The EC_{50} value in the effluent of the CSTR reactor increased to 1033 mg/L at a 111.11 g/m^3d AMX loading (Figures 6.167 (c)). This showed that acute toxicity decreased from the influent of AMCBR to the effluent of CSTR reactor. The acute toxicity removal efficiencies increased from 48% to 70% and to 84% from the influent of the AMCBR reactor to the effluent of the CSTR reactor in the sequential AMCBR/CSTR reactor system.

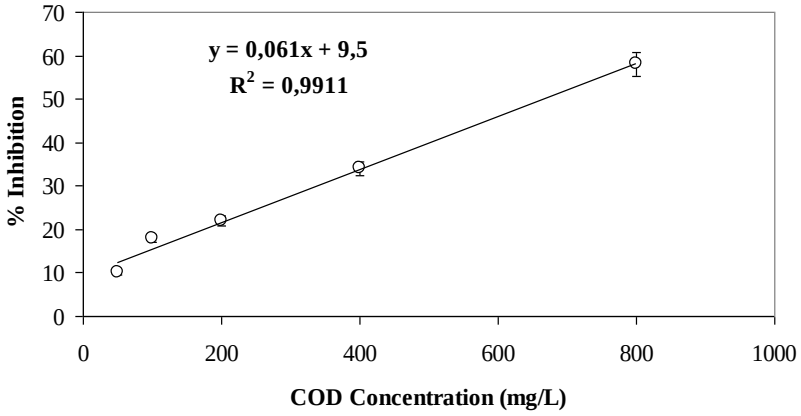

(a)

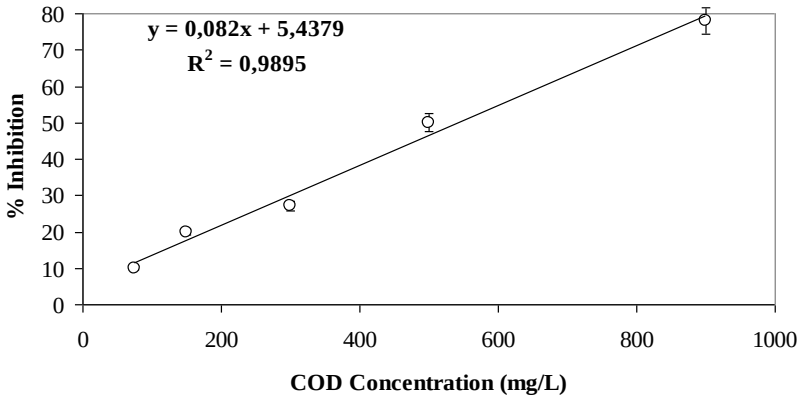

(b)

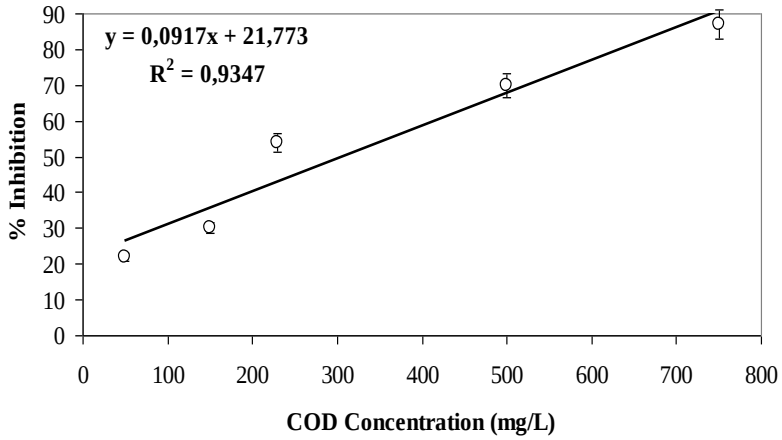

(c)

Figure 6.166 Variations of acute toxicity percentages and EC_{50} values in the effluent of the AMCBR reactor **(a)** AMX loading 22.22 g/m^{3}d, EC_{50}= 667 mg/L; **(b)** AMX loading 66.67 g/m^{3}d, EC_{50}=543 mg/L and **(c)** AMX loading 111.11 g/m^{3}d, EC_{50}= 310 mg/L (HRT=4.5 days, SRT=49-95 days).

As the AMX loadings increased from 22.22 to 44.44, 66.67, 88.89 and to 111.11 g/m^{3}d the EC_{50} values in the influent of the AMCBR reactor decreased from 323 to 302, 273, 200 and to 161 mg/L. Similarly, as the AMX loadings increased from 22.22 up to 111.11 g/m^{3}d the EC_{50} values decreased from 664 mg/L to 310 mg/L in the effluent of the AMCBR reactor. The EC_{50} values also decreased from 2647 mg/L to 1033 mg/L in the effluent of the CSTR reactor. High EC_{50} values show the resistance of *Vibrio fischeri* to the synthetic pharmaceutical wastewater containing low AMX concentrations. The acute toxicity removals increased from the effluent of the AMCBR to the effluent of the CSTR reactor.

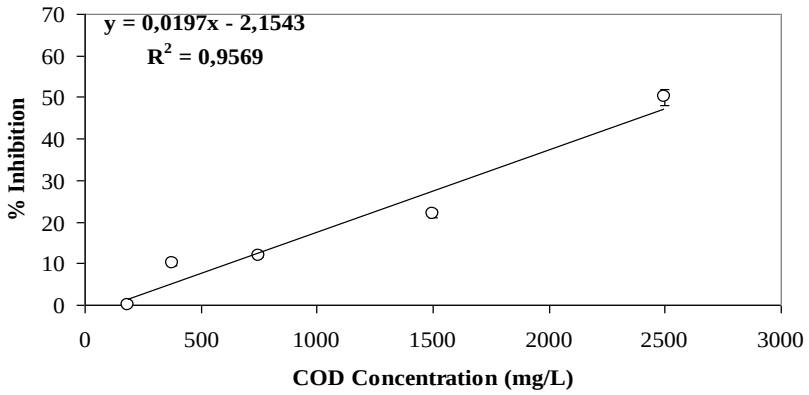

(a)

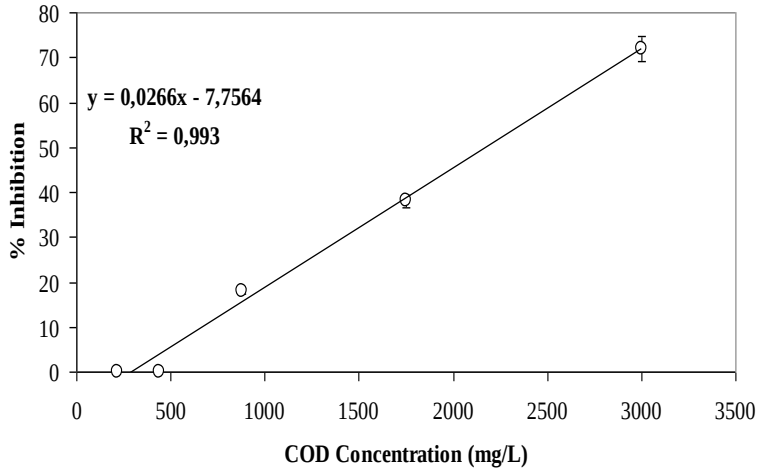

(b)

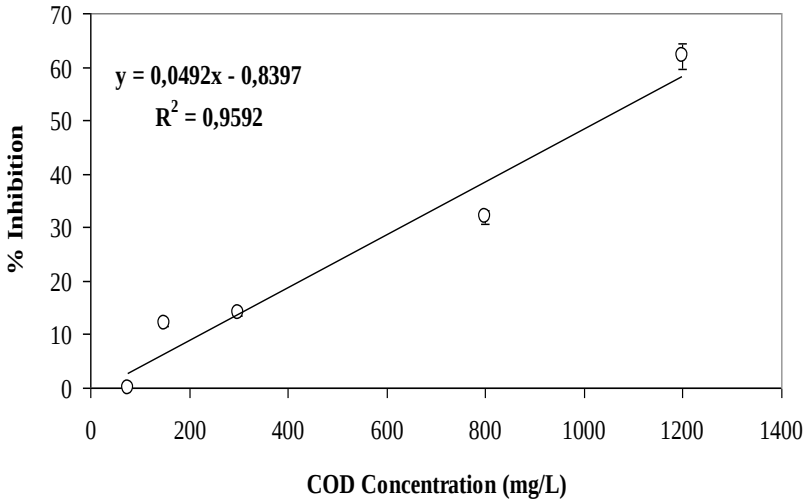

(c)

Figure 6.167 Variations of acute toxicity percentages and EC_{50} values in the effluent of the CSTR reactor for **(a)** AMX loading 22.22 g/m^{3}d, EC_{50}= 2647 mg/L; **(b)** AMX loading 66.67 g/m^{3}d, EC_{50}=2172 mg/L and **(c)** AMX loading 111.11 g/m^{3}d, EC_{50}= 1033 mg/L (HRT=9.0 days, SRT=20 days).

The maximum total acute toxicity reduction in the sequential AMCBR/CSTR reactor system effluent was 88% for 22.22 g/m^{3}d AMX loading rate (see Table 6.65). The minimum total acute toxicity reduction in the sequential AMCBR/CSTR reactor system effluent was 84% for 111.11 g/m^{3}d AMX loading rate (see Table 4.17). In this study, high AMX (>150 mg/L) concentrations caused inhibitory effect on *Vibrio fischeri* (LCK 491; strain NRRL-B-11177) in the sequential AMCBR/CSTR system (Table 6.65).

The studies performed in recent literature showed that the β-lactam antibiotics exhibited acute toxicity to different test organisms in wastewaters. The acute toxicities of AMX (12.82-39.48 mg/L) were investigated on the *Vibrio fischeri* by Bolelli et al., (2006). The EC_{50} values for AMX varied between 18.37 and 34.45 mg/L under anaerobic conditions in the study performed by Bolelli et al., (2006). Kümmerer et al., (2004) investigated the suitability of the bioluminescence inhibition test to assess the effect of AMX acute toxicity on *Vibrio fischeri* (bioluminescence bacteria). The EC_{50} value for AMX was >100 mg/L in the aquatic environment. Liu et al., (2012) investigated the acute toxicity effects (EC_{50}) of 0.08-1.00 mg/L AMX

on *Microcystis aeruginosa*. The EC_{50} on *Microcystis aeruginosa* varied between 0.07 and 1 mg/L. The EC_{50} values obtained in the aforementioned study are low in comparison to the EC_{50} values found in our study (EC_{50}=161-664 mg/L). The differences between trophic levels [*Vibrio fischeri* (bioluminescence bacteria) and *Microcystis aeruginosa* (Cyanobacteria)] can affect the EC_{50} values with different responses to AMX.

6.5.7 Acute Toxicity Evaluation of Increasing TYL Concentrations in the Sequential AMCBR/CSTR Reactor System with Vibrio fischeri

Microtox test is an acute toxicity test. Therefore the acute toxicity results of this test could be obtained in short times (maximum 30 min). Table 6.43 shows the EC_{50} values and the acute toxicity removals in samples taken from the influent of the synthetic pharmaceutical wastewater containing TYL of 50, 100, 150, 200, 250 mg/L from the anaerobic AMCBR and aerobic CSTR reactors through continuous operation at HRT=2.25 days, SRT=71-117 days for AMCBR reactor and HRT=4.5 days, SRT=20 days for CSTR reactor (see section "Materials and Methods"). The EC_{50} values and the acute toxicity reductions found in the influent, effluent of the AMCBR reactor and effluent of the CSTR reactor were given in Figures 6.168 (a-b-c), 6.169 (a-b-c) and 6.170 (a-b-c) for 50, 150 and 250 mg/L TYL concentrations, respectively.

The initial EC_{50} values increased from 275 to 546 mg/L from the influent of the anaerobic AMCBR reactor to the effluent of the AMCBR reactor at 50 mg/L TYL concentration (Table 6.66; Figures 6.168, 6.169 and 6.170 (a-b-c)). At the same TYL concentration the EC_{50} value in the effluent of the CSTR reactor increased to 2030 mg/L (Figures 6.170 (a)). This showed that acute toxicity decreased from the influent of the AMCBR reactor to the effluent of the CSTR reactor. The acute toxicity removal efficiencies increased from 51% to 73% and to 86% from the influent of the AMCBR reactor to the effluent of the CSTR reactor in the sequential AMCBR/CSTR reactor system at a 50 mg/L TYL concentration (see Table 6.43). The EC_{50} values increased from 205 to 410 mg/L from the influent of the anaerobic

AMCBR reactor to the effluent of the AMCBR reactor at 100 mg/L TYL concentration (Figures 6.168 (b) and 6.169 (b)). The EC_{50} value in the effluent of the CSTR reactor increased to 1216 mg/L at a 100 mg/L TYL concentration (Figures 6.170 (b)). The acute toxicity removal efficiencies increased from 50% to 66% and to 83% from the influent of the AMCBR reactor to the effluent of the CSTR reactor in the sequential AMCBR/CSTR reactor system (Table 6.43). At 250 mg/L TYL concentration the EC_{50} values increased from 122 to 230 mg/L from the influent of the AMCBR reactor to the effluent of the AMCBR reactor (Figures 6.168 (c) and 6.169 (c)). At the same TYL concentration the EC_{50} value in the effluent of the CSTR reactor increased to 650 mg/L (Figure 6.170 (c)). This showed that acute toxicity decreased from the influent of the AMCBR to the effluent of the CSTR reactor. The acute toxicity removal efficiencies increased from 47% to 64% and to 81% from the influent of the AMCBR reactor to the effluent of the CSTR in the sequential AMCBR/CSTR reactor system.

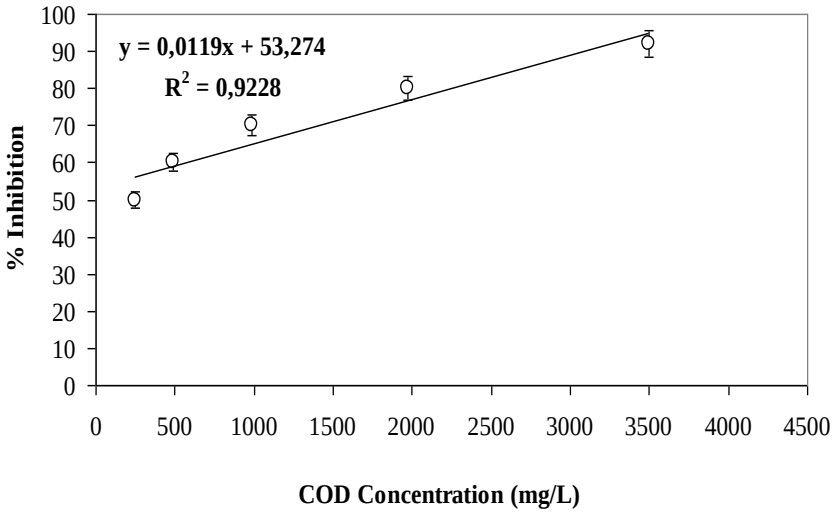

(a)

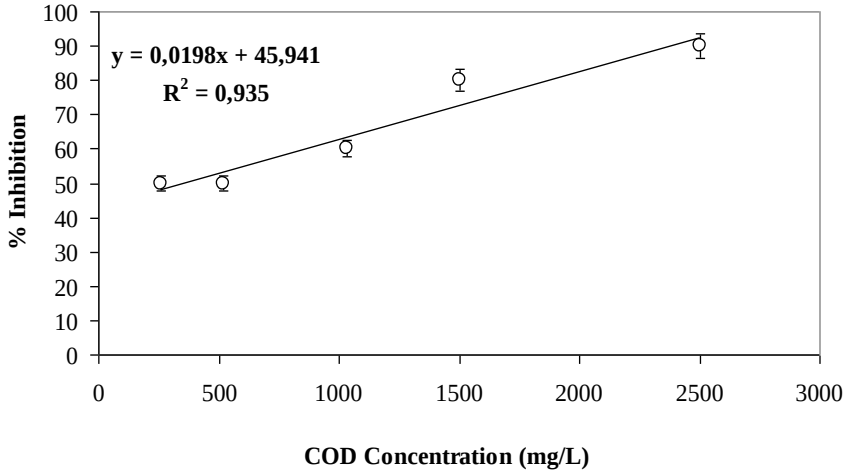

(b)

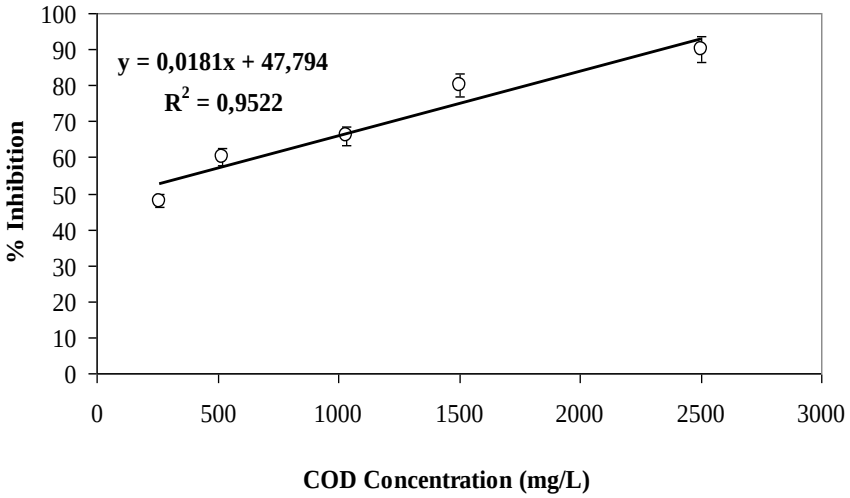

(c)

Figure 6.168 Variations of acute toxicity percentages and EC_{50} values in the influent of the AMCBR reactor for **(a)** TYL concentration 50 mg/L, EC_{50}=275 mg/L; **(b)** TYL concentration 150 mg/L, EC_{50}=205 mg/L and **(c)** TYL concentration 250 mg/L, EC_{50}=122 mg/L (HRT=2.25 days; SRT=71-117 days).

As the TYL concentrations increased from 50 to 100, 150, 200 and to 250 mg/L the EC_{50} values in the influent of the AMCBR reactor decreased from 275 to 250, 205, 164 and to 122 mg/L. Similarly, as the TYL concentrations increased from 50 up to 250 mg/L the EC_{50} values decreased from 546 mg/L to 230 mg/L in the effluent of the AMCBR reactor. The EC_{50} values also decreased from 2030 mg/L to

650 mg/L in the effluent of the CSTR reactor. Low EC_{50} values indicated the sensitivity of the *Vibrio fischeri* to the synthetic pharmaceutical wastewater at high TYL concentrations. The acute toxicity removals increased from the effluent of the AMCBR reactor to the effluent of the CSTR reactor. The acute toxicity removals decreased at all reactor system as the TYL concentration increased from 50 to 250 mg/L.

Table 6.43 Variations of acute toxicity values in the influent and effluents of the AMCBR, CSTR and sequential AMCBR/CSTR system (HRT=2.25 days, SRT=71-117 days for AMCBR reactor and HRT=4.5 days, SRT=20 days for CSTR reactor)

TYL **Conc. (mg/L)**	**AMCBR reactor**		**CSTR reactor**	**Acute Toxicity Removal in the reactor system**		
	***EC_{50} value in the inf. (mg/L)**	***EC_{50} value in the eff. (mg/L)**	***EC_{50} value in the eff. (mg/L)**	**AMCBR reactor (%)**	**CSTR reactor (%)**	**AMCBR/CSTR reactor (%)**
50	275	546	2030	51	73	86
100	250	500	1563	50	68	84
150	205	410	1216	50	66	83
200	164	315	911	48	65	82
250	122	230	650	47	64	81

* EC_{50} values were calculated based on COD (mg/L).

This shows that the effluent of the anaerobic AMCBR reactor was less toxic (EC_{50}=230-546 mg/L) than the feed containing TYL. After aerobic treatment, the EC_{50} values increased from 650 to 2030 mg/L in the aerobic effluent. The CSTR reactor effluent was less toxic compared to the influent. It was observed that the acute toxicity of influent of the anaerobic AMCBR reactor were high, whereas after sequential treatment the acute toxicity was decreased.

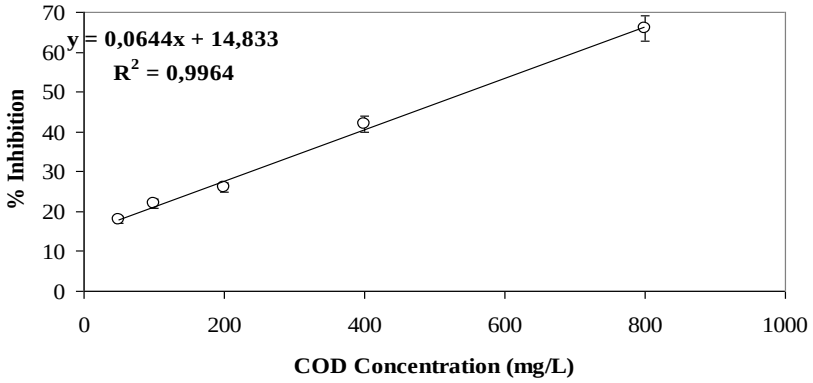

(a)

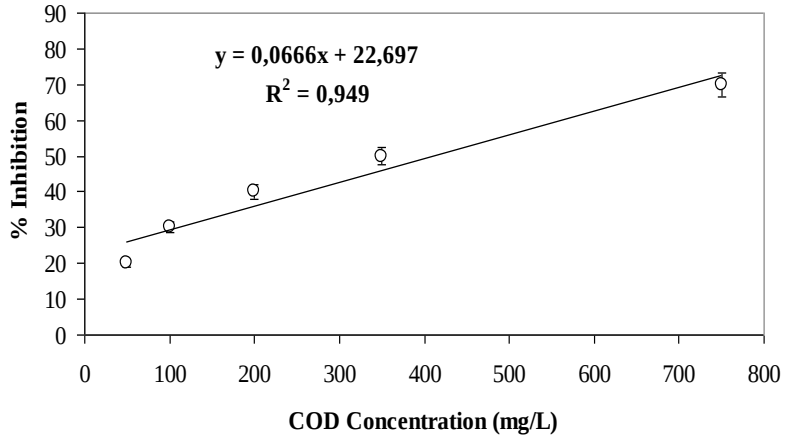

(b)

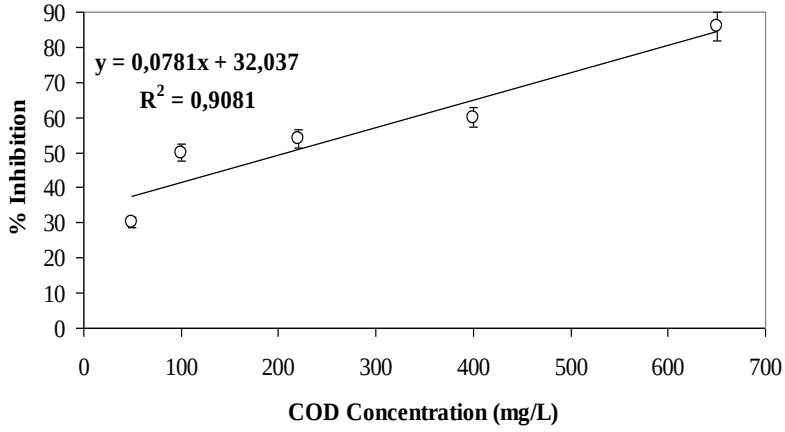

(c)

Figure 6.169 Variations of acute toxicity percentages and EC_{50} values in the effluent of the AMCBR reactor for **(a)** TYL concentration 50 mg/L, EC_{50}=546 mg/L; **(b)** TYL concentration 150 mg/L, EC_{50}=410 mg/L and **(c)** TYL concentration 250 mg/L, EC_{50}= 230 mg/L (HRT=4.5 days, SRT=71-117 days)

Low EC_{50} values found at high TYL concentrations could be attributed to their detrimental effect on the *Vibrio fischeri* (strain NRRL-B-11177; LCK 491) cells the high TYL concentrations caused plasmolysis in *Vibrio fischeri* cells by increasing the osmotic pressure in the Microtox test medium. The maximum acute toxicity removal efficiency in the effluent of the sequential AMCBR/CSTR reactor system was 86% for 50 mg/L TYL concentration (Table 6.66). The minimum acute toxicity removal efficiency in the effluent of the sequential AMCBR/CSTR reactor system effluent was 81% for 250 mg/L TYL concentration (see Table 6.66).

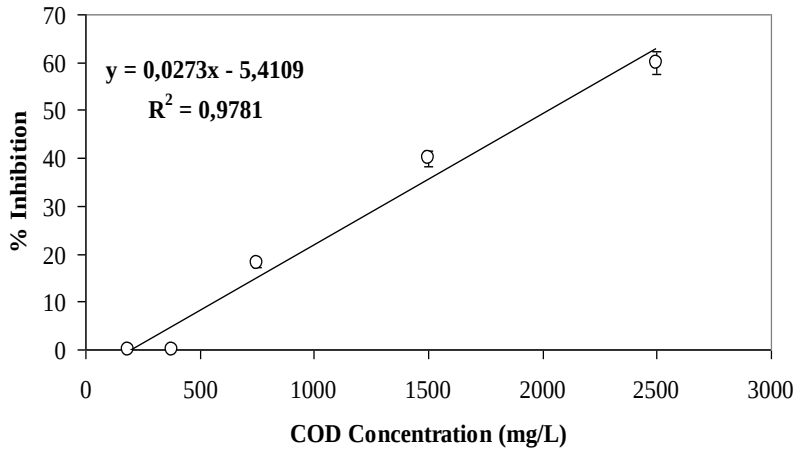

(a)

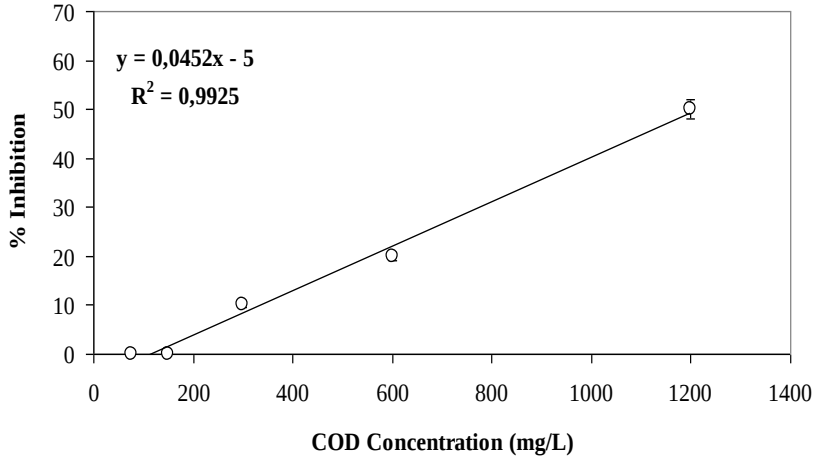

(b)

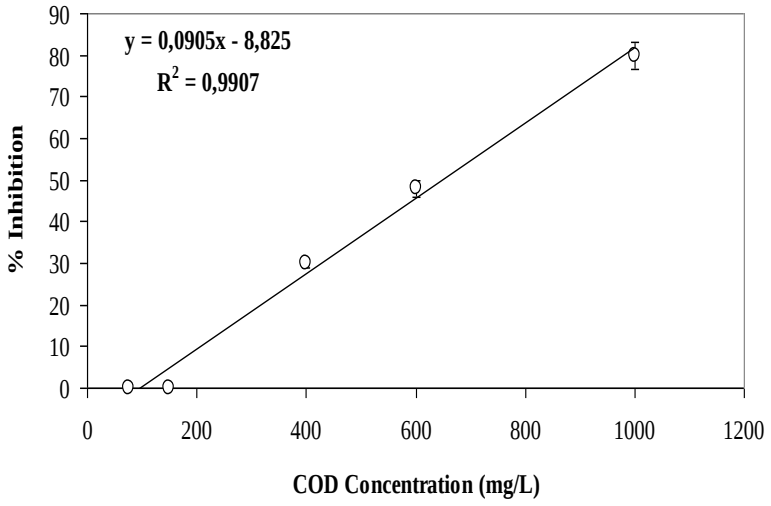

(c)

Figure 6.170 Variations of acute toxicity percentages and EC_{50} values in the effluent of the CSTR reactor for **(a)** TYL concentration 50 mg/L, EC_{50}=2030 mg/L; **(b)** TYL concentration 150 mg/L, EC_{50}=1216 mg/L and **(c)** TYL concentration 250 mg/L, EC_{50}=650 mg/L (HRT=4.5 days, SRT=20 days for CSTR reactor)

The acute toxicity of TYL (50-160 mg/L) was investigated on water flea *Daphnia magna* by Wollenberger et al. (2000). The EC_{50} value for TYL varied between 56 and 483 mg/L under anaerobic conditions in this study performed by Wollenberger et al. (2000). In our study, the EC_{50} values were between 230 and 546 mg/L, at TYL concentrations varying between 50 and 250 mg/L in the effluent of the AMCBR reactor system. The EC_{50} values for TYL obtained in the aforementioned study are low in comparison to the EC_{50} values found in our study. The low EC_{50} values found at high TYL concentrations could be explained by TYL inhibitions or lethal effect of high TYL concentrations on *Daphnia magna* cells.

Brain et al., (2004) reported that the acute toxicity effect of 50 mg/L TYL on *Lemma gibba* (duckweed). The effective concentration cause 50% mortality (EC_{50}) on *Lemma gibba* was 10.28 mg/L. The EC_{50} values obtained in the aforementioned study are low in comparison to the EC_{50} values found in our study (EC_{50}=650-2030 mg/L). The differences in operational conditions and the differences in the TYL concentrations can affect the EC_{50} values.

6.5.8 Acute Toxicity Evaluation of Increasing ERY Concentrations in the Sequential AMCBR/CSTR Reactor System with Vibrio fischeri

The Microtox test is accepted as an acute toxicity test. Acute toxicity test was estimated in terms of EC_{50}, defined as the concentration of the toxicant causing 50% reduction in activity of the *Vibrio fischeri* (strain NRRL-B-11177; LCK 491). The effective COD concentrations caused 50% mortality in *Vibrio fischeri* (strain NRRL-B-11177; LCK 491) cells was defined as EC_{50} (mg/L) in pharmaceutical wastewater samples. The EC_{50} values were calculated by taking into consideration the dilution ratios. Table 6.44 shows the EC_{50} values and the acute toxicity removals in samples taken from the influent of the AMCBR reactor (from the synthetic pharmaceutical wastewater) containing 50, 100, 150, 200, 250 mg/L ERY, from the anaerobic AMCBR and aerobic CSTR reactors through continuous operation at HRT=1.50 days, SRT=85-106 days for AMCBR reactor and HRT=3.0 days, SRT=20 days for CSTR reactor. The EC_{50} values and the acute toxicity reductions found in the influent, effluent of the AMCBR reactor and effluent of the CSTR reactor were given in Figures 6.171 (a-b-c), 6.172 (a-b-c) and 6.173 (a-b-c) for 50, 150 and 250 mg/L ERY concentrations, respectively.

The initial EC_{50} values increased from 275 to 546 mg/L from the influent of the anaerobic AMCBR reactor to the effluent of the AMCBR reactor at 50 mg/L ERY concentration (Table 6.44; Figures 6.171, 6.172 and 6.173 (a-b-c)). At the same ERY concentration the EC_{50} value in the effluent of the CSTR reactor increased to 2030 mg/L (Figures 6.173 (a)). This showed that acute toxicity decreased from the influent of the AMCBR reactor to the effluent of the CSTR reactor. The acute toxicity removal efficiencies increased from 51% to 73% and to 86% from the influent of the AMCBR reactor to the effluent of the CSTR reactor in the sequential AMCBR/CSTR reactor system at a 50 mg/L ERY concentration (see Table 6.44). The EC_{50} values increased from 205 to 410 mg/L from the influent of the anaerobic AMCBR reactor to the effluent of the AMCBR reactor at 100 mg/L ERY concentration (Figures 6.171 (b) and 6.172 (b)). The EC_{50} value in the effluent of the CSTR reactor increased to 1216 mg/L at a 100 mg/L ERY concentration (Figure

6.173 (b)). The acute toxicity removal efficiencies increased from 50% to 66% and to 83% from the influent of the AMCBR reactor to the effluent of the CSTR reactor in the sequential AMCBR/CSTR reactor system (Table 6.44). At 250 mg/L ERY concentration the EC_{50} values increased from 122 to 230 mg/L from the influent of the AMCBR reactor to the effluent of the AMCBR reactor (Figures 6.171 (c) and 6.172 (c)). At the same ERY concentration the EC_{50} value in the effluent of the CSTR reactor increased to 650 mg/L (Figure 6.173 (c)). This showed that acute toxicity decreased from the influent of the AMCBR to the effluent of the CSTR reactor. The acute toxicity removal efficiencies increased from 47% to 64% and to 81% from the influent of the AMCBR reactor to the effluent of the CSTR reactor in the sequential AMCBR/CSTR reactor system.

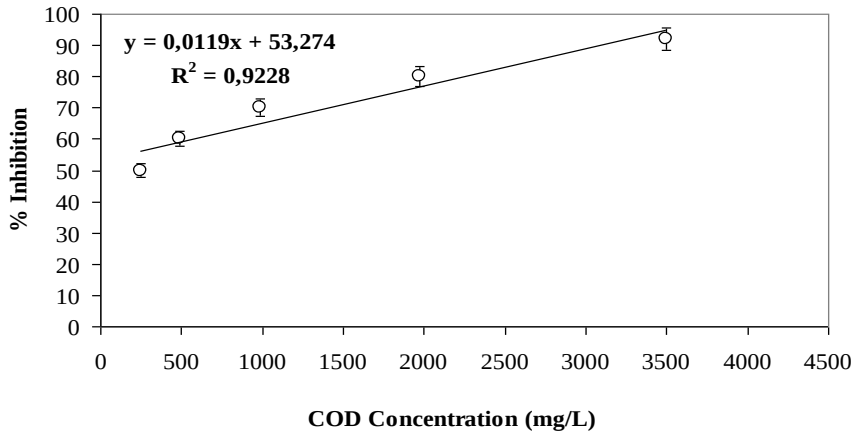

(a)

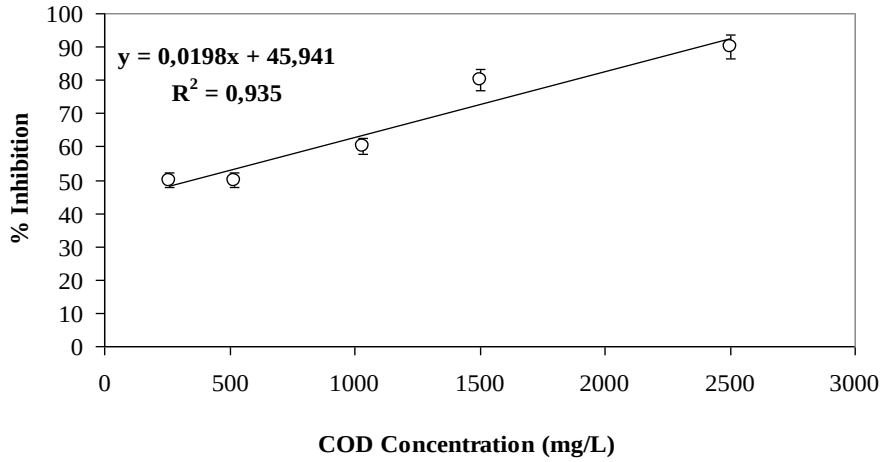

(b)

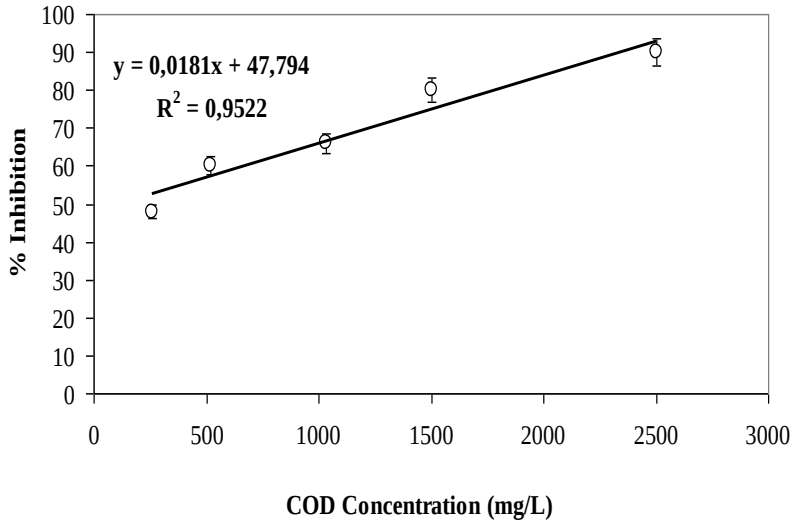

(c)

Figure 6.171 Variations of acute toxicity percentages and EC_{50} values in the influent of the AMCBR reactor for **(a)** ERY concentration 50 mg/L, EC_{50}=275 mg/L; **(b)** ERY concentration 150 mg/L, EC_{50}=205 mg/L and **(c)** ERY concentration 250 mg/L, EC_{50}=122 mg/L (HRT=1.50 days; SRT=85-106 days).

As the ERY concentrations increased from 50 to 100, 150, 200 and to 250 mg/L the EC_{50} values in the influent of the AMCBR reactor decreased from 275 to 250, 205, 164 and to 122 mg/L. Similarly, as the ERY concentrations increased from 50 up to 250 mg/L the EC_{50} values decreased from 546 mg/L to 230 mg/L in the effluent of AMCBR reactor. The ERY concentrations increased from 50 up to 250 mg/L the EC_{50} values decreased from 2030 mg/L to 650 mg/L in the effluent of the CSTR reactor. The acute toxicity removals increased from the effluent of the AMCBR to the effluent of the CSTR reactor. The acute toxicity removals decreased at all reactor system as the ERY concentration increased from 50 to 250 mg/L.

Table 6.44 Variations of acute toxicity values in the influent and effluents of the AMCBR, CSTR and sequential AMCBR/CSTR system (HRT=1.5 days, SRT=85-106 days for AMCBR reactor and HRT=3.0 days, SRT=20 days for CSTR reactor)

ERY **Conc. (mg/L)**	**AMCBR reactor**		**CSTR reactor**	**Acute Toxicity Removal in the reactor system**		
	***EC_{50} value in the inf. (mg/L)**	***EC_{50} value in the eff. (mg/L)**	***EC_{50} value in the eff. (mg/L)**	**AMCBR reactor (%)**	**CSTR reactor (%)**	**AMCBR/CSTR reactor (%)**
50	275	546	2030	51	73	86
100	250	500	1563	50	68	84
150	205	410	1216	50	66	83
200	164	315	911	48	65	82
250	122	230	650	47	64	81

* EC_{50} values were calculated based on COD (mg/L).

This shows that the effluent of the anaerobic AMCBR reactor was less toxic (EC_{50}=230-546 mg/L) than the feed containing ERY. After aerobic treatment, the EC_{50} values increased from 650 to 2030 mg/L in aerobic effluent. The aerobic CSTR reactor effluent was less toxic compared to the influent. It was observed that the acute toxicity of influent of anaerobic AMCBR reactor were high, whereas after sequential anaerobic/aerobic treatment the acute toxicity was decreased.

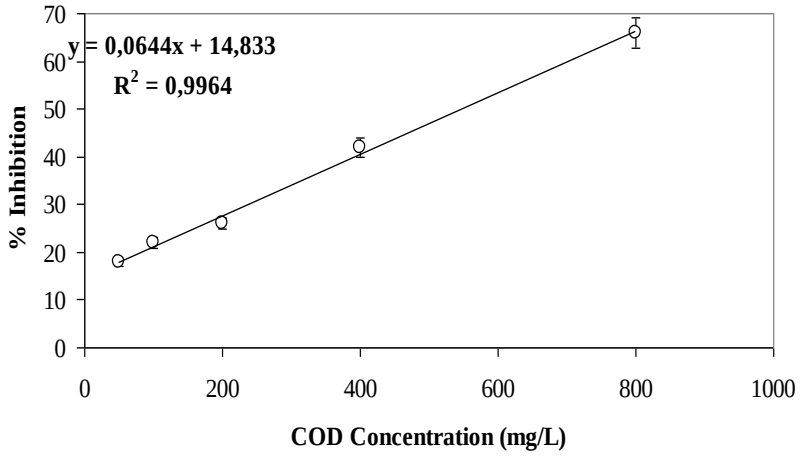

(a)

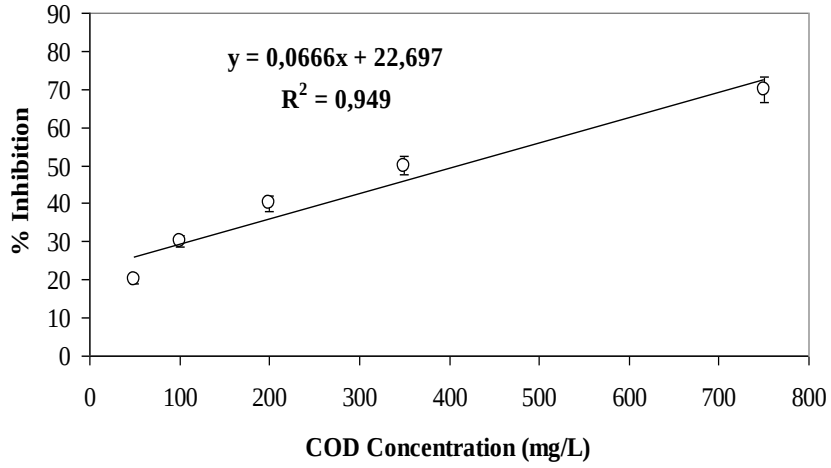

(b)

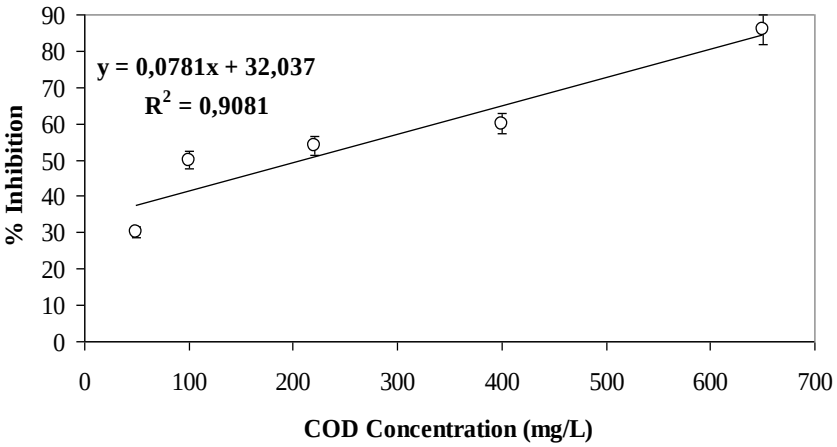

(c)

Figure 6.172 Variations of acute toxicity percentages and EC_{50} values in the effluent of the AMCBR reactor for **(a)** ERY concentration 50 mg/L, EC_{50}=546 mg/L; **(b)** ERY concentration 150 mg/L, EC_{50}=410 mg/L and **(c)** ERY concentration 250 mg/L, EC_{50}= 230 mg/L from the anaerobic AMCBR and aerobic CSTR reactors through continuous operation (HRT=1.50 days; SRT=85-106 days)

Low EC_{50} values found at high ERY concentrations could be attributed to their detrimental effect on the *Vibrio fischeri* (strain NRRL-B-11177; LCK 491) cells. The high ERY concentrations caused plasmolysis in *Vibrio fischeri* cells by increasing the osmotic pressure in the *Vibrio fischeri* (strain NRRL-B-11177; LCK 491)

medium. The maximum acute toxicity removal efficiency in the effluent of the sequential AMCBR/CSTR reactor system was 86% for 50 mg/L ERY concentration (Table 6.67). The minimum acute toxicity removal efficiency in the effluent of the sequential AMCBR/CSTR reactor system was 81% for 250 mg/L ERY concentration (see Table 6.67).

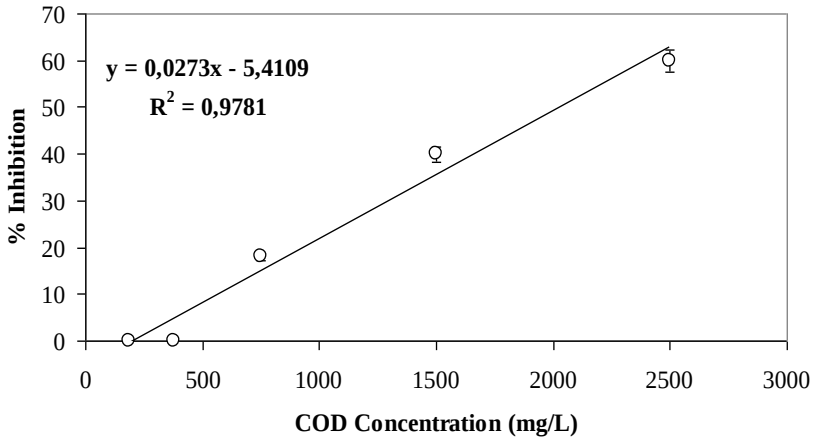

(a)

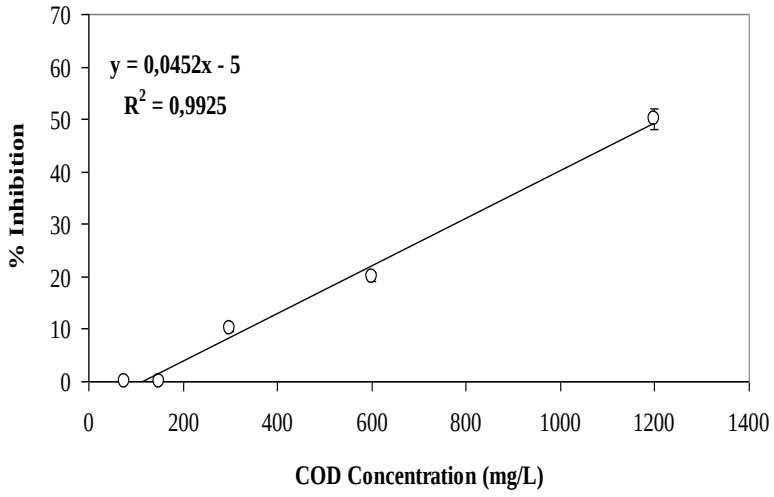

(b)

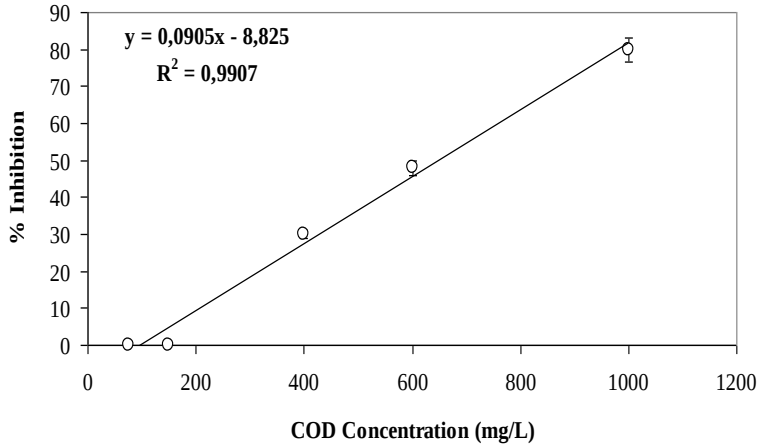

(c)

Figure 6.173 Variations of acute toxicity percentages and EC_{50} values in the effluent of the CSTR reactor for **(a)** ERY concentration 50 mg/L, EC_{50}=2030 mg/L; **(b)** ERY concentration 150 mg/L, EC_{50}=1216 mg/L and **(c)** ERY concentration 250 mg/L, EC_{50}=650 mg/L from the anaerobic AMCBR and aerobic CSTR reactors through continuous operation (HRT=3.0 days, SRT=20 days).

Kümmerer et al., (2004) investigated the suitability of the bioluminescence inhibition test to assess the effect of ERY acute toxicity on *Vibrio fischeri* (bioluminescence bacteria). The EC_{50} on *Vibrio fischeri* was >100 mg/L in the environment. Holten Lützhoft et al., (1999) found that a weak acute toxicity of 50 mg/L ERY to *Daphnia magna* in 48-hour (EC_{50}= 30.5 mg/L). In our study, the EC_{50} values were between 230 and 546 mg/L, at ERY concentrations varying between 50 and 250 mg/L in the effluent of the AMCBR reactor system. The EC_{50} values for ERY obtained in the aforementioned study are low in comparison to the EC_{50} values found in our study. Flaherty and Dodson (2005) investigated the acute toxicity effects of 0.1-10 mg/L ERY on *Daphnia magna*. The EC_{50} values on *Daphnia magna* were 3.5 and 5 mg/L, respectively. In another study, Halling-Sørensen, (2001) investigated the acute toxicity effects of 100 mg/L ERY to different species and found EC_{50} values to *Daphnia magna*, *Microcystis Aeruginosa*, *Selenastrium Capricarnitum* to be 54.7, 13.8 and 34 mg/L, respectively. Christensen et al., (2006) investigated the acute toxicity of macrolide antibiotic used in aquaculture. They found that a strong acute toxicity with *Daphnia magna* in 24 hour EC_{50} value of 41 mg/L.

6.5.9 Sensitivity of Antibiotics (OTC, AMX, TYL and ERY)

In order to determine the sensitivity of *Daphnia magna* for the acute toxicity tests described above and to show the responses of two different organisms, to anaerobic and aerobic treatment wastewater samples the acute toxicity test was also performed with *Vibrio fischeri* (strain NRRL-B-11177, LCK 491). Sensitivity ranking indicates the sum of toxicity responses of every organism used in acute toxicity tests (Sponza, 2002a; 2002b; 2006). To explain the sensitivity of acute toxicity test results based on *Daphnia magna* and *Vibrio fischeri* (strain NRRL-B-11177, LCK 491) a table was constructed ranking the samples in order of acute toxicity (Sponza, 2002a; 2006; Sponza and Kuşçu, 2011). A score of ***"1"*** was assigned to the most sensitive test for each sample down to ***"2"*** for the least sensitive organism representing two trophic levels which were classified according to the acute toxicity test results (Sponza, 2002a; 2006). The comparison of toxicity response and sensitivity ranking was assessed in synthetic pharmaceutical wastewater sequential AMCBR/CSTR reactor system.

The acute toxicity classification of an effluent should always be based on the toxicity results of testing all trophic levels at least once. The direct comparison of sensitivity of *Daphnia magna, Vibrio fischeri* (strain NRRL-B-11177, LCK 491) to OTC, AMX, TYL and ERY revealed that the *Vibrio fischeri* (strain NRRL-B-11177, LCK 491) acute toxicity test is significantly more sensitive to OTC, AMX, TYL and ERY than the *Daphnia magna* acute toxicity tests. The most resistant organism was found to be *Daphnia magna*. Comparative sensitivity ranking of *Daphnia magna, Vibrio fischeri* (strain NRRL-B-11177, LCK 491) to OTC, AMX, TYL and ERY are given in Tables 6.45 and 6.46.

Table 6.45 Comparison of EC_{50} values (mg/L; 95% Confidence limits between brackets) reported in the present study. Effect concentrations are listed for the *Vibrio fischeri* (strain NRRL-B-11177, LCK 491) and *Daphnia magna* for the four tested antibiotics in the AMCBR reactor system.

Antibiotic	**Concentration (mg/L)**	***Daphnia magna***		**Exposure Time**	**Sensitivity Ranking**	***Vibrio fischeri (strain NRRL-B-11177, LCK 491)***		**Exposure Time**	**Sensitivity Ranking**
		Influent	**Effluent**			**Influent**	**Effluent**		
OTC	50-250	250-263 (235-260; 248-270)	580-665 (550-606; 630-697)	24 hour	2	155-208 (145-158; 192-214)	345-520 (322-360; 490-541)	30 min.	1
AMX	50-250	318-510 (300-332; 482-535)	472-764 (445-492; 724-800)	24 hour	2	161-323 (148-165; 301-335)	310-664 (290-322; 630-695)	30 min.	1
TYL	50-250	250-329 (235-260; 312-344)	500-620 (472-520; 585-648)	24 hour	2	122-275 (112-126; 260-285)	230-546 (218-240; 516-571)	30 min.	1
ERY	50-250	250-329 (235-260; 312-344)	500-620 (472-520; 585-648)	24 hour	2	122-275 (112-126; 260-285)	230-546 (218-240; 516-571)	30 min.	1

The acute toxicities of 4 antibiotics namely; OTC (50-250 mg/L), AMX (50-250 mg/L), TYL (50-250 mg/L) and ERY (50-250 mg/L) were investigated on the *Daphnia magna* and *Vibrio fischeri* (strain NRRL-B-11177, LCK 491). The EC_{50} values for OTC, AMX, TYL and ERY antibiotics were 250-263, 318-510, 250-329 mg/L for *Daphnia magna* and 155-208, 161-323, 122-275 mg/L for *Vibrio fischeri* (strain NRRL-B-11177, LCK 491), respectively in the influent samples (see Table 6.45). The EC_{50} values measured for *Daphnia magna* differed significantly from *Vibrio fischeri* (strain NRRL-B-11177, LCK 491) in the decline of sensitivity scores and exhibited lower mortalities in the influent samples (t-test 4.08, $p \leq 0.05$). The t-test statistics showed that *Daphnia magna* had higher EC_{50} values and lower sensitivity scores than *Vibrio fischeri* (strain NRRL-B-11177, LCK 491). The *Vibrio fischeri* (strain NRRL-B-11177, LCK 491) and *Daphnia magna* had different responses to toxicity and mortalities (t-test 4.10, $p=0.09$) and this difference was significant (t-test 12.06, $p \leq 0.05$).

In other words, the *Daphnia magna* was found to be resistant compared to *Vibrio fischeri* (strain NRRL-B-11177, LCK 491). From the acute toxicity tests it can be seen that different organisms were affected differently by the influent and effluent wastewaters. It should be pointed out, however, that the *Vibrio fischeri* (strain NRRL-B-11177, LCK 491) and *Daphnia magna* tests are reference standards used world-wide for toxicity testing and represent one of the trophic level tests required in toxicity evaluation. The increment in EC_{50} values indicated the reduction in toxicity from the influent and effluent of the AMCBR reactor. The total sensitivity scores were 1 and 2 for *Vibrio fischeri* (strain NRRL-B-11177, LCK 491) and *Daphnia magna*, respectively, indicating that *Vibrio fischeri* (strain NRRL-B-11177, LCK 491) is more sensitive than *Daphnia magna* (Table 6.46). The differences in test sensitivities could be attributed to the differences in the responses of the two different trophic organisms in synthetic pharmaceutical wastewater. As a conclusion, this study showed that the Microtox test (*Vibrio fischeri* (strain NRRL-B-11177, LCK 491)) is more sensitive than that *Vibrio fischeri* (strain NRRL-B-11177, LCK 491) in the treated synthetic pharmaceutical wastewater samples containing OTC, AMX, TYL and ERY (Table 6.45 and 6.46).

Table 6.46 Sensitivity ranking of *Daphnia magna*, *Vibrio fischeri* to selected antibiotics

Selected Antibiotics	**Sensitivity ranking (based on EC_{50} values)**
OTC	*Vibrio fischeri* > *Daphnia magna*
AMX	
TYL and ERY	

6.6 Determination of Kinetic Constants

Kinetic analysis is an accepted route for describing the performance of biological treatment systems and for predicting their performance (Yetilmezsoy and Sakar, 2008; Debik and Coskun, 2009). Kinetic studies are very important for anaerobic reactor design. Generally, the results of kinetic studies obtained from experimental studies can be used to estimate the treatment efficiencies of laboratory-scale anaerobic reactors (Pandian et al. 2011). For this purpose, the experimental data obtained from six HRTs in the AMCBR reactor treating the antibiotics were applied to various kinetic models such as, Monod, Grau second order, Stover-Kincannon, zero order, first order, second order, Contois, Michelis-Menten to determine the optimum substrate removal and biogas kinetics.

6.6.1 Substrate Removal Kinetic Models in the AMCBR Reactor for Synthetic Wastewaters

In order to obtain the kinetic coefficients for different kinetic models the laboratory-scale anaerobic AMCBR reactor was operated with synthetic pharmaceutical wastewater containing constants OTC and COD concentrations of 100 and 4000 mg/L, respectively, at six different HRTs (5.50-4.50-2.25-1.50-1.13-0.90 days) under steady state conditions.

6.6.1.1 Monod Kinetic Model for COD Biodegradation in the AMCBR Reactor

The experimental data under steady-state conditions were used and kinetic parameters were evaluated using the linear expressions and their meaningful concentrations. The values of growth yield coefficient Y (mgVSS/mgCOD) and endogenous decay coefficient k_d (d^{-1}) can be obtained by plotting (S_o-S)/HRT*X versus 1/SRT in Eq. 5.25 (see chapter 5.8.1.1.4). HRT and SRT are the hydraulic retention time (d) and the solid retention time (d), respectively. S_0 and S are influent and effluent COD (mg/L) concentrations, respectively. Y and k_d values calculated from the intercept and the slope of the straight line illustrated in Figure 6.174 as 4.22 mgVSS/mgCOD and 0.0031 d^{-1}, respectively. The linear regression coefficient value (R^2) of this plot was 0.944 (y=4.4965x-0.0139) for AMCBR reactor treating 100 mg/L OTC (see Figure 6.174).

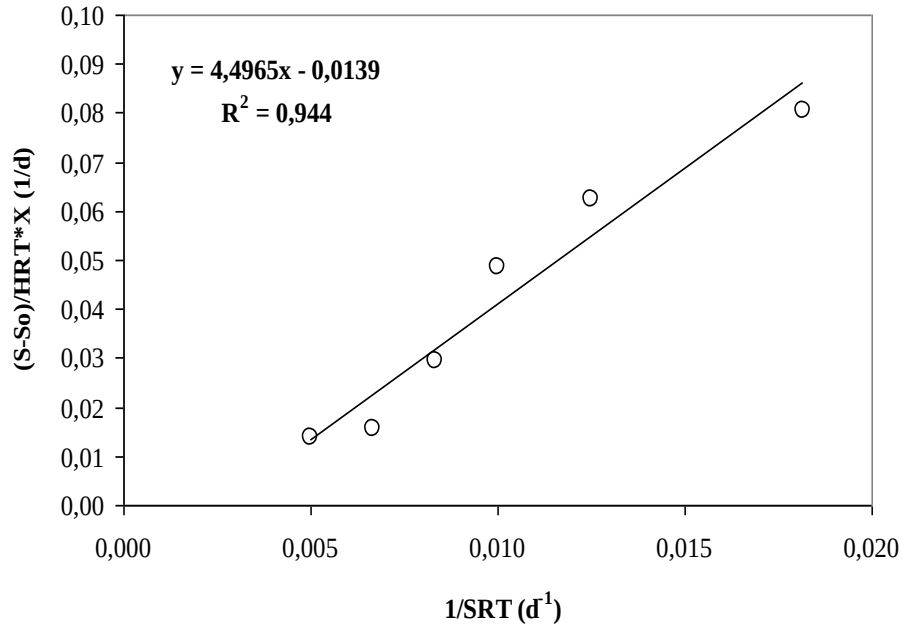

Figure 6.174 Determination of growth yield coefficient (Y) and endogenous decay coefficient (k_d) values for AMCBR reactor treating 100 mg/L OTC

The values of maximum specific growth rate (μ_{max}) (d^{-1}) and half saturation constant (K_S) (mg/L) can be obtained by plotting SRT/1+(SRT*k_d) versus 1/S in Eq. (5.27) (see chapter 5.8.1.1.4). The slope of the line gives the K_S. The intercept point of the line gives the μ_{max}. The μ_{max} and K_S values calculated from the intercept and

the slope of the straight line illustrated in Figure 6.175 for AMCBR reactor treating 100 mg/L OTC as 1.31 d^{-1} and 0.92 mg/L, respectively. The linear regression coefficient value (R^2) was 0.944 (y=19.904x+0.7592) for AMCBR reactor treating 100 mg/L OTC in this plot (see Figure 6.175).

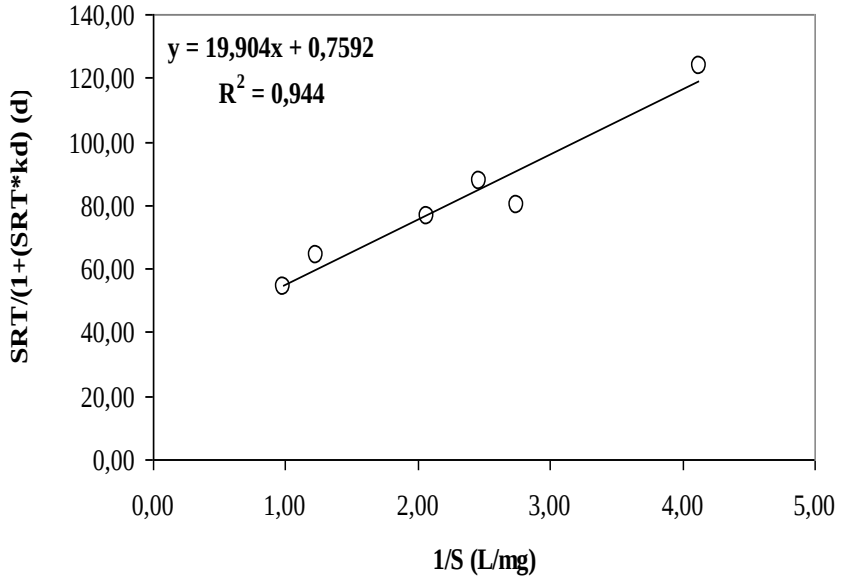

Figure 6.175 Determination of maximum specific substrate utilization rate (μ_{max}) and half saturation constant (K_S) values for AMCBR reactor treating 100 mg/L OTC

6.6.1.2 Monod Kinetic Model for OTC Biodegradation in the AMCBR Reactor

Figure 6.176 shows the pair of coordinates (A0-A)/HRT*X versus 1/SRT, to obtain the growth yield coefficient Y (mgVSS/mgOTC) and the endogenous decay coefficient k_d (d^{-1}). HRT and SRT are hydraulitic retention time (d) and the solid retention time (d), respectively. A_0 and A are influent and effluent OTC (mg/L) concentrations, respectively. The Y and k_d values were calculated as 1.92 mgVSS/mgOTC and 0.0053 d^{-1}, respectively. The linear regression coefficient value (R^2) of this plot was 0.8104 (y=9.8261x-0.0547) for AMCBR reactor treating 100 mg/L OTC (see Figure 6.176).

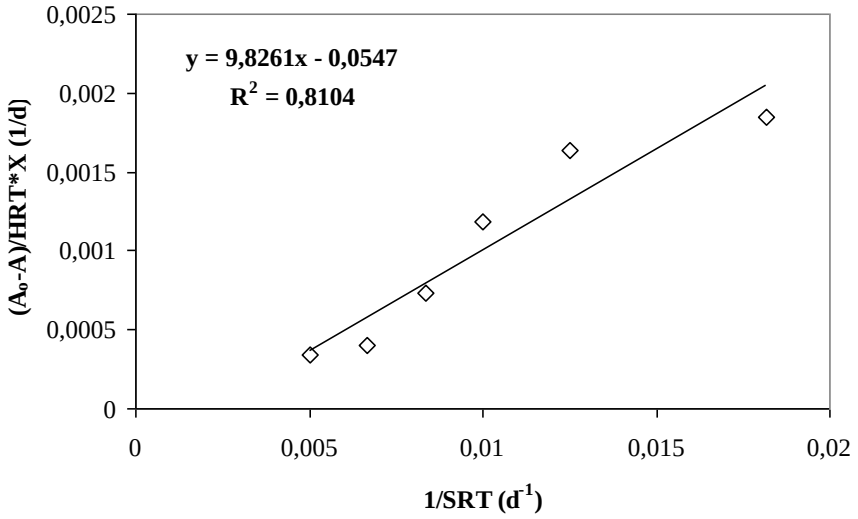

Figure 6.176 Determination of growth yield coefficient (Y) and endogenous decay coefficient (k_d) values for AMCBR reactor treating 100 mg/L OTC

Figure 6.177 shows a pair of coordinates SRT/1+(SRT*k_d) versus 1/A to determine the maximum specific substrate utilization rate (μ_{max}) (d^{-1}), and the half saturation constant (K_S) (mg/L) values. The μ_{max} and K_S for OTC were calculated as 0.22 d^{-1} and 0.032 mg/L, respectively. The linear regression coefficient value (R^2) was 0.9682 (y=0.0242x+4.5143) for AMCBR reactor treating 100 mg/L OTC in this plot (see Figure 6.177).

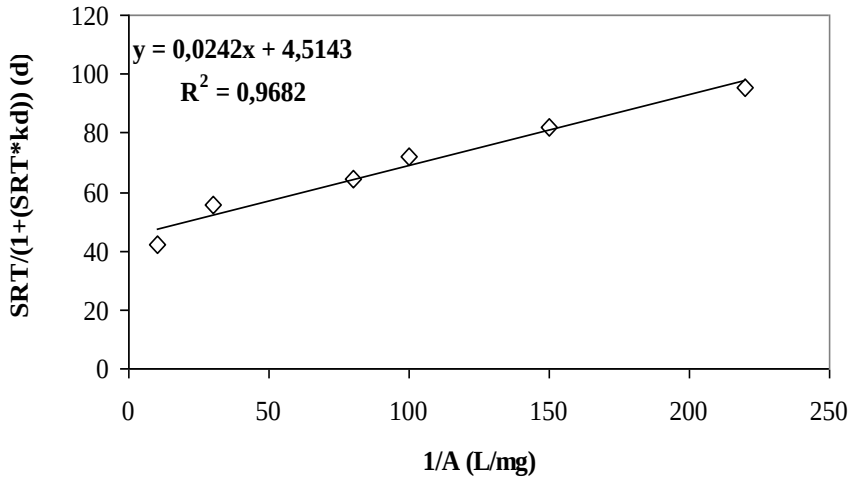

Figure 6.177 Determination of maximum specific substrate utilization rate (μ_{max}) and half saturation constant (K_S) values for AMCBR reactor treating 100 mg/L OTC

6.6.1.3 Grau Second-order Kinetic Model for COD Removal in the AMCBR Reactor

In order to determine the Grau second-order kinetic constants "a" (d), "b" (dimensionless) and Grau second-order substrate removal rate constant (k_s) (d^{-1}) Eq. 5.40 (see chapter 5.8.1.1.7) was plotted (Figure 6.178). The values of "a" and "b" were calculated from the intercept and slope of the straight line on the graph given in Figure 6.154. The values of "a" and "b" were found to be 0.21 d and 1.04, respectively. "a" is also defined with Exp. 6.1. S_0 and X are the influent COD concentration (mg/L) and the biomass concentration (mg/L), respectively. The k_s value was then calculated from the expression (Exp.) given in Exp. 6.1 as 0.08 d^{-1} indicating the substrate removal by the microorganisms in the AMCBR reactor depends on k_s.

$$a = \frac{S_0}{(k_S \times X)} \qquad \text{Exp. 6.1}$$

The linear regression coefficient value (R^2) was 0.99 for the plot given in Eq. (3.40) (y=1.0337x+0.2114) for AMCBR reactor treating 100 mg/L OTC.

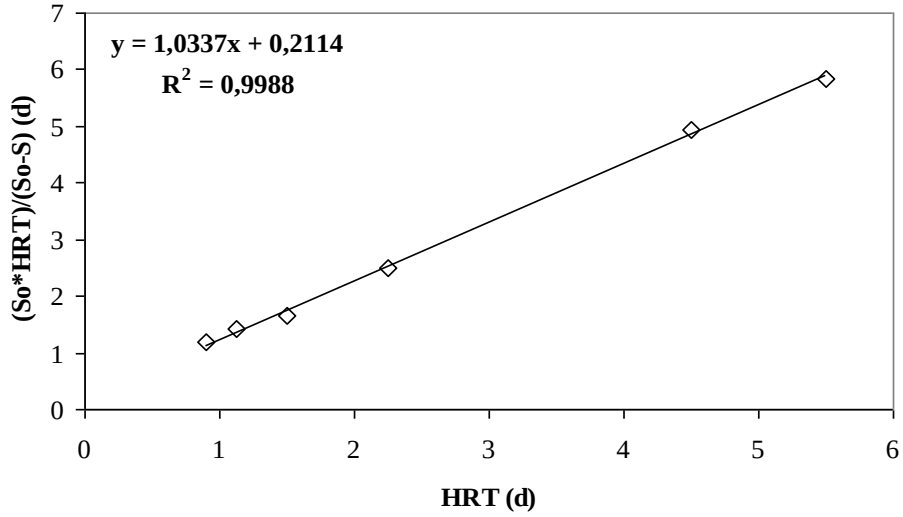

Figure 6.178 Determination of kinetic constants (a, b and k_s) in Grau second-order model for AMCBR reactor treating 100 mg/L OTC

6.6.1.4 Grau Second-order Kinetic Model for OTC Removal in the AMCBR Reactor

In order to determine the Grau second-order kinetic constants "a" (d), "b" (dimensionless) and Grau second-order substrate removal rate constant (k_s) (d^{-1}) Eq. 5.40 (see chapter 5.8.1.1.7) was plotted in Figure 6.179. The values of "a" and "b" were calculated from the intercept and slope of the straight line on graph. S_{0TC} and X are influent OTC concentration (mg/L) and the biomass concentration (mg/L), respectively. The k_s value was then calculated from the expression given in Exp. 6.2 as 0.0021 d^{-1} indicating the substrate removal by the microorganisms in the AMCBR reactor depends on k_s.

$$a = \frac{S_{OTC}}{(k_S \times X)} \qquad \text{Exp. 6.2}$$

The values of "a" and "b" were found to be 0.24 d and 1.00, respectively. The linear regression coefficient value (R^2) was 0.99 (y=1.003x+0.2392) for AMCBR reactor treating 100 mg/L OTC in this plot.

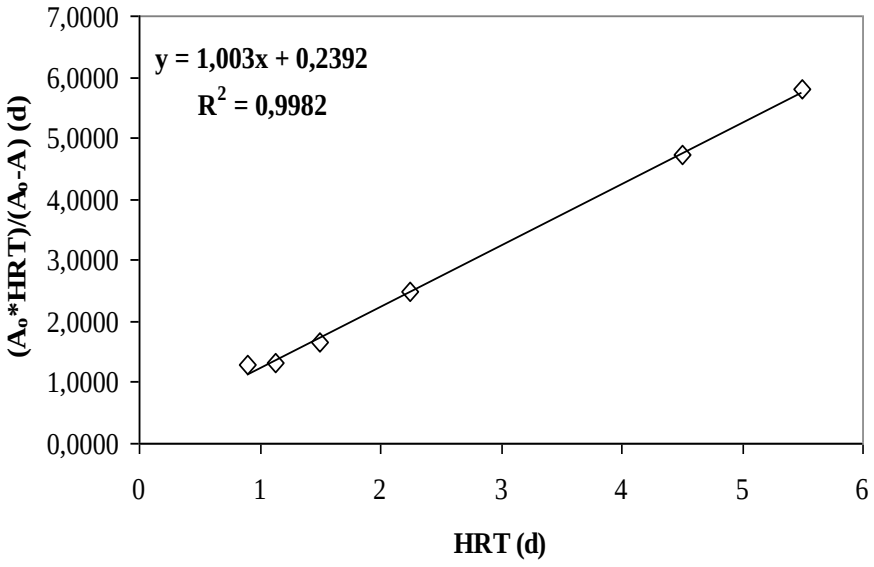

Figure 6.179 Determination of kinetic constants (a, b and k_s) in Grau second-order model for AMCBR reactor treating 100 mg/L OTC

6.6.1.5 Contois Kinetic Model for COD Removal in the AMCBR Reactor

Figure 6.180 was plotted from the Eq. 5.37 (see section 5.8.1.1.6) for determining the values of maximum specific growth rate (μ_{max}) (d^{-1}) and Contois kinetic constant (β) (gCOD/gbiomass) in Contois kinetic model. S and X are effluent COD concentration (mg/L) and the biomass concentration (mg/L), respectively. The μ_{max} and β values calculated from the intercept and the slope of the straight line illustrated in Figure 6.180. The μ_{max} and β values were calculated as 0.0261 d^{-1} and 20.20 gCOD/gbiomass, respectively. The linear regression coefficient value (R^2) was 0.9301, (y=0.3076x+38.068) for AMCBR reactor treating 100 mg/L OTC in this plot.

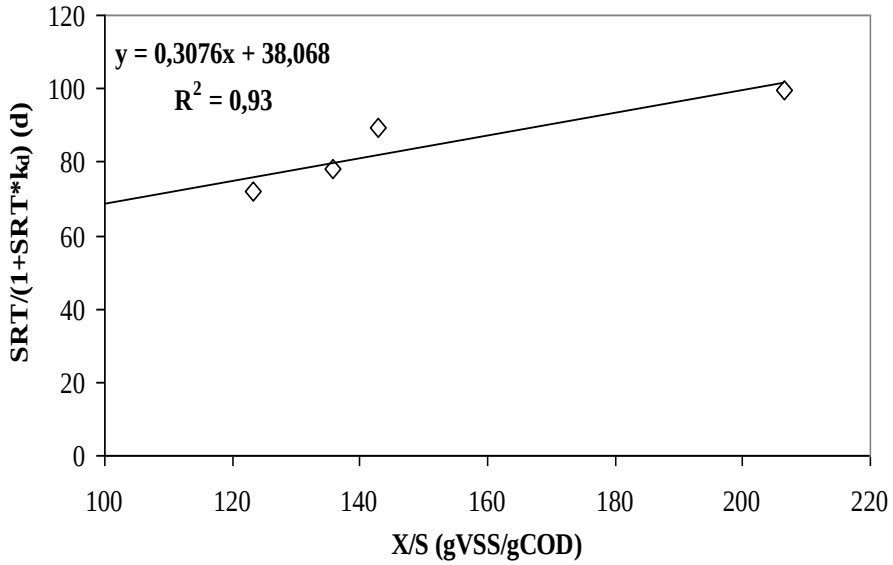

Figure 6.180 Determination of kinetic constants (μ_{max} and β) in Contois Kinetic Model for AMCBR reactor treating 100 mg/L OTC

6.6.1.6 Contois Kinetic Model for OTC Removal in the AMCBR Reactor

The values of maximum specific growth rate (μ_{max}) (d^{-1}) and Contois kinetic constant (β) (gCOD/gbiomass) can be obtained by plotting SRT/1+(SRT*k_d) versus X/A in Eq. 5.37 (see section 5.8.1.1.6). A and X are effluent OTC concentration (mg/L) and the biomass concentration (mg/L), respectively. Figure 6.181 was plotted from the Eq. 5.37 for determining the values of μ_{max} and β in the Contois kinetic

model. The slope of the line gives the β. The intercept point of the line gives the μ_{max}. The values of μ_{max} and β were found as 0.023 d^{-1} and 1.40 gOTC/gbiomass, respectively. The linear regression coefficient value (R^2) was 0.9358, (y=0.0059x+43.661) for AMCBR reactor treating 100 mg/L OTC in this plot.

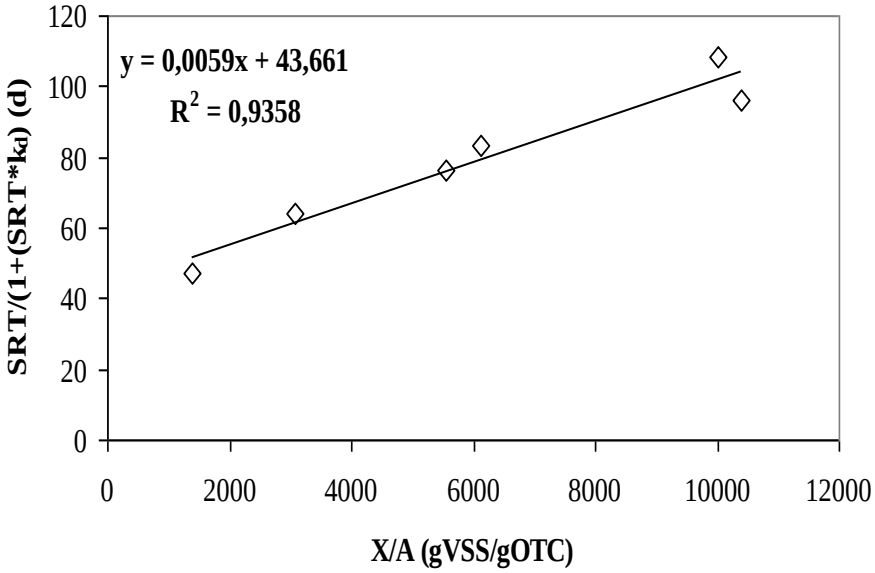

Figure 6.181 Determination of kinetic constants (μ_{max} and β) in Contois Kinetic Model for AMCBR reactor treating 100 mg/L OTC

6.6.1.7 Stover-Kincannon Kinetic Model for COD Biodegradation in the AMCBR Reactor

Figure 6.182 shows the Stover-Kincannon kinetic model in its linearized form for the six data series HRTs. The values of saturation constant (K_B) (g/L.d) and maximum utilization rate (R_{max}) (g/L.d) can be obtained by plotting $V/Q*(S_0-S)$ versus $V/Q*S_0$ in Eq. 5.45 (see section 5.8.1.1.8). Q and V are the inflow rate (L/day) and the volume of the anaerobic reactor (L), respectively. S_0 and S are influent and effluent COD (mg/L) concentrations, respectively. Figure 6.182 shows the graph plotted between reciprocal of total removed organic loading removal rate, $V/Q*(S_0-S)$ against to the reciprocal of the total organic loading rate, $V/Q*S_0$ using Eq. (5.45). Since the plot of $V/Q*(S_0-S)$ versus $V/Q*S_0$ was found to be linear, therefore, linear regressions were used to determine the intercept $1/R_{max}$ and the slope K_B/R_{max}. The values of R_{max} and K_B were found as 9.23 and 9.87 gCOD/L d,

respectively. The linear regression coefficient value (R^2) was 0.9988 (y=1.0335x+0.052) for AMCBR reactor treating 100 mg/L OTC in this plot (see Figure 6.182).

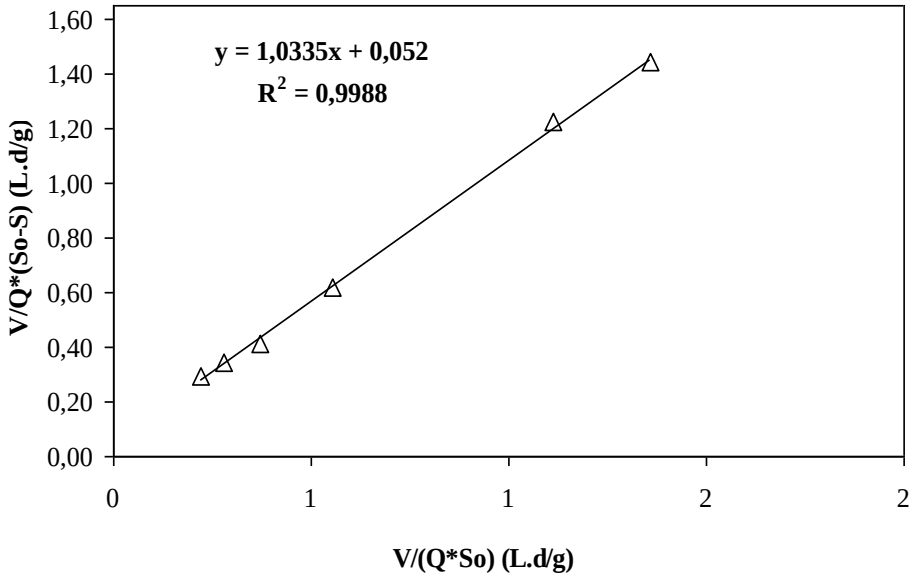

Figure 6.182 Determination of kinetic constants (R_{max} and K_B) in Stover Kincannon model for AMCBR reactor treating 100 mg/L OTC

6.6.1.8 Stover-Kincannon Kinetic Model for OTC Biodegradation in the AMCBR Reactor

The values of saturation value constant (K_B) (g/L.d) and maximum utilization rate (R_{max}) (g/L.d) can be obtained by plotting $V/Q^*(A_0-A)$ versus V/Q^*A_0 in Eq. 5.45 (section 5.8.1.1.8). Q and V are the inflow rate (L/d) and the volume of the AMCBR reactor (L), respectively. A_o and A are the influent and effluent OTC (mg/L) concentrations, respectively. Figure 6.183 shows the graph plotted between reciprocal of total removed organic loading removal rate, $V/Q^*(A_0-A)$ against to the reciprocal of total organic loading rate, V/Q^*A_0 using Eq (3.45). Since the plot of $V/Q^*(A_0-A)$ versus V/Q^*A_0 was found to be linear, A linear regression plot were used to determine the intercept $1/R_{max}$ and the slope K_B/R_{max}. The values of R_{max} and K_B were found as 0.91 and 0.42 gOTC/L d, respectively. The linear regression coefficient value (R^2) was 0.9358, (y=1.003x+2.3902) for AMCBR reactor treating 100 mg/L OTC in this plot (see Figure 6.183).

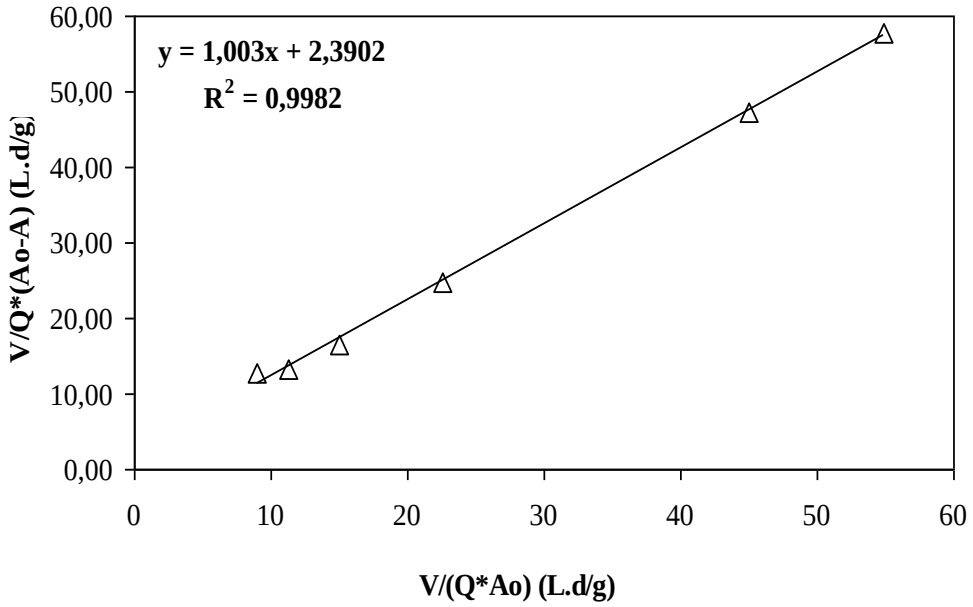

Figure 6.183 Determination of kinetic constants (R_{max} and K_B) in Stover Kincannon model for AMCBR reactor treating 100 mg/L OTC

6.6.1.9 Zero Order Kinetic Model for COD Biodegradation in the AMCBR Reactor

Zero order kinetic constant (k_0) (mg/L.d) was obtained from the slope of the line by plotting (S_0-S) versus (HRT) in Eq. (5.10) (see Section 5.8.1.1.1). S_o and S are influent and effluent COD (mg/L) concentrations, respectively. Figure 6.184 shows the plot between (S_0-S) and (HRT). The k_0 was calculated as 0.1159 mg/L.d. The linear regression coefficient value (R^2) was 0.5703, (y=0.1159x+3.2065) for AMCBR reactor treating 100 mg/L OTC in this plot (see Figure 6.184).

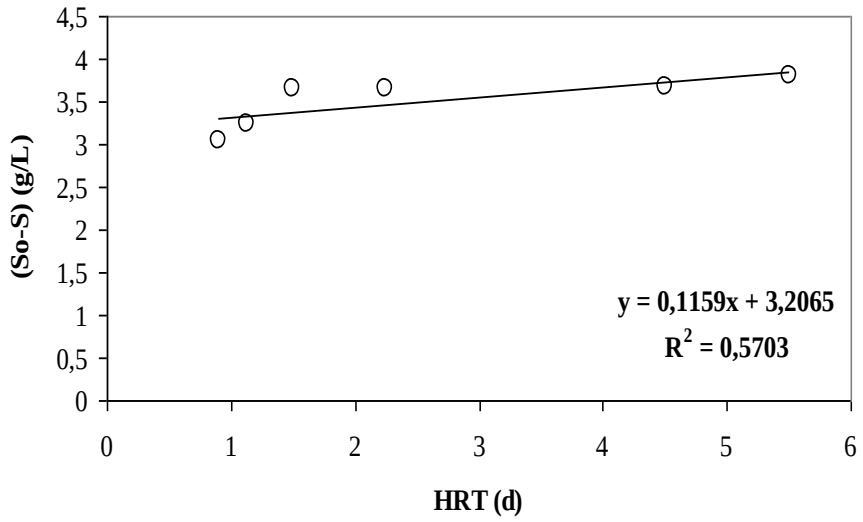

Figure 6.184 The plot of zero order kinetic model for AMCBR treating 100 mg/L OTC

6.6.1.10 Zero Order Kinetic Model for OTC Biodegradation in the AMCBR Reactor

The value of zero order kinetic constant (k_0) (mg/L.d) was obtained from the slope of the line by plotting (A_0-A) versus (HRT) in Eq. (5.10) (see Section 5.8.1.1.1). A_o and A are the influent and effluent OTC (mg/L) concentrations, respectively. Figure 6.185 shows the plot between (A_0-A) and (HRT). The k_0 was calculated as 0.0035 mg/L.d. The linear regression coefficient value (R^2) was 0.5005, (y=0.0035x+0.0786) for AMCBR reactor treating 100 mg/L OTC in this plot.

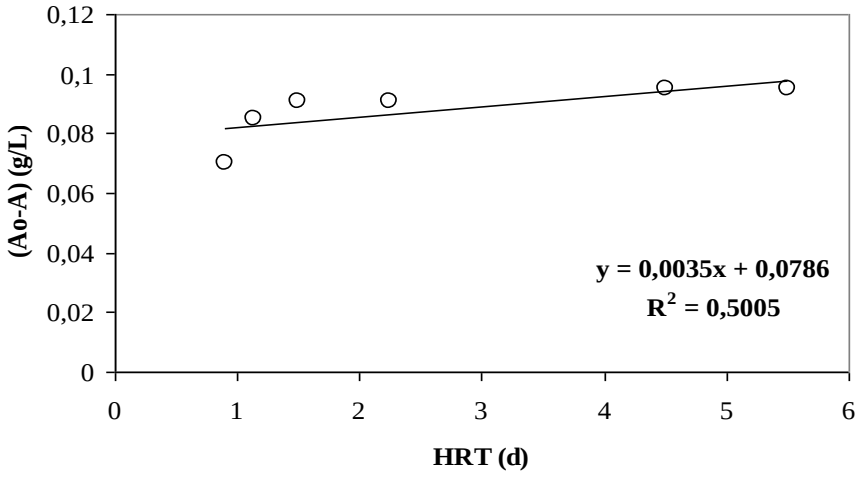

Figure 6.185 The plot of zero order kinetic model for AMCBR treating 100 mg/L OTC

6.6.1.11 First Order Kinetic Model for COD Biodegradation in the AMCBR Reactor

First order kinetic constant (k_1) (d^{-1}) was obtained from the slope of the line by plotting (S_o-S)/HRT versus (S) in Eq. (5.12) (see Section 5.8.1.1.2). S_o and S are the influent and effluent COD (mg/L) concentrations, respectively. Figure 6.186 shows the plot between (S_o-S)/HRT and S. The k_1 was calculated as 2.7915 d^{-1}. The linear regression coefficient value (R^2) was 0.565, (y=2.7915x+0.7968) for AMCBR reactor treating 100 mg/L OTC in this plot (Figure 6.186).

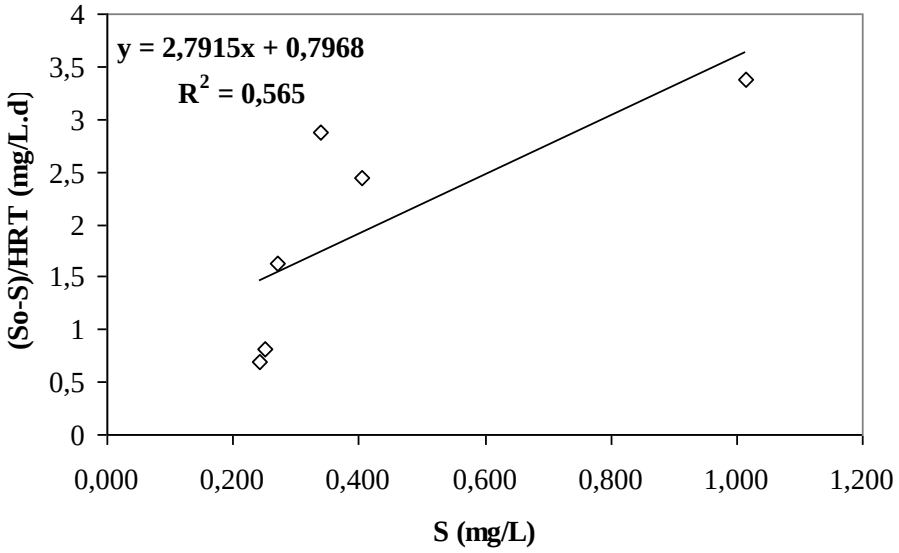

Figure 6.186 Determination of first order kinetic model for AMCBR treating 100 mg/L OTC

6.6.1.12 First Order Kinetic Model for OTC Biodegradation in the AMCBR Reactor

First order kinetic constant (k_1) (d^{-1}) was obtained from the slope of the line by plotting (A_0-A)/HRT versus (A) in section 5.8.1.1.2 (Eq 5.12). A_o and A are the influent and effluent OTC (mg/L) concentrations, respectively. Figure 6.187 shows the plot between (A_0-A)/HRT and A. The k_1 value for OTC was calculated as 0.0022 d^{-1} and the linear regression coefficient value (R^2) was 0.6412, (y=0.0022x+0.0215) for AMCBR reactor treating 100 mg/L OTC in this plot (see Figure 6.187).

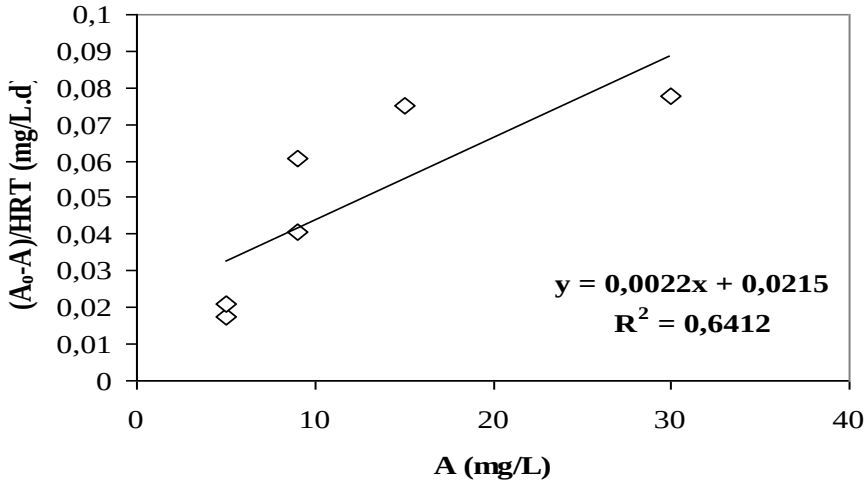

Figure 6.187 Determination of first order kinetic model for AMCBR treating 100 mg/L OTC

6.6.1.13 Second Order Kinetic Model for COD Biodegradation in the AMCBR Reactor

The general equation of the Second-order kinetic model is given in chapter 5.8.1.1.3 (Eq. 5.14). Second-order rate constant (k_2) (L/mg.d) was obtained from the slope of the line by plotting (S_o-S)/HRT versus S^2 in Eq. (3.14) (see chapter 5.8.1.1.3). S_o and S are the influent and effluent COD (mg/L) concentrations, respectively. Figure 6.188 shows the plot between (S_o-S)/HRT and S^2. The k_2 value for COD was calculated as 0.19 L/mg.d. The linear regression coefficient value (R^2) was 0.476, (y=1.9875x+1.472) for AMCBR reactor treating 100 mg/L OTC in this plot (Figure 6.188).

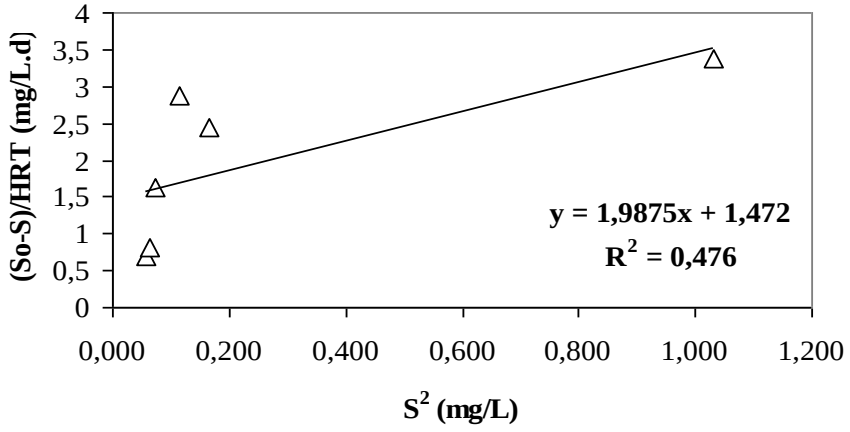

Figure 6.188 Determine of second order kinetic model for AMCBR treating 100 mg/L OTC

6.6.1.14 Second Order Kinetic Model for OTC Biodegradation in the AMCBR Reactor

Second-order rate constant (k_2) (L/mg.d) was obtained from the slope of the line by plotting (A_0-A)/HRT versus A_e^2 in Eq. (5.14) (see chapter 5.8.1.1.3). A_o and A are the influent and effluent OTC (mg/L) concentrations, respectively. The k_2 value for OTC was calculated as 0.00005 L/mg.d and the linear regression coefficient value (R^2) was 0.4714, (y=0.00005x+0.0368) for AMCBR reactor treating 100 mg/L OTC in this plot (see Figure 6.189).

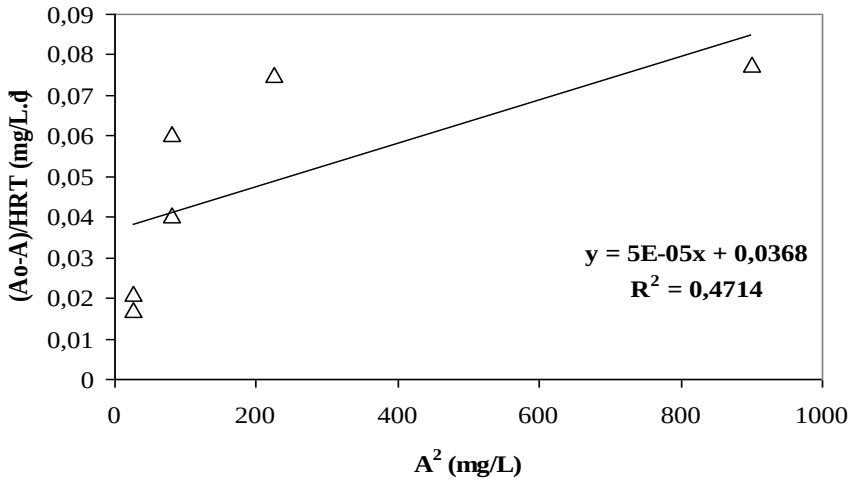

Figure 6.189 Determine of second order kinetic model for AMCBR treating 100 mg/L OTC

6.6.1.15 Assessment of the Results of the Substrate Removal Kinetic Models Used in the AMCBR Reactor to Treat the COD and the OTC in Synthetic Wastewater

The regression coefficient (R^2) was chosen as the criterion for choosing the most suitable model to represent substrate removal kinetics in an anaerobic AMCBR reactor together with the values of kinetic constants. All the regression coefficients and the kinetic parameters calculated from the Monod, Zero-First-Second order, Contois, Stover-Kincannon and Grau second order substrate removal kinetic models are summarized in Table 6.47. The kinetic data showed that Stover-Kincannon and Grau second order substrate removal kinetics were more appropriate models than the other kinetic models (Zero-First-Second order, Monod, Contois) for predicting the

performance of the laboratory-scale anaerobic AMCBR reactor (treating 4000 mg/L COD and 100 mg/L OTC) when the regression coefficients and the kinetic parameters were compared with each other.

In the determination of kinetic constants the calculations were performed according to the primary substrate (COD) and co-substrate (OTC) in the Monod kinetic model. The Monod kinetic constants based on COD were calculated as follows: Y=4.22 mgVSS/mgCOD, k_d=0.0031 d^{-1}, μ_{max}=1.31 d^{-1}, K_s=0.92 mgCOD/L. The kinetic constants evaluated based on OTC were as follows: Y=1.92 mgVSS/mgOTC, k_d=0.0053 d^{-1}, μ_{max}=0.22 d^{-1}, K_S=0.032 mgOTC/L, respectively. The growth yield coefficient (Y) was extremely higher in the Monod kinetic model. Maximum specific growth rate (μ_{max}) was excessively higher compared to the endogenous decay coefficient (k_d). Although low K_S value indicates higher affinities of anaerobic methanogens to COD and OTC in this study very low K_S values (0.92 mgCOD/L, 0.032 mgOTC/L) does not reflect the utilization of COD. According to Metcalf and Eddy (2003), the K_S values varied between 15 and 70 mg/L in the anaerobic reactors. The K_S values varied between 11 and 421 mg/L in the anaerobic reactors for toxic industrial wastewaters (Speece, 1996). In other words, the K_S value for COD was not observed between acceptable values suggested by Metcalf and Eddy (2003) and Speece, (1996) for anaerobic treatment for toxic industrial wastewaters since the wastewater studied in this research contained 100 mg/L OTC.

The maximum substrate utilization rate (R_{max}) is higher and the saturation constant (K_B) is lower during COD and OTC biodegradation in Stover Kincannon kinetic model. High COD and OTC utilization rates (R_{max}) increase the reactor efficiency while the low saturation constant (K_B) indicates the utilization of COD and OTC by the methanogens in the anaerobic AMCBR reactor. In this study, K_B =9.87 g/L.d for COD and K_B=0.42 g/L.d for OTC. The R_{max}=9.23 g/L.d for COD and R_{max}=0.91 g/L.d for OTC in the Stover-Kincannon model.

a, b and k_s kinetic constants were calculated from the Grau second order kinetic model showed that "a" kinetic constant depends to influent COD, OTC concentrations and it was influenced by the inverse of second order substrate removal rate constant (k_s) and microorganism concentrations. The maximum substrate removal rate constant (k_s) and "a" kinetic constant will be increased as the COD and OTC removal efficiencies increased, depending to initial substrate (S_o) and biomass concentration (X) in the anaerobic AMCBR reactor.

The coefficient regression (R^2) of Zero, First and Second order kinetic models are low and Zero order kinetic constant (k_o) values are extremely low for COD and OTC biodegradation. First order (k_1) and Second order (k_2) kinetic constants values are extremely low in the AMCBR reactor treating 100 mg/L OTC. The Zero order kinetic constant (k_o) are not so relevant with substrate (COD) and co-substrate (OTC) versus decreasing HRTs. The First order kinetic constant (k_1) are not so relevant with the ratio of substrate removal to HRT versus the effluent substrate concentration. The Second order kinetic constant (k_2) are not so relevant with the ratio of substrate removal to HRT versus square of substrate concentration in the effluent. Therefore, Zero, First and Second order kinetic models are not appropriate to describe the OTC and COD biodegradation in the AMCBR reactor treating a synthetic pharmaceutical wastewater.

Maximum specific growth rate (μ_{max}) in Monod kinetic and Contois kinetic constant (β) obtained from the Contois kinetic models are not appropriate to describe the anaerobic metabolization of COD and OTC in the AMCBR reactor. The maximum specific growth rate (μ_{max}) and Contois kinetic constant (β) values are high indicating that the OTC removal could be defined with these kinetic values.

Table 6.47 Kinetic parameters of anaerobic AMCBR reactor treating 100 mg/L OTC

Kinetic models	**Kinetic parameters**	**COD removal**		**OTC removal**	
		Values	**R^2**	**Values**	**R^2**
Monod	Y (mgVSS/mgCOD)	4.22	0.94	1.92	0.81
	k_d (d^{-1})	0.0031		0.0053	
	μ_{max} (d^{-1})	1.31		0.22	0.96
	K_S (mg/L)	0.92		0.032	
Grau second-order	k_s (d^{-1})	0.08	0.99	0.0021	0.99
	a (d)	0.21		0.2392	
	b (dimensionless)	1.037		1.0030	
Stover-Kincannon	K_B (g COD/L d)	9.87	0.99	0.42	0.99
	R_{max} (g COD/L d)	9.23		0.91	
Zero-order	k_0 (mg /L d)	0.1159	0.57	0.0035	0.50
First-order	k_1 (d^{-1})	2.7915	0.56	0.0022	0.64
Second-order	k_2 (L /mg d)	0.19	0.47	0.00005	0.47
Contois	μ_{max} (d^{-1})	0.0261	0.93	0.0230	0.93
	β (g COD/g biomass)	20.20		1.4	

Table 6.48 contains the results of kinetic studies of different wastewater obtained from different anaerobic reactors including the different kinetic models (Monod, Zero-First-Second order, Contois, Stover-Kincannon and Grau second order). It is important to note that only few studies were found about of substrate removal kinetics in anaerobic reactors treating pharmaceutical wastewaters: Hu et al., (2007) investigated the substrate removal kinetics in an anaerobic reactor treating pharmaceutical wastewaters using Zero-order and Contois kinetic models. The K_S=0.92 mg/L and k_d=0.0031 d^{-1} values obtained in this study for Monod kinetic model was lower than reported by Deshphande et al. (2012) (K_S=129.3 mg/L, k_d=0.013 d^{-1}) in an anaerobic fixed film fixed bed (AFFFBR) reactor treating pharmaceutical wastewater at three HRTs of 1, 2, 3 days, by Pandian et al. (2011) (K_S=183 mg/L, k_d=0.562 d^{-1}) in an anaerobic hybrid (AHR) reactor treating pharmaceutical wastewater at six HRTs of 30, 18, 12, 8, 6, 3 hours and by Coşkun et al. (2012) (K_S=32 mg/L, k_d=0.010 d^{-1}) in up-flow anaerobic sludge blanket (UASB) reactor treating antibiotic fermentation broth wastewater at HRT of 13 days (see Table 6.48). The differences could be attributed to the differences in wastewater

characteristics and top the operational conditions (HRT, SRT etc.) used in the studies.

In this study, the saturation constant (K_B=9.87 g/L.d for COD) and the maximum substrate utilization rate (R_{max}=9.23 g/L.d for COD) values obtained from the Stover-Kincannon model are lower than those obtained by Deshpande et al. (2012) (R_{max}=13.10 g/L.d, K_B=13.87 g/L.d) in an AFFFBR reactor treating pharmaceutical wastewater at three HRTs of 1, 2, 3 days (see Table 6.48). The possible reasons for the differences could be the variations in the anaerobic reactor configurations, wastewater characteristics and microorganisms used in the study. Low saturation values (K_B) showed that there is no any accumulation of COD and OTC in the anaerobic AMCBR reactor resulting in high affinity of substrate to the anaerobic methanogenic bacteria. The R_{max} and K_B values obtained in this study were lower than values found by Pandian et al. (2011) (R_{max}=108.69 g/L.d, K_B=115.66 g/L.d) in an anaerobic hybrid (AHR) reactor treating pharmaceutical wastewater at six HRTs of 30, 18, 12, 8, 6, 3 hours and Coşkun et al. (2012) (R_{max}=399 g/L.d, K_B=445.5 g/L.d) in up-flow anaerobic sludge blanket (UASB) reactor treating antibiotic fermentation broth wastewater at HRT of 13 days (see Table 4.26). The differences could be explained by the wastewater characteristics and operational conditions (HRT, SRT etc.) used in the study.

Although in our study it was mentioned that the first order kinetic was not suitable for OTC biodegradation, the first order kinetic coefficient value (k_1) found in this study (2.79 d^{-1} for COD) was compared with other studies: The kinetic coefficient k_1 was found to be 0.45 d^{-1} by Coşkun et al. (2012) in an up-flow anaerobic sludge blanket (UASB) reactor treating antibiotic fermentation broth wastewater at a HRT of 13 days (see Table 6.48). In another study, the kinetic coefficient k_1 was calculated as 2.7480 d^{-1} by Degirmentas and Deveci, (2004) in a laboratory-scale bioreactor (LSBR) treating pharmaceutical wastewater at two different HRTs (see Table 6.48).

In this study, the substrate rate constant (k_s) (0.08 d^{-1} for COD) and kinetic constants “a” and “b” relevant to anaerobic AMCBR reactor (0.21 d and 1.04 for COD values) obtained from the Grau second order model are higher than those obtained by Pandian et al. (2011) (k_s=0.07 d^{-1}, a=0.03 d and b=1.07, respectively) in an anaerobic hybrid reactor (AHR) treating fermentation based pharmaceutical wastewater (see Table 6.48). The reasons in the differences in kinetic constant values could be attributed to the differences in anaerobic reactor configurations.

Table 6.48 Comparison of kinetic constants in the Grau second order, Stover Kincannon, First, Second-order and Monod models for substrate in different

Models	Wastewater	Reactor type	Influent COD (mg/L)	Influent OTC (mg/L)	HRT (day)	Kinetic parameters				Reference
						μ_{max}	Y	k_d	K_s	
Monod	Pharmaceutical wastewater	AFFFBR	26150-34400	-	1-3	0.159	0.087	0.013	129.3	Deshpande et al. (2011)
Monod	Pharmaceutical wastewater	AHR	4000-4500	-	0.13-1.25	0.050	0.020	0.562	183	Pandian et al. (2011)
Monod	Antibiotic fermentation broth wastewater	UASB	150000	-	1-13	0.394	3.101	0.010	32	Coşkun et al. (2012)
Monod	Synthetic wastewater (OTC)	AMCBR	4000	100	0.9-5.5	1.310	4.22	0.0031	0.92	This Study
Models	**Wastewater**	**Reactor type**	**Influent COD (mg/L)**	**Influent OTC (mg/L)**	**HRT (day)**	**Kinetic parameters**				**Reference**
						k_1				
First-order	Antibiotic fermentation broth wastewater	UASB	150000	-	1-13	0.4480				Coşkun et al. (2012)
First-order	Synthetic wastewater (OTC)	AMCBR	4000	100	0.9-5.5	2.79				This Study
Models	**Wastewater**	**Reactor type**	**Influent COD (mg/L)**	**Influent OTC (mg/L)**	**HRT (day)**	**Kinetic parameters**				**Reference**
						k_2				
Second-order	Pharmaceutical wastewater	LSBR	3000-10000	-	4-25	2.7480				Degirmentas and Deveci, (2004)
Second-order	Synthetic wastewater (OTC)	AMCBR	4000	100	0.9-5.5	0.19				This Study
Models	**Wastewater**	**Reactor type**	**Influent COD (mg/L)**	**Influent OTC (mg/L)**	**HRT (day)**	**Kinetic parameters**				**Reference**
						R_{max}		K_B		
Stover Kincannon	Pharmaceutical wastewater	AFFFBR	26150-34400	-	1-3	13.10		13.87		Deshpande et al. (2011)
Stover Kincannon	Antibiotic fermentation broth wastewater	UASB	150000	-	1-13	399		445.5		Coşkun et al. (2012)
Stover Kincannon	Pharmaceutical wastewater	AHR	4000-4500	-	0.13-1.25	108.69		115.66		Pandian et al. (2011)
Stover Kincannon	Synthetic wastewater (OTC)	AMCBR	4000	100	0.9-5.5	9.23		9.87		This Study
Models	**Wastewater**	**Reactor type**	**Influent COD (mg/L)**	**Influent OTC (mg/L)**	**HRT (day)**	**Kinetic parameters**				**Reference**
						k_s	**a**	**b**		
Grau second-order	Pharmaceutical wastewater	AHR	4000-4500	-	0.13-1.25	0.052	0.031	1.067		Pandian et al. (2011)
Grau second-order	Synthetic wastewater (OTC)	AMCBR	4000	100	0.9-5.5	0.080	0.212	1.037		This Study

AFFFR= anaerobic fixed film fixed bed reactor, AHR=anaerobic hybrid reactor, UASB=upflow anaerobic sludge blanked reactor, AMCBR=anaerobic multichamber bed reactor, MBR=multistage bioreactor, a and b=Grau second-order constant, k_s=Grau second-order substrate removal rate (d^{-1}), R_{max}=maximum utilization rate (g COD/L d), K_B=saturation value constant (g COD/L d), μ_{max}=maximum specific growth rate (day-1), Y=growth yield coefficient (g VSS /g COD), k_d=endogenous decay coefficient (d^{-1}), Ks=half saturation conc. (mg/L), k_1= first order rate constant (d^{-1}), k_2= second order kinetic constant (L/mg.d).

6.6.2 Biogas (total and methane gas) Production Kinetic Models in the AMCBR Reactor

In this study two biogas production kinetic models namely, Stover Kincannon and Van der Meer-Heertjes were evaluated in the AMCBR reactor.

6.6.2.1 Stover-Kincannon model for Total Gas Production in the AMCBR Reactor

In order to determine the Stover Kincannon kinetic constant, the inverse of the total gas production rate was plotted against the inverse of the organic loading rate (OLR) (g/Ld) in Eq. (5.50) (section 5.8.1.2.1) (Figure 6.190). The values of maximum specific total gas production rate (G_{max}) (ml/L/d) and gas kinetic constant (G_B) (mg/L/d) can be obtained by plotting 1/G versus 1/OLR in Eq. (5.50) (section 5.8.1.2.1). The intercept and slope of the plotline resulted in $1/G_{max}$ and G_B/G_{max}, respectively (see Figure 6.190). The G_{max} and G_B were determined to be 1862 ml/L/d and 2.08 mg/L/d, respectively. The linear regression coefficient value (R^2) was 0.99 (y=0.0011x+0.0005) for AMCBR reactor treating 100 mg/L OTC in this plot (see Figure 6.190).

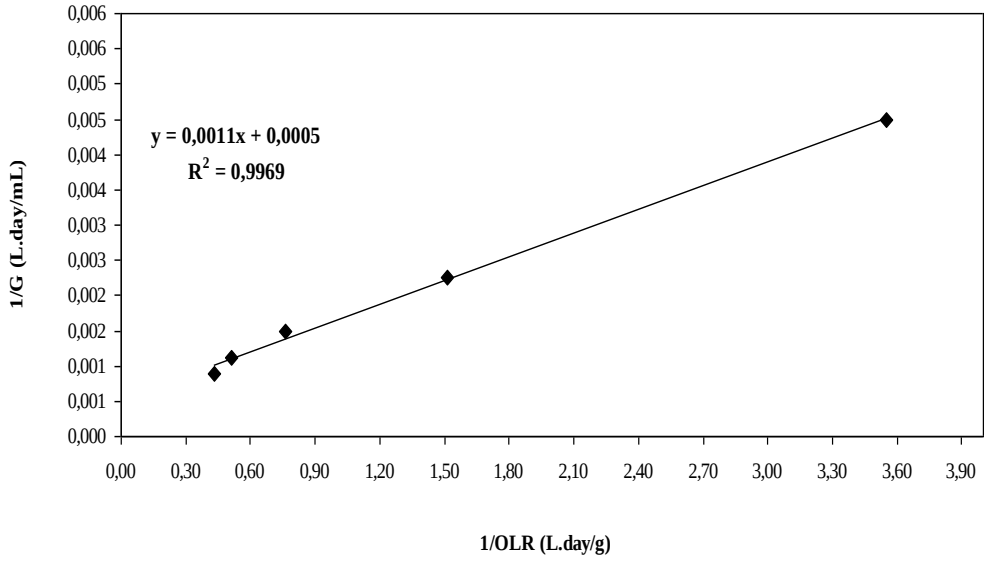

Figure 6.190 Determination of G_{max} and G_B values in Stover Kincannon model for AMCBR treating 100 mg/L OTC

6.6.2.2 Stover-Kincannon kinetic model for methane gas production in the AMCBR reactor

The values of maximum specific methane gas production rate (M_{max}) (ml/L.d) and kinetic constant (M_B) (mg/L.d) can be obtained by plotting 1/M versus 1/OLR in Eq. (5.51) (section 5.8.1.2.1). The intercept and slope of the plotline resulted in $1/M_{max}$ and M_B/M_{max}, respectively (see Figure 6.191). The M_{max} and M_B were determined to be 598 ml/L/d and 0.63 mg/L/d, respectively. The linear regression coefficient value (R^2) was 0.97 (y=0.0011x+0.0017) for AMCBR reactor treating 100 mg/L OTC in this plot (see Figure 6.191).

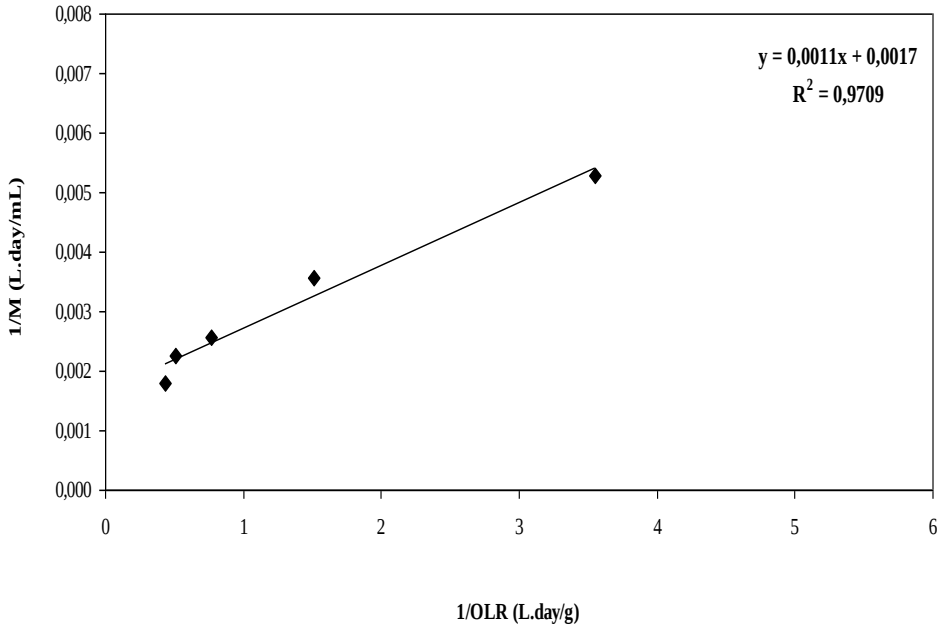

Figure 6.191 Determination of M_{max} and M_B values in Stover Kincannon model for AMCBR treating 100 mg/L OTC

6.6.2.3 Van der Meer-Heertjes model for Methane Gas Oroduction in the AMCBR Reactor

In this study, the Van der Meer-Heertjes kinetic model was applied to methane gas production in the anaerobic AMCBR reactor. In this model the methane gas production is related with gas kinetic constant, flow rate applied to the anaerobic

AMCBR reactor and removed substrate concentrations. The value of Van der Meer-Heertjes kinetic constant (k_{sg}) (ml/mg) can be obtained by plotting $Q^*(S_0-S)$ versus G_{CH4} in Eq. 5.55 (see chapter 5.8.1.2.2). Q is the flow rate (L/d), and G_{CH4} is the methane gas production (L/d). S_0 and S are the influent substrate concentration (mg/L) and the effluent substrate concentration (mg/L), respectively. The k_{sg} was calculated as 0.79 $mlCH_4$/mgCOD removal. The linear regression coefficient value (R^2) of this plot was 0.96 (y=0.1408x+0.7261) for AMCBR reactor treating 100 mg/L OTC (see Figure 6.192).

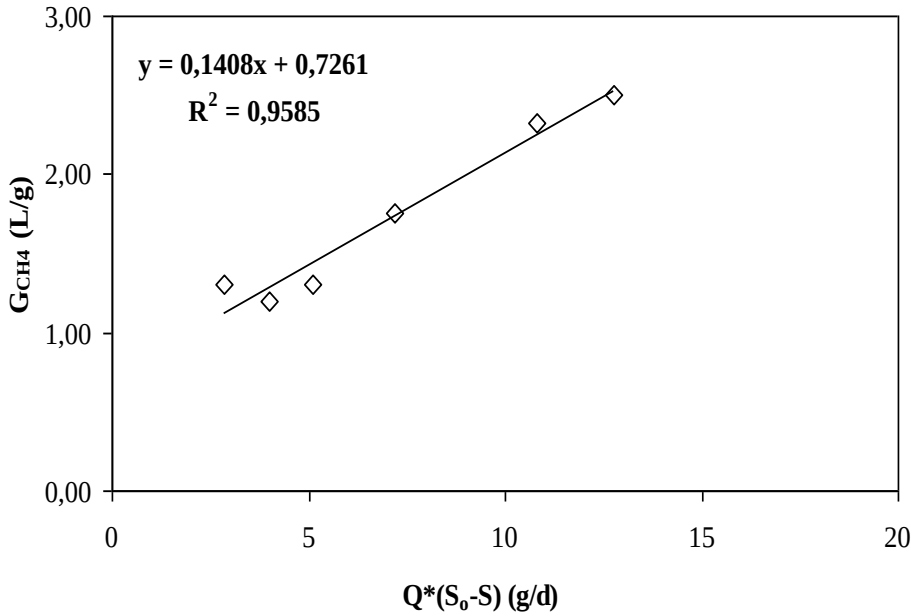

Figure 6.192 Determination of k_{sg} in Van der Meer and Heertjes model for AMCBR reactor treating 100 mg/L OTC

6.6.2.4 Evaluation of the Biogas *Production Kinetic Models* Used in the AMCBR *Reactor*

Biogas production is the most attractive feature of anaerobic technology as it contains methane, which methane is potential source of energy. Therefore, the quantity of biogas was also regularly monitored at all the OLRs and HRTs. The methane and total gas productions calculated from the experimental studies were compared in two different kinetic models. The kinetic constants calculated from the kinetic models are summarized in Table 6.49.

The maximum specific total gas and methane gas production rates (G_{max} and M_{max}) are higher and the total and methane gas kinetic constants (G_B and M_B) are lower during COD and OTC biodegradation in Stover Kincannon kinetic model. High total gas and methane gas production rates (G_{max} and M_{max}) increase the anaerobic AMCBR reactor efficiency while low total and methane gas kinetic constants (G_B and M_B) indicates the utilization of COD and OTC by the methanogens via methanogenesis in the anaerobic AMCBR reactor. The M_B value was calculated as 0.63 mg/Ld in this kinetic model. In the comparison of the kinetic constants of the Stover Kincannon and Van der Meer-Heertjes kinetic models it was found that the Van der Meer-Heertjes kinetic constant ($k_{sg,}$ 0.79 ml CH4/mg COD) exhibits similarity with the methane production rate (M_B, 0.63 mg/L d) (see Table 6.49).

Table 6.49 Comparison of kinetic constants for Stover-Kincannon and Van der Meer-Heertjes kinetic models for total and methane gas productions

Kinetic models	**Kinetic parameters**	**Methane Gas**		**Total Gas**	
		Values	**R^2**	**Values**	**R^2**
Stover-Kincannon	G_{max} (ml/L d)	-	0.97	1862	0.99
	G_B (mg/L d)	-		2.08	
	M_{max} (ml/L d)	598		-	
	M_B (mg/L d)	0.63	0.96		
Van der Meer-Heertjes	ksg (ml CH_4/mg COD)	0.79		-	

In this study, the gas kinetic constant (G_B=2.08 mg/Ld) and the maximum total gas production rate (G_{max}=1862 ml/Ld) values obtained from the Stover-Kincannon model exhibited similarities with the data obtained by Deshpande et al. (2012) (G_{max}=6080 ml/Ld and G_B=1.18 mg/Ld) in an anaerobic fixed film fixed bed reactor (AFFFBR) treating pharmaceutical wastewater.

As aforementioned in previous sections, there is not much published information about the methane production rate in the anaerobic reactor treating pharmaceutical wastewater using Van der Meer-Heertjes kinetic model.

6.6.2.4.1 Evaluation of the Experimental and Theoretical Total Gas Productions in Stover-Kincannon Kinetic Model. The experimental total gas production varied between 1000 and 5000 ml/d versus increasing HRTs (see Table 6.50). The theoretical total gas productions in the anaerobic AMCBR reactor were calculated according to the Eq. 5.53 and varied between 1073 and 4048 ml/d versus increasing HRTs (Table 6.50) as described in "Material and Methods" (see chapter 5.8.1.2.1).

$$\frac{1}{G} = \frac{G_B}{G_{\max}} \times \frac{1}{OLR} + \frac{1}{G_{\max}} \qquad \text{Eq. (5.53)}$$

The theoretical total gas production can be estimated from the Eq. (6.8) by substituting some gas kinetic constants calculated previously in an AMCBR reactor treating 100 mg/L OTC.

$$\frac{1}{G} = \frac{2.08}{1862} \times \frac{1}{OLR} + \frac{1}{1862} \qquad \text{Eq. (6.8)}$$

G is specific total gas production rate (mL/L.d) and OLR is organic loading rate (g/L.d). G_{max} is the maximum specific total gas (ml/Ld) and G_B is the total gas kinetic constant (mg/Ld) The theoretical total gas production values from the Stover-Kincannon kinetic model was very close to the experimental total gas production values in the anaerobic AMCBR reactor system with an regression coefficient of (R^2) 0.98 (see Table 6.50).

Table 6.50 Evaluation of theoretical and experimental results for total gas productions in the Stover-Kincannon Kinetic Model.

Parameter	**Experimental results**	**Theoretical results**	Regression coefficient (R^2)
		Stover-Kincannon Kinetic Model	
HRT (day)	Total gas (ml/d)	Total gas (ml/d)	
5.5	5000	4048	0.98
4.5	4000	3515	
2.25	3000	2784	
1.5	2000	1995	
1.13	1000	1073	

6.6.2.4.2 Evaluation of the Experimental and Theoretical Methane Gas Production of Stover-Kincannon Kinetic Model. The experimental methane gas productions varied between 850-2500 ml/d versus decreasing HRTs. The theoretical methane gas productions in the AMCBR reactor were calculated according to Eq. (5.54) and varied between 448-2070 ml/d versus decreasing HRTs (see Table 6.51) as described in "Material and Methods" (see chapter 5.8.1.2.1).

$$\frac{1}{M} = \frac{M_B}{M_{max}} \times \frac{1}{OLR} + \frac{1}{M_{max}} \qquad \text{Eq. (5.54)}$$

The Eq. (6.9) could be proposed to estimate the theoretical methane gas production in the Stover-Kincannon kinetic model by replacing the kinetic constant values in the AMCBR reactor treating 100 mg/L OTC. M is specific methane gas production rate (mL/L.d) and OLR is organic loading rate (g/L.d). M_{max} is the maximum specific methane gas (ml/Ld) and M_B is the methane gas kinetic constant (mg/Ld). The theoretical methane gas production values from the Stover-Kincannon kinetic model was very close to the experimental methane gas production values in the anaerobic AMCBR reactor system with an regression coefficient of (R^2) 0.97 (see Table 6.51)

$$\frac{1}{M} = \frac{0.63}{598} \times \frac{1}{OLR} + \frac{1}{598} \qquad \text{Eq. (6.9)}$$

Table 6.51 Evaluation of theoretical and experimental results for methane gas productions in the Stover-Kincannon Kinetic Model

Parameter	**Experimental results**	**Theoretical results**	Regression coefficient (R^2)
		Stover-Kincannon Kinetic Model	
HRT (day)	Methane gas (ml/d)	Methane gas (ml/d)	
5.5	2500	2070	0.97
4.5	2000	1745	
2.25	1750	1163	
1.5	1260	588	
1.13	850	448	

6.6.2.4.3 Evaluation of the Experimental and Theoretical Methane Gas Production of Van derMeer-Heertjes Kinetic Model. The experimental methane gas productions varied between 850-2500 ml/d versus decreasing HRTs. The theoretical methane gas productions in the AMCBR reactor were calculated according to Eq. (5.55) and varied between 448-2070 ml/d versus decreasing HRTs (see Table 6.52) as described in "Material and Methods" (see chapter 5.8.1.2.2).

$$G_{CH_4} = k_{sg} \times Q \times (S_0 - S) \qquad \text{Eq. (5.55)}$$

The Eq. (6.10) could be proposed to estimate the theoretical methane gas production in the Van derMeer-Heertjes kinetic model by replacing the kinetic constant values in the AMCBR reactor treating 100 mg/L OTC.

$$G_{CH_4} = 0.1408 \times Q \times (S_0 - S) \qquad \text{Eq. (6.10)}$$

M is specific methane gas production rate (mL/L.day). G_{CH4} is the methane gas production (L/d). Q is the flow rate (L/d). k_{sg} is the Van der Meer and Heertjes kinetic constant (mL/mg). S_0 and S are explained as the influent substrate concentration (mg/L) and the effluent substrate concentration (mg/L), respectively. The theoretical methane gas production values from the Van der Meer and Heertjes kinetic model was close to the experimental methane gas production values in the AMCBR reactor system with an regression coefficient of (R^2) 0.96 (see Table 6.52).

Table 6.52 Evaluation of theoretical and experimental results for methane gas productions in the Van derMeer-Heertjes Kinetic Model

Parameter	**Experimental results**	**Theoretical results**	Regression coefficient (R^2)
		Van derMeer-Heertjes Kinetic Model	
HRT (day)	Methane gas (ml/d)	Methane gas (ml/d)	
5.5	2500	1852	0.96
4.5	2000	1561	
2.25	1750	1041	
1.5	1260	526	
1.13	850	445	

6.6.2.4.4 Comparison of Theoretical Results for Methane Gas Productions in the Stover-Kincannon and Van derMeer-Heertjes Kinetic Models. All the regression coefficients and the theoretical methane gas production calculated from the Stover-Kincannon and Van derMeer-Heertjes kinetic models are summarized in Table 6.53.

Table 6.53 Comparison of theoretical results for methane gas productions in the Stover-Kincannon and Van derMeer-Heertjes Kinetic Models

Parameter	**heoretical methane gas productions**		
	Stover-Kincannon Kinetic Model		**Van derMeer-Heertjes Kinetic Model**
HRT (day)	Methane gas values (ml/d)	Methane gas values (ml/d)	Regression coefficient (R^2)
5.5	2070	1852	0.97
4.5	1745	1561	
2.25	1163	1041	
1.5	588	526	
1.13	448	445	

The theoretical methane gas productions calculated from the Stover-Kincannon kinetic model was very close to the theoretical methane gas production datas compared to the Van der Meer-Heertjes kinetic model. The linear relationships showed that the regression coefficient (R^2) between Modified Stover-Kincannon kinetic model and Van der Meer-Heertjes kinetic model is higher (see Table 6.53).

6.6.3 Substrate Removal Kinetic Models of Real Raw Pharmaceutical Wastewater in the AMCBR Reactor

In order to obtain the kinetic coefficient for different kinetic models the AMCBR reactor was operated with real pharmaceutical wastewater containing 65 mg/L OTC at six different HRTs through 216 days of the operation period**.** Monod, Grau second order, Stover-Kincannon, zero order, first order, second order, Contois kinetic models were applied to the experimental datas obtained from AMCBR reactor treating OTC at six different HRTs (5.5-4.5-2.25-1.5-1.13-0.9 days). All kinetic

coefficients calculated from the kinetic models are given in Table 6.54 with regression (R^2) coefficients in the AMCBR reactor.

In the experiment of Monod kinetic constants determination, influent substrate (COD) and co-substrate (OTC) were selected. The Monod kinetic constants based on COD were calculated as follows: Y=0.027 mgVSS/mgCOD, k_d=0.0037 d^{-1}, μ_{max}= 0.068 d^{-1}, K_S=5000 mgCOD/L. The kinetic constants based on OTC were calculated as follows: Y=0.011 mgVSS/mgOTC, k_d=0.0045 d^{-1}, μ_{max}=0.020 d^{-1}, K_S=42 mgOTC/L, respectively (Table 6.54).

The maximum substrate utilization rate (R_{max}) is higher and the saturation constant (K_B) is lower during COD and OTC biodegradation in Stover Kincannon kinetic model. High R_{max} indicates the reactor efficiency while low K_B indicates the utilization of COD and OTC by the methanogens in the anaerobic AMCBR reactor. In this study, K_B for COD and OTC biodegradation was found as 33.00 g/L.d and 0.52 g/L.d, respectively. The R_{max} values for COD and OTC were calculated as 29.42 g/L.d and 0.41 g/L.d, respectively in Stover-Kincannon kinetic model (Table 6.54).

"a" kinetic constant in Grau-second order kinetic model depends to COD, OTC concentrations and it was influenced by the inverse of second order substrate removal rate constant (k_s) and microorganism concentrations. The maximum substrate removal rate constant (k_s) and "a" kinetic constant will be increased as the COD and OTC removal efficiencies increased, depending to initial substrate (S_o) and biomass concentration (X) in the anaerobic AMCBR reactor (see Table 6.54).

The Zero, First and Second order kinetic models are not appropriate to describe the OTC and COD biodegradations in a real raw pharmaceutical wastewater. Maximum specific growth rate (μ_{max}) in Monod kinetic model and Contois kinetic constant (β) obtained from the Contois kinetic model are not appropriate to describe the anaerobic metabolization of COD and OTC in the anaerobic AMCBR reactor.

The maximum specific growth rate (μ_{max}) in Monod kinetic model and Contois kinetic constant (β) in Contois kinetic model are very low indicating that the OTC removal could not be defined with these kinetic constant values (see Table 6.54). Furthermore the Y values are enormously low and the K_S values are extremely high in Monod kinetic. As a result it is obvious that the Monod kinetic model is not suitable for OTC biodegradation.

Table 6.54 Kinetic parameters of anaerobic AMCBR reactor treating 65 mg/L OTC

Kinetic models	**Kinetic parameters**	**COD removal**		**OTC removal**	
		Values	**Regression coefficients**	**Values**	**Regression coefficients**
Monod	Y (mgVSS/mgCOD)	0.027	0.91	0.011	0.92
	k_d (d^{-1})	0.0037		0.0045	
	μ_{max} (d^{-1})	0.068		0.020	
	K_S (mg/L)	**5000**		**42**	
Grau second order	k_s (d^{-1})	0.07	0.98	0.003	0.97
	a (d)	0.30		0.32	
	b (dimensionless)	1.13		1.00	
Stover-Kincannon	K_B (g COD/L d)	33.00	0.98	0.52	0.97
	R_{max} (g COD/L d)	29.42		0.41	
Zero-order	k_0 (mg /L d)	0.14	0.59	0.004	0.50
First-order	k_1 (d^{-1})	3.02	0.60	0.002	0.61
Second-order	k_2 (L /mg d)	2.12	0.51	0.0002	0.50
Contois	μ_{max} (d^{-1})	0.03	0.90	0.033	0.90
	β (g COD/g biomass)	0.001		0.0002	

The kinetic data showed that Stover-Kincannon and Grau second order substrate removal kinetics were more appropriate models than the other models for predicting the performance of the lab scale AMCBR reactor when the regression coefficients and kinetic constants were compared with each other (see Table 6.54).

6.6.4 Biogas Production Kinetics for Real Raw Pharmaceutical Wastewater in the AMCBR Reactor

The methane and total gas productions calculated from the experimental studies were compared in two different kinetic models. The kinetic constants calculated from the kinetic models are summarized in Table 6.55. The maximum specific total gas and methane gas production rates (G_{max} and M_{max}) are higher and the total and methane gas kinetic constants (G_B and M_B) are lower during COD and OTC biodegradation in Stover Kincannon kinetic model.

In this study, the total gas kinetic constant (G_B) and the maximum total gas production rate (G_{max}) were found as 30 mg/Ld and 3200 ml/Ld, respectively, in Stover-Kincannon kinetic model. Similarly, the methane gas kinetic constant (M_B) and the maximum total gas production rate (M_{max}) were determined as 0.36 mg/Ld and 1582 ml/Ld respectively in the Stover-Kincannon model. In Van der Meer and Heertjes kinetic model, the methane gas kinetic constant (k_{sg}) was found as 0.39 (ml CH_4/mg COD) (see Table 6.55). Low methane gas kinetic constants (M_B and k_{sg}) indicate the utilization of COD and OTC by the methanogens in the AMCBR reactor for Stover-Kincannon and Van der Meer and Heertjes kinetic models. In the comparison of the kinetic constants of the Stover Kincannon and Van der Meer-Heertjes kinetic models it was found that the Van der Meer-Heertjes kinetic constant ($k_{sg,}$ 0.39 ml CH4/mg COD) exhibits similarity with the methane production rate (M_B, 0.36 mg/L d) in Stover Kincannon kinetic model (see Table 6.55).

The methane gas productions calculated from the Stover-Kincannon kinetic model was very close to the methane gas production data compared to the Van der Meer-Heertjes kinetic model. The linear relationships showed that the regression coefficient (R^2) is higher in the Stover-Kincannon kinetic model compared to the Van der Meer-Heertjes kinetic model (Table 6.55).

Table 6.55 Comparison of the kinetic constants for Modified Stover-Kincannon and Van der Meer kinetic models for total and methane gas productions

Kinetic models	**Kinetic parameters**	**CH_4 Gas**		**Total Gas**	
		Values	**R^2**	**Values**	**R^2**
Stover-Kincannon	G_{max} (ml/L d)	-	0.95	3200	0.96
	G_B (mg/L d)	-		1.30	
	M_{max} (ml/L d)	1582		-	
	M_B (mg/L d)	0.36	0.93		
Van der Meer and Heertjes	k_{sg} (ml CH_4/mg COD)	0.39		-	

6.6.4.1 Evaluation of the Experimental and Theoretical Total Gas Production in the AMCBR Reactor According to Stover-Kincannon Kinetic Model for Real Raw Pharmaceutical Wastewater

The theoretical total gas productions in the anaerobic AMCBR reactor were calculated according to the Eq. 5.53 and varied between 2013 and 5012 ml/d versus increasing HRTs (Table 6.56) as described in "Material and Methods" (see chapter 5.8.1.2.1). The theoretical total gas production can be estimated from the Eq. (6.11) by substituting some gas kinetic constants calculated previously in an AMCBR reactor treating 65 mg/L OTC.

$$\frac{1}{G} = \frac{1.30}{3200} \times \frac{1}{OLR} + \frac{1}{3200} \qquad \text{Eq. (6.11)}$$

The theoretical total gas production values from the Stover-Kincannon kinetic model was very close to the experimental total gas production values in the anaerobic AMCBR reactor system with an regression coefficient of (R^2) 0.96 (see Table 6.56). The theoretical total gas production can be estimated from the Eq. (6.11) by substituting some total gas kinetic constants calculated previously in an AMCBR reactor treating 100 mg/L OTC.

Table 6.56 Comparison of theoretical and experimental results for total gas productions in the Stover-Kincannon Kinetic Model

Parameter	**Experimental results**	**Theoretical results**	Regression coefficient (R^2)
		Stover-Kincannon Kinetic Model	
HRT (day)	Total gas (ml/d)	Total gas (ml/d)	
5.5	7000	5012	0.96
4.5	6420	4846	
2.25	5130	3925	
1.5	4600	3034	
1.13	2800	2013	

6.6.4.2 Evaluation of the Experimental and Theoretical Methane Gas Production of Stover-Kincannon Kinetic Model for Real Raw Pharmaceutical Wastewater.

The theoretical methane gas productions in the AMCBR reactor were calculated according to Eq. (5.54) and varied between 848-2865 ml/d versus decreasing HRTs (see Table 6.57) as described in "Material and Methods" (see chapter 5.8.1.2.1). The Eq. (6.12) could be proposed to estimate the theoretical methane gas production in the Stover-Kincannon kinetic model by replacing the kinetic constant values in the AMCBR reactor treating 65 mg/L OTC.

$$\frac{1}{M} = \frac{0.95}{1582} \times \frac{1}{OLR} + \frac{1}{1582} \qquad \text{Eq. (6.12)}$$

The theoretical methane gas production values from the Stover-Kincannon kinetic model was very close to the experimental methane gas production values in the anaerobic AMCBR reactor system with an regression coefficient of (R^2) 0.95 (see Table 6.57)

Table 6.57 Comparison of theoretical and experimental results for methane gas productions in the Stover-Kincannon Kinetic Model

Parameter	**Experimental results**	**Theoretical results**	Regression coefficient (R^2)
		Stover-Kincannon Kinetic Model	
HRT (day)	Methane gas (ml/d)	Methane gas (ml/d)	
5.5	4600	2865	0.95
4.5	3100	2000	
2.25	2500	1421	
1.5	2000	1080	
1.13	1260	848	

6.6.4.3 Evaluation of the Experimental and Theoretical Methane Gas Production of Van derMeer-Heertjes Kinetic Model for Raw Pharmaceutical Wastewater

The theoretical methane gas productions in the AMCBR reactor were calculated according to Eq. (5.55) and varied between 448-2070 ml/d versus decreasing HRTs (see Table 6.58) as described in "Material and Methods" (see chapter 5.8.1.2.2). The Eq. (6.13) could be proposed to estimate the theoretical methane gas production in the Van derMeer-Heertjes kinetic model by replacing the kinetic constant values in the AMCBR reactor treating 65 mg/L OTC.

$$G_{CH_4} = 0.1408 \times Q \times (S_0 - S) \qquad \text{Eq. (6.13)}$$

The theoretical methane gas production values from the Van der Meer and Heertjes kinetic model was close to the experimental methane gas production values in the anaerobic AMCBR reactor system with an regression coefficient of (R^2) 0.93 (see Table 6.58).

Table 6.58 Comparison of theoretical and experimental results for methane gas productions in the Van derMeer-Heertjes Kinetic Model

Parameter	**Experimental results**	**Theoretical results**	Regression coefficient (R^2)
		Van derMeer-Heertjes Kinetic Model	
HRT (day)	Methane gas (ml/d)	Methane gas (ml/d)	
5.5	4600	1965	0.93
4.5	3100	1800	
2.25	2500	1200	
1.5	2000	946	
1.13	1260	745	

6.6.4.4 Comparison of Theoretical Results for Methane Gas Productions in the Stover-Kincannon and Van derMeer-Heertjes Kinetic Models for Raw Pharmaceutical Wastewater

The regression coefficient and the theoretical methane gas productions calculated from the Stover-Kincannon and Van derMeer-Heertjes kinetic models are summarized in Table 6.59.

Table 6.59 Comparison of theoretical results for methane gas productions in the Stover-Kincannon and Van derMeer-Heertjes Kinetic Models

Parameter	**Theoretical methane gas productions**		
	Stover-Kincannon Kinetic Model		**Van derMeer-Heertjes Kinetic Model**
HRT (day)	Methane gas values (ml/d)	Methane gas values (ml/d)	Regression coefficient (R^2)
5.5	2865	1965	0.93
4.5	2000	1800	
2.25	1421	1200	
1.5	1080	946	
1.13	848	745	

The theoretical methane gas productions calculated from the Stover-Kincannon kinetic model was very close to the theoretical methane gas production datas compared to the Van der Meer-Heertjes kinetic model. The linear relationships showed that the regression coefficient (R^2) between Modified Stover-Kincannon kinetic model and Van der Meer-Heertjes kinetic model is higher (see Table 6.59).

6.6.5 Variations of the Volumetric Methane Gas Production Rates versus Substrate Concentrations in the AMCBR Reactor According to Michelis-Menten Kinetic Model for Real Raw Pharmaceutical Wastewater

The values of volumetric methane gas production rate (R_{CH4}) ($mlCH_4/d.L$) can be obtained by plotting $R_{CH4}=q_{CH4}/V$ versus S in Eq. 5.56 (see chapter 5.8.1.2.3). q_{CH4} and V are the daily methane production ($mlCH_4/d$) and the AMCBR reactor volume (L), respectively. S is the biodegradable total COD (mg/L) concentration (see Figure 6.193). As can be seen, R_{CH4} values obtained from the experimental methane measurements fitted a hyperbolic function, an indication of Michaelis-Menten kinetic model (see chapter 5.8.1.2.3). The q_{CH4} values increased from 0.60 ml CH_4/d up to a constant q_{CH4} value of 1.42 ml CH_4/d versus biodegradable COD concentrations. Increasing of substrate concentration (>0.90 g/L) does not affect the q_{CH4} values. The linear regression coefficient value (R^2) was 0.9538 ($y=1.9842x/0.3492+x$) for AMCBR reactor treating 100 mg/L OTC in this plot (see Figure 6.193).

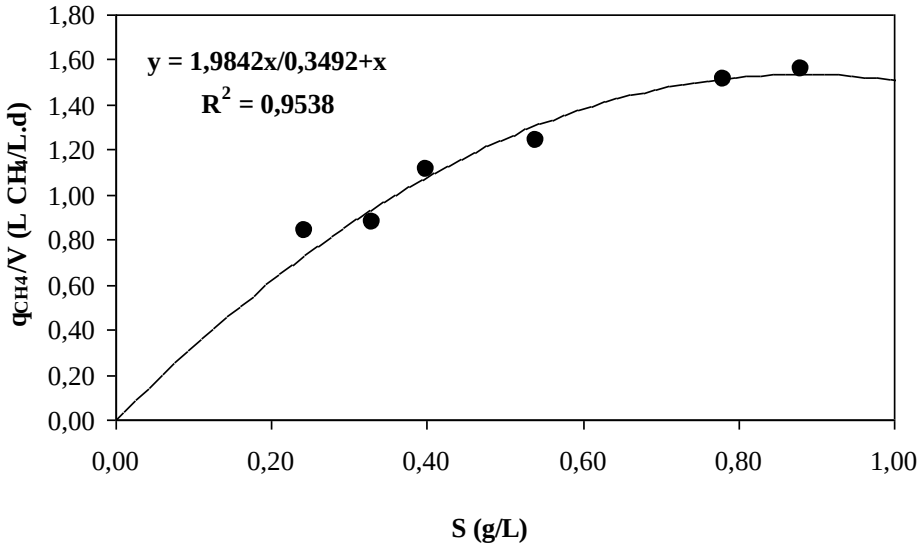

Figure 6.193 Variations of the volumetric methane gas production rates as a function of the biodegradable total COD concentration in the effluent of the AMCBR reactor in Michelis-Menten kinetic model

6.6.5.1 Validation of Experimental and Theoretical Methane Production Rates in the AMCBR Reactor for Michelis-Menten Kinetic Model

From Eq. 5.56 the volumetric methane gas production rate ($R_{CH4)}$ values were calculated for tentative and theoretical values were compared in the anaerobic AMCBR reactor used in this study. It was found that the experimental gas productions agree with the theoretical gas productions. The experimental R_{CH4} values are plotted against those observed theoretical R_{CH4} values using a linear regression plot with slopes of 0.9684 and of 0.9692, respectively in the AMCBR reactor (see Figure 6.194). The linear regression coefficient values (R^2) were 0.9674 (therotical R_{CH4}) and 0.9702 (experimental R_{CH4}) for AMCBR reactor treating 65 mg/L OTC in this plot (see Figure 6.194). A good linear relationship was observed between experimental and theoretical methane gas productions in the Michaelis-Menten model. Additionally, all the points in the plot were in the coverage area of the dotted lines obtained from ±5% of the slope of the linear line. Nevertheless, there is not much published information about the methane production rate in the anaerobic reactor treating pharmaceutical wastewater using Michaelis-Menten model.

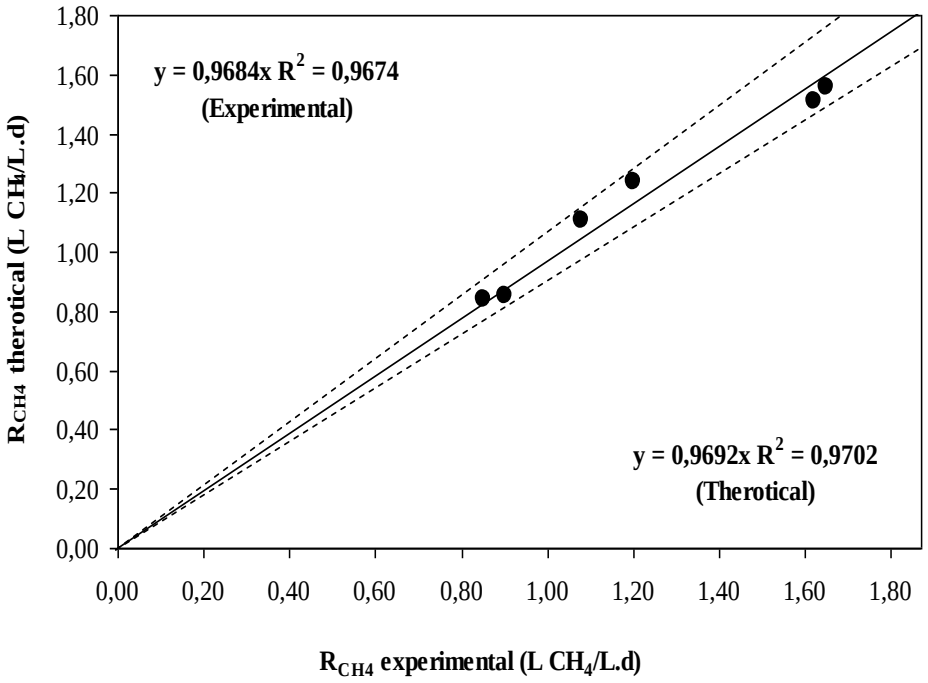

Figure 6.194 Validation of theoretical and experimental volumetric methane gas production rates in Michaelis-Menten kinetic for AMCBR reactor treating 65 mg/L OTC

6.6.6 Evaluation of Biodegradation and Inhibition Kinetics Parameters throughout Anaerobic Treatment of Molasses-COD and OTC in the AMCBR Reactor Based on Methanogens and Acidogens

The kinetic results of this part of Ph.D thesis include the constants obtained from the acidogenic and methanogenic sampling points of the AMCBR reactor at five OTC loadings when the VSS concentrations of the aforementioned bacteria are low (50 g/L) after 163 days of operation period only for OTC:

The hydrolytic rate of molasses-COD (k) was observed both in the absence and in the presence of increasing OTC concentrations. The presence of OTC until an OTC loading rate of 177.78 gOTC/m^3d did not affect the hydrolytic rate constant of molasses-COD, significantly, in the first compartment of the AMCBR reactor. The value of k was measured as 0.99 d^{-1} in the first compartment of the control AMCBR while the k value were between 1.18 and 1.21 d^{-1} at OTC loading rates of 22.22 and 133.33 gOTC/m^3d, respectively. Then it decreased in the same compartment (Table

6.60). The OTC loadings up to 177.78 gOTC/m^3d improved the hydrolysis of molasses-COD. The k values obtained in the AMCBR reactor for the OTC loadings mentioned above were comparably higher than in the control reactor without OTC. This showed that OTC besides molasses–COD could be used as carbon and energy source by the biomass with co-metabolism. This could be attributed to the increase in MLVSS concentrations from 16.7 to 18.21 g/L as the OTC loadings increased from 22.22 to 133.33 gOTC/m^3d. The k value decreased in the second and third compartments of the AMCBR reactor since in these compartments acidogenesis and methanogenesis take place (Table 6.60).

The inhibition of pH on hydrolysis was not considered in this study because the measured pH was in the range of 7.1-8.0 and the inhibition of pH could be negligible. Therefore, the inhibition constants of pH on acidogens ($K_{I\text{-}pH\text{-}acid}$) and methanogens ($K_{I\text{-}pH\text{-}meth}$) were calculated as approximately close to zero (Table 6.60)

As seen in Table 6.52 the maximum specific utilization of hydrolysis products of molasses-COD (k_{mh}) increased from 0.8 up to 1.8 d^{-1} as the OTC loading rate increased from 22.22 up to 133.33 gOTC/m^3d. The maximum k_{mh} was observed at OTC loading rates of 111.11 and 133.33 gOTC/m^3d in the first compartment of AMCBR reactor. The reason for this may be the favorable co-metabolism of OTC for growth of acidogens resulting in TVFA production in the first chamber of the AMBR reactor. The reason for lower k_{mh} at OTC loadings higher than 133.33 gOTC/m^3d could be attibuted to the toxic effects of higher OTC concentration on acidogenic bacteria to produce TVFA in the AMCBR reactor. The TVFA production is higher (800-900 mg L^{-1}) at OTC loading rates between 44.44 and 133.33 gOTC/m^3d due to highest k, k_{mh}, and maximum specific utilization of TVFA (k_{TVFA}). At these OTC loadings OTC could be used as a co-substrate together with TVFA. Therefore the TVFA produced by acidogens consumed by acetogen bacteria.

The TVFA production decreased at OTC loadings higher than133.33 gOTC/m^3d due to lower k_{mh} and k_{TVFA} at higher OTC loadings. At high OTC loadings the reason for lower k_{mh} and TVFA production were both the high half-saturation constant for

acidogenic bacteria growth ($K_{s\text{-}acid}$) and the decay rate of acidogenic bacteria ($k_{d\text{-}acid}$) in the first compartment of the AMCBR. These agree with the studies performed by Fountoulakis et al., (2008) in an anaerobic reactor in the presence of tetracycline and oflaxine group antibiotics. The k_{mh} decreased while the $K_{s\text{-}acid}$ increased for acetate and propionate degradations in the presence of both antibiotics. The K_s values increased to 34 mg/L in a full scale anaerobic digester in the precence of some pharmaceuticals (O'Flaherty et al., 1998). The low value of μ_{max} and high value of K_s showed that the typical wastes were slowly biodegraded in the comparison to more easily degraded substrate (Truax et al., 1995). These finding are of particular importance because low K_s values are essential for achieving a good treatment efficiency in anaerobic treatment of toxic wastewaters.

The k_{TVFA} increased significantly with the increase of OTC loading rates up to 177.78 gOTC/m^3d then it decreased indicating that high OTC concentrations inhibited the TVFA utilization significantly by acetoclastic methanogens. These bacteria were affected strongly by high OTC concentrations. This resulted in decrease of k_{TVFA} and methane production at high OTC loading rates. These agree with the studies performed by Delgadillo-Mirquez et al., (2011) in an anaerobic reactor treating micropollutants and antibiotics.

The k value for OTC found in this study was considered higher as compared to the k values obtained by Wu et al., (2011) during the swine manure composting ($k=0.26\ d^{-1}$), by Rodante et al., (2002) ($k=0.67\ d^{-1}$) in an anerobic contact reactor and by Arıkan et al., (2008) for CTC in the anaerobic manure samples ($k=0.56\ d^{-1}$). Furthermore, the k value found in this study is significantly higher for the biodegradation rate constant of TC ($k=0.034\ d^{-1}$) (Yahiat et al., 2011) and tetracycline antibiotics ($k=0.07\ d^{-1}$) (Fountoulakis et al., 2008).This could be due to the AMCBR was a high rate reactor for the anaerobic growth yield under high OTC concentrations. The anaerobic bacteria were immobilized by dense compact granules due to higher substrate-cell surface interaction and higher microorganism activity in separate compartments.

The half-saturation constant of methanogenic bacteria ($K_{s\text{-}meth}$) increased to 90 mg/L while the inhibition constant of methanogens caused by OTC ($K_{I\text{-}OTC\text{-}meth}$) decreased to 0.001 mg/L (Table 6.60) in the second compartment of the AMCBR at an OTC loading rate of 177.78 gOTC/m^3d. On the other hand, high OTC concentrations significantly affect the balance between the heterothrophic, acidogenic, acetogenic and methanogenic bacteria. As a result, the symbiotic relationships between the major bacteria groups throughout hydrolysis, acid production, acedogenesis and methanogenesis of the anaerobic degradation changed.

The decay rate of acidogenic bacteria ($k_{d\text{-}acid}$) represents lysis and endogenous respiration processes in the conversion of molasses-COD throughout anaerobic treatment. As seen in Table 6.52, the values of $k_{d\text{-}acid}$ up to an OTC loading rate of 177.78 gOTC/m^3d were lower than increased with the increase of OTC. The inhibition constants of TVFA on methanogens ($K_{I\text{-}\ TVFA\text{-}\ meth}$) and of OTC on methanogens ($K_{I\text{-}\ OTC\text{-}meth}$) decreased at high OTC loadings since the methanogens were strongly affected by the TVFA accumulation and high OTC concentrations.

Table 6.60 Substrate removal and inhibition kinetics for anaerobic bacteria in AMCBR reactor system at increasing OTC

parameter		AMCBR, 1st compartment					AMCBR, 2nd compartment					AMCBR, 3rd compartment				
		OTC loading rate (gOTC $m^{-3}.d^{-1}$)					OTC loading rate (gOTC $m^{-3}.d^{-1}$)					OTC loading rate (gOTC $m^{-3}.d^{-1}$)				
	C	22.22	44.44	111.11	133.33	177.78	22.22	44.44	111.11	133.33	177.78	22.22	44.44	111.11	133.33	177.78
k	0.99	1.18	1.20	1.20	1.21	0.78	0.04	0.05	0.03	0.01	0	0	0	0	0	0
k_{mh}	0.7	0.8	0.9	1.8	1.8	0.67	0.2	0.2	0.3	0.4	0.03	0	0	0	0	0
$K_{s\text{-}acid}$	20	40	30	20	18	400	20	20	20	30	80	0	0	0	0	0
$k_{d\text{-}acid}$	0.03	0.08	0.08	0.04	0.05	1.2	0.03	0.03	0.02	0.03	0.09	0	0	0	0	0
k_{TVFA}	1.50	1.20	1.33	1.39	1.56	0.80	1.02	1.03	1.04	1.49	0.66	0.01	0.01	0.01	0.01	0.01
$K_{s\text{-}meth}$	40	40	45	40	30	80	5	6	7	3	90	4	3	2	1	1
$k_{d\text{-}acid}$	0.01	0.01	0.01	0.01	0.01	0.09	0.02	0.02	0.02	0.02	0.09	0	0	0	0	0
$K_{d\text{-}meth}$	0	0	0	0	0	0	0.001	0.001	0.001	0.001	0.09	0	0	0	0	0
$K_{I\text{-}TVFA\text{-}acid}$	0.14	0.17	0.18	0.18	0.22	0.08	0.04	0.04	0.04	0.07	0.01	0	0	0	0	0
$K_{I\text{-}TVFA\text{-}meth}$	0.06	0.06	0.07	0.09	0.21	0.03	0.05	0.06	0.06	0.82	0.04	0.70	0.72	0.79	0.89	0.01
$K_{I\text{-}OTC\text{-}acid}$	0.78	0.88	0.89	0.94	1.03	0.23	0.03	0.03	0.04	0.06	0.01	0	0	0	0	0
$K_{I\text{-}OTC\text{-}meth}$	0.43	0.02	0.02	0.02	0.03	0.002	0.02	0.10	0,24	0,27	0.001	0.56	0.67	0.87	0.98	0.29
μ_{acid}	0.56	0.67	0.61	0.73	0.11	0.10	0.77	0.78	0.79	0.89	0.21	0.01	0.01	0.01	0.01	0
μ_{meth}	0.001	0.001	0.001	0.001	0.003	0.0001	0.002	0.003	0.004	0.009	0.001	0.09	0.011	0.023	0.045	0.02
Y_{acid}	0.33	0.35	0.47	0.49	0.59	0.10	0.69	0.69	0.69	0.69	0.72	0.10	0.001	0.001	0.001	0.001
Y_{meth}	0.17	0	0	0	0	0.22	0.34	0.44	0.44	0.56	0.08	0.54	0.56	0.60	0.76	0.02
$R_{max\text{-}acid}$	5.2	5.3	5.4	5.6	5.8	1.1	5.8	5.9	5.9	6.23	2.01	0.4	0.5	0.4	0.5	0.1
$R_{max\text{-}meth}$	2.8	2.9	3.1	3.1	3.9	0.7	4.3	4.4	4.5	5.6	1.7	5.4	5.8	5.9	6.3	1.9
$\mu_{max\text{-}acid}$	0.58	0.68	0.69	0.79	0.15	0.01	0.79	0.81	0.82	0.91	0.22	0.02	0.02	0.02	0.02	0
$\mu_{max\text{-}meth}$	0.002	0.002	0.002	0.002	0.004	0.0009	0.003	0.004	0.005	0.010	0.02	0.011	0.017	0.039	0.055	0.03
$K_{ID\text{-}OTC\text{-}acid}$	33	33	33	34	35	2	51	51	52	54	4	48	47	49	52	4
$K_{ID\text{-}OTC\text{-}meth}$	2	2	2	3	5	1	7	8	8	14	1	19	22	39	43	2
$K_{I\text{-}pH\text{-}acid}$	$1x10^{-4}$	$1x10^{-4}$	$1x10^{-4}$	$1x10^{-4}$	$1x10^{-4}$	$1x10^{-4}$	$1x10^{-4}$	$1x10^{-4}$	$1x10^{-4}$	$1x10^{-4}$	$1x10^{-4}$	$1x10^{-4}$	$1x10^{-4}$	$1x10^{-4}$	$1x10^{-4}$	$1x10^{-4}$
$K_{I\text{-}pH\text{-}meth}$	$1x10^{-5}$	$1x10^{-5}$	$1x10^{-5}$	$1x10^{-5}$	$1x10^{-5}$	$1x10^{-5}$	$1x10^{-5}$	$1x10^{-5}$	$1x10^{-5}$	$1x10^{-5}$	$1x10^{-5}$	$1x10^{-5}$	$1x10^{-5}$	$1x10^{-5}$	$1x10^{-5}$	$1x10^{-5}$

C: Control without OTC

The μ_{acid} values are higher at OTC loading rates between 44.44 and 133.33 gOTC/m^3d in the first and in the second compartments of the AMCBR reactor up to 177.78 gOTC/m^3d while the μ_{meth} constants are higher in the third compartment of the AMCBR reactor were methanogenesis is predominant for the OTC loadings in suspension. Similarly the Y_{acid} values are higher in the first and in the second compartments of the AMCBR reactor for OTC loadings between 44.4 and 133.33 gOTC/m^3d when acidogenesis is prodeminant. The Y_{meth} is higher in the third compartment where methane production is at the highest ranges. Samuel Suman Raj and Anjaneyulu, 2005 investigated the biokinetic parameters like Y, K_s, k, μ_{max} and k_d for the treatment of pharmaceutical wastewater under anoxic conditions. Lower Y, k and μ_{max} values was observed compared to the present study during the anaerobic treatment while high K_s and k_d values was reported for the tetracycline group antibiotics (Samuel Suman Raj and Anjaneyulu, 2005).

First order reaction kinetic for OTC, TC and CTC biodegradations was observed in the studies performed by Wu et al., (2011) during the swine manure composting, by Rodante et al., (2002) in an anerobic contact reactor, by Yahiat et al., (2011), Arıkan et al., (2008) and by Foundalakis et al., (2008) in the anaerobic manure samples with low biodegradation rates. In this study the biodegradation of molasses-COD together with OTC was explained in Monod kinetic with higher biodegradation rates. This could be attributed to the dominancy of the resistant granulated anaerobic bacteria to the high OTC concentrations and to the AMCBR reactor configuration.

In this study it was found that the possible direct effect of high OTC concentrations on methanogen and acidogens could be explained by the Haldane inhibition kinetic. The kinetic constants in the control reactor without OTC were obtained with Lineweaver–Burk plot by the linearization of Eqs. (5.30)-(5.33) for hydrolytic bacteria, acidogens and methanogens. As summarized in Table 6.52, the parameters estimated using integrated Monod kinetic are, 0.58 d^{-1} for the maximum specific growth rate of acidogens ($\mu_{max\text{-}acid}$), 0.002 d^{-1} for the maximum specific growth rate of methanogens ($\mu_{max\text{-}meth}$), 20 mg/L and 40 g/L for the half saturation constant of acidogens and methanogens ($K_{s\text{-}acid}$ and $K_{s\text{-}meth}$) and 5.2 and 2.8 g/L.d for

the maximum substrate removals rates of acidogens and methanogens ($R_{max-\ acid}$ and $R_{max-meth}$) through anaerobic degradation of 4000 mg L^{-1} molasses-COD without OTC in the control AMCBR reactor. The R_{max} and K_s values found from the integrated Monod equations for both bacteria in the control reactor without OTC were substituted into the Haldane kinetic to determine the K_s, K_{ID} and R_{max} at increasing OTC concentrations from 350 to 400 mg/L (OTC loadings: 155.56-177.78 gOTC/m^3.d)

The results of this step showed that the Haldane equation gave the correct fit since the model fitted the experimental data very well with an r^2 greater than 99%. In the presence of OTC the maximum specific growth rates for acidogens and methane bacteria ($\mu_{max-acid,}$ $\mu_{max-meth}$), varied in the range of 0.01 d^{-1} and 0.0009 d^{-1} for 400 mg/L OTC concentration (OTC loading rate: 177.78 gOTC/m^3.d) while the half saturation constant of acidogens and methanogens bacteria ($K_{s-acid,}$ K_{s-meth}) increased from 20 and 40 mg/L to 400 and 80 mg/L, respectively, throughout anaerobic degradation of 400 mg/L OTC in the first compartment of the AMCBR reactor. At high OTC concentrations (350 and 400 mg/L) the threshold limitations for Haldane inhibitions are: $K_s \leq K_{ID}$; $K_s \leq 2000$ mg/L; $\mu \leq \mu_{max} \leq 3\mu \leq$ for 4000 mg/L molasses-COD; $K_s \leq K_{ID}$; $K_s \leq 50$ mg/L OTC. In this inhibition the inhibition coefficients for acidogen and methanogens ($K_{ID-acid,}$ $K_{ID-meth}$) decreased to 2-4 mg/L and 1-2 mg/L from 35, 54,52 and 5,14, 43 mg/L at an OTC concentration of 400 mg/L (OTC loading rate: 177.78 gOTC/m^3d) in all compartments. No inhibition of OTC to bacterial cells was observed at OTC concentration varying between 50-300 mg/L. Table 6.60 shows that the inhibition coefficients (K_{ID}) increased at low OTC concentrations (50-300 mg/L) (OTC loading rate: 44.44-133.33 gOTC/m^3d). From this data, it can be concluded that the Haldane inhibition occurs between 350 and 400 mg/L OTC. Because the inhibition effect is inversely proportional to the inhibition constant it will decrease as the toxicant concentration increases. The half saturation constant in both bacteria (K_{s-acid}, K_{s-meth}) reflects the fact that the low K_s values of 18-40 mg/L and 1-45 mg/L imply that there is a strongly affinity of substrate to bind the bacteria for OTC concentrations 50-300 mg/L. Therefore, it can be said that no OTC accumulation was observed in the AMCBR reactor for OTC concentration 50-300

mg/L. From the above results the K_{ID} values indicated that the inhibition effects are observed only at higher OTC concentrations. The bacterial growth increased with increasing of OTC concentration to its maximum and then decreased with further increase in OTC concentration. Low K_s values are essential for achieving good treatment efficiency in anaerobic treatment of antibiotics. It is evident that the kinetic represented by Haldane model is very suitable for OTC inhibition than the other inhibition models reported in the recent literature by Maurer et al., (2007) (competitive inhibition), Han and Levenspiel, (1987) and Rodante et al., (2002). 100 mg/L OTC reduced the methane production by 62% and increased the K_s value from 34 to 89 mg/L following a Haldane inhibition kinetic (Alvarez et al., 2010). In a study performed by Shi et al., (2011) the biodegradation performance of 80 mg/L OTC decreased the COD yields from 79 to 30% and increased the K_s value from 297 to 847 mg/L following the Haldane kinetic. Haldane kinetic exhibited high inhibition for OTC.

The non-linear behaviour of antibiotic inhibition has been also shown in previous studies. Sanz et al., (1996) studied the impact of several antibiotics on the anaerobic digestion process and observed that increasing concentrations of neomycin and hydromycin B produced a constant increase of inhibition. Han and Levenspiel, (1987) modified the uncompetitive type of inhibition function to account for the nonlinearity of the inhibition with respect to the inhibitor concentration. The modified non-competitive kinetic model succeeds to evaluated the experimental data in the presence of pharmaceuticals for a wide range of concentrations (Yahiat et al., 2011). In the Haldane type inhibition the OTC acting on bacterial cell membranes probably caused changes in permeability and protein structure and resulting in membrane disruption at higher OTC concentrations (Maurer et al., 2007).

6.6.7 Inhibition Kinetic Models for Real Raw Pharmaceutical Wastewaters Containing OTC

In order to obtain the inhibition kinetic constants for different inhibition kinetic models the AMCBR reactor was operated with real pharmaceutical wastewater

containing OTC concentrations of 50, 65 and 85 mg/L, respectively, at a HRT of 2.25 days under steady state conditions. The most commonly used biodegradation kinetic model is the Monod which is relates with the maximum substrate utilization rate (R_{max}), with the maximum specific growth rate (μ_{max}) and with the half saturation constant (K_S), (Eq. (6.3); Han and Levenspiel, 1988) (Table 6.61). Competitive, Non-competitive, Un-competitive and Haldane inhibition kinetic models are classified according to the effect of toxic compounds on the R_{max}, and K_S and derived from Eq. (6.3) (see chapter 5.8.1.3, Table 5.46) (Lehninger, 1997). Inhibition kinetic functions Eqs. (6.4-6.7) was fitted with the experimental data using Microsoft Excel 2003 (Table 6.61). The Line weaver-Burk plot is the linearized form of the Monod graphical presentation is described by Line weaver and Burk, (1934).

Table 6.61 The slope and to the intercepts and the type of inhibition kinetic models

Kinetic	**kinetic formulae**	**Slope**	**Intercepts**	**Eqs**
Without inhibition (no OTC)				
Monod	$-\frac{dS}{dt} = -R = -\frac{R_{max} \times S}{K_S + S}$	$\frac{K_S}{R_{max}}$	$\frac{1}{R_{max}}$	6.3
With inhibition (50-65-85 mg/L OTC)				
Competitive	$-\frac{dS}{dt} = -R = -\frac{R_{max} \times S}{K_S \times \left(1 + \left(\frac{I_A}{K_{IA}}\right)\right) + S}$	$\frac{K_S}{R_{max}} \times \left(1 + \frac{I_A}{K_{IA}}\right)$	$\frac{1}{R_{max}}$	6.4
Noncompetitive	$-\frac{dS}{dt} = -R = -\frac{R_{max}}{\left(1 + \left(\frac{K_S}{S}\right)\right) \times \left(1 + \left(\frac{I_A}{K_{IA}}\right)\right)}$	$\frac{K_S}{R_{max}} \times \left(1 + \frac{I_A}{K_{IA}}\right)$	$\frac{1}{R_{max}} \times \left(1 + \frac{I_A}{K_{IA}}\right)$	6.5
Uncompetitive	$-\frac{dS}{dt} = -R = -\frac{\frac{R_{max} \times S}{\left(1 + \left(\frac{I_A}{K_{IA}}\right)\right)}}{\left(\frac{K_S}{\left(1 + \left(\frac{I_A}{K_{IA}}\right)\right)}\right) + S}$	$\frac{K_S}{R_{max}}$	$\frac{1}{R_{max}} \times \left(1 + \frac{I_A}{K_{IA}}\right)$	6.6
Haldane	$\mu = \frac{\mu_{max} \times S}{K_S + S + \frac{S^2}{K_i}}$	$\frac{K_S}{\mu_{max}}$	$\frac{1}{\mu_{max}} \times \left(1 + \frac{I_A}{K_{IA}}\right)$	6.7

When the inverse of co-substrate (OTC) utilization rate 1/R is plotted against the reciprocal of co-substrate (OTC) 1/S, a straight line is obtained (Line weaver–Burk plot) in Eq. (6.3) (chapter 5.8.1.3; Figure 5.6) (Table 6.61). This line will have a slope of K_S/R_{max}, an intercept of $1/R_{max}$ on the 1/R axis, and an intercept of $-1/K_S$ on the 1/S axis. Such a double reciprocal plot has the advantage of allowing much more accurate determination of R_{max} and K_S. The double reciprocal plot of the Line weaver–Burk plot can give valuable information on inhibition. The possible effects of increasing OTC concentrations on Line weaver-Burk plot can be seen by the linearization of Eqs. (6.4)-(6.7) (see Table 6.61).

The parameters estimated using integrated Monod kinetic constants are, 0.66 d^{-1} for the maximum specific growth rate (μ_{max}) and 38.12 g/L d for the maximum substrate removals (R_{max}) through anaerobic degradation of a real pharmaceutical wastewater without OTC at a HRT of 2.25 days and at OTC concentrations of 50, 65 and 85 mg/L (see Table 6.62). Subsequently the initial R_{max} and K_S values obtained from the Lineawer-Burk plot were substituted into the integrated competitive, non-competitive and uncompetitive equations to obtain the relationships between K_S, inhibition constant (K_I) and R_{max} at increasing OTC concentrations from 50 to 85 mg/L.

The calculated R_{max} values are unreastically high in competitive (5.8-8.7 g/Ld), non-competitive (6.0-10.2 g/Ld), and uncompetitive (9.6-15.0 g/Ld) inhibition kinetic models as seen in Table 6.62. In the determination of competitive inhibition kinetic model constants the calculations were performed according to the co-substrate (OTC). The competitive inhibition kinetic constants based on increasing OTC concentrations were calculated as follows: the R_{max} varied in the range of 5.8, 7.0 and 8.7 g/Ld, the K_S varied in the range of 45, 47 and 52 mg/L, the K_I varied in the range of 12, 20 and 75 mg/L, respectively in the AMCBR reactor system. In this study, R_{max}=6.0-10.2 g/L.d, K_S=10-92 mg/L and K_I=15-108 mg/L for OTC concentrations in the non-competitive inhibition kinetic model. Table 6.62 shows that the inhibition coefficient (K_I) increased unreastically as the OTC concentration increased from 50 to 85 mg/L in uncompetitive inhibition kinetic model. The K_I

values increased from 12, 36 and to 120 mg/L at OTC concentrations of 50, 65 and 85 mg/L in uncompetitive inhibition kinetic model. The R_{max} varied in the range of 9.6, 11.0 and 15.0 g/Ld and the K_S varied in the range of 8, 14 and 80 mg/L, respectively at OTC concentrations of 50, 65 and 85 mg/L in the AMCBR reactor. Table 6.62 shows that the inhibition coefficient (K_I) increased as the OTC concentration increased from 50 to 85 mg/L in Competitive, Non-competitive and Uncompetitive inhibition kinetic models. μ_{max} and K_S values were placed in integrated Monod equations to determine μ_{max}, K_S and inhibition coefficient (K_I) values in Haldane inhibition kinetic model. The results of this step showed that the Haldane equation gave the correct fit since the model fitted the experimental data very well with an regression coefficient (R^2) greater than 0.99. The μ_{max}, K_S and K_I for OTC were illustrated in Table 6.62. In the presence of OTC the μ_{max}, varied in the range of 0.005 d^{-1} and 0.0003 d^{-1} for OTC concentrations 50-85 mg/L while the K_S increased from 7 to 60 mg/L throughout anaerobic biodegradation (Table 6.62) at a HRT of 2.25 days.

Table 6.62 shows that the inhibition coefficient (K_I) decreased as the OTC concentration increased from 50 to 85 mg/L in Haldane inhibition kinetic model. For this reason Eqs. (6.4)-(6.5) have to be rejected. The threshold limitations for Haldane inhibition are: $K_S \geq K_I$; $Ks \leq 65$ mg/L for 50-85 mg/L and $\mu \leq \mu_{max} \leq 3\mu$ for OTC anaerobic biodegradation. The K_I values decreased from 23 to 6 mg/L at OTC concentrations of 65 and 85 mg/L in Haldane inhibition kinetic model. From this data, it can be concluded that the OTC inhibition heavily occurs between 65 and 85 mg/L. Because the inhibition effect is inversely proportional to the inhibition constant it will decrease as the OTC concentration increases. The half saturation constant (K_S) values increase from 7 to 45 and to 60 mg/L in the presence of 50, 65 and 85 mg/L OTC, respectively.

Table 6.62 Inhibition kinetic constants calculated for OTC in the AMCBR reactor system at increasing OTC concentrations (50-65-85 mg/L) at a HRT of 2.25 days

OTC (mg/L)	**Type of inhibition**	**Maximum specific growth rate**	**Maximum substrate utilization rate**	**Half saturation constant**	**Inhibition constant**	**R^2**
		μ_{max} (d^{-1})	**R_{max} (g/L d)**	**K_S (mg/L)**	**K_I (mg/L)**	
0	No-inhibition	0.66	38.12	-	-	0.99
50	Competitive	-	5.8	45	12	0.75
50	Non-competitive	-	6.0	10	15	0.81
50	Un-competitive	-	9.6	8	13	0.80
50	**Haldane inhibition**	**0.005**	**-**	**7**	**30**	**0.99**
65	Competitive	-	7.0	47	20	0.60
65	Non-competitive	-	8.6	15	42	0.70
65	Un-competitive	-	11.0	14	38	0.77
65	**Haldane inhibition**	**0.012**	**-**	**45**	**20**	**0.99**
85	Competitive	-	8.7	52	75	0.69
85	Non-competitive	-	10.2	90	108	0.71
85	Un-competitive	-	15.0	78	120	0.53
85	**Haldane inhibition**	**0.0003**	**-**	**60**	**8**	**0.99**

6.6.7.1 Evaluation of the Results of the Inhibition Kinetic Models Used in the AMCBR Reactor to Treat the OTC

The regression coefficient was chosen as the criterion for choosing the most suitable model to represent inhibition kinetic models in an AMCBR reactor together with the values of inhibition kinetic constants. All the regression coefficients and the kinetic constants calculated from the Competitive, Noncompetitive, Uncompetitive and Haldane inhibition kinetic models are summarized in Table 6.62. Higher K_S and lower K_I values, in the Haldane inhibition, can be characterized as a system with low affinity to co-substrate and with more inhibition. Low values of K_I in OTC higher than 65 mg/L indicates high inhibition potential because K_I is in the denominator in the Haldane inhibition equation. Lower K_I in samples containing high concentrations of OTC (65-85 mg/L), represent the degree to which the microorganisms are significantly inhibited by increasing OTC concentrations compared to low concentrations of the OTC. From the above results the K_I values indicated that the

inhibition effects are observed only at higher OTC concentrations. The bacterial growth increased with increasing OTC concentration to its maximum and then decreased with further increase in OTC concentration. Very little kinetic data for OTC inhibition is reported in the specialized literature and a direct comparison is difficult and not completely reliable due to the fact that different inhibition kinetic models were employed for data correlation. Recent studies have not investigated the inhibition kinetic model of the OTC under anaerobic conditions. Arikan et al. (2009) found 27% inhibition in methane production in the presence of 100 mg/L OTC under anaerobic conditions. It is evident that the inhibition kinetic represented by the Haldane inhibition kinetic model is more suitable for OTC inhibition than the other inhibition kinetic models reported in the recent literature by Maurer et al., (2007) (competitive inhibition). 100 mg/L OTC reduced the methane production by 62% and increased the K_S value from 34 to 89 mg/L following a Haldane inhibition kinetic model (Alvarez et al. 2010). In a study performed by Shi et al., (2011) the biodegradation performance of 80 mg/L OTC decreased the COD yields from 79 to 30% and increased the Ks value from 297 to 847 mg/L following the Haldane inhibition kinetic model. The differences in Haldane inhibition kinetic models and kinetic constants could be attributed to the OTC concentrations, to the additional carbon sources, to the microorganism, metabolic pathways of microorganism, metabolites and to the operational conditions such as temperature, HRT and SRT.

Substantial inhibitory effects on K_S and K_I values were observed, as evidenced by a decrease in K_I values for OTC higher than 65 mg/L in Haldane inhibition kinetic model. As the OTC concentration increased to 85 mg/L the K_S value increased to 60 mg/L. The Haldane inhibition kinetic model could be used to calculate the inhibitory concentrations of the antibiotics in the AMCBR system, which could then be used to advice on the design of the anaerobic treatment of drug wastewaters containing antibiotics.

6.7 Cost Analysis for Sequential Reactor System

6.7.1 Cost Estimation for Sequential Reactor Anaerobic/Aerobic System

Cost estimation was done for the present sequential anaerobic/aerobic reactor system throughout treatment of the real pharmaceutical wastewater. The overall costs are represented by the sum of capital costs, chemicals costs, analysis costs, labor costs, costs for the apparatus (heater, air pump, peristaltic pump) and electricity costs. For the lab-scale sequential anaerobic/aerobic reactor system these costs strongly depend on the nature and the concentrations of the pollutants, on the flow rate of the influent and on the configuration of the sequential anaerobic/aerobic reactor system. An estimation cost has been made in this section regarding the operation costs for the sequential anaerobic/aerobic reactor system used for the biodegradation of OTC and AMX for 365 days of continuous operation period.

6.7.1.1 Chemical Costs

As shown in Table 6.63, the chemical costs include the $NaHCO_3$ expenses (0.20 €/year) ($NaHCO_3$ alkalinity is necessary to methanogens for a pH value around 7.7); the Sodium thioglycolate expenses (0.25 €/year) (to maintain the anaerobic conditions) and the Vanderbilt mineral medium expenses (0.15 €/year) (trace and mineral elements for growth of methanogens). The total chemical cost for the anaerobic treatment of the real pharmaceutical wastewater in sequential anaerobic/aerobic reactor system was calculated as 0.60 €/year.

Table 6.63 Chemical costs for the real pharmaceutical wastewater treatment in the sequential anaerobic/aerobic reactor system

Chemicals consumption	**Quantity (kg/year)**	**Unit Price (**€/kg**)**	**Cost (**€/year**)**
$NaHCO_3$	0.04	5	0.20
Sodium thioglycolate	0.02	12	0.25
Vanderbilt mineral medium	0.01	15	0.15
TOTAL COST	**Sequential system**		**0.60**

6.7.1.2 Analysis Costs

The analysis costs for the anaerobic treatment of the real pharmaceutical wastewater in sequential anaerobic/aerobic reactor system are shown in Table 6.64. The total analysis costs was calculated as 1000 €/year for OTC and AMX analysis in the laboratory in the sequential anaerobic/aerobic system.

Table 6.64 Analysis costs for the real pharmaceutical wastewater treatment in sequential anaerobic/aerobic system

Analysis consumption	**Sample frequency (sample/week)**	**Sample frequency (sample/year)**	**Unit Price (€/sample)**	**Cost (**€/year**)**
OTC	1	50	10	500
AMX	1	50	10	500
TOTAL COST	**Sequential anaerobic/aerobic system**			**1000**

6.7.1.3 Labor Costs

The labor costs for the treatment of real raw pharmaceutical wastewater in sequential anaerobic/aerobic reactor system are shown in Table 6.65. The total labor cost was calculated as 650 €/year for one person.

Table 6.65 Labor costs for the real raw pharmaceutical wastewater treatment in the sequential anaerobic/aerobic system

Labor consumption	**Labor hours (hours/week)**	**Labor hours (hours/year)**	**Labor cost (€/hours)**	**Cost (€/year)**
1 person	2.5	130	5	650
TOTAL COST	**Sequential anaerobic/aerobic system**			**650**

6.7.1.4 Capital Costs

The capital costs including the costs of anaerobic and aerobic reactors, feed tanks and the apparatus (air, peristaltic pumps and heater) used in this study is shown in Table 6.66.

Table 6.66 Capital costs including the costs of anaerobic and aerobic reactors, feed tanks and the apparatus for treat the real pharmaceutical wastewater in sequential anaerobic/aerobic system

Type of apparatus	**Capacity (L)**	**Quantity**	**Material**	**Cost (€)**
Anaerobic reactor	4.5	1	Stainless steel	500
Aerobic reactor	9	1	Stainless steel	100
Feed tank	20	1	Polystyrene	5
Air pump	-	1	-	40
Peristaltic Pump	-	1	-	40
Heater	-	1	-	20
TOTAL COST	**Sequential anaerobic/aerobic system**			**705**

6.7.1.5 Electricity Expenses in the Sequential Anaerobic/Aerobic System

The engine electricity consumed from the apparatus is as follows: the peristaltic pump consumes 22 Wh of electric energy per hour. Since the peristaltic pump was operated 15 minute in an hour the total electric energy used in this apparatus is approximately 5.5 Wh/15 min. The air pump in the aeration tank of the aerobic reactor system consumes 40 Wh of electric energy per hour. The heater in the sequential anaerobic/aerobic reactor system consumes 10 Wh of electric energy per hour. The electric energy consumed by the total sequential anaerobic/aerobic reactor is equal to 8.03 kWh per year (see Table 6.67) while the total electricity cost was 0.78 €/year.

Table 6.67 Electricity consumption costs for the apparatus used in the sequential anaerobic/aerobic reactor system the treat the real raw pharmaceutical wastewater treatment

electricity consumption	**Unit**	**Sequential Anaerobic/Aerobic System**
Air pump	kWh	0.01 (only aerobic CSTR reactor)
Peristaltic pump		0.002
Heater		0.01
Total electricity consumption		0.01+0.002+0.01=**0.022**
Total electricity consumption	kWh/year	8.03
Specific electricity costs	€/kWh	0.098
Total electricity costs	€/year	0.78

6.7.1.5.1 Electric Energy Obtained from the CH_4 Gas and Electricity Equivalent of CH_4 Gas. The CH_4 produced from the anaerobic reactor treating OTC and AMX concentrations of 65 mg/L at a HRT of 2.25 days are equal to 0.003 m^3/d, respectively. The electric energy produced from 1 m^3 CH_4 is equal to 2.90 kWh (Ozdemir et al., 2006). Therefore, the electric energy productions from the methane are equal to 0.0087 kWh/d, respectively in the anaerobic reactor throughout biodegradation of OTC and AMX antibiotics, respectively. The 1 kWh electric energy cost was 0.098 €. The electric energy equivalents of CH_4 are shown in Table 6.68. The total biogas cost was calculated by multiplying the electricity production (kWh/year) with specific energy cost (€/kWh).

Table 6.68 The electric energy equivalents of CH_4 in the anaerobic reactor system

Biogas utilization		
$P_{electrical}$	kWh/d	0.0087
$P_{electrical}$	kWh/year	3.18
Specific energy costs	€/kWh	0.098
Biogas costs total (Energy recovery)	€/ year	0.31

$P_{electrical}$: Electricity energy equivalent of methane gas

If the energy obtained from methane in the anaerobic reactor in the sequential anaerobic/aerobic reactor system is compared to the consumed electric energy the electricity obtained from the methane is the half (3.18 kWh/year) of the energy consumed as electric energy (8.03 kWh/year) (see Table 6.67 and 6.68). The total

operational cost consists of the chemical, of the electricity expenses, of the antibiotics analysis (AMX and OTC) and of the labor costs in the sequential anaerobic/aerobic reactor system (Table 6.69). The total operational cost was 1651.4 €/year for treating the real pharmaceutical wastewaters containing OTC and AMX with removal efficiencies higher than 95% in the AMCBR reactor.

Table 6.69 Total operational costs (electricity consumption, chemicals, OTC-AMX analysis and labor cost) for the sequential anaerobic/aerobic system

Type of costs	**Informations for Consumption**	**Cost (**€/year**)**
Electricity	Electricity consumption for apparatus and heating of the anaerobic reactor	0.78
Chemicals	$NaHCO_3$, Sodium thioglycolate, Vanderbilt	0.60
OTC-AMX analysis	Analysis consumption for OTC and AMX	1000
Labor	The labor consumption for 1 person	650
TOTAL COST	**sequential anaerobic/aerobic system**	**1651.4**

As a conclusion, it can be said that the total cost of the sequential anaerobic/aerobic reactor consisting of the capital cost including the apparatus (705 €), chemical costs (0.60 €/year), analysis costs (1000 €/year), labor costs (650 €/year) and the electricity costs (0.78 €/year) was 2356.4 €/year. The electric energy obtained from the methane in the anaerobic reactor was calculated as 0.31 €/year while the electric energy consumption was 0.78 €/year. Therefore, it can be concluded that 39% of the total electric energy expenses could be received from the CH_4 production.

$$UnitTreatmentCost = \frac{Oper.Costs\ (Chemicals + Electricit\,yConsump.)\ (\in / year)}{Flow\ Rate\ (m^3\ / year)}$$

Unit treatment cost for 1 m^3 real raw pharmaceutical wastewater was calculated [(1.38(€/year)/0.73 (m^3/year)] 1.89 €/m^3 wastewater at optimum operation conditions in the sequential anaerobic/aerobic reactor for treating the real raw pharmaceutical wastewater.

CHAPTER SEVEN
CONCLUSIONS

This Ph.D thesis was performed to investigate the treatability of the antibiotics namely OTC, AMX, TYL and ERY from synthetic and real pharmaceutical wastewaters in a sequential reactor system consisting of anaerobic AMCBR/aerobic CSTR and sequential anaerobic ABFR/aerobic CSTR. The results from these reactors are summarized below:

7.1 Batch Studies for OTC, AMX, TYL and ERY Antibiotics under Anaerobic Conditions

The toxic effect of OTC, AMX, TYL and ERY on methane *Archaea* was investigated using ATA test under batch conditions in the beginning of the study in order to determine the IC_{50} values of the OTC, AMX, TYL and ERY. The IC_{50} values of OTC, AMX, TYL and ERY were calculated as 224.18, 216.78, 192.00 mg/L and 152.00 mg/L, respectively in the batch reactors. According to the ATA test among the antibiotics used in this study it was found that the most toxic antibiotic was OTC while AMX, TYL and ERY were the less toxic antibiotics to the methanogenic bacteria.

The SMA values of OTC, AMX, TYL and ERY were investigated under anaerobic batch conditions. The maximum SMA values for OTC, AMX, TYL and ERY were calculated as 1.13, 1.05, 0.87 and 1.20 g CH_4-COD/gVSS.d respectively.

The main removal mechanisms of OTC, AMX, TYL and ERY were biodegradation. Around 99% biodegradations were obtained for OTC, AMX, TYL and ERY antibiotics under batch anaerobic conditions. The contributions of volatilization and adsorption to the removals of OTC, AMX, TYL and ERY were found to be not significant.

7.2 Continuous Studies for OTC, AMX, TYL and ERY in the Sequential AMCBR/CSTR for Synthetic Wastewater

7.2.1 The Removal of OTC in the AMCBR, CSTR and Sequential AMCBR/CSTR System in Synthetic Wastewater

7.2.1.1 AMCBR Reactor

Among the OTC loadings (22.22-44.44-66.67-88.89-111.11-133.33-155.56-177.78 g/m^{3}d) applied to the AMCBR reactor it was found that the maximum OTC and COD yields was obtained at a OTC loading of 133.33 g/m^{3}d at a HRT of 5.5 days. The maximum COD and OTC removal efficiencies were 95% and 99% at a OTC loading rate of 133.33 g/m^{3}d (OTC concentration=300 mg/L) and a HRT of 5.5 days, respectively in the AMCBR reactor. The majority of COD was removed in the 1st compartment of the AMCBR reactor while low COD removal efficiencies occurred in the subsequent compartments. 81% of COD was removed of 1st compartment while the COD yields were 49% in subsequent 2nd and 3rd compartments for the aforementioned operational conditions. 300 mg/L OTC was transformed to 2 mg/L α-Apo-OTC and 4 mg/L ß-Apo-OTC with an OTC removal efficiency of 96% in the AMCBR reactor at an OTC loading rate of 133.33 g/m^{3}d.

The COD_{inert} concentrations in the effluent of the AMCBR reactor decreased by 44% and 57% compared to the influent, for OTC loading rates between 88.89 and 133.33 g/m^{3}d (OTC concentration 200 and 300 mg/L). This showed that the COD_{inert} is taken up by the cells of anaerobic granule bacteria together with biodegradable COD and OTC throughout anaerobic treatment in the AMCBR at a HRT of 2.5 days. The COD_{imp} increased at high OTC loadings (>133.33 g/m^{3}d) due to the toxicity of high OTC concentrations since the death of the biomass produced more inert metabolites and extracellular organics. The COD_{imp} converted into stored material in bacterial cells when the substrate is metabolized effectively.

The maximum total, methane gas productions and methane percentage were found as 14 L/d, 9.36 L/d and 65%, respectively at an OTC loading rate of 133.33 g/m^3d (OTC concentration=300 mg/L) at a HRT of 5.5 days, respectively. The TVFA, HCO_3 alkalinity concentrations and TVFA/HCO_3 Alk. ratios were between the limit values given for anaerobic AMCBR reactor although it was studied at high OTC concentrations. Acetic acid (485 mg/L) was the main TVFAs in the AMCBR reactor following the propionic acid (280 mg/L), butryric acid (100 mg/L) and lactic acid (0 mg/L) at an OTC loading rate of 133.33 g/m^3d (OTC concentration= 300 mg/L) in the first compartment of the AMCBR reactor. Thus, contributes reaching to high methane productions via methanogenesis from acedogenesis.

7.2.1.2 CSTR Reactor

The contribution of aerobic CSTR reactor to the OTC biodegradation in the sequential anaerobic AMCBR/aerobic CSTR system is to remove the COD, OTC and OTC metabolites remaining from the anaerobic AMCBR reactor. From the initial 4088 mg/L COD, 3883 mg/L COD was removed in the anaerobic AMCBR reactor, the remaining 205 mg/L COD was biodegraded in the aerobic CSTR reactor. From the initial 300 mg/L OTC concentration, 297 mg/L OTC was removed in the anaerobic AMCBR reactor, the remaining 3 mg/L OTC was biodegraded in the aerobic CSTR reactor with an OTC concentration of 0.30 mg/L in the effluent of the aerobic CSTR reactor. The maximum COD and OTC removal efficiencies were 91% and 90% at an OTC loading rate of 133.33 g/m^3d (OTC concentration= 300 mg/L) at a HRT of 10.97 days, respectively in the CSTR reactor. From 2 mg/L of α-Apo-OTC and from 4 mg/L of ß-Apo-OTC remaining from the anaerobic AMCBR reactor were biodegraded with high removal efficiencies (99.9%) in the CSTR reactor. 1.98 mg/L α-Apo-OTC and 3.99 mg/L ß-Apo-OTC were removed in the aerobic CSTR reactor resulting in 0.02 and 0.01 mg/L α-Apo-OTC and ß-Apo-OTC concentrations in the effluent of the aerobic CSTR reactor.

7.2.1.3 Sequential Reactor

The maximum COD and OTC removal efficiencies were 99% and 100% at a loading rate of 133.33 g/m^3d and a total HRT of 16.47 days, respectively in the sequential anaerobic AMCBR/aerobic CSTR reactor system.

7.2.2 The Removal of AMX in the AMCBR, CSTR and Sequential AMCBR/CSTR System in Synthetic Wastewater

7.2.2.1 AMCBR Reactor

Among the AMX loadings (22.22, 44.44, 66.67, 88.89, 111.11 and 133.33 g/m^3d) applied to the AMCBR reactor it was found that the maximum AMX and COD yields was obtained at an AMX loading of 66.67 g/m^3d at a HRT of 5.5 days. The maximum COD and AMX removal efficiencies were 94% and 93% at an AMX loading rate of 66.67 g/m^3d (AMX concentration=150 mg/L) at a HRT of 5.5 days, respectively, in the AMCBR reactor.

The maximum total, methane gas productions and methane content were found as 12 L/d and 6.5 L/d and 55%, at an AMX loading rate of 66.67 g/m^3d (AMX concentration=150 mg/L) at a HRT of 5.5 days respectively, in the AMCBR reactor. The methane yield of the AMCBR reactor treating the AMX was 0.34 $m^3CH_4/kgCOD_{removed}$. The TVFA, HCO_3 concentrations and TVFA/HCO_3 Alk. ratios in the effluent and in the compartments of AMCBR reactor were between the limit values although it was studied at high AMX concentrations.

7.2.2.2 CSTR Reactor

The aerobic CSTR reactor was used to biodegraded the remaining COD and AMX from AMCBR reactor in the sequential anaerobic AMCBR/aerobic CSTR system. From the initial 4050 mg/L COD, 3765 mg/L COD was removed in the AMCBR reactor, the remaining 285 mg/L COD was biodegraded in the aerobic CSTR reactor.

From the initial 150 mg/L AMX concentration, 140 mg/L AMX was removed in the AMCBR reactor, the remaining 10 mg/L AMX was biodegraded in the aerobic CSTR reactor with an OTC concentration of 1 mg/L in the effluent of the aerobic CSTR reactor. The maximum COD and AMX removal efficiencies were 88% and 90% at an AMX loading rate of 66.67 g/m^3d (AMX concentration=150 mg/L) at a HRT of 10.97 days, respectively in the CSTR reactor.

7.2.2.3 Sequential Reactor

The maximum COD and AMX removal efficiencies were 98% and 100% at an AMX loading rate of 66.67 g/m^3d (AMX concentration=150 mg/L) at a total HRT of 16.47 days, respectively in the sequential anaerobic AMCBR/aerobic CSTR reactor system.

7.2.3 The Removal of TYL in the AMCBR, CSTR and Sequential AMCBR/CSTR System in Synthetic Wastewater

7.2.3.1 AMCBR Reactor

Among the TYL loading rates (22.22, 44.44, 66.67, 88.89, 111.11 and 133.33 g/m^3d) applied to the AMCBR reactor it was found that the maximum COD and TYL yields were obtained at a TYL loading rate of 22.22 g/m^3d. The maximum COD and TYL yields were 96% and 94% in the synthetic pharmaceutical wastewater at 22.22 g/m^3d TYL loading rate (TYL concentration=50 mg/L) at a HRT of 5.5 days respectively in the anaerobic AMCBR reactor.

The maximum total gas, methane gas productions and methane percentage were found as 15 L/d and 9.4 L/d and 60%, respectively, at a TYL loading rate of 22.22 g/m^3d (TYL concentration=50 mg/L) at a HRT of 5.5 days in the anaerobic AMCBR reactor. The methane yield of the AMCBR reactor treating the TYL was 0.37 $m^3CH_4/kgCOD_{removed}$. The TVFA, HCO_3 alkalinity concentrations, TVFA/HCO_3 Alk. ratios were between the limit values given for anaerobic AMCBR reactor

although it was studied at high TYL concentrations. The H_{pr}/H_{ac} ratio was lower than 1.4 indicating the state-steady H_{ac} concentrations (lower than 800 mg/L) and the successful methane production in the AMCBR reactor. The predominant TVFA were H_{ac}, H_{pr}, H_{ba} and H_{la} with percentages of 47.36%, 30.00%, 12.35% and 5.80%, respectively, at a TYL loading rate of 22.22 g/m^3d in the AMCBR reactor.

7.2.3.2. CSTR Reactor

From the initial 3925 mg/L COD, 3768 mg/L COD was removed in the AMCBR reactor, the remaining 157 mg/L COD was biodegraded in the aerobic CSTR reactor. From the initial 50 mg/L TYL concentration, 47 mg/L TYL was removed in the AMCBR reactor, the remaining 3 mg/L TYL was biodegraded in the aerobic CSTR reactor with a TYL concentration of 1 mg/L in the effluent of the aerobic CSTR reactor. The maximum COD and TYL removal efficiencies were 86% and 67% at a TYL loading rate of 22.22 g/m^3d (TYL concentration=50 mg/L) and a HRT of 10.97 days, respectively in the CSTR reactor.

7.2.3.3 Sequential Reactor

The maximum COD and the TYL removal efficiency in the sequential AMCBR/CSTR reactor system were measured as 99% and 98% at a TYL loading rates of 22.22 g/m^3d (TYL concentration=50 mg/L) at a total HRT of 16.47 days, respectively.

7.2.4 The Removal of ERY in the AMCBR, CSTR and Sequential AMCBR/CSTR System in Synthetic Wastewater

7.2.4.1 AMCBR Reactor

Among the ERY loading rates (22.22, 44.44, 66.67, 88.89, 111.11 and 133.33 g/m^3d) applied to the AMCBR reactor it was found that the maximum COD and ERY yields were obtained at an ERY loading rate of 44.44 g/m^3d. The maximum

COD and TYL yields were 95% and 95% in the synthetic pharmaceutical wastewater at 44.44 g/m^{3}d ERY loading rate (ERY concentration=100 mg/L) at a HRT of 5.5 days, respectively, in the anaerobic AMCBR reactor. The COD was mainly removed in the 1st compartment with a yield of 86%, at an ERY loading rate of 44.44 g/m^{3}d.

The maximum total, methane gas productions and methane percentage were found as 12 L/d, 7.5 L/d and 62%, respectively at an ERY loading rate of 44.44 g/m^{3}d (ERY concentration=100 mg/L) at a HRT of 5.5 days in the AMCBR reactor. The methane yield of the AMCBR reactor treating the ERY was 0.36 $m^3CH_4/kgCOD_{removed}$. The TVFA, HCO_3 alkalinity concentrations, TVFA/HCO_3 Alk., and H_{pr}/H_{ac} ratios were between the limit values given for anaerobic AMCBR reactor although it was studied at high ERY concentration. Four major TVFAs, namely H_{ac}, H_{pr}, H_{ba} and H_{la} were produced throughout the operation of the 1st and 2nd compartments of the AMCBR. The other TVFAs were not detected at significant concentrations.

7.2.4.2 CSTR Reactor

From the initial 4040 mg/L COD, 3838 mg/L COD was removed in the AMCBR, the remaining 202 mg/L COD was biodegraded in the CSTR. From the initial 100 mg/L ERY concentration, 95 mg/L ERY was removed in the AMCBR, the remaining 5 mg/L ERY was biodegraded in the CSTR with an ERY concentration of 1 mg/L in the effluent of the CSTR. The maximum COD and ERY removal efficiencies were 90% and 80% at an ERY loading rate of 44.44 g/m^{3}d (ERY concentration=100 mg/L) at a HRT of 10.97 days, respectively in the CSTR.

7.2.4.3 Sequential Reactor

The maximum COD and the ERY removal efficiencies in the sequential AMCBR/CSTR system were measured as 95% and 97%, respectively, at an ERY loading rate of 44.44 g/m^{3}d at a total HRT of 16.47 days.

7.3 Continuous Studies for OTC, AMX, TYL and ERY in the Sequential ABFR/CSTR Systems for Synthetic Wastewater

7.3.1 The Removal of OTC in the ABFR, CSTR and Sequential ABFR/CSTR System in Synthetic Wastewater

7.3.1.1 ABFR Reactor

The optimum OTC loading rate was found as 8.33 g/m^3d for maximum COD (94%) and OTC (90%) yields in the ABFR reactor. The COD removal efficiencies were higher (78%) in the 1^{st} sampling point of the lower part of the ABFR reactor than the others sampling points (2^{nd}, 3^{rd}) of the lower part (28%, 21%) of the ABFR reactor at an OTC loading rate of 8.33 g/m^3d.

The maximum total gas, methane gas productions and methane content were recorded as 12.30 L/d and 9.12 L/d and 65%, respectively at an OTC loading rate of 8.33 g/m^3d (OTC concentration=50 mg/L), respectively in the ABFR reactor. The methane yield effluent of the AMCBR reactor treating the OTC was 0.31 $m^3CH_4/kgCOD_{removed}$. The TVFA, HCO_3 alkalinity concentrations, TVFA/HCO_3 Alk., and H_{pr}/H_{ac} ratios were between the limit values given for anaerobic reactor although it was studied at high OTC concentrations. The H_{pr}/H_{ac} ratio was lower than 1.4 indicating the state-steady H_{ac} concentrations (lower than 800 mg/L) and the successful methane production in the ABFR reactor. The predominant TVFAs were H_{ac} (530 mg/L), H_{pr}, (320 mg/L), H_{ba} (110 mg/L), and H_{la} (102 mg/L), respectively, at an OTC loading rate of 8.33 g/m^3d in the 1^{st} sampling point of the ABFR reactor.

7.3.1.2 CSTR Reactor

From the initial 3925 mg/L COD, 3690 mg/L COD was removed in the AMCBR reactor, the remaining 236 mg/L COD was biodegraded in the aerobic CSTR reactor. From the initial 50 mg/L OTC concentration, 45 mg/L OTC was removed in the AMCBR reactor, the remaining 5 mg/L OTC was biodegraded in the aerobic CSTR

reactor with an OTC concentration of 0.5 mg/L in the effluent of the aerobic CSTR reactor. The maximum COD and OTC removal efficiencies were 90% and 90% at an OTC loading rate of 8.334 g/m^3d (OTC concentration=50 mg/L) at a HRT of 4.5 days, respectively in the CSTR reactor.

7.3.1.3 Sequential Reactor

The maximum COD and OTC yields were 99% and 99% at an OTC loading rate of 8.33 g/m^3d (OTC concentration=50 mg/L) at a total HRT of 10.5 days in the sequential anaerobic ABFR/aerobic CSTR reactor system.

7.3.2 The Removal of AMX in the ABFR, CSTR and Sequential ABFR/CSTR System

7.3.2.1 ABFR Reactor

Among the AMX loading rates (8.33, 16.67, 25.00, 33.33 g/m^3d) applied to the AMCBR reactor it was found that the maximum COD and AMX yields were obtained at an AMX loading rate of 16.67 g/m^3d. The maximum COD and AMX yields were 85% and 85% in the synthetic pharmaceutical wastewater at 16.67 g/m^3d AMX loading rates (AMX concentration=100 mg/L) at a HRT of 6.0 days, respectively, in the anaerobic AMCBR reactor. The COD was mainly removed in the 1^{st} sampling point with a yield of 74%, at an AMX loading rate of 16.67 g/m^3d. The effluent COD removal profile across the ABFR reactor followed the sampling point 1^{st} > sampling point 2^{nd} > sampling point 3^{rd} > sampling point 4^{th} > sampling point 5^{th}. 100 mg/L AMX was transformed to 7 mg/L AMX-diketopiperazine-2,5 with an AMX removal efficiency of 95% in the AMCBR reactor at an AMX loading rate of 16.67 g/m^3d.

The maximum total, methane gas productions and methane content were found about 11.42 L/d, 8.12 L/d and 58%, respectively at an AMX loadings of 16.67g/m^3d (AMX concentration=100 mg/L) at a HRT of 6.0 days, respectively. The methane

yield effluent of the ABFR treating the AMX was 0.32 $m^3CH_4/kgCOD_{removed}$. The HCO_3 and TVFA concentrations and TVFA/ HCO_3 ratio were between the limit values know for ABFR although it was studied at high OTC concentrations.

7.3.2.2 CSTR Reactor

The CSTR was used to biodegraded the remaining COD and AMX from ABFR in the sequential ABFR/CSTR system. From the initial 4025 mg/L COD, 3421 mg/L COD was removed in the ABFR, the remaining 604 mg/L COD was biodegraded in the CSTR. From the initial 100 mg/L AMX concentration, 43 mg/L AMX was removed in the ABFR, the remaining 7.5 mg/L AMX was biodegraded in the CSTR with an OTC concentration of 1.5 mg/L in the effluent of the CSTR. The maximum COD and AMX removal efficiencies were 86% and 80% at an AMX loading rate of 16.67 g/m^3d (AMX concentration=100 mg/L) at a HRT of 4.5 days, respectively in the CSTR.

7.3.2.3 Sequential Reactor

The maximum COD and AMX yields were 98% and 97% at an AMX loading rate of 16.67 g/m^3d (AMX concentration=100 mg/L) at a total HRT of 10.5 days in the sequential ABFR/CSTR reactor system.

7.3.3 The Removal of TYL in the ABFR, CSTR and Sequential ABFR/CSTR System

7.3.3.1 ABFR Reactor

Among the TYL loading rates (8.33, 16.67, 25.00, 33.33 g/m^3d) applied to the ABFR it was found that the maximum COD and TYL yields were obtained at a TYL loading rate of 16.67 g/m^3d. The maximum COD and TYL yields were 93% and 92% in the synthetic pharmaceutical wastewater at 16.67 g/m^3d TYL loading rate (TYL concentration=100 mg/L) at a HRT of 6.0 days respectively in the ABFR.

The maximum total gas, methane gas productions and methane percentage were found as 4.50 L/d and 2.50 L/d and 60%, respectively, at a TYL loading rate of 16.67 g/m^3d (TYL concentration=100 mg/L) at a HRT of 6.0 days in the anaerobic ABFR reactor. The methane yield of the AMCBR reactor treating the TYL was 0.33 $m^3CH_4/kgCOD_{removed}$. The TVFA, HCO_3 alkalinity concentrations, TVFA/HCO_3 Alk. ratios were between the limit values given for AMCBR reactor although it was studied at high TYL concentrations.

7.3.3.2 CSTR Reactor

From the initial 4140 mg/L COD, 3850 mg/L COD was removed in the ABFR reactor, the remaining 290 mg/L COD was biodegraded in the CSTR reactor. From the initial 100 mg/L TYL concentration, 92 mg/L TYL was removed in the ABFR reactor, the remaining 8 mg/L TYL was biodegraded in the CSTR reactor with a TYL concentration of 1.92 mg/L in the effluent of the CSTR reactor. The maximum COD and AMX removal efficiencies were 85% and 76% at a TYL loading rate of 16.67 g/m^3d (TYL concentration=100 mg/L) at a HRT of 4.5 days, respectively in the CSTR reactor.

7.3.3.3 Sequential Reactor

The maximum COD and TYL yields were 99% and 98% at a TYL loading rate of 16.67 g/m^3d (TYL concentration=100 mg/L) at a total HRT of 10.5 days in the sequential ABFR/CSTR reactor system.

7.3.4 The Removal of ERY in the ABFR, CSTR and Sequential ABFR/CSTR System

7.3.4.1 ABFR Reactor

Among the ERY loading rates (8.33, 16.67, 25.00, 33.33 g/m^3d) applied to the ABFR reactor it was found that the maximum COD and ERY yields were obtained at

an ERY loading rate of 16.67 g/m^3d. The maximum COD and ERY yields were 92% and 90% in the synthetic pharmaceutical wastewater at 16.67 g/m^3d ERY loading rate (ERY concentration=100 mg/L) at a HRT of 6.0 days respectively in the anaerobic ABFR reactor.

The maximum total gas, methane gas productions and methane percentage were found as 3.64 L/d and 2.00 L/d and 55%, respectively, at an ERY loading rate of 16.67 g/m^3d (ERY concentration=100 mg/L) at a HRT of 6.0 days in the anaerobic ABFR reactor. The methane yield of the AMCBR reactor treating the ERY was 0.27 $m^3CH_4/kgCOD_{removed}$. The TVFA, HCO_3 alkalinity concentrations, TVFA/HCO_3 Alk. ratios were between the limit values given for anaerobic AMCBR reactor although it was studied at high ERY concentrations.

The VSS analysis showed that the anaerobic ABFR performance was directly related with the VSS accumulated surrounding of the polystyrene balls as carrier material. The contribution of VSS in the mixed liquor of the ABFR to the antibiotics and to the COD yields was found to be minor. The properties of the carriers used in the ABFR contributed significantly to the treatment of OTC, AMX, TYL and ERY from the pharmaceutical wastewater with an optimum biomass thickness around polystrene balls.

7.3.4.2 CSTR Reactor

From the initial 4140 mg/L COD, 3809 mg/L COD was removed in the ABFR reactor, the remaining 331 mg/L COD was biodegraded in the aerobic CSTR reactor. From the initial 100 mg/L ERY concentration, 90 mg/L ERY was removed in the ABFR reactor, the remaining 10 mg/L ERY was biodegraded in the aerobic CSTR reactor with an ERY concentration of 3 mg/L in the effluent of the aerobic CSTR reactor. The maximum COD and AMX removal efficiencies were 83% and 70% at an ERY loading rate of 16.67 g/m^3d (ERY concentration=100 mg/L) at a HRT of 4.5 days, respectively in the CSTR reactor.

7.3.4.3 Sequential Reactor

The maximum COD and ERY yields were 99% and 97% at an ERY loading rate of 16.67 g/m^{3}d (ERY concentration=100 mg/L) at a total HRT of 10.5 days in the sequential anaerobic ABFR/aerobic CSTR reactor system.

7.4 Evaluation of the Sequential Reactors

Although the OTC antibiotic was found to be more toxic than the other three antibiotics it was removed with high yields. It was found that the COD in the effluent of the sequential AMCBR/CSTR reactor (18.45 mg/L) was low compared to the COD (23.60 mg/L) in the effluent of the sequential ABFR/CSTR reactor system. Although the OTC loading in the AMCBR reactor was as high as 133.33 g/m^{3}d, the OTC loading in the ABFR reactor was only 8.33 g/m^{3}d indicating the AMCBR reactor was operated with an OLR of 16 times higher than that the OLR in the ABFR reactor. This showed that the AMCBR reactor is more resistant to the OTC than that ABFR. Although both AMCBR and ABFR reactors are high-rate anaerobic reactors the separation of acedogenesis and methanogenesis exhibit strong protection against to toxicity of OTC in the AMCBR reactor. Furthermore, lower HRTs in the AMCBR reactor provide high resistance to the organic shocks with special gas and sludge separations. The AMX, TYL and ERY antibiotic concentrations in the effluent of the sequential AMCBR/CSTR reactor were 34.2 mg/L, 22 mg/L and 20.2 mg/L at AMX, TYL and ERY loading rates of 66.67, 22.22, 44.44 g/m^{3}d, respectively. The AMX, TYL and ERY antibiotic concentrations in the effluent of the sequential ABFR/CSTR reactor system were 85 mg/L, 43.5 mg/L and 56.3 mg/L at AMX, TYL and ERY loading rates of 16.67 g/m^{3}d, respectively. This results showed that the AMCBR reactor is more stable that that ABFR reactor in the biodegradation of AMX, TYL and ERY antibiotics.

In the treatment of real raw pharmaceutical wastewater the biodegradation of OTC and AMX antibiotics were only performed in the anaerobic AMCBR and ABFR reactors. It was found that the AMCBR reactor exhibited high performance

than that ABFR reactor although it was studied at high OTC and AMX loadings (14.44 g/m^3d) compared to the ABFR reactor (5.42 g/m^3d). The COD, AMX and OTC yields in the AMCBR reactor were 86%, 88% and 88% resulting in effluent COD, AMX and OTC concentrations of 2065 mg/L, 7.80 mg/L and 7.80 mg/L in the effluent of AMCBR reactor. The yields in the ABFR reactor were low (COD=82%, AMX=85%, OTC=85%) with effluent concentration of 2753 mg/L, 9.50 mg/L and 9.50 mg/L in the effluent of ABFR reactor. The biodegradable data obtained from the real raw pharmaceutical wastewater are higher than that obtained in the synthetic wastewater for both anaerobic reactors. It is important note that the COD value of synthetic antibiotic wastewater was around 4000 mg/L while the COD of the real raw pharmaceutical wastewater was recorded as 15135 mg/L. This showed that the main carbon source (COD) used by the anaerobic bacteria to generate energy in the real raw pharmaceutical wastewater was extremely high and affect negatively the COD yields. The AMX and OTC antibiotics used as co-substrate in the real raw pharmaceutical wastewater are low and it was not think that they are inhibitory.

7.5 Acute Toxicity Evaluation in the Sequential AMCBR/CSTR Reactor System in Synthetic Wastewater

7.5.1 Acute Toxicity Evaluation of Increasing OTC, AMX, TYL and ERY Concentrations in the Effluent of the Sequential AMCBR/CSTR Reactor System with Daphnia magna

The maximum acute toxicity removals were 60% , 46%, 50%, 50% for OTC, AMX, TYL and ERY concentrations of 100 mg/L, 150 mg/L, 50 mg/L and 50 mg/L, respectively in the AMCBR reactor. After aerobic treatment in the CSTR reactor the acute toxicity yields were recorded as 70%, 76%, 75% and 75% for the aforementioned antibiotics in the CSTR reactor. The maximum total acute toxicity removals were 88%, 87% ,88% and 88% for 100 mg/L OTC, 150 mg/L AMX, 50 mg/L TYL and 50 mg/L ERY, respectively, in the sequential AMCBR/CSTR reactor system.

7.5.2 Acute Toxicity Evaluation of Increasing OTC, AMX, TYL and ERY Concentrations in the Effluent of the Sequential AMCBR/CSTR Reactor System with Vibrio fischeri

The maximum acute toxicity removals were 60%, 51%, 51%, 51% for OTC, AMX, TYL and ERY concentrations of 50 mg/L, respectively in the AMCBR reactor. After aerobic treatment in the CSTR reactor the acute toxicity yields were recorded as 74%, 75%, 73% and 73% for the aforementioned antibiotics in the CSTR reactor. The maximum total acute toxicity removals were 90%, 88% ,86% and 86% for 50 mg/L OTC, 50 mg/L AMX, 50 mg/L TYL and 50 mg/L ERY, respectively, in the sequential AMCBR/CSTR system. The antibiotic doses used in the acute toxicity test performed by *Daphnia magna* could not be used in the *Vibrio fisheri* test since mortalities were detected at the antibiotic doses used in *Daphnia magna*.

7.5.3 Sensitivity Ranking of Daphnia magna, Vibrio fischeri to OTC, AMX, TYL and ERY in the Effluent of the Sequential AMCBR/CSTR Reactor System

The *Vibrio fischeri* acute toxicity test was found to be more sensitive than the acute toxicity test performed by *Daphnia magna* to the raw and to the treated pharmaceutical wastewaters in the influent and effluent samples at all antibiotics used in this study. In other words, the *Daphnia magna* was found to be resistant compared to *Vibrio fischeri*.

7.6 Continuous Studies for OTC and AMX in the AMCBR Reactor for Real Raw Pharmaceutical Wastewater

7.6.1 The Treatment of Real Raw Pharmaceutical Wastewater Including OTC and AMX in the AMCBR Reactor

Antibiotic analysis result showed that the real raw pharmaceutical wastewater contained 65 mg/L OTC and 65 mg/L AMX. Among the OTC and AMX loadings (14.44, 28.89, 43.33 g/m^3d) applied to the AMCBR reactor it was found that the

maximum OTC-AMX and COD yields was obtained at an OTC and AMX loading of 14.44 g/m^{3}d at a HRT of 4.5 days. The maximum COD and OTC removal efficiencies were 86% and 88% at an OTC and AMX loading rates of 14.44 g/m^{3}d (OTC and AMX concentration 65 mg/L) at a HRT of 4.5 days at an OLR 3.40 gCOD/m^{3}d (COD concentration=15135 mg/L), respectively in the AMCBR reactor.

The maximum total gas, methane gas and methane content were found as 3.08 and 1.6 L/d and 52%, respectively, at an OTC and AMX loading rate of 14.44 g/m^{3}d (OTC and AMX concentrations=65 mg/L) respectively in the ABFR reactor. The TVFA, HCO_3 alkalinity concentrations and TVFA/HCO_3 Alk. ratios were between the limit values given for AMCBR reactor although it was studied at a toxic wastewater with OTC and AMX concentrations of 65 mg/L.

7.6.2 The Treatment of Real Raw Pharmaceutical Wastewater Including OTC and AMX in the ABFR Reactor

Among the OTC and AMX loadings (5.42, 10.83, 16.25 g/m^{3}d) applied to the AMCBR reactor it was found that the maximum OTC-AMX and COD yields was obtained at an OTC and AMX loading of 5.42 g/m^{3}d at a HRT of 12 days. The maximum COD and OTC removal efficiencies were 82% and 85% at OTC and AMX loading rates of 5.42 g/m^{3}d (OTC, AMX concentrations 65 mg/L) at a HRT of 12 days at an OLR 1.30 gCOD/m^{3}d (COD=15135 mg/L), respectively in the ABFR reactor.

The maximum total gas, methane gas productions and methane content were found about 3.42 L/d, 1.71 L/d and 50%, respectively at an OTC and AMX loading rate of 5.42 g/m^{3}d in the ABFR reactor. The OTC, AMX and the COD in real pharmaceutical wastewaters were ultimately biodegraded to H_2O and CO_2 in the methanogenesis phase of the anaerobic treatment in the ABFR reactor with high methane gas yields. The TVFA, HCO_3 alkalinity concentrations and TVFA/HCO_3 Alk. ratios were between the limit values given for anaerobic ABFR reactor although it was studied at a toxic wastewater with OTC and AMX concentrations of 65 mg/L.

7.7 Determination of Kinetic Constant for AMCBR Reactor in Synthetic Wastewater

Among the kinetic models applied to the experimental data obtained from the continuous operation of the anaerobic AMCBR system it was found that the Stover-Kincannon and Grau second-order kinetic models were more appropriate than Monod, Zero, First, Second order and to Contois kinetic models to the describe the anaerobic biodegradation of COD and OTC at six HRTs varying between 0.9 and 5.5 days, in the comparison of the value of kinetic constants and the regression coefficient (R^2). K_B and R_{max} was 19.87 and 19.23 g/L.d, respectively with high regression coefficient (R^2=0.99) for COD in the Stover-Kincannon kinetic model in synthetic wastewater. Similarly, the R_{max} and K_B values for OTC were obtained as 0.42 and 0.41 g/L.d, respectively, with high regression coefficient (R^2=0.99) in the Stover-Kincannon kinetic model. ks, a and b was 0.08 d^{-1}, 0.21 d and 1.04 (dimensionless), respectively with high regression coefficient (R^2=0.99) for COD in the Grau second-order kinetic model. Similarly, the k_s, a and b values for OTC were obtained as 0.002 d^{-1}, 0.24 d and 1.00 (dimensionless), respectively with high regression coefficient (R^2=0.99) in the Grau second-order kinetic model. Therefore, these models could be used in the design of the AMCBR reactor. It is important to note that the COD and OTC were biodegraded according to Monod kinetic when the kinetic constants were evaluated according to pure methane, acidogenic bacteria where the growth of these bacteria, the TVFA and the methane production and the OTC utilization were defined with the equations 5.32, 5.33 5.70 and 5.71 in section "Material methods" (see Chapter 5.8.1.1.5 and 5.8.1.3.3).

The substrate kinetic constants found from the real pharmaceutical wastewater exhibited similarities with the synthetic pharmaceutical wastewater. The antibiotics and COD in real wastewater were biodegraded according to Stover-Kincannon and Grau-Second order kinetic models. Among the biogas kinetic models applied to the AMCBR reactor it was found that the Stover-Kincannon model was more appropriate to determine the total and methane gas productions compared to the Van der Meer-Heertjes kinetic model in synthetic wastewater. The maximum methane gas

production rate (M_{max}) and gas kinetic constant (M_B) were calculated as 598 mL/L.d and 0.63 mg/L.d, respectively. The following equation could be used to estimate the methane gas productions in the AMCBR treating wastewater with 100 mg/L OTC at a HRT of 5.5 days yielding 95% OTC (1/M=0.63/598x1/OLR+1/598).

The biogas kinetic constants found from the real raw pharmaceutical wastewater exhibited similarities with synthetic pharmaceutical wastewater. The total and methane gas in real raw pharmaceutical wastewater were produced according to Stover Kincannon kinetic model. The maximum methane gas production rate (M_{max}) and gas kinetic constant (M_B) were calculated as 1582 mL/L.d and 0.95 mg/L.d, respectively. The following equation could be used to estimate the methane gas productions in the AMCBR reactor treating pharmaceutical wastewater with 65 mg/L OTC at a HRT of 6.0 days yielding 88% OTC, (1/M=0.95/1582x1/OLR+1/1582).

Among the inhibition kinetics used in the AMCBR (competitive, non-competitive, un-competitive and Haldane) it was observed that the biodegradation of OTC in the pharmaceutical wastewaters were inhibited by Haldane inhibition at OTC concentrations >50 mg/L. The results of this step showed that the Haldane equation gave the correct fit since the model fitted the experimental data very well with an r^2 greater than 99%. Because the inhibition effect is inversely proportional to the inhibition constant it will decrease as the toxicant concentration increases. The bacterial growth increased with increasing of OTC concentration to its maximum and then decreased with further increase in OTC concentration. The Haldane inhibition kinetic model could be used to calculate the inhibitory concentrations of the antibiotics in the AMCBR system, which could then be used to advice on the design of the anaerobic treatment of drug wastewaters containing antibiotics.

7.8 Total Annual Costs for the Pharmaceutical Wastewater Treatment According to Sequential Anaerobic/Aerobic Reactor System

The total annual cost of the sequential anaerobic/aerobic reactor consisting of the capital cost including the apparatus (705 €), chemical costs (0.60 €/year), analysis

costs (1000 €/year), labor costs (650 €/year) and the electricity costs (0.78 €/year) was 2356.4 €/year. The electric energy obtained from the methane in the anaerobic reactor was calculated as 0.31 €/year while the electric energy consumption was 0.78 €/year. Therefore, it can be concluded that 39% of the total electric energy expenses could be received from the CH_4 production.

7.9 Recommendations

In the framework of this Ph.D thesis the sequential anaerobic treatability of the OTC, AMX, TYL and ERY in the AMCBR and ABFR reactors were performed first time in the recent literature. The acute toxicity responses of *Vibrio fischeri* and *Daphnia magna* to the OTC, AMX, TYL and ERY antibiotics were performed for the first time in an anaerobic/aerobic sequential system.

Although AMCBR and ABFR reactors are high rate reactors with high biomass concentrations the AMCBR reactor exhibited more performance to treat the OTC, AMX, TYL and ERY with high yields and small volumes although the antibiotic loadings in the AMCBR reactor are high compare to the ABFR reactor.

The sequential AMCBR/CSTR system can be recommended to treat the synthetic and real raw pharmaceutical wastewaters containing antibiotics at high rates. This reactor system was effectively removed the acute toxicities originated from the antibiotics. Furthermore, the methane gas productions are high in this sequential system providing the recovery of the spending energy throughout continuous operation. This could be due to three separate compartments, to resistance to shock organic loads and pH with dominated methanogen biomass. However, the sequential ABFR/CSTR system can be also proposed to treat the antibiotic wastewaters since in the ABFR reactor the methanogens are separated from the acidogens.

The average methane yield was 0.36 $m^3CH_4/kgCOD_{removed}$ in the AMCBR reactor while this yield was found as 0.31 $m^3CH_4/kgCOD_{removed}$ in the ABFR reactor. The methane productions and methane gas percentages are high in the AMCBR reactor

compare to the ABFR reactor. The expenses in the AMCBR reactor consist of the chemical cost (0.60 €/year), of the analysis costs (500 €/year), of the labor costs (650 €/year), of the capital costs (500 €/year), of the instrumental costs (65 €/year), and of the electricity costs 0.78 €/year) while the methane recovery energy obtained from the AMCBR reactor was 0.31 €/year. The half of the electricity expenses could be obtained from the methane production in the AMCBR reactor.

Since the Turkish Water Pollution Control regulation has no limitation for antibiotic concentrations in the effluent of the antibiotic discharges, the antibiotics could be safely sending to the receiving environments after sequential AMCBR-(ABFR)/CSTR treatment. As a result, the antibiotics could be sending safely to the receiving bodies after treated in the suggested sequential AMCBR-(ABFR)/CSTR reactor system. Thus, prevent the antibiotic accumulations in the receiving aquatic ecosystems.

The results obtained from the substrate removal, biogas and inhibition kinetics in a laboratory scale model system could be used to estimate the treatment efficiencies in full-scale reactors when the similar operational conditions was applied to the pharmaceutical, food, chemistry industrial wastewaters.

REFERENCES

Ağdağ, O.N. (2004). *Factors Affecting the Treatment Efficiency of Municipal Solid Wastes in Simulated Landfill Bioreactors*. Ph.D Thesis. Dokuz Eylül University, Izmir, Turkey.

Ahring, B.K., Sandberg, M., & Angelidaki, I. (1995). Volatile fatty acids as indicators of process imbalance in anaerobic digestors. *Applied Microbiology and Biotechnology, 43 (3),* 559-565

Akarsubasi AT, Ince O, Kirdar B, Oz NA, Orhon D, Curtis TP, et al. (2005). Effect of wastewater composition on archaeal population diversity. *Water Research, 39,* 1576-1584

Akbarpour, A.T., & Mehrdadi, N. (2011). Wastewater treatment from antibiotics plant (UASB Reactor). *International Journal of Environmental Research, 5 (1),* 241-246.

Akunna, J.C., & Clark, M. (2000). Performance of a granular bed anaerobic baffled reactor (GRABBR) treating whisky distillery wastewater. *Bioresource Technology*, *74,* 257-261.

Alltech Chromatography. (n.d.). Retrieved, 2012, from http://www.alltechWEB.com

Alvarez, J.A., Otero, L., Lema, J.M., & Omil. F. (2010). The effect and fate of antibiotics during the anaerobic digestion of pig manure. *Bioresource Technology, 101*, 8581-8586

Amin, M.M. (2004). *Performance Evaluation of Three Anaerobic Bioreactors: ASBR, HAIS, and UASB.* Ph.D Thesis. Isfahan University, Isfahan, Iran.

Amin, M.M., Zilles, J.L., Greiner, J., Charbonneau, S., Raskin, L., & Morgenroth, E. (2006). Influence of the antibiotic erythromycin on anaerobic treatment of a pharmaceutical wastewater. *Environmental Science & Technology, 40 (12),* 3971-3977.

Anderson, G.K., & Yang, G. (1992). Determination of bicarbonate and total volatile acid concentration in anaerobic digesters using a simple titration. *Water Environment Research, 64*, 53-59.

Andreozzi, R., Caprio, V., Ciniglia, C., De Champdorea, M., Giudice, R. L., Marotta, R., et al. (2004). Antibiotics in the Environment: Occurrence in Italian STPs, Fate, and Preliminary Assessment on Algal Toxicity of Amoxicillin. *Environmental Science & Technology*, *38*, 6832-6838.

Andrews, J.F. (1968). A mathematical model for the continuous culture of microorganisms utilizing inhibitory substance. *Biotechnology & Bioengineering***,** *10 (6)*, 707-723

Angenent, L.T., Banik, G.C., & Sung, S. (2001). Development of anaerobic migrating blanket reactor (AMBR), a novel anaerobic treatment system. *Water Research*, *35 (7)*, 1739-1747.

APHA-AWWA-WEF, (2005). *Standard Methods for the Examination of Water and Wastewater*, (21th ed). Washington, DC, USA; American Public Health Association/American Water Works Association/Water Environment Federation

Aquino, S.F., & Stuckey, D.C. (2004). Soluble microbial products formation in anaerobic chemostats in the presence of toxic compounds. *Water Research, 38,* 255-266

Arikan, O.A. (2008). Degradation and metabolization of chlortetracycline during the anaerobic digestion of manure from medicated calves. *Journal of Hazardous Materials, 158*, 485-490

Arikan, O.A., Sikora, L.J., Mulbry, W., Khan, S.U., Rice, C., & Foster, G.D. (2006). The fate and effect of oxytetracycline during the anaerobic digestion of manure from therapeutically treated calves. *Process Biochemistry, 41,* 1637-1643

Arikan, O.A., Walter, M., & Clifford, R. (2009). Management of antibiotic residues from agricultural sources: use of composting to reduce chlortetracycline residues in beef manure from treated animals. *Journal of Hazardous Materials, 164,* 483-489.

Azbar, N., & Speece, R. (2001). Two-phase, two-stage and single-stage anaerobic process comparison. *Journal of Environmental Engineering, 26,* 240-248.

Backhaus, T., & Grime, L.H. (1999). The toxicity of antibiotic agents to the luminescent bacterium *Vibrio Fischeri*. *Chemosphere, 38 (14),* 3291-3301.

Balcioglu, I. A., & Otker, M. (2002). Treatment of pharmaceutical wastewater containing antibiotics by O_3 and O_3/H_2O_2 processes. *Chemosphere,* 50, 85-95.

Baloch, M.I., & Akunna, J.C. (2003). Granular bed baffled reactor (GRABBR): solution to a two-phase anaerobic digestion system. *Journal of Environmental Engineering, 129,* 1015-1021.

Barampouti, E.M., Mai, S.T., & Vlyssides, A.G. (2005). Dynamic Modeling of the Ratio Volatile Fatty Acids/Bicarbonate Alkalinity in a UASB Reactor for Potato Processing Wastewater Treatment. *Environmental Monitoring and Assessment, 110,* 121-128.

Batt, A.L. (2006). *Investigating the occurrence and fate of human and veterinary antibiotics in environmental water systems.* Ph.D Thesis. The State University, New York, USA.

Behling, E., Diaz, A., Colina, G., Herrera, M., Gutierrez, E., & Chacin, E. (1997). Domestic wastewater treatment using a UASB reactor. *Bioresource Technology, 61,* 239-245.

Benefield, L.D. (1980). *Biological process design for wastewater treatment*. Prentice-Hall, Inc., Englewood, Cliffs, N.J. O7632.

Benito-Pena, E., Partal-Rodera, A.I., Leon-Gonzalez, M.E., & Moreno-Bond, M.C. (2006). Evaluation of mixed mode solid phase extraction cartridges for the preconcentration of beta-lactam antibiotics in wastewater using liquid chromatography with UV-DAD Detection. *Analytica Chimica Acta, 556 (2),* 415-422.

Bertino, A. (2010). *Study one-stage partial nitritation-Anammox process in moving bed biofilm reactors: A Sustainable Nitrogen Removal.* Ph.D Thesis. Royal Institute of Technology (KTH), Stockholm, Sweden.

Beydilli, M.I., Pavlostathis, S.G., & Tincher, W.C. (1998). Decolorization and toxicity screening of selected reactive azo dyes under methanogenic conditions. *Water Science & Technology, 38,* 225-232.

Blackwell, P.A., Kay, P., Boxall, & Alistair B.A. (2007). The dissipation and transport of veterinary antibiotics in a sandy loam soil. *Chemosphere, 67,* 292-299.

Bolelli, L., Bobrovova, Z., Feri, E., Fini, F., Menotta, S., Scandurra, S., et al. (2006). Bioluminescent bacteria assay of veterinary drugs in excreta of food-producing animals. *Journal of Pharmaceutical and Biomedical Analysis, 42 (1),* 88-93.

Bonakdarpour, B., Vyrides, I., & Stuckey, D.C. (2011). Comparison of the performance of one stage and two stage sequential anaerobic/aerobic biological processes for the treatment of reactive-azo-dye-containing synthetic wastewaters. *International Biodeterioration & Biodegradation, 65*, 591-599

Brain, R.A., Johnson, D.J., Richards, S.M., Sanderson, H., Sibley, P.K., & Solomon, K.R. (2004). Effects of 25 pharmaceutical compounds to lemma gibba using a seven-day static-renewal test. *Environmental Toxicology and Chemistry, 23 (2)* 371-382.

Buitron, G., Melgoza, R. M., & Jimenez, L. (2003). Pharmaceutical wastewater treatment using an anaerobic/aerobic sequencing batch biofilter. *Journal of Environmental Science and Health, Part A. Toxic/Hazardous Substances and Environmental Engineering, 38,* 2077-2088.

Busetti F., & Heitz A. (2011). Determination of human and veterinary antibiotics in indirect potable reuse systems. *International Journal of Environmental Analytical Chemistry, 91 (10),* 989-1012.

Buyukkamaci, N., & Filibeli, A. (2004). Volatile fatty acid formation in an anaerobic hybrid reactor. *Process Biochemistry, 39 (11),* 1491-1494

Callaghan, F.J., Wase, D.A.J., Thayanithy, K., & Forsten, C.F. (2002). Continuous co-digestion of cattle slurry with fruit and vegetable wastes and chicken manure. *Biomass and Bioenergy*, *27*, 71-77

Capellos, C., & Bielski, B. H. J. (1972). *Kinetic systems: Mathematical description of chemical kinetics in solution*. Wiley publisher, New York, London, Sidney.

Cetecioglu, Z., Ince, B., Orhon, D., & Ince, O. (2012). Acute inhibitory impact of antimicrobials on acetoclastic methanogenic activity. *Bioresource Technology, 114*, 109-116

Chang, C., Chang, J., Vigneswaran, S., & Kandasamy, J. (2008). Pharmaceutical wastewater treatment by membrane bioreactor process-a case study in southern Taiwan. *Desalination, 234 (1-3),* 386-392.

Chee-Sanford, J.C., Aminov, R.I., Krapac, I.J., Garrigues-Jeanjean, N., & Mackie, R.I. (2001). Occurrence and diversity of tetracycline resistance genes in lagoons and groundwater underlying two swine production facilities. *Applied and Environmental Microbiology*, *67 (4),* 1494-1502.

Chelliapan, S., & Sallis, P.J. (2011). Application of anaerobic biotechnology for pharmaceutical wastewater. *The IIOAB Journal-Institute of Integrative Omics and Applied Biotechnology (IIOAB), 2 (1),* 13-21.

Chelliapan, S., Wilby, T., & Sallis, P. (2006). Performance of an up-flow anaerobic stage reactor (UASR) in the treatment of pharmaceutical wastewater containing macrolide antibiotics. *Water Research, 40 (3),* 507-516

Chelliapan, S., Wilby, T., & Sallis, P. (2010). Treatment of Pharmaceutical Wastewater Containing Tylosin in an Anaerobic-Aerobic Reactor System. *Water Practice & Technology, 5 (1),* 1165-166

Chelliapan, S., Wilby, T., & Sallis, P. (2011). Effect of hydraulic retention time on up-flow anaerobic stage reactor performance at constant loading in the presence of antibiotic tylosin. *Brazilian Journal of Chemical Engineering, 28 (1),* 51-61,

Chelliapan, S., Wilby, T., Yuzir, A. & Sallis, P. J. (2011). Influence of organic loading on the performance and microbial community Structure of an anaerobic stage reactor treating pharmaceutical wastewater. *Desalination, 271,* 257-264.

Chelliapan, S., Wilby, T., Sallis, P., & Yuzir, A. (2011). Tolerance of the antibiotic Tylosin on treatment performance of an Up-flow Anaerobic Stage Reactor (UASR). *Water Science & Technology, 63 (8),* 1599-1606

Chen, H.C., & Ding, W.H. (2008). *LC-MS/MS in Trace Analysis of Selected Emerging Contaminants-Method Development and Applications.* Retrieved 2008, from http://ivy1.epa.gov.tw/Dioxin_Toxic_Instruction/ap3/poster/Poster04.pdf

Chen, Q. (2010). *Kinetics of Anaerobic Digestion of Selected C_1 to C_4 Organic Acids.* Ph.D Thesis. University of Missouri-Columbia

Chen, W-R., & Huang, C-H. (2011). Transformation kinetics and pathways of tetracycline antibiotics with manganese oxide. *Environmental Pollution, 159,* 1092-1100

Chen, Z., Ren, N., Wang, A., Zhang, Z. P., & Shi, Y. (2008). A novel application of TPAD-MBR system to the pilot treatment of chemical synthesis-based pharmaceutical wastewater. *Water Research, 42,* 3385-3392

Chen, Z., Wang, H., Chena, Z., Ren, N., Wang, A., Shi, Y., et al. (2011). Performance and model of a full-scale up-flow anaerobic sludge blanket (UASB) to treat the pharmaceutical wastewater containing 6-APA and amoxicillin. *Journal of Hazardous Materials, 185*, 905-913.

Chen, Z., Wang, H., Ren, N., Cui, M., Nie, S., & Hu, D. (2011). Simultaneous removal and evaluation of organic substrates and NH3-N by a novel combined process in treating chemical synthesis-based pharmaceutical wastewater. *Journal of Hazardous Materials, 197*, 49-59.

Chernicharo, C. A. L. (2007). *Anaerobic reactors, biological wastewater treatment series*. (4 ed.). IWA Publication, London

Christensen, A.M., Ingerslev, F., & Baun, A. (2006). Ecotoxicity of mixtures of antibiotics used in aquacultures. *Environmental Toxicology and Chemistry, 25 (8),* 2208–2215

Contois, D. E. (1959). Kinetics of bacterial growth: relationship between population density and space growth rate of continuous cultures. *Journal of General Microbiology, 21*, 40-50.

Coşkun, T., Kabuk, H.A., Varinca, K.B., Debik, E., Durak, I., & Kavurt, C. (2012). Antibiotic Fermentation Broth Treatment by a pilot up flow anaerobic sludge bed reactor and kinetic modeling. *Bioresource Technology, 121*, 31-35.

Costanzo, S.D., Murby, J., & Bates, J. (2005). Ecosystem response to antibiotics entering the aquatic environment. *Marine Pollution Bulletin, 51 (1-4)*, 218-223.

Daughton, C.G., & Ternes, T.A. (1999). Pharmaceuticals and personal care products in the environment: agents of subtle change? *Environmental Health Perspectives Supplements, 107 (6)*, 907-938.

De Baere, S., Wassink, P., Croubles, S., De Boever, S., Baer't, K., & De Backer, P. (2005). Quantitative liquid chromatographic-mass spectrometric analysis of amoxicillin in broiler edible tissues. *Analytica Chimica Acta, 529*, 221-227.

Debik, E., & Coskun, T. (2009). Use of the static granular bed reactor (SGBR) with anaerobic sludge to treat poultry slaughterhouse wastewater and kinetic modeling. *Bioresource Technology, 100,* 2777-2782.

Deegan, A. M., Shaik, B., Nolan, K., Urell, K., Oelgemöller, M., Tobin, J., et al. (2011). Treatment options for wastewater effluents from pharmaceutical companies. *International Journal of Environmental Science and Technology, 8 (3),* 649-666

Değirmentaş, İ., & Deveci, N. (2004). Anaerobic Treatment of Antibiotic Production Wastewater and Kinetic Evaluations. *Journal of Biochemistry, 136,* 177-182

Del Nery, V., Pozzi, E., Damianovic, M.H.R.Z., Domingues, M.R., & Zaiat, M. (2008). Granules Characteristics in the vertical profile of a full-scale up flow anaerobic sludge blanket reactor treating poultry slaughterhouse wastewater. *Bioresource Technology, 99 (6),* 2018-2024.

Delgadillo-Mirquez L., Lardon, L., Steyer, J.P., & Patureau, D. (2011). A new dynamic model for bioavailability and cometabolism of micropollutants during anaerobic digestion. *Water Research, 45,* 4511–4521

Deng, Y., Zhang, Y., Gao, Y., Li, D., Liu, R., Liu, M., et al. (2012). Microbial Community Compositional Analysis for Series Reactors Treating High Level Antibiotic Wastewater. *Environmental Science & Technology, 46 (2),* 795-801.

Deshpande, A.M., Satyanarayan, S., & Ramakant. (2012). Kinetic analysis of an anaerobic fixed-film fixed bed reactor treating wastewater arising from production of a chemically synthesized pharmaceutical. *Environmental Technology, 33 (10-12),* 1261-1270.

Dinopoulou, G., Rudd T., & Leste J.N. (1988). Anaerobic Acidogenesis of a Complex Wastewater: The Influence of Operational Parameters on Reactor Performance. *Biotechnology and Bioengineering, 31,* 958-968.

DiPersio, L.P., & DiPersio, J.R. (2006). High rates of erythromycin and clindamycin resistance among OBGYN isolates of group B Streptococcus. *Diagnostic Microbiology and Infectious Disease, 54 (1),* 79-82.

Dlamini, S. (2009). Process Development for Co-Digestion of Toxic Effluents; Development of Screening Procedures. *Ph.D Thesis.* Durban University, KwaZulu-Natal, South Africa.

Donlon, B.A., Razo-Flores, E., Field, J.A., & Lettinga, G. (1995). Toxicity of N-substituted aromatics to acetoclastic methanogenic activity in granular sludge. *Applied and Environmental Microbiology, 61*, 3889-3893

DRLANGE LUMIXmini type luminometer, Dr. LANGE Company, (1996).

Ekama, G.A., Dold, P.L., & Marais, G.V. (1986). Procedures for determining influent COD fractions and the maximum specific growth-rate of heterotrophs in activated sludge systems. *Water Science & Technology, 18,* 91-114.

El-Deeb Ghazy, M.M., & Fayed, S.E. (2011). Acute and Chronic Toxic Effects of a Waste Stabilization Pond Wastewater on *Daphnia magna. Australian Journal of Basic and Applied Sciences, 5 (8),* 1371-1376

Elefsiniotis, P., & Oldham, W.K., 1994. Effect of HRT on acidogenic digestion of primary sludge. *Journal of Environmental Engineering, 120 (3),* 645-660.

Elmolla, E.S., & Chaudhuri, M. (2011). The feasibility of using combined TiO_2 photocatalysis-SBR process for antibiotic wastewater treatment. *Desalination, 272*, 218-224

Elmolla, E.S., Chaudhuri, M., & Eltoukhy, M.M. (2010). The use of artificial neural network (ANN) for modeling of COD removal from antibiotic aqueous solution by the Fenton process. *Journal of Hazardous Materials, 179,* 127-134

Enright, A., McHugh, S., Collins, G., & O'Flaherty, V. (2005). Low-temperature anaerobic biological treatment of solvent containing pharmaceutical wastewater. *Water Research, 39 (19)*, 4587-4596.

EPA (1998). *Antibiotics by high pressure liquid chromatography 56371B and 1694-1698 methods*. Retrieved 1998, from http://www.epa.gov/fem/methcollectns.htm

EPA (2010a). *Treating Contaminants of Emerging Concern. A Literature Review Database.* http://water.epa.gov/scitech/swguidance/ppcp/upload/cecliterature.pdf

Fatta-Kassinos, D., Meric, S., & Nikolaeu, A. (2011). Pharmaceutical residues in environmental waters and wastewater: current state of knowledge and future research. *Analytical and Bioanalytical Chemistry*, *399*, 251-275

FDA, (2006). http://www.fda.gov/AnimalVeterinary/default.htm

Fernández, I., Mosquera-Corral, A., Campos, J.L., & Méndez, R. (2009). Operation of an Anammox SBR in the presence of two broad-spectrum antibiotics. *Process Biochemistry, 44 (4)*, 494-498

Ferreira, C.S., Nunes, B.A., Henriques-Almeida, J.M., & Guilhermino, L. (2007). Acute toxicity of oxytetracycline and florfenicol to the microalgae Tetraselmis chuii and to the crustacean Artemia parthenogenetica. *Ecotoxicology and Environmental Safety, 67(3)*, 452-458.

Flaherty, C.M., & Dodson, S.I. (2005). Effects of pharmaceuticals on Daphnia survival, growth and reproduction. *Chemosphere, 61 (2)*, 200-207

Fountoulakis, M.S., Stamatelatou, K., & Lyberatos, G. (2008). The effect of pharmaceuticals on the kinetics of methanogenesis and acetogenesis. *Bioresource Technology*, *99*, 7083-7090

Fox, P., & Venkatasubbiah, V. (1996). Coupled anaerobic/aerobic treatment of high-sulfate wastewater with sulfate reduction and biological sulfide oxidation. *Water Science and Technology*, *34*, 359-366.

Gangagni, A., Venkata Naidu, G., Krishna Prasad, K., Chandrasekhar Rao, N. Venkata Mohan, S., Jetty, A., et al. (2005). Anaerobic treatment of wastewater with high suspended solids from a bulk drug industry using fixed film reactor (AFFR). *Bioresource Technology, 96 (1),* 87-93.

Gao, P., Ding, Y., Li, H., & Xagoraraki, I. (2012). Occurrence of pharmaceuticals in a municipal wastewater treatment plant: Mass balance and removal processes. *Chemosphere*, *88*, 17-24

Gartiser, S., Urich, E., Alexy, R., & Kümmerer, K. (2007). Anaerobic inhibition and biodegradation of antibiotics in ISO test schemes. *Chemosphere, 66,* 1839-1848.

Ghaniyari-Benis, S., Borja, R., Ali Monemian S., & Goodarzi, V. (2009). Anaerobic treatment of synthetic medium-strength wastewater using a multistage biofilm reactor. *Bioresource Technology, 100,* 1740-1745

Glassmeyer, S.T., Furlong, E.T., Kolpin, D.W., Cahill, J.D., Zaugg, S.D., Werner, S.L., et al. (2005). Transport of Chemical and Microbial Compounds from Known Wastewater Discharges: Potential for Use as Indicators of Human Fecal Contamination. *Environmental Science and Technology, 39 (14),* 5157-5169.

Gobel, A., Thomsen, A., Mcardell, C.S., Joss, A., & Giger, W. (2005). Occurence and Sorption Behavior of Sulfonamides, Macrolides, and Trimethoprim in Activated Sludge Treatment. *Environmental Science & Technology, 39,* 3981-3989.

Golet, E.M., Alder, A.C., & Giger, W. (2002). Environmental Exposure and Risk Assessment of Fluoroquinolone Antibacterial Agents in Wastewater and River Water of the Glatt Valley Watershed, Switzerland. *Environmental Science and Technology, 36 (17),* 3645-3651.

Grau, P., Dohanyas, M., & Chudoba, J. (1975). Kinetic of mlticomponant substrate removal by activated sludge, *Water Research, 9,* 337-342.

Gulkowska, A., Leung, H.W., So, M.K., Taniyasu, S., Yamashita, N., Yeung, L.W.Y., et al. (2008). Removal of antibiotics from wastewater by sewage treatment facilities in Hong Kong and Shenzhen, China. *Water Research, 42 (1-2)*, 395-403

Haldane, J. B. S. (1965). *Enzymes*, MIT, Cambridge, Mass.

Halling-Sørensen, B. (2001). Inhibition of aerobic growth and nitrification of bacteria in sewage sludge by antibacterial agents. *Archives of Environment Contamination and Toxicology, 40*, 451-460.

Halling-Sorensen, B., Sengelov, G., & Tjornelund, J. (2002). Toxicity of tetracyclines and tetracycline degradation products to environmentally relevant bacteria, including selected tetracycline-resistant bacteria. *Archives of Environmental Contamination and Toxicology*, *42*, 263-271.

Han, K., & Levenspiel, O. (1988). Extended Monod Kinetics for Substrate, Product, and Cell Inhibition. *Biotechnology and Bioengineering, 32 (4)*, 430 - 437

Haridas, A., Suresh, S., Chitra, K.R., & Manilal, V.B. (2005). The Buoyant Filter Bioreactor: a high-rate anaerobic reactor for complex wastewater-process dynamics with dairy effluent. *Water Research, 39*, 993-1004

Heidari, M., Saffari Khouzani, H., Amin, M.M., Ghasemian, M., Taherian, E. Attari, L., et al. (2011). Inhibition Effect of Antibiotics Ciprofloxacin and Ofloxacin and Hormone β-stradiol 17 Valerat on the Methanogenic Activity of Anaerobic Biomass. *Iranian Journal of Environmental Health Science & Engineering*, *4 (2)*, 1-12.

Hill, D. T., Gobb, S. A, & Bolte, J. P. (1987). Using Volatile Fatty Acid Relationships to Predict Anaerobic Digester Failure, *Transactions of the ASAE, 30 (2)*, 496-501.

Hirsch, R., Ternes, T., Haberer, K., & Kratz, K.L. (1999). Occurrence of antibiotics in the aquatic environment. *Science of the Total Environment, 225 (1,2)*, 109-118.

Holm, J.V., Ruegge, K., Bjerg, P.L., & Christensen, T.H. (1995). Occurrence and distribution of pharmaceutical organic compounds in the groundwater down gradient of a landfill (Grindsted, Denmark). *Environmental Science & Technology, 29 (5),* 1415-20.

Holten Lutzhoft, H.C., Halling-Sorensen, B., & Jorgensen, S.E. (1999). Algal Toxicity of Antibacterial Agents Applied in Danish Fish Farming. *Archives of Environmental Contamination & Toxicology, 36,* 1-6.

Holtz, S. (2006). *There Is No "Away."* Pharmaceuticals, Personal Care Products, and Endocrine-Disrupting Substances: Emerging Contaminants Detected in Water. *Research Report*. Canadian Institute for Environmental Law and Policy, Canada.

Hsu, M. C., & Hsu, P. W. (1992). High-Performance Liquid Chromatographic Method for Potency Determination of Amoxicillin in Commercial Preparations and for Stability Studies. *Antimicrobial Agents & Chemotherapy, 36 (6),* 1276-1279.

Hu, D., Fulton, B., Henderson, K., & Coats, J. (2008). Identification of Tylosin Photoreaction Products and Comparison of ELISA and HPLC Methods for Their Detection in Water. *Environmental Science & Technology, 42 (8*), 2982-2987

Hyun, S.H., Young, J.C., & Kim, I.S. (1998) Inhibition kinetics for propionate degradation using propionate-enriched mixed cultures. *Water Science and Technology 38*, 443-451.

Ince, B.K., Selcuk, A., & Ince, O. (2002). Effect of a chemical synthesis-based pharmaceutical wastewater on performance, acetoclastic methanogenic activity and microbial population in an up flow anaerobic filter. *Journal of Chemical Technology and Biotechnology, 77 (6),* 711-719.

Ingerslev, F., Torang, L., Loke, M.-L., Stollingen-Sorensen, B., & Nylom, N. (2001). Primary biodegradation of veterinary antibiotics in aerobic and anaerobic surface water simulation systems. *Chemosphere, 44*, 865-872.

Isidori, M., Lavorgna, M., Nardelli, A., Pascarella, L., & Parrella, A. (2005). Toxic and genotoxic evaluation of six antibiotics on non-target organisms. *Science of the Total Environment, 346 (1-3*), 87-98.

Işık, M., & Sponza, D. T. (2005). Substrate removal kinetics in an up flow anaerobic sludge blanket reactor decolorizing simulated textile wastewater. *Process Biochemistry*, *40*, 1189-1198.

Jessick A.M., Moorman T.B., & Coats J.R. (2011). Optimization of analytical methods to improve detection of erythromycin from water and sediment. *Journal of Environmental Science and Health, Part B, 46 (8),* 735-740.

Jin, H., Kumar, A.P., Paik, D.H., Ha, K.C., Yoo, YJ., & Lee, Y. (2010). Trace analysis of tetracycline antibiotics in human urine using UPLC–QToF mass spectrometry. *Microchemical Journal, 94 (2),* 139-147.

Jin, R-C., & Zheng, P. (2009). Kinetics of nitrogen removal in high rate anammox up flow filter. *Journal of Hazardous Materials*, *170*, 652-656

Jorgensen, S.E., & Halling-Sorensen, B. (2000). Drugs in the environment. *Chemosphere*, *40 (7)*, 691-699.

Kaparaju, P., Serrano, M., & Angelidaki, I. (2009). Effect of reactor configuration on biogas production from wheat straw hydrolysate. *Bioresource Technology*, *100 (24),* 6317-6323

Karthikeyan, K.G., & Meyer, M.T. (2006). Occurrence of antibiotics in wastewater treatment facilities in Wisconsin, USA. *Science of the Total Environment, 361*, 196-207.

Kassab, G., Halalsheh, M., Klapwijk, A., Fayyad, M., & van Lier, J.B. (2010). Sequential anaerobic-aerobic treatment for domestic wastewater-A Review. *Bioresource Technology, 101,* 3299-3310

Kay, P., Blackwell, P.A., & Boxall, A.B.A. (2005). A lysimeter experiment to investigate the leaching of veterinary antibiotics through a clay soil and comparison with field data. *Environmental Pollution (Amsterdam, Netherlands), 134 (2)*, 333-341.

Khanal, S.K. (2008). *Anaerobic Biotechnology for Bioenergy Production Principles and Applications.* ISBM 13: 978-0-8138-2346-1. A John Wiley & Sons, Ltd., Publication, Iowa, USA.

Kim, S., & Aga, D.S. (2007). Potential ecological and human health impacts of antibiotics and antibiotic-resistant bacteria from wastewater treatment plants. *Journal of Toxicology and Environmental Health, Part B, 10*, 559-573.

Kim, S., Eichhorn, P., Jensen, J.N., Weber, A.S., & Aga, D.S. (2005). Removal of Antibiotics in Wastewater: Effect of Hydraulic and Solid Retention Times on the Fate of Tetracycline in the Activated Sludge Process. *Environmental Science & Technology*, *39 (15)*, 5816-5823.

Kim, Y., Jung, J., Kim, M., Park, J., Boxall, A.B.A., & Choia, K. (2008). Prioritizing veterinary pharmaceuticals for aquatic environment in Korea. *Environmental Toxicology and Pharmacology, 26*, 167–176

Kim, Y., Choi, K., Jung, J., Park, S. Kim, P.G., & Park, J. (2007). Aquatic toxicity of acetaminophen, carbamazepine, cimetidine, diltiazem and six major sulfonamides, and their potential ecological risks in Korea. *Environment International, 33*, 370-375.

Kolpin, D.W., Furlong, E.T., Meyer, M.T., Thurman, E.M., Zaugg, S.D., Barber, L.B., et al. (2002). Pharmaceuticals, Hormones, and Other Organic Wastewater Contaminants in U.S. Streams, 1999-2000: A National Reconnaissance. *Environmental Science and Technology*, *36 (6)*, 1202-1211.

Kolz, A.C., Ong, S.K. & Moorman, T.B. (2005). Sorption of tylosin onto swine manure. *Chemosphere*, *6*0, 284-289

Krishna, G.V.T., Kumar, P., & Kumar, P. (2009). Treatment of low-strength soluble wastewater using an anaerobic baffled reactor (ABR). *Journal of Environmental Management, 90*, 166-176

Kuai, L., De Vreese, L., & Vandevivere, P. (1998). GAC amended UASB reactor for the stable treatment of toxic textile wastewater. *Environmental Technology, 19*, 1111-1117.

Kulshrestha, P., Giese, R.F., & Aga, D.S. (2004). Investigating the Molecular Interactions of Oxytetracycline in Clay and Organic Matter: Insights on Factors Affecting Its Mobility in Soil. *Environmental Science & Technology, 38 (15)*, 4097-4105.

Kümmerer, K., Alexy, R., Hüttig, J., & Scholl, A. (2004). Standardized tests fail to assess the effects of antibiotics on environmental bacteria. *Water Research, 38 (8)*, 2111-2116

Kuo, W.C., & Parkin, G.F. (1996). Characterization of soluble microbial products from anaerobic treatment by molecular weight distribution and nickel-chelating properties. *Water Research*, 3*0*, 915–922.

Kurosawa, N., Kuribayashi, S., Owada, E., Ito, K., Nioka, M., Arakawa, M., et al. (1985). Determination of streptomycin in serum by high-performance liquid chromatography. *Journal of Chromatography, 343(2)*, 379-85.

Kuşçu Selçuk, Ö. (2007). *Comparison of Anaerobic Baffled (ABR) and Migrating Blanket Reactors (AMBR) in the Anaerobic Treatability of Nitroorganic Compounds.* Ph.D Thesis, Dokuz Eylül University, Izmir, Turkey

Kuşçu Selçuk, Ö., & Sponza D.T. (2009). Effect of increasing nitrobenzene loading rates on the performance of anaerobic migrating blanket reactor and sequential anaerobic migrating blanket reactor/completely stirred tank reactor system. *Journal of Hazardous Materials, 168*, 390-399

Lahav, O., Morgan, B.E., & Loewenthal, R.E. (2002). Rapid, simple and accurate method for measurement of VFA and carbonate alkalinity in anaerobic reactors. *Environmental Science & Technology, 36 (12)*, 2736-2741.

Lallai, A., Mura, G., & Onnis, N. (2002). The effects of certain antibiotics on biogas production in the anaerobic digestion of pig waste slurry. *Bioresource Technology*, *82 (2), 205-208*

Lalumera, G.M., Calamari, D., Galli, P., Castiglioni, S., Crosa, G., & Fanelli, R. (2004). Preliminary investigation on the environmental occurrence and effects of antibiotics used in aquaculture in Italy. *Chemosphere*, *54 (5)*, 661-668

Lamm, A., Gozlan, I., Rotstein, A., & Avısar, D. (2009). Detection of amoxicillin-diketopiperazine-2-5 in wastewater samples. *Journal of Environmental Science and Health Part, 44*, 1512-1517

Lange, B. (1994). LUMISmini, Operating Manual. Dr. Bruno, Lange, Düsseldorf, Germany.

Lansky, P., & Halling-Sorensen, B. (1997). The toxic effect of the antibiotic metronidazol on aquatic organisms. *Chemosphere*, *35*, 2553-2561.

Lapara, T. M., Nakatsu, C. H., Pantea, L. M., & Alleman, J. E. (2001). Aerobic biological treatment of a pharmaceutical wastewater: effect of temperature on cod removal and bacterial community development. *Water Research*, 35 (18), 4417-4425.

Larsen, T.A., Lienert, J., Joss, A., & Siegrist, H. (2004). How to avoid pharmaceuticals in the aquatic environment. *Journal of Biotechnology*, *113* 295–304

Lecture 16. (n.d.). Retrieved, 2012, from http://www.slideserve.com/brygid/lecture16

Lehninger, A.L., (1977). *The Molecular Basis of Cell Structure and Function Biochemistry*, (3rd ed.). New York, Worth Publishers.

Li, K., Yediler, A., Yang, M., Schulte-Hostede, S., & Wong, M.H. (2008). Ozonation of oxytetracycline and toxicological assessment of its oxidation by-products. *Chemosphere, 72 (3),* 473-478

Liguoro, M.D., Poltronieri, C., Capolongo, F., & Montesissa, C. (2003). Use of oxytetracycline and tylosin in intensive calf farming: Evaluation of transfer to manure and soil. *Chemosphere, 52 (1),* 203-212

Lindberg, R., Jarnheimer, P.A., Olsen, B., Johansson, M., & Tysklind, M. (2004). Determination of antibiotic substances in hospital sewage water using solid phase extraction and liquid chromatography/mass spectrometry and group analogue internal standards. *Chemosphere, 57 (10),* 1479-1488.

Lindberg, R.H., Bjorkloundb, K., Johanssond, P.R., Tysklinda, M., & Anderson, M.B.A.V. (2007). Environmental risk assessment of antibiotics in the Swedish environment with emphasis on sewage treatment plants. *Water Research, 41,* 613-619.

Lindsey, M.E., Meyer, M., & Thurman, E.M. (2001). Analysis of trace levels of sulfonamide and tetracycline antimicrobials in groundwater and surface water using solid-phase extraction and liquid chromatography/mass spectrometry. *Analytical Chemistry, 73 (19),* 4640-4646.

Lineweaver, H., & Burk, D. (1934). The Determination of Enzyme Dissociation Constants. *Journal of the American Chemical Society, 56 (3),* 658-666.

Liu C., Li L., Yang J.L., Yang H.N., & Zhang R. (2011). Inhibitory effects of streptomycin and erythromycin on methane production of anaerobic granular sludge. *Bioinformatics and Biomedical Engineering, 5th International Conference,* 1-4.

Liu, R., Tian, Q., & Chen, J. (2010). The developments of anaerobic baffled reactor for wastewater treatment: A Review. *African Journal of Biotechnology, 9 (11),* 1535-1542

Liu, X., Ren, N., & Yuan, Y. (2009). Performance of a periodic anaerobic baffled reactor fed on Chinese traditional medicine industrial wastewater. *Bioresource Technology, 100*, 104-110

Liu, Y., & Shen, L. (2008). From Langmuir Kinetics to First- and Second-Order Rate Equations for Adsorption. *Langmuir, 24*, 11625-11630

Liu, Y., Gao, B., Yue, Q., Guan, Y., Wang, Y., & Huang, L. (2012). Influences of two antibiotic contaminants on the production, release and toxicity of microcystins. *Ecotoxicology and Environmental Safety, 77 (1)*, 79-87.

Loke, M.L., Jespersen, S., Vreeken, R., Halling-Sørensen, & Tjornelund, J. (2003). Determination of oxytetracycline and its degradation products by high-performance liquid chromatography–tandem mass spectrometry in manure-containing anaerobic test systems. *Journal of Chromatography B, 783*, 11-23

Lorestani, A.A.Z., Mohamed, A.R., Mashitah, M.D., Abdullah, A.Z., & Isa, M.H. (2006). Effects of Organic Loading Rate on Palm Oil Mill Effluent Treatment in an Up-Flow Anaerobic Sludge Fixed Film Bioreactor. *Environmental Engineering and Management Journal, 5 (3)*, 337-350.

Majewsky M, Galle T, Yargeau V., & Fischer K, Active heterotrophic biomass and sludge retention time (SRT) as determining factors for biodegradation kinetics of pharmaceuticals in activated sludge. *Bioresource Technology, 102*, 7415-7421

Malina, J., & Pohland, F. (1992). *Design of anaerobic processes for the treatment of industrial and municipal wastes*. Water Quality Management, Taylor François.

Martín, A., Borja, R., & Chica, A., 1993. Kinetic study of an anaerobic fluidized bed system used for the purification of fermented olive mill wastewater. *Journal of Chemical Technology & Biotechnology, 56*, 155-62.

Maszenan, A.M., Liu, Y., & Jern N.G.W. (2011). High-Performance Anaerobic Granulation Processes for Treatment of Wastewater-Containing Recalcitrant Compounds. *Critical Reviews in Environmental Science and Technology, 41*, 1271-1308

Maurer M, Escher BI, Richle P, Schaffner C., & Adler, A.C. (2007). Elimination of R-blockers in sewage treatment. *Water Research, 41*, 1614-1622

McCarty, P.L., & Mosey, F.E. (1991) Modelling of anaerobic digestion processes (a discussion of concepts). *Water Science and Technology, 24(8)*, 17-33.

McInerney, M.J. (1988). *Anaerobic hydrolysis and fermentation of fats and proteins.* In *Biology of anaerobic microorganisms*. Jon Wiley & Sons.

Metcalf & Eddy Inc. (2003). *Wastewater Engineering: Treatment and Reuse.* (4th ed.). McGraw-Hill, New York.

Miege, C., Choubert, J.M., Ribeiro, L., Eusebe, M., & Coquery, M. (2009). Fate of pharmaceuticals and personal care products in wastewater treatment plants-conception of a database and first results. *Environmental Pollution, 157 (5)*, 1721-1726

Mohan, S.V., Prakasham, R.S., Satyavathi, B., Annapurna, J., & Ramakrishna, S.V. (2001). Biotreatability studies of pharmaceutical wastewater using an anaerobic suspended film contact reactor. *Water Science and Technology, 43*, 271-276.

Monod, J. (1949). The growth of bacterial cultures. *Annual Review of Microbiology, 3*, 371-376.

Myers, R.C. (2009). Modeling the fate of emerging contaminants and investigating the importance of their physical, chemical, and biological properties in water and wastewater treatment. *Ph.D Thesis,* Southern Methodist University, United States.

Nachaiyasit S., & Stuckey D.C. (1997b). The effect of shock loads on the performance of an anaerobic baffled reactor (ABR): 2. step and transient hydraulic shocks at constant feed strength. *Water Research, 31*, 2747-2755.

Nagele, E., & Moritz, R. (2005). Structure elucidation of degradation products of the antibiotic amoxicillin with ion trap MSn and accurate mass determination by ESI TOF. *Journal of the American Society for Mass Spectrometry, 16*, 1670-1676.

Nandy, T., & Kaul, S.N. (2001). Anaerobic pre-treatment of herbal-based pharmaceutical wastewater using fixed-film reactor with recourse to energy Recovery. *Water Research*, *35*, 351-362.

Nandy, T., Kaul, S.N., & Szpyrkowicz, L. (1998). Treatment of herbal pharmaceutical wastewater with energy Recovery. *International Journal of Environmental Studies, 54*, 83-105.

Noble, J., (2006). GE ZeeWeed MBR technology for pharmaceutical wastewater treatment. *Membrane Technology*, *9*, 7-9.

Novaes, R.F.V. (1986). Microbiology of anaerobic digestion. *Water Science and Technology, 18 (12)*, 1-14.

O'Flaherty, V., Mahony, T., O'Kennedy, R., & Colleran, E. (1998). Effect of pH on growth kinetics and sulphide toxicity thresholds of a range of methanogenic, syntrophic and sulphate-reducing bacteria. *Process Biochemistry,* 33, 555–569

Oktem YA, Ince O, Sallis P, et al. (2008). Anaerobic treatment of a chemical synthesis-based pharmaceutical wastewater in a hybrid up flow anaerobic sludge blanket reactor. *Bioresource Technology, 99*, 1089-1096.

Oktem, Y., Ince, O., Sallis, P., Donnelly, T., & Ince, B. (2007). Anaerobic treatment of a chemical synthesis-based pharmaceutical wastewater in a hybrid up flow anaerobic sludge blanket reactor. *Bioresource Technology, 99 (5),* 1089-1096.

Owen, W.F., Stuckey, D.C., Healy, J.B., Young, L.Y., & McCarty, P.L. (1979). Bioassay for monitoring biochemical methane potential and anaerobic toxicity. *Water Research, 13,* 485-492.

Oz, N.A., Ince, O., & Ince, B.K. (2004). Effect of wastewater composition on methanogenic activity in an anaerobic reactor. *Journal of Environmental Science and Health, Part A. Toxic/Hazardous Substances and Environmental Engineering, 39 (11-12),* 2941-2953.

Özdemir, C., Dursun, S. & Sen, N. (2006). Methane Production from Anaerobic Treatment of Volatile Organic Compounds (Voc). *Energy Exploration & Exploitation,24,* 259-270.

Öztürk, I., Altinbas, M., Arikan, O., & Demir, A. (1998). Anaerobic UASBR Treatment of Young Landfill leachate. *1st International Workshop on Environmental Quality and Environmental Engineering in the Middle East Region*, Konya, Turkey.

Pallavi, V., Daga, K., Gehlot, P., & Chaudhary, S. (2009). Anaerobic treatability of pharmaceutical wastewaters. *Asian Journal of Chemistry, 21*, 1979-1982.

Pandey, P.K., Ndegwa, P.M., Soupir, M.L., Alldredge, J.R., & Pitts, M.J. (2011). Efficacies of inocula on the startup of anaerobic reactors treating dairy manure under stirred and unstirred conditions. *Biomass and Bioenergy, 35 (7),* 2705-2720.

Pandian, M., NGO, H-H., & Pazhaniappan, S. (2011). Substrate Removal Kinetics of an Anaerobic Hybrid Reactor Treating Pharmaceutical Wastewater. *Journal of Water Sustainability, 1 (3),* 301-312

Panicker, S.J., Philipose, M. C., & Haridas, A. (2008). Buoyant Filter Bio-Reactor (BFBR)-a novel anaerobic wastewater treatment unit. *Water Science & Technology, 58 (2),* 373-377.

Park, S., & Choi, K. (2008). Hazard assessment of commonly used agricultural antibiotics on aquatic ecosystems. *Ecotoxicology, 17,* 526-538.

Patel, C., & Madamwar, D. (1998). Biomethanation of salty cheese whey using multichamber anaerobic bioreactor. *Energy & Environmental Science, 9,* 225-231.

Patel, C., & Madamwar, D. (2001). Single and multichamber fixed film anaerobic reactors for biomethanation of acidic petrochemical wastewater-systems performance. *Process Biochemistry, 36,* 613-619

Pavlostathis, S. G., & Giraldo-Gomez, E. (1991). Kinetics of anaerobic treatment. *Water Science and Technology, 24 (8),* 35-59

Penaud, V., Delgenes, J.P., Torrijos, M., Moletta, R., Vanhoutte, B., & Cans, P. (1997). Definition of optimal conditions for the hydrolysis and acidogenesis of a pharmaceutical microbial biomass. *Process Biochemistry, 32 (6),* 515-521.

Petrovic, M., Gonzalez, S., & Barcelo, D. (2003). Analysis and removal of emerging contaminants in wastewater and drinking water. *Trends in Analytical Chemistry, 22 (10),* 685-696.

Radjenovic, J., Petrovic, M., & Barcelo, D. (2009). Fate and distribution of pharmaceuticals in wastewater and sewage sludge of the conventional activated sludge (CAS) and advanced membrane bioreactor (MBR) treatment. *Water Research, 43,* 831-841.

Razo-Flores, E., Luijten, M., Donlon, B., Lettinga, G., & Field, J. (1997). Biodegradation of selected azo dyes under methanogenic conditions. *Water Science & Technology, 36,* 65-72.

Ren, N., Liu, M., Wang, A., Ding, J., & Li, H. (2003) Organic acids conversion in methanogenic-phase reactor of the two-phase anaerobic process. *Huanjing Kexue/Environmental Science, 24 (4),* 89.

Rincon, B., Borja, R., Martin, M.A., & Martin, A. (2009). Evaluation of the methanogenic step of a two-stage anaerobic digestion process of acidified olive mill solid residue from a previous hydrolytic–acidogenic step. *Waste Management, 29 (9),* 2566-2573

Rittmann, B.E., & McCarty, P.L. (2001). *Environmental biotechnology: principles and applications*. McGraw-Hill International Edition, New York, USA

Robinson J.A., & Tiedje J.M. (1983). Non-linear estimation of Monod growth kinetic parameters from a single substrate depletion curve. *Applied and Environmental Microbiology, 45,* 1453-1458.

Rodante, F., Vecchio, S., & Tomassetti, M. (2002). Multi-step decomposition processes for some antibiotics: a kinetic study. *Thermochimica Acta, 394*, 7-18

Rodríguez-Martinez J, Garza-Garcia Y, Aguilera-Carbo A, et al. (2005). Influence of nitrate and sulphate on the anaerobic treatment of pharmaceutical wastewater. *Engineering Life Science, 5*, 568-573.

Rubert, K., & Pedersen, J.A. (2006). Kinetics of oxytetracycline reaction with a hydrous manganese oxide. *Environmental Science & Technology, 40,* 7216-7221

Samuel Suman Raj D., & Anjaneyulu Y. (2005). Evaluation of biokinetic parameters for pharmaceutical wastewaters using aerobic oxidation integrated with chemical treatment. *Process Biochemistry, 40*, 165-175

Sanchez, E., Borja, R., Travieso, L., Martin, A., & Colmenarejo, M.F. (2005). Effect of organic loading rate on the stability, operational parameters and performance of a secondary up flow anaerobic sludge bed reactor treating piggery waste. *Bioresource Technology, 96*, 335-344.

Santos, L.H.M.L.M., Araujo, A.N., Fachini, A., Pena, C., Delerue-Matos, M.C.B.S., & Montenegro, M. (2010). Ecotoxicological aspects related to the presence of pharmaceuticals in the aquatic environment. *Journal of Hazardous Materials, 175*, 45-95.

Sanz, J.L., Rodriguez, N., & Amils, R. (1996). The action of antibiotics on the anaerobic digestion process. *Applied Microbiology and Biotechnology, 46*, 587-592

Sarmah, A.K., Meyer, M.T., & Boxall, A.B.A. (2006). A global perspective on the use, sales, exposure pathways, occurrence, fate and effects of veterinary antibiotics (VAs) in the environment. *Chemosphere, 65 (5),* 725-759

Sato, N., Okubo, T., Onodera, T., Ohashi, A., & Harada, H. (2006). Prospects for a self sustainable sewage treatment system: a case study on full-scale UASB system in India's Yamuna River Basin. *Journal of Environmental Management, 80,* 198-207.

Satyanarayan, S., & Kaul, S.N. (2002). Kinetics of an anaerobic moving bed reactor system treating synthetic milk wastewater. *Journal of environmental science and health. Part A. Toxic/hazardous Substances & Environmental Engineering, 37 (9),* 1737-1755.

Sawyer, L.L, McCarty, P.L., & Parkin, G.F. (2002). *Chemistry for environmental engineering*. (5^{th} ed.). McGraw Hill.

Seghezzo L, Gutierrez, M.A., Trupiano, A.P., Figueroa, M.E., Cuevas, C.M., & Zeeman, G., et al. (1998). A review: the anaerobic treatment of sewage in UASB and EGSB reactors. *Bioresource Technology, 65,* 175-190.

Senta, I., Matosic, M., Jakopovic, K.H., Terzic, S., Curko, J., Mijatovic, I. et al. (2011). Removal of antimicrobials using advanced wastewater treatment. *Journal of Hazardous Materials, 192 (1),* 319-328

Sentürk, E., İnce, M., & Engin Onkal, G. (2010). Kinetic evaluation and performance of a mesophilic anaerobic contact reactor treating medium-strength food-processing wastewater. *Bioresource Technology, 101,* 3970-977

Senyuva, H., Ozden, T., & Sarıca, D.Y. (2000). High performance liquid chromatographic determination of oxytetracycline in cured meat products. *Turkish Journal of Chemistry, 24,* 395-400.

Shaojun, J., Zhang, S., Yin, D., Wang, L., & Chen, L. (2008). Aqueous oxytetracycline degradation and the toxicity change of degradation compounds in photo irradiation process. *Journal of Environmental Sciences, 20*, 806–813

Shi, J.C., Liao, X.D., Wu, Y.B., & Liang, J.B. (2011). Effect of antibiotics on methane arising from anaerobic digestion of pig manure. *Animal Feed Science and Technology, 166-167*, 457-463

Shimada, T., Zilles, J.L., Morgenroth, E., & Raskin, L. (2006). Effects of Macrolide Antimicrobials on the Performance of Anaerobic Treatment Systems. *WEFTEC-2006*, 1543-1547.

Shimada, T., Zilles, J.L., Morgenroth, E., & Raskin, L. (2008). Inhibitory Effects of the Macrolide Antimicrobial Tylosin on Anaerobic Treatment. *Biotechnology & Bioengineering, 101 (1),* 73-82.

Shimada, T., Zilles, J.L., Morgenroth, E., & Raskin, L. (2011). Effects of the antimicrobial tylosin on the microbial community structure of an anaerobic sequencing batch reactor. *Biotechnology and Bioengineering, 108 (2)*, 296-305.

Siegrist, H., Vogt, D., Garcia-Heras, J.L., & Gujer, W. (2002). Mathematical model for mesophilic and thermophilic anaerobic sewage sludge digestion. *Environmental Science & Technology*, *36*, 1113-1123.

Snyder, S.A., Adham, S., Redding, A.M., Cannon, F.S., DeCarolis, J., Oppenheimer, J., et al. (2007). Role of membranes and activated carbon in the removal of endocrine disruptors and pharmaceuticals. *Desalination, 202*, 156-181.

Speece, R.E. (1996). *Anaerobic biotechnology for industrial wastewaters*, (1st ed.). Archae Press, Nashville, Tennessee, USA

Sponza, D.T. (2002a). Incorporation of toxicity tests to the discharges of pulp and paper industry in Turkey. *Bulletin of Environmental Contamination and Toxicology, 69*, 719-726.

Sponza, D.T. (2002b). Necessity of toxicity assessment in Turkish industrial discharges (examples from metal and textile industry effluents). *Environmental Monitoring and Assessment, 73*, 41-66.

Sponza, D.T. (2006). Toxicity studies in a chemical dye production industry in Turkey. *Journal of Hazardous Materials A, 138*, 438-447.

Sponza, D.T., & Selcuk-Kuscu, O. (2011). Relationships between acute toxicities of paranitrophenol (p-NP) and nitrobenzene (NB) to *Daphnia magna* and Photobacterium phosphoreum: Physicochemical properties and metabolites under anaerobic/aerobic sequentials. *Journal of Hazardous Materials, 185*, 1187-1197.

Sponza, D.T., & Demirden, P. (2007). Treatability of sulfamerazine in sequential up flow anaerobic sludge blanket reactor (UASB)/completely stirred tank reactor (CSTR) processes. *Separation and Purification Technology*, *56*, 108-117

Sponza, D.T., & Demirden, P. (2010). Relationships between chemical oxygen demand (COD) components and toxicity in a sequential anaerobic baffled reactor/aerobic completely stirred reactor system treating Kemicetine. *Journal of Hazardous Materials*, *176*, 64-75

Sponza, D.T., & Işık, M. (2004). Monitoring of toxicity and intermediates of C.I. Direct Black 38 azo dye through decolorization in an anaerobic/aerobic sequential reactor system. *Journal of Hazardous Materials B, 114*, 29-39

Sreekanth, D., Sivaramakrishna, D., Himabindu, V., & Anjaneyulu, Y. (2009) Thermophilic treatment of bulk drug pharmaceutical industrial wastewaters by using hybrid up flow anaerobic sludge blanket reactor. *Bioresource Technology, 100*, 2534-2539.

Steyer, J.P., Bernard, O., Batstone, D.J., & Angelidaki, I. (2006). Lessons learnt from 15 years of ICA in anaerobic digesters. *Water Science and Technology, 53 (4-5)*, 25-33.

Suarez, S., Carballa, M., Omil, F., & Lema, J.M. (2008). How are pharmaceutical and personal care products (PPCPs) removed from urban wastewaters? *Reviews in Environmental Science and Biotechnology, 7(2),* 125-138.

Suarez, S., Lema, J.M., Suarez Omil, F. (2009). Pre-treatment of hospital wastewater by coagulation-flocculation and flotation. *Bioresource Technology*, *100*, 2138-2146.

Sulaiman, A., Tabatabaei, M., Zulkhairi Mohd Yusoff, M., Faizal Ibrahim, M., Hassan, M.A., & Shirai, Y. (2010). Accelerated Start-up of a Semi-commercial Digester Tank Treating Palm Oil Mill Effluent with Sludge Seeding for Methane Production. *World Applied Sciences Journal, 8 (2),* 247-258

Switzenbaum, M.S., Girald-Gomez, E., & Hickey, R.F. (1990). Monitoring of the anaerobic methane fermentation process. *Enzyme and Microbial Technology*, *12*, 722-730.

Tay, J., & Zhang, X. (2000). Stability of high rate anaerobic systems. I: Performance under shocks. *Journal of Environmental Engineering, 126 (8),* 713-725

Teixeira, S., Delerue-Matos, C., Alves, A., & Santos, L. (2008). Fast screening procedure for antibiotics in wastewaters by direct HPLC-DAD analysis. *Journal of Separation Science, 31 (16-17),* 2924-2931

Ternes, T.A., Joss, A., & Siegrist, H. (2004). Scrutinizing pharmaceuticals and personal care products in wastewater treatment. *Environmental Science and Technology, 38 (20),* 392-399.

Trovo, A. G., Pupo-Nogueira, R. F., Aguilera, A., Fernandez-Alba, A. R., & Malato, S. (2011). Degradation of the antibiotic amoxicillin by photo-Fenton process-chemical and toxicological assessment. *Water Research, 45*, 1394-1402.

Truax, D.D., Britto, R., & Sherrard, J.H. (1995). Bench-scale studies of reactor based treatment of fuel-contaminated soils. *Waste Management, 15*, 351–357

Tsung-Hsien, Y., Yu-Chen, L., Sri Chandana, P., Pui-Kwan, A.H., Ping-Yi, Y., & Cheng-Fang, L. (2011). Biodegradation and bio-sorption of antibiotics and non-steroidal anti-inflammatory drugs using immobilized cell process. *Chemosphere, 8*, 23-29.

USDA/APHIS/Veterinary Services, (1999). *Antibiotic Use in U.S. Livestock Production*, http://www.aphis.usda.gov/vs/ceah/cei/health.htm#antimicrobial.

USFDA, (2004). *Electronic Orange Book: Approved Drug Products*, in *(U.S. Food and Drug Administration).* http://www.fda.gov/cder/ob/default.htm

Uyaguari, M., Key, P., Moore, J., Jackson, K., & Scott, G. (2009). Acute effects of the antibiotic oxytetracycline on the bacterial community of the grass shrimp, palaemonetes pugio. *Environmental Toxicology and Chemistry, 28 (12)*, 2715-2724

Uyanik, S., Sallis, P.J., & Anderson, G.K. (2002). The effect of polymer addition on granulation in an anaerobic baffled reactor (ABR). Part I: process performance. *Water Research*, *36*, 933-943.

Valvo, L., Ciranni, E., Alimenti, R., Alimonti, S., Draisci, R., Gianneti, L., et al. (1998). Development of a simple liquid chromatographic method with UV and mass spectrometric detection for the separation of substances related to amoxicillin sodium. *Journal Chromatography A, 797*, 311-316.

Van der Meer, R.R., & Heertjes, P.M. (1983). Mathematical description of anaerobic treatment of wastewater in up flow reactors. *Biotechnology and Bioengineering, 25 (11),* 2531-2556.

Van Lier, J.B., Van Der Zee, F.P., Tan, N.C.G., Rebac, S., & Kleerrebezem, R. (2001). Advances in high-rate anaerobic treatment: staging of reactor systems. *Water Science and Technology*, *44*, 15-25.

Vavilin, V.A., & Lokshina, L.Y. (1996). Modeling of volatile fatty acids degradation kinetics and evaluation of microorganism activity. *Bioresource Technology,* 57 (1), 69-80

Walsh, C. (2003). *Antibiotics: actions, origins, and resistance* (hardcover). ASM Press, Washington

Wang, S., Rao, N.C., Qiu, R., & Moletta, R. (2009). Performance and kinetic evaluation of anaerobic moving bed biofilm reactor for treating milk permeate from dairy industry. *Bioresource Technology, 100,* 5641-5647.

Wang, Y., Zhang, Y., Wang, J., & Meng, L. (2009) Effects of volatile fatty acid concentrations on methane yield and methanogenic bacteria. *Biomass and Bioenergy, 33 (5),* 848-853.

Watkinson, A.J., Murby, E.J., & Costanzo, S.D. (2007). Removal of antibiotics in conventional and advanced wastewater treatment: Implications for environmental discharge and wastewater recycling. *Water Research, 41 (18),* 4164–4176

Wollenberg, L., Halling-Sorensen, B., & Kusk, K.O. (2000). Acute and chronic toxicity of veterinary antibiotics to *Daphnia magna***.** *Chemosphere, 40,* 723-730

Wong, B-T., Show, K-Y., Su, A., Wong, R-J., & Lee, D-J. (2008). Effect of Volatile Fatty Acid Composition on Up flow Anaerobic Sludge Blanket (UASB) Performance. *Energy & Fuels, 22,* 108-112

Wu, Q. (1985). Mathematical modeling analysis of floating bead biofilter applications to domestic wastewater treatment. *Ph.D Thesis,* Xiang Tan University, China.

Wu, X., Wei, Y., Zheng, J., Zhao, X., & Zhong, W. (2011). The behavior of tetracyclines and their degradation products during swine manure composting. *Bioresource Technology, 102 (10),* 5924-5931

Yahiat, S., Fourcade, F., Brosillon, S., & Amrane, A. (2011). Removal of antibiotics by an integrated process coupling photocatalysis and biological treatment – Case of tetracycline and tylosin. *International Biodeterioration & Biodegradation, 65 (7),* 997-1003

Yang, S., & Carlson, K.H. (2004). Solid-phase extraction high performance liquid chromatography ion trap mass spectrometry for analysis of trace concentrations of macrolide antibiotics in natural and wastewater matrices. *Journal of Chromatography, A, 1038 (1-2),* 141-155.

Yetilmezsoy, K., & Sakar, S. (2008). Development of empirical models for performance evaluation of UASB reactors treating poultry manure wastewater under different operational conditions. *Journal of Hazardous Materials, 153,* 532-543.

Yu, H, Wilson, F., & Tay, J. (1998). Kinetic analysis of an anaerobic filter treating soybean wastewater. *Water Research, 32*, 3341-3352.

Zaldívar, J-M., & Baraibar, J. (2011). A biology-based dynamic approach for the reconciliation of acute and chronic toxicity tests: Application to *Daphnia magna*. *Chemosphere*, *82 (11),* 1547-1555.

Zaman, N.Q. (2010). *The Applicability of Batch Tests to Assess Biomethanation Potential of Organic Waste and Assess Scale up to Continuous Reactor Systems.* Ph.D Thesis. Environmental Engineering, University of Canterbury, New Zealand

Zhang, P., Chen, Y., & Zhou, Q. (2010). Effect of surfactant on hydrolysis products accumulation and short-chain fatty acids (SCFA) production during mesophilic and thermophilic fermentation of waste activated sludge: kinetic studies. *Bioresource Technology*, *101,* 6902-6909.

Zhang, Y., Cai, X., Lang, X., Qiao, X., Li, X., & Chen, J. (2012). Insights into aquatic toxicities of the antibiotics oxytetracycline and ciprofloxacin in the presence of metal: Complexation versus mixture. *Environmental Pollution, 166,* 48-56

Zhou, L., Ji, M., Zhang, G., & Yin, C. (2009). Treatment of Chemical Synthesis-Based Pharmaceutical Wastewater with Combined ABR and MBR System. *3rd International Bioinformatics and Biomedical Engineering Conference*, 1-5.

Zhou, P., Su, C., Li, B., & Qian, Y. (2006). Treatment of high-strength pharmaceutical wastewater and removal of antibiotics in anaerobic and aerobic biological treatment processes. *Journal of Environmental Engineering, 132*, 129-136.